BIOCHEMICAL AND FUNCTIONAL CHARACTERIZATION OF RPA2 N-TERMINAL PHOSPHORYLATION DURING DNA REPAIR AND CHECKPOINT ADAPTATION IN SACCHAROMYCES CEREVISIAE

A Dissertation
Submitted to the Graduate Faculty
of the
North Dakota State University
of Agriculture and Applied Science

By

Timothy Michael Wilson

In Partial Fulfillment of the Requirements
for the Degree of
DOCTOR OF PHILOSOPHY

Major Program:
Biochemistry

March 2018

Fargo, North Dakota

North Dakota State University
Graduate School

Title

BIOCHEMICAL AND FUNCTIONAL CHARACTERIZATION OF RPA N-TERMINAL PHOSPHORYLATION DURING DNA REPAIR AND CHECKPOINT ADAPTATION IN SACCHAROMYCES CEREVISIAE

By

TIMOTHY MICHAEL WILSON

The Supervisory Committee certifies that this ***disquisition*** complies with North Dakota State University's regulations and meets the accepted standards for the degree of

DOCTOR OF PHILOSOPHY

SUPERVISORY COMMITTEE:

Stuart Haring
Chair

D.K. Srivastava

Pinjing Zhao

Glenn Dorsam

Approved:

03/30/2018	Gregory Cook
Date	Department Chair

ABSTRACT

In response to DNA damage, a signaling cascade is activated within cells that promotes cell cycle arrest in order to provide adequate time for DNA repair to occur. Replication Factor A (RFA) is an essential, heterotrimeric complex that acts as a primary sensor of DNA damage, localizes to sites of and binds to broken DNA, and serves as a platform for several DNA damage repair proteins. RFA-coated ssDNA leads to activation of the sensor kinase Mec1. Activation of Mec1 leads directly to phosphorylation of the checkpoint regulator Rad53, which in turn activates several downstream effectors that halt cell growth and promote DNA repair.

In response to a permanent, irreparable DNA lesion yeast cells undergo Rad53-dependent checkpoint arrest for approximately 12 hours. After this prolonged arrest, cell cycle restart occurs sometime between 12-15 hours, promoting mitosis despite the presence of an unrepaired lesion. This aberrant checkpoint exit is known as checkpoint adaptation. Checkpoint adaptation deficiency, or the inability to override the established Rad53-dependent checkpoint, can be conferred through deletion of non-essential but important genes involved in DNA damage repair (*e.g.*, *ku70*Δ*, rdh54*Δ). The molecular mechanism(s) by which checkpoint adaptation occurs remains poorly understood; however, a single point mutation (K45E) in the Rfa1 subunit of the RFA complex is capable of rescuing adaptation deficiencies.

During the DNA damage response, the RFA complex is known to be post-translationally modified through phosphorylation, ubiquitination, and sumoylation. Despite robust characterization of these modifications to RFA, the physiological role of phosphorylation within the N-terminal (NT) domain of the second subunit of the RFA complex, Rfa2, remains elusive. My studies using phospho-mimetic Rfa2 mutants demonstrates that phosphorylation of the NT is: *1)* dispensable for activation of the Rad53-dependent checkpoint, *2)* is readily detected during the temporal window within which checkpoint adaptation occurs and *3)* promotes checkpoint adaptation in all adaptation-deficient mutations tested. Furthermore, analysis of Rfa2 phospho-mutants in sensor kinase deletions *mec1*Δ and *tel1*Δ reveal phosphorylation of the Rfa2 NT may directly impede Mec1 activity, thereby inhibiting maintenance of the Rad53-dependent checkpoint and providing a mechanism by which cells can escape an established DNA damage-dependent checkpoint.

ACKNOWLEDGEMENTS

During the Ph.D. process, I learned that gambles rarely, if at all, ever pay off to the degree that one might expect them to when leaving things to chance. When I was accepted to NDSU's graduate program, I knew in the back of my mind that someone was taking a chance on me, gambling their future to benefit my own. To that end, I would like to acknowledge and directly thank Dr. Stuart Haring, not only for taking that gamble in 2012 and bringing me into his lab but also for the years of mentorship, thought-provoking discussion, friendship, and raw energy that enabled me to be successful within his laboratory. Dr. Haring always made sure that his students were held to the absolute highest standard, and I hope that in my future work I can emulate the degree of perfection and precision that he expects of his students. All that you did for me will never be forgotten Dr. Haring, and I will be forever grateful.

I would also like to thank all of the people within the Haring lab that helped me along the way – former graduate student Dr. Padmaja L. Ghospurkar; current graduate students Angela M. Adsero and Trevor L. Baumgartner, and Wendy A. Larson, as well as all the undergraduate researchers who I have been lucky enough to mentor and work with throughout my graduate career, Erin M. Richards, Cristian M. Hernandez, Barbara L. Senger, Nolan M. Miles, Noelle P. Torrence, Allison K. Christensen, Anna K. Reinholz, Courtney M. Karnopp, Francis P. Landman, and Brian L. Samuelson. Without your diligence, help, and feedback, none of the work I have done would have been possible.

Thank you all for lifting me up and being the giants whose shoulders I could stand upon.

DEDICATION

For Family. For Moose. For Science.

TABLE OF CONTENTS

ABSTRACT iii

ACKNOWLEDGEMENTS iv

DEDICATION v

LIST OF TABLES xii

LIST OF FIGURES xiii

LIST OF ABBREVIATIONS xvii

LIST OF SYMBOLS xix

LIST OF APPENDIX FIGURES xx

CHAPTER 1: INTRODUCTION 1

1.1. Introduction to the DNA damage response 1

1.2. Replication Protein A – guardian of the genome 2

1.2.A. Basic biochemical properties of RPA 2

1.2.B. RPA domains required for LPR- and DDC-specific interactions 4

1.3. Post-translational modification of RPA and relevant mutant phenotypes 8

1.3.A. Sumoylation of RPA 9

1.3.B. Ubiquitination of RPA 11

1.4. Phosphorylation of the human RPA complex and related mutant phenotypes 12

1.4.A. Phosphorylation of Rpa2 in other model systems 15

1.4.B. Phosphorylation of RFA in budding yeast 15

1.5. Meiotic process and meiotic recombination 16

1.5.A. Meiotic recombination is essential for proper chromosomal segregation 19

1.5.B. RPA interactions with LPR and meiosis-specific factors during meiosis 20

1.5.C. Phosphorylation of RPA during meiosis 21

1.6. The DNA damage response 21

1.6.A. Initiation of the DNA damage response – lesion processing and repair 22

1.6.B. DNA damage repair through non-homologous end joining 25

1.6.C. DNA damage repair through homologous recombination 27

1.6.D. Other types of DNA repair (NER, BER, MMR, and BIR) 30

1.7. DNA damage-dependent checkpoint (DDC) 30

1.7.A. Establishment of the DDC in *Saccharomyces cerevisiae* 31

1.7.B. Checkpoint arrest in yeast prevents anaphase, entry into mitosis via Rad53/Chk1 activity 32

1.7.C. The currently undefined role for RPA phosphorylation during the DDC 33

1.8. Description of Thesis 34

CHAPTER 2: RFA2 PHOSPHORYLATION DURING LESION PROCESSING AND DNA REPAIR 36

2.1. Abstract 36

2.2. Introduction 36

2.3. Materials and Methods 41

2.3.A. Strains and Plasmids 41

2.3.B. DNA damage spot-plating assays 43

2.3.C. *In vitro* site-directed mutagenesis 43

2.3.D. Plasmid shuffle to generate mutant RPA strains 43

2.3.E. DNA damage induction and collection of whole-cell lysate 44

2.3.F. Phosphatase treatment of whole cell lysates 44

2.3.G. SDS-PAGE and Immunoblotting 44

2.3.H. Phospho-specific Immunoblotting of *rfa2-h2NT* 45

2.4. Results 45

2.4.A. Examination of sequential phosphorylation and site-dependent phosphorylation mechanisms in *Saccharomyces cerevisiae* using *rfa2-h2NT* 45

2.4.B. Analysis of Rfa2-h2NT mutant function in *Saccharomyces cerevisiae* 46

2.4.C. Analysis of Rfa2 NT extensive mutations in kinase deletion mutant yeast 49

2.4.D. Detection of Rfa2 modifications during prolonged genotoxic stress 50

2.4.E. Delayed modification observed upon prolonged DNA damage is phosphorylation 63

2.4.F. Delayed Rfa2 NT phosphorylation is localized to the NT domain and is not dependent on early S122 phosphorylation 63

2.4.G. Damage-sensitive Rfa2 NT extensive mutations are prominently phosphorylated at S122 66

2.4.H. Rfa2 NT mutations display differential effects on Mec1 activity 67

2.4.I. Examination of Rfa2 phosphorylation in DNA damage response kinases deletions 68

2.4.J. Rfa2 NT phosphorylation is observed under various genotoxic conditions 68

2.4.K. Rfa2 NT phosphorylation is readily detectable in an *rfa1-t11* mutation 70

2.5. Discussion 71

2.5.A. Rfa2 is phosphorylated via two temporally distinct mechanisms 71

2.5.B. Rfa2 phosphorylation at S122 as a marker for Mec1/Tel1 activity 74

2.5.C. Delayed Rfa2 NT phosphorylation is not dependent on the Rfa1 NT (DBD-F) 75

2.5.D. Yeast as a model system to study Rfa2 dynamics of other eukaryotic organisms and the physiological relevance of Rfa2 phosphorylation within those organisms 75

2.5.E. Implications for delayed Rfa2 NT phosphorylation 76

2.6. Acknowledgements 77

CHAPTER 3: RFA2 NT PHOSPHORYLATION DURING CHECKPOINT ADAPTATION PROMOTES MITOTIC EXIT IN THE PRESENCE OF AN IRREPARABLE LESION 78

3.1. Abstract 78

3.2. Introduction 78

3.3. Materials and Methods 82

3.3.A. Strains and Plasmids 82

3.3.B. Single DSB induction and collection of whole-cell lysate 82

3.3.C. Checkpoint adaptation plating assays 83

3.3.D. SDS-PAGE and Immunoblotting 84

3.4. Results 85

3.4.A. *rdh54*Δ mutations recapitulate known damage sensitives that are exacerbated by the phospho-state of the Rfa2 NT 85

3.4.B. The native Replication Factor A2 amino-terminus is phosphorylated in response to a single, irreparable double-strand break. 88

3.4.C. Checkpoint adaptation efficiency is dependent on the Rfa2 NT and its phospho-state. 89

3.4.D. Rfa2 NT mutations that mimic NT phosphorylation or are naturally phosphorylated promote checkpoint adaptation in adaptation-deficient *rdh54*Δ cells. 90

3.4.E. Phosphorylation at serine 122 of Rfa2 has little influence on the checkpoint adaptation function of RFA. 94

3.4.F. A naturally phosphorylated Rfa2 NT mutation also drives checkpoint adaptation in otherwise adaptation-deficient *rdh54*Δ cells. 97

3.4.G. Regions of the Rpa2 NT and their importance in checkpoint adaptation 100

3.5. Discussion 103

3.5.A. Rfa2 NT phosphorylation mediates checkpoint and mitotic exit 103

3.5.B. Certain subregions of the Rfa2 NT may be preferential phospho-targets during mitotic exit 106

3.5.C. Ubiquitination and sumoylation of RPA is dispensable during the DDC 106

3.5.D. Phosphorylation of the Rfa2 NT rescues adaptation-deficient *rdh54*Δ 107

3.6. Acknowledgements 108

CHAPTER 4: RFA2 N-TERMINAL PHOSPHORYLATION RESCUES CHECKPOINT ADAPTATION-DEFICIENT YEAST 109

4.1. Abstract 109

4.2. Introduction 109

4.3. Materials and Methods 112

4.3.A. Strains and Plasmids 112

4.3.B. Diagnostic replica plating used in analysis of deletion mutants 113

4.3.C. Single DSB induction and collection of whole-cell lysate 114

4.3.D. Checkpoint adaptation plating assays 114

4.3.E. SDS-PAGE and Immunoblotting 114

4.3.F. Yeast genomic DNA isolation for qPCR resection assays 115

4.3.G. Analysis of resection via qPCR 116

4.4. Results 116

4.4.A. Adaptation proficiency conferred by Rfa2 NT extensive mutations is not dependent on DSB resection 116

4.4.B. The Rfa2 NT is required for checkpoint adaptation 119

4.4.C. Rfa2 NT extensive mutations promote rescue of adaptation-deficient *rtt107*Δ and *slx4*Δ 120

4.4.D. Effects of Rfa2 NT extensive mutations on *sae2*Δ adaptation-deficient mutations 129

4.4.E. *rfa2-D$_X$* and *rfa2-h2NT* promote adaptation rescue more efficiently than *rfa1-t11* in *ckII*Δ adaptation-deficient mutations 135

4.4.F. Rpa2 NT phosphorylation during checkpoint adaptation is distinct from phosphorylation during genotoxic stress 149

4.5. Discussion 149

4.5.A. Checkpoint adaptation promoted by Rfa2 NT phospho-mutations is not dependent on resection 149

4.5.B. Phospho-mimetic Rfa2 promotes adaptation rescue better than *rfa1-t11* 151

4.5.C. Potential therapeutic value in targeting Rpa2 phosphorylation during chemoradiation therapy in human disease 152

CHAPTER 5: FUNCTION OF THE RFA2 NT IN MEIOSIS AND OTHER UNSOLVED MYSTERIES 154

5.1. Introduction 154

5.2. Materials and Methods 155

5.2.A. Construction and *In vitro* site-directed mutagenesis of pRS315-Rfa2 NT extensive vectors 155

5.2.B. Integration of *pRS306*-Rfa2 NT extensive mutations into haploid yeast 156

5.2.C. Mating of haploid yeast to create diploid cells 157

5.2.D. Sporulation of diploid yeast and tetrad dissection 157

5.2.E. Diagnostic replica plating 158

5.2.F. Analysis of heteroallelic recombination 158

5.2.G. qPCR of *MAT* locus during mating type switching 158

5.2.H. Generation of yeast two hybrid vectors 158

5.3. Results 159

5.3.A. Examination of the effects of Rfa2 NT extensive mutations during meiosis 159

5.3.B. Effects of Rfa2 NT extensive mutations on heteroallelic recombination 162

5.3.C. Effects of Rfa2 NT extensive mutations on mating type switching 163

5.3.D. Auto-activation of pJG4-5 bait vector prevented identification of Rfa2 interacting partners 165

5.4. Discussion 166

5.5. Acknowledgements 168

CHAPTER 6: CONCLUDING DISCUSSION AND FINAL REMARKS 169

6.1. The role of the Rpa2 NT in LPR 169

6.1.A. Phosphorylation of the Rfa2 NT appears to be dispensable for LPR 170

6.1.B. The Rfa2 NT is physically required for LPR 171

6.1.C. Role for the Rfa2 NT in genome maintenance at telomeres 173

6.2. Defining the role of Rfa2 NT phosphorylation during mitotic exit 174

6.2.A. Rfa2 NT phosphorylation causes aberrant checkpoint exit in the presence of a persistent lesion 174

6.2.B. A simple model for Rfa2 NT phosphorylation promoting checkpoint exit 175

6.2.C. Phospho-mimetic Rfa2 NT mutations promote adaptation more efficiently than *rfa1-t11* 176

6.2.D. Rfa2 NT phosphorylation may drive signaling away from kinases and towards phosphatases 178

6.3. Role of the Rfa2 NT during meiosis unclear 181

6.3.A. Rfa2 NT extensive mutations lead to different meiotic phenotypes 181

6.3.B. Timing of meiotic divisions may be affected by Rfa2 NT phosphorylation 184

6.4. Final Remarks 185

REFERENCES 188

APPENDIX A. YEAST STRAINS 210

APPENDIX B. PLASMIDS 221

APPENDIX C. PRIMERS 228

APPENDIX D. APPENDIX FIGURES 239

LIST OF TABLES

Table		Page
1.1.	DNA repair proteins in budding yeast and their human homologs.	5
3.1.	Average Adaptation Percentages in NMM104 cells.	93
3.2.	Average Adaptation Percentages observed in *rdh54*Δ cells containing Rfa2 NT mutations.	95
3.3.	Mutation of a known, Mec1-phospho-target site on Rpa2 does not greatly impact adaptation proficiency or deficiency conferred by Rfa2 phospho-mutants.	99
3.4.	Average Adaptation Percentages conferred by *rfa2-h2NT* in *rdh54*Δ cells.	101
3.5.	Average Adaptation Percentages conferred by Rfa2 subregion mutations.	105
4.1.	Average Adaptation Percentages in NMM104 cells.	118
4.2.	Average Adaptation Percentages observed in NMM104 *tel1*Δ.	122
4.3.	Average Adaptation Percentages observed in NMM104 *rtt107*Δ cells.	128
4.4.	Average Adaptation Percentages observed in NMM104 *slx4*Δ.	131
4.5.	Average Adaptation Percentages observed in NMM104 *sae2*Δ.	134
4.6.	Average Adaptation Percentages observed in NMM104 *cka1*Δ.	145
4.7.	Average Adaptation Percentages observed in NMM104 *cka2*Δ.	146
4.8.	Average Adaptation Percentages observed in NMM104 *ckb1*Δ.	147
4.9.	Average Adaptation Percentages observed in NMM104 *ckb2*Δ.	148
5.1.	List of yeast two hybrid vectors generated.	155
5.2.	Effect of Rfa2 NT extensive mutations on tetrad formation in budding yeast.	160
5.3.	Effect of Rfa2 NT extensive mutations on meiosis in budding yeast.	160
5.4.	Effect of Rfa2 NT extensive mutations on spore survival ratio in budding yeast.	162
5.5.	Effect of Rfa2 NT extensive mutations on spore viability in budding yeast.	162

LIST OF FIGURES

Figure		Page
1.1.	RPA Schematics and Crystal Structure of RPA-ssDNA Complex from *U. maydis*	3
1.2.	The Five Stages of Meiosis.	18
1.3.	Initiation of Lesion Processing and Repair in Saccharomyces cerevisiae.	23
1.4.	Mec1/Tel1 sensor kinase signaling and Checkpoint Establishment.	24
1.5.	Non-Homologous End Joining.	26
1.6.	Initiation of Homologous Recombination in Budding Yeast	28
1.7.	Process of Homologous Recombination.	29
2.1.	Phosphorylation of eukaryotic Rpa2 NT in budding yeast.	40
2.2.	One-step gene replacement and verification strategy.	42
2.3.	Borowiec and Oakley models for sequential phosphorylation of the Rpa2 NT.	47
2.4.	Human-specific antibody recognition of damage dependent and mitotic *rfa2-h2NT* phosphorylation.	47
2.5.	*rfa2-h2A$_I$* mutations have no discernable effect on sequential phosphorylation of *rfa2-h2NT*.	48
2.6.	Mec1 phosphorylates *rfa2-h2NT* at known damage-dependent sites (T21 and S33).	49
2.7.	Alignment of Rfa2 NT ‘extensive’ mutations with Rfa2-h2 NT ‘extensive’ mutations.	51
2.8.	Additional phosphorylation of Rfa2-h2 NT mutations is not observed in ‘extensive’ NT mutations.	51
2.9.	Rfa2-h2 NT mutations produce phenotypes in line with Rfa2 NT extensive mutations.	52
2.10.	Diagnostic spot assay of *tel1*Δ, *chk1*Δ, *dun1*Δ mutants containing the *rfa2-D$_X$* mutation	53
2.11.	Diagnostic spot assay of *tel1*Δ, chk1Δ, *dun1*Δ mutants containing the *rfa2-A$_X$* mutation.	54
2.12.	Diagnostic spot assay of *tel1*Δ mutations (*rfa2-D$_X$* and *rfa2-h2NT*).	55
2.13.	Diagnostic spot assay of *tel1*Δ mutations (*rfa2-A$_X$* and *rfa2-*Δ*N$_X$)*.	56
2.14.	Diagnostic spot assay of *dun1*Δ Rfa2 NT extensive mutations (*rfa2-D$_X$* and *rfa2-h2NT*).	57
2.15.	Diagnostic spot assay of *dun1*Δ Rfa2 NT extensive mutations (*rfa2-A$_X$* and *rfa2-*Δ*N$_X$)*	58

2.16. Diagnostic spot assay of *chk1*Δ Rfa2 NT extensive mutations (*rfa2-D$_X$* and *rfa2-h2NT*). 59

2.17. Diagnostic spot assay of *chk1*Δ Rfa2 NT extensive mutations (*rfa2-A$_X$* and *rfa2-*Δ*N$_X$*)..... 60

2.18. Diagnostic spot assay of *sml1*Δ, *mec1*Δ, *rad53*Δ mutants containing the *rfa2-D$_X$* mutation. 61

2.19. Diagnostic spot assay of *sml1*Δ, *mec1*Δ, *rad53*Δ mutants containing the *rfa2-A$_X$* mutation. 62

2.20. Rfa2 NT phosphorylation is detectable in challenged with phleomycin. 64

2.21. Rfa2 NT phosphorylation is removed by lambda protein phosphatase. 64

2.22. Known Mec1-dependent phosphorylation sites have no discernable function in the Lesion and DNA repair program. 65

2.23. Rfa2 phosphorylation is not detected in Rfa2 NT extensive mutations containing *S122$_{A/D}$*..... 69

2.24. Rfa2-D$_X$ phosphorylation at S122 is impeded in *tel1*Δ. 70

2.25. Rfa2 NT phosphorylation occurs independent of Tel1, Chk1, and Dun1. 70

2.26. Rfa2 phosphorylation in response to low-levels of genotoxic stress. 72

2.27. Rfa2 phosphorylation in response to high-levels of genotoxic stress. 73

3.1. One-step gene replacement and verification strategy used in the creation of *rdh54*Δ. 83

3.2. Diagnostic spot assay of *rdh54*Δ Rfa2 NT phospho-mimetic mutations at various clastogen concentrations. 86

3.3. Diagnostic spot assay of *rdh54*Δ Rfa2 NT unphosphorylatable mutations at various clastogen concentrations..... 87

3.4. Rfa2 phospho-mimetics impact checkpoint adaptation differentially. 89

3.5. Hyper-phosphorylation of Rfa2 during checkpoint adaptation. 90

3.6. Comparison of Rfa2 NT extensive mutant integrations versus plasmid-borne expression 92

3.7. The N-terminus and its phospho-state affect checkpoint adaptation. 93

3.8. The phospho-state of the Rfa2 NT affects the ability of checkpoint adaptation to be rescued in the adaptation-deficient *rdh54*Δ mutation. 95

3.9. Rad53 activation corresponds to the ability of the Rfa2 NT mutation to rescue checkpoint adaptation in the adaptation-deficient *rdh54*Δ mutation. 96

3.10. Hyper-phosphorylation of the Rfa2 NT occurs but is reduced in the adaptation-deficient *rdh54*Δ mutation. 96

3.11. A known phosphorylation target (S122) outside of the Rfa2 NT does not affect checkpoint adaptation. 98

3.12. Natural hyper-phosphorylation of the Rfa2 NT occurs indistinguishably in both the adaptation-proficient *RDH54* strain and the adaptation-deficient *rdh54*Δ mutation. 99

3.13. Natural hyper-phosphorylation of the Rfa2 NT drives adaptation proficiency in the adaptation-deficient *rdh54*Δ mutation. 100

3.14. Rad53 activation corresponds to the ability of the Rfa2 NT mutation to rescue checkpoint adaptation in the adaptation-deficient *rdh54*Δ mutation. 101

3.15. Schematic of Rfa2 NT subregion mutations. 102

3.16. Rfa2 NT subregion mutations and their effect on adaptation in *RDH54* and *rdh54*Δ mutant cells. 104

4.1. Rfa2 NT phosphorylation is required for checkpoint adaptation in wild-type cells. 118

4.2. Rad53 phospho-state is correlated with checkpoint adaptation. 119

4.3. Proof of concept for resection qPCR assay. 120

4.4. Rfa2 NT is dispensable for long-range resection of MAT locus. 121

4.5. The Rfa2 NT is required for checkpoint adaptation in *tel1*Δ. 122

4.6. Diagnostic spot assay of *rtt107*Δ mutations (*rfa2-D$_X$* and *rfa2-h2NT*). 124

4.7. Diagnostic spot assay of rtt107Δ mutations (*rfa2-A$_X$* and *rfa2-*Δ*N$_X$)*. 125

4.8. Diagnostic spot assay of slx4Δ mutations (*rfa2-D$_X$* and *rfa2-h2NT*). 126

4.9. Diagnostic spot assay of slx4Δ mutations (*rfa2-A$_X$* and *rfa2-*Δ*N$_X$*). 127

4.10. Rfa2 NT phosphorylation is required for checkpoint adaptation in *rtt107*Δ cells. 128

4.11. Rad53 inactivation during checkpoint adaptation requires Rfa2 NT phosphorylation in *rtt107*Δ. 129

4.12. Rfa2 NT phosphorylation is required for checkpoint adaptation in *slx4*Δ cells. 130

4.13. Rad53 inactivation during checkpoint adaptation requires Rfa2 NT phosphorylation in *slx4*Δ. 131

4.14. Diagnostic spot assay of *sae2*Δ mutations (*rfa2-D$_X$* and *rfa2-h2NT*). 132

4.15. Diagnostic spot assay of *sae2*Δ mutations (*rfa2-A$_X$* and *rfa2-*Δ*N$_X$)*. 133

4.16. Rfa2 NT phosphorylation is required for checkpoint adaptation in *sae2*Δ cells. 134

4.17. Rad53 inactivation during checkpoint adaptation requires Rfa2 NT phosphorylation in *sae2*Δ. 135

4.18. Diagnostic spot assay of *cka1*Δ mutations (*rfa2-D$_X$* and *rfa2-h2NT*). 137

4.19. Diagnostic spot assay of *cka1*Δ mutations (*rfa2-A$_X$* and *rfa2-*Δ*N$_X$*). 138

4.20. Diagnostic spot assay of *cka2*Δ mutations (*rfa2-D$_X$* and *rfa2-h2NT*). 139

4.21. Diagnostic spot assay of *cka2*Δ mutations (*rfa2-A$_X$* and *rfa2-*Δ*N$_X$)*. 140

4.22. Diagnostic spot assay of *ckb1*Δ mutations (*rfa2-D$_X$* and *rfa2-h2NT*). 141

4.23. Diagnostic spot assay of *ckb1*Δ mutations (*rfa2-A$_X$* and *rfa2-*Δ*N$_X$*). 142

4.24. Diagnostic spot assay of *ckb2*Δ mutations (*rfa2-D$_X$* and *rfa2-h2NT*). 143

4.25. Diagnostic spot assay of *ckb2*Δ mutations (*rfa2-A$_X$* and *rfa2-*Δ*N$_X$*). 144

4.26. Rfa2 NT phosphorylation is required for checkpoint adaptation in adaptation-deficient *cka1*Δ mutations..... 145

4.27. Rfa2 NT phosphorylation is required for checkpoint adaptation in adaptation-deficient *cka2*Δ mutations..... 146

4.28. Rfa2 NT phosphorylation is required for checkpoint adaptation in adaptation-deficient *ckb1*Δ mutations..... 147

4.29. Rfa2 NT phosphorylation is required for checkpoint adaptation in adaptation-deficient *ckb2*Δ mutations..... 148

4.30. Rfa2 NT phosphorylation during checkpoint adaptation is distinct from that observed during genotoxic stress. 150

5.1. Restriction digest verification of Rfa2 NT extensive mutations in pRS306 integrating vectors..... 157

5.2. Effect of Rfa2 NT extensive mutations on meiosis in budding yeast. 160

5.3. Effect of Rfa2 NT extensive mutations on spore viability in budding yeast. 161

5.4. Effect of Rfa2 NT extensive mutations on heteroallelic recombination in budding yeast via diagnostic replica plating. 163

5.5. Effect of Rfa2 NT extensive mutations on heteroallelic recombination in budding yeast. 164

6.1. Model for Rfa2 NT phospho-regulation of ubiquitin and sumo ligase activity during LPR and adaptation 172

6.2. Rfa2 NT phosphorylation inhibits Mec1 potentiation of Rad53 phosphorylation leading to aberrant checkpoint exit 177

6.3. Model for Rfa2 NT phospho-regulation of kinase activity during LPR and adaptation 183

LIST OF ABBREVIATIONS

aa ..... amino acids

BER..... Base excision repair

BIR ..... Break induced replication

bp ..... base pairs

CPT ..... Camptothecin

Da ..... Dalton (molecular weight)

DBD ..... DNA binding domain

DDC ..... DNA damage-dependent checkpoint

DDR ..... DNA damage response

dHJ..... Double Holliday junction

DNA ..... Deoxyribonucleic acid

GAL..... galactose

HO..... Heterothallic

HR..... Homologous recombination

HU..... Hydroxyurea

kbp ..... kilobase pairs (1000 bases per kilobase)

kDa..... kilodalton (molecular weight, 1000 daltons per kilodalton)

LPR ..... Lesion processing and repair

MMR..... Mismatch repair

MMS..... Methyl methane sulfonate

MWM..... Molecular weight marker

NER ..... Nucleotide excision repair

NHEJ..... Non-homologous end joining

NT ..... N-terminus/N-terminal

nt..... nucleotide

OB..... oligonucleotide binding

PD ..... Phosphorylation domain

PHL ..... Phleomycin

RFA..... Replication Factor A

RIC ..... Recombination initiation complex

RPA ..... Replication Protein A

SD- ..... Synthetic complete media with dextrose

SSA ..... Single-strand annealing

ssDNA ..... Single-stranded DNA

WHD ..... winged-helix domain

YPD ..... Yeast extract peptone dextrose

YPR ..... Yeast extract peptone raffinose

YPRG ..... Yeast extract peptone raffinose galactose

LIST OF SYMBOLS

Δ	Upper-case Delta; used to describe deletions, defining the DNA polymerase Δ holoenzyme
α	Alpha; used in defining helical secondary structure, defining the DNA polymerase α protein
μ	Mu; used to described DNA polymerase μ
δ	Lower-case delta; used to define DNA polymerase δ
λ	Lambda; used in defining Lambda protein phosphatase, short-hand for MWMs in agarose gels
ºC	Degree symbol, used to define degrees Celsius

LIST OF APPENDIX FIGURES

Figure		Page
D.1.	Distribution of cells in Rfa2 NT extensive mutations during adaptation time course.	239
D.2.	Distribution of cells in *rdh54*Δ Rfa2 NT extensive mutations during adaptation time course.	240
D.3.	Distribution of cells in *rdh54*Δ rfa2-h2NT mutations during adaptation time course.	241
D.4.	Distribution of cells in *rfa2-S122*$_{D/A}$ mutations during adaptation time course.	242
D.5.	Distribution of cells in *rfa2-D*$_X$*-S122*$_{D/A}$ mutations during adaptation time course.	243
D.6.	Distribution of cells in *rfa2-ΔN*$_X$*-S122*$_{D/A}$ mutations during adaptation time course.	244
D.7.	Distribution of cells in *rfa2-D*$_M$ mutations during adaptation time course.	245
D.8.	Distribution of cells in *rfa2-A*$_M$ mutations during adaptation time course.	246
D.9.	Distribution of cells in NMM104 Rfa2 NT extensive mutations during adaptation time course.	247
D.10.	Distribution of cells in *tel1*Δ Rfa2 NT extensive mutations during adaptation time course.	248
D.11.	Distribution of cells in *sae2*Δ Rfa2 NT extensive mutations during adaptation time course.	249
D.12.	Distribution of cells in *rtt107*Δ Rfa2 NT extensive mutations during adaptation time course.	250
D.13.	Distribution of cells in *slx4*Δ Rfa2 NT extensive mutations during adaptation time course.	251
D.14.	Distribution of cells in *cka1*Δ Rfa2 NT extensive mutations during adaptation time course.	252
D.15.	Distribution of cells in *cka2*Δ Rfa2 NT extensive mutations during adaptation time course.	253
D.16.	Distribution of cells in *ckb1*Δ Rfa2 NT extensive mutations during adaptation time course.	254
D.17.	Distribution of cells in *ckb2*Δ Rfa2 NT extensive mutations during adaptation time course.	255

CHAPTER 1: INTRODUCTION

1.1. Introduction to the DNA damage response

The transfer of unadulterated genetic material from cell-to-cell (mitosis) or parent-to-offspring (meiosis) is dependent on the ability of each cell to maintain the integrity of its own genome prior to these processes. Fortunately, each cell comes equipped with signaling pathways and proteins, many of which are highly conserved, responsible for the detection and processing of DNA lesions that might otherwise compromise the integrity of an organism's genome. Once a DNA lesion has been detected, an intracellular program known as the DNA damage response (DDR) is initiated, where lesion processing and repair (LPR) triggers the activation and establishment of the DNA damage-dependent checkpoint (DDC). While the primary purpose of the LPR is to facilitate faithful repair of the DNA lesion, the DDC provides the DNA repair machinery adequate time to process any and all lesions detected by halting cellular growth with the goal of preventing aberrant chromosomal division and genomic instability (Ciccia *et al.* 2010).

At the center of all DNA metabolism is the essential, conserved, heterotrimeric complex Replication Protein A (RPA). Replication Protein A's primary biochemical function is to bind any single-stranded DNA (ssDNA) detected in the cell (Blackwell *et al.* 1994). Originally identified as being essential for *in vitro* DNA replication of *SV40* viral DNA (Wold *et al.* 1988), RPA also functions as a genuine guardian of the genome by playing an indispensable role in mediating LPR in every phase of the cell cycle (Wold 1997). As the first line of defense against potentially mutagenic lesions, RPA is required for generating the initial scaffold that promotes error-free DNA repair through a process known as homologous recombination (HR) (Zou *et al.* 2003). During both LPR and the DDC, RPA's activity appears to be mediated through post-translational modification of the heterotrimeric complex. These modifications are thought to control repair by regulating the interactions between RPA and its partners (Marechal *et al.* 2015). Recent work, and work within this thesis suggest that post-translational modification, particularly phosphorylation, of RPA also temporally regulates the DDC and mitotic exit in response to irreparable DNA lesions.

1.2. Replication Protein A – guardian of the genome

Replication Protein A (RPA) is a highly conserved heterotrimeric protein complex that plays essential roles in DNA replication, repair and homologous recombination. The RPA complex is comprised of the Rpa1, Rpa2, and Rpa3 proteins (Figure 1.1A and 1.1B), and in budding yeast, RPA is known as Replication Factor A (RFA) containing the analogous subunits Rfa1, Rfa2, and Rfa3. As guardian of the genome, RPA binds and protects any single-stranded DNA (ssDNA) intermediates that arise during DNA replication, DNA repair, and homologous recombination to prevent nucleolytic digestion of ssDNA or the formation of repair- or replication-impeding secondary structures (*e.g.*, hairpins) (Yuzhakov *et al.* 1999, Kowalczykowski 2000). RPA plays dynamic and indispensable roles in the coordination and assembly of replication machinery, such as the DNA polymerase Δ holoenzyme and DNA polymerase α-primase (Dornreiter *et al.* 1992, Yuzhakov *et al.* 1999), the initial signaling platform utilized in during DDR in activating the DDC (Zou *et al.* 2003), and even in the maintenance of telomeres (Smith *et al.* 2000, Schramke *et al.* 2004, Grudic *et al.* 2007, Luciano *et al.* 2012).

1.2.A. Basic biochemical properties of RPA

The heterotrimeric RPA complex has been demonstrated to bind ssDNA in a sequence non-specific manner with 5'→3' polarity and very high (sub-nanomolar) affinity (Kim *et al.* 1994, Bochkarev *et al.* 1997, Arunkumar *et al.* 2003). Rpa1 (616 amino acids (aa), 70 kDa) is the largest subunit of the RPA complex and contains the modular domain architecture and flexible arrangement, when compared with the other RPA subunits (Figure 1.1B). An oligonucleotide binding (OB)-fold amino-terminal (N-terminal) domain, known as DBD-F (DNA binding domain F), is linked to the rest of the core Rpa1 peptide through a flexible linker region. The core Rpa1 protein consists of OB-fold domains A, B, and C (DBD-A, DBD-B, and DBD-C), where DBD-A and DBD-B promote the strongest ssDNA interactions for the RPA complex (Kim *et al.* 1992, Kim *et al.* 1994). DBD-C of Rpa1 is also capable of binding ssDNA, and is primarily required for trimerization of the RPA complex with Rpa2 and Rpa3 through conserved alpha helical bundles that exist at the C-terminal regions within DBD-C of Rpa1, DBD-D of Rpa2, and DBD-E of Rpa3 (Bochkareva *et al.* 2002). Rpa2 (270 aa, 32 kDa) is comprised of a short, unstructured 40 amino acid phosphorylation domain within its N-terminus that leads into a high affinity oligonucleotide binding fold (DBD-D) and terminates with a specialized winged-helix domain (WHD) composed of a winged helix-loop-

helix motif (Mer *et al.* 2000). Rpa3 (121 aa, 14 kDa), the smallest of the RPA subunits, is composed of an oligonucleotide binding fold (DBD-E) that appears to have very low affinity for DNA (similar to DBD-F), and its major role appears to be stabilization of the heterotrimeric complex (Iftode *et al.* 1999, Bochkareva *et al.* 2002).

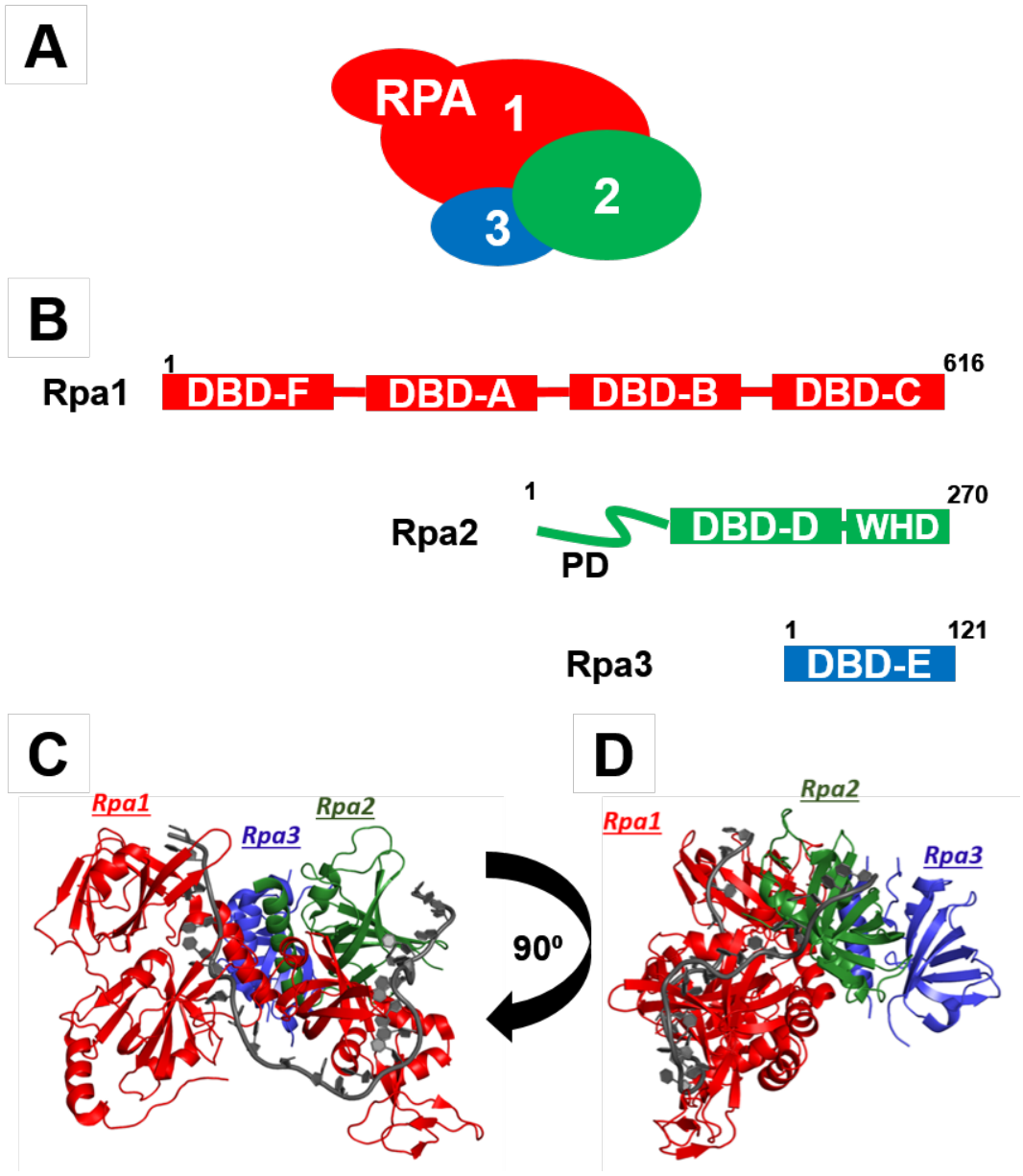

Figure 1.1. RPA Schematics and Crystal Structure of RPA-ssDNA Complex from *U. maydis*. **A.** Pictorial representation of the RPA heterotrimer as utilized throughout this thesis**. B.** Schematic diagram of the three individual RPA subunits Rpa1, Rpa2, and Rpa3. Rpa1 is comprised of DBD-F, DBD-A, DBD-B, DBD-C and is 616 amino acids (aa) long. Rpa2 is 270 aa long and made up of an N-terminal phosphorylation domain (PD), DBD-D, and the winged-helix domain (WHD). **C** and **D.** Representation of RPA bound to ssDNA from structural data isolated from *U. maydis* RPA. PDB: 4GOP.

Replication Protein A complex binding to ssDNA is thought to proceed through a two-step binding mode process. First, RPA binds ssDNA in 8-10 nucleotide (nt) increments, representative of DBD-A and DBD-B interaction with ssDNA (Bochkarev *et al.* 1997, Arunkumar *et al.* 2003). This first binding mode is thought to be a short binding mode that affords RPA the ability to transition to its long binding mode that occludes 23-30 nucleotides of ssDNA through the additive binding of DBD-C and DBD-D (Bastin-Shanower *et al.* 2001). Interestingly, DBD-A and DBD-B of Rpa1 have been demonstrated to have nearly 100-fold higher affinity for ssDNA than that of the remaining RPA DBDs *in vitro* (Arunkumar *et al.* 2003). Moreover, mutation of aromatic residues within DBD-A (*rpa1-aroA*; F238/F269A) and DBD-B (*rpa1-aroB*; W361/F382A) confer significant defects in DNA replication leading to damage sensitive cells that accumulate in S- and G2-phases (Haring *et al.* 2008). Binding of the RPA complex to ssDNA has been shown via structural studies to transition from an elongated structure in the short 8-10 nt binding mode, to a condensed, almost horseshoe-like structure in the condensed, long 23-30 nt binding mode (Figure 1.1C and 1.1D) (Bochkareva *et al.* 2002, Fan *et al.* 2012).

1.2.B. RPA domains required for LPR- and DDC-specific interactions

While the core DBDs are required for RPA's primary ssDNA binding activity, other regions of the RPA complex have been demonstrated to be required for RPA's activity during LPR and establishment of the DDC. The most well studied and arguably most important domain of RPA involved DNA repair is DBD-F of Rpa1. While possessing an OB-fold structure, DBD-F does not contribute to binding of RPA to ssDNA or DNA replication, as RPA mutants lacking DBD-F (*rpa1-*Δ*FL)* or containing the *rpa1-t11* (R45E and Y52F) mutation are proficient for both RPA localization to repair foci and DNA replication following endogenous Rpa1 knockdown (Haring *et al.* 2010). While it is unclear in human cells whether this leads to inviability of the cells, deletion of DBD-F in yeast results in inviability (Philipova *et al.* 1996). In human cells, deletion of DBD-F has been demonstrated to lead to an aberrant cell cycle distribution post-exposure to DNA damaging agents, indicating a checkpoint deficiency, despite the mutant RPA complex being able to localize to DSB sites, similar to that observed for *rpa1-t11* (Haring *et al.* 2008). It is unclear whether cells are able to establish a proper DDC with *rpa1-t11* or *rpa1-*Δ*FL*, or if they initiate checkpoint establishment and then, through an unknown mechanism, bypass the established checkpoint. Because deletion of DBD-F in budding yeast results in inviable cells, the most well characterized DBD-F mutation

Table 1.1. DNA repair proteins in budding yeast and their human homologs.

Functional Class	*S. cerevisiae*	*H. sapiens*	Function	Source
ssDNA sensor	Rfa1 Rfa2 Rfa3	Rpa1 Rpa2 Rpa3	Binds ssDNA, platform for checkpoint activation and Repair	Lisby and Rothstein 2004
DSB sensor	Mre11 Rad50 Xrs2	Mre11 Rad50 Nbs1	Endonuclease; ATPase	Lisby and Rothstein 2004
Clamps	Rad24/Rfc2-5	Rad17/Rfc2-5	Clamp loader complex Loads 9-1-1- clamp	Lisby and Rothstein 2004
Clamps	Ddc1 Mec3 Rad17	Rad9 Hus1 Rad1	9-1-1 clamp, interacts with Effector kinases	Lisby and Rothstein 2004
Adaptors	Mrc1	Claspin	Rad53/Chk1 Chaperone	Lisby and Rothstein 2004
Adaptors	Rad9	BRCA1 MDC1 53BP1	Rad53/Chk1 Chaperone	Lisby and Rothstein 2004
Sensor Kinase	Mec1/Ddc2	ATR/ATRIP	Required for checkpoint activation; stimulates Rad53/Chk1 activity	Lisby and Rothstein 2004
Sensor Kinase	Tel1	ATM	Phosphorylates several effectors; promotes checkpoint activation	Lisby and Rothstein 2004
Effector Kinase	Rad53	Chk2	Cell cycle arrest	Lisby and Rothstein 2004
Effector Kinase	Chk1	Chk1	Cell cycle arrest, inhibition of anaphase entry	Lisby and Rothstein 2004
Recombination Protein	Rad52	Rad52	RPA-Rad51 Exchange Strand Annealing during HR	Kowalczykowski 2015

Table 1.1. DNA repair proteins in budding yeast and their human homologs (continued).

Functional Class	*S. cerevisiae*	*H. sapiens*	Function	Source
Recombination Protein	Rad51	Rad51	Displaces RPA with Rad52; binds ssDNA, pairs homologous DNA during HR	Kowalczykowski 2015
Recombination Protein	Rdh54	Rad54B	Required for proper HR repair	Kowalczykowski 2015
End Joining Proteins	Yku70/Yku80	Ku70/Ku80	End tethering and End Joining	Kowalczykowski 2015
End Joining Proteins	Dnl4/Lif1	Lig4/Xrcc4	DNA ligase IV complex	Kowalczykowski 2015
Resection Protein	Sae2	CtiP	Component of MRXS/MRN-CtiP. Required for resection	Kowalczykowski 2015
Resection Protein	Sgs1-Top3-Rmi1 (STR)	BLM-TopIIIα-Rmi1 (BTR)	Nuclease/Helicase complex	Kowalczykowski 2015
Resection Protein	Dna2	Dna2	Nuclease/Helicase; functions with STR/BTR & Exo1	Kowalczykowski 2015
Resection Protein	Exo1	Exo1	MRX/MRN-independent exonuclease	Kowalczykowski 2015
Scaffolding Protein	Rtt107	PTIP	Required for checkpoint activation Scaffolding protein	Kowalczykowski 2015
Scaffolding Protein	Slx4	Slx4	Holliday junction resolution Endonuclease	Leung *et al.* 2014
Scaffolding Protein	Dpb11	TopBP1	Mec1/ATR activation; interacts with 9-1-1 Clamp; scaffold assembly at DSB	Leung *et al.* 2014

in DNA metabolism and cell cycle regulation is *rfa1-t11* (K45E) (Umezu *et al.* 1998). The *rfa1-t11* mutation confers hypersensitivity to DNA damaging agents (Chen *et al.* 1998, Umezu *et al.* 1998) and has been reported to have an inability to load Rad24-RFC onto damage-like substrates *in vitro* (Majka *et al.* 2006). However, it remains unclear as to whether a physical interaction between Rad24 and *rfa1-t11* is abrogated or whether RFA containing *rfa1-t11* interacts with the DNA properly to facilitate the proper loading of Rad24. Moreover, the *rpa1-t11* (R41E and Y42F) mutation in human cells has been demonstrated to disrupt or impede interactions that are critical for checkpoint establishment, including ATR/ATRIP (Ball *et al.* 2005, Nakada *et al.* 2005), Rad17-RFC loading (Zou *et al.* 2003, Majka *et al.* 2006), Rad9 (component of the Rad9-Rad1-Hus1 '9-1-1' PCNA-like clamp; Zou *et al.* 2003, Xu *et al.* 2008) , as well as the MRN complex (Mre11-Rad50-Nbs1, essential complex for DSB processing; Robison *et al*. 2004, Robison *et al*. 2005, Olson *et al*. 2007) . DBD-F has also been reported to interact with TopBP1, a scaffolding protein required for activation of ATR (Kumagai *et al.* 2006, Mordes *et al.* 2008, Navadgi-Patil *et al.* 2008, Germann *et al.* 2011). Table 1.1 lists all the known homologs between yeast and human proteins involved in the DDR.

In yeast, *rfa1-t11* has been demonstrated to promote checkpoint adaptation, or the ability of cells to enter into mitosis despite the continued presence of DNA lesions, in cells containing adaptation-deficient mutations (Lee *et al.* 2001, Pellicioli *et al.* 2001, Lee *et al.* 2003, Ghospurkar *et al.* 2015). The interaction between Ddc2 (Mec1 chaperone/interacting partner) and RFA has been reported to be impeded by *rfa1-t11*, suggesting that Mec1 cannot become fully activated in *rfa1-t11* cells (Zou *et al.* 2003, Grandin *et al.* 2007, Deshpande *et al.* 2017); however, *rfa1-t11* cells can still activate the Rad53-dependent checkpoint suggesting a defect in checkpoint maintenance rather than checkpoint establishment.

DBD-F is not the only domain thought to be essential for protein-protein interactions during the DDR. Rpa2 contains a C-terminal winged helix-loop-helix motif known as the winged-helix domain (WHD) (Mer *et al.* 2000). In human cells, the WHD has been demonstrated to interact with a number of proteins essential for proper genome maintenance such as Rad52 (strand-annealing protein required for homologous recombination; Park *et al*. 1996, Sung 1997, Gasior *et al*. 1998, Shinohara et al 1998 New *et al*. 2002, Sugiyama et al. 2006, Sleeth *et al*. 2007) , XPA (protein required for nucleotide excision repair;

Li *et al.* 1995, Stigger *et al.* 1998, Wang *et al.* 2000) , Ung2 (uracil-DNA glycosylase, prevents uracil incorporation into the genome during nucleotide excision repair; Mer *et al*. 2000, Hagen *et al*. 2008, Ali *et al*. 2010, Torseth *et al*. 2012, Herate *et al.* 2016) , SMARCAL1, and TIPIN (replication fork protection and replication restart; Ali *et al.* 2010, Kemp *et al.* 2010, Betous *et al*. 2013, Feldkamp *et al*. 2014, Witosch *et al*. 2014, Xie *et al*. 2014, Poole *et al*. 2015). In budding yeast, cells containing WHD truncations are hypersensitive to DNA damaging agents and exhibit hyper-recombination phenotypes that lead to excessive mutation of the genome (Santocanale *et al.* 1995, Maniar *et al.* 1997). RPA has also been demonstrated to interact with the XPF-ERCC1 endonuclease in order to initiate the processing of inter-strand crosslinks present in DNA (Abdullah *et al.* 2017).

Another domain that has been well characterized during the DDR is the N-terminal (NT) phosphorylation domain (PD) of Rpa2. This domain is unstructured and has not yet been demonstrated to become more ordered upon post-translational modification. Phospho-mimetic mutation of the Rpa2 NT has been demonstrated to weaken Rpa1 DBD-Fs interaction with the MRN complex *in vitro,* specifically with Mre11 and Nbs1, whereas an unphosphorylatable mutation of the same phospho-sites did not impede RPA-MRN complex interaction or localization to breaks but did increase persistence of the complex at the DSB site (Oakley *et al.* 2009). However, this data is somewhat conflicting to another report demonstrating that hyper-phosphorylated Rpa2 (and by extension, the RPA complex) co-localizes with phosphorylated Mre11 (and by extension the MRN complex) at stalled replication forks *in vivo* (Robison *et al.* 2004). Mechanistically, recruitment of MRN to break-sites has been shown to be dependent on the RPA complex, and disruptions in the MRN-RPA complex interactions lead to increased DNA replication after DSB induction with ionizing radiation (Olson *et al.* 2007). More recently, the Rpa2 NT has been shown to, upon DDR-dependent phosphorylation, influence the interaction with the ubiquitin ligase Prp19 (Dubois *et al.* 2017). Ubiquitination of RPA, as described in section 1.3.B, has been shown to be a requirement of proper checkpoint activation.

1.3. Post-translational modification of RPA and relevant mutant phenotypes

In response to a variety of DNA metabolic processes, as well as during the cell cycle, RPA is known to be post-translationally modified, and this post-translational modification of RPA is thought to mediate its dynamic intracellular activities. Post-translational modifications (PTMs) allow for rapid

changes in protein function without the energetic cost of degrading and resynthesizing useable proteins. Examples of post-translational modification include ubiquitination (addition of ubiquitin, a small 8 kDa peptide), sumoylation (addition of small ubiquitin-like modifier, a small 12 kDa peptide), and methylation/acetylation (addition of small carbon chains, typically via N- or O- linkages on amino acid side chains). Each modification alters protein function in in different ways. For example, acetylation of the RPA complex is thought to promote DNA repair through the Nucleotide Excision Repair (NER) pathway (He *et al.* 2017, Zhao *et al.* 2017). This process is mediated by PCAF/GCN-5 acetylase complex and occurs on Rpa1 at K163 (*ibid*). RPA acetylation has also been deemed important during DNA repair, cells containing an *rpa1-K163R* mutation exhibit hypersensitivity to UV-induced DNA damage (*ibid*). However, Rpa1 K163 is also a known ubiquitin ligase target during the DDR program (*ibid*), and it is unknown whether preventing acetylation or ubiquitination of Rpa1 is more important during the DDR. Ubiquitination has been demonstrated to target proteins for degradation via the proteasome (Thrower *et al.* 2000) and is suggested to form a molecular 'glue' to keep proteins in close proximity with one another (Kim *et al.* 2007). Sumoylation is thought to be important for nuclear transport of proteins (Rodriguez *et al.* 2001), transcriptional regulation (Kagey *et al.* 2003), and enhancement of protein stability (Desterro *et al.* 1998). Methylation and acetylation of amino acids on peptides can be used to neutralize side-group charges, impede phosphorylation of phospho-targets, and/or alter protein-protein interactions by disrupting docking contacts (Schubert *et al.* 2006).

1.3.A. Sumoylation of RPA

The RPA complex becomes robustly sumoylated and ubiquitinated during the DDR. Previous studies have reported that ubiquitination and sumoylation of RPA have been demonstrated to be important for proper LPR progression (Galanty *et al.* 2012, Yin *et al.* 2012, Marechal *et al.* 2014, Chung *et al.* 2015, Elia *et al.* 2015, Dubois *et al.* 2017), as well as proper establishment of the DDC (Marechal *et al.* 2014, Wan *et al.* 2014, Dubois *et al.* 2017). However, the aforementioned studies were performed in ubiquitin- or sumo-ligase deletion/null mutations or using RNAi knockdown of the ligase itself, making it difficult to discern whether the defect lies with the inability to modify RPA or an inability to modify other LPR targets of these ligases. Moreover, these small protein additions are thought to function by recruiting and retaining the required DDR components at the lesion site to promote repair. In yeast cells,

sumoylation of RPA occurs on both Rfa1 and Rfa2 at and is achieved by Siz2, an E3 sumo ligase (Chung *et al.* 2015) and is regulated by the Slx5-Slx8 sumo-targeted ubiquitin ligase complex (Burgess *et al.* 2007). In human cells, Rpa1 has been demonstrated to be sumoylated with sumo-2/3 at K449 and K577 by a yet unidentified sumo ligase and is prevented by Senp6, a sumo protease (Dou *et al.* 2010, García-Rodríguez *et al.* 2016). In human cells, a double mutation of K449 and K557 of Rpa1 leads to increased sensitivity to genotoxic agents, such as camptothecin, demonstrating that sumoylation of Rpa1 is essential for a proper DDR (Dou *et al.* 2010). Sumoylation of Rpa1 has been shown to be necessary for RPA-Rad51 exchange at DSBs, as deletion of Siz2 has been demonstrated to not only inhibit RPA sumoylation, but also impair RPA interaction with the strand-annealing protein Rad52 (Psakhye *et al.* 2012). The interaction with RPA through Rad52 is thought to be critical in mediating the exchange between RPA and the Rad51 recombinase on ssDNA during homologous recombination (Psakhye *et al.* 2012, Shima *et al.* 2013). Impediment of RPA desumoylation leads to the formation of DSBs during DNA replication and causes accumulation of cells in S- and G_2/M phases (Dou *et al.* 2010). Sumoylation and desumoylation of RPA, in a controlled and coordinated fashion, is thus required for regulation of RPA's activity during DNA replication, repair, and cell cycle progression. Similar to phosphorylation (discussed in section 1.4), permanent changes in a cell's ability to readily modify RPA prevent cells from properly executing DNA replication, checkpoint activation, and mitotic exit. In both yeast and human cells, sumoylation of RPA, and other DDR machinery, has been implicated to be important for Mec1 and ATR activation, respectively (Galanty *et al.* 2009, Cremona *et al.* 2012, Cremona *et al.* 2012, Galanty *et al.* 2012). It is unclear, however, whether sumoylation of RPA, or the lack of the E3 sumo ligases modifying targets outside of RPA are the direct drivers of these phenotypes. In human cells, depletion of Pias1 and Pias4 (sumo E3 ligases) lead to reduced ATR activation and reduced ATM-dependent phosphorylation of Rpa2 at S4/S8, indicating that sumoylation of RPA is required for proper checkpoint signaling (Galanty *et al.* 2009). Furthermore, depletion of Rnf4 (sumo-targeted ubiquitin E3 ligase) has been demonstrated to impair RPA turnover and impede Rad51 filament formation, inhibiting homologous recombination repair (Galanty *et al.* 2012).

1.3.B. Ubiquitination of RPA

Ubiquitination of RPA occurs primarily via Rfwd3 and Prp19 (Gong *et al.* 2011, Liu *et al.* 2011, Marechal *et al.* 2014, Wan *et al.* 2014, Elia *et al.* 2015, Dubois *et al.* 2017, Feeney *et al.* 2017, Inano *et al.* 2017). Rfwd3 and Prp19 are E3 ubiquitin ligases required for DNA repair. Rfwd3 has been demonstrated to have a constitutive interaction with RPA, whereas Prp19 interaction only occurs during the DDR following phosphorylation of the Rpa2 NT (Dubois *et al.* 2017). Prp19 has been demonstrated to ubiquitinate RPA bound to ssDNA and is required for efficient activation of Chk1 (Marechal *et al.* 2014). Preventing ubiquitination via Prp19 knockdown has been shown to lead to reduced Rpa2 phosphorylation, as well as Chk1 activation, suggesting ubiquitination plays an important role in the recruitment and activation of ATR/ATRIP. ATR/ATRIP has been shown to preferentially interact with K63 tetra-ubiquitin molecules which is the type of ubiquitination Prp19 has been demonstrated to stimulate on Rpa1 and Rpa2 (Marechal *et al.* 2014, Dubois *et al.* 2017). Preventing ubiquitination of RPA via knockdown or mutation of Prp19 or Rfwd3, or mutation of known RPA ubiquitin sites (specifically Rpa2: K37, K38 (Elia *et al.* 2015) has been shown to lead to a slight increase in γ-H2AX after hydroxyurea treatment, impaired checkpoint activation, and repair through homologous recombination leading to replication fork collapse and replication catastrophe, demonstrating a role for ubiquitination of RPA in the DDR (Marechal *et al.* 2014, Elia *et al.* 2015, Dubois *et al.* 2017). An interaction between RFA and the yeast homolog to human Prp19 (Prp19/Pso4) has not yet been demonstrated; however, yeast containing a *pso4-1* mutation display sensitivity to ultraviolet radiation (UV) and exhibit deficiencies in mitotic recombination (Henriques *et al.* 1989, Grey *et al.* 1996).

Ubiquitination of RPA is also reported to be driven by Rnf4, a sumo-targeted ubiquitin ligase (STUbL) that is thought to regulate and ubiquitinate sumoylated DDR proteins such as Mdc1 (Mediator of DNA damage checkpoint protein 1, Luo *et al.* 2012) CtIP (C-terminal binding protein 1 (CtBP1) interacting protein; Sartori *et al.* 2007, Himmels *et al.* 2016) (Galanty *et al.* 2009, Galanty *et al.* 2012, Luo *et al.* 2012, Yin *et al.* 2012). However, Rnf4 is only able to ubiquitinate proteins that have already received prior sumoylation modifications, and typically ubiquitinates the sumo groups that have been covalently attached to its targets (Galanty *et al.* 2012, Yin *et al.* 2012). Preventing ubiquitination of Mdc1 or CtIP leads to reduced resection of the DSB and inhibition of both the generation of RPA coated ssDNA and

homologous recombination (Galanty *et al.* 2009, Galanty *et al.* 2012, Luo *et al.* 2012, Yin *et al.* 2012). Replication Protein A, as described above, is sumoylated on K449 and K577, and mutation of these residues to the non-sumoylatable K449/K577R leads to reduced RPA turnover (degradation) and an increase in RPA occupancy on ssDNA generated at DSBs, analogous to results observed for Rnf4-deficient cells (Galanty *et al.* 2012). The most common phenotype observed in preventing sumoylation or ubiquitination of RPA or other complexes during the DDR is reduced checkpoint activation through sensor kinases and deficiency in homologous recombination repair. However, it is unknown whether this is due to reduced RPA modification or reduced modification of the multitude of enzymes functioning during the DDR, as several components require small ubiquitin-like modifiers for proper function. However, if DNA repair proteins are held together through a variety of sumoylation and ubiquitination events that act to coordinate the repair process, then the aforementioned phenotypes are somewhat expected.

1.4. Phosphorylation of the human RPA complex and related mutant phenotypes

Phosphorylation of proteins is a rapid way cells use to alter protein function by the addition of an 80 Dalton (Da) phosphate group to Serine/Threonine/Tyrosine (S/T/Y) side-chains. Phosphorylation of proteins can occur on multiple S/T/Y sites and can dynamically change protein function. Phosphorylation can be inhibitory to activity, as is the case with Dun1-mediated phosphorylation of Sml1 (causing degradation of Sml1) during the DDR (Gardner *et al.* 1999), or stimulatory to activity, as is the case with Mec1-mediated phosphorylation of Rad53 during establishment of the DDC in yeast (Sanchez *et al.* 1996, de la Torre-Ruiz *et al.* 1998, Gardner *et al.* 1999, Sanchez *et al.* 1999, Pellicioli *et al.* 2001, Sweeney *et al.* 2005, Clerici *et al.* 2014). Phosphorylation of RPA is also thought to mediate RPA's activity throughout the DDR. While Rpa1 in humans has been shown via large-scale screens to be phosphorylated at T180, T191, and S384 (Matsuoka *et al.* 2007, Olsen *et al.* 2010), the most important and physiologically relevant phosphorylation events that occur to the RPA complex appear to occur within the NT phosphorylation domain of Rpa2, as alteration of phospho-acceptor sites produce synthetic phenotypes.

Most of what is understood about Rpa2 phosphorylation comes from experiments performed in human cells. Cells containing the phospho-deficient *rpa2-S4/S8A* mutation display reduced phosphorylation of critical DDR factors Chk1, Mre11, and TopBP1 (Liu *et al.* 2012), as well as aberrant replication restart following etoposide-induced DNA damage (Ashley *et al.* 2014). Additionally, *rpa2-*

S4/S8A mutants fail to phosphorylate T21 of the Rpa2 NT, suggesting a site-dependency or sequential phosphorylation mechanism may be responsible for achieving an optimal Rpa2 NT phospho-state (Oakley *et al.* 2009). Cells containing S23/S29A phospho-deficient mutations display increased γ-H2AX and apoptosis (Anantha *et al.* 2007), and reduced Rad51 loading in response to genotoxic insult (Anantha *et al.* 2008), suggesting phosphorylation of these residues may be important for the RPA-Rad51 exchange during homologous recombination. Rpa2 mutations containing T21/S33A prevent DNA synthesis during recovery from HU-induced replication stress or DNA damage caused by UV-radiation (Olson *et al.* 2006, Vassin *et al.* 2009). Further highlighting the importance of Rpa2 phosphorylation in DNA repair after HU-induced replication stress, a severely phospho-deficient extensive Rpa2 mutation *rpa2-Ala7* (S4/S8/S11/S12/S13/T21/S33A) generates phenotypes that display reduced Rad51 filament formation (Shi *et al.* 2010), analogous to, but more severe than, that observed in the S23/S29A mutation. Additionally, it was reported that the *rpa2-Ala7*, and *rpa2-S23/29A* mutations accumulate in either S- or G2- phases of the cell cycle, without any sort of DNA damage stimulus (Anantha *et al.* 2007, Anantha *et al.* 2008, Shi *et al.* 2010); however, the significance of this result is unclear, as it has been demonstrated that cell cycle distribution in untreated *rpa2-Ala9* cells (where all nine S/T residues in the NT are mutated to A), does not appear to be greatly affected (unpublished results, SJH). Taken together, preventing phosphorylation of the Rpa2 NT during either cell cycle progression or the DDR program leads to reduced/impaired homologous recombination and aberrant replication restart.

Phospho-mimetic mutation of Rpa2 has provided additional mechanistic insight into the regulatory role that the RPA complex plays during cell cycle regulation during the DDR. In yeast, the physical presence and subsequent phosphorylation of the Rfa2 NT has been implicated to play a role in telomere maintenance, as an NT deletion mutation of Rfa2 (*rfa2-*ΔN_{40}) displayed severely shortened telomeres via decreased Est1 recruitment to telomeric DNA (Schramke *et al.* 2004). In human cells, cells containing *rpa2-S8/S33D*, *rpa2-T21/S33D,* or *rpa2-S8/S23/S29/S33D* mutations decreased viability and RPA foci formation at DSBs following camptothecin exposure indicating a defect in DNA repair efficiency and suggesting that the phospho-state of Rpa2 mediates RPA complex recruitment to DSB sites (Lee *et al.* 2010). Rpa2 has been demonstrated to be dephosphorylated by the PP4 phosphatase complex (PP4R2, PP4C), and inhibition of PP4 components via transient knockdown has been shown to cause inefficient

Rad51 loading and a prolonged G_2/M checkpoint, suggesting that PP4-mediated dephosphorylation is required for efficient progression of homologous recombination repair. Knockdown of another phosphatase complex PP2A/C (components of the PP2 phosphatase complex) has been shown to lead to increased RPA foci after HU exposure, suggesting that PP2-mediated dephosphorylation is required for efficient repair and resolution of HU-induced stalled replication forks (Feng *et al.* 2009). Consistently, the aforementioned Rpa2 mutations also display deficiencies in the ability to resolve HU-induced fork damage during replication stress. However, it is somewhat unclear as to whether mediation of the Rpa2 phospho-state or broad inhibition of phosphatase activity is responsible for the aforementioned phenotypes, as each of the Rpa2 mutations mentioned above have been noted to lead to proper establishment of the damage-dependent checkpoint.

Phospho-mimetic studies of the Rpa2 NT phospho-state using ectopically expressed *rpa2* mutations have revealed that phosphorylation of Rpa2 prevents RPA from participating in chromosomal DNA replication (Vassin *et al.* 2004, Olson *et al.* 2006), and leads to defects in DNA synthesis during HU-induced replication stress causing apoptosis (Vassin *et al.* 2009) despite observed increases in RPA binding to ssDNA (Vassin *et al.* 2009). *In vitro*, phosphorylation of Rpa2 has been shown to recruit Palb2 (partner and localizer of BRCA2), an interaction that is thought to mediate replication restart at and stabilize stalled replication forks, as use of phospho-mimetic Rpa2 or transient knockdown of PP4R2 cause impaired or slowed replication fork movement during HU-induced replication stress and during recovery once hydroxyurea is removed (Murphy *et al.* 2014). Moreover, phosphorylation or phospho-mimetic mutation of the Rpa2 NT has been demonstrated, through *in vitro* interaction assays, to impede interaction with the MRN complex (specifically Mre11 and Nbs1; Oakley *et al.* 2009) . However, much of the data generated using phospho-mimetic mutation of Rpa2 is conflicting in that constitutively mimicking phosphorylation leads to replication or repair deficient phenotypes that mirror those observed in cells containing unphosphorylatable Rpa2 mutations. Taken together, the above phenotypes for phospho-mimetic or unphosphorylatable Rpa2 NT mutations highlight the critical nature of *rapidly* modulating the Rpa2 NT phospho-state in order to successfully mediate the processes of DNA replication and repair, as well as RPA's dynamic activity as a sensor of DNA damage, essential replication factor, and cell cycle regulatory complex.

1.4.A. Phosphorylation of Rpa2 in other model systems

Rpa2 in *Xenopus laevis* egg extracts and in the pathogenic yeast *Candida albicans* has been shown to be phosphorylated during mitotic entry, mitotic exit, and during the DDR. It is unclear which of the conserved kinases phosphorylates Rpa2 in *Xenopus laevis*, however it is thought that this phosphorylation is mediated by ATR and CDK (Recolin *et al.* 2012). Phosphorylation of Rpa2 in *Candida albicans* has been demonstrated to occur by both Mec1- and Cdc28-dependent mechanisms. In mutant cells where Mec1 expression is inhibited, or that containing the *cdc28-as* mutation that is inhibited by 1NM-PP_1 (ATP analog), display reduced Rpa2 phosphorylation during HU-induced replication stress as well as upon entry into mitosis (Gao *et al.* 2014).

In *Candida albicans*, phosphorylation SQ/TQ sites within the Rfa2 NT (S18 and S30) by Mec1, and to a lesser extent phosphorylation of the Rfa2 NT by Cdc28, were implicated to be important during replication stress caused by hydroxyurea (HU) (Gao *et al.* 2014). Cells expressing a phospho-deficient *rfa2-4A* mutation (T11A, S18A, S29A, S30A) were reported to be more sensitive to HU-induced stress and in some instances were unable to deactivate the Rad53-dependent checkpoint when compared with *rfa2-4D* (T11D, S18D, S29D, S30D) mutant cells (*ibid*). In *Xenopus* extracts, Rpa2 phospho-mimetics (S26D, S31D, T35D) exhibit deficiency in checkpoint activation in response to aphidicolin treatment (leading to fork unwinding and replication stress), whereas phospho-deficient Rpa2 mutation could still faithfully activate Chk1 during S-phase (Recolin *et al.* 2012). As mentioned in section 1.4, the phospho-mimetic Rfa2 mutations used mirror phenotypes of unphosphorylatable Rfa2 mutations suggesting that rapidly modulating the phospho-state of Rfa2 is essential for proper RPA complex function in all DNA metabolic processes.

1.4.B. Phosphorylation of RFA in budding yeast

In budding yeast, RFA has been demonstrated to be phosphorylated at S178 of Rfa1 (similar in position to Rpa1 T180, Matsuoka *et al.* 2007) and S122 of Rfa2 by the sensor kinase Mec1 (Kim *et al.* 2003). The physiological role of phosphorylation at the known Mec1 sites (Rfa1-S178 and Rfa2-S122) is unclear due to the observation that these sites appear to be completely dispensable for the DDR in yeast (Ghospurkar *et al.* 2015). While this will be covered more in-depth in chapter 3, aspartate- or alanine-mutagenesis of S122 (Rfa2) and S178 (Rfa1) revealed that every possible combination of $S178_{A/D}$ and

$S122_{A/D}$ mutations were as proficient as wild-type cells in tolerating clastogen challenge. Furthermore, while S122 phosphorylation is a common marker for Mec1 activity, each *rfa2-S122*$_{A/D}$ mutation is capable of performing checkpoint arrest in an indistinguishable manner from WT cells suggesting that Mec1-dependent phosphorylation of RPA at S122 is not required for proper checkpoint activation (see Chapter 3). Additionally, the only identified phosphorylation events that occur in budding yeast on the Rfa2 NT occur during meiosis by Ime2 (Brush *et al.* 2001, Clifford *et al.* 2004, Bartrand *et al.* 2006) or in a *set1*Δ or *mec3*Δ mutant by Rad53 (Schramke *et al.* 2001). Phosphorylation of RFA also occurs during meiosis and will be discussed in section 1.5.C.

1.5. Meiotic process and meiotic recombination

Paramount to the propagation of any sexually reproducing species is the stable exchange of genetic information from parent to offspring through the process of meiosis. Broadly, the process of meiosis involves duplication of a diploid genome, followed by recombination between homologous chromatids, which is necessary to ensure proper chromosome segregation during the reductional division critical for the generation of viable haploid gametes. This differs from mitotic recombination in that mitotic recombination is primarily driven between sister chromatids. Replication Protein A, by virtue of its ssDNA-binding role in DNA replication and the DDR, plays essential but somewhat poorly understood roles in the meiotic process. Not only does RPA interact with proteins that play a significant role during meiosis, but it is phosphorylated during the meiotic program by some of its interacting partners. Described in the following sections are the process of meiosis and its importance in proper chromosome segregation and the known extent and context of RPA's meiotic protein interactions.

The process of meiosis is essential for all sexually reproducing organisms, and leads to increased genetic variability among organisms (Martini *et al.* 2002). In order for meiosis to occur properly, five major cellular programs must be executed in a precise and step-wise manner (Figure 1.2) (Page *et al.* 2003). First, the genetic information of the diploid organism must be duplicated during premeiotic DNA synthesis. Second, as the cells enter prophase of meiosis I (MI), the formation of DSBs and pairing of homologous chromosomes occurs leading to meiotic recombination. Meiotic recombination must occur between paired homologous chromosomes (interhomologs) in order to guarantee proper chromosome segregation during meiotic divisions (Baker *et al.* 1976, Hollingsworth *et al.* 1990). Prophase I is typically broken up into five

stages, based on the physical state of the chromosomes: (1) leptotene – pairing and synaptonemal complex (SC) assembly occurs, (2) zygotene – synapsis of homologs mediated by the SC, (3) pachytene – homologous recombination between synapsed homologs, (4) diplotene – SC degradation and initial untethering of recombined homologs, and (5) diakinesis – complete untethering of recombined homologs. Third, recombined homologous chromosomes align during metaphase I, are attached to the kinetochore components during anaphase I, and are segregated in a reductional division during telophase I, resulting in separation of homologous chromosomes to opposite poles and halving of the genomic content (hence the name reductional division). Fourth, the daughter cells undergo an equational division known as MII, in which the sister chromatids of the recombined chromosomes are aligned and segregated (prophase II – telophase II), in order to segregate the recombined chromosomes into four haploid gametes (cytokinesis). Finally, the haploid gametes (spores) are packaged, which in budding yeast includes the development of a tough ascal coat that surrounds the four spores and protects them from harsh environmental conditions.

During meiotic homologous recombination in yeast, nearly 200 DSBs are intentionally introduced to the paired chromosomes through the activity of an evolutionarily conserved type II topoisomerase known as Spo11 (Keeney *et al.* 1997). In yeast cells, Spo11 acts in concert with nine other meiotic DSB processing factors (Ski8/Rec103, Mre11-Rad50-Xrs2, Rec102-Rec104, Mer2, Rec114, Mei4; Keeney 2008) to bind more frequently than average regions of the genome known as “meiotic recombination hot spots”, where Spo11 cleaves one or more of the four chromatids. Once DSBs are formed, resection of each of the ~180-200 DSBs is achieved through the 5’→3’ exonuclease activity of the Exo1 exonuclease in a manner similar to that observed during the mitotic DDR (discussed in 1.6.A; (Mimitou *et al.* 2008, Mimitou *et al.* 2010, Shim *et al.* 2010), followed by brief occupancy of the generated ssDNA by RPA (Ribeiro *et al.* 2016). Replication Protein A is then actively replaced with Dmc1, the meiosis-specific Rad51 protein required for interhomolog strand invasion (Bishop *et al.* 1992, Dresser *et al.* 1997, Hong *et al.* 2001, Martinez *et al.* 2016). Dmc1-coating of the ssDNA promotes strand invasion of the homologous chromosomes, as opposed to Rad51 filaments that promote strand invasion of the sister chromatid (Dresser *et al.* 1997, Arbel *et al.* 1999).

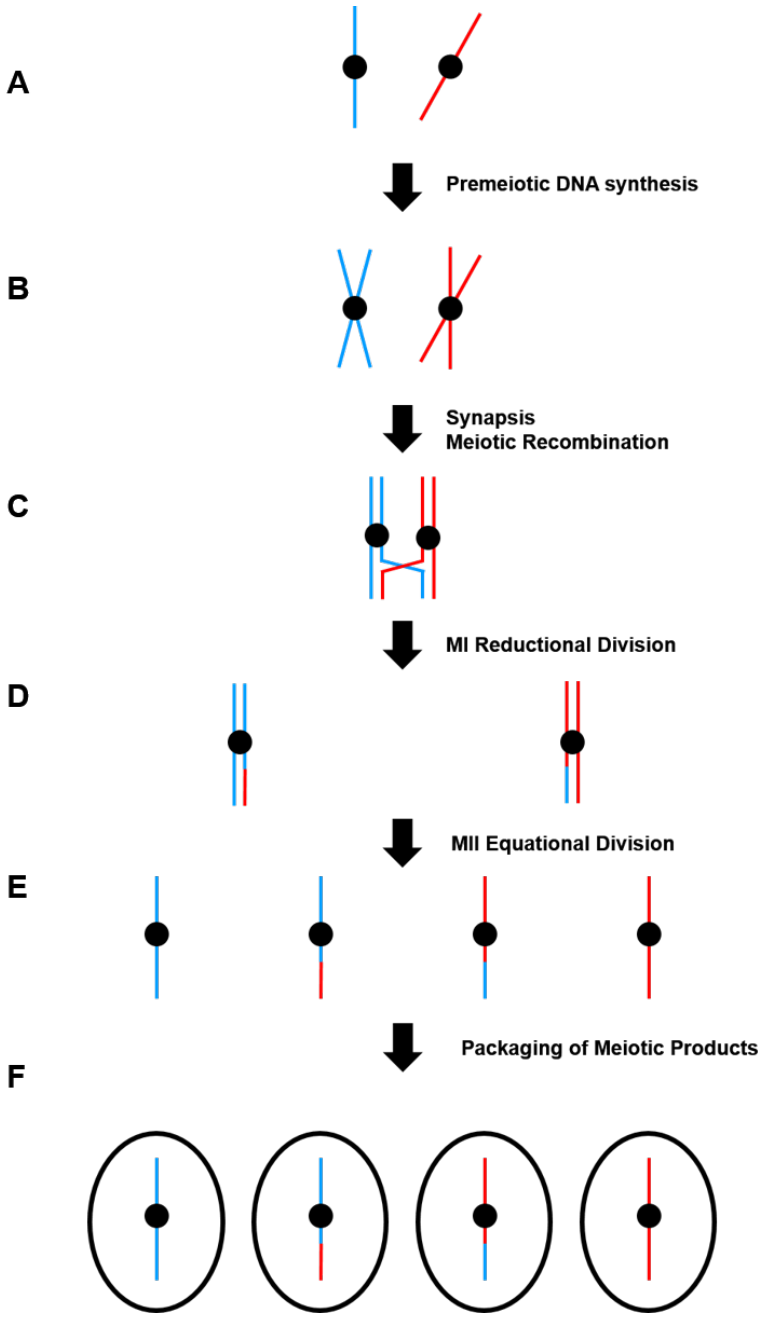

Figure 1.2. The Five Stages of Meiosis.
A. Premeiotic DNA synthesis occurs on homologous chromosomes (red and blue). **B.** Entry into prophase I leads to pairing of homologous chromosomes and SC assembly during leptotene, followed by DSB formation by RIC (Spo11 *et al*). **C.** Synapsis, or fusion of the chromosomes, occurs during zygotene followed by meiotic recombination during pachytene. **D.** Degradation of the SC promotes initial segregation of synapted chromosomes during diplotene, and full separation of recombined chromosomes occurs during diakinesis, leading to two cells with haploid chromosomes after the MI reductional division (cytokinesis I) **E.** MII equational division further segregates sister chromatids into individual gametes (cytokinesis II) **F.** Haploid gametes are then packaged, which in yeast leads to the formation of the ascal coat surrounding the four haploid spores.

Once strand-invasion and homologous base pairing to form heteroduplex DNA are complete, DNA synthesis and second-strand capture occurs to repair the Spo11-generated DSBs and link the chromosomes together through the generation of double Holliday Junctions (dHJ) across each break (Bizard *et al.* 2014). The dHJs are then resolved through the employment of 'resolvases' or 'dissolvases' that untether the chromosomes from one another (Heyer *et al.* 2003, Heyer 2004, Bizard *et al.* 2014, Bocquet *et al.* 2014, Matos *et al.* 2014, Sarbajna *et al.* 2014, Wyatt *et al.* 2014, West *et al.* 2015), leading to the formation of crossover or noncrossover products that are segregated during the reductional division. Failure to properly induce Spo11-dependent DSBs, defects in strand invasion, or defects in dHJ resolution typically lead to incomplete or inviable meiotic products (Baudat *et al.* 2000). In human cells, it is presumed that defects in meiotic recombination lead to aberrant chromosome segregation events that lead to cellular disease and developmental defects (Ratcliffe 1981, Zaki *et al.* 2005, Templado *et al.* 2011, Adams *et al.* 2015).

1.5.A. Meiotic recombination is essential for proper chromosomal segregation

In order for meiotic recombination to be executed, homologous chromosomes must be aligned through the formation of the tripartite synaptonemal complex (SC), composed of two axial elements (on each homologous chromosome) and a central core element (Page 2003). While formation of the SC axial elements on each chromosome occurs during early leptotene, synapsis between chromosomes only occurs once a homology search has concluded successfully. The homology search occurs through DSB formation and strand invasion, and as such, cells defective for meiotic recombination are also defective for SC formation (*ibid*). Following the homology search, transverse filaments are formed during pachytene (Zickler *et al.* 1999, Fraune *et al.* 2012), resulting in fully paired homologous chromosomes. Furthermore, improper SC assembly inhibits proper crossover formation and can lead to inviable meiotic products and embryonic lethality (Page 2003, Kouznetsova *et al.* 2011).

Much of what we know about the meiotic program, however, does not come from the study of human gametogenesis, but rather the study of yeast progressing through meiosis. Several of the components required to elicit programmed DSBs during meiosis, as well as the factors required to repair the lesions generated, have been demonstrated to be essential in preventing aberrant recombination phenotypes, and some have even been demonstrated to completely inhibit meiosis when deleted. For

example, *spo11*Δ yeast are unable to complete meiotic recombination due to a lack of adequate DSBs being formed to promote resection and recombination (Keeney *et al.* 1997, McKee *et al.* 1997, Baudat *et al.* 2000, Romanienko *et al.* 2000, Diaz *et al.* 2002), however, microscopic analysis of nuclear genome content in *spo11*Δ yeast revealed that these mutants are still able to complete meiotic divisions through MI and MII but are inviable. Moreover, deletion of the meiosis specific recombinase Dmc1 prevents proper meiotic progression due to a lack of recombination between interhomologs (Bishop *et al.* 1992, Diener *et al.* 1996, McKee *et al.* 1997, Shinohara *et al.* 1997, Xu *et al.* 1997, Thompson *et al.* 1999, Fukushima *et al.* 2000). Replication Protein A is also an essential protein for proper meiotic recombination (Soustelle *et al.* 2002). Cells containing the *rfa1-t11* mutation have been demonstrated to exhibit a marked reduction in spore survival after meiosis, as well as a 10- to 100-fold reduction in total genome recombination (*ibid*). As described in section 1.5.C., RPA is known to be phosphorylated on Rpa2 by Ime2 on S27 (Clifford *et al.* 2004), as well as S122 by Mec1 (Brush *et al.* 2001, Bartrand *et al.* 2006) during early meiotic signaling and the initial resection events post-Spo11 catalyzed breaks, respectively. The physiological significance of Rpa2 phosphorylation by Ime2 remains unknown.

1.5.B. RPA interactions with LPR and meiosis-specific factors during meiosis

During meiotic DNA replication and recombination, as well as during the initial entry into meiosis, RPA has been demonstrated to interact with a number of meiosis-specific proteins. As described previously, RPA been shown to become phosphorylated by the meiosis-specific Cdc28 homolog Ime2, and the physiological function of this early phosphorylation remains unclear (Clifford *et al.* 2004). Replication Protein A has also been shown to interact with the meiosis specific proteins MeioB and Spata22 in mice (Luo *et al.* 2013, Souquet *et al.* 2013, Ribeiro *et al.* 2016). MeioB is a meiosis-specific homolog to Rpa1, containing 3'$\rightarrow$5' exonuclease and ssDNA-binding activity as well as structural domain similarity to Rpa1. Spata22 is a meiosis-specific protein that interacts with MeioB and RPA in order to promote recombination during meiosis I (*ibid*).

During meiotic recombination, RPA also interacts with Rad51 and Dmc1, each of which are required for proper strand invasion during mitosis and meiosis, respectively (Golub *et al.* 1998, Murayama *et al.* 2013). Furthermore, RPA has been shown to interact with Rad52 during meiosis, promoting the assembly of Rad51 and the Rad55/Rad57 heterodimer at Rad52-RPA foci that are thought to lead to

exchange hand-off to Dmc1 (Shinohara *et al.* 1997, Sung 1997, Gasior *et al.* 1998). Further mediation of Dmc1-foci formation and protofilament assembly is thought to be driven by interaction with Mei5-Sae3 heterodimer, RPA, and Dmc1 (Hayase *et al.* 2004, Tsubouchi *et al.* 2004, Ferrari *et al.* 2009). Taken together, the above interactions highlight an important role for RPA in meiosis in the governance and regulation of assembly of highly ordered and organized protein-DNA complexes that execute the meiotic program on nuclear substrates.

1.5.C. Phosphorylation of RPA during meiosis

Rfa2 is phosphorylated during the earliest stages of meiosis by the meiosis-specific Cdc28-related cyclin-dependent kinase Ime2 at S27 located within N-terminal phosphorylation domain (Clifford *et al.* 2004). Unlike the above mentioned PTMs, phosphorylation of Rfa2 by Ime2 during meiosis can occur when RPA is not bound to ssDNA (*ibid*). The function of Rfa2 NT phosphorylation during meiosis remains unclear. During meiosis, Rfa2 has also been demonstrated to be phosphorylated at S122 by Mec1 in a similar manner to that observed in mitotic cells experiencing a double-strand break (DSB) (Brush *et al.* 1996, Brush *et al.* 2001, Bartrand *et al.* 2004). Spo11-dependent meiotic break processing leads to RPA-coated ssDNA in a similar fashion to that observed during the mitotic DDR and leads to additional phosphorylation of Rfa2 at S122 through transient activation of Mec1 (*ibid*). Previously, it was shown that mutation of S122 of Rfa2 does not affect the ability of cells to perform DNA repair in response to multiple different DNA damaging agents, demonstrating that Mec1-dependent phosphorylation of S122 is likely not required for repair through homologous recombination (Ghospurkar *et al.* 2015). Thus, while it has been reported that mutation of S122 seems to produce a modest impact on crossover frequency during meiosis compared to wild-type (WT) cells, this impact in crossover frequency did not impact the viability of these cells after meiosis had been completed suggesting that phosphorylation of RPA outside of the Rfa2 NT doesn't play a major role in regulating the meiotic program (Brush *et al.* 2001, Bartrand *et al.* 2006).

1.6. The DNA damage response

The DNA damage response (DDR) is a critical signaling pathway used by cells to prevent mutation of the genome. Without the DDR program, simple genotoxic stressors like UV-radiation (*e.g.;* exposure to sun light or tanning beds) would cause severe genomic instability that could lead to mutations that might otherwise lead to cellular diseases, like cancer, in humans. Replication Protein A

acts as a primary activator of the DDR program as the primary sensor of broken or single-stranded DNA in cells. As mentioned previously in section 1.1, Replication Protein A binds this broken DNA and establishes the initial scaffold used both in the repair process and for preventing entry into mitosis through establishment of the DNA damage checkpoint. Replication Protein A's indispensable role in the DDR is underscored by the numerous RPA phenotypes that lead to aberrant LPR or improper DDC signaling.

1.6.A. Initiation of the DNA damage response – lesion processing and repair

To prevent cells from dividing with unstable genomic information, whether caused by errors in DNA replication or by genotoxic stressors caused by clastogens, a complex series of signals are elicited that activate the intracellular LPR, which broadly encompasses all of the proteins responsible for the physical repair of a DNA lesion. A pictorial overview of LPR leading to the establishment of the DDC are diagrammed in Figure 1.3 and Figure 1.4, respectively. The DDR program involves four general steps: (1) recognition of the DNA lesion, (2) establishment of the intracellular DNA damage checkpoint (DDC), (3) physical repair of the DSB, and (4) release of the DDC to facilitate cell cycle re-entry.

In response to DNA double-strand breaks (DSBs) specifically, the DDR program starts with the recognition or detection of the DSB, followed by programmed resection of the DSB by the MRX (Mre11-Rad50-Xrs2) complex (Trujillo *et al.* 2003, Lisby *et al.* 2004, Deshpande *et al.* 2014). ATPase activity within the Rad50 subunit of the MRX complex is thought to induce and regulate MRX endonuclease activity at break sites (*ibid*). ATP-bound Rad50, within the MRX complex, has been demonstrated to promote DNA end binding and end tethering, whereas ATP hydrolysis is required for Mre11 endonuclease activity and the promotion of DNA resection at the DSB site (Deshpande *et al.* 2014). MRX endonuclease recruitment and activity at the DSB end not only leads to activation of the sensor kinase Tel1 (Nakada *et al.* 2003, Lee *et al.* 2005, Paull *et al.* 2005), but also provides access by the multifunctional Dna2 helicase/nuclease and the Sgs1-Top3-Rmi1 (STR) nuclease complex that unwind and digest DNA in a 5' $\rightarrow$3' directionality creating a 3' overhang on the unprocessed strand (Shim *et al.* 2010). The newly formed 3' ssDNA overhang structure is then bound by the RPA complex, and extensive resection at the DSB allows for additional RPA molecules to be loaded onto the elongated 3' ssDNA overhang. The formation of RPA-coated ssDNA is then recognized by the sensor kinase Mec1/Ddc2 (Zou *et al.* 2003).

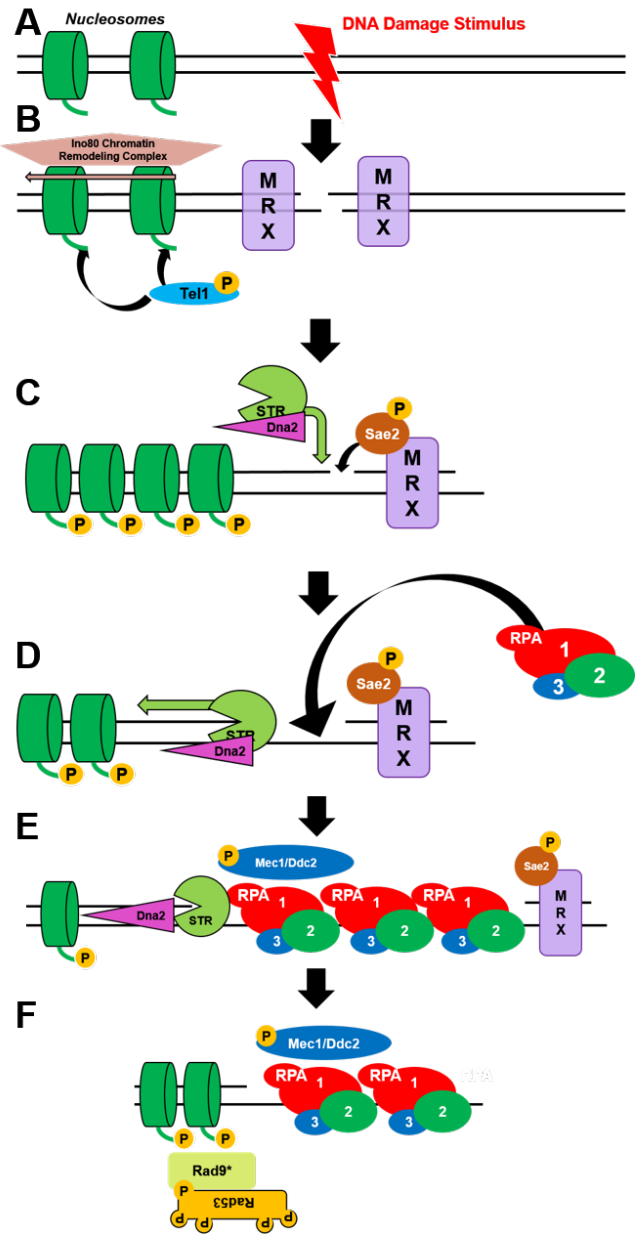

Figure 1.3. Initiation of Lesion Processing and Repair in *Saccharomyces cerevisiae.*
A. Induction of DNA damage, facilitated by a chemical clastogen or various types of radiation, leads to the formation of a double-strand break (DSB). **B.** The free ends of the DSB are rapidly bound by the Mre11-Rad50-Xrs2 (MRX) complex. Localization of MRX to DSB ends leads to the activation of the Tel1 sensor kinase, which phosphorylates H2AX at S129, and stimulates Ino80-dependent chromatin remodeling around the DSB. **C.** Phosphorylation of Sae2 by Tel1 recruits it to MRX and stimulates MRX-S endonucleolytic processing of the break. This enables loading of the Sgs1-Top3-Rmi1 (STR) and Dna2 nuclease-helicase complexes for 5'→3' resection of the DSB, creating a 3' overhang ssDNA structure. **D.** RPA rapidly coats 3' ssDNA generated during STR-Dna2 resection. **E.** Mec1/Ddc2 sensor kinase is recruited to RPA-coated ssDNA platform, attenuates Tel1-MRX-S signaling at the DSB terminus, and halts resection. **F.** Mec1-dependent activation and recruitment of Rad9-Rad53 heterodimer to the DSB initiates the DNA damage checkpoint by causing release Mec1-phosphorylated Rad53 from Rad9.

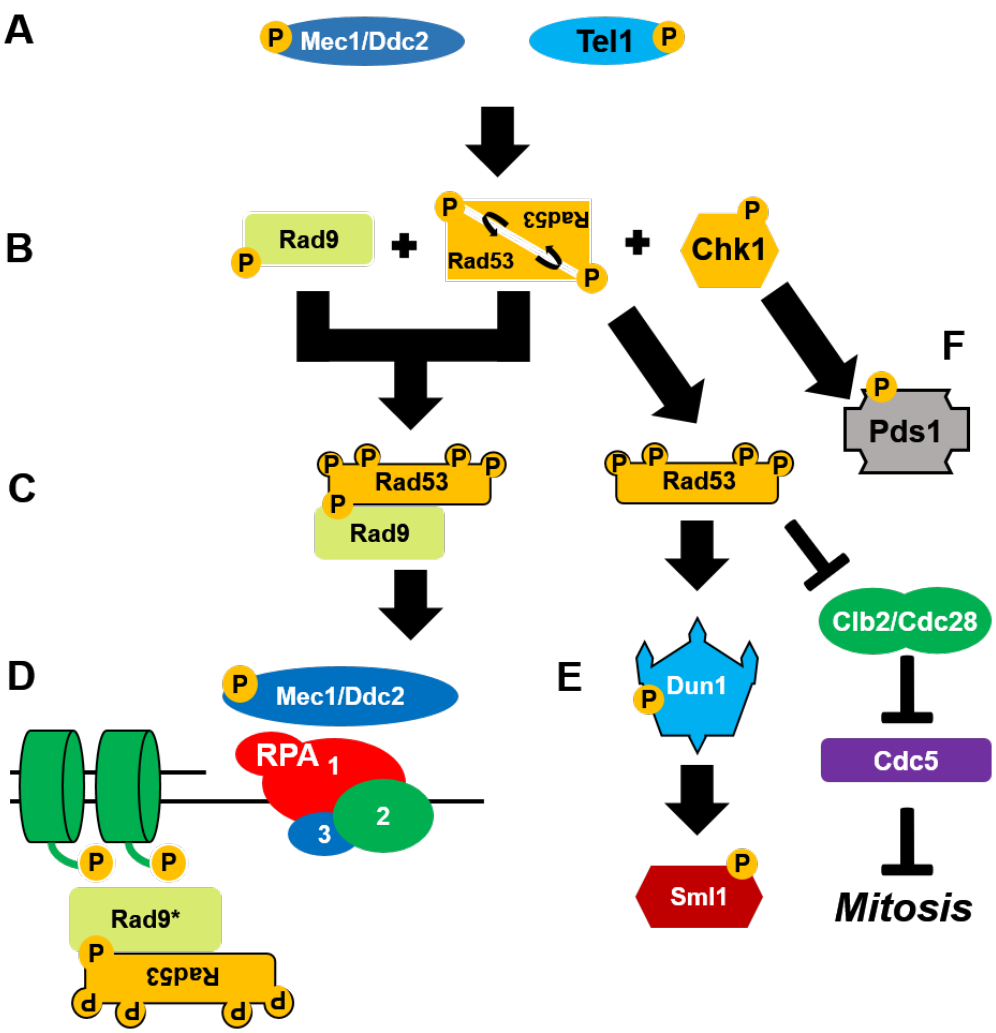

Figure 1.4. Mec1/Tel1 sensor kinase signaling and Checkpoint Establishment.
A. Activation of Mec1 and Tel1 lead to the establishment of the DDC in budding yeast by phospho-activation of Rad9, Rad53, and Chk1. **B.** Phospho-activation of Rad9 leads to complex formation with inactive Rad53 hetero-dimers that undergo *trans* auto-phosphorylation. **C.** Rad9-Rad53 heterodimers co-localize to the DSB via Rad9 association with γ-H2AX, leading to Mec1-dependent Rad53 hyper-phosphorylation. Hyper-phosphorylation of Rad53 causes its dissociation from Rad9 and promotes cell cycle arrest signaling alongside Chk1. **D.** Schematic assembly of Rad9-Rad53 at the 5' Junction of ssDNA platform generated by RPA/Mec1/Ddc2 **E.** Hyper-phosphorylated Rad53 activates Dun1, an effector kinase that phosphorylates and inhibits the activity of Sml1, a potent inhibitor of ribonucleotide reductase. Inhibition of Sml1 allows for conversion of rNTPs to dNTPs for DNA synthesis during repair. Rad53 also directly inhibits the kinase activity of Cdc5, by inhibiting Clb2/Cdc28 cyclin activity on Cdc5 and preventing entry into mitosis. **F.** Activation of Chk1 (from **C**) promotes phosphorylation of Pds1. Pds1 phosphorylation prevents its degradation by the APC^{CDC20} complex, preventing entry into anaphase and subsequently premature chromosome segregation.

Tel1 activity at the DSB site that leads to the generation of the RPA-coated ssDNA platform, and the generation of the RPA-ssDNA platform is then able to recruit the Mec1 sensor kinase through an interaction between RPA and Ddc2 (Zou *et al.* 2003). Activation of Mec1 kinase activity is also dependent

on the recruitment of Dpb11 (Navadgi-Patil *et al.* 2008), Ddc1 (Majka *et al.* 2006, Navadgi-Patil *et al.* 2009), and the Dna2 nuclease/helicase (Wanrooij *et al.* 2015, Wanrooij *et al.* 2016), discussed in 1.6.C. Mec1 and Tel1 activity at DSB sites has been demonstrated to activate a number of different effector molecules necessary for DNA repair, including phosphorylation of the histone variant H2AX at S129, the Ino80 chromatin remodeling complex (Gospodinov *et al.* 2011), the nuclease Sae2 (Baroni *et al.* 2004), and adaptor molecules Rad9 (Vialard 1998) or Mrc1 (Osborn *et al.* 2003, Grandin *et al.* 2005, Chen *et al.* 2009, Berens *et al.* 2012), and the yeast master checkpoint regulators Rad53 and Chk1 (Cortez *et al.* 2001, Nakada *et al.* 2003, Nakada *et al.* 2003, Nakada *et al.* 2004, Clerici *et al.* 2005, Lee 2005, Nakada 2005, Javaheri *et al.* 2006, Namiki *et al.* 2006, Toh *et al.* 2006, Hammet *et al.* 2007). Activation of Rad53 and Chk1 initiate the establishment of the DNA damage checkpoint (DDC) and will be discussed in-depth in sections 1.7.A and 1.7.B. Once activated, the DDC affords cells adequate time to process and repair the DSB, preserving the integrity of the genome.

1.6.B. DNA damage repair through non-homologous end joining

Not all repair processes are the same, and as such, do not always lead to the activation of the DDC in cells. One such mechanism cells employ to rapidly repair their genome is the *error-prone* Non-Homologous End Joining (NHEJ) pathway (Figure 1.5). NHEJ is the preferred repair mechanism used by cells that encounter DNA damage in the G1 phase of the cell cycle, when end resection of broken ends is less active likely due to reduced CDK signaling, as well as the lack of a viable sister chromatid with which to perform homologous recombination (Chiruvella *et al.* 2013). Ku70/Ku80 heterodimers localize to the DSB site, along with the MRX complex and the DNA ligase IV complex (Dnl4/Lig4), forming the canonical NHEJ complex (Clerici *et al.* 2008). At this point, the DNA ligase IV complex can then stimulate the loading of DNA polymerase μ and λ to perform fill in synthesis of the damaged genetic material, leading to a *fairly* accurate repair of the DNA (Chiruvella *et al.* 2013).

However, under conditions of prolonged occupancy of the MRX complex at the break, the Ku heterodimer is removed from the DSB site and alternative NHEJ, also known as microhomology-mediated end joining (MMEJ), is performed (Chiruvella *et al.* 2013). During MMEJ, mutagenic rearrangement of the DNA is possible due to small homologous overlaps less than 18 nucleotides in length (Sfeir *et al.* 2015) formed by the displacement of the Ku complex from the break site. If the homologous nucleotide repeats

that flank the DSB are greater than 30 nucleotides in length, then the complimentary 3' overhangs are annealed through a process known as single-strand annealing (SSA) (Paques *et al.* 1999), which requires the strand-annealing protein Rad52.

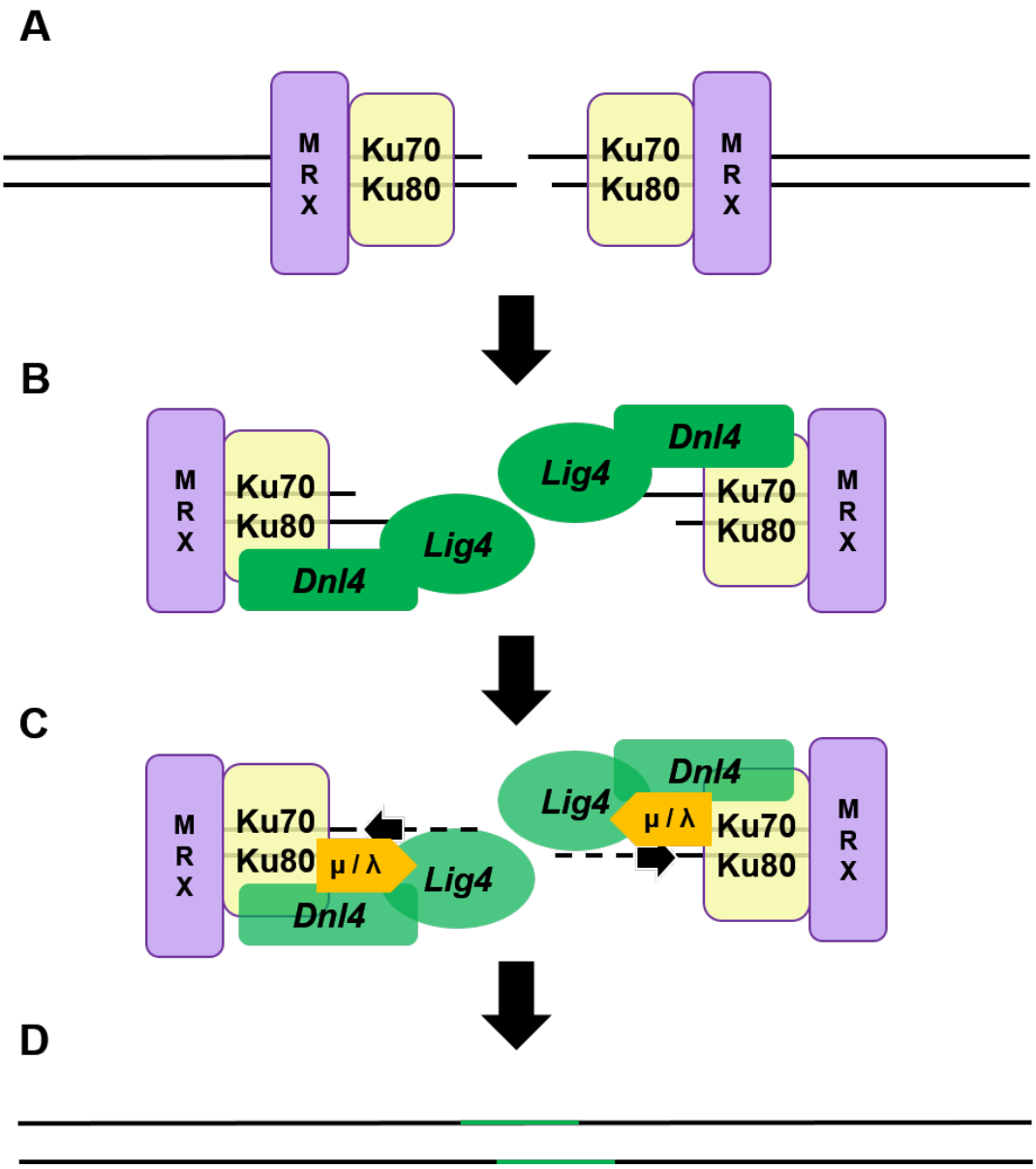

Figure 1.5. Non-Homologous End Joining.
A. Ku70/Ku80 complex, along with MRX, localize to the DSB site. Lack of homologous template material or lack of S- or G2-phase cyclins enable stable Ku association at the DSB. **B.** MRX-KU is recognized by the DNA Ligase IV complex (Dnl4/Lig4), which localizes to the ends of the DSB and begins filling in nucleotide gaps generated by the DSB **C.** DNA Ligase IV complex stimulates DNA polymerase μ and λ loading and the polymerases complete DNA synthesis through the DSB **D.** Repaired DNA achieved through NHEJ, where replaced nucleotides are represented by green regions on the DNA.

In either of these three error-prone type repair mechanisms, fusion of the broken DNA ends causes permanent loss off the material not contained within the homologous overlap, can be regarded as highly mutagenic, and may contribute to genome instability as homologous template is not used for repair. However, when homologous recombination repair is unable to be performed, either due to lack of template or lack of essential repair components, NHEJ mechanisms must be used to preserve the greater whole of the genome within a cell.

1.6.C. DNA damage repair through homologous recombination

During the S- or G2-phases of the cell cycle, DSBs are typically processed through the homologous recombination (HR) due to the availability of the necessary homologous genetic material required for HR, kept within close proximity by the cohesion complex (Symington *et al.* 2014), as well as the protein machinery required to execute HR. A pictorial diagram of HR can be found in Figure 1.6 and Figure 1.7. Homologous recombination repair starts with the formation of the RPA-coated ssDNA platform, generated by resection, which is then recognized by Mec1/Ddc2, as depicted in Figure 1.3D-F (Zou *et al.* 2003). The RPA molecules proximal to the 5' junction of the processed DNA interact with and load the Rad24-RFC2-5 clamp loader complex and facilitate loading of the Rad17-Mec3-Ddc1 clamp (Majka *et al.* 2006). Replication Protein A is then exchanged for Rad51, forming the presynaptic nucleofilament, a process that is dependent on Rad52 (Sung 1997, Gasior *et al.* 2001, Gaines *et al.* 2015). Formation of the Rad51/Rad52 proto-filament allows for strand- pairing and invasion of homologous genetic material to prime repair synthesis, a process that is stabilized by the presence of RPA binding of the displaced loop (D-loop) of homologous, single-stranded DNA, similar in structure to a replication bubble (Sung 1997, Gasior *et al.* 2001, Eggler *et al.* 2002, Sneeden *et al.* 2013, Gaines *et al.* 2015).

Homologous template copying via DNA synthesis is stimulated by D-loop localized RPA and achieved via DNA polymerase α (alpha) and δ (delta) loading and activity (Eggler *et al.* 2002, Wang *et al.* 2004, Sneeden *et al.* 2013). Completion of DNA synthesis leads to the formation of complex DNA structures known as Holliday Junctions (Holliday 2007). Processing of the Holliday junctions formed during repair uncouples the homologous genetic material, forming crossover or non-crossover products

that can be uncoupled through branch migration and/or decatenation, completing error-free repair of the DSB and preserving the integrity of the cellular genome (Bizard *et al.* 2014).

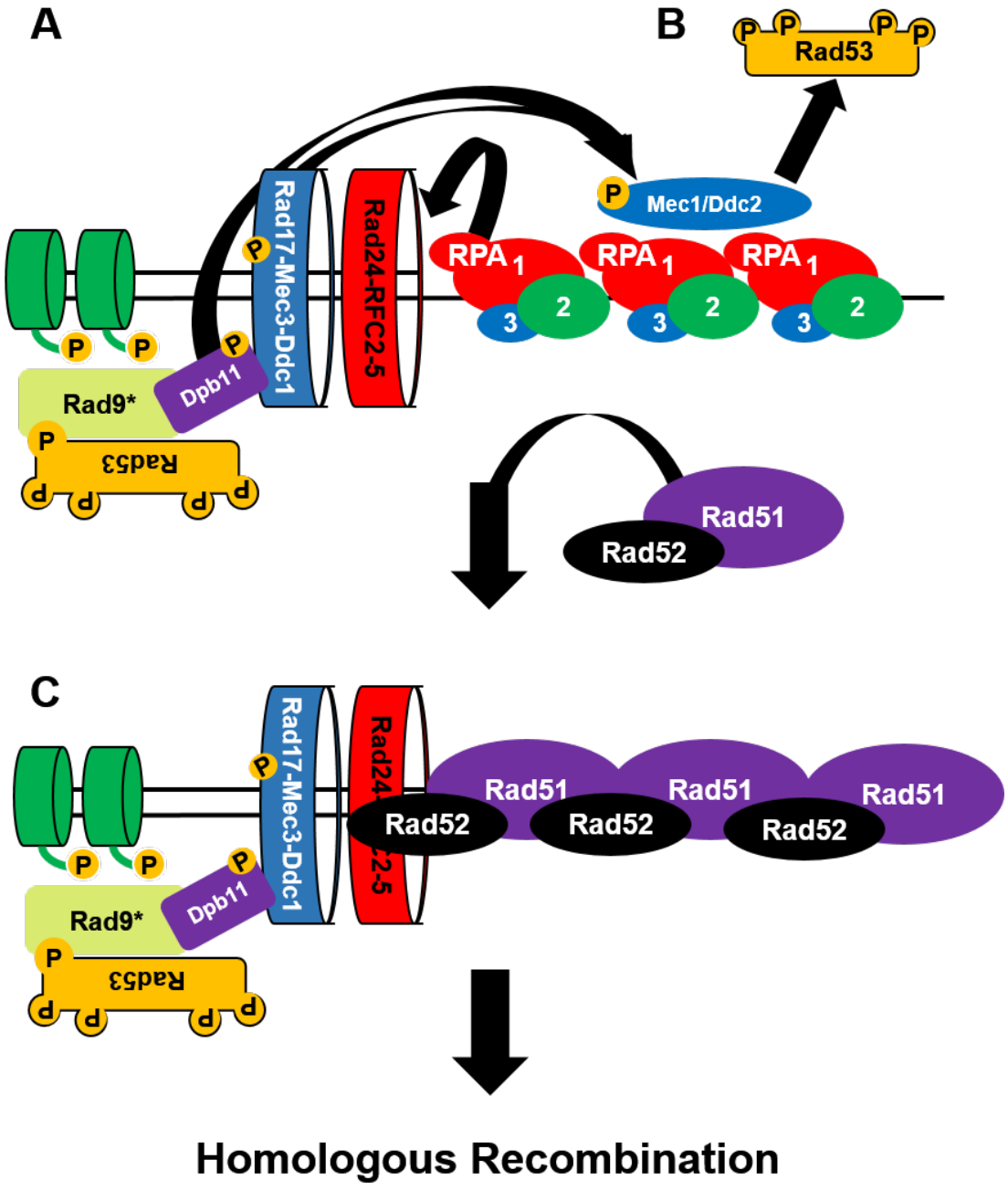

Figure 1.6. Initiation of Homologous Recombination in Budding Yeast.
A. Loading of the Rad24-RFC2-4 clamp loader complex (CLC) by RPA stimulates loading of the 9-1-1 Clamp (Rad17-Mec3-Ddc1), allows for loading of the scaffold protein Dpb11 (via Rad9 and 9-1-1 complex dependent interactions) and subsequently Mec1 activation. **B.** Mec1 hyper-phosphorylates Rad53, causing its dissociation from Rad9 and leads to checkpoint establishment (Fig 1.2). **C.** RPA is exchanged for Rad51/Rad52 heterodimers, creating the Rad51 protofilament and establishing a cellular commitment to homologous recombination repair.

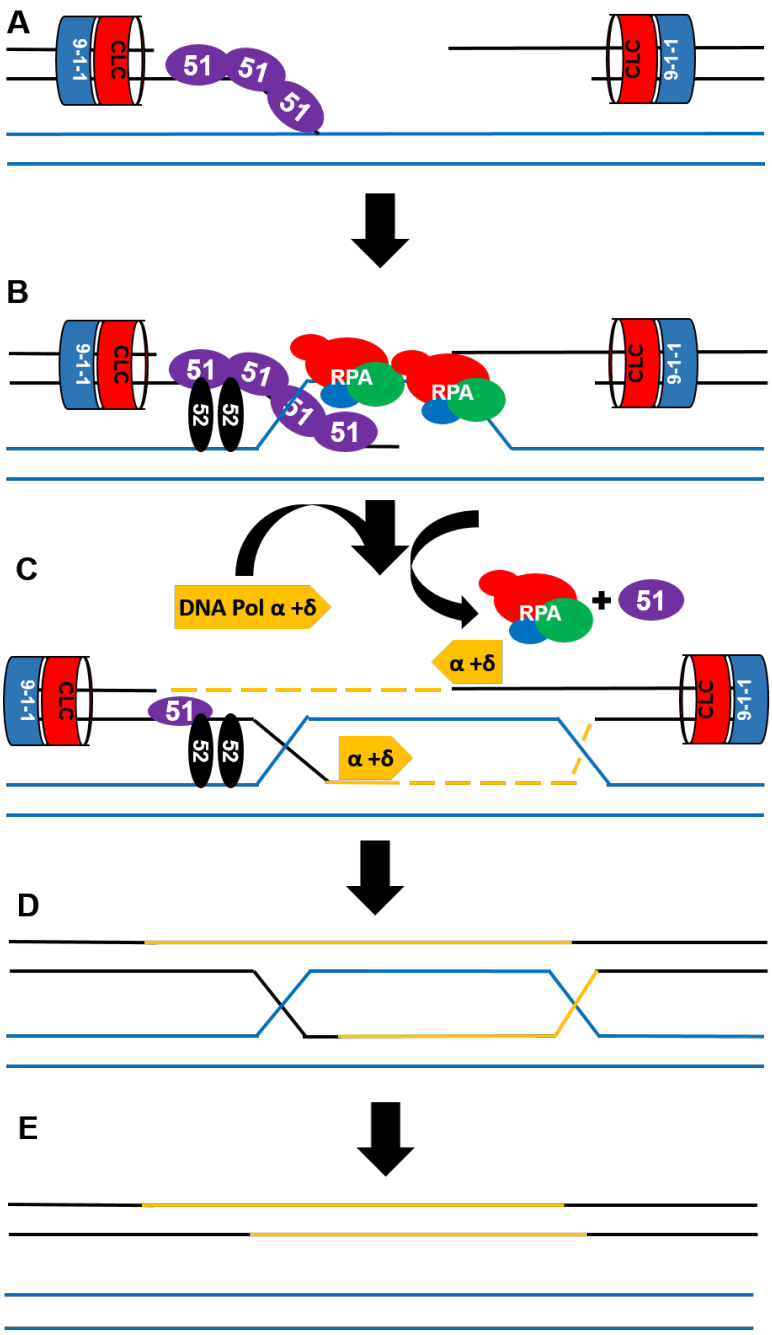

Figure 1.7. Process of Homologous Recombination.
A. Rad51 proto-filament, alongside the strand-annealing protein Rad52, perform strand invasion of homologous template material used for repair. **B.** Invasion by the Rad51 protofilament leads to the formation of a loop of displaced ssDNA from the homologous template, known as the D-loop, which is bound by RPA. **C.** The RPA-bound D-loop serves as a recruitment platform for DNA polymerase α and Δ which perform DNA synthesis from the free 3' hydroxyl group from each end of the DSB. **D.** Completion of DNA synthesis leads to the generation of the double Holliday structure joint molecule. **E.** Resolvases act on the DHJ joint molecule, restoring the DNA into fully repaired duplex DNA.

1.6.D. Other types of DNA repair (NER, BER, MMR, and BIR)

Certain types of clastogens elicit differential chemical effects on the DNA they act upon. In some instances, NHEJ or HR are not required to or are unable to be utilized repair the break. These repair mechanisms consist of Nucleotide Excision Repair (NER), Base Excision Repair (BER), and Mismatch Repair (MMR). In NER, BER, or MMR, single or small numbers of nucleotides are excised from the genomic material through similar mechanisms. In each, the exonuclease Exo1 provides resection through the excised material and provides access to DNA ligase I (MMR) or III (NER/BER) to perform gap synthesis to restore the genetic material. In each of these cases, the repair is thought to be *mostly* error free, as the donor template for repair is the remaining, intact strand of the duplex (the one not being repaired). However, in some instances, each of these mechanisms can lead to permanent changes in the genome if the *correct* strand of DNA is not repaired. These processes are reviewed in depth in (Li 2008) and (Iyama *et al.* 2013) and are mostly beyond the scope of this thesis.

Break-induced replication (BIR) is a final type of DNA repair that is utilized by cells when normal repair of the DNA through homologous recombination (HR) fails. Break-induced replication involves similar steps to HR repair in that the DSB must be resected and eventually coated by Rad51, as described in 1.6.C. However, unlike HR repair, BIR occurs when only one arm of the DSB can find homologous template. In this instance, BIR is used to synthesize new DNA from the homologous template and proceeds through the end of the template material (which is often the end of a chromosome). Break-induced replication is thought to be carried out through a D-loop migration mechanism, by which the D-loop becomes a pseudo-replication bubble (Sakofsky *et al.* 2017). This process is detailed and reviewed in Sakofsky and Malkova (Sakofsky *et al.* 2017). Replication Protein A's role in the later steps of BIR remains unclear.

1.7. DNA damage-dependent checkpoint (DDC)

The DNA Damage Checkpoint (DDC) is a conserved process that is designed to prevent entry into mitosis during the DDR program, preserving genomic stability and reducing mutation frequency in cells that have experienced some form of genotoxic insult. As described below, entry into mitosis in yeast is a much simpler process than in more complex organisms like human cells which depend on the inhibition of multiple cyclins to prevent anaphase and mitotic entry/exit. Replication Protein A plays critical

roles in the DDR program and the establishment and maintenance of the DDC. Not only is RPA required for the initial events that lead to establishment of the DDC, but mutant forms of RPA have been shown to alleviate checkpoint signaling and/or promote aberrant or premature replication restart in cells. Understanding how RPA is regulated during the establishment, maintenance, and recovery from the DDC leading to mitotic entry may provide researchers with novel targets to inhibit mitotic entry in cells that grow uncontrollably (*i.e.* cancer cells), as developing therapeutics that directly improve checkpoint function may lead to a reduction in mutations caused by improper or incomplete lesion processing, and thus increase genomic fidelity. This is especially prevalent as current therapeutic practices in the treatment of cancer involve the use of broad spectrum DNA damaging agents with the rationale that cancer cells will be unable to tolerate the added genomic instability while normal cells will faithfully repair any lesions that are generated during chemotherapy.

1.7.A. Establishment of the DDC in *Saccharomyces cerevisiae*

In *Saccharomyces cerevisiae*, the DNA Damage Checkpoint (DDC) is established rapidly to prevent cells from entering mitosis with incomplete or damaged genetic information and affords the DNA repair machinery adequate time to repair the DNA to preserve genomic integrity. As discussed briefly in 1.6.B, DSBs that are repaired in the G1 phase of the cell cycle, typically by NHEJ, often do not elicit a DDR from the cells, which prevents the establishment of a DDC. During the S- or G2-phases of the cell cycle; however, the establishment of the DDC is essential in preventing unwanted mutagenesis of the genome due to genotoxic insult. As described in section 1.1, initiation of the DDR program leads to establishment of the DDC through activation of the master checkpoint regulators in yeast, Rad53 and Chk1.

In order to fully activate Rad53, a number of conditions must first be met. First, the DNA damage response must have proceeded far enough along to generate the RPA-ssDNA platform that is recognized by Mec1/Ddc2. Replication Protein A stimulates loading of the Rad24-RFC2-5 clamp loader complex, which leads to the loading of 9-1-1 clamp (Rad17-Mec3-Ddc1) (Majka *et al.* 2006, Majka *et al.* 2006, Navadgi-Patil *et al.* 2009, Navadgi-Patil *et al.* 2011). An additional scaffold protein, Dpb11, interacts with the 9-1-1 clamp, and helps facilitate activation of Mec1/Ddc2 kinase activity (Mordes *et al.* 2008, Navadgi-Patil *et al.* 2008, Puddu *et al.* 2008, Navadgi-Patil *et al.* 2009, Navadgi-Patil *et al.* 2011). Mec1 is known

to phosphorylate a host of downstream effector molecules, most important of which for this thesis are Rad9 and Rad53 (de la Torre-Ruiz *et al.* 1998, Naiki *et al.* 2004, Sweeney *et al.* 2005, Bonilla *et al.* 2008, Clerici *et al.* 2014). Rad9 phosphorylation promotes its association to Rad53 and to damage-modified histones (H2AX S129 phosphorylation by Tel1/Mec1 (Downs *et al.* 2000, Burma *et al.* 2001, Ward *et al.* 2001) and H3K79 methylation by the Dot1 methyltransferase (Huyen *et al.* 2004, Grenon *et al.* 2007, Lazzaro *et al.* 2008, Puddu *et al.* 2008). Rad9 association with inactive Rad53 dimers leads to *trans* auto-phosphorylation of Rad53 and dissociates the heterodimers from one another (Gilbert *et al.* 2001). Localization of the Rad9-Rad53 dimer to DSB sites allows for Mec1-dependent hyper-phosphorylation of Rad53, causing it's dissociation from the Rad9 adaptor and eliciting Rad53's checkpoint arrest signaling activity.

1.7.B. Checkpoint arrest in yeast prevents anaphase, entry into mitosis via Rad53/Chk1 activity

Once fully activated, Rad53 activates Dun1 to promote the conversion of ribonucleotide triphosphates into deoxyribonucleotide triphosphates through the inhibition of Sml1. The increased dNTP pools are then used during DNA synthesis after the DSB is processed (Gardner *et al.* 1999). Rad53 inhibits Cdc5 kinase activity by maintaining elevated levels of CDK activity in the cell (Sanchez *et al.* 1999, Ira *et al.* 2004). Cdc5, an essential Polo-like kinase within the mitotic exit network (MEN) of kinases, facilitates entry into mitosis through the phospho-targeted destruction of a number of cyclins that Rad53 upregulates during establishment and maintenance of the DDC (Charles *et al.* 1998, Shirayama *et al.* 1998, Sanchez *et al.* 1999). Rad53's activity on Clb2/Cdc28 inhibits Clb2/Cdc28 phosphorylation of the mitosis-promoting Cdc5 Polo-like kinase (Cdc5 is an active target of Clb2/Cdc28 phospho-activation; Schleker *et al.* 2010) (Sanchez *et al.* 1999). Mitotic exit also requires interaction between APC^{CDC20} and Pds1 targets Pds1 for degradation through ubiquitination and allows entry into anaphase (Cohen-Fix *et al.* 1996, Cohen-Fix *et al.* 1997, Cohen-Fix *et al.* 1999, Agarwal *et al.* 2003). Rad53 also acts with Chk1 and phosphorylates Pds1, inhibiting Pds1 association with Cdc20 (Agarwal *et al.* 2003). Chk1 activity has been determined to be the predominant cause of phosphorylation on Pds1 in order to inhibit anaphase by preventing Pds1 ubiquitination, and prevents aberrant chromosome segregation through inhibition of spindle pole body dissolution (Cohen-Fix *et al.* 1996, Cohen-Fix *et al.* 1997, Cohen-Fix *et al.* 1999, Sanchez *et al.* 1999, Wang *et al.* 2001, Agarwal *et al.* 2003). In more complex organisms, activation of

the master checkpoint regulators Chk1 and Chk2 (Chk1 and Rad53 respectively) not only leads to the inhibition of anaphase, but also leads to the inhibition of cyclin signaling that would continue to move the cell cycle forward. This is in contrast to yeast, as yeast primarily halt cell growth by preventing degradation of Pds1 and inhibition of Cdc5 signaling activity which directly inhibits entry into anaphase, chromosome segregation, and entry into mitosis (*ibid*).

1.7.C. The currently undefined role for RPA phosphorylation during the DDC

RPA's role in the checkpoint response seems relatively straightforward at first glance. Replication Protein A is required for Mec1-dependent recognition of DSBs (Rouse *et al.* 2002, Rouse *et al.* 2002, Zou *et al.* 2003, Dubrana *et al.* 2007), loading of the Rad24-RFC2-5 clamp (Kim *et al.* 2001, Majka *et al.* 2006, Majka *et al.* 2006, Piya *et al.* 2015), as well as recruitment and stabilization of the DNA repair polymerases DNA pol α and DNA pol δ (Wang *et al.* 1999, Eggler *et al.* 2002, Wang *et al.* 2004, Sneeden *et al.* 2013). Previous research has suggested a more important role for RPA in mediating the DDC during DNA repair, as the *rfa1-t11* mutation or phospho-mimetic mutation of the Rfa2 NT appear to promote aberrant checkpoint exit (Lee *et al.* 2001, Pellicioli *et al.* 2001, Ghospurkar *et al.* 2015). This aberrant checkpoint exit is known as checkpoint adaptation and occurs approximately 10-12 hours after the initial DDR in yeast (Sandell *et al.* 1993, Toczyski *et al.* 1997). During checkpoint adaptation, the primary signals keeping Rad53 hyper-phosphorylated are deactivated, leading to entry into mitosis despite the presence or persistent of lesions with the genetic material (Sanchez *et al.* 1999, Pellicioli *et al.* 2001, Vidanes *et al.* 2010, Ferrari *et al.* 2013). In some instances, checkpoint adaptation can be inhibited by mutations of certain yeast genes. Some of these include the deletion or mutation of Cdc5 (kinase involved in mitotic exit; Toczyski *et al.* 1997) CKII (casein kinase II complex, *ibid*), Rdh54 (Swi2/Snf2 chromatin remodeler; Lee *et al.* 2001, Ferrari *et al.* 2013) , Srs2 (helicase involved in recombination; Vaze *et al.* 2002) , Rtt107 and Slx4 (scaffolding proteins involved in reversal of Rad53 signaling by competing for Rad9 proximal to the DSB; Ohouo et al. 2010, Ohouo et al. 2013, Cussiol et al. 2015, Dibitetto et al. 2016), Ku70 (essential for repair through NHEJ; Lee *et al.* 1998) , Mre11 and Rad50 (components of the MRX complex that initiate resection and checkpoint signaling through Tel1 sensor kinase; Lee et al. 1998, Grenon et al. 2001, Nakada et al. 2004, Paull and Lee 2005), Sae2 (nuclease component of MRXS, thought to be required for resection; Baroni et al. 2004, Gobbini et al. 2015, Dibitetto et al. 2016).

Currently, it has been demonstrated that a point mutation of the large subunit of RPA, *rfa1-t11* (K45E), checkpoint adaptation is promoted in the adaptation-deficient mutations *rdh54*Δ (Lee *et al.* 2001) or *yku70*Δ (Lee *et al.* 2001, Pellicioli *et al.* 2001), but not in cells containing the *cdc5-ad* mutation (Pellicioli *et al.* 2001). Furthermore, recent evidence has demonstrated that phospho-mimetic mutations or mutations that promote natural phosphorylation within the Rpa2 N-terminal (NT) phosphorylation domain are able to rescue the adaptation deficiency conferred by *yku70*Δ (Ghospurkar *et al.* 2015). Understanding the basic mechanisms and conditions by which RPA can promote checkpoint adaptation was a major focus of and impetus for this thesis.

1.8. Description of Thesis

The goal of this thesis was to better understand the function of the Rfa2 NT during DNA repair, checkpoint adaptation and meiosis, as well as the physiological consequences behind the observed, robust phosphorylation that occurs to Rfa2 during checkpoint adaptation. This thesis focuses on these problems. Chapter 2 addresses how, when, where, and why Rfa2 is phosphorylated during genotoxic stress. Chapter 3 addresses Rfa2 phosphorylation, specifically during checkpoint adaptation. Chapter 4 addresses global rescue of resection- and adaptation- deficient phenotypes using Rfa2 phospho-mimetic proteins. Chapter 5 addresses the role of Rfa2 NT phosphorylation as it contributes to meiosis and the meiotic recombination events that are essential for proper chromosomal segregation.

My work on the biochemical properties governing Rfa2 phosphorylation reveals that Rfa2 phosphorylation during the DDR is not only difficult to detect, but also occurs in the absence of many of the primary kinases involved in the DDR program, as demonstrated in *tel1*Δ*, dun1*Δ*, chk1*Δ*, mec1*Δ*,* and *rad53*Δ mutations. Furthermore, Rfa2 phosphorylation during checkpoint adaptation occurs more robustly than that observed during mitotically growing cells challenged with clastogens, suggesting that prolonged or irreparable DNA lesions are the major trigger of this post-translational modification of Rfa2. Studies performed here on the role phosphorylation plays during recombination refute the long-standing hypothesis that Rfa2 NT phosphorylation is both required for, and preferentially drives, DNA repair directly. My work on Rpa2 in checkpoint adaptation suggest a paradigm shifting new role for Rpa2 phosphorylation in cell cycle regulation, specifically that RPA is the primary coordinator of checkpoint entry, but that Rpa2 phosphorylation specifically is what is primarily coordinating checkpoint exit,

particularly in the face of persistent, irreparable DNA lesions. Moreover, Rfa2 NT phospho-mimetic or naturally phosphorylatable Rfa2 NT mutations preferentially drive checkpoint adaptation in resection-deficient mutations. I also demonstrate Rpa2 NT mutations do not appear to greatly impact resection of DSBs in checkpoint adaptation, suggesting that the adaptation rescue observed in *Saccharomyces cerevisiae* is independent of the ability of cells to resect the generated DSB. The findings detailed in this thesis provide evidence that Rfa2 NT phosphorylation plays a more important role in the temporal regulation of the DNA damage-dependent checkpoint during DNA repair, rather than mediating the repair process.

CHAPTER 2: RFA2 PHOSPHORYLATION DURING LESION PROCESSING AND DNA REPAIR

2.1. Abstract

Replication Protein A (RPA) is an essential single-stranded DNA (ssDNA) binding complex found in all eukaryotic organisms. In human cells, the amino-terminus (NT) of the Rpa2 subunit is phosphorylated by checkpoint kinases in response to DNA lesions. Phosphorylation of a residue outside of the yeast Rfa2 NT has been previously characterized. Although the yeast Rfa2 NT is serine/threonine-rich, similar to the human Rpa2 NT, phosphorylation within this domain had not been well-characterized. In this study, characterization of the yeast Rfa2 NT revealed that a "delayed" phosphorylation of this domain occurs in response to prolonged exposure to multiple clastogens. Mutation or removal of all serines/threonines within the Rfa2 NT eliminates the observed delayed phosphorylation event. Interestingly, cells containing either an NT phospho-mimetic form or an NT deletion form are sensitive to DNA damaging agents and display an early phosphorylation event. In both of these mutations, the major phospho-target is an SQ motif at serine 122 (a Mec1/Tel1 target site). However, Mec1 activity appears to be reduced in the Rfa2 NT phospho-mimetic mutation. Furthermore, delayed Rfa2 NT phosphorylation is not dependent on the Rfa1 NT (DBD-F), nor is it dependent on checkpoint kinases that initiate the DNA damage-dependent checkpoint. When human and other eukaryotic Rpa2 NT are fused to the Rfa2 protein, they exhibit earlier phosphorylation events that correlate with the presence of S/TQ motifs, which the yeast Rfa2 NT lacks. The delayed Rfa2 NT phosphorylation suggests a novel role for Rfa2 downstream of the initial DNA damage response.

2.2. Introduction

Critical for the prevention of mutations in the genetic blueprint of all eukaryotic organisms and all DNA metabolic processes is the heterotrimeric ssDNA-binding protein Replication Protein A (RPA). Composed of three subunits, called Rpa1 (70 kDa), Rpa2 (32 kDa), and Rpa3 (14 kDa), the RPA complex was originally isolated as a factor essential for *in vitro* SV40 DNA replication (REF). Since its discovery, RPA's biochemical role has been characterized as a single-stranded DNA (ssDNA) binding complex that facilitates cellular genome duplication and the maintenance of all genetic material (Wold *et al.* 1988, Heyer *et al.* 1990, Brill *et al.* 1991, Seroussi *et al.* 1993, Ghospurkar *et al.* 2015). Although RPA's primary biochemical role is ssDNA binding, RPA also plays diverse molecular roles, via post-

translational modification, in coordinating DNA replication, repair/recombination, and cell cycle regulatory responses to DNA damage (Marechal *et al.* 2015). Thus far phosphorylation remains the most well-characterized post-translational modification of the RPA complex. Rpa2 is phosphorylated at multiple serine and threonine residues within its N-terminus by several checkpoint kinases, including, but not limited to, ATR-ATRIP, ATM, CDK, and DNA-PK (Liu *et al.* 2012).

While Rpa2 is readily phosphorylated in response to genotoxic stress, the intracellular consequences and physiological role of these phosphorylation events play have remained elusive. Previous research has demonstrated that S23 and S29 of Rfa2 are phosphorylated by CDK during normal mitotic cell cycle progression, as well as upon cellular exposure to ionizing radiation (Brill *et al.* 1989, Din *et al.* 1990). Unsurprisingly, cells containing an Rpa2 S23/S29A double mutation accumulated in G_2-phase following camptothecin treatment indicating a cell cycle defect (Anantha *et al.* 2007) and also display reduced hyper-phosphorylation of the Rpa2 NT (Liu *et al.* 2012), suggesting a role for Rpa2 NT phosphorylation in mediating proper cell cycle progression. Additionally, phospho-mimetic studies of T21 and S33 suggest that phosphorylation of these residues may be required for inhibition of DNA replication during UV-induced DNA damage (Olson *et al.* 2006).

Studies performed using a phospho-mimetic NT (*rfa2-D*) mutation has been demonstrated to show reduced RPA complex association with replication centers, but show no detectable change in RPA complex association to repair foci (Vassin *et al.* 2004). Phospho-mimetic NT Rpa2 mutations have also been demonstrated to disrupt interaction with the MRN complex, specifically through Mre11, *in vitro* (Oakley *et al.* 2009). Moreover, Rpa2 phosphorylation may play a critical role in normal checkpoint initiation and maintenance, as S4/S8A mutations are defective for Chk1, Mre11 and TopBP1 phosphorylation (Liu *et al.* 2012) – all of which are required for normal checkpoint activation in human cells. More recently, Rpa2 NT phosphorylation has been proposed as a biomarker for human oral cancer progression and prognosis, with abundant Rpa2 hyper-phosphorylation at S4 and/or S8 as an indicator of poorer diagnostic outcomes (Rector *et al.* 2016).

While Rpa2 phosphorylation has been well characterized in human cells, the same level of biochemical characterization and corroboration of Rpa2 mutation phenotypes is lacking in other model systems. In advanced model systems such as *Xenopus laevis,* Rpa2 phosphorylation occurs in an

ssDNA-dependent manner during S-phase by Cdk2, as well as during mitotic entry in a DNA-independent mechanism by Cdc2 (Fang *et al.* 1993). Upon exit from mitosis, Rpa2 becomes dephosphorylated, and is re-phosphorylated upon RPA association with the pre-initiation complex (Francon *et al.* 2004). Furthermore, control of Rpa2 phosphorylation has been demonstrated to be important for S-phase-dependent checkpoint signaling, as phospho-mimetic Rpa2 mutations are deficient in promoting checkpoint activation at unwound replication forks (Recolin *et al.* 2012, Recolin *et al.* 2012).

In plant model systems, like *Arabidopsis thaliana* (thale cress) or *Oryza sativa* (rice), there are multiple copies of RPA subunit genes, particularly Rpa1 and Rpa2, and it has been hypothesized that the different forms are necessary to perform distinct functions involving an RPA complex in the cell. For example, plants may have a replication-specific Rpa2, a DNA damage-specific Rpa2, and have been shown to form distinct RPA complexes with precise combinations of RPA subunits to perform explicit functions. Consistent with this hypothesis are observations that Rpa1 and Rpa2 paralogs form differential complexes in plants that regulate meiotic crossover, DNA replication, and DNA repair (Marwedel *et al.* 2003, Chang *et al.* 2009, Li *et al.* 2013, Aklilu *et al.* 2014, Eschbach *et al.* 2014, Aklilu *et al.* 2016). Post-translational modifications of plant RPA subunits have not been studied. Consistent with other organisms, mutations of Rpa2 in *Arabidopsis* lead to hyper-sensitivity to DNA damaging agents (Elmayan *et al.* 2005).

In *Candida albicans*, Rpa2 phosphorylation has been detected in response to genotoxic stress (Wang *et al.* 2013), with residues in the N-terminal phosphorylation domain (T11, S18, S29, S30) being important during the intracellular response to clastogens. Phosphorylation of the aforementioned NT residues on Rpa2 is has been shown to be achieved through Mec1- and Clb2-Cdc28-dependent phosphorylation (Gao *et al.* 2014), analogous to that observed in human cells. Furthermore, Rpa2 obtained from unchallenged, mitotically growing cells has been demonstrated by mass spectrometry to be phosphorylated differentially from cells treated with the DNA replication inhibitor hydroxyurea (HU) (Wang *et al.* 2013). In contrast to human cells, however, *C. albicans* cells containing either phospho-mimetic (T11D, S18D, S29D, S30D) or unphosphorylatable (T11A, S18A, S29A, S30A) mutations exhibit an increased sensitivity to DNA damaging agents, and defects in checkpoint recovery, but not checkpoint activation (Gao *et al.* 2014).

During her thesis work, Padmaja L. Ghospurkar tested phosphorylation of various eukaryotic N-termini fused to the Rfa2 core peptide (DBD-D and WHD) in response to phleomycin challenge (Figure 2.1; Ghospurkar 2015). Some of the most striking differences in Rfa2 post-translational modification are observed when comparing Rfa2-NT mutations within plants. *Oryza sativa*, as well *Arabidopsis thaliana*, contain multiple copies of RFA2 within their respective genomes. Biochemical studies involving Rfa2 in *O. sativa* and A*. thaliana* are non-existent, most likely because antibodies to each of the individual Rfa2 isoforms do not exist. Our yeast system provides a unique opportunity to study Rfa2 NT domain function in vivo. Unsurprisingly, not only do each of these Rfa2 forms support mitotic growth and properly activate a DNA damage-induced checkpoint, each appears to be modified differentially in a DNA damage-dependent manner. Rfa2-OS1 shows significant modification of the fusion protein in both unstressed and stressed conditions, whereas Rfa2-OS2 shows minimal or barely detectable modification under genotoxic stress. Rfa2-ATa shows robust modification in both unstressed and stressed conditions, while Rfa2-ATb shows robust modification of Rfa2 only in a stressed condition. Taken together, her results have two major implications for studying Rfa2 phosphorylation in budding yeast. First, Rfa2 phosphorylation from other eukaryotic organisms can be studied rapidly and cost-effectively in a *Saccharomyces cerevisiae* model, especially for model organisms where antibodies to the individual Rfa2 proteins do not exist. Secondly, her data correlates well with the idea that 'redundant' copies of genes may not be redundant but in fact may have specific functions within the cell that are separate and regulated in different ways from their duplicate counterparts. Moreover, the presence of phospho-species observed in Figure 2.1 may be due to the presence of SQ/TQ (serine-glutamine/threonine-glutamine) kinase consensus phosphorylation sites within each respective Rpa2 paralog.

In the budding yeast *Saccharomyces cerevisiae*, there are two known target sites for phosphorylation in RFA, both of which have been reported to be phosphorylated by the checkpoint kinase Mec1. The first lies at S178 of Rfa1, within a flexible linker between the N-terminus (DBD-F) and the core ssDNA binding domain (DBD-A) (Brush *et al.* 2000). The second, reported to be a Mec1-dependent phosphorylation site, lies at S122 of Rfa2 (within the unstructured loop 3-4 region) (Brush *et al.* 1996, Brush *et al.* 2000, Mallory *et al.* 2003). Despite their relative ease of identification, there is no observed physiological role for these residues in mitosis (Ghospurkar *et al.* 2015), and only a minor role reported in

meiosis (Brush *et al.* 1996, Brush *et al.* 2000, Brush *et al.* 2001, Clifford *et al.* 2004). Similar to observations made in *Candida*, the budding yeast Rfa2 NT is dispensable for checkpoint activation and mitotic growth (Gao *et al.* 2014, Ghospurkar *et al.* 2015).

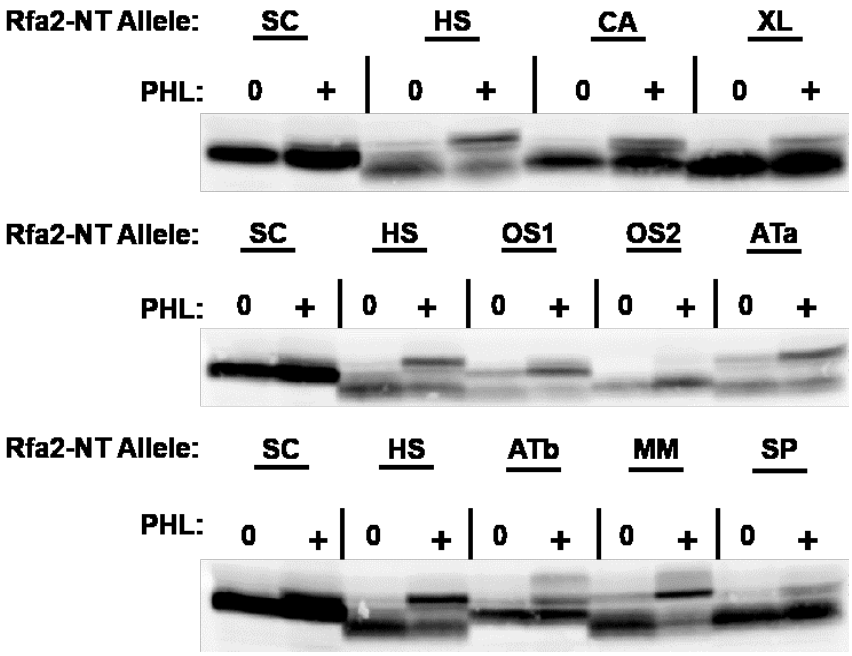

Figure 2.1. Phosphorylation of eukaryotic Rpa2 NT in budding yeast.
Adapted from Padamaja L. Ghospurkar's thesis (Ghospurkar 2015). Immunoblot depicting Rfa2 NT mutations using NT sequence from other eukaryotic organisms. Phosphorylation of eukaryotic Rpa2 NT occurs in response to phleomycin (PHL) treatment and differs between different paralogs of Rpa2 found within their respective organisms. Equivalent numbers of cells were harvested prior to phleomycin (PHL) exposure (0) or four hours post-PHL exposure (+). Species are indicated as follows: SC – *Saccharomyces cerevisiae*, HS – *Homo sapiens*, CA – *Candida albicans*, XL – *Xenopus laevis*, AT – *Arabidopsis thaliana*, OS – *Oryza sativa*, MM – *Mus musculus*.

Previous studies have demonstrated that the *Saccharomyces* Rfa2 N-terminus is important in the DNA damage response (Ghospurkar *et al.* 2015) and that in some special cases (*ie*, *set1*Δ mutations; Schramke *et al.* 2001, and during meiosis; Brush *et al.* 2001), it can be post-translationally modified by phosphorylation. However, identification of mitotic phosphorylation of RFA had been limited to serine residues that lie outside the N-terminus. In a study of the physiological importance of the yeast Rfa2 NT, it was demonstrated that an *rfa2* mutation (*rfa2-D*$_X$) that contained aspartate substitutions of serines/threonines in the N-terminus lead to checkpoint adaptation (Ghospurkar *et al.* 2015); however, this effect occurred 12-16 hr after induction of DNA damage and 8-12 hr following checkpoint activation. This led us to test whether Rfa2 NT-dependent phosphorylation was occurring after prolonged exposure

to DNA damage. Delayed Rfa2 phosphorylation occurs, and is readily detected, after prolonged genotoxic challenge. This additional phosphorylation is dependent on the physical presence of the N-terminal phosphorylation domain, but not the N-terminus of the larger RPA subunit, Rpa1, as Rfa2 NT phosphorylation occurs in the damage-sensitive *rfa1-t11* (K45E) point mutation. Furthermore, this delayed phosphorylation does not appear to be dependent on the activity of kinases known to play essential roles during the initiation of the DNA damage-dependent checkpoint, such as Mec1 or Tel1.

2.3. Materials and Methods

2.3.A. Strains and Plasmids

Yeast strains and plasmids used in these studies are listed in Appendix A and Appendix B, respectively. All yeast strains used within this study are isogenic derivatives of JKM179 (*hoΔ MATα hmlΔ::ADE1 hmrΔ::ADE1 ade1-100 leu2-3,112 lys5 trp1::hisG' ura3-52 ade3::GAL-HO*; Lee *et al.* 1998) containing either *rfa2Δ::kanMX* (NMM104) or *rfa1Δ::kanMX* (NMM101). To generate NMM104 (JKM179 *rfa2Δ::kanMX*) or NMM101 (JKM179 *rfa1Δ::kanMX)*, PCR of the *kanMX* cassette was performed using pEG202K (Appendix B) as a template and appropriate primers to *RFA1* or *RFA2* (Appendix C) containing an additional 40 nucleotides (nt) of homologous sequence located immediately upstream and downstream of the coding region of *RFA2* or *RFA1*. This PCR product was co-transformed with pJM132, a centromeric vector containing wild-type *RFA1*, *RFA2*, and *RFA3* genes expressed from their native promoters (Maniar *et al.* 1997), into competent JKM179 cells to facilitate one-step gene replacement at the *RFA2* or *RFA1* locus. Chromosomal knockout of *RFA2* or *RFA1* was verified by PCR using appropriate primers (Appendix C), using a strategy similar to that for the generation of yeast gene deletions (Kelly *et al.* 2001). PCR products were also sequenced to verify genomic replacement.

The generation of *TEL1*, *CHK1*, and *DUN1* kinase deletions in the NMM104 background was done using PCR amplification of the *natMX* cassette from plasmid pFA6-natNT2 (Euroscarf; Janke *et al* 2004) with primers (Appendix C) containing an additional 40 nt of homologous sequence immediately upstream and downstream of the coding regions of each gene and one-step gene replacement. *tel1Δ*, *chk1Δ*, and *dun1Δ* candidates were screened via diagnostic replica plating and by PCR using diagnostic primers (Figure 2.2) (Appendix C).

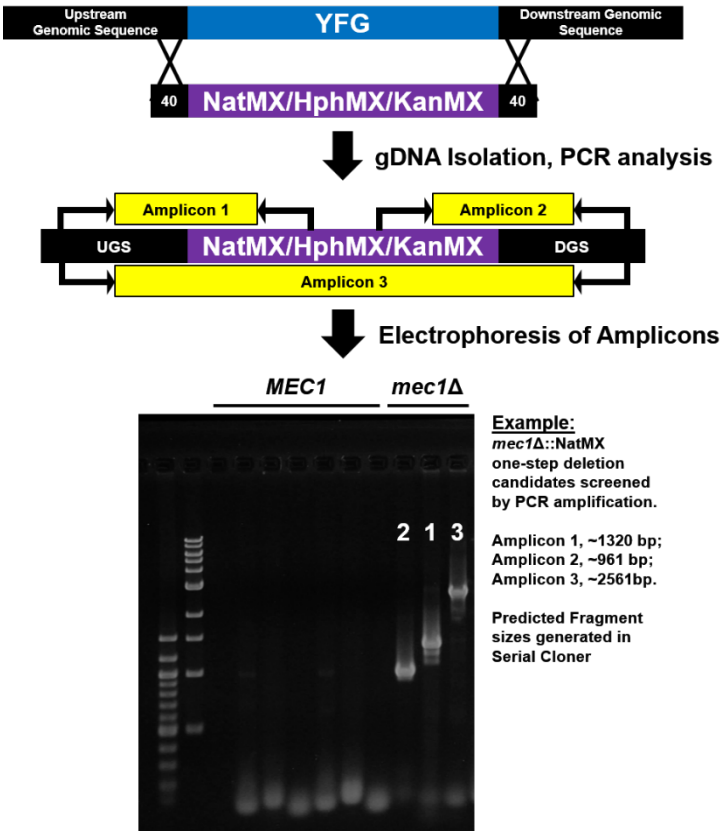

Figure 2.2. One-step gene replacement and verification strategy.
A schematic representation of the one-step gene replacement strategy used for the generation of deletion mutations used in this study (Top Panels). PCR product containing a resistance cassette (natMX, kanMX, hphNX) and at least 40 nt of homologous sequence upstream and downstream of YFG (your favorite gene), was generated as described in section 2.3.A. This PCR fragment was transformed into lithium acetate competent yeast cells and incubated for 5 hours. Following selection and genomic isolation, PCR amplification using appropriate primers (Appendix C) confirmed each gene deletion (bottom panel). Displayed is the *mec1*Δ mutation amplified against *MEC1* cells. Three amplicons were examined. Amplicon 1 is produced from a forward primer outside the deletion site and a reverse primer starting within the natMX cassette. Amplicon 2 is produced from a forward primer within the natMX cassette and a reverse primer outside of the gene deletion. Amplicon 3 is the full-length product produced a forward external primer at the 5' end of the chromosome sequence and a reverse external primer at the 3' end of the chromosome sequence.

The *MEC1* kinase deletion strain utilized in this study was also generated by one-step gene replacement. However, before attempting deletion of *MEC1,* the *SML1* gene was first deleted by PCR amplification of *hphN* from pFA6-hphN (Euroscarf; Janke *et al* 2004) using a similar method to that described above. Once verified, the *sml1*Δ*::hphN* NMM104 derivative strain was transformed with *mec1*Δ*::natMX* PCR product amplified using the appropriate primers as described above. *mec1*Δ *sml1*Δ candidates were screened via diagnostic replica plating and PCR using diagnostic primers (Appendix C).

2.3.B. DNA damage spot-plating assays

Wild-type or mutant cells were grown overnight at 30°C in liquid YPD media (1% yeast extract, 2% peptone, 2% dextrose) and were initially diluted to an OD_{600} of 1.0 in 1x PBS. Six 10-fold serial dilutions from each initial sample were then performed, and 5 uL of the initial dilution and serial dilutions for each strain were spotted onto the following media: YPD, YPD + 0.0075–0.06% methyl methanesulfonate (MMS), YPD + 0.2–25 mg/ml camptothecin (CPT), YPD + 40–360 mM hydroxyurea (HU), YPD + 0.2–25 mg/ml phleomycin (PHL). Plates were incubated for 2–4 days at 30°C, and growth differences between the mutant and wild-type cells were documented.

2.3.C. *In vitro* site-directed mutagenesis

To generate $S122_{D/A}$ mutations in Rfa2 NT mutation vectors, *in vitro* site-directed mutagenesis was performed using Q5 High-Fidelity polymerase (New England Biolabs) and primers O-284 (S122D) or O-285 (S122A) on the appropriate pRS315-*RFA2*-derived template. Following *Dpn*I digestion, mutagenesis reactions were transformed into bacterial cells and plasmid DNA was harvested from viable transformants. Vectors generated by mutagenesis were then digested with diagnostic enzymes (*Bst*EII or *Bam*HI) and sequenced (Eton Biosciences). Vectors identified to have S122D or S122A mutations were then transformed into NMM104 via plasmid shuffle (described below).

2.3.D. Plasmid shuffle to generate mutant RPA strains

Centromeric *rfa2* mutant plasmids (pRS315 derivatives; *LEU2*) (Appendix B) were transformed into NMM104 cells. Transformants were selected on synthetic complete media (0.5% ammonium sulfate, 0.17% yeast nitrogen base w/o amino acids, 2% dextrose) lacking leucine, resulting in transformants that contained two plasmids. Cells were grown in liquid SD-Leu media overnight, selecting for *rfa2* mutant vectors, and subsequently plated and recovered on media containing 1.0 ug/mL 5-fluoroorotic acid (5-FOA). Use of 1.0 ug/mL 5-FOA is specific for JKM179 derivative strains. Recovered colonies were then picked to a YPD master plate and subsequently replica plated to synthetic complete media lacking uracil or leucine to verify loss of pJM132 (*URA3*). Cells that were uracil auxotrophs (*ura3*) and leucine prototrophs (*LEU2*) were then used in further studies.

2.3.E. DNA damage induction and collection of whole-cell lysate

Induction of DNA damage in cells for biochemical assays was performed in liquid culture. Yeast cells were grown for 20 hours (hr) in liquid YPD (1% yeast extract, 2% peptone, 2% dextrose) to an OD_{600} of 1.0. Each culture was then exposed to one of the following DNA-damaging agents: 0.03 or 0.06% v/v methyl methanesulfonate (MMS), 5 or 25 ug/mL camptothecin (CPT), 5 or 25 ug/mL phleomycin (PHL), 80 or 360 mM hydroxyurea (HU). In order to harvest an equivalent number of cells from each culture, 25 ODs of cells were harvested from each culture at 0, 2, 4, 6, 8, 10, 12, 16, and 24 hr post-exposure to each damaging agent. Harvested cells were treated with 0.3 M NaOH for 5 minutes at room temperature, pelleted at 10K RPM for 2 minutes (min), and aspirated to remove NaOH from the pellet. The pelleted cells were then resuspended in 500 uL of K-Buffer (0.06 M Tris-HCl, ph 6.8, 5% glycerol, 2% SDS, 4% β-mercaptoethanol, 10 mM DTT; Kushnirov 2000), and each protein sample was boiled at 100°C for 3 min. A modified Lowry assay (RC-DC Assay Kit; Bio-Rad) was used to quantify protein concentration within each sample to ensure even protein loading during SDS-PAGE.

2.3.F. Phosphatase treatment of whole cell lysates

Whole cell lysate obtained as described above was quantified and 100 ug total whole cell lysate was precipated in 100% ice cold acetone and harvested via centrifugation at 15,000 RPM for 10 minutes. Following aspiration of the supernatant, the pellet was resuspended in 100 uL of Buffer A (BA) + Protease Inhibitor Cocktail (G-Biosciences). An aliquot of 40 uL (approximately 40 ug) of the Buffer A protein suspension was added to a new centrifuge tube, to which 5 uL of 10X PMP buffer (NEB) and 5 uL of 10 mM MnCl2 was added. 400 units (2 uL) of Lambda Protein Phosphatase (NEB) was then added to each sample. Samples were incubated at 30°C for 2 hours to allow full dephosphorylation of lysate. 50 uL of 2x K-buffer was then added to each sample and boiled for 3 min at 100°C. 20 uL (approximately 5 ug total protein) of the boiled suspension was then used in SDS-PAGE.

2.3.G. SDS-PAGE and Immunoblotting

Whole-cell lysate containing 10 ug total protein from each sample was loaded into SDS-PAGE gels containing a 4% (37.5:1 mono:bis) stacking gel and 12% (150:1 mono:bis) or 15% (29:1 mono:bis) resolving gel. Electrophoresis was then performed at 10-30 mA constant current for 15 minutes, 20-60 mA constant current for 2-4 hours allowing the 25 kDa band (PageRuler Plus Prestained Protein Ladder;

Thermo Scientific) to reach the base of the gel. Each gel was equilibrated in Towbin Transfer Buffer (10 mM Tris-HCl, 100 mM glycine, 10% Methanol) for 15 min and transferred onto a 0.2-micron nitrocelllose membrane (Bio-Rad) at 40 mA constant current for 16 hours at 4°C.

Once transfer was complete, nitrocellulose membranes were then stained with Ponceau S (0.5% w/v Ponceau S, 1% v/v acetic acid) for 10 min to visualize total protein content to determine equivalent loading within each lane. Once membranes were imaged, the Ponceau S stain was removed by washing with Western Wash Buffer (WWB) (0.3% Tween-20, 5 uM NaF, 0.05 uM Na_3VO_4) for 15 minutes. Blocking buffer (WWB, 1% w/v BSA) was then added and the blot was incubated for 2 hours at room temperature. Blocking buffer was removed, and Primary Antibody Buffer (PAB) (WWB, 0.5% w/v nonfat dry milk, 0.5% BSA) containing a 1:40,000 dilution of α-Rfa2 antibody (kindly provided by Dr. Steve Brill) was added to the blots. Following a 16 hr incubation at 4°C, the PAB was removed and washes were performed using WWB. Secondary Antibody Buffer (SAB) (WWB, 0.2% w/v nonfat dry milk), containing a 1:40,000 dilution of goat-α-rabbit-HRP (Abcam; ab97051, 1:40,000, Bethyl; A120-101P, 1:40,000) was then added to each blot and allowed to incubate for 2 hr at room temperature. The SAB was then removed and washes using WWB were performed. All blots were developed using a fluorescent substrate (ECL2 Plus; Thermo Scientific) and visualized on a STORM imager (GE Healthcare).

2.3.H. Phospho-specific Immunoblotting of *rfa2-h2NT*

SDS-PAGE and western blotting was performed as described above, with the following changes. Phospho-specific antibodies to the human Rpa2 epitopes of pS4/pS8 (Bethyl; A300-245A, 1:5,000, 40 ug total protein), pT21 (Abcam; ab109394, 1:40,000, 2 ug total protein), pS29 (kindly provided by Jim Borowiec, 1:10,000, 10 ug total protein), pS33 (Bethyl; A300-246A, 1:5,000, 20 ug total protein) were used to probe site specific phosphorylation changes. All the above primary antibodies were generated in rabbits, and as such, were detected using the same secondary antibodies described above.

2.4. Results

2.4.A. Examination of sequential phosphorylation and site-dependent phosphorylation mechanisms in *Saccharomyces cerevisiae* using *rfa2-h2NT*

Previous research performed in human cells suggest the existence of a sequential phosphorylation mechanism as a means by which to propagate phosphorylation throughout the N-

terminal domain (Anantha et al. 2008, Liu et al. 2012). This has led to the proposal of two sequential phosphorylation models by the Borowiec (Figure 2.3A) and Oakley (Figure 2.3B) lab groups. The Borowiec model suggests that phosphorylation at S33 is the priming event that leads to phosphorylation at S23/29, which facilitates phosphorylation T21, S11/12/13, S8, and/or S4. The Oakley model suggests that while phosphorylation can occur initially at several different residues on the N-terminus individually, one primed event is necessary to propagate phosphorylation throughout the rest of the phosphorylation domain. Using our Rfa2-h2NT fusion protein, we probed whether sequential phosphorylation of the human NT occurs in budding yeast (Figure 2.4).

Using a genetic approach, we modified each of the serine/threonine residues within the phosphorylation domain of *rfa2-h2NT* to alanine to determine site-specific dependency of phosphorylation by monitoring adjacent sites. Cells challenged with phleomycin, containing single serine to alanine or threonine to alanine mutations of the yeast Rfa2 protein exhibited near-identical levels of Rfa2 hyper-phosphorylation (Figure 2.5A). Using human-peptide phospho-specific antibodies to probe the serine or threonine to alanine mutations within *rfa2-h2NT*, we demonstrate that preventing of phosphorylation at one site does not impede phosphorylation at adjacent or distal sites (Figure 2.5B). Both results, taken together, suggest two things: *1)* sequential, primed phosphorylation of the N-terminal domain is not a mechanism employed in yeast to fully hyper-phosphorylate the Rfa2-h2NT protein, and *2)* phosphorylation at all other residues examined was observed for each of the Rfa2-h2A$_I$ single mutants tested. Further analysis of Rfa2-h2NT phosphorylation revealed that phosphorylation at T21 and S33 were achieved by Mec1 (Figure 2.6). Phosphorylation at T21 became more intense in a *rad53*Δ strain, similar to wild-type Rfa2 NT phosphorylation observed in a *rad53*Δ mutation (Schramke *et al.* 2001).

2.4.B. Analysis of Rfa2-h2NT mutant function in *Saccharomyces cerevisiae*

During our study of the function of the human Rpa2 NT in budding yeast, we also analyzed the function of human phospho-mimetic NT mutations (Figure 2.7 and 2.8). We found that each of the human NT mutations (*rfa2-h2NT, rfa2-h2D$_X$, rfa2-h2A$_X$, rfa2-h2*Δ*N$_X$*) promoted proper checkpoint activation in yeast, as measured by Rad53 phosphorylation via immunoblot. Furthermore, modification of the humanized Rfa2 NT was only observed in the *rfa2-h2NT* mutant (Figure 2.8; (Ghospurkar *et al.* 2015).

Moreover, we found that each of the respective *rfa2-h2* mutations recapitulated known phenotypes for Rfa2 NT mutations via diagnostic spot assays (Figure 2.9).

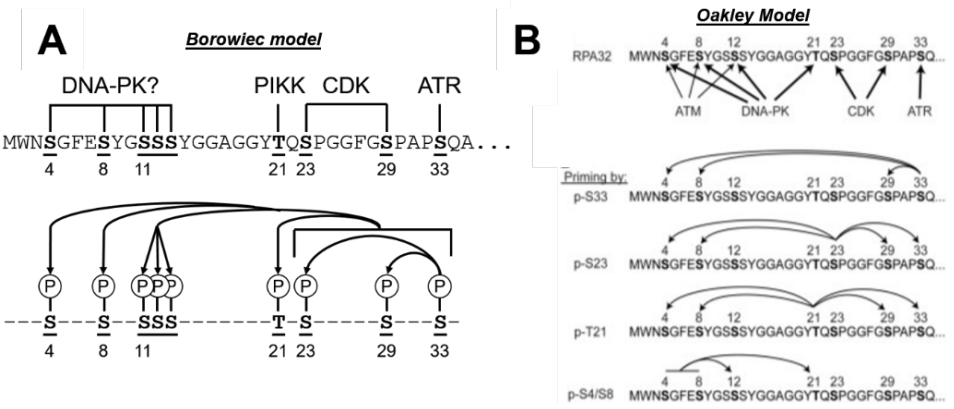

Figure 2.3. Borowiec and Oakley models for sequential phosphorylation of the Rpa2 NT.
A. Borowiec model of sequential phosphorylation adapted from (Anantha *et al.* 2009). Top panel displays known kinase activity at Rpa2 NT sites. Bottom panel is the Borowiec Model for sequential phosphorylation emanating from S33, and propagating phosphorylation to S29 and S33. This additional phosphorylation leads to T21 phosphorylation, which then promotes phosphorylation at S11, S12, S13 and S4 and S8 **B.** The Oakley model (Liu *et al.* 2012) for sequential phosphorylation suggests that phosphorylation at *any* site is required for priming of phosphorylation at adjacent or distal sites (reprinted with permission from Oxford Academic Journals: Liu *et al.*, *Nucleic Acids Research,* 2012).

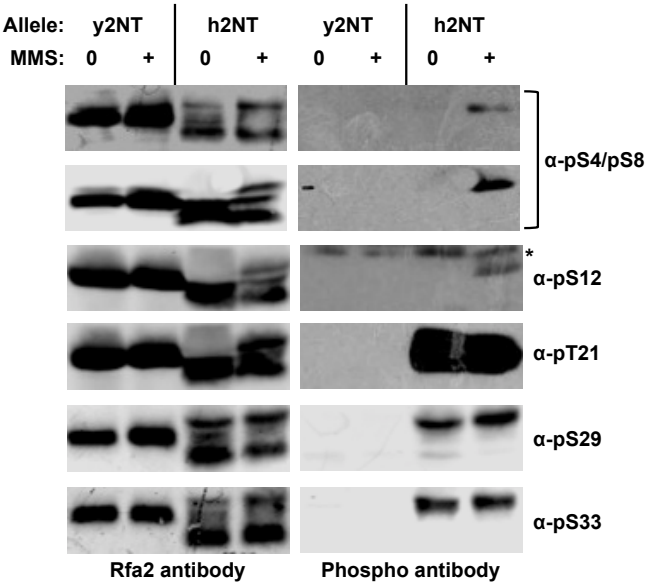

Figure 2.4. Human-specific antibody recognition of damage dependent and mitotic *rfa2-h2NT* phosphorylation.
Phosphorylation of *rfa2-h2NT* occurs in response to PHL treatment and in mitotically growing cells. MMS treatment (0.03%) is indicated by '+', untreated cells '0'. Western blotting with human Rpa2 phospho-specific antibodies (right-side blots with specific antibody used denoted to the right of each blot) was performed. Blots on left half represent resolution of approximately equal amounts of total Rfa2 or Rfa2-h2NT (not total protein). Phosphorylation at S4/S8 occurs in response to PHL treatment. Human phospho-specific antibodies do not recognize the yeast Rfa2 peptide natively. This blot was done by Shenqin Liu of the Oakley lab and published in Ghospurkar *et al.* 2015.

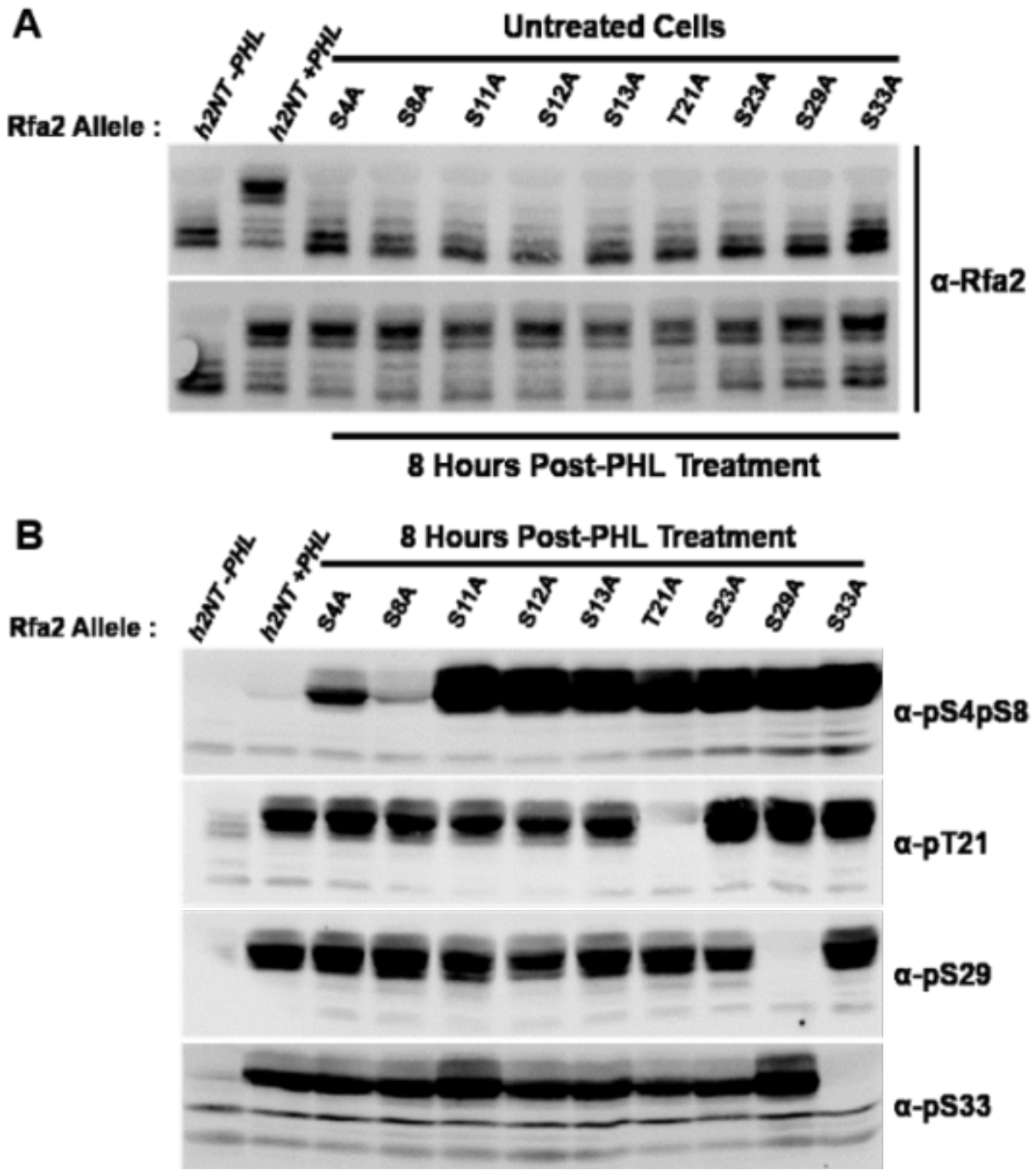

Figure 2.5. *rfa2-h2A$_l$* mutations have no discernable effect on sequential phosphorylation of *rfa2-h2NT.*

A. Analysis of *rfa2-h2A$_l$* mutations during phleomycin challenge displays near identical biochemical phenotypes for each individual mutation, suggesting that sequential phosphorylation of the *rfa2-h2NT* in budding yeast is not occurring. **B.** Human phospho-specific antibody probes of *rfa2-A$_l$* mutations from **A.** further demonstrate that sequential phosphorylation of the *rfa2-h2NT* in budding yeast is not occurring or is not impacted by single-site mutations. Phospho-site-specific antibodies are denoted to the right of the immunoblots.

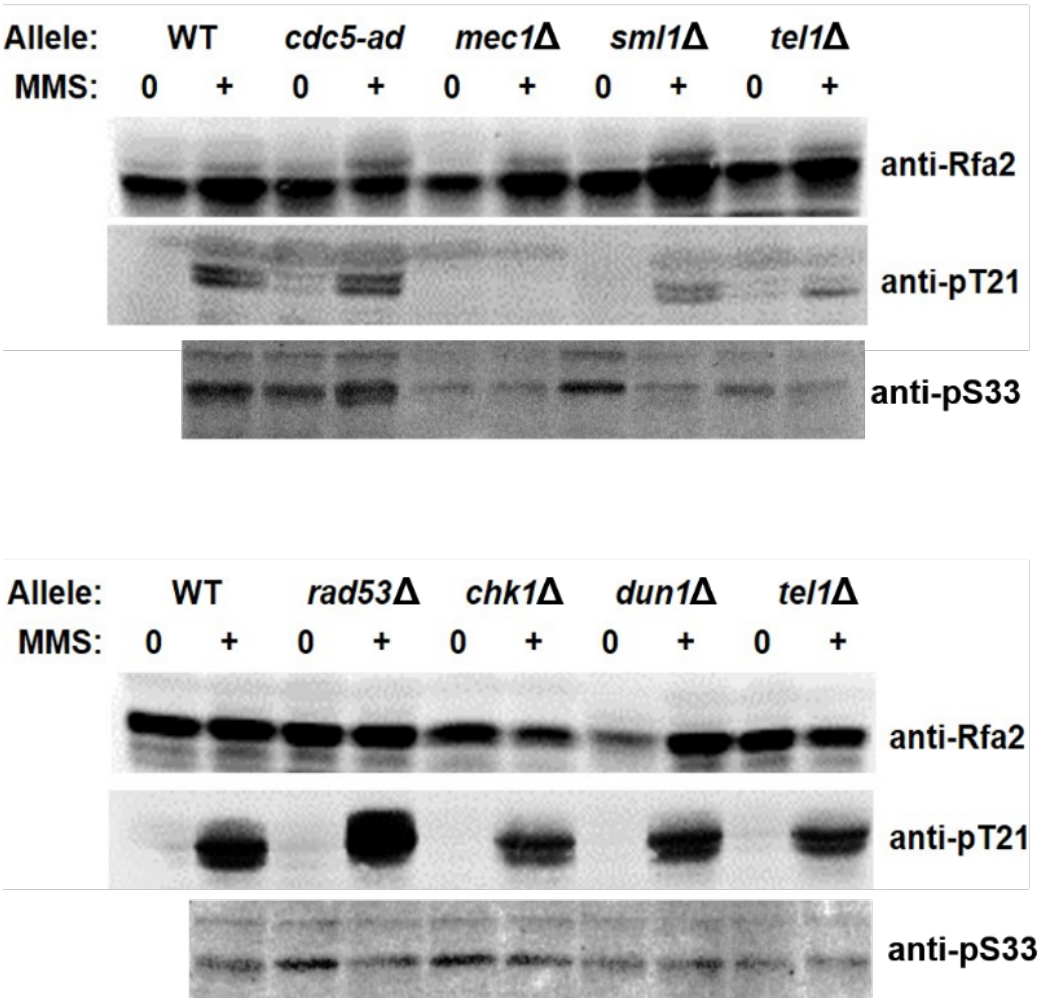

Figure 2.6. Mec1 phosphorylates *rfa2-h2NT* at known damage-dependent sites (T21 and S33). Kinase deletion mutations in the JKM179 background (AWY strains) were subjected to PHL treatment, harvested, and analyzed using a human phospho-specific antibody to Rpa2-T21 phosphorylation. *mec1*Δ cells are unable to phosphorylate T21 and S33, suggesting Mec1 is the primary kinase phosphorylating the SQ/TQ kinase consensus sites on Rfa2-h2NT in budding yeast.

2.4.C. Analysis of Rfa2 NT extensive mutations in kinase deletion mutant yeast

Through our collaboration with the Andre Walther Lab at Cedar Crest College (Allentown, PA, USA), we obtained several JKM179 derivative strains containing chromosomal integrations of two Rfa2 NT extensive mutations (*rfa2-D*$_X$ and *rfa2-A*$_X$) to analyze. Overnight cultures *tel1*Δ, *chk1*Δ, *dun1*Δ, *sml1*Δ, *mec1*Δ, or *rad53*Δ containing either *RFA2*, *rfa2-D*$_X$ (Figures 2.10 and 2.12) or *rfa2-A*$_X$ (Figures 2.11 and 2.13) were harvested and an OD_{600} was determined. Six 10-fold serial dilutions were performed starting at an OD_{600} = 1.0 and spotted on YPD media or YPD media containing MMS, PHL, CPT, or HU at various concentrations. In nearly every case examined the presence of the *rfa2-D*$_X$ mutation led to an increase the kinase deletion mutant sensitivity to genotoxic agents. Surprisingly, the *rfa2-D*$_X$ mutation supported

some resistance to phleomycin in *tel1*Δ, *chk1*Δ, *dun1*Δ mutants, and was more effective at promoting genotoxic resistance to phleomycin than the *rfa2-A$_X$* mutation.

Deletion of the *MEC1* and *RAD53* genes is only possible after deleting *SML1* (suppressor of Mec1 lethal). Yeast mutants containing the *sml1*Δ, *mec1*Δ *sml1*Δ, or *rad53*Δ *sml1*Δ deletions were sensitive to genotoxic agents and became more sensitive to HU, MMS, and CPT. Similar to that observed for *tel1*Δ, *chk1*Δ, *dun1*Δ the *mec1*Δ *sml1*Δ, or *rad53*Δ *sml1*Δ double mutants containing *rfa2-D$_X$* were tolerant to phleomycin-induced genotoxic stress, whereas the same double mutants containing *rfa2-A$_X$* were as sensitive to each genotoxic agent as the double mutants containing *RFA2*.

These results are inconsistent with previous observations that the *rfa2-D$_X$* mutation broadly increases sensitivity to genotoxic agents. Moreover, recreating these strains in the JKM179 background using one-step gene replacement (Figures 2.12, 2.14, and 2.16) revealed that *rfa2-D$_X$* does lead to increased genotoxic sensitivity in *tel1*Δ, *chk1*Δ, *dun1*Δ mutants in all clastogens tested. Similarly, the *rfa2-A$_X$* mutation (Figures 2.13, 2.15, 2.17) supports clastogen resistance in line with *RFA2* in each of the deletion mutants tested, and *tel1*Δ, *chk1*Δ, *dun1*Δ deletion mutants do not tolerate genotoxic challenge better than the same deletion mutants containing *RFA2* in any of the genotoxic conditions analyzed.

2.4.D. Detection of Rfa2 modifications during prolonged genotoxic stress

In a previous study, phosphorylation of the yeast Rfa2 NT was unobservable in response to genotoxic stress carried out for up to 4 hours. However, a chimeric Rfa2 containing the human Rpa2 N-terminus is robustly phosphorylated in this region in response to genotoxic stress (Ghospurkar *et al.* 2015). This indicated that a sequence attached to the NT region of Rfa2 was capable of being phosphorylated, but that the native yeast Rfa2 NT was not detectably modified within the 4-hour time course. Characterization of Rfa2 NT phospho-mutations in a *yku70*Δ background revealed that the phospho-mimetic form stimulated checkpoint adaptation approximately 12-15 hours after the generation irreparable DSB and nearly 8-10 hours after initial checkpoint establishment (Ghospurkar *et al.* 2015). As a result of these previous experiments, we aimed to determine if delayed Rfa2 phosphorylation might be occurring in response to prolonged clastogen exposure. When treated with phleomycin (PHL), a chemical analog of bleomycin, *rfa2-h2NT* cells show robust phosphorylation of N-terminus approximately 2 hours after exposure. Additional modification of the Rfa2-h2NT protein does not appear to change with

prolonged exposure to phleomycin (Figure 2.20). Although we can detect minimal modification of Rfa2 at 2 hours, the intensity of this modification increases until maximum modification is observed at 12 hours. Furthermore, we are able to detect two slower migrating species of Rfa2 in wild-type cells when damaged with phleomycin. We suggest that one or more of these slower migrating species also contains phosphorylation occurring at S122, which has been demonstrated previously (Brush et al. 1996).

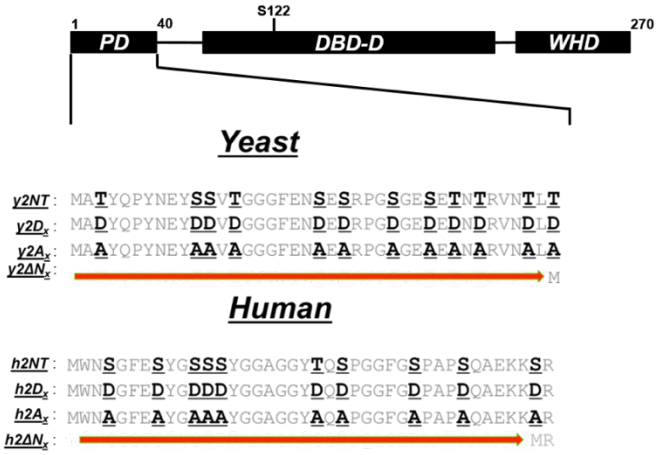

Figure 2.7. Alignment of Rfa2 NT 'extensive' mutations with Rfa2-h2 NT 'extensive' mutations.
A schematic of Rfa2 depicting the region of the Rfa2 NT that was mutated in each strain (top panel) and an alignment of the residues changed in each respective mutation (bottom panel). Sequence schematics are a zoom-in of the Rfa2/Rpa2 phosphorylation domain (PD). S/T indicates serines or threonines within the PD. A or D substitutions below indicate alanine or aspartate mutations, respectively.

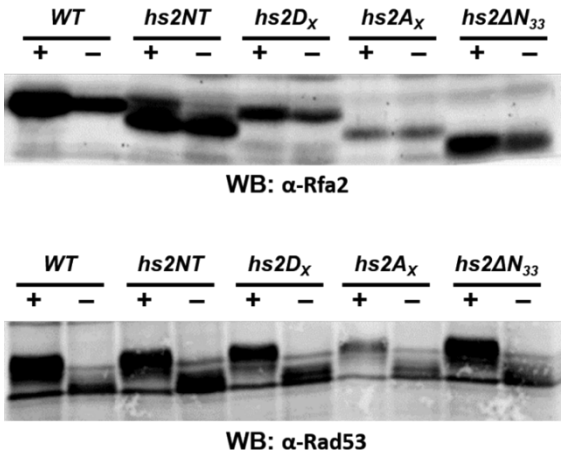

Figure 2.8. Additional phosphorylation of Rfa2-h2 NT mutations is not observed in 'extensive' NT mutations.
Top Panel: Rfa2 phosphorylation is only observed in *rfa2-h2NT* extensive mutation, whereas *rfa2-h2D$_X$, rfa2-h2A$_X$,* and *rfa2-h2ΔN$_{33}$* produce biochemical phenotypes in-line with that observed for the Rfa2 NT extensive variants (Figure 2.14), suggesting phosphorylation occurs on the NT of Rfa2-h2NT. Bottom Panel: Rad53 phosphorylation in response to PHL treatment occurs indistinguishably from WT cells in each of the *rfa2-h2* NT extensive mutations, indicating NT extensive mutations do not impair checkpoint activation in budding yeast.

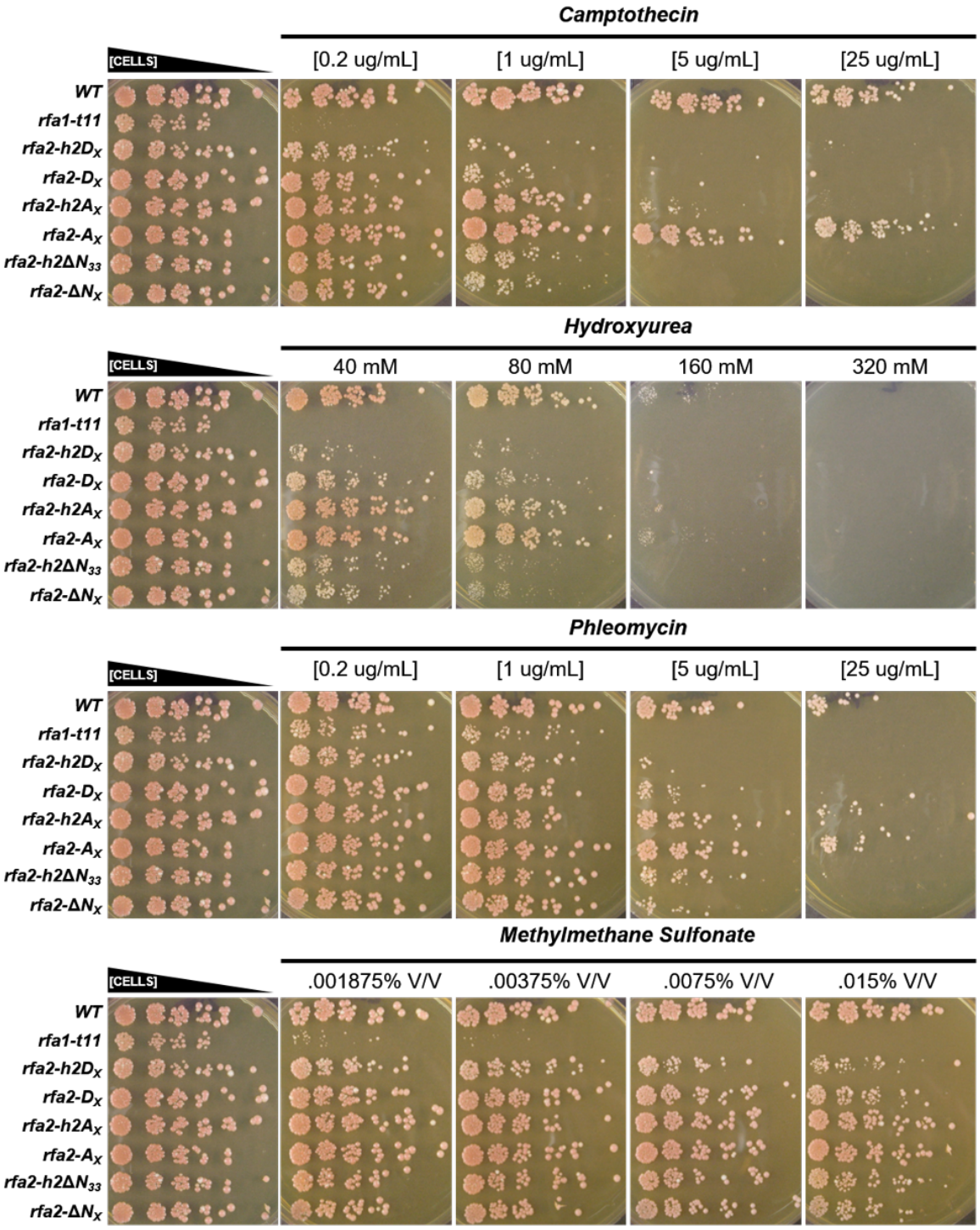

Figure 2.9. Rfa2-h2 NT mutations produce phenotypes in line with Rfa2 NT extensive mutations. Six 10-fold serial dilutions of cells containing extensive Rfa2 NT mutations were plated on YPD media or YPD media containing genotoxic agents at various concentrations against *rfa2-h2* NT extensive mutations to assess their phenotype. Each *rfa2-h2* NT extensive mutation recapitulates the phenotype of its yeast Rfa2 NT extensive counterpart. Each D_X and ΔN_X extensive mutation is damage sensitive, whereas *h2NT* or A_X extensive mutations support clastogen resistance in-line with WT Rfa2.

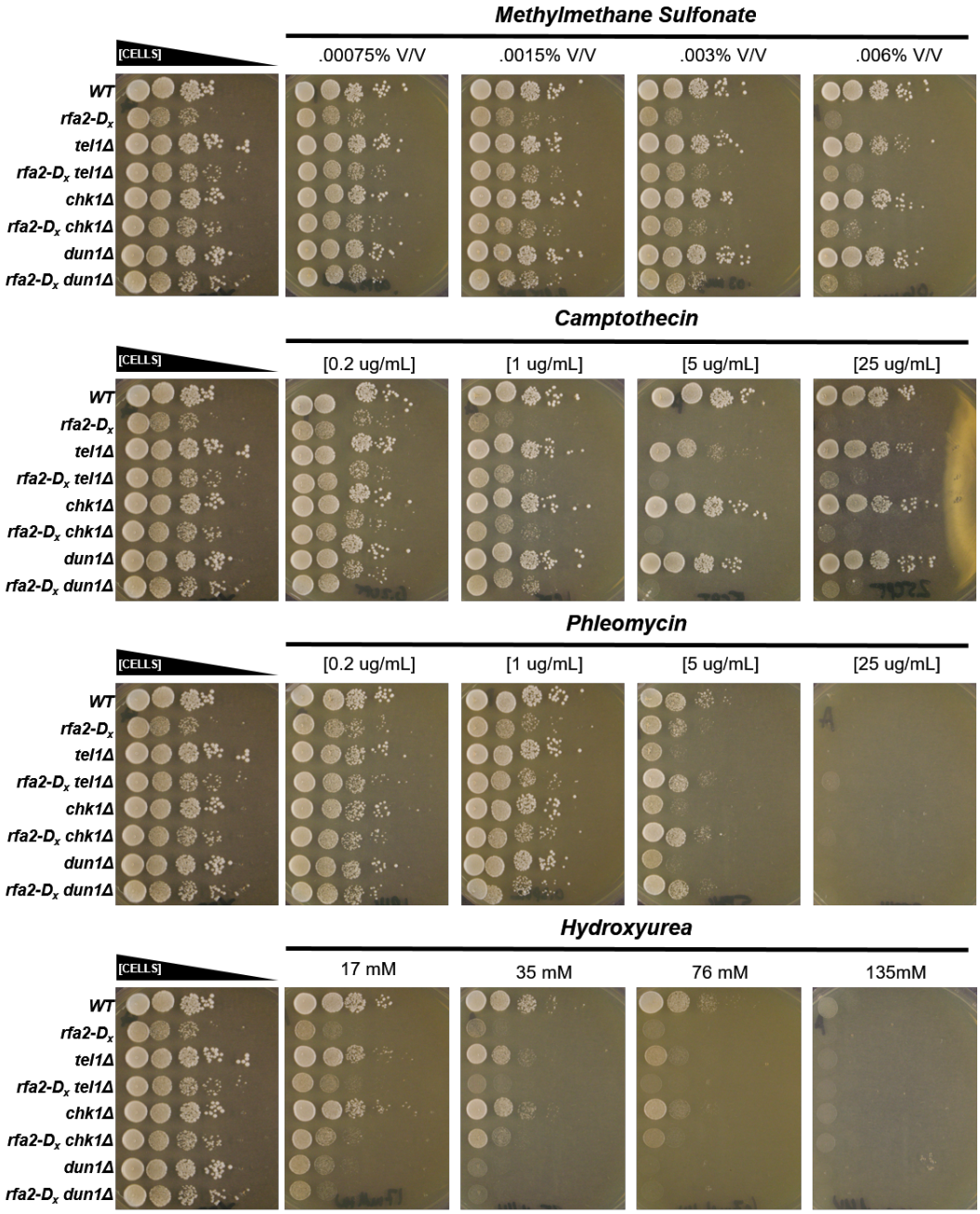

Figure 2.10. Diagnostic spot assay of *tel1*Δ, *chk1*Δ, *dun1*Δ mutants containing the *rfa2-Dx* mutation

JKM179 derivative mutants containing *tel1*Δ, *chk1*Δ, *dun1*Δ mutations and *RFA2* or the *rfa2-Dx* mutation were grown overnight in YPD media. The following day, an OD_{600} reading was taken, and cells six 10-fold serial dilutions were performed, starting at an OD_{600} = 1.0. 200 uL of each dilution was added to a 96-well micro-titer plate and 5 uL of each sample was spotted on YPD media or YPD media containing genotoxic agents at various concentrations. The *rfa2-Dx* mutation leads to an increase in sensitivity to the genotoxic agents MMS, CPT, and HU, but not PHL in each strain analyzed.

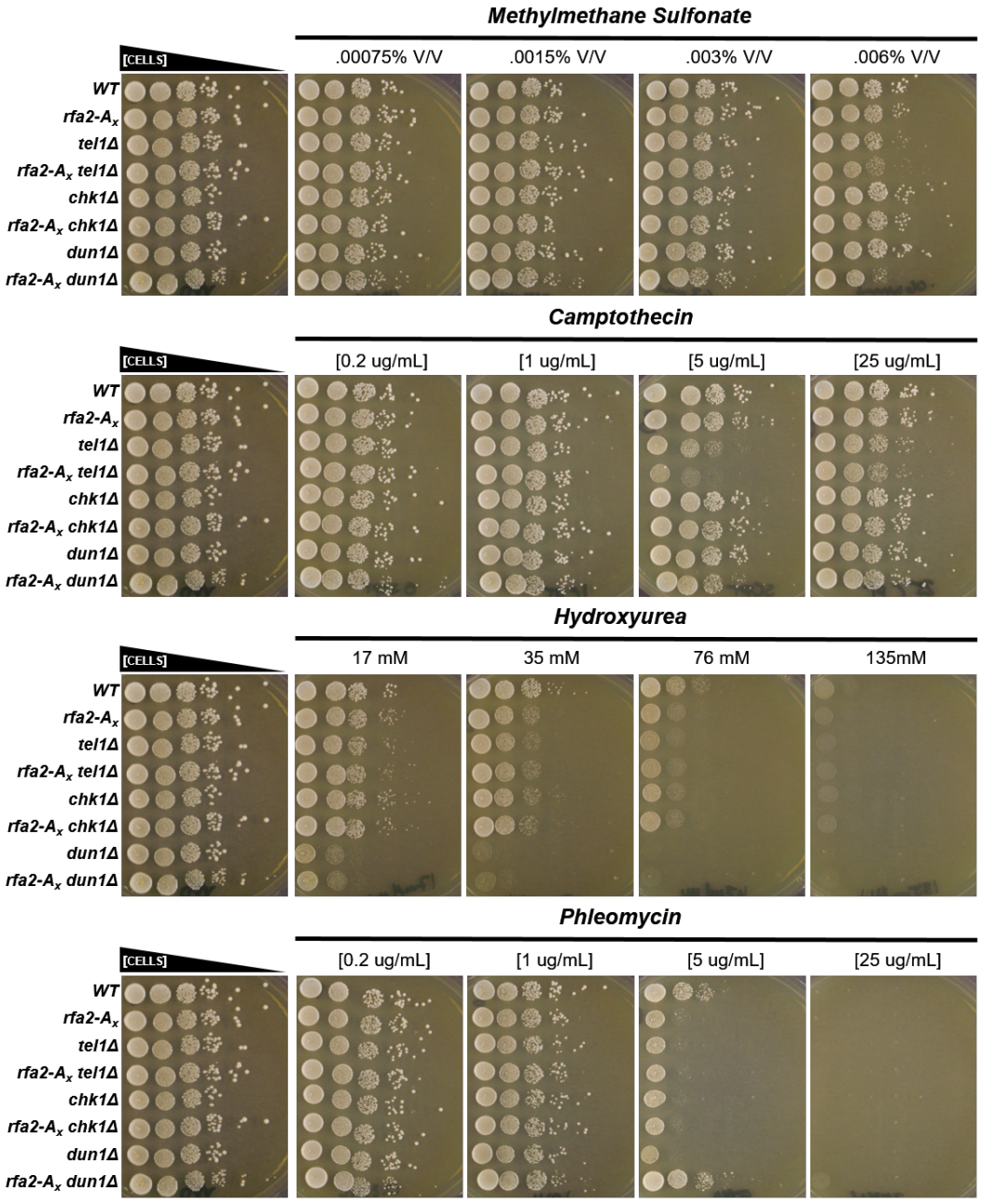

Figure 2.11. Diagnostic spot assay of *tel1*Δ, *chk1*Δ, *dun1*Δ mutants containing the *rfa2-A*$_X$ mutation.
JKM179 derivative strains containing *tel1*Δ, *chk1*Δ, *dun1*Δ mutations and *RFA2* or the *rfa2-A*$_X$ mutation were grown overnight in YPD media. The following day, an OD_{600} reading was taken, and cells six 10-fold serial dilutions were performed, starting at an OD_{600} = 1.0. 200 uL of each dilution was added to a 96-well micro-titer plate and 5 uL of each sample was spotted on YPD media or YPD media containing genotoxic agents at various concentrations. The *rfa2-A*$_X$ mutation supports clastogen resistance in each strain in-line with wild-type Rfa2.

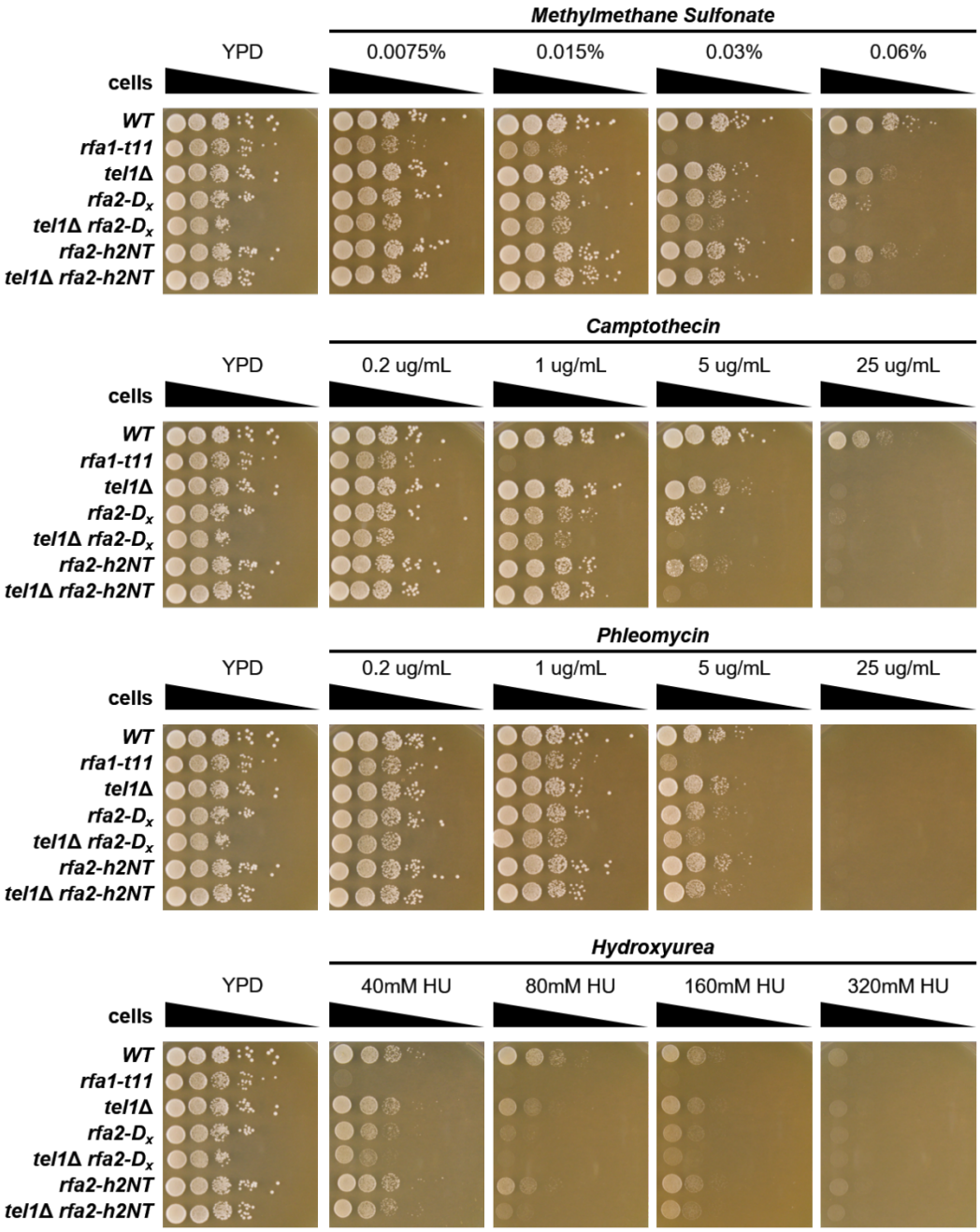

Figure 2.12. Diagnostic spot assay of *tel1*Δ mutations (*rfa2-Dx* and *rfa2-h2NT*).
*tel1*Δ Rfa2 NT mutations were harvested and an OD_{600} for the exponentially growing culture was determined. Starting at an OD_{600} of 1.0, six ten-fold serial dilutions were performed in sterile filtered water. 200 uL of the diluted culture was added to a 96-well microtiter plate and 5 uL of the dilution was then spotted onto the YPD plates and YPD plates containing genotoxic agents at indicated concentrations using a multi-channel pipetman. *tel1*Δ mutant cells containing the *rfa2-Dx* or *rfa2-h2NT* mutations are hypersensitive to genotoxic agents.

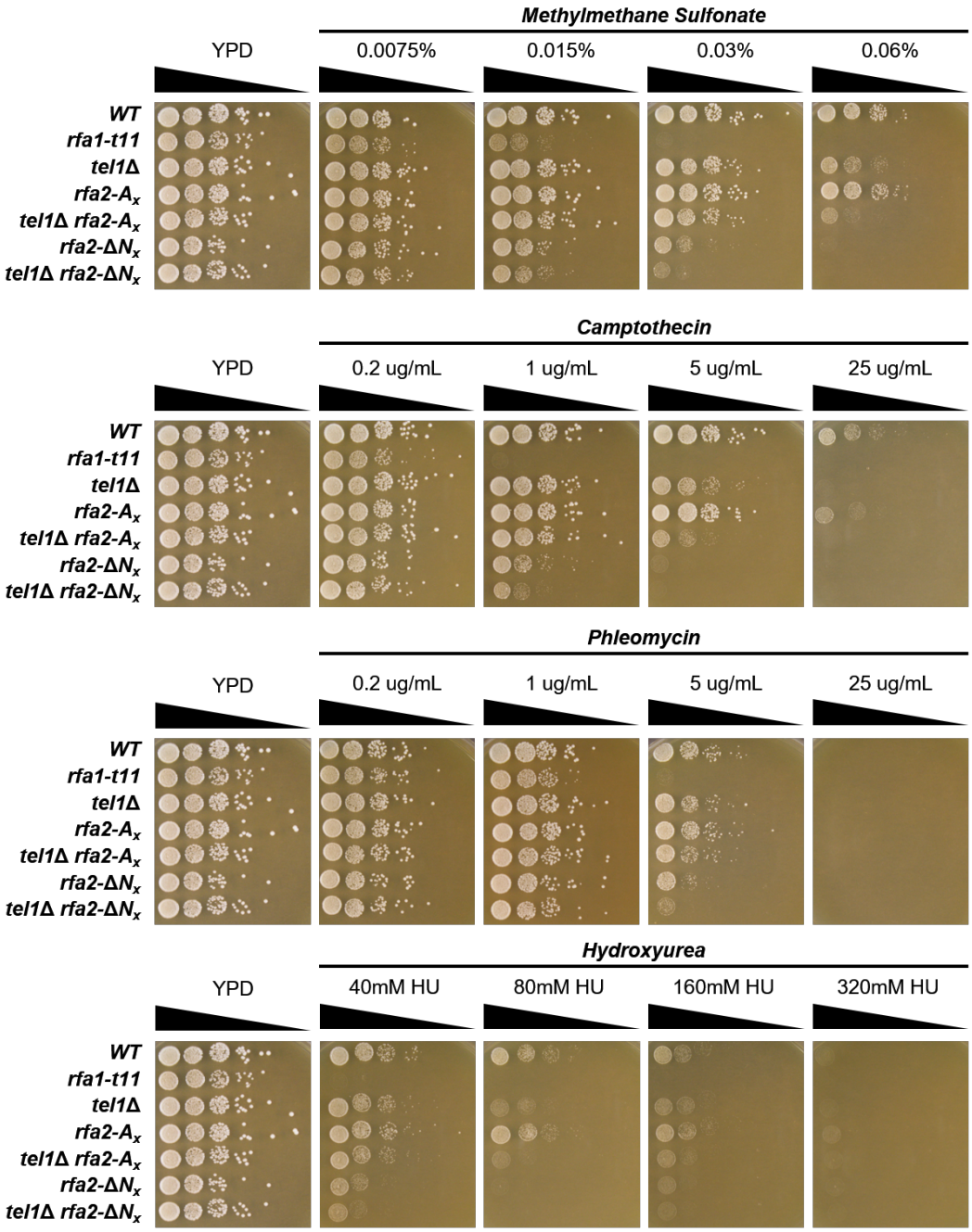

Figure 2.13. Diagnostic spot assay of *tel1*Δ mutations (*rfa2-A*$_X$ and *rfa2-*Δ*N*$_X$).
*tel1*Δ Rfa2 NT mutations were harvested and an OD_{600} for the exponentially growing culture was determined. Starting at an OD_{600} of 1.0, six ten-fold serial dilutions were performed in sterile filtered water. 200 uL of the diluted culture was added to a 96-well microtiter plate and 5 uL of the dilution was then spotted onto the YPD plates and YPD plates containing genotoxic agents at indicated concentrations using a multi-channel pipetman. *tel1*Δ mutant cells containing the *rfa2-A*$_X$ support clastogen resistance in-line with wild-type Rfa2. *tel1*Δ mutant cells containing the *rfa2-*Δ*N*$_X$ mutation are hypersensitive to genotoxic agents.

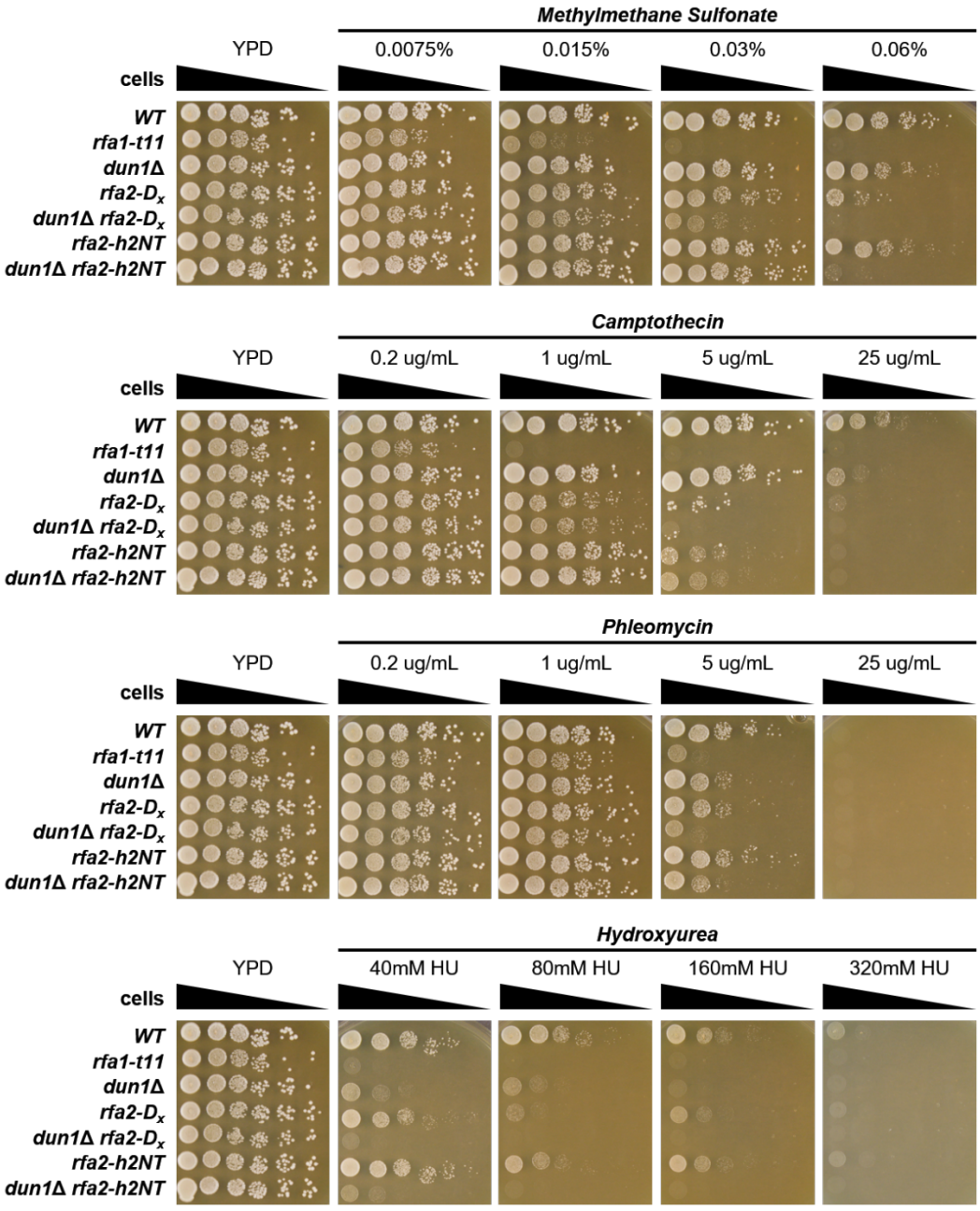

Figure 2.14. Diagnostic spot assay of *dun1*Δ Rfa2 NT extensive mutations (*rfa2-D*$_X$ and *rfa2-h2NT*). *dun1*Δ Rfa2 NT extensive mutations were harvested and an OD_{600} for the exponentially growing culture was determined. Starting at an OD_{600} of 1.0, six ten-fold serial dilutions were performed in sterile filtered water. 200 uL of the diluted culture was added to a 96-well microtiter plate and 5 uL of the dilution was then spotted onto the plates using a multi-channel pipetman. *dun1*Δ mutant cells containing the *rfa2-D*$_X$ mutation are hyper-sensitive to genotoxic agents, whereas the Rfa2-h2NT mutant appears to support genotoxic resistance in line with WT Rfa2.

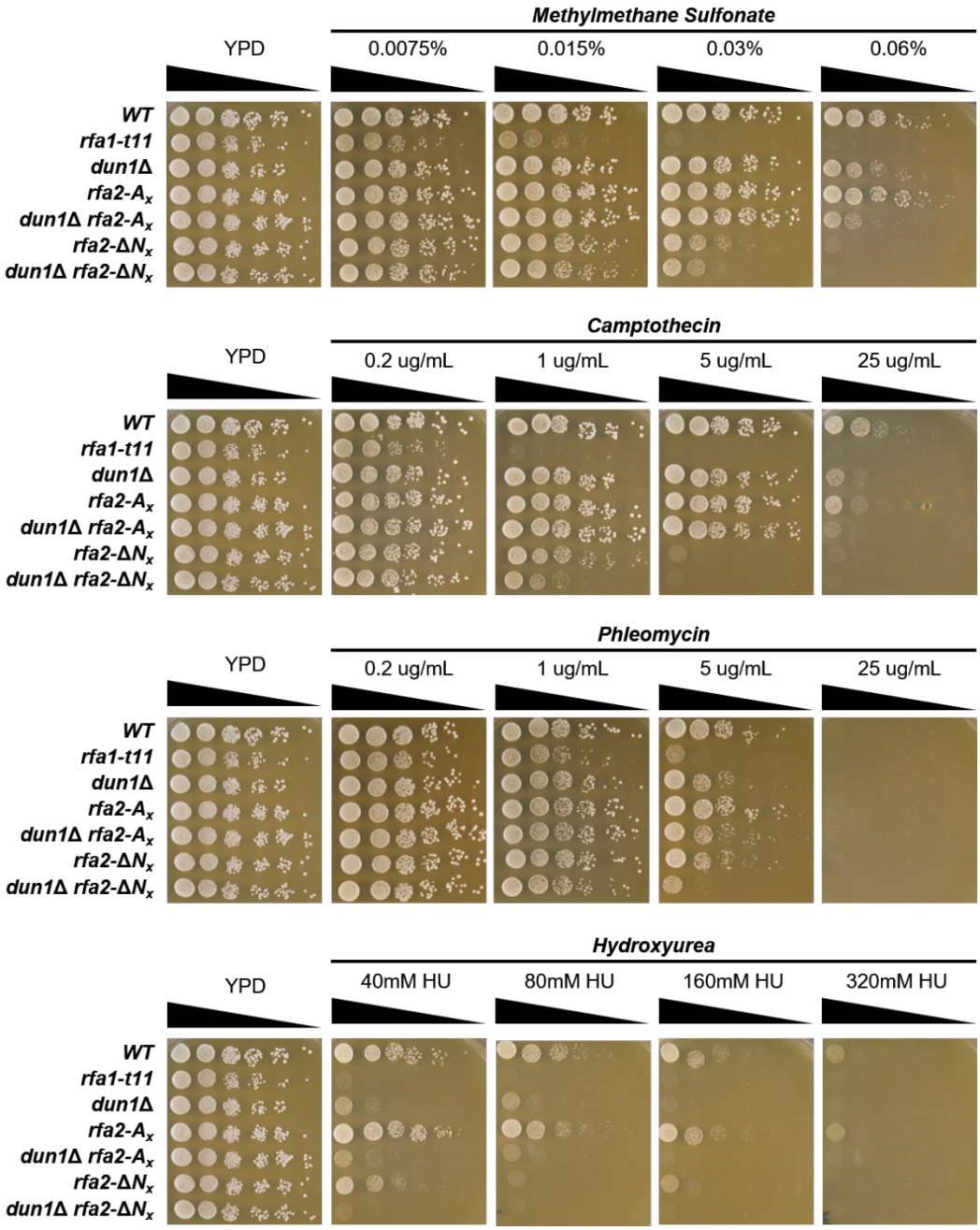

Figure 2.15. Diagnostic spot assay of *dun1*Δ Rfa2 NT extensive mutations (*rfa2-A*$_X$ and *rfa2-*Δ*N*$_X$). *dun1*Δ Rfa2 NT extensive mutations were harvested and an OD_{600} for the exponentially growing culture was determined. Starting at an OD_{600} of 1.0, six ten-fold serial dilutions were performed in sterile filtered water. 200 uL of the diluted culture was added to a 96-well microtiter plate and 5 uL of the dilution was then spotted onto the plates using a multi-channel pipetman. *dun1*Δ mutant cells containing the *rfa2-A*$_X$ mutation are no more sensitive to genotoxic agents than *dun1*Δ mutants containing Rfa2, whereas the *rfa2-*Δ*N*$_X$ mutation leads to hyper-sensitivity to genotoxic agents.

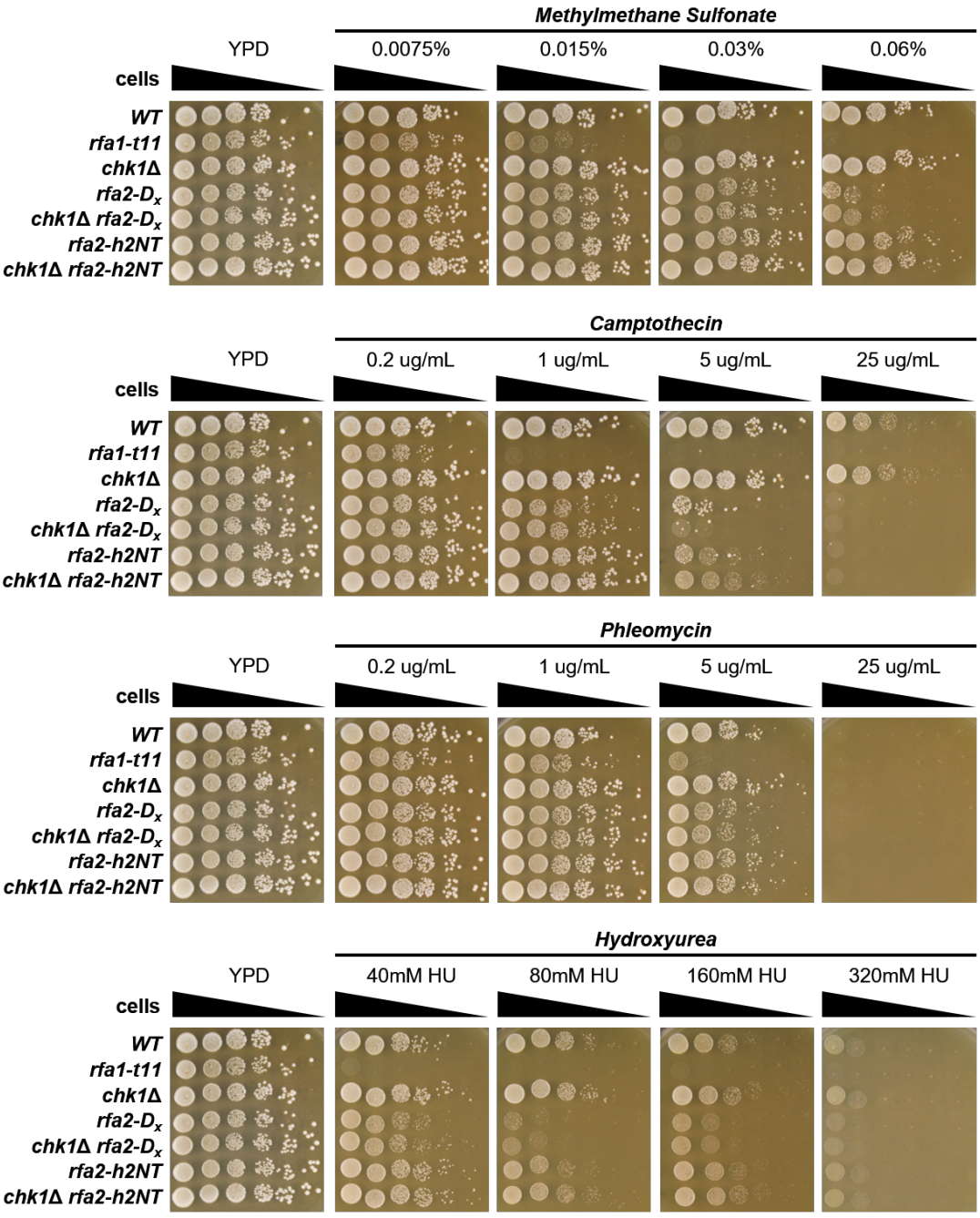

Figure 2.16. Diagnostic spot assay of *chk1*Δ Rfa2 NT extensive mutations (*rfa2-Dx* and *rfa2-h2NT*). *chk1*Δ Rfa2 NT extensive mutations were harvested and an OD_{600} for the exponentially growing culture was determined. Starting at an OD_{600} of 1.0, six ten-fold serial dilutions were performed in sterile filtered water. 200 uL of the diluted culture was added to a 96-well microtiter plate and 5 uL of the dilution was then spotted onto the plates using a multi-channel pipetman. *chk1*Δ mutant cells containing the *rfa2-Dx* mutation are hyper-sensitive to genotoxic agents, whereas the Rfa2-h2NT mutant supports genotoxic resistance in line with WT Rfa2.

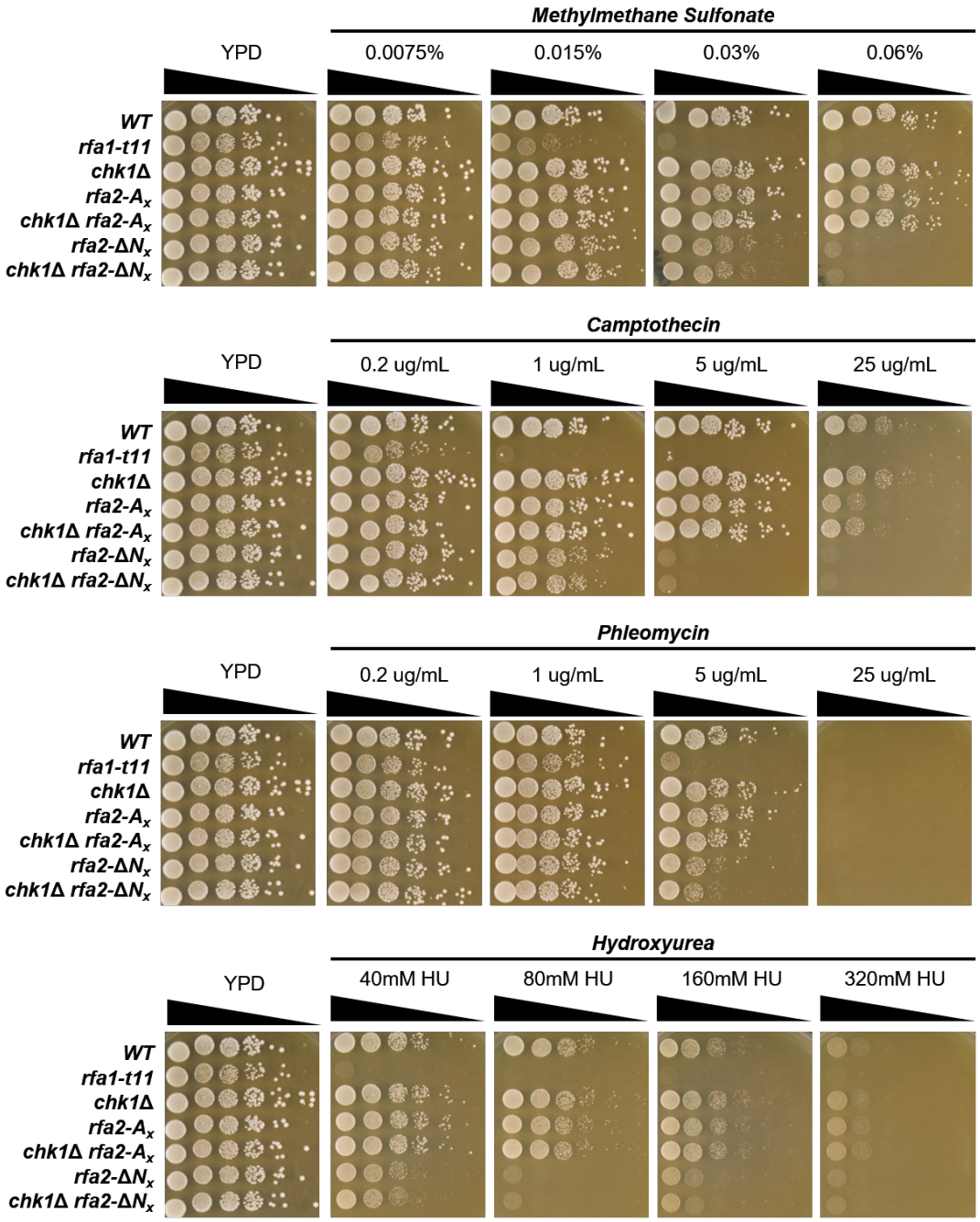

Figure 2.17. Diagnostic spot assay of *chk1*Δ Rfa2 NT extensive mutations (*rfa2-A*$_X$ and *rfa2-*Δ*N*$_X$). *chk1*Δ Rfa2 NT extensive mutations were harvested and an OD_{600} for the exponentially growing culture was determined. Starting at an OD_{600} of 1.0, six ten-fold serial dilutions were performed in sterile filtered water. 200 uL of the diluted culture was added to a 96-well microtiter plate and 5 uL of the dilution was then spotted onto the plates using a multi-channel pipetman. *chk1*Δ mutant cells containing the *rfa2-A*$_X$ mutation are no more sensitive to genotoxic agents than *chk1*Δ mutants containing Rfa2, whereas the *rfa2-*Δ*N*$_X$ mutation leads to hyper-sensitivity to genotoxic agent

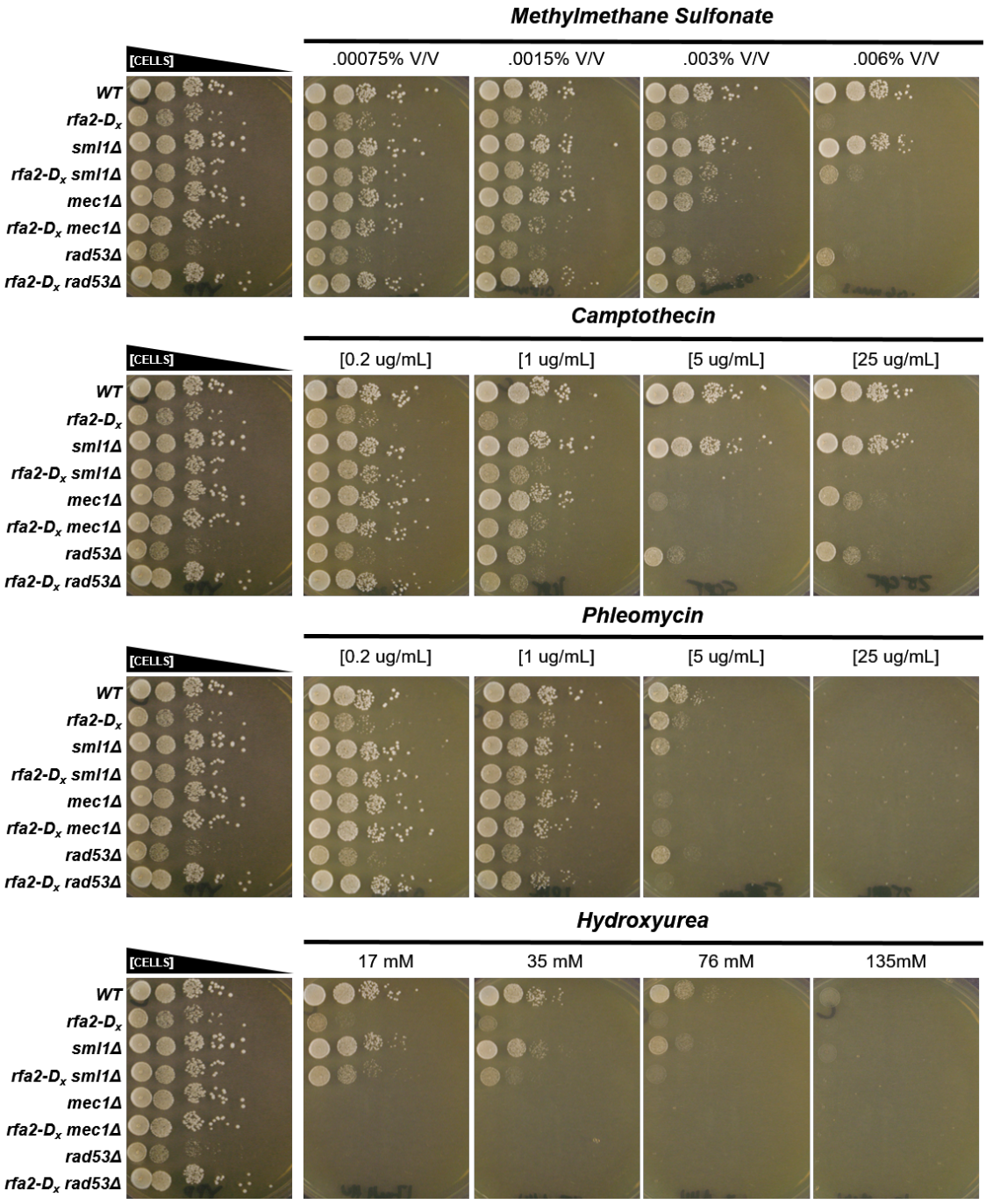

Figure 2.18. Diagnostic spot assay of *sml1*Δ, *mec1*Δ, *rad53*Δ mutants containing the *rfa2-Dx* mutation.
JKM179 derivative strains containing *sml1*Δ, *mec1*Δ, *rad53*Δ mutations and *RFA2* or the *rfa2-Dx* mutation were grown overnight in YPD media. The following day, an OD_{600} reading was taken, and cells six 10-fold serial dilutions were performed, starting at an OD_{600} = 1.0. 200 uL of each dilution was added to a 96-well micro-titer plate and 5 uL of each sample was spotted on YPD media or YPD media containing genotoxic agents at various concentrations. The *rfa2-Dx* mutation leads to increased sensitivity to genotoxic agents in all strains analyzed. Cells containing *mec1*Δ and *rad53*Δ mutations are hyper-sensitive to genotoxic agents irrespective of the Rfa2 form present.

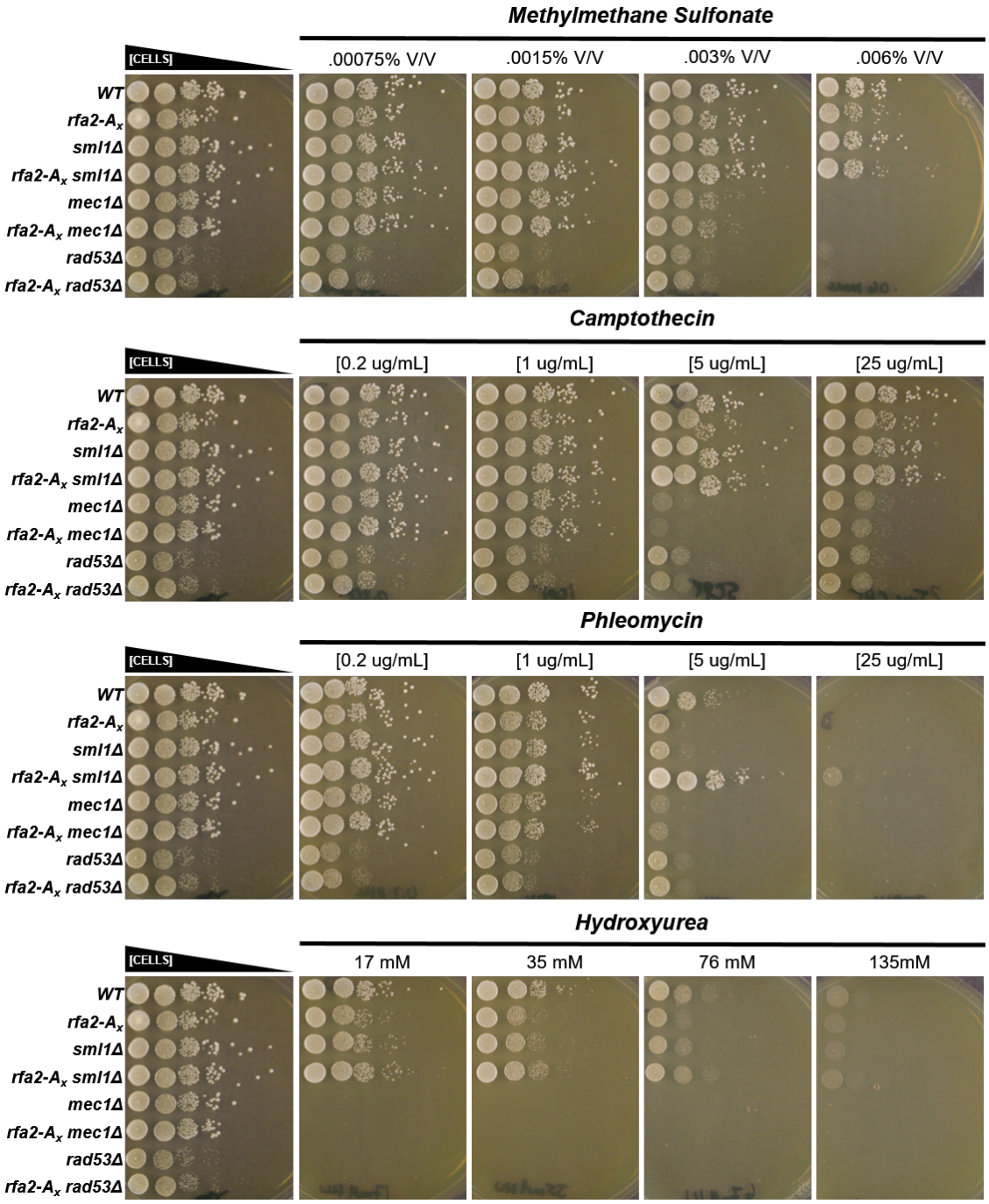

Figure 2.19. Diagnostic spot assay of *sml1*Δ, *mec1*Δ, *rad53*Δ mutants containing the *rfa2-A$_X$* mutation.
JKM179 derivative strains containing *sml1*Δ, *mec1*Δ, *rad53*Δ mutations and *RFA2* or the *rfa2-A$_X$* mutation were grown overnight in YPD media. The following day, an OD_{600} reading was taken, and cells six 10-fold serial dilutions were performed, starting at an OD_{600} = 1.0. 200 uL of each dilution was added to a 96-well micro-titer plate and 5 uL of each sample was spotted on YPD media or YPD media containing genotoxic agents at various concentrations. The *rfa2-A$_X$* mutation supports clastogen resistance in each strain in-line with Rfa2. Cells containing *mec1*Δ and *rad53*Δ mutations are hyper-sensitive to genotoxic agents irrespective of the Rfa2 form present.

2.4.E. Delayed modification observed upon prolonged DNA damage is phosphorylation

The detectable modification of Rfa2 is suggestive of a phosphorylation event. To test this phosphorylation, whole cell lysates obtained from damage-induced cells were subjected to lambda protein phosphatase (λPP) treatment (Figure 2.21). Two types of prolonged damage were examined: phleomycin treatment that induces multiple DSBs throughout the genome and a galactose-inducible HO-endonuclease generates a single, irreparable DSB due to a lack of silent mating loci in the yeast strain NMM104.

Figure 2.21 demonstrates that highest molecular weight species of Rfa2 present in response to global DSB induction is removed by λPP and is present when the λPP inhibitor sodium orthovanadate is added to the reaction. Additionally, generation of a single, persistent DSB is also sufficient to induce Rfa2 phosphorylation by 12 hours, as this higher molecular weight species is observed and subsequently removed by λPP. To ensure that λPP activity was occurring, samples were examined containing Rfa2-h2NT, which is known to be phosphorylated on the NT in response to DSB agents. The slower migrating species in these samples are removed by λPP.

2.4.F. Delayed Rfa2 NT phosphorylation is localized to the NT domain and is not dependent on early S122 phosphorylation

Using Rfa2 'extensive' mutations from previous studies (Figure 2.7), we sought to understand whether the additional, delayed phosphorylation of Rfa2 was occurring within the N-terminal phosphorylation domain. To determine whether the NT is a phospo-target during genotoxic stress, an alanine-scanning approach was used. The unphosphorylatable Rfa2-A_X mutant has all 11 serines/threonines mutated to alanine. In this *rfa2-A$_X$* cells, no detectable modification of the Rfa2 protein is observed via immunoblot (Figure 2.20) in response to prolonged exposure to phleomycin. This demonstrates that serines/threonines within the NT region are necessary for delayed phosphorylation of Rfa2.

It has been demonstrated previously that Rfa2 becomes phosphorylated at serine 122 approximately 2 hours after a DSB has been generated in cells (Bartrand et al. 2004). S122, however, does not appear to play a major role in the DNA damage response as S122 mutations display no discernable phenotype when challenged with a variety of DNA damaging agents (Figure 2.22)

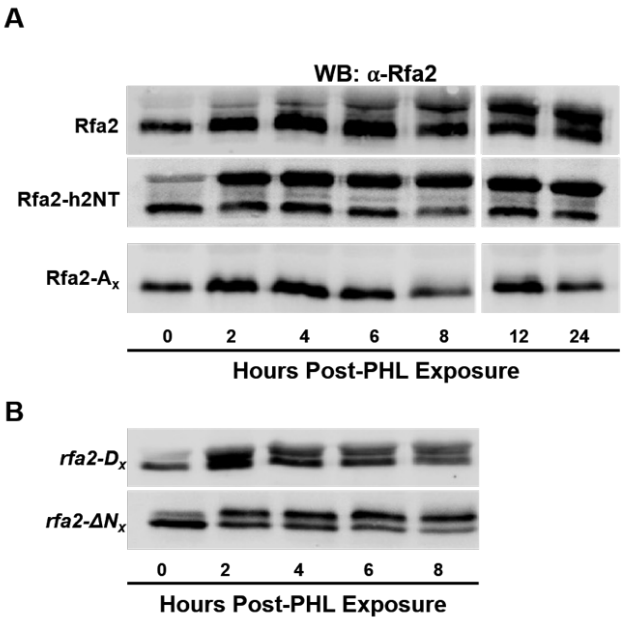

Figure 2.20. Rfa2 NT phosphorylation is detectable in challenged with phleomycin.
A. Immunoprobe using α-Rfa2 antibody. Phospho-modification of Rfa2 is observed in response to PHL treatment starting at approximately 4 hours and becomes maximized by 12 hours. Phosphorylation of *rfa2-h2NT* is observed at 2 hours post-PHL exposure and maintains a similar intensity throughout the observed time course. *rfa2-A*$_X$ does not appear to be modified under the same conditions. **B.** *rfa2-D*$_X$ and *rfa2-*Δ*N*$_X$ are still modified in response to PHL treatment, suggesting phosphorylation occurs outside of the NT phosphorylation domain on these mutant proteins.

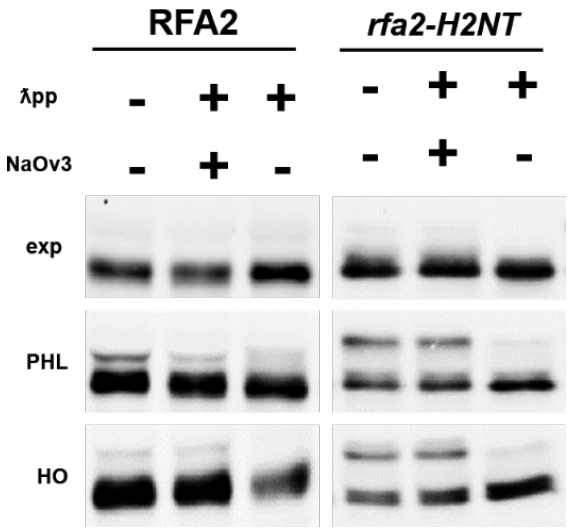

Figure 2.21. Rfa2 NT phosphorylation is removed by lambda protein phosphatase.
Immunoprobe using α-Rfa2 antibody. Modification observed on Rfa2 during PHL treatment or in response to an HO-induced DSB at the *MAT* locus is phosphorylation. Incubation of 40 ug total protein from whole cell lysates with lambda protein phosphatase (λpp) in Buffer A eliminates the observed phospho-shift. This demonstrates that the observed modifications to Rfa2 and Rfa2-h2NT are phosphorylation. Lamda protein phosphatase inhibitor Sodium Orthovanadate (NaOv3) was used as a control for λpp activity. Samples containing λpp retain the observed modification, further indicating that this modification is phosphorylation.

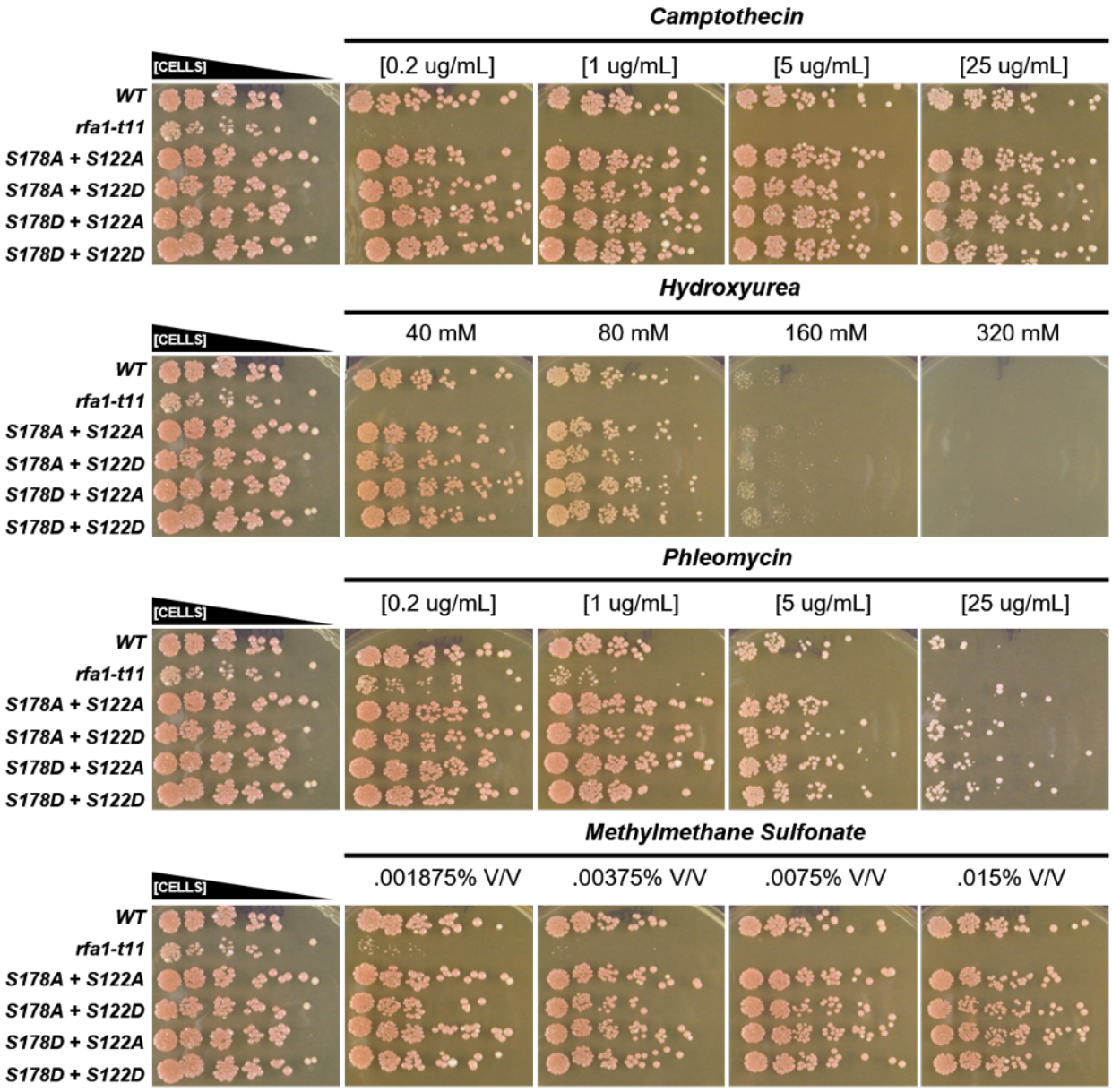

Figure 2.22. Known Mec1-dependent phosphorylation sites have no discernable function in the Lesion and DNA repair program.
Six 10-fold serial dilutions of cells containing combinations of *rfa1-S178*$_{A/D}$ and *rfa2-S122*$_{A/D}$ were plated on YPD media or YPD media containing genotoxic agents at various concentrations. Each combination produces phenotypes in-line with wild-type cells and support genotoxic stress much more effectively than *rfa1-t11*, demonstrating that phosphorylation at Rfa1 on S178 or Rfa2 on S122 appear to be dispensable for the lesion and repair program (LPR).

(Ghospurkar et al. 2015). To determine if S122 regulates the delayed phosphorylation observed within the NT, we employed an aspartic acid/alanine-scanning approach to S122. We hypothesized that if S122 phosphorylation is required for the delayed NT phosphorylation observed, mutating this residue to the phospho-mimetic S122D mutation would cause additional NT phosphorylation, and that mutating it to the

unphosphorylatable S122A mutation would prevent delayed Rfa2 NT phosphorylation. However, delayed phosphorylation of Rfa2 is still observed in both *rfa2-S122D* and *rfa2-S122A* in response to prolonged phleomycin challenge (Figure 2.23A). When compared with Rfa2 from wild-type cells, one of the two observed phospho-species is absent. We presume that the missing phospho-species is due to an inability of S122 to be modified. This demonstrates that the observed delayed Rfa2 NT phosphorylation is still achieved without prior, early modification of S122.

2.4.G. Damage-sensitive Rfa2 NT extensive mutations are prominently phosphorylated at S122

Two additional extensive NT mutations were also examined to characterize Rfa2 phosphorylation. The first being a phospho-mimetic extensive mutation, *rfa2-D$_X$*, was created by mutating all of the serines/threonines to aspartates. The second is an NT deletion mutation in which amino acids 2-38 of the Rfa2 NT are deleted (*rfa2-ΔN$_X$*). Previous studies have demonstrated that *rfa2-D$_X$* or *rfa2-ΔN$_X$* cells exhibit increased sensitivity to DNA damaging agent, but in these cells the mutant Rfa2 proteins are still phosphorylated in response to genotoxic stress (Ghospurkar et al. 2015). However, phosphorylation of these mutant proteins had been observed after MMS treatment for 4 hours (Ghospurkar et al. 2015). Consistent with previous data, early, damage-dependent modification of Rfa2-D$_X$ and Rfa2-ΔN$_X$ is also observed upon treatment with phleomycin (Figure 2.23B and C). Phosphorylation of Rfa2-D$_X$ and Rfa2-ΔN$_X$ is minimally observed in untreated, exponentially growing cells – a result that is consistent with the fact that these NT mutations harbor a cellular growth defect, even when unchallenged by genotoxic stress (Ghospurkar *et al.* 2015). Similar to that observed for Rfa2-h2NT, Rfa2-D$_X$ and Rfa2-ΔN$_X$ show maximal phosphorylation between 2-4 hours. We propose that the phosphorylation observed on Rfa2-D$_X$ and Rfa2-ΔN$_X$ is occurring at S122. S122 has been demonstrated to be a Mec1 target site of SQ/TQ consensus on Rfa2 that becomes phosphorylated in response to DNA damage and mitotic growth (Brush *et al.* 1996). Because all the serines/threonines within the NT have been mutated to aspartic acids or removed entirely in these mutations, the observed phosphorylation of *rfa2-D$_X$* and *rfa2-ΔN$_X$*, therefore, cannot be occurring within the NT domain.

Although we observe phosphorylation in *rfa2-D$_X$* and *rfa2-ΔN$_X$* cells, the ratio of phosphorylated Rfa2 to unmodified Rfa2 appears to differ between the two mutations, especially after 8 hours. In particular, the ratio of phosphorylated to unphosphorylated Rfa2 is much greater in the *rfa2-ΔN$_X$* mutation

than in the *rfa2-D$_X$* mutation. This is perhaps unsurprising as it has been demonstrated that these two mutations, despite both being sensitive to DNA damage, demonstrate different synthetic genetic interactions and ability to exit a checkpoint in response to persistent DNA damage (Ghospurkar *et al.* 2015). To determine if S122 is the site being modified on these mutations, we mutated S122 to S122D or S122A. Independent of whether S122 is in the phospho-mimetic or unphosphorylatable state, no observable damage-dependent phosphorylation of Rfa2 is detected.

2.4.H. Rfa2 NT mutations display differential effects on Mec1 activity

Although both Mec1 and Tel1 have been shown to phosphorylate Rfa2, Mec1 is the primary kinase demonstrated to target Rfa2 at serine 122 in response to both mitotic and meiotic DNA damage (Brush *et al.* 1996, Brush *et al.* 2001, Clifford *et al.* 2004, Bartrand *et al.* 2006). In this study, we observed S122 phosphorylation in the Rfa2 NT mutations *rfa2-D$_X$* and *rfa2-*Δ*N$_X$*, in response to phleomycin-induced DSBs. To characterize whether Mec1 or Tel1 activity is differentially affected by the phospho-state of the Rfa2 NT, we examined Rfa2 S122 phosphorylation in *rfa2 mec1*Δ *sml1*Δ or *rfa2 tel1*Δ double mutations in response to phleomycin induced DSBs. Specifically, we focused on the *rfa2-D$_X$* and *rfa2-*Δ*N$_X$* mutants.

We suspected that if Mec1 or Tel1 kinase activity is dependent on the phospho-state of the Rfa2 NT, then eliminating either of these kinases, or the physical presence of the Rfa2 NT, would reduce the appearance of S122 phospho-species. Immunoblots of Rfa2-D$_X$ and Rfa2-ΔN$_X$ in *mec1*Δ or *tel1*Δ indicated that phosphorylation efficiency of S122 is affected differentially. Cells containing *mec1*Δ were able to phosphorylate Rfa2-D$_X$ or Rfa2-ΔN$_X$, in response to phleomycin challenge, indistinguishably from *MEC1* cells. Cells containing *tel1*Δ were able to readily phosphorylate *rfa2-*Δ*N$_X$* indistinguishably from *MEC1/TEL1* cells but were unable to phosphorylate Rfa2-D$_X$ to the same level observed in wild-type cells (Figure 2.24). In *tel1*Δ cells, Mec1 is still active and this may explain why phosphorylation is still observed on *rfa2-*Δ*N$_X$*. The observation that *rfa2-D$_X$* is not readily phosphorylated in *tel1*Δ indicates that the phospho-state of the Rfa2 NT may regulate Mec1 activity at DSBs. *rfa2-D$_X$* has been previously demonstrated to promote checkpoint exit in response to a persistent DSB, and it is possible that this phenomenon is a direct result of a hyper-phosphorylated Rfa2 NT attenuating Mec1 activity at DSB sites.

2.4.I. Examination of Rfa2 phosphorylation in DNA damage response kinases deletions

Previous data has suggested a role for Mec1/Ddc2 and Tel1 in phosphorylation of Rfa2 in response to DNA damage. In an effort to further elucidate what kinases might be acting upon Rfa2, we deleted *TEL1*, *CHK1*, and *DUN1* individually and assayed the Rfa2 phospho-state upon 2 different types of clastogen challenge (Figure 2.19). To reduce potential discrepancy between S122 phosphorylation and NT phosphorylation, 12% (150:1 mono:bis) acrylamide gels were used that allow the S122 phospho-species to run with the same mobility as unphopshorylated Rfa2. Phosphorylation of Rfa2 in response to global DSBs induced by phleomycin appears to produce only one observable phospho-species, whereas a single DSB induced by HO-endonuclease appears to produce two distinct phospho-species. Together, these results demonstrate that phosphorylation of the Rfa2 NT occurs in response to DSBs in yeast.

2.4.J. Rfa2 NT phosphorylation is observed under various genotoxic conditions

Rfa2 N-terminal phosphorylation does not readily occur in response to genotoxic challenge within a previously analyzed 4-hour exposure to genotoxic agents (Ghospurkar *et al.* 2015). We sought to assay whether Rfa2 hyper-phosphorylation would occur in response to prolonged genotoxic stress or in a dose-dependent fashion, as had been previously reported, with genotoxic agents (MMS, PHL, and CPT). Each genotoxic agent used leads to the generation of ssDNA intermediates that RFA would be required to bind and protect. In WT cells, Rfa2 hyper phosphorylation is observed roughly 4-8 hours after clastogen exposure, specifically when cells are exposed to phleomycin (Figure 2.26 and 2.27), and to a lesser extent when cells are exposed to methyl methanesulfonate (MMS) or camptothecin (CPT). This phosphorylation appears to increase in a dose-dependent manner, as increasing the concentration of DNA damaging agent used lead to an increase in observed Rfa2 phosphorylation (Figure 2.27) Cells expressing the Rfa2-h2NT fusion protein challenged under the same genotoxic conditions yield hyper-phosphorylated Rfa2-h2NT. Maximal phosphorylation of Rfa2-h2NT is observed by 4-8 hours in nearly every condition, likely due to the appearance of SQ/TQ consensus phospho-target sites within the NT.

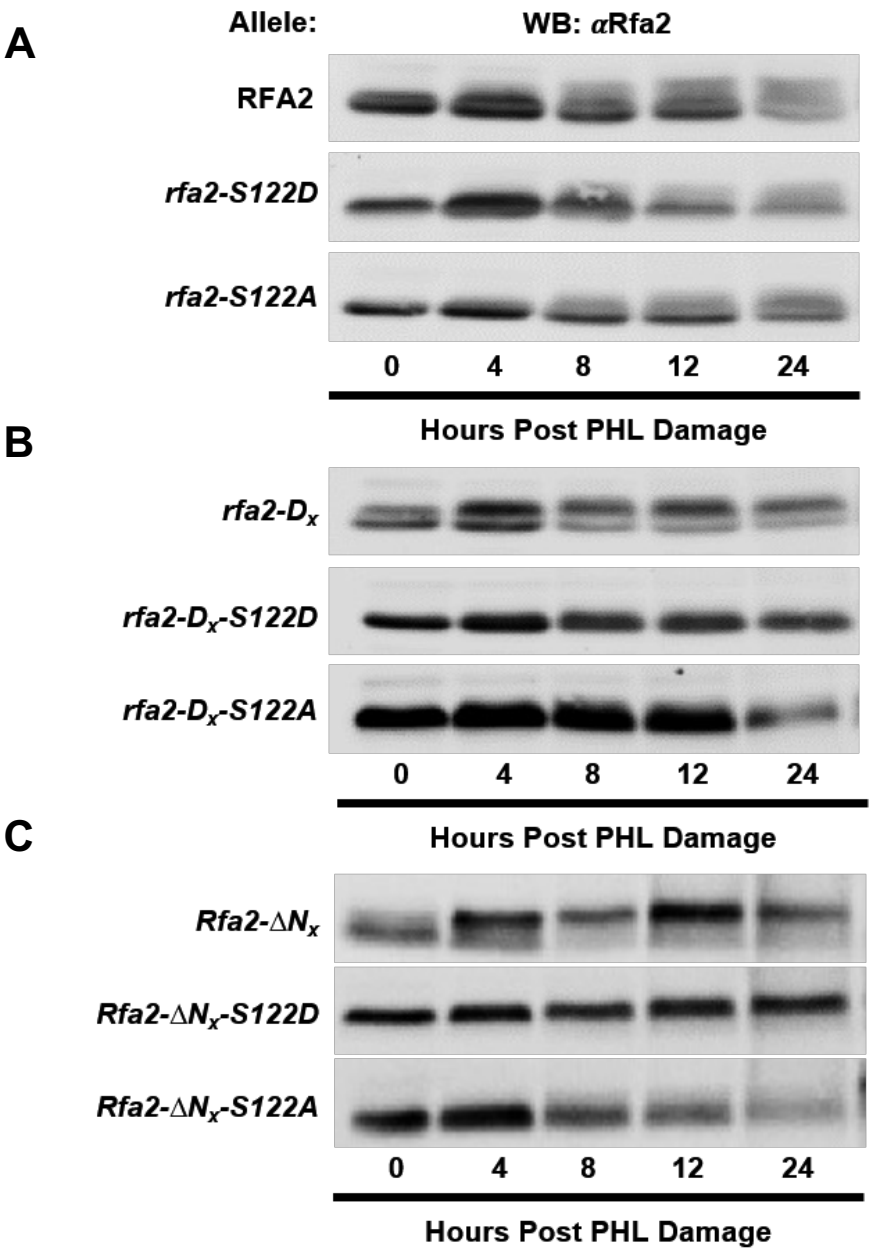

Figure 2.23. Rfa2 phosphorylation is not detected in Rfa2 NT extensive mutations containing S122$_{A/D}$.
A. Immunoprobe using α-Rfa2 antibody. 10 ug total protein from whole cell lysates was used for immunoblotting. Early phosphorylation of Rfa2 is observed by 4 hours, with an additional, late phospho-shift occurring by 8 hours. Rfa2 phosphorylation occurs in response to PHL treatment in *rfa2-S122$_{A/D}$* mutations. The additional, late phospho-shift observed on Rfa2 is eliminated in Rfa2-S122D or Rfa2-S122A, but each mutant protein is still detectably phosphorylated. **B.** The additional phospho-shift observed in *rfa2-S122$_{A/D}$* mutations is eliminated when the Rfa2 NT is mutated to *rfa2-D$_X$*. The additional phospho-shift observed in *rfa2-D$_X$* occurs at S122 and is eliminated when S122 is mutated indicating that S122 is the early phosphorylation event that occurs in cells. **C.** *rfa2-ΔN$_X$,* similar to *rfa2-D$_X$,* is phosphorylated at S122 in response to PHL treatment, and this additional phospho-shift is eliminated when S122 is mutated.

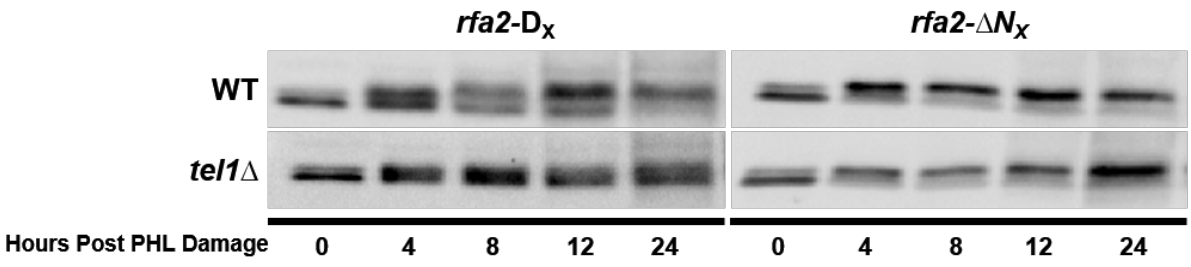

Figure 2.24. Rfa2-D$_X$ phosphorylation at S122 is impeded in *tel1*Δ.
Immunoprobe using α-Rfa2 antibody and 10 ug total protein from whole cell lysates. Phospho-mimetic *rfa2-D$_X$* is phosphorylated in response to PHL treatment in WT cells indistinguishably from *rfa2-*Δ*N$_X$*. Phosphorylation at S122 appears to be impaired in cells containing *tel1*Δ *rfa2-D$_X$* when compared to *rfa2-*Δ*N$_X$*, where a greater majority of the *rfa2* isolated appears to be phospho-shifted, suggesting that Mec1 activity is impaired in *rfa2-D$_X$* cells.

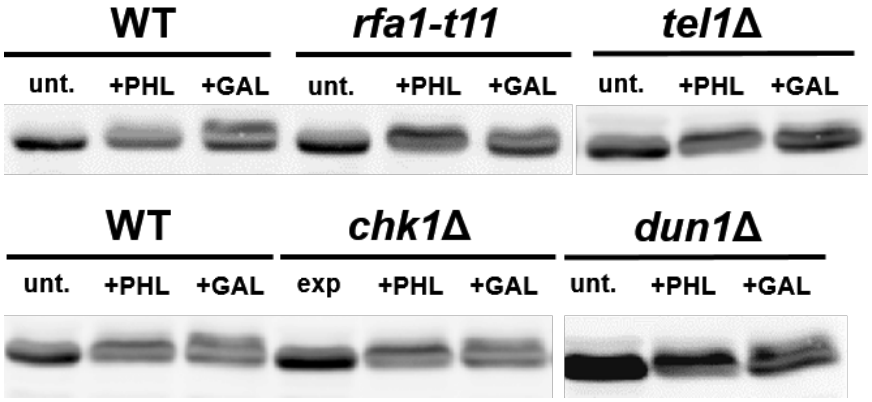

Figure 2.25. Rfa2 NT phosphorylation occurs independent of Tel1, Chk1, and Dun1.
Immunoprobe using α-Rfa2 antibody and 10 ug total protein from whole cell lysates. Cells were grown to an OD_{600} of 1.0 and global genotoxic stress was induced using phleomycin. A single DSB was stimulated by adding galactose to a final concentration of 2% to induce HO-endonuclease expression. Phleomycin induced damage produces two distinct bands, whereas a single DSB created by HO-endonuclease leads to the formation of three distinct phospho-species. This demonstrates that phosphorylation of the Rfa2 NT occurs in response to global DSBs, but more extensively in response to a single irreparable lesion. Phosphorylation of Rfa2 in *tel1*Δ*, chk1*Δ, and *dun1*Δ mutations occurs indistinguishably from WT cells. Immunoblots were produced from 12% (150:1 mono:bis) acrylamide gels that allow the observed early phosphorylation of S122 to run with unmodified Rfa2, allowing for more focused analysis of Rfa2 phospho-species generated during genotoxic stress.

2.4.K. Rfa2 NT phosphorylation is readily detectable in an *rfa1-t11* mutation

Central to RFA complex function is RFA1 DBD-F's ability to load the 9-1-1 Clamp loader complex (Rad24-RFC2-5 in yeast) to the 5' proximal junction, as well as facilitate loading of the 9-1-1 clamp (Rad17-Mec3-Ddc1) by stabilizing the clamp loader-5' junction interaction (Kumagai *et al.* 2006, Delacroix *et al.* 2007, Lee *et al.* 2007, Mordes *et al.* 2008, Navadgi-Patil *et al.* 2008, Puddu *et al.* 2008, Lee *et al.* 2010, Liu *et al.* 2011). These protein interactions are thought to be mediated via the N-terminus of Rfa1, known as DBD-F, and previous research has demonstrated that many DDR-specific protein interactions

which are dependent on the physical presence of a functional DBD-F within Rfa1. A point mutation of Rfa1, known as *rfa1-t11* (K45E), is known to ablate several of these protein interactions, leading to defective checkpoint signaling and severe genotoxic sensitivity (Zou *et al.* 2003, Zou *et al.* 2003, Lucca *et al.* 2004, Majka *et al.* 2006). Furthermore, *rfa1-t11* has been demonstrated to promote checkpoint exit in the presence of a persistent DNA lesion (Lee et al. 2001), similar to that observed for *rfa2-D$_X$* (Ghospurkar et al. 2015). We postulated that if DBD-F of Rfa1 was essential for Rfa2 NT phosphorylation that Rfa2 would not become phosphorylated in *rfa1-t11* mutations. Figures 2.25, 2.26 and 2.27 demonstrate that Rfa2 phosphorylation is not reduced in *rfa1-t11* mutations, suggesting that the delayed phosphorylation event observed on Rfa2 is not dependent on protein-protein interactions driven through the NT of Rfa1. Moreover, since *rfa2-D$_X$* and *rfa1-t11* promote checkpoint adaptation, and phosphorylation of Rfa2 is still observed in *rfa1-t11* mutants, it is conceivable that phosphorylation of the Rfa2 NT may be the direct cause of checkpoint adaptation in *rfa1-t11* mutants in response to prolonged genotoxic stress.

2.5. Discussion

The RPA complex is indispensable for all DNA metabolic processes due to its function in binding to single-stranded DNA (ssDNA) with nanomolar affinity, allowing RPA to act as a sensor of non-duplex DNA intermediates, and providing an essential role in the regulation of DNA damage-dependent checkpoint function. Coordinately, the amino-terminus (NT) of Rpa2 is hyper-phosphorylated by checkpoint kinases in response to lesions in DNA. However, the function post-translational phosphorylation of Rpa2 plays in cells remains elusive. Moreover, the long-term, generational consequences of Rpa2 in human cells are limited as expression and knockdown studies only produce phenotypes that can be observed transiently. It is clear that Rpa2 NT phosphorylation plays a critical role in mediating particular aspects of checkpoint signaling, namely delayed replication restart and checkpoint establishment and maintenance.

2.5.A. Rfa2 is phosphorylated via two temporally distinct mechanisms

In this study, examination of post-translational phosphorylation of Rfa2 in *Saccharomyces cerevisiae* revealed that there are two distinct phosphorylation events that Rfa2 experiences in response to the generation of DNA lesions. First, upon the generation of ssDNA intermediates Rfa2 becomes

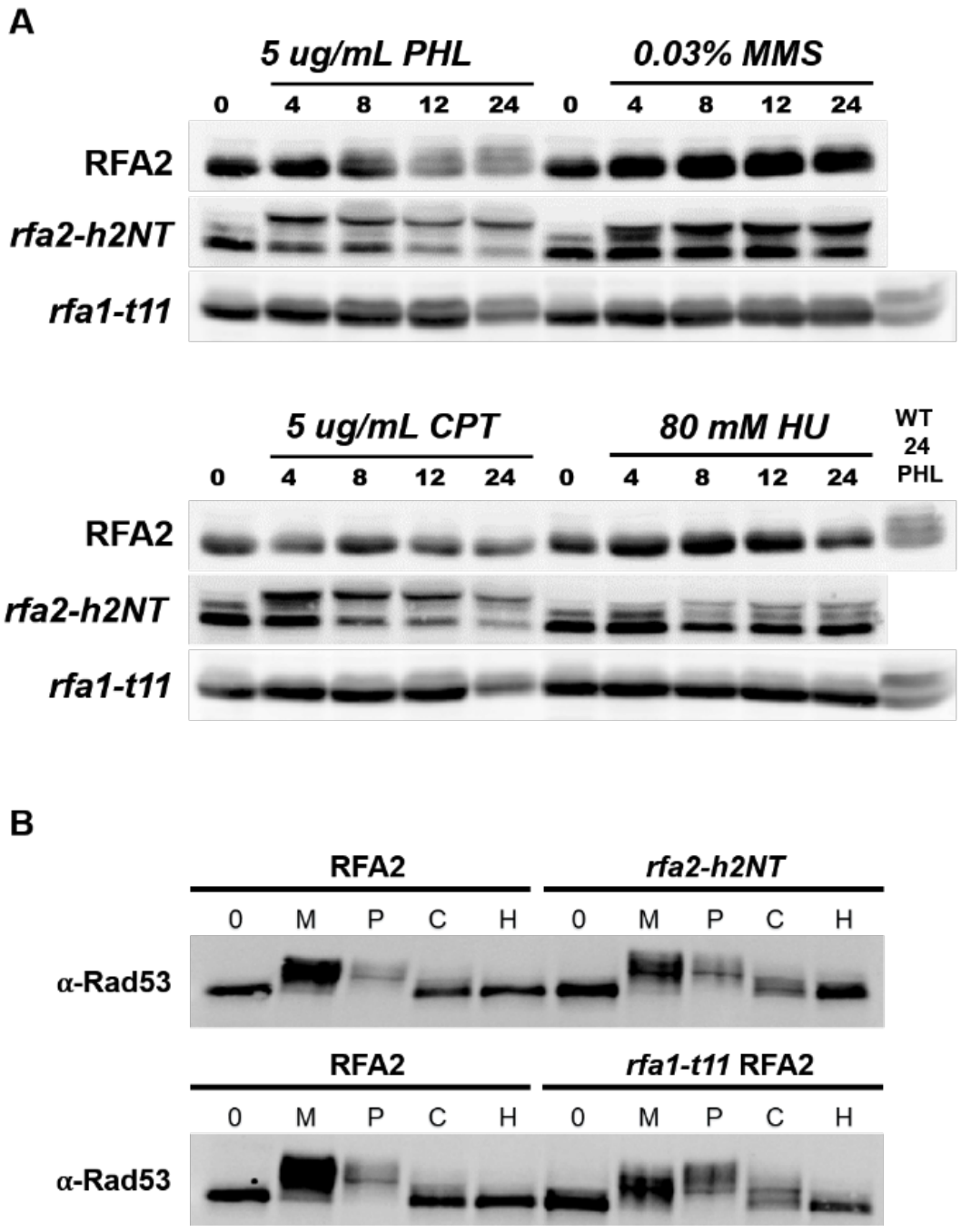

Figure 2.26. Rfa2 phosphorylation in response to low-levels of genotoxic stress.
A. Immunoprobe using α-Rfa2 antibody and 20 ug total protein from whole cell lysates. Rfa2 phosphorylation is readily detectable upon cellular exposure to low levels of PHL, CPT and MMS concentrations indicated at 8 hours in WT and *rfa1-t11* cells and occurs by 4 hours in *rfa2-h2NT*. Phosphorylation of Rfa2, *rfa2-h2NT*, or Rfa2 isolated from *rfa1-t11* cells is not hyper-phosphorylated in response to HU-induced replication stress. **B.** Rad53 immunoblots from strains in **A.** depicting Rad53 activation occurring in MMS and PHL treated cells, but not CPT or HU treated cells, indistinguishably in each condition. Phospho-activation of Rad53 does not occur in response to low levels of genotoxic stress induced by CPT or HU but occurs robustly in response to PHL or MMS treatment.

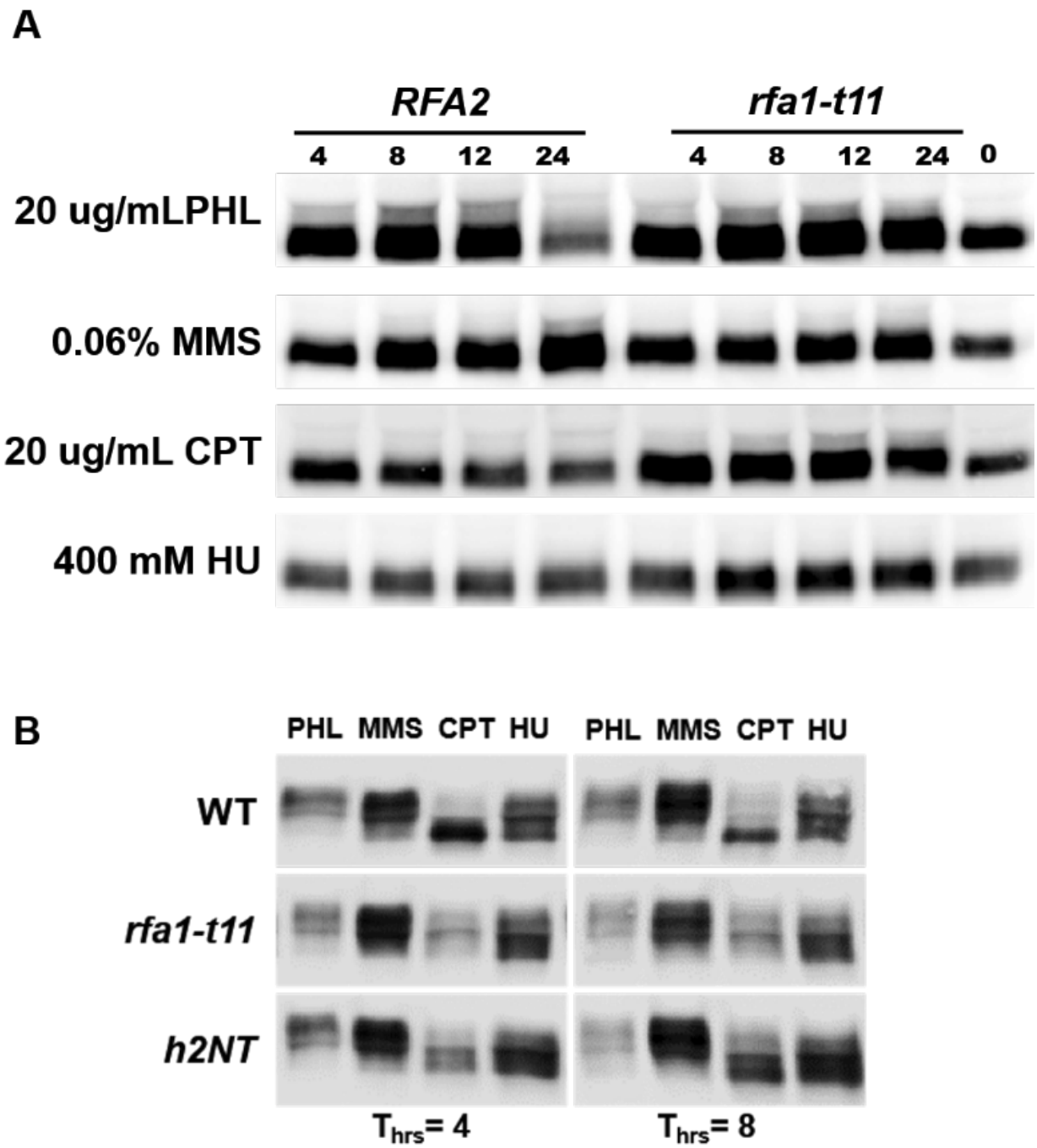

Figure 2.27. Rfa2 phosphorylation in response to high-levels of genotoxic stress.
A. Immunoprobe using α-Rfa2 antibody using 20 ug total protein from whole cell lysates. Rfa2 phosphorylation in NMM104 cells and NMM101 *rfa1-t11* cells in response to various clastogens at high doses. Rfa2 phosphorylation is observed in response to PHL, MMS, and CPT, but not HU. **B.** Immoblot of Rad53 activation in the aforementioned strains occurs indistinguishably in response to high doses of genotoxic agents used in **A.** Phospho-activation of Rad53 does not occur in response to genotoxic stress induced by CPT, but occurs robustly in response to PHL, MMS, or HU treatment.

phosphorylated at S122 by Mec1. In response to prolonged genotoxic challenge, Rfa2 undergoes a late phosphorylation event on the NT phosphorylation domain. This phosphorylation only occurs in response to prolonged challenge and is thus delayed and likely not a function of the initial DNA damage response. Furthermore, examination of mutant strains containing deletions of kinases known to be involved in the initial DNA damage response (Mec1/Tel1), or immediately downstream of the initial downstream response (Chk1/Dun1), reveals that delayed Rfa2 NT phosphorylation is still readily detected in a manner indistinguishable from wild-type cells. This demonstrates that there is an unidentified kinase acting upon Rfa2, promoting delayed phosphorylation of the NT.

2.5.B. Rfa2 phosphorylation at S122 as a marker for Mec1/Tel1 activity

In this study, we examined Rfa2 S122 phosphorylation in Rfa2 NT phospho-mutations *rfa2-D$_X$* and *rfa2-*Δ*N$_X$*, and in *mec1*Δ or *tel1*Δ mutants. Analysis of phosphorylation of Rfa2-D$_X$ or Rfa2-ΔN$_X$ reveals that S122 phosphorylation occurs readily and accumulates in response to prolonged genotoxic stress. However, phosphorylation of S122 may not serve any physiological function as phospho-mimetic Rfa2-S122 mutations do not display any increased sensitivity to DNA damaging agents. Instead, phosphorylation of S122 may serve as a biomarker for Mec1/Tel1 kinase activity during checkpoint initiation and maintenance.

Cells containing either *rfa2-D$_X$* or *rfa2-*Δ*N$_X$* mutations exhibit increased sensitivity to DNA damaging agents, however their sensitivities may be due to a role for Rfa2 NT function in checkpoint exit. In cells containing the *rfa2-*Δ*N$_X$* mutation, checkpoint initiation occurs indistinguishably from wild-type cells; however, in the presence of a persistent lesion these mutants experience permanent checkpoint arrest. As phosphorylation of S122 accumulates on *rfa2-*Δ*N$_X$* through the observed 24-hour window, we postulate that Mec1 and Tel1 activity is maintained in these mutants, promoting the observed permanent arrest.

The *rfa2-D$_X$* mutation is known to promote checkpoint exit in yeast experiencing a permanent arrest caused by an irreparable lesion, whereas *rfa2-*Δ*N$_X$* promotes checkpoint maintenance/arrest under the same conditions. Concomitant with this idea is the observation that *rfa2-DX* appears to inhibit accumulation of phosphorylation at S122 in a *tel1*Δ mutation, where only Mec1 activity on Rfa2 is expected. Mec1 is known to activate the master checkpoint regulator Rad53 and promote checkpoint

establishment and maintenance until a detected genotoxic insult has been repaired. The *rfa2-D$_X$* mutation causes cells that encounter a persistent DNA lesion to exit the checkpoint prematurely, an observation that correlates well with a reduced presence of hyper-phosphorylated Rad53. It is enticing to speculate, based on these combined results, that the phospho-state of the Rfa2 NT may downregulate Mec1 activity at the site of DNA lesions, promoting checkpoint exit through Rad53 deactivation.

2.5.C. Delayed Rfa2 NT phosphorylation is not dependent on the Rfa1 NT (DBD-F)

The NT of Rfa1, known as DBD-F, serves as host to several protein-protein interactions that have been identified to be essential to the repair on lesions in DNA. DBD-F is known to interact with Rad24, a component of the Rad24-RFC2-5 clamp-loader complex, the MRX complex, and perhaps most importantly the checkpoint kinase complex Mec1/Ddc2 (Marechal *et al.* 2015). In a point mutation of the Rfa1 NT, known as *rfa1-t11* (K45E), these interactions are reduced or eliminated, leading to an increased genotoxic sensitivity and instability in *rfa1-t11* cells. Furthermore, the *rfa1-t11* mutation has been demonstrated to promote relief of a permanent checkpoint induced by an irreparable lesion through a process known as checkpoint adaptation.

In this study we observed Rfa2 NT phosphorylation in response to prolonged genotoxic challenge or an irreparable DSB in cells containing the *rfa1-t11* mutation that was indistinguishable from wild-type cells. This observation has two major implications. The first major implication is that DBD-F is not responsible for the recruitment of the kinase(s) that produce delayed Rfa2 NT phosphorylation. This likely excludes Mec1/Ddc2 as the most likely culprit for delayed Rfa2 NT phosphorylation, as *rfa1-t11* negatively impacts Mec1/Ddc2 activity at DSB sites. The second implication is that the checkpoint adaptation-proficient phenotype conferred by *rfa1-t11* may be caused directly by delayed Rfa2 NT phosphorylation. Further study will be required in order to elucidate the exact mechanism by which *rfa1-t11* and *rfa2-D$_X$* promote checkpoint adaptation.

2.5.D. Yeast as a model system to study Rfa2 dynamics of other eukaryotic organisms and the physiological relevance of Rfa2 phosphorylation within those organisms

Saccharomyces cerevisiae can afford researchers a unique opportunity to study Rfa2 function from their own model organisms in a rapid and controlled fashion. As described in section 2.4.A, budding yeast Rfa2 is phosphorylated during genotoxic stress by two temporally distinct mechanisms, whereas

the Rfa2-h2NT mutant is robustly phosphorylated in response to genotoxic stress on the NT. While this phosphorylation occurs at T21 and S33 by Mec1, it has been difficult to characterize which kinases promote phosphorylation of the Rfa2-h2NT mutant at other sites like S4 or S8, etc. Moreover, as described in Padmaja Ghospurkar's thesis, yeast transformed with a variety of eukaryotic *rfa2* NT mutations are both mitotically viable and produce independent phosphorylation patterns in response to clastogen challenge. However, individual paralogs from the same species may be used in different processes such as DNA replication or DNA repair. Analysis of Rpa2 paralogs in *Arabidopsis* and *Oryza*, for example, demonstrated that each paralog experiences distinct modification events during genotoxic stress suggesting that the paralogs Rpa2-OS1 and Rpa2-ATa may be required for DNA repair in these organisms. Moreover, and consistent with this hypothesis are observations that Rpa1 and Rpa2 paralogs form differential complexes in plants that regulate meiotic crossover, DNA replication and DNA repair (Marwedel *et al.* 2003, Chang *et al.* 2009, Li *et al.* 2013, Aklilu *et al.* 2014, Eschbach *et al.* 2014, Aklilu *et al.* 2016). Our results together, however, do not rule out the simplest possibility of Mec1 phosphorylating SQ/TQ consensus motifs where they exist on each domain. Further study will be required to determine which specific eukaryotic NT promote checkpoint adaptation in yeast, which residues are required to be phosphorylated to drive adaptation, and which kinases are modifying these other eukaryotic N-termini in an effort to correlate which paralog of Rpa2 regulates checkpoint exit in each respective organism.

2.5.E. Implications for delayed Rfa2 NT phosphorylation

In this study, delayed Rfa2 NT phosphorylation was observed in response to prolonged genotoxic challenge in several checkpoint kinase deletions (*tel1*Δ, *chk1*Δ, *dun1*Δ), as well as in cells containing *rfa1-t11* (K45E). Human Rpa2 is known to be phosphorylated by DNA-PK, as well as CDK. While yeast do not possess a readily identifiable homolog to DNA-PK, yeast does have a clear CDK homolog in Cdc28. Delayed Rfa2 NT phosphorylation appears to be maximized around 12 hours in cells experiencing prolonged genotoxic challenge, the same window by which checkpoint adaptation occurs in yeast. We hypothesize that whichever kinase is producing maximally phosphorylated Rfa2 in this temporal window is not involved in the DNA damage response to checkpoint initiation, but critical for checkpoint exit and resumption to normal mitotic growth. As demonstrated in Figure 2.15 single deletions of the initial DSB sensor kinase Tel1, or downstream effector kinases Dun1 and Chk1, produce Rfa2 that is phosphorylated

indistinguishably from WT cells. It is possible then that Cdc28, or Cdc5, as a cell cycle regulatory kinase that promotes mitotic exit then phosphorylates the Rfa2 NT to promote checkpoint adaptation in response to a persistent DNA lesion. It is also curious that the phospho-state of the Rfa2 NT appears regulate Mec1 activity at break sites. We postulate that whichever kinase is phosphorylating the Rfa2 NT does so to relieve Mec1-dependent checkpoint maintenance to promote checkpoint recovery after a lesion has been repaired. Further study will be required to determine which kinase is directly responsible for producing the delayed Rfa2 NT phosphorylation observed.

2.6. Acknowledgements

Timothy M. Wilson was responsible for the creation or oversaw production of all yeast deletion mutations used in this study, performed most experiments, analysis, and supervised all undergraduate research experiments. **Barbara L. Senger** (undergraduate) created the *pRS315-rfa2-D$_X$-S122$_{A/D}$*, *pRS315-rfa2-A$_X$-S122$_{A/D}$* mutation vectors via *in vitro* site-directed mutagenesis used in this study and assisted with plasmid shuffle into strains tested. **Noelle P. Torrence** (undergraduate) helped with plasmid shuffle and analysis of the *rfa2-A$_l$* mutations used in this study. She also assisted in protein collection and SDS-PAGE preparation. **Nolan M. Miles** (undergraduate) helped with the construction and verification of NMM101 (JKM179 *rfa1*Δ::kanMX) and NMM104 (JKM179 *rfa2*Δ::kanMX) strains used in this study. **Erin M. Richards** (undergraduate) assisted with plasmid shuffle of *mec1*Δ strains used in this study and performed independent protein collection, SDS-PAGE, and Immunoblots demarcated in their respective figures. EMR also performed created the *pRS315-rfa2-*Δ*N$_X$-S122$_{A/D}$* vectors via *in vitro* site-directed mutagenesis and performed plasmid shuffle into strains tested.

CHAPTER 3: RFA2 NT PHOSPHORYLATION DURING CHECKPOINT ADAPTATION PROMOTES MITOTIC EXIT IN THE PRESENCE OF AN IRREPARABLE LESION

3.1. Abstract

In response to DNA damage, cells enter a checkpoint to provide adequate time for a DNA lesion to be processed properly. Upon repair of the lesion, cells exit the checkpoint and re-enter the cell cycle. However, cells can also exit the checkpoint despite the continued presence of a DNA lesion – termed checkpoint adaptation. This mechanism provides a balance between permanent checkpoint arrest and the potential for a cell to grow and divide, despite the lesion. One of the factors that senses disrupted DNA structure through its ability to bind to single-stranded DNA and mediates the activation of checkpoint arrest through interactions with key checkpoint proteins is Replication Protein A (RPA). It has been demonstrated in yeast that both the 70 kDa (Rfa1) and 32 kDa (Rfa2) subunits of RPA are also involved in the decision to exit a checkpoint with a lesion. In this study, we show that the Rfa2 N-terminus (NT) is phosphorylated during checkpoint adaptation. Furthermore, Rfa2 mutants that contain a phospho-mimetic NT, naturally-occurring NT phosphorylation, or that stimulate Rfa2 hyper-phosphorylation all drive checkpoint adaptation in an otherwise adaptation-deficient mutant. Certain subregions of the Rfa2 NT are important in this checkpoint adaptation phenotype, while post-translational modifications of other residues, particularly lysines, within Rfa2 are dispensable for the DNA damage response and may actually regulate the extent of Rfa2 phosphorylation.

3.2. Introduction

When cells are subjected to genotoxic stress, a signaling cascade is activated to halt cell growth and provide time for DNA repair machinery to properly process broken DNA (Hartwell *et al.* 1989, Elledge 1996, Toczyski *et al.* 1997). In budding yeast, this signaling occurs in a conserved process known as the DNA damage response (DDR) and activates the sensory kinases Tel1 and Mec1 which can then phosphorylate the transducer kinases Chk1 and Rad53 (Longhese *et al.* 1998, Rhind *et al.* 1998, Weinert 1998, Sanchez *et al.* 1999, Lowndes *et al.* 2000, O'Connell *et al.* 2000). Rad53 is activated by both Tel1 (in response to DNA double-strand breaks; DSBs) and by Mec1 (in response to single-stranded DNA intermediates) in a Rad9- or Mrc1- dependent manner (de la Torre-Ruiz *et al.* 1998, Alcasabas *et al.* 2001). Once activated, Rad53 drives cell cycle arrest through the phosphorylation of many known and

unknown downstream targets (Cohen-Fix *et al.* 1997, Smolka *et al.* 2007, Barnum *et al.* 2014). Ideally, checkpoint arrest would stall cell cycle progression until all DNA lesions have been repaired. However, under conditions of prolonged checkpoint arrest due to an irreparable DNA break, cells eventually initiate a program to exit the checkpoint and promote cell division. This process has been termed checkpoint adaptation (Sandell *et al.* 1993, Toczyski *et al.* 1997).

In *Saccharomyces cerevisiae* (budding yeast), checkpoint activation can be driven by a single, controlled DSB (Toczyski 2006). In otherwise wild-type (WT) yeast, homologous recombination involving the silent mating loci (*HML* and *HMR*) is employed to repair an HO-induced break at the *MAT* locus. However, in this scenario, a checkpoint response through Rad53 phosphorylation (activation) is not detectable (Pellicioli *et al.* 2001). Rad53 activation is only detected in cells where repair of the HO-induced break is delayed due to engineered, ectopic homologous sequences that lie at some distance from the break or on another chromosome (Haber 2000, Pellicioli *et al.* 2001). When cells are engineered to completely lack homologous sequence to recombine with sequence surrounding an HO-induced DNA break, the DNA break persists indefinitely, and checkpoint activation (Rad53 phosphorylation) is readily observed. Despite the persistence of a break, Rad53 becomes inactivated (dephosphorylated) in WT cells, and these cells attempt to divide (*i.e.*, they exit checkpoint arrest) (Toczyski *et al.* 1997, Lee *et al.* 1998, Lee *et al.* 2001). This phenomenon of checkpoint adaptation as a last-resort mechanism allowing cell growth and division while also leading to an increase in DNA mutations appears to also occur in mammalian cells (Swift *et al.* 2014) and is a potential cause for mutagenesis-induced cellular disease, including uncontrolled cellular proliferation (Kubara *et al.* 2012, Swift *et al.* 2014, Lewis *et al.* 2016, Serrano *et al.* 2016).

A number of factors involved directly in repair of DNA or in the regulation of the cell cycle in response to DNA damage have been identified to either increase or decrease a cell's ability to exit a checkpoint in the face of a persistent lesion. Some factors that when deleted inhibit checkpoint adaptation include: Yku70/Hdf1 (involved in non-homologous end joining; NHEJ; Lee *et al*. 1998) , Rdh54/Tid1 (involved in recombination repair of DSBs; Lee *et al.* 2001) , Sgs1-Dna2 (helicase/nuclease involved directly in 5'→3' resection of DNA; Zhu et al. 2008, Cejka et al. 2010) , Slx4-Rtt107 (complex that competes with Rad9 for interaction with Dpb11 and γ-H2AX to mute Rad53 activation; Cussiol et al. 2016,

Dibitetto et al. 2016) , subunits of casein kinase II (CKII; Toczyski et al. 1997) , and the phosphatases Pph3-Psy2 and Ptc2 (involved in dephosphorylating Rad53 and Mec1; O'Neill et al. 2007, Kim et al. 2011, Jablonowski et al. 2015) . Furthermore, adaptation-deficient mutations of the polo-like kinase Cdc5 and the sensory kinase Mec1 have been identified (*cdc5-ad* and *mec1-ad*; Toczyski et al. 1997, Clerici et al. 2014) . Factors that when deleted promote checkpoint adaptation include Mre11 and Rad50 (components of the MRX complex that recognizes DSB ends and promotes resection; Lee et al. 1998, Viscardi et al. 2007, Niu et al. 2010, Shim et al. 2010) and Tel1 (sensor kinase that phosphorylates Rad53; Vialard 1998, Nakada et al. 2003, Nakada et al. 2003, Clerici et al. 2014) . Although DNA resection ability is often positively correlated with checkpoint adaptation proficiency, and in some instances appears to influence Rad53 dephosphorylation and checkpoint exit (*e.g.*, overexpression of *EXO1*; Mimitou and Symington 2010) , this is not always the case; a deletion of *MRE11* (resulting in reduced resection) also leads to checkpoint adaptation proficiency. It is of interest that Mre11-Rad50-Xrs2 assists in the recruitment of Tel1, and that deletion of three of these four genes not only promotes adaptation, but does so in some adaptation-deficient strains (Clerici *et al.* 2014). In addition, a mutation (*rfa1-t11*) in the 70 kDa subunit of yeast Replication Factor A (RFA; the eukaryotic single-stranded binding complex; Umezu *et al.* 1998) , promotes adaptation proficiency in otherwise adaptation-deficient *yku70*Δ or *rdh54/tid1*Δ cells; however, adaptation in *cdc5-AD* cells could not be rescued by the *rfa1-t11* mutation (Lee *et al.* 2001, Pellicioli *et al.* 2001).

Rdh54 (Rad54 homolog) is an ATPase/translocase member of the Swi2-like family of proteins and is thought to function as a nucleosome remodeler during the initial DSB processing events that occur immediately upon activation of the DDR (Lee *et al.* 2001). During the lesion and repair program (LRP), Rdh54 has been demonstrated to be important for the dissociation of Rad51 from chromatin during homologous recombination, which required for DNA polymerase activity during repair synthesis (Santa Maria *et al.* 2013). Enzymes within the Swi2-like family have been reported to be critical for homologous recombination, mediating processes such as DNA supercoiling/unwinding, D-loop formation, and branch migration (New *et al.* 1998, Mazin *et al.* 2000, Petukhova *et al.* 2000, Van Komen *et al.* 2000). Interestingly, it has been demonstrated that Rdh54 is phosphorylated by Mec1 and Rad53, specifically during the DDR during meiosis (Dresser *et al.* 1997, Shinohara *et al.* 2000). Mutant cells containing an

ATPase-dead form of Rdh54 (*rdh54*-K318R) or a deletion of the *RDH54* gene are adaptation-deficient – this is to say that these cells cannot facilitate coordinated dephosphorylation and inactivation of Rad53 in the presence of an irreparable lesion during G2/M to bypass the established checkpoint and restart the cell cycle (Lee *et al.* 2001).

Replication Factor A is an essential, heterotrimeric, single-stranded DNA (ssDNA) binding complex that is actively recruited to resected DSBs and establishes the signaling platform utilized to recruit in checkpoint machinery, including Ddc2-Mec1 (Zou *et al.* 2003), the Rad24-RFC2-5 clamp loader (Majka *et al.* 2006, Piya *et al.* 2015), the Rad17-Mec3-Ddc1 clamp (Zou *et al.* 2003, Majka *et al.* 2006), in addition to recruitment of additional resection machinery including Sgs1 helicase and Dna2 nuclease (Marechal *et al.* 2015), (Marechal *et al.* 2015). RFA/RPA is a target for many post-translational modifications, including sumoylation, ubiquitination, and phosphorylation (Marechal *et al.* 2015), with phosphorylation of the N-terminus (NT) of the 32 kDa human RPA subunit, Rpa2, being the most well-characterized (Vassin *et al.* 2009, Liu *et al.* 2012, Marechal *et al.* 2015). While human Rpa2 NT phosphorylation is readily observed following DNA damage, detectable phosphorylation and characterization of the yeast Rfa2 NT has been limited at best (Wilson *et al.* 2018). The only conditions where Rfa2 NT phosphorylation was previously detected is in a *set1Δ* or *mec3*Δ mutation (Schramke *et al.* 2001), during meiosis (Clifford *et al.* 2004), and upon prolonged DNA damage (Wilson *et al.* 2018). However, like *rfa1-t11*, an amino-terminal phospho-mimetic form of Rfa2 (Rfa2-D_X) also promotes checkpoint adaptation in *yku70*Δ cells (Ghospurkar *et al.* 2015). Conversely, an unphosphorylatable form of Rfa2 (Rfa2-A_X) not only prevents checkpoint adaptation in *yku70*Δ cells but it also appears to enhance the adaptation deficiency in these double-mutant cells (Ghospurkar *et al.* 2015).

Correlative and causative studies have indicated that phosphorylation of yeast Rfa2 NT (and human Rpa2 NT) plays a role in the DNA damage response; however, exactly what role(s) and their significance remain unclear. In this study, the function of the Rfa2 NT was probed to determine its role in checkpoint exit, particularly when DNA damage persists. We put forth the idea that RFA is not only instrumental in checkpoint activation, but that it is a prime candidate for driving checkpoint exit as well. In this study, we demonstrate that observed Rfa2 hyper-phosphorylation occurs around the time in which checkpoint adaptation begins to occur. Furthermore, using three different *rfa2* mutant constructs (two of

which are naturally phosphorylated in yeast cells), we demonstrate that phosphorylation (or mimicking phosphorylation) does indeed drive checkpoint adaptation in another adaptation-deficient mutation (*rdh54*Δ), suggesting that promotion of checkpoint exit in the face of persistent DNA damage by Rfa2 phosphorylation may be a generally applicable phenomenon. Finally, characterization of subregions of the Rfa2 NT reveals that two subregions, previously identified to have DNA damage-sensitivity or display synthetic genetic interactions, have the greatest influence on checkpoint adaptation efficiency.

3.3. Materials and Methods

3.3.A. Strains and Plasmids

Yeast strains and plasmids used in these studies are listed in Appendix A and B, respectively. All yeast strains used within this study are isogenic derivatives of JKM179 (*ho*Δ *MAT*α *hml*Δ*::ADE1 hmr*Δ*::ADE1 ade1-100 leu2-3,112 lys5 trp1::hisG ura3-52 ade3::GAL::HO*; Lee *et al.* 1998) containing *rfa2*Δ*::kanMX* (NMM104; Wilson *et al.* 2018).

The generation of an *RDH54* deletion in NMM104 was completed using PCR amplification (Figure 3.1) of the *natMX* cassette from plasmid pFA6-natNT2 (Euroscarf) with appropriate primers (Appendix C) containing an additional 40 nt of homologous sequence immediately upstream and downstream of the coding regions of each gene and one-step gene replacement. Deletion candidates were then screened via diagnostic replica plating and by PCR using diagnostic primers (Appendix C) using a strategy like that for the generation of yeast gene deletions (Kelly *et al.* 2001).

3.3.B. Single DSB induction and collection of whole-cell lysate

All induction of DNA damage in cells for biochemical assays was performed in liquid culture. Yeast cells were grown for 20 hours (hr) in liquid YPD (1% yeast extract, 2% peptone, 2% dextrose) to an OD_{600} of 1.0, and subsequently sub-cultured the next day into YPR (1% yeast extract, 2% peptone, 2% raffinose) and grown for 20 hours to an OD_{600} of 2.0. A single break at the *MAT* locus via HO endonuclease was induced by adding 20% galactose to the YPR cultures to a final concentration of 2%.

To harvest an equivalent number of cells, 10 ODs of cells were harvested from each culture at time-points indicated in figures. Harvested cells were treated with 0.1 M NaOH for 10 minutes at room temperature, pelleted at 10K RPM for 2 minutes (min), and aspirated to remove NaOH from the pellet. The pelleted cells were then resuspended in 500 uL of K-Buffer (0.06 M Tris-HCl, ph 6.8, 5% glycerol, 2%

SDS, 4% β-mercaptoethanol, 10 mM DTT; Kushnirov 2000), and each protein sample was boiled at 100°C for 3 min. A Lowry assay (RC-DC Assay Kit; Bio-Rad) was used to quantify protein concentration within each sample to ensure even protein loading during SDS-PAGE.

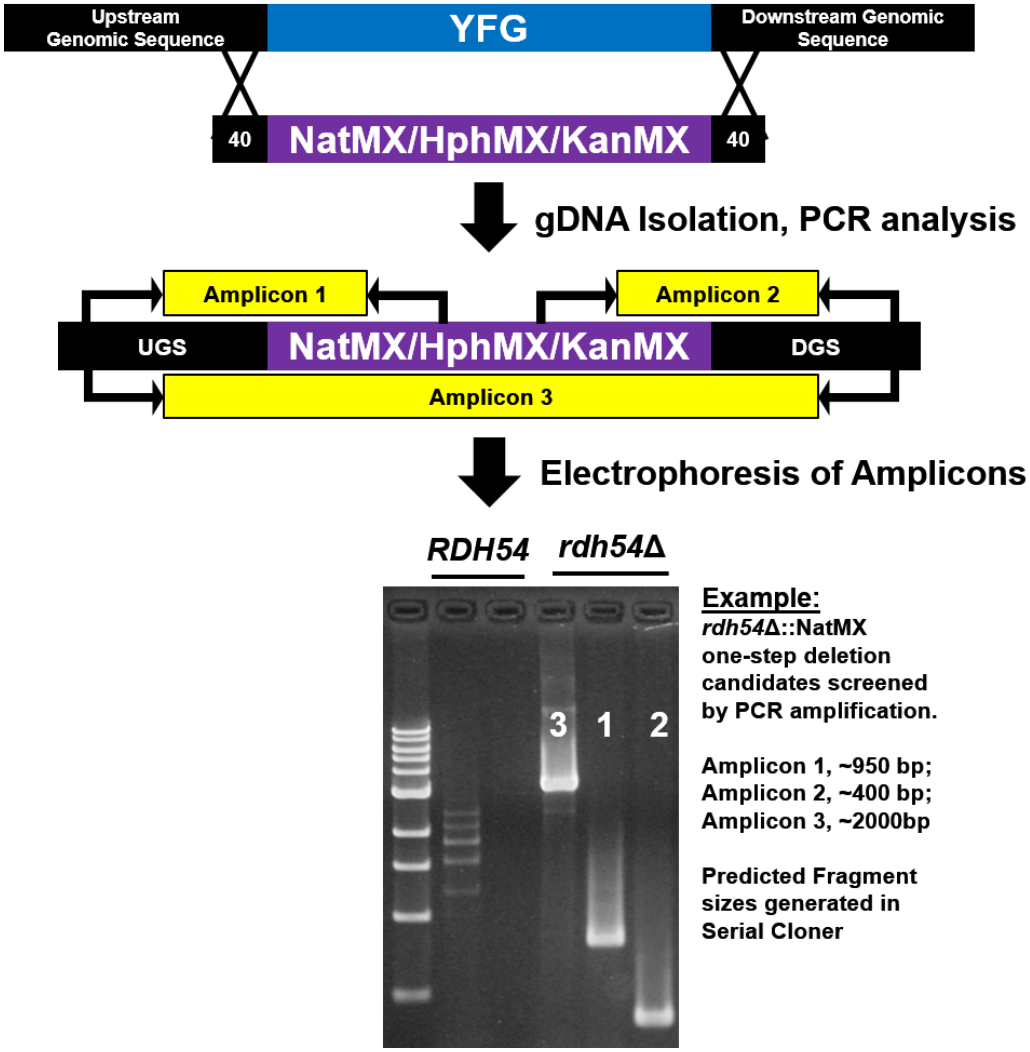

Figure 3.1. One-step gene replacement and verification strategy used in the creation of *rdh54*Δ. The one-step gene replacement and verification strategy used in the creation of *rdh54*Δ is identical that described in Chapter 2, Figure 2.2. Amplicon sizes for *rdh54*Δ are 1: 961 bp, 2: 388 bp, 3; 1981 bp as generated by Serial Cloner. Fragments were generated via PCR, as described, and analyzed on a 1% agarose gel.

3.3.C. Checkpoint adaptation plating assays

Cells for the checkpoint adaptation plating assays were grown in liquid culture as described above. A single break at the *MAT* locus via HO endonuclease was induced by adding 20% galactose to the YPR cultures to a final concentration of 2%. Cells were grown for 8 hours in YPR-Gal media to sync cells at the G2/M checkpoint.

To observe cellular adaptation, 0.05 OD_{600} of cells were plated onto YPRG (1% yeast extract, 2% peptone, 2% raffinose, 2% galactose) media and spread using glass beads. Cells were counted under 20x optical zoom on an Olympus microscope, and then categorized based on observed counts. At 8 hours cells were counted as 1 cell (single cell), 2 cell (bilobal big buds), 3 cell, 4 cell, and 5+ cell clusters. At 24 and 48 hours cells were counted as 1-2 cell, 3-4 cell, 5-6 cell, 7-8 cell, and 9+ cell clusters. Colonies that formed as a result of NHEJ events were not counted. Average adaptation was calculated by averaging three independent data sets. Clusters ≥3 cells were eliminated from 24 and 48-hour averages.

3.3.D. SDS-PAGE and Immunoblotting

K-Buffered Whole-cell lysate from each sample was loaded into SDS-PAGE gels containing a 4% stacking gel (37.5:1 mono:bis) and 12% (150:1 mono:bis) or 15% resolving gel (29:1 mono:bis). 60 ug total whole cell lysate was used in SDS-PAGE to observe Rad53, 20 ug total whole cell lysate was used to observe Rfa2. Electrophoresis was then performed at 30 mA constant current for 15 minutes, 60 mA constant current for 2 hours allowing the 25 kDa band (PageRuler Plus Prestained Protein Ladder; Thermo Scientific) to reach the base of the gel. Each gel was equilibrated in Towbin Transfer Buffer (10 mM Tris-HCl, 100 mM glycine, 10% Methanol) for 15 min and transferred onto a 0.2-micron nitrocellulose membrane (Bio-Rad) at 40 mA constant current for 16 hours at 4°C.

Once transfer was complete, nitrocellulose membranes were then stained with Ponceau S (0.5% w/v Ponceau S, 1% v/v acetic acid) for 10 min to visualize total protein content to determine equivalent loading within each lane. Once membranes were imaged, the Ponceau S stain was removed by washing with Western Wash Buffer (WWB) (0.3% Tween-20, 5 uM NaF, 0.05 uM Na_3VO_4) for 15 minutes. Blocking buffer (WWB, 1% w/v BSA) was then added and the blot was incubated for 2 hours at room temperature. Blocking buffer was removed, and Primary Antibody Buffer (PAB) (WWB, 0.5% w/v nonfat dry milk, 0.5% BSA) was added to the blots.

To probe Rfa2 phosphorylation, a 1:40,000 dilution of α-Rfa2 antibody (kindly provided by Dr. Steve Brill) was used in PAB. To probe Rad53 phosphorylation, a 1:6000 dilution of α-Rad53 antibody (ab104232, AbCam) was used in PAB.

Following a 16 hr incubation at 4°C the PAB was removed and washes were performed using WWB. Secondary Antibody Buffer (SAB) (WWB, 0.2% w/v nonfat dry milk), containing a 1:40,000 dilution

of goat-α-rabbit-HRP (Abcam; ab97051, 1:40,000, Bethyl; A120-101P, 1:40,000) was then added to each blot and allowed to incubate for 2 hr at room temperature. The SAB was then removed and washes using WWB were performed. All blots were developed using a fluorescent substrate (ECL2 Plus; Thermo Scientific) and visualized on a STORM imager (GE).

3.4. Results

3.4.A. *rdh54*Δ mutations recapitulate known damage sensitives that are exacerbated by the phospho-state of the Rfa2 NT

Previous research demonstrated that *rdh54*Δ mutants are sensitive to genotoxic agents via diagnostic spot assays (Klein 1997). In order to ensure that the *rdh54*Δ mutation and *rdh54*Δ *rfa2* NT extensive mutation combinations created in this study would recapitulate known phenotypes, we performed a diagnostic spot assay (Figures 3.2 and 3.3). The *rdh54*Δ mutant used in this study is sensitive to genotoxic stress produced by MMS, CPT, PHL, and HU. Moreover, as observed in other studies, combination of *rdh54*Δ with *rfa2-D*$_X$ or *rfa2*-Δ*N*$_X$ produces hyper-sensitive phenotypes at lower doses, whereas *rfa2-A*$_X$ does not support clastogen resistance in *rdh54*Δ cells, suggesting that the *rdh54*Δ phenotype is dominant to the phenotypes produced by the Rfa2 NT extensive mutations during mitotic DNA damage.

Through our collaboration with the Andre Walther Lab at Cedar Crest College (Allentown, PA, USA), we obtained two adaptation-deficient mutations, *cdc5-AD* and *rdh54*Δ with chromosomal integrations of the *rfa2-D*$_X$ or *rfa2-A*$_X$ extensive mutations in each background. Initial analysis of the Rad53 phosphorylation state during checkpoint adaptation (Figure 3.4) revealed that the phospho-mimetic *rfa2-D*$_X$ promotes more rapid dephosphorylation of Rad53 in both *cdc5-AD* and *rdh54*Δ cells, specifically around 12-16 hours post-HO induction. The *rfa2-A*$_X$ mutation promoted a more robust checkpoint in *rdh54*Δ and led to a stronger initial activation of Rad53 in *cdc5-AD* cells. Moreover, *rdh54*Δ *rfa2-A*$_X$ double mutant cells also displayed hyper-phosphorylated Rad53 throughout the observed 36-hour time course, indicating that these cells were deficient for checkpoint exit. This led us to further test the effect of the Rfa2 NT phospho-state in *rdh54*Δ, as these mutants appeared to have a more significant checkpoint adaptation deficiency than *cdc5-AD* cells.

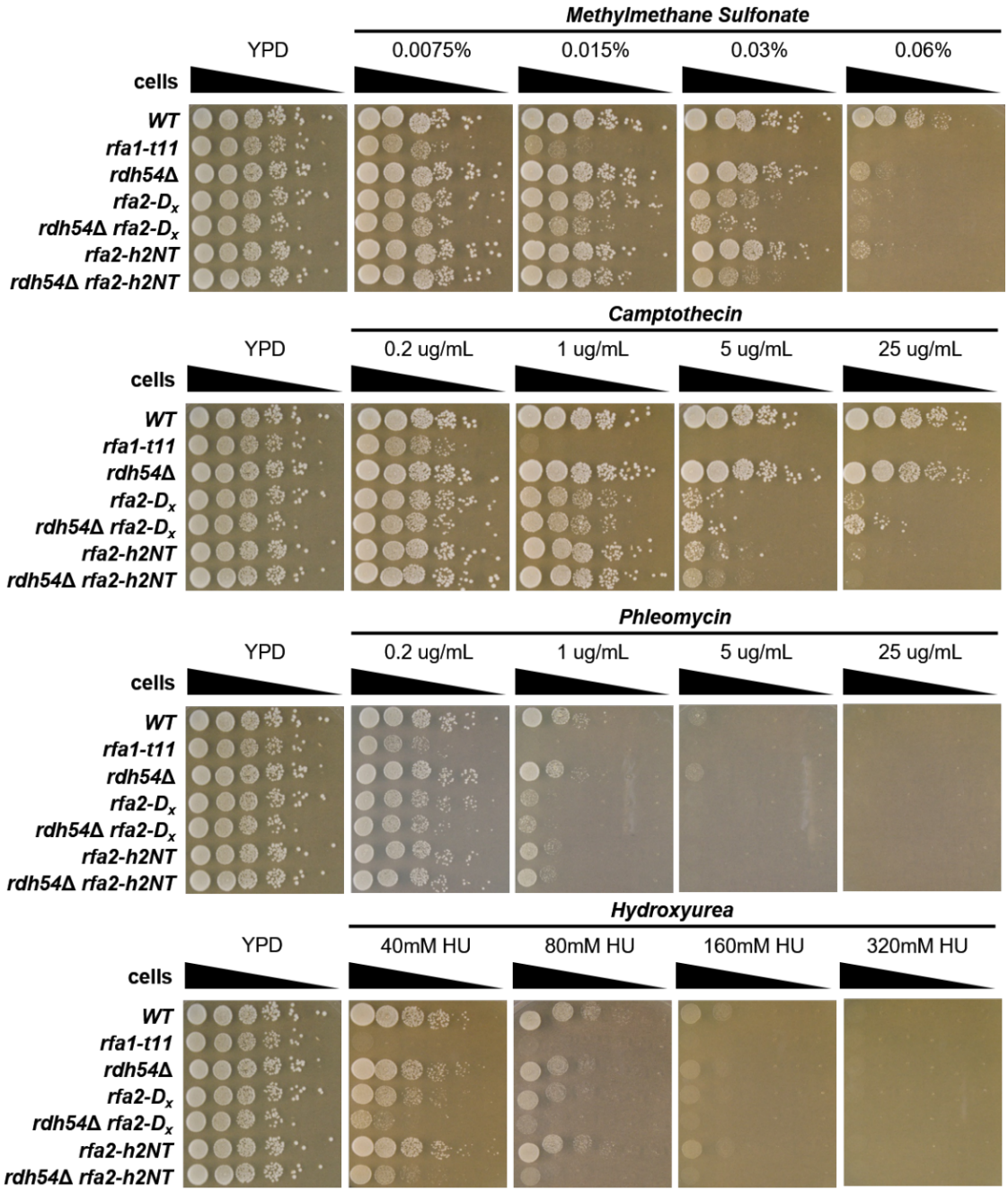

Figure 3.2. Diagnostic spot assay of *rdh54*Δ Rfa2 NT phospho-mimetic mutations at various clastogen concentrations.
NMM104 cells containing *rdh54*Δ Rfa2 NT mutations were harvested and an OD_{600} for the exponentially growing culture was determined. Starting at an OD_{600} of 1.0, six ten-fold serial dilutions were performed in sterile filtered water. 200 uL of the diluted culture was added to a 96-well microtiter plate and 5 uL of the dilution was then spotted onto the plates using a multi-channel pipetman. *rdh54*Δ mutant cells containing the *rfa2-D*$_X$ mutation are hyper-sensitive to genotoxic agents and the *rfa2-h2NT* mutation increases sensitivity to genotoxic agents.

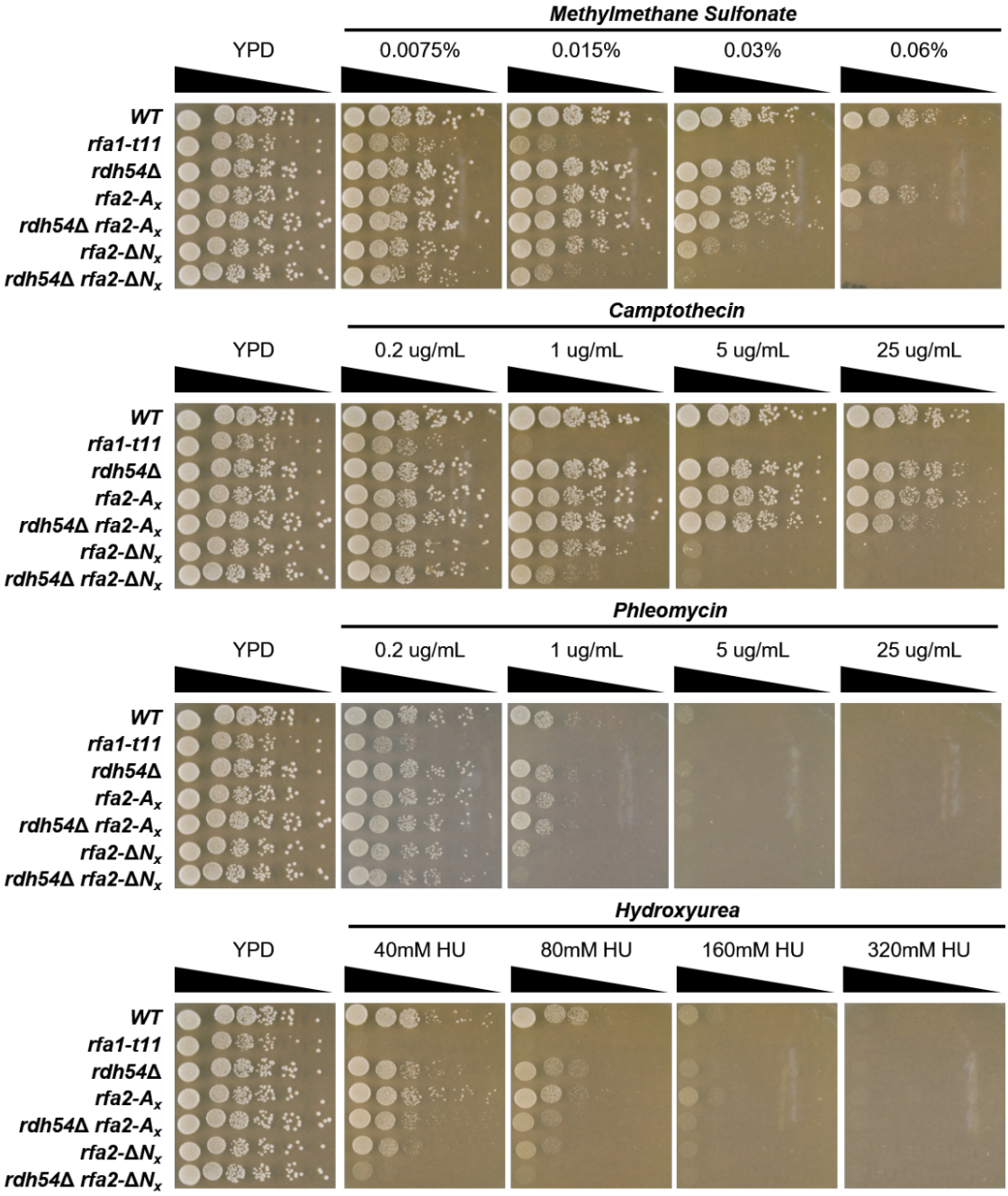

Figure 3.3. Diagnostic spot assay of *rdh54*Δ Rfa2 NT unphosphorylatable mutations at various clastogen concentrations.

NMM104 cells containing *rdh54*Δ Rfa2 NT mutations were harvested and an OD_{600} for the exponentially growing culture was determined. Starting at an OD_{600} of 1.0, six ten-fold serial dilutions were performed in sterile filtered water. 200 uL of the diluted culture was added to a 96-well microtiter plate and 5 uL of the dilution was then spotted onto the plates using a multi-channel pipetman. *rdh54*Δ mutant cells containing the *rfa2-A*$_X$ mutation are no more sensitive to genotoxic agents than *rdh54*Δ mutants containing Rfa2, whereas the *rfa2-*Δ*N*$_X$ mutation leads to hyper-sensitivity to genotoxic agents.

3.4.B. The native Replication Factor A2 amino-terminus is phosphorylated in response to a single, irreparable double-strand break.

Although phosphorylation of the human Rpa2 N-terminus in response to DNA damage is overt and readily detectable, there has been little report of phosphorylation in the yeast Rfa2 NT. Previously, detectable DNA damage-dependent phosphorylation of *S. cerevisiae* Rfa2 during mitosis has only been characterized for serine 122 (S122; (Brush *et al.* 1996, Brush *et al.* 2000, Bartrand *et al.* 2004). However, as described in Chapter 2 my study using *rfa2-S122$_{A/D}$* mutations demonstrates that this damage-dependent phosphorylation is dispensable for DNA repair and checkpoint activation. Phosphorylation within the Rfa2 NT has only been detected in meiosis (prior to programmed DSB formation; (Clifford *et al.* 2004) and in specific mutations (*set1*Δ and *mec3*Δ; (Schramke *et al.* 2001). To our knowledge, Rfa2 NT phosphorylation in otherwise WT cells in response to DNA damage had never been characterized prior to the evidence presented in Chapter 2 (Wilson *et al.* 2018). Previous attempts to measure Rfa2 NT phosphorylation had been unsuccessful (Ghospurkar *et al.* 2015); however, these studies had only assessed the Rfa2 phospho-state after 2-4 hr post DNA damage. It was demonstrated that the phospho-state of the Rfa2 NT has bearing on the ability of a cell to adapt to a checkpoint, which occurs roughly 12-15 hr post DNA damage. Therefore, it was reasonable to address whether detection of more overt Rfa2 phosphorylation simply required a longer period following DNA damage induction. Protein isolation from WT cells over a 24 hr time course revealed that Rfa2 phosphorylation is detectable by around 8 hr post DSB induction and becomes nearly maximally phosphorylated by 12-16 hr following a DNA break (Figure 3.5, top panel). This is similar to the time in which checkpoint adaptation typically occurs and is just prior to when Rad53 dephosphorylation is observed (Figure 3.5, bottom panel).

This correlative evidence is consistent with the previous observation that mimicking phosphorylation drives checkpoint adaptation in the otherwise adaptation-deficient *yku70/hdf1*Δ strain (Ghospurkar *et al.* 2015). This delayed phosphorylation also occurs much later (8-12 hr *vs.* 2-4 hr) than the S122 phosphorylation reported previously ((Brush *et al.* 1996, Brush *et al.* 2000, Bartrand *et al.* 2004). The observed delayed phosphorylation in response to prolonged phleomycin treatment is dependent on the presence of S/T residues in the Rfa2 NT (Chapter 2, Figure 2.7), as no phospho-species are detected for *rfa2-A$_X$* (similar to that observed for prolonged phleomycin treatment of cells (Chapter 2, Figure 2.10;

Wilson *et al.* 2018a) . Analysis of post-translational modification of Rfa2-A_X under HO-induced damage conditions has not been studied.

3.4.C. Checkpoint adaptation efficiency is dependent on the Rfa2 NT and its phospho-state.

A previous study demonstrated that mimicking phosphorylation or preventing phosphorylation of the Rfa2 N-terminus positively and negatively affected checkpoint adaptation, respectively. However, the adaptation deficiency of a unphosphorylatable Rfa2 NT had only a minor (~10%) reduction in checkpoint adaptation efficiency (Figure 3.6; Ghospurkar *et al.* 2015) . Previous studies of a unphosphorylatable *rfa2-*A_X mutation *vs*. another unphosphorylatable *rfa2-*ΔN_X mutation (which is also missing this domain) revealed that of these two only the NT deletion mutant had a discernable DNA damage sensitivity (Ghospurkar *et al.* 2015). Therefore, these function differently in the DNA damage response. With respect to checkpoint adaptation efficiency, the *rfa2* NT deletion mutation displayed a much more severe adaptation deficiency (Figure 3.6, Table 3.1), indicating that both the presence of the domain and phosphorylatable S/T residues are required for full checkpoint adaptation.

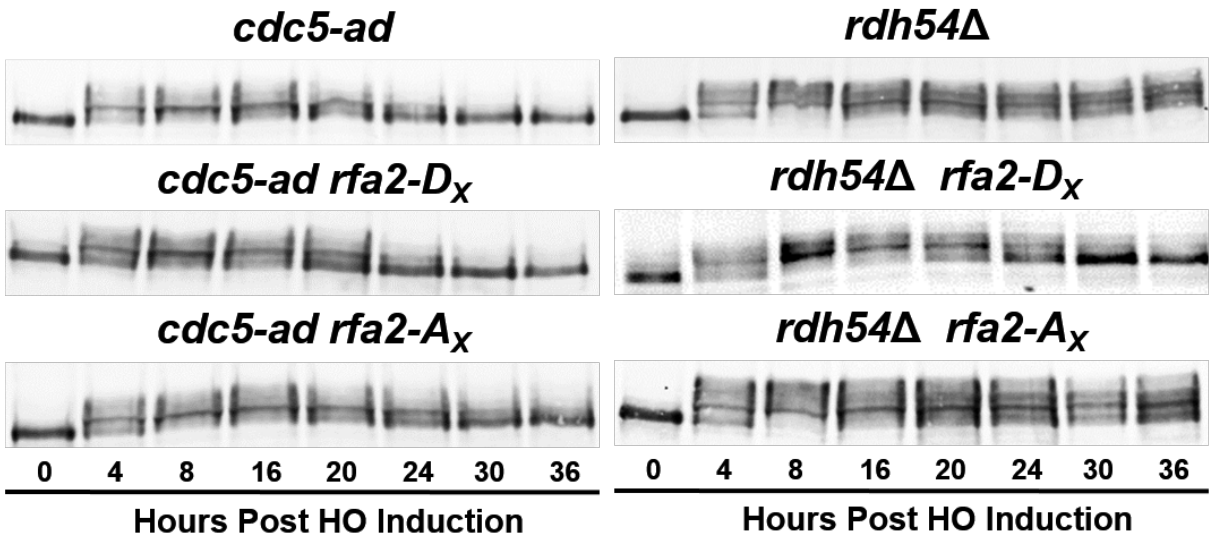

Figure 3.4. Rfa2 phospho-mimetics impact checkpoint adaptation differentially.
cdc5-AD (Left Panels) and *rdh54*Δ are established adaptation-deficient mutations that are rescued by *rfa2-*D_X. Rescue is classified as the ability to dephosphorylate Rad53 and enter mitosis. *rfa2-*A_X mutations promote extended checkpoint maintenance in each mutation, as observed by hyper-phosphorylated Rad53 throughout the time course.

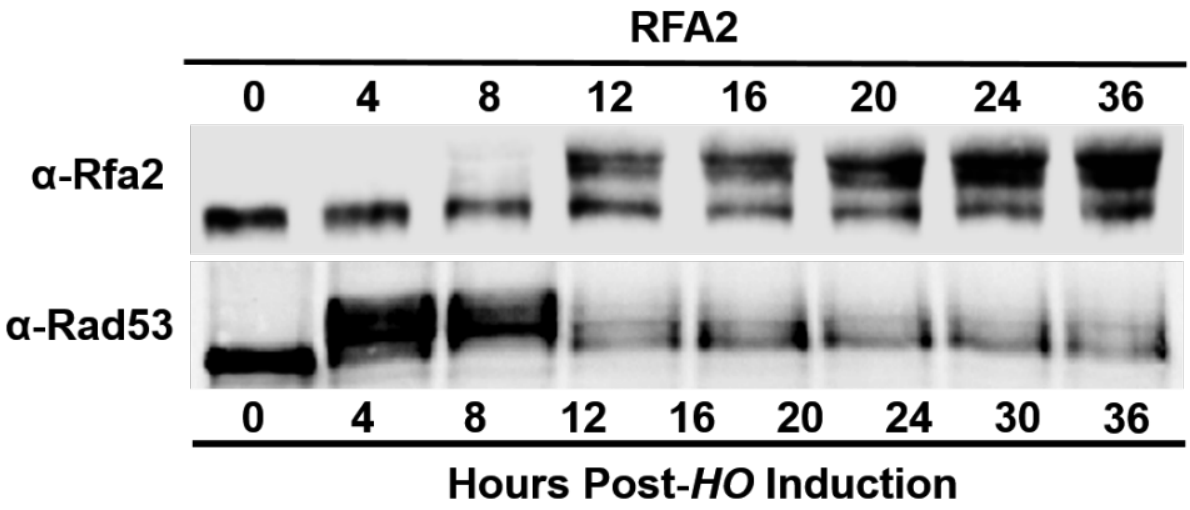

Figure 3.5. Hyper-phosphorylation of Rfa2 during checkpoint adaptation.
Rfa2 hyper-phosphorylation and Rad53 dephosphorylation during checkpoint adaptation are correlatively linked. A. Immunoblots depicting phospho-shift of Rfa2 during checkpoint adaptation (Top Panel) and Rad53 phosphorylation and dephosphorylation during checkpoint adaptation (Bottom Panel). Maximal Rad53 phosphorylation is achieved by 4 hours post-HO induction, whereas optimal Rfa2 hyper-phosphorylation is observed by 12-16 hours. HO induction was achieved by adding 2% galactose to the media. At indicated time points, 10 ODs of cells were harvested, and protein was isolated via K-Buffer extraction. For Rfa2 blots, 10 ug total protein was used. For Rad53 blots, 40 ug total protein was used.

3.4.D. Rfa2 NT mutations that mimic NT phosphorylation or are naturally phosphorylated promote checkpoint adaptation in adaptation-deficient *rdh54*Δ cells.

To examine *rfa2* mutations in the presence of other gene mutation/deletion strains, especially in the JKM179 background (Lee *et al.* 1998), we utilized the NMM104 strain (JKM179 derivative with *RFA2* deleted containing pJM132, which can be used for plasmid shuffle of *rfa2* mutant alleles). We ensured that NMM104 containing *rfa2* NT mutant alleles expressed from the native *RFA2* promoter on plasmid pRS315 (Sikorski *et al.* 1989) behaved similarly to integrated forms of these alleles by performing a comparative DNA damage assay. The results of plasmid-expressed *vs.* integrated copies of *rfa2* NT mutations were indistinguishable (Figure 3.6). Both *rfa2-D*$_X$ and *rfa2-*Δ*N*$_X$ reveal DNA damage sensitivity, similar to that observed not only for the JKM179 strain background, but also for other strain backgrounds we have tested (Ghospurkar et al. 2015).

Integrated copies of Rfa2 NT mutant alleles had been examined in a *yku70*Δ strain previously, with the *rfa2-D*$_X$ mutation restoring adaptation proficiency and the *rfa2-A*$_X$ mutation enhancing the observed adaptation deficiency (Ghospurkar et al. 2015). To determine if the effects of Rfa2 NT mutations on checkpoint adaptation were more widely applicable the *rdh54*Δ checkpoint adaptation-deficient

mutation was generated. We first sought to ensure that our NMM104-derived *rdh54*Δ mutation recapitulated its known adaptation-deficient phenotype via microscopy (Figure 3.7, Table 3.2). Wild-type NMM104 (expressing *RFA2* from pRS315) adapts at approximately 87-90% by 24 hours, 95% by 48 hours post-HO induction (Figure 3.7, Table 3.1), whereas the NMM104 *rdh54*Δ mutant (expressing *RFA2* from pRS315) in these assays adapts at approximately 33% by 24 hours, 38% by 48 hours (Figure 3.7, Table 3.2). This data is consistent with previous observations that the deletion of *RDH54* confers significant adaptation deficiency in response to an unrepaired lesion (Lee et al. 2001).

Microscopy also revealed that *rdh54*Δ mutants containing an N-terminally truncated form of Rfa2 (Rfa2-ΔN_X), or an unphosphorylatable NT form (Rfa2-A_X), display further reduced total adaptation (Figure 3.8. Table 3.2). However, in the presence of a hyper-phospho-mimetic NT form of Rfa2 (Rfa2-D_X), adaptation in *rdh45*Δ mutants increased markedly to approximately 66% by 24 hours, 75% by 48 hours post-HO induction (Figure 3.8, Table 3.2). Consistent with the observed adaptation rescue or adaptation prevention, analysis of Rad53 phosphorylation (indicative of checkpoint activation) and dephosphorylation(indicative of checkpoint exit) revealed two features (Figure 3.9): *1)* adaptation-deficient cells display a more pronounced activation of Rad53, as indicated by even slower mobility species observed for *rdh54*Δ, *rdh54*Δ *rfa2-A*$_X$, and *rdh54*Δ *rfa2-*Δ*N*$_X$ mutants, and *2) rdh54*Δ *rfa2-D*$_X$ mutant cells result in detection of dephosphorylated Rad53 by 16 hrs post-HO induction. If Rfa2 NT phosphorylation helps facilitate checkpoint adaptation, then it was possible that in adaptation-deficient cells that Rfa2 phosphorylation would be reduced. Examination of Rfa2 phosphorylation in *rdh54*Δ cells revealed that Rfa2 is still detectably phosphorylated; however, this phosphorylation is consistently delayed and/or reduced (Figure 3.10). Furthermore, the mobility of the phospho-species is not as reduced as in WT adaptation-proficient cells (Figure 3.5), indicating more phosphorylation of Rfa2 in WT *vs. rdh54*Δ cells. As observed in WT cells, Rad53 dephosphorylation begins to occur within the temporal window within which we observed Rfa2 NT phosphorylation. A similar phenomenon was observed in *rdh54*Δ mutants where detectable Rfa2 phosphorylation at 16-20 hours also display reduced Rad53 phosphorylation at the same times. This suggests that Rfa2 phosphorylation is the direct cause of Rad53 dephosphorylation during adaptation.

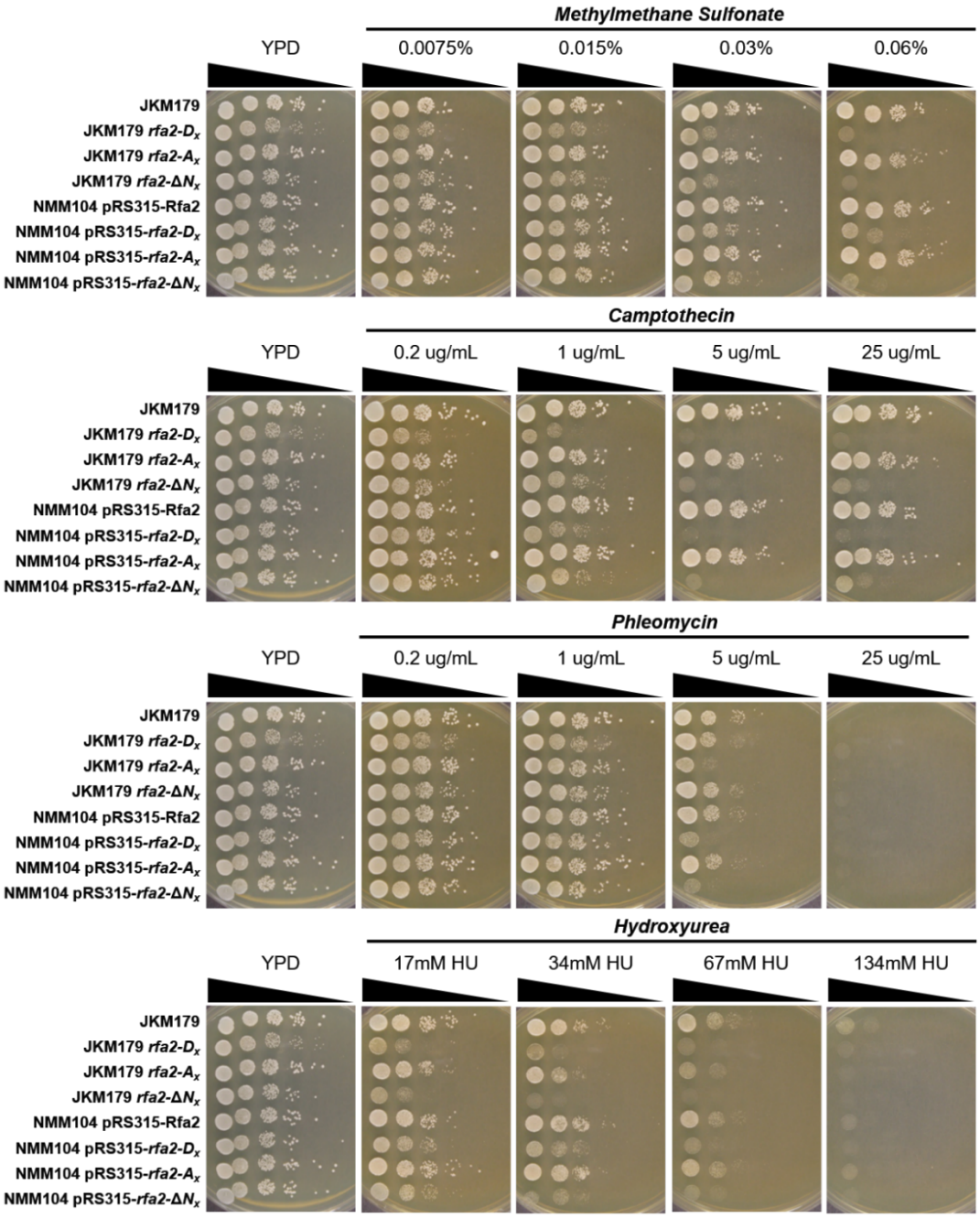

Figure 3.6. Comparison of Rfa2 NT extensive mutant integrations versus plasmid-borne expression

JKM179 cells containing *RFA2, rfa2-D*$_X$, *rfa2-A*$_X$, or *rfa2-*Δ*N*$_X$ and NMM104 cells containing pRS315-derivative Rfa2 NT extensive mutation vectors were grown overnight and harvested the next day. Six 10-fold serial dilutions were performed starting at an OD_{600} = 1.0 and spotted on YPD media or YPD media containing genotoxic agents at indicated concentrations. After 2 days, plates were analyzed and photographed. Cells containing the *rfa2-D*$_X$ or *rfa2-*Δ*N*$_X$ mutations were sensitive to genotoxic agents irrespective of whether the mutation was conferred by chromosomal integration or through ectopic expression via pRS315. Cells containing *rfa2-A*$_X$ were no more sensitive to genotoxic stress than cells containing *RFA2*, consistent with previous observations.

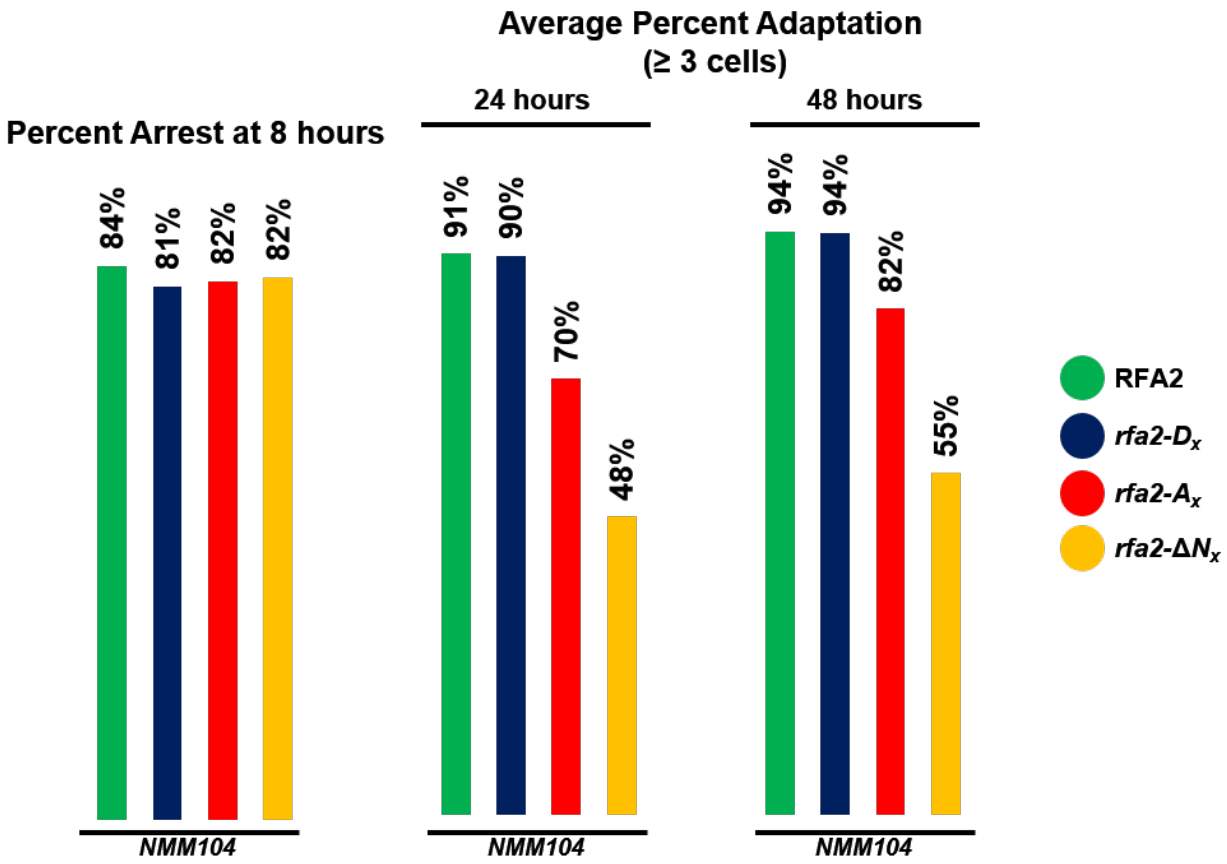

Figure 3.7. The N-terminus and its phospho-state affect checkpoint adaptation.
NMM104 cells containing Rfa2 NT mutations were grown in YPR media for 16 hours to an OD_{600} = 1.0 and 20% galactose was added to each culture to a final concentration of 2% to induce expression of HO endonuclease. Cells were then harvested from HO-induced culture at 8 hours, diluted, spread on YPRG plates using glass beads, and then analyzed microscopically and quantitated at 8, 24, and 48 hours post-HO induction. Averages are from three independent replicate data sets. HO expression was induced in exponentially growing cells by adding 2% galactose to the media. *rfa2-A$_X$* or *rfa2-ΔN$_X$* display reduced average adaptation compared to RFA2 cells. *rfa2-D$_X$* adapts indistinguishably from RFA2 cells.

Table 3.1. Average Adaptation Percentages in NMM104 cells.

Strain	Percentage of clusters ≥ 3 Cells at 8 hours	Average Adaptation by 24 hours	Average Adaptation by 48 hours
WT	8%	82%	86%
rfa2-D$_X$	11%	79%	83%
rfa2-A$_X$	11%	59%	71%
rfa2-ΔN$_X$	10%	38%	45%

Average adaptation was calculated by subtracting the total number of cells greater than or equal to three cells at 8 hours from total observed adaptation at 24 and 48 hours. Averages are from three independent experiments.

3.4.E. Phosphorylation at serine 122 of Rfa2 has little influence on the checkpoint adaptation function of RFA.

It is clear that Rfa2 becomes phosphorylated in response to prolonged DNA damage, whether it be a single, irreparable DSB (this study) or prolonged exposure to a clastogen, such as phleomycin (Ghospurkar *et al.* 2015, Wilson *et al.* 2018). It has also been demonstrated that this phosphorylation occurs in addition to that at serine (S) 122 (Brush *et al.* 1996, Brush *et al.* 2000, Bartrand *et al.* 2004), and that mutation of this site has no detectable effect on the mitotic DNA damage response, as measured by DNA damage sensitivity assays (Ghospurkar *et al.* 2015). However, it did remain possible that post-translational modification of S122 could influence checkpoint adaptation, especially given the observation that an *rfa2-A$_X$* mutant displays very little DNA damage sensitivity, yet it shows reduced adaptation efficiency and further reduces the efficiency in already adaptation-deficient mutations. Examination of *rfa2-S122A* and *rfa2-S122D* mutations microscopically to measure adaptation efficiency revealed that neither of these mutations had a role in checkpoint adaptation in otherwise WT cells (Figure 3.11). When combined with an Rfa2 NT mutant (*rfa2-D$_X$*) that rescues adaption in two adaptation-deficient mutations, the addition of the *rfa2-S122* mutation had little effect (Figure 3.11B). When combined with the *rfa2* NT deletion mutation (*rfa2-*ΔN_x) that already displays a 50% reduction in checkpoint adaptation, the addition of an *rfa2-S122* mutation only had an effect when S122 was unphosphorylatable (slight reduction of 9-10% compared to *rfa2-*ΔN_x alone; Figure 3.11C, Table 3.3).

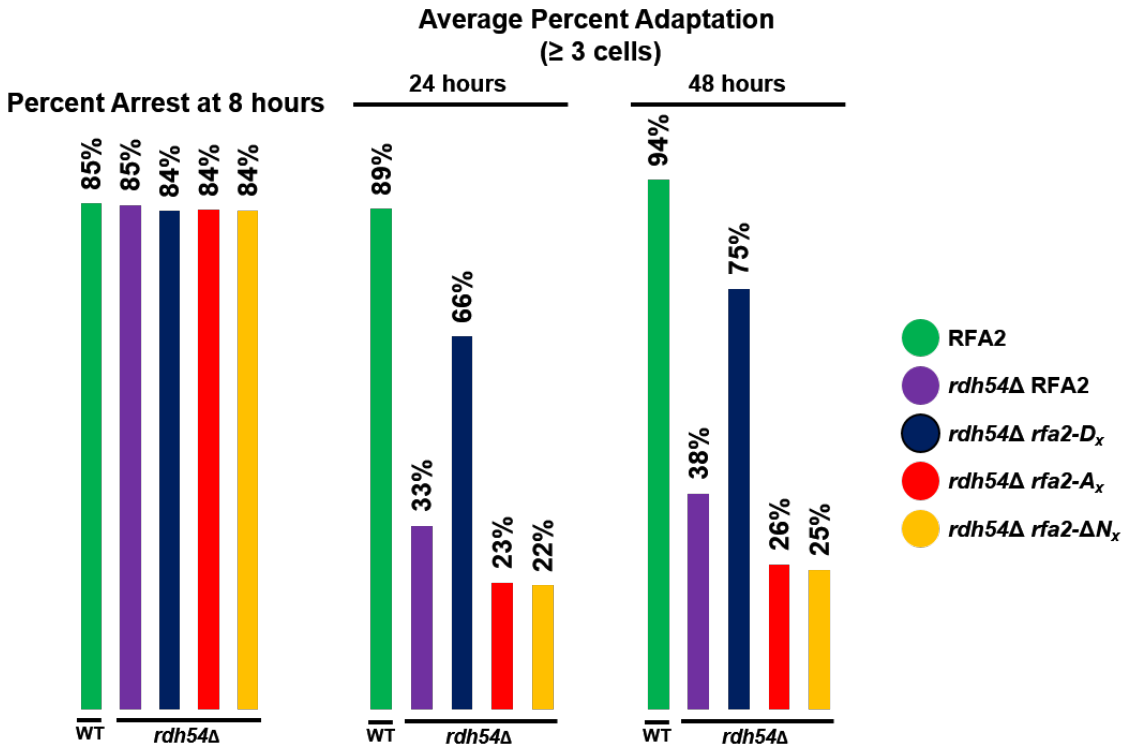

Figure 3.8. The phospho-state of the Rfa2 NT affects the ability of checkpoint adaptation to be rescued in the adaptation-deficient *rdh54*Δ mutation.
Rfa2 NT phospho-state determines rescue of *rdh54*Δ cells during checkpoint adaptation. *rdh54*Δ cells containing Rfa2 NT mutations were grown to an OD_{600} = 1.0 in YPR media and 20% galactose was added to a final concentration of 2% to induce HO-endonuclease expression. Cells were then harvested from HO-induced culture and analyzed microscopically as described. *rdh54*Δ cells containing *rfa2-A*$_X$ or *rfa2-*Δ*N*$_X$ display reduced average adaptation compared to *rdh54*Δ RFA2. *rfa2-D*$_X$ confers greatly increased adaptation proficiency to *rdh54*Δ cells. Averages are from three independent replicate data sets.

Table 3.2. Average Adaptation Percentages observed in *rdh54*Δ cells containing Rfa2 NT mutations.

Strain	Percentage of clusters ≥ 3 Cells at 8 hours	Average Adaptation by 24 hours	Average Adaptation by 48 hours
WT	7%	83%	88%
rdh54*Δ *Rfa2	8%	23%	32%
***rdh54*Δ *rfa2-D*$_X$**	8%	55%	67%
***rdh54*Δ *rfa2-A*$_X$**	7%	16%	19%
***rdh54*Δ *rfa2-*Δ*N*$_X$**	7%	15%	18%

Average adaptation was calculated by subtracting the total number of cells greater than or equal to three cells at 8 hours from total observed adaptation at 24 and 48 hours. Averages are from three independent experiments.

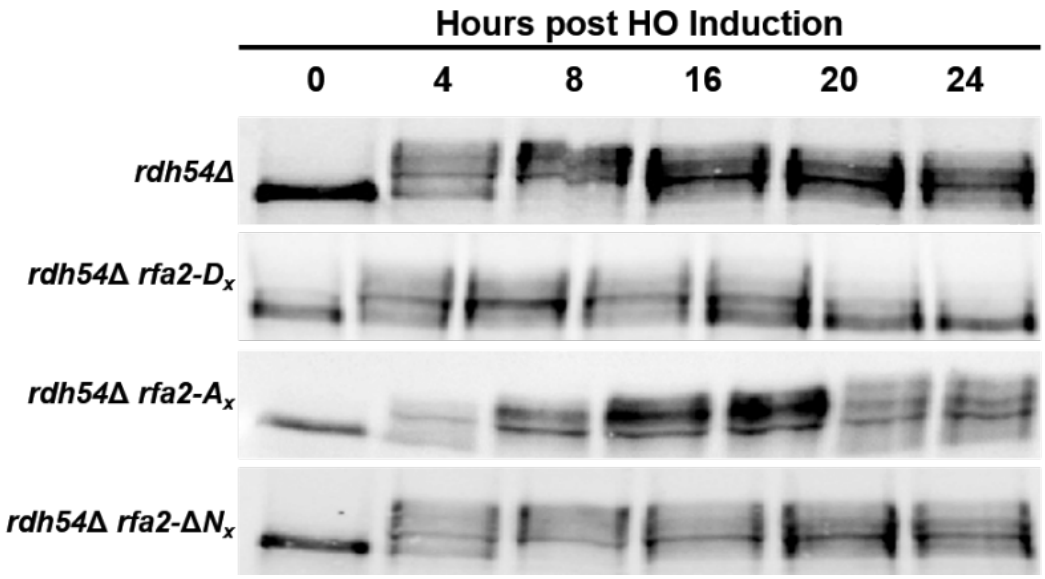

Figure 3.9. Rad53 activation corresponds to the ability of the Rfa2 NT mutation to rescue checkpoint adaptation in the adaptation-deficient *rdh54*Δ mutation.
Rad53 activation corresponds with Rfa2 NT mutation rescue in checkpoint adaptation-deficient *rdh54*Δ*.* Immunoblots depicting Rad53 phosphorylation and dephosphorylation during checkpoint adaptation in *rdh54*Δ cells containing Rfa2 NT mutations. Mutant cells were grown in YPR for 16 hours and HO-endonuclease expression was induced by adding 20% galactose to the culture to a final concentration of 2%. At indicated time points, 10 OD_{600} of cells were harvested and whole cell lysate was isolated via K-buffer extraction. Following quantitation of protein concentration using an RC-DC kit, 40 ug total protein was used in SDS-PAGE.

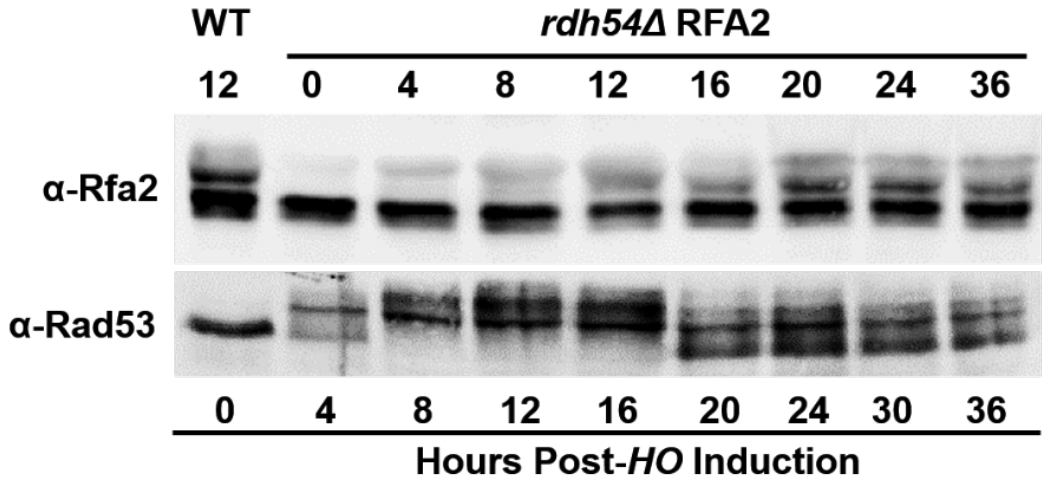

Figure 3.10. Hyper-phosphorylation of the Rfa2 NT occurs but is reduced in the adaptation-deficient *rdh54*Δ mutation.
Hyper-phosphorylation of the Rfa2 NT occurs, but is impaired in the adaptation-deficient *rdh54*Δ mutation*. A.* Immunoblots depicting Rfa2 NT hyper-phosphorylation (Top Panel) and Rad53 phosphorylation and dephosphorylation (Bottom Panel) during checkpoint adaptation in *rdh54*Δ cells containing Rfa2 NT mutations. As Rfa2 phosphorylation increases Rad53 phosphorylation is decreases, specifically between 20-24 hours. Induction of HO, protein collection, and total protein used in immunoblots was performed as described.

3.4.F. A naturally phosphorylated Rfa2 NT mutation also drives checkpoint adaptation in otherwise adaptation-deficient *rdh54*Δ cells.

A previous study demonstrated that the domain substitution of the yeast Rfa2 NT for the human Rpa2 NT (Rfa2-h2NT) resulted in the chimeric Rfa2 protein in yeast cell being phosphorylated on the N-terminus in a similar fashion to that measured in human cells for human Rpa2 (Ghospurkar *et al.* 2015). Similarities include not only the residues modified and whether or not they are in a DNA damage-dependent manner, but they also include the timing of the events. Within 2-4 hr, the chimeric Rfa2 containing the human Rpa2 NT is maximally phosphorylated in this domain (Ghospurkar *et al.* 2015).We took advantage of this mutant, as it is naturally phosphorylated in its N-terminus in response to clastogen exposure (Ghospurkar *et al.* 2015). To determine if a single, irreparable DSB would also trigger its natural phosphorylation in yeast cells, we induced HO expression in NMM104 containing only the *rfa2-h2NT* allele. Examination of Rfa2 phosphorylation in these cells revealed strong phosphorylation of *rfa2-h2NT* by 4 hrs post-HO induction (Figure 3.12, top panel). An additional slower-mobility species was also observed at 20 hr post-HO induction. Phosphorylation observed for *rfa2-h2NT* in *rdh54*Δ cells was indistinguishable from that in *RDH54* cells, suggesting that the *rdh54*Δ did not impact the ability for the human Rpa2 NT to be modified (Figure 3.12, top panel compared with bottom panel). This is different than the phosphorylation of WT Rfa2 in *rdh54*Δ cells, and perhaps reflects a difference in the enzymes that modify these two domains in yeast.

Because *rfa2-h2NT* is readily phosphorylated in JKM179 derivatives, we addressed whether this modification of the N-terminus could drive checkpoint adaptation in otherwise adaptation-deficient *rdh54*Δ cells. Microscopic examination of *rdh54*Δ *rfa2-h2NT* cells following induction of HO endonuclease revealed that adaptation proficiency in *rdh54*Δ can be restored to approximately 70% by 24 hr, 80% by 48 hr (compared to 34% by 24 hr and 38% by 48 hr observed for *rdh54*Δ cells; Figure 3.13, Table 3.4). This data suggests that *naturally driven* phosphorylation, and not just a phospho-mimetic mutation form, of the Rfa2 NT can override the prolonged checkpoint arrest that occurs in *rdh54*Δ cells.

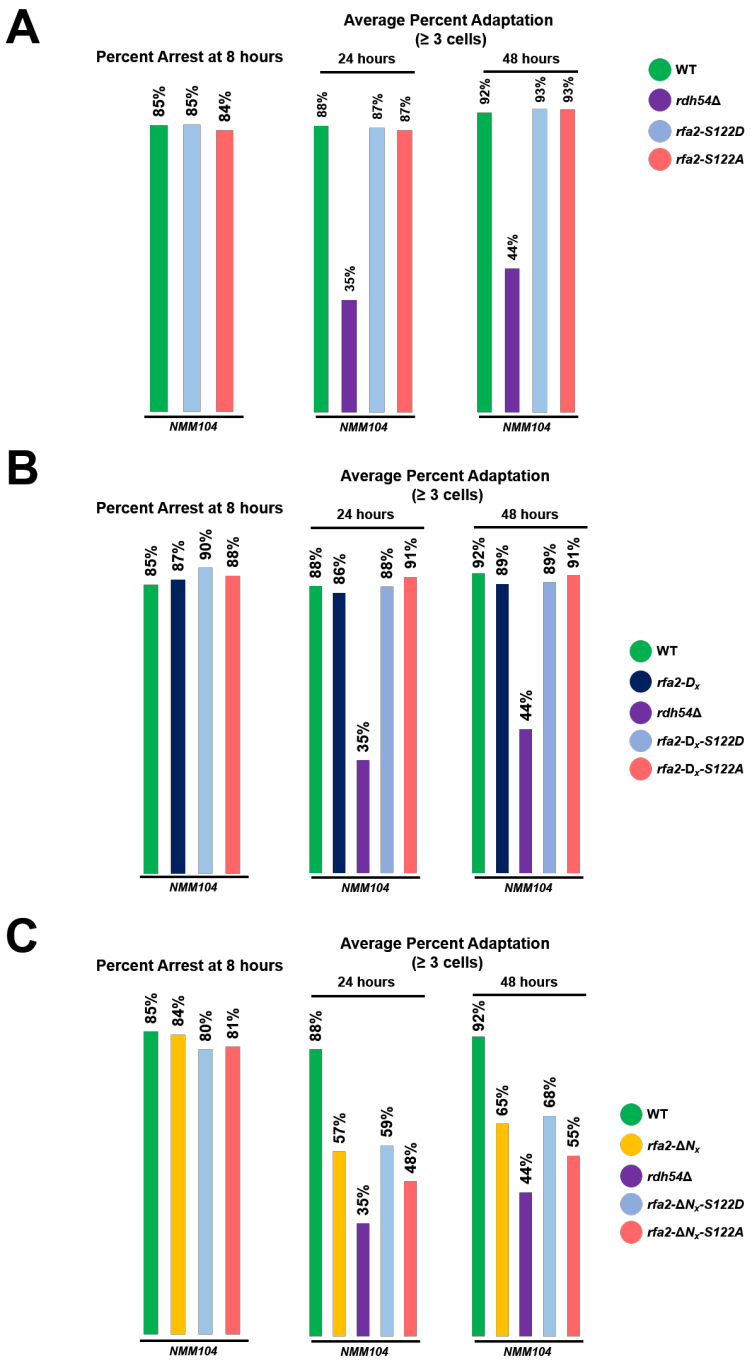

Figure 3.11. A known phosphorylation target (S122) outside of the Rfa2 NT does not affect checkpoint adaptation.

Hyper-phosphorylation of the Rfa2 NT occurs, but is impaired in the adaptation-deficient *rdh54*Δ mutation. ***A.*** Phospho-mimetic mutation of S122, a known Mec1 phospho-site, does not impact checkpoint adaptation frequency in otherwise wild-type cells. ***B.*** Phospho-mimetic mutation of S122, combined with *rfa2-D*$_X$, does not change observed adaptation rescue conferred by *rfa2-D*$_X$. ***C.*** Adaptation deficiency conferred by *rfa2-*Δ*N*$_X$ is unable to be overcome by phospho-mimetic mutation of S122. Averages presented are from three independent replicate data sets. Induction of HO and microscopic analysis was performed as described. Averages are from three independent replicate data sets.

Table 3.3. Mutation of a known, Mec1-phospho-target site on Rpa2 does not greatly impact adaptation proficiency or deficiency conferred by Rfa2 phospho-mutants.

Strain	Percentage of clusters ≥ 3 Cells at 8 hours	Average Adaptation by 24 hours	Average Adaptation by 48 hours
rfa2-S122D	15%	73%	78%
rfa2-S122A	16%	70%	76%
rfa2-D$_X$	13%	73%	75%
rfa2-D$_X$-S122D	10%	78%	79%
rfa2-D$_X$-S122A	12%	78%	79%
rfa2-ΔN$_X$	16%	41%	49%
rfa2-ΔN$_X$-S122D	20%	38%	48%
rfa2-ΔN$_X$-S122A	19%	28%	36%

Average adaptation was calculated by subtracting the total number of cells greater than or equal to three cells at 8 hours from total observed adaptation at 24 and 48 hours. Averages are from three independent experiments.

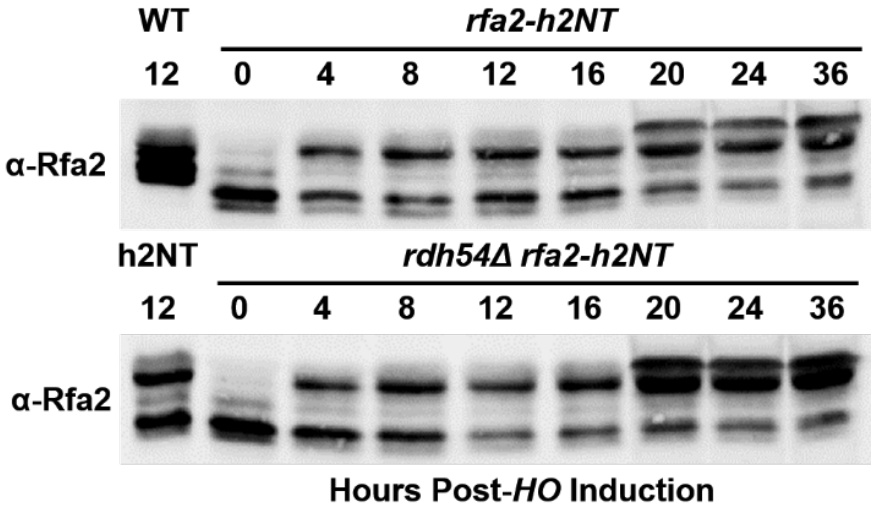

Figure 3.12. Natural hyper-phosphorylation of the Rfa2 NT occurs indistinguishably in both the adaptation-proficient *RDH54* strain and the adaptation-deficient *rdh54*Δ mutation.
Natural hyper-phosphorylation of the Rfa2 NT occurs indistinguishably in *RDH54* and *rdh54*Δ cells. Immunoblots depicting *rfa2-h2NT* hyper-phosphorylation in *RDH54* (Top Panel) and *rdh54*Δ cells (Bottom Panel). Optimal *rfa2-h2NT* hyper-phosphorylation is observed by 20 hours in each mutation, with significant hyper-phosphorylation occurring by 4 hours. Induction of HO, protein collection, and total protein used in immunoblots was performed as described.

Biochemical monitoring of Rad53 reveals a coordinate decrease in phosphorylated (activated) Rad53 in *rdh54*Δ *rfa2-h2NT* cells (Figure 3.14), suggestive that phosphorylation of the Rfa2 NT in these cells is causative of Rad53 dephosphorylation resulting in restoration of checkpoint adaptation. The

adaptation proficiency conferred by Rfa2 NT phospho-mutations in *rdh54*Δ is reduced when compared to proficiency conferred by an Rfa1 mutation, *rfa1-t11*. *rdh54*Δ cells containing *rfa1-t11* adapt at nearly 90% by 24 hours (Lee *et al.* 2001).

3.4.G. Regions of the Rpa2 NT and their importance in checkpoint adaptation

It is clear that a phospho-mimetic form (*rfa2-D*$_X$), and now a naturally-phosphorylated NT form (*rfa2-h2NT*), can both drive checkpoint adaptation in *rdh54*Δ cells. It has been difficult to identify which residue(s) in the yeast Rfa2 NT are being modified, presumably due to overlap of modification of some of the residues. In an attempt to identify which residues might be targets during prolonged DNA damage, we used *rfa2* NT mutations where clusters of 3-4 residues were mutated to aspartates (D) or alanines (A) (Figure 3.14); these mutations have been previously characterized with respect to DNA damage sensitivity and synthetic genetic interaction (Ghospurkar *et al.* 2015). In all cases tested previously, mutations of subregions 1 and 3 were responsible for all observed damage sensitivities and/or synthetic genetic interactions.

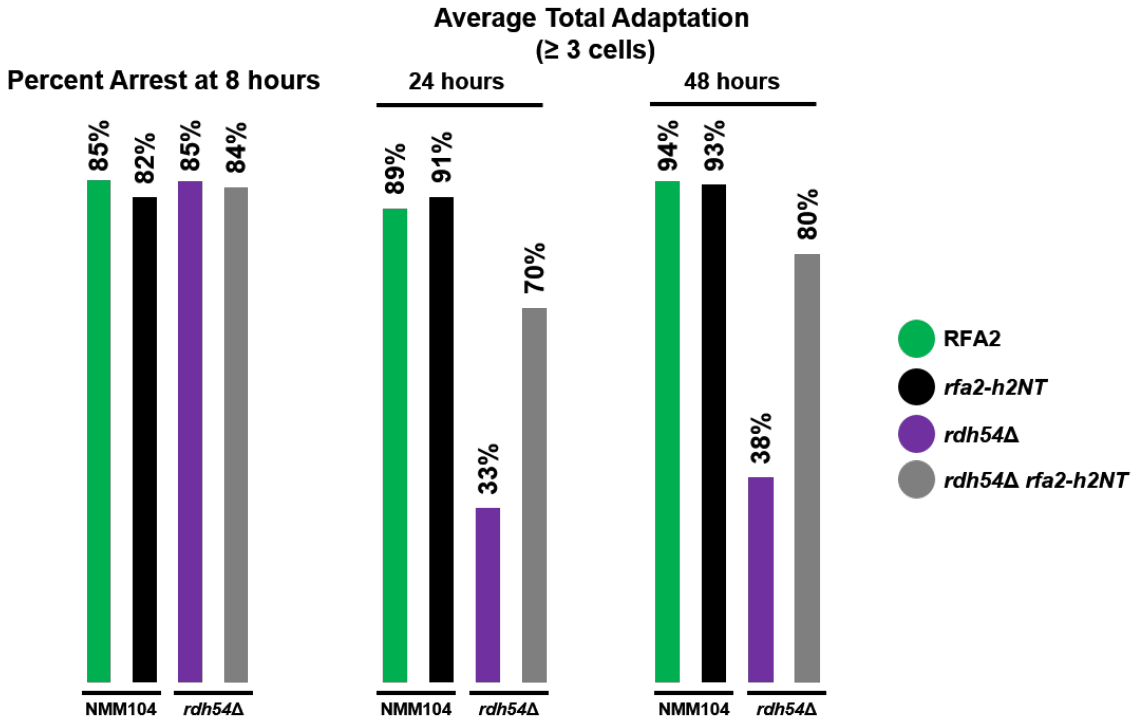

Figure 3.13. Natural hyper-phosphorylation of the Rfa2 NT drives adaptation proficiency in the adaptation-deficient *rdh54*Δ mutation.
*rdh54*Δ cells containing the *rfa2-h2NT* mutation were harvested from HO-induced culture and analyzed microscopically as described. *rfa2-h2NT* mutation confers modest increases in adaptation proficiency to *rdh54*Δ cells compared with *rfa2-D*$_X$ (Figure 3.6).

Table 3.4. Average Adaptation Percentages conferred by *rfa2-h2NT* in *rdh54Δ* cells.

Strain	Percentage of clusters ≥ 3 Cells at 8 hours	Average Adaptation by 24 hours	Average Adaptation by 48 hours
WT	7%	83%	88%
rfa2-h2NT	9%	82%	84%
rdh54Δ Rfa2	8%	23%	32%
rdh54Δ rfa2-h2NT	7%	62%	74%

Average adaptation was calculated by subtracting the total number of cells greater than or equal to three cells at 8 hours from total observed adaptation at 24 and 48 hours. Averages are from three independent experiments.

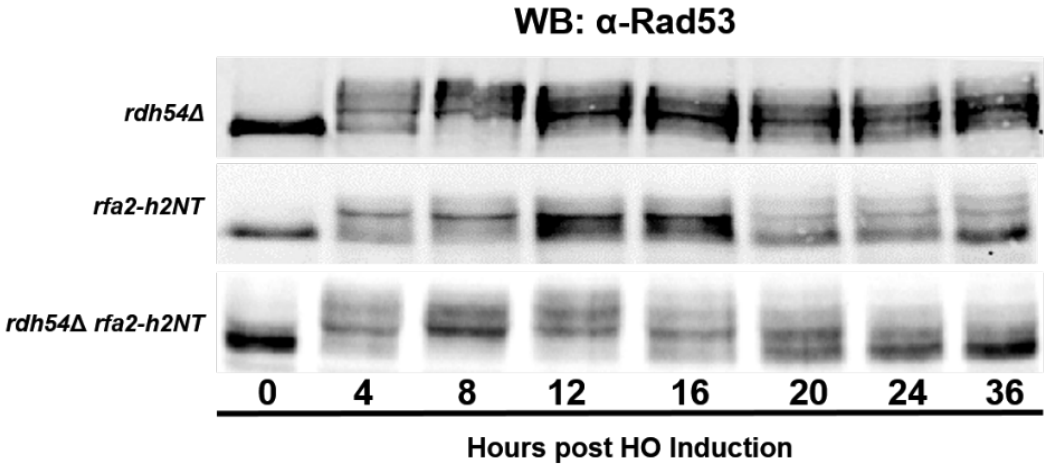

Figure 3.14. Rad53 activation corresponds to the ability of the Rfa2 NT mutation to rescue checkpoint adaptation in the adaptation-deficient *rdh54*Δ mutation.
rfa2-h2NT promotes Rad53 dephosphorylation indistinguishably in *RDH54* and *rdh54*Δ cells*. A.* Immunoblots depicting *Rad53* phosphorylation and dephosphorylation in *rdh54*Δ RFA2 cells (Top Panel), *RDH54 rfa2-h2NT* cells (Middle Panel) and *rdh54*Δ *rfa2-h2NT* cells. Optimal Rad53 activation occurs by 4 hours in each mutation, however, *RDH54 rfa2-h2NT* and *rdh54*Δ *rfa2-h2NT* appear to promote more rapid inactivation of Rad53 by 12 and 16 hours, respectively. Induction of HO, protein collection, and total protein used in immunoblots was performed as described.

To identify which region(s) might be important during checkpoint adaptation and potential targets for phosphorylation, we examined whether mimicking phosphorylation (*rfa2-D_M* mutations) in each Rfa2 NT could promote checkpoint adaptation. Mutations in subregion 1 (*rfa2-D_{M1}*) or subregion 3 (*rfa2-D_{M3}*) displayed the most efficient checkpoint adaptation in both *RDH54* and *rdh54*Δ cells (Figure 3.16, Table 3.5), whereas mutations in subregion 2 (*rfa2-D_{M2}*) led to a slight reduction in adaptation efficiency in *RDH54* cells compared to WT *RFA2* or the other subregion mutations. Despite this, mimicking phosphorylation in any of the three subregions led to an increase in checkpoint adaptation efficiency in *rdh54*Δ mutations of 6-20% by 24 hr and 16-24% by 48 hr post-HO induction (Figure 3.16A). The level of

adaptation rescue in any of the the *rfa2-D*$_M$ mutations by 24 and 48 hr post-HO induction in an *rdh54*Δ strain is somewhat reduced from that observed for *rfa2-D*$_X$ (66% and 75%), indicating that mimicking phosphorylation in any of the subregions has a similar effect on checkpoint adaptation rescue as mutating all three subregions simultaneously (Figure 3.16).

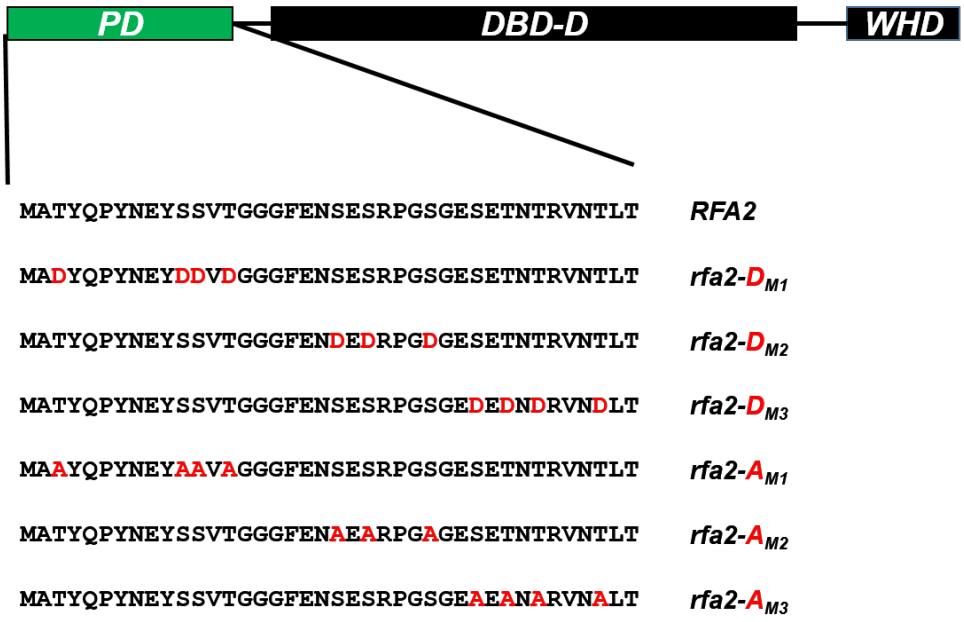

Figure 3.15. Schematic of Rfa2 NT subregion mutations.
Schematic of rfa2 NT subregion mutations. *rfa2-D*$_{M1}$ consists of S3/S11/S12/T14D, *rfa2-D*$_{M2}$ consists of S21/S23/S27D, and *rfa2-D*$_{M3}$ consists of S30/T32/T34/T38D. Analogous residues are mutated to alanine to achieve respective *rfa2-A*$_M$ mutations.

Although phospho-mimetics of any of the three subregions can promote checkpoint adaptation, phospho-mimetics of subregions 1 and 3 consistently promote slightly higher adaptation efficiency, consistent with those subregions being identified previously as those that lead to damage-sensitive and/or synthetic genetic phenotypes when mutated. Our data is also consistent with data demonstrating phosphorylation of key residues within these subregions being essential for normal mitotic growth and mitotic exit following DNA damage (Anantha et al. 2007, Anantha et al. 2008).

Conversely, preventing phosphorylation within those same subregions (*rfa2-A*$_M$ mutations) was also examined for its effect on promoting checkpoint adaptation. In *RDH54* cells, a slight reduction in checkpoint adaptation efficiency is observed at both 24 hr and 48 hr post-HO induction for *rfa2-A*$_{M1}$ (76% and 85%) and *rfa2-A*$_{M3}$ (81% and 82%) compared to WT *RFA2* cells (91% and 94%; Fig 10), suggesting that an inability to phosphorylate S/T residues in these subregions has the most influence on checkpoint

adaptation efficiency. *rfa2-A$_{M2}$* mutation adaption efficiency (89% by 24 hr and 91% by 48 hr) is nearly indistinguishably compared to WT *RFA2* cells (Figure 3.16). In the *rdh54*Δ mutation, the *rfa2-A$_{M1}$* mutation shows a slight reduction (24% *vs*. 34% for *rdh54*Δ cells) in checkpoint adaptation by 24 hr, but by 48 hr, all three, with subregion mutations adapt (43%, 37%, and 40% for *rfa2-A$_{M1}$*, *rfa2-A$_{M2}$*, and *rfa2-A$_{M3}$*, respectively) with a similar efficiency to *rdh54*Δ cells (38%). Interestingly, *rfa2-A$_{M1}$* cells appear to have a slower progression of adaptation, as 9% and 19% differences in adaptation efficiency are observed between 24 and 48 hr in the *RDH54* or *rdh54*Δ background, respectively. The other subregion mutations do not display more than a 3% change from 24 to 48 hr. Again, mutation of subregions 1 and 3 led to the most discernible reduction of adaptation efficiency in *RDH54* cells, suggesting these are the most important regions for checkpoint adaptation and potentially the most relevant targets for phosphorylation, promoting the strongest rescue of the *rdh54*Δ adaptation deficiency observed.

3.5. Discussion

3.5.A. Rfa2 NT phosphorylation mediates checkpoint and mitotic exit

Prior to this study, it was previously demonstrated that mimicking phosphorylation of the Rfa2 NT promoted checkpoint adaptation in adaptation-deficient *yku70*Δ mutant cells (Ghospurkar *et al.* 2015). In this study, adaptation rescue was observed in *rdh54*Δ cells containing the phospho-mimetic *rfa2-D$_X$* mutation. While it has been known that mutant forms of RPA can promote checkpoint adaptation (Lee *et al.* 2001, Ghospurkar *et al.* 2015), it is possible that the mechanism by which each RPA mutant promotes rescue does so in unique ways. Furthermore, *RDH54* has been deemed essential in alleviating checkpoint arrest in response to a permanent DNA lesion, however, this study demonstrates that phospho-mimetic Rfa2 NT mutations are sufficient to promote adaptation rescue in this severely adaptation-deficient strain. Based on our findings, we suggest that RPA, as the primary sensor of ssDNA in eukaryotic cells and the phospho-state of the Rfa2 NT, must play a key role in the decision to exit the DNA damage-dependent checkpoint in response to irreparable lesions.

The hypothesis that phosphorylation of RPA drives mitotic exit is not entirely novel. In fact, previous studies done in human U2-OS osteocarcinoma and HCT116 colorectal cancer cells have determined that the phospho-state of Rpa2 does play a role in mediating mitotic exit. Rpa2 NT phosphorylation during mitosis has been demonstrated to occur at S23 and S29 by cyclin B-Cdc2, or

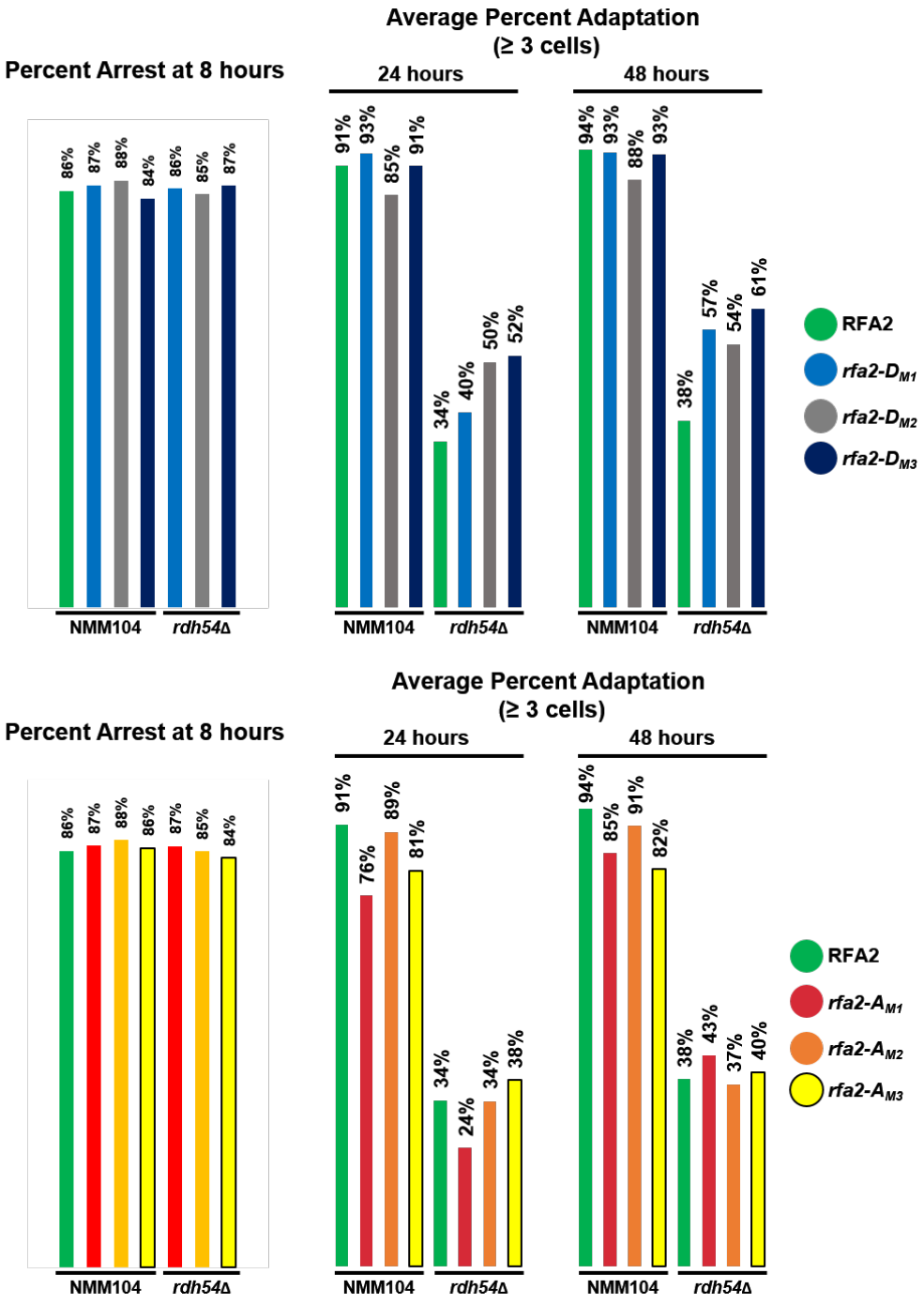

Figure 3.16. Rfa2 NT subregion mutations and their effect on adaptation in *RDH54* and *rdh54*Δ mutant cells.
A. *rfa2-D$_M$* mutations promote checkpoint adaptation in *rdh54*Δ cells, albeit with reduced effect when compared to *rfa2-D$_X$*. Averages are from three independent replicate data sets. **B.** Checkpoint adaptation is generally inhibited in *rdh54*Δ *rfa2-A$_M$* mutations, conferring minimal increases in adaptation proficiency when compared to that observed for *rdh54*Δ *rfa2-A$_X$* cells. Averages are from three independent replicate data sets.

Table 3.5. Average Adaptation Percentages conferred by Rfa2 subregion mutations.

Strain	Percentage of clusters ≥ 3 Cells at 8 hours	Average Adaptation by 24 hours	Average Adaptation by 48 hours
rfa2-A$_{m1}$	13%	63%	72%
rfa2-A$_{m2}$	12%	77%	78%
rfa2-A$_{m3}$	14%	67%	68%
rfa2-D$_{m1}$	13%	80%	80%
rfa2-D$_{m2}$	12%	72%	76%
rfa2-D$_{m3}$	16%	75%	77%
rdh54Δ	11%	23%	27%
rdh54Δ + rfa2-A$_{m1}$	13%	11%	30%
rdh54Δ + rfa2-A$_{m2}$	15%	19%	23%
rdh54Δ + rfa2-A$_{m3}$	16%	22%	24%
rdh54Δ + rfa2-D$_{m1}$	14%	26%	43%
rdh54Δ + rfa2-D$_{m2}$	15%	35%	39%
rdh54Δ + rfa2-D$_{m3}$	13%	38%	48%

Average adaptation was calculated by subtracting the total number of cells greater than or equal to three cells at 8 hours from total observed adaptation at 24 and 48 hours. Averages are from three independent experiments.

CDK (Anantha *et al.* 2008) and is thought do drive mitotic exit in response to late G_2/M encountered DNA damage. This mitotically-phosphorylated Rpa2 was also demonstrated to not be associated with chromatin-bound fractions, suggesting that phospho-Rpa2 may elicit a signaling program that is not DNA dependent during mitotic exit. Further implication of S23 and S29 phosphorylation driving mitotic exit can be found in the observation that *rpa2-S23/S29A* mutations accumulate in G2/M, indicating that cells unable to phosphorylate Rpa2 after the initial DNA damage response stall during mitotic entry (Anantha *et al.* 2008). Phosphorylation of the Rpa2 NT has been suggested to impede interaction with ATM and DNA-PK (Oakley *et al.* 2003), as well as the MRN complex (Oakley *et al.* 2009). Moreover, *in vitro* data suggests that dephosphorylation of Rpa2 restores the ability of RPA to interact with the aforementioned DNA damage response proteins (Oakley *et al.* 2003).

In a previous study, it was demonstrated that *rfa2-h2NT* in yeast cells is able to become phosphorylated in a damage-dependent manner at the S4, S8, S12, T21, S29, and S33 (Ghospurkar *et*

al. 2015) – phospho-sites that are also observed in human cells (Anantha *et al.* 2008, Marechal *et al.* 2015). Similar to that observed for *rdh54*Δ *rfa2-D*$_X$, *rdh54*Δ mutant cells containing *rfa2-h2NT* mutation also adapt at a much higher frequency than those that contain Rfa2 or unphosphorylatable forms of the Rfa2 NT (*rfa2-A*$_X$ or *rfa2-*Δ*N*$_X$, Figure 3.9, Table 3.2 and Figure 3.14, Table 3.4). This demonstrates that, when the Rfa2 NT is in a more readily phosphorylatable state, the phospho-state of Rpa2/Rfa2 are likely key in the initial molecular decisions involved in mitotic exit.

3.5.B. Certain subregions of the Rfa2 NT may be preferential phospho-targets during mitotic exit

Certain subregions of the Rfa2 NT, when mutated to a phospho-mimetic state (*rfa2-D*$_{M1}$ and *rfa2-D*$_{M3}$, Figure 3.17, Table 3.5), are also capable of promoting checkpoint adaptation in *rdh54*Δ cells, albeit reduced to that observed for *rfa2-D*$_X$. This evidence suggests that phosphorylation or phospho-mimetic mutation of just a few residues within the Rfa2 NT are sufficient to promote adaptation-deficient rescue. Moreover, preventing phosphorylation in these regions through alanine mutagenesis (*rfa2-A*$_{M1}$ and *rfa2-A*$_{M3}$, Figure 3.17, Table 3.5) also appear to impede checkpoint exit due to an irreparable lesion. This further implicates the Rfa2 NT phospho-state as a key regulator of the decision to enter mitosis when damaged DNA is present in cells.

3.5.C. Ubiquitination and sumoylation of RPA is dispensable during the DDC

Other post-translational modification of RPA has been implicated as being essential for regulating the DNA damage response (replication restart, resumption to normal mitotic growth) and resistance to clastogen challenge, namely sumoylation and ubiquitination (Dou *et al.* 2010, Elia *et al.* 2015, Marechal *et al.* 2015). However, as stated previously, these studies were performed in E3 sumo/ubiquitin ligase deletions or RNAi knockdowns, making it difficult to distinguish whether modification of the RPA complex, or other E3 ligase targets, are the dominant drivers of the observed checkpoint and repair deficiencies. Moreover, ubiquitination or sumoylation of Rfa2, in budding yeast, appears to be dispensable for DNA repair. Cells containing a 'lysine-less' Rfa2 mutation (Rfa2-R$_X$) appear to have DNA damage sensitivities in line with unmodified cells (unpublished data, WAL; Wilson *et al.* 2018b) suggesting that ubiquitin-dependent modification of Rfa2 is dispensable for the DNA damage response. However, preventing ubiquitin-dependent modification of Rfa1 does lead to a synthetic defect in cells challenged with typical clastogens (data not shown). The observation of additional phospho-species in *rfa2-R*$_X$ mutants suggests

that ubiquitin-dependent modification of Rfa2 may control the extent of phosphorylation the Rfa2 NT is subjected to. We speculate that additional phosphorylation of an otherwise unmodified Rfa2 would promote checkpoint adaptation in *rdh54*Δ cells. Promoting additional phosphorylation of Rfa2, through elimination of ubiquitin-dependent modification, facilitates checkpoint exit in *rdh54*Δ cells (unpublished data, WAL; Wilson *et al.* 2018b).

3.5.D. Phosphorylation of the Rfa2 NT rescues adaptation-deficient *rdh54*Δ

Rescue of *rdh54*Δ checkpoint adaptation deficiency has been demonstrated to be possible with mutation of large subunit, Rfa1, of the RPA complex (*rfa1-t11,* Lee *et al.* 2001). However, it has been reported that this is likely due to reduced checkpoint signaling, or checkpoint dampening, caused by inefficient interaction between RFA and Rad24-RFC2-5 that impairs loading of the 9-1-1 clamp which would impede full Mec1 activation (Zou *et al.* 2003, Majka *et al.* 2006, Majka *et al.* 2006, Piya *et al.* 2015). Cells containing *rfa1-t11* have been demonstrated to be hyper-sensitive to clastogens; however, Rfa2 NT mutations have variable sensitivity to clastogens (Ghospurkar *et al.* 2015). Cells containing *rfa2-D$_X$* or *rfa2-*Δ*N$_X$* mutations exhibit clastogen sensitivities in line with *rfa1-t11* (Ghospurkar *et al.* 2015); however, Rfa2-h2NT (Ghospurkar *et al.* 2015), Rfa2-R$_X$ (Wilson *et al.* 2018), Rfa2-A$_X$ (Ghospurkar *et al.* 2015) all appear to be resistant to DNA damaging agents to the same degree as unmodified cells. This demonstrates that phosphorylation of Rfa2 is not correlated with whether or not a cell will be sensitive to DNA damaging agents and suggests that phosphorylation of Rfa2 during DNA repair is dispensable and may also provide rationale as to why Rfa2 NT phosphorylation is difficult to detect in clastogen-challenged mitotic cells. While Rfa2 NT phosphorylation may not influence the ability of cells to perform DNA repair, it may influence the ability of cells to overcome irreparable lesions that might otherwise lead to permanent arrest or apoptosis.

Phosphorylation of the Rfa2 NT may become critical when cells have experienced a prolonged DNA damage response or in the face of an irreparable lesion. *rdh54*Δ cells containing unphosphorylatable Rfa2 NT mutations (Rfa2-A$_X$ or Rfa2-ΔN$_X$) never recover from the irreparable lesion, suggesting that some modification of the Rfa2 NT is necessary to recover from a prolonged DNA damage-dependent checkpoint response. Moreover, *naturally* phosphorylatable Rfa2 mutations appear to

drive robust checkpoint adaptation in *rdh54*Δ, alluding to the requirement of Rfa2 NT phosphorylation in driving checkpoint exit in the presence of an irreparable lesion.

Ultimately, cells need to commit to a molecular decision that either commit cells to permanent arrest and eventual death or leads to an aberrant mitotic division in the presence of DNA damage, in the hope that during subsequent rounds of DNA replication that that lesion can be repaired. In adaptation-deficient cells, Rfa2 NT phosphorylation is observed between 4-8 hours post-HO induction (Figure 3.5, Figure 3.10 and Figure 3.12), suggesting that phosphorylation of the NT does not occur during the initial DNA damage response, but rather occurs much later. Our data also suggests that phosphorylation of the Rfa2 NT is at the forefront of this molecular decision-making process, rather than being essential for DNA repair or the initial DNA damage response. Moreover, while ablation of the established DNA damage-dependent checkpoint may provide the cell with a last-ditch mechanism to survive, in the context of a more complex organism this may lead to significant genome instability that gives rise to mutations that, in human cells, lead to cellular disease such as cancer. Identifying the mechanism(s) of how Rfa2 NT phosphorylation facilitates the molecular commitment to override an established DNA damage-dependent checkpoint may yet reveal a novel signaling pathway, driven by RPA, which promotes checkpoint override and mitotic exit in the presence of genomic catastrophe.

3.6. Acknowledgements

Timothy M. Wilson created the *rdh54*Δ used in this study and planned and performed most experiments. **Angela M. Adsero** performed diagnostic spot assays on JKM179 Rfa2 NT extensive mutations (Figure 3.6) **Erin M. Richards** (undergraduate) performed plasmid shuffle of *rdh54*Δ to generate mutations containing *rfa2-D$_X$-S122$_{A/D}$* or *rfa2-*Δ*N$_X$-S122$_{A/D}$* and evaluated each mutation microscopically during adaptation (Figure 3.11). **Wendy A. Larson** (graduate) performed plasmid shuffle in *rdh54*Δ to generate mutations containing Rfa2-R$_X$ and analyzed *rdh54*Δ *rfa2-R$_X$* mutants in adaptation. **Barbara L. Senger** (undergraduate) performed *in vitro* site-directed mutagenesis to create *rfa2-D$_X$-S122$_{A/D}$* and *rfa2-R$_X$* plasmids. **Nolan M. Miles** (undergraduate) performed initial adaptation counts on *rdh54*Δ *rfa2-D$_M$/A$_M$* mutations.

CHAPTER 4: RFA2 N-TERMINAL PHOSPHORYLATION RESCUES CHECKPOINT ADAPTATION-DEFICIENT YEAST

4.1. Abstract

Checkpoint adaptation is broadly classified as the ability of cells to subvert a DNA damage-dependent checkpoint and enter mitosis despite the presence of DNA damage. While this may benefit the cell, as it provides additional rounds for mitotic division, it may be detrimental to an organism and uncontrolled cellular growth that is a hallmark of many cellular disease such as cancer. The Replication Protein A (RPA) complex has been demonstrated to interact with several critical repair and checkpoint factors during the DNA damage response. It has also been demonstrated in yeast that mutation or post-translational modification of individual RPA subunits can promote checkpoint adaptation. In this study, we show that phospho-mimetic or naturally phosphorylatable Rfa2 NT mutations cause checkpoint exit in adaptation- and resection-deficient mutations. We demonstrate that Rfa2 is natively and robustly phosphorylated during checkpoint adaptation in response to a single, controlled DSB in all mutants tested, in a manner that is different from that observed during global genotoxic stress. Furthermore, we demonstrate that Rfa2 NT phosphorylation is essential for checkpoint exit in the presence of a persistent DNA lesion in mutants containing documented adaptation deficiencies.

4.2. Introduction

Aberrant checkpoint exit in the presence of DNA damage, also known as checkpoint adaptation (Sandell *et al.* 1993, Toczyski *et al.* 1997), is thought to be dependent on several critical repair and checkpoint factors. Previous studies in budding yeast have demonstrated that mutation or deletion of CKII (heterotetrameric kinase complex; Tocyzski *et al.* 1997), Sae2 (component of MRXS endonuclease; Clerici *et al.* 2006, Gobbini *et al.* 2015), the Rtt107/Slx4 scaffold complex (dampens active checkpoints by competing with Rad9 for Dpb11 and γ-H2AX binding preventing continual Rad53 hyper-phosphorylation; Dibitetto *et al.* 2016), PP4 phosphatase complex (Pph3/Psy2 phosphatases; O'Neill *et al.* 2007) or Ptc2 (PP2C-like phosphatase required for checkpoint recovery; Leroy *et al.* 2003) lead to checkpoint adaptation deficiency and prevent aberrant mitotic exit in the presence of a persistent lesion.

Typically, in order to maintain genomic integrity, a complex, conserved signaling network is activated to stall cell growth during DNA repair. These include the first-responder complexes RPA

(Replication Protein A; Marechal and Zou 2015), MRX (Mre11-Rad50-Xrs2; Gobbini *et al.* 2016), STR-Dna2 (Sgs1-Top3-Rmi1-Dna2 Helicase/Nuclease complex; Cejka *et al.* 2010), sensor kinases Mec1 and Tel1 (Morrow *et al.* 1995, Sanchez *et al.* 1996, Gobbini *et al.* 2013), and effector kinases Rad53 and Chk1 (Sanchez *et al.* 1999, Agarwal *et al.* 2003). Rad53 and Chk1, once activated, work in concert to both inhibit Cdc5 and Clb2/Cdc28 mitotic entry signaling (Sanchez *et al.* 1999, Schleker *et al.* 2010) as well as to maintain Pds1 phosphorylation, preventing it's degradation by the APC^{CDC20} complex and entry into anaphase (Cohen-Fix *et al.* 1996, Yamamoto 1996, Cohen-Fix *et al.* 1999, Gardner *et al.* 1999, Wang *et al.* 2001).

Entry into anaphase and mitotic exit cannot be delayed indefinitely, however, and budding yeast provide a unique opportunity to readily study the processes of checkpoint establishment, recovery, and exit. Checkpoint establishment and activation can be facilitated through a single, controlled DSB at the *MAT* locus with HO endonuclease (Toczyski 2006). In unmodified yeast, homologous recombination is employed to repair the *MAT* locus, Rad53 never becomes phosphorylated (Pellicioli *et al.* 2001), and cell cycle progression resumes normally. In mutant cells, where the homologous *MAT* sequences HMR and HML have been deleted, checkpoint activation occurs and remarkably, 12-15 hours after the irreparable double-strand break (DSB) is formed, cell cycle restart occurs in a process known as checkpoint adaptation (Toczyski *et al.* 1997, Lee *et al.* 1998, Lee *et al.* 2001). Cell cycle restart in the face of a persistent lesion has been implicated in several, mutagenesis-induced cellular diseases, including cancer (Kubara *et al.* 2012, Swift *et al.* 2014, Lewis *et al.* 2016, Serrano *et al.* 2016). Checkpoint adaptation deficiency can be conferred to yeast cells through various deletions of non-essential genes thought to play important roles in their respective LPR and DDC pathways. In this study, we examined checkpoint adaptation deficiency and rescue, via genetic interaction with mutant RPA complexes, in *rtt107*Δ*, sae2*Δ*, slx4*Δ*, cka1*Δ*, cka2, ckb1*Δ*, ckb2*Δ, *pph3*Δ*, ptc2*Δ*,* and *psy2*Δ mutations. This is of significant interest, as prolonged checkpoint arrest in cells seems to promote a last-resort division mechanism that can lead to uncontrolled cellular proliferation (Serrano *et al.* 2016).

It was hypothesized previously that extensive hyper-resection of an irreparable DSB would lead to checkpoint adaptation (Lee *et al.* 1998) through alternative repair pathways like single-strand annealing (SSA), where microhomology within the resected DNA tracts allows for stable enough association of the

damaged ends to promote repair-dependent synthesis and religation of the broken DNA fragments (Bhargava *et al.* 2016). Many proteins required for DSB resection when mutated or deleted, like Sae2 or Fun30, lead to a resection-dependent adaptation-deficiency (Clerici *et al.* 2005, Eapen *et al.* 2012, Gobbini *et al.* 2015), whereas others, like Mre11, lead to resection-proficient adaptation-deficiency (Lee *et al.* 1998) despite being able to establish the Rad53-dependent checkpoint indistinguishably from normal cells. Thus, the link between resection of DSB ends and the ability of a cell to override an established damage-dependent checkpoint is unclear.

Understanding the regulatory networks involved in the DDR and DDC are essential to our understanding of how cells exit a checkpoint despite the presence of damaged genetic information. In human cells, RPA and the phospho-state of Rpa2 are thought to regulate mitotic exit (Anantha *et al.* 2008), replication restart (Liu *et al.* 2012, Ashley *et al.* 2014), and even DNA repair pathway choice (Marechal *et al.* 2015). In budding yeast Rtt107 and Slx4, as a dimer, compete for Dpb11 and γ-H2AX binding with the Rad53 chaperone Rad9 in order to dampen the established checkpoint once repair starts (Ohouo *et al.* 2010, Ohouo *et al.* 2013, Dibitetto *et al.* 2016). Sae2 deletions lead to both resection deficiency and adaptation deficiency that can be overcome through Dna2-Exo1-dependent resection (Symington 2016). Casein kinase II (CKII) is a heterotetrameric kinase complex comprised Cka1, Cka2, Ckb1, and Ckb2. The ‘A’ subunits of CKII have been demonstrated to function as the catalytic units of the Ser/Thr kinase complex, while the CKB subunits have been demonstrated to regulate kinase complex activity (Ackermann *et al.* 2001). CKII is also thought to play a critical role in mediating cell cycle entry, as deletions of individual components of the tetrameric complex *cka1*Δ and *cka2*Δ, or deletion of both *ckb1*Δ and *ckb2*Δ, disrupt expression of several cell cycle regulatory proteins (Pyerin *et al.* 2005). Furthermore, downregulation of CKII genes via RNAi in human cells has been demonstrated to induce apoptosis in tumorigenic tissues, highlighting the importance of CKII activity in mediating both cellular growth and programmed cell death (Wang *et al.* 2005). Moreover, the Ckb1 and Ckb2 subunits of CKII have been demonstrated to interact *in vitro* and *in vivo* with the Ptc2 phosphatase (Guillemain *et al.* 2007), strongly suggesting that CK2 activation of the PP2C phosphatase complex is required to dephosphorylate and inactivate Rad53 during checkpoint recovery and mitotic exit. The multifunctional role each of these

complexes and their components play during the initial LPR, the establishment of the DDC, and relief of the DDC promoting mitotic exit are also of interest.

Previous studies have demonstrated that Rfa2 N-terminal phosphorylation leads to checkpoint adaptation in adaptation-deficient mutations (Ghospurkar *et al.* 2015) Wilson *et al.* 2018b). In this study we broadly characterized the adaptation deficiencies of multiple resection-deficient and adaptation-deficient mutations. We also monitored checkpoint adaptation proficiency through immunoblot analysis of the phospho-state of Rad53. We found that not only is the Rpa2 NT required for checkpoint exit, as demonstrated previously, but natural phosphorylation or phospho-mimetic forms of the Rpa2 NT actively promote checkpoint adaptation in phosphatase- and resection-deficient cells. We demonstrate that the Rpa2 NT becomes phosphorylated in a manner distinct from that observed under global genotoxic stress with the DSB-inducer phleomycin. We show that, despite the presence of a persistent DNA lesion, Rad53 hyper-phosphorylation becomes reduced in cells containing Rpa2 phospho-mimetic mutations, and that this event induces additional rounds of cellular division. Taken together, the results from this study suggest a defined role for hyper-phosphorylation of the Rpa2 NT in regulating the DDC, which facilitates cell cycle restart as a last-resort survival mechanism, leading to aberrant cell growth and genomic instability.

4.3. Materials and Methods

4.3.A. Strains and Plasmids

Yeast strains and plasmids used in these studies are listed in Appendix A and Appendix B, respectively. All yeast strains used within this study are isogenic derivatives of JKM179 (*ho*Δ *MAT*α *hml*Δ*::ADE1 hmr*Δ*::ADE1 ade1-100 leu2-3,112 lys5 trp1::hisG ura3-52 ade3::GAL::HO*; Lee *et al*. 1998) containing *rfa2*Δ*::kanMX* (NMM104, Wilson *et al.* 2018A).

The generation o*f CKA1, CKA2, CKB1, CKB2, CHK1, DUN1* deletions in NMM104 was completed using PCR amplification of the *natMX* cassette from plasmid pFA6-NatNT2 (Euroscarf) with appropriate primers (Appendix C) containing an additional 40 nt of homologous sequence immediately upstream and downstream of the coding regions of each gene and one-step gene replacement. The same strategy was used to delete *SLX4, RTT107,* and *SAE2* using PCR amplification of the hphNX cassette from plasmid pFA6-hphNX (Euroscarf) using appropriate primers (Appendix C). Deletion

candidates were then screened via diagnostic replica plating (section 4.3.B.) and by PCR using diagnostic primers (Appendix C) using a strategy like that for the generation of yeast gene deletions (Kelly *et al.* 2001).

MEC1 kinase deletion strains utilized in this study were also generated by one-step gene replacement. However, before attempting deletion of the respective kinase gene, the *SML1* gene was first deleted by single-step gene replacement using PCR amplicon of *hphN* from pFA6-hphN (Euroscarf) using a similar method to that described above. Once verified, the *sml1*Δ::*hphN* NMM104 derivative strain was transformed *mec1*Δ*::natMX* PCR amplicons as described above. *mec1*Δ *sml1*Δ candidates were screened via diagnostic replica plating and by PCR using diagnostic primers (Table S3).

CKII *rfa1-t11* mutations were generated via two-step gene replacement as follows. pRS315-*rfa1-t11*-BsaHI was digested with MfeI to linearize the vector and target integration to the *RFA1* locus. The digested plasmid was then transformed into JKM179 *yku70*Δ cells and transformants were selected for on synthetic complete media (0.5% ammonium sulfate, 0.34% yeast nitrogen base without amino acids) containing dextrose (2%) and lacking uracil (SD-Ura). The integrants were then grown overnight in liquid YPD (1% yeast extract, 2% peptone, 2% dextrose) and plated onto media containing 0.8 µg/mL 5-fluoroorotic acid (SD+5-FOA). Genomic DNA from 5-FOA-resistant cells was isolated and PCR was performed using appropriate primers (Appendix C). This PCR product was then digested with BsaHI to determine correct integration of the *rfa1-t11* mutant allele and was subsequently sequenced (Eton Bioscience) to verify proper integration of the mutation. *rfa1-t11* damage sensitivity was also confirmed via diagnostic replica plating.

4.3.B. Diagnostic replica plating used in analysis of deletion mutants

Deletion of *SLX4, SAE2, RTT107,* CKII genes, *MEC1, TEL1, CHK1,* and *DUN1* all lead to DNA damage sensitive phenotypes. Screening of transformants picked to a master plate prior to PCR was performed via diagnostic replica plating. YPD media with or without genotoxic agents and SD- media with strain specific amino-acid dropouts were used in replica plating. Damage-sensitive candidates, or yeast that grew poorly on YPD media containing 5 ug/mL PHL or CPT were then analyzed via PCR following genomic DNA isolation as described in section 4.3.A.

4.3.C. Single DSB induction and collection of whole-cell lysate

All induction of DNA damage in cells for biochemical assays was performed in liquid culture. Yeast cells were grown for 20 hours (hr) in liquid YPD (1% yeast extract, 2% peptone, 2% dextrose) to an OD_{600} of 1.0, and subsequently sub-cultured the next day into YPR (1% yeast extract, 2% peptone, 2% raffinose) and grown for 20 hours to an OD_{600} of 2.0. A single break at the *MAT* locus via HO endonuclease was induced by adding 20% galactose to the YPR cultures to a final concentration of 2%.

To harvest an equivalent number of cells, 10 ODs of cells were harvested from each culture at time-points indicated in figures. Harvested cells were treated with 0.1 M NaOH for 10 minutes at room temperature, pelleted at 10K RPM for 2 minutes (min), and aspirated to remove NaOH from the pellet. The pelleted cells were then resuspended in 500 uL of K-Buffer (0.06 M Tris-HCl, ph 6.8, 5% glycerol, 2% SDS, 4% β-mercaptoethanol, 10 mM DTT; Kushnirov 2000), and each protein sample was boiled at 100°C for 3 min. A Lowry assay (Bio-Rad RC-DC Assay Kit) was used to quantify protein concentration within each sample to ensure even protein loading during SDS-PAGE.

4.3.D. Checkpoint adaptation plating assays

Cells for the checkpoint adaptation plating assays were grown in liquid culture as described above. A single break at the *MAT* locus via HO endonuclease was induced by adding 20% galactose to the YPR cultures to a final concentration of 2%. Cells were grown for 8 hours in YPR-Gal media to sync cells at the G2/M checkpoint.

To observe cellular adaptation, 0.05 OD_{600} of cells were plated onto YPRG (1% yeast extract, 2% peptone, 2% raffinose, 2% galactose) media and spread using glass beads. Cells were counted under 20x optical zoom on an Olympus microscope, and then categorized based on observed counts as described in Chapter 3, section 3.3.C.

4.3.E. SDS-PAGE and Immunoblotting

K-Buffered Whole-cell lysate from each sample was loaded into SDS-PAGE gels containing a 4% stacking gel (37.5:1 mono:bis) and 12% (150:1 mono:bis) or 15% resolving gel (29:1 mono:bis). 40-60 ug total whole cell lysate was used in SDS-PAGE to observe Rad53, 10-20 ug total whole cell lysate was used to observe Rfa2. Electrophoresis was then performed at 30 mA constant current for 15 minutes, 60 mA constant current for 2 hours allowing the 25 kDa band (PageRuler Plus Prestained Protein Ladder;

Thermo Scientific) to reach the base of the gel. Each gel was equilibrated in Towbin Transfer Buffer (10 mM Tris-HCl, 100 mM glycine, 10% Methanol) for 15 min and transferred onto a 0.2-micron nitrocellulose membrane (Bio-Rad) at 40 mA constant current for 16 hours at 4°C.

Once transfer was complete, nitrocellulose membranes were then stained with Ponceau S (0.5% w/v Ponceau S, 1% v/v acetic acid) for 10 min to visualize total protein content to determine equivalent loading within each lane. Once membranes were imaged, the Ponceau S stain was removed by washing with Western Wash Buffer (WWB) (0.3% Tween-20, 5 uM NaF, 0.05 uM Na_3VO_4) for 15 minutes. Blocking buffer (WWB, 1% w/v BSA) was then added and the blot was incubated for 2 hours at room temperature. Blocking buffer was removed, and Primary Antibody Buffer (PAB) (WWB, 0.5% w/v nonfat dry milk, 0.5% BSA) was added to the blots.

To probe Rfa2 phosphorylation, a 1:40,000 dilution of α-Rfa2 antibody (kindly provided by Dr. Steve Brill) was used in PAB. To probe Rad53 phosphorylation, a 1:6000 dilution of α-Rad53 antibody (ab104232, AbCam) was used in PAB.

Following a 16 hr incubation at 4°C the PAB was removed and washes were performed using WWB. Secondary Antibody Buffer (SAB) (WWB, 0.2% w/v nonfat dry milk), containing a 1:40,000 dilution of goat-α-rabbit-HRP (Abcam; ab97051, 1:40,000, Bethyl; A120-101P, 1:40,000) was then added to each blot and allowed to incubate for 2 hr at room temperature. The SAB was then removed and washes using WWB were performed. All blots were developed using a fluorescent substrate (ECL2 Plus; Thermo Scientific) and visualized on a STORM imager (GE).

4.3.F. Yeast genomic DNA isolation for qPCR resection assays

Ten OD_{600} of cells were harvested prior to HO induction and every hour for four hours post-HO induction with galactose. Cells were pelleted at 2500 RPM and the media was aspirated away from the pellet. Pellets were then resuspended in 500 uL of YEX buffer (Yeast Extraction Buffer: 100 mM Tris-HCl, pH 8.0, 50 mM EDTA, 2% SDS), 500 uL of glass beads, and 500 uL of P:C:I (phenol:chloroform:isoamyl alcohol; 25:24:1) was added to each tube. Cells were bead-beat on maximum speed at 4ºC for 30 minutes. Tubes were then placed in a centrifuge at max speed for 10 minutes to separate the solubilized DNA (aqueous phase) away from cellular debris and phenol. The aqueous phase was then extracted twice in ice-cold 24:1 chloroform:isoamyl alcohol, and then precipitated using 3M NaAC and 2.5 volumes

of ice-cold 95% ethanol. Nucleic acids were harvested by centrifuging the reaction tubes at 4ºC, max speed for 10 minutes. Ethanol was aspirated away, and the nucleic acid pellets were washed once with ice-cold 70% ethanol. Following another centrifugation and aspiration, nucleic acid pellets were dried for 10 minutes in a vacuum centrifuge and resuspended in 100 uL of TE, pH = 8.0. 1 uL of RNase A was then added to each tube and the tubes were incubated at 37ºC for 30 minutes to eliminate RNA. 3M NaAC and 2.5 volumes of ice-cold 95% ethanol was then added to the tubes to precipitate DNA, which was harvested and dried as described. Following the final drying step, DNA was resuspended in 100 uL of ddH_2O, quantitated via spectroscopy, and 100 ng of DNA was used in each qPCR reaction, with appropriate primers (Appendix C).

4.3.G. Analysis of resection via qPCR

DNA isolated as described in section 4.3.F was 2 mg of DNA was digested with *Ssp*I enzyme at 37°C for 2 hours. DNA was then diluted to 20ng/uL and 5 uL (100ng) of diluted DNA was used in qPCR as follows. *EvaGreen* SYBR qPCR master mix (abm), appropriate primers for each *Ssp*I restriction site at the *MAT* locus (Appendix C), and filter-sterile ddH_2O were used to create a qPCR master mix. Primers were utilized at a final concentration of 300 nM each. 15 uL of each master mix was added to a 96-well qPCR plate. 5 uL (100ng) of dilute DNA sample was then added to each well, and qPCR was performed on an AB7500 system (Applied Biosystems).

4.4. Results

4.4.A. Adaptation proficiency conferred by Rfa2 NT extensive mutations is not dependent on DSB resection

Previously, it was demonstrated that Rfa2 NT extensive mutations have significant impacts on the ability of cells to undergo checkpoint adaptation or enter mitosis with broken/damaged DNA (Chapter 3; Ghospurkar *et al.* 2015, Wilson *et al.* 2018b) . Characterization of ectopically expressed Rfa2 NT extensive mutations in otherwise unmodified cells during checkpoint adaptation reveals that, as observed previously, the *rfa2-*D_X and *rfa2-h2NT* mutations promote checkpoint adaptation in-line with wild-type cells (Figure 4.1, Table 4.1). The *rfa2-*A_X mutation leads to an approximate 10% decrease in adaptability of cells, whereas *rfa2-*ΔN_X leads to a 40% reduction in cells aberrantly entering mitosis. Biochemical analysis of the phospho-state of Rad53 reveals that, in each of the Rfa2 NT extensive mutations,

checkpoint activation occurs indistinguishably from wild-type, however, *rfa2-A*$_X$ and *rfa2-*Δ*N*$_X$ mutations lead to an additional Rad53 phospho-species that persists through 12-16 hours post-DSB induction (Figure 4.2).

Previous research has speculated that the process of resection, or controlled nucleolytic digestion of the 5' strand proximal to the DSB, impacts the ability of cells to undergo checkpoint adaptation (Lee *et al.* 1998, Eapen *et al.* 2012). This hypothesis was largely driven by the observation that *yku70*Δ adaptation deficiency could be rescued by *rfa1-t11* and led to extensive long-range resection 3-6 hours after a single DSB was introduced at the *MAT* locus in the *rfa1-t11 yku70*Δ double mutation (Lee *et al.* 1998). However, recent research has demonstrated that promoting extensive or long-range resection through either deletion of *RAD9* (Rad53 chaperone during G_2/M; Dibitetto *et al.* 2016) or via over-expression of Exo1 exonuclease (Eapen *et al.* 2012, Clerici *et al.* 2014) can rescue adaptation-deficiency by inhibiting or promoting extensive resection of the DSB, respectively. Moreover, preventing extensive resection through over-expression of Rad9 successfully inhibits checkpoint adaptation in adaptation-deficient mutants suggestive that the extent of which resection proceeds at a DSB may mediate the checkpoint adaptation process (Dibitetto *et al.* 2016). This led us to test whether resection of the HO-induced DSB at the *MAT* locus was affected by Rfa2 NT extensive mutations (Figure 4.3 and 4.4). Using primers identical to that used in Dibitetto *et al.* (2016), we first performed a proof of concept PCR on undigested and *Ssp*I digested DNA to ensure that the products generated for the assay were able to be synthesized only if undigested DNA was present. We discovered that spurious amplification of R2, R3, and R7 (Figure 4.3, panel 2 and 3) occurred in the absence of any template DNA. Ultimately, we decided to commit to using primers for the R1, R4, and R6 resection products as they exist at 1.7, 5.9, and 8.9 kbp distal to the *MAT* locus, on the right arm of chromosome III (Figure 4.4A). By selecting different range positions on the chromosome, we assessed that we would be able to measure both short-range (1-5 kbp) and long-range resection (5 kbp+) with high confidence.

Using the qPCR strategy described in Figure 4.4A, we were able to determine that both short-range and long-range resection of the *MAT* locus is not significantly impacted by Rfa2 NT extensive mutations. Analysis of short-range resection reveals that each mutant *rfa2* form, as well as *rfa1-t11* have a minor defect (~10% reduction) in fold-enrichment of product at R1, or 1.7 kbp distal *MAT*. Long-range

resection appears to be most greatly impacted by *rfa1-t11*, a mutation that was previously reported to generate hyper-resection phenotypes, or *rfa2-A*$_X$. Resection in *rfa2-D*$_X$*, rfa2-h2NT,* or *rfa2-ΔN*$_X$ was reduced when compared to wild-type at 1.7, 5.9, and 8.9 kbp from the DSB site. Taken together, these data suggest that: *1)* resection of the DSB is not the primary determinant for checkpoint adaptation and *2)* that phosphorylation and the physical presence of the Rfa2 NT may only play a minor role during DSB resection.

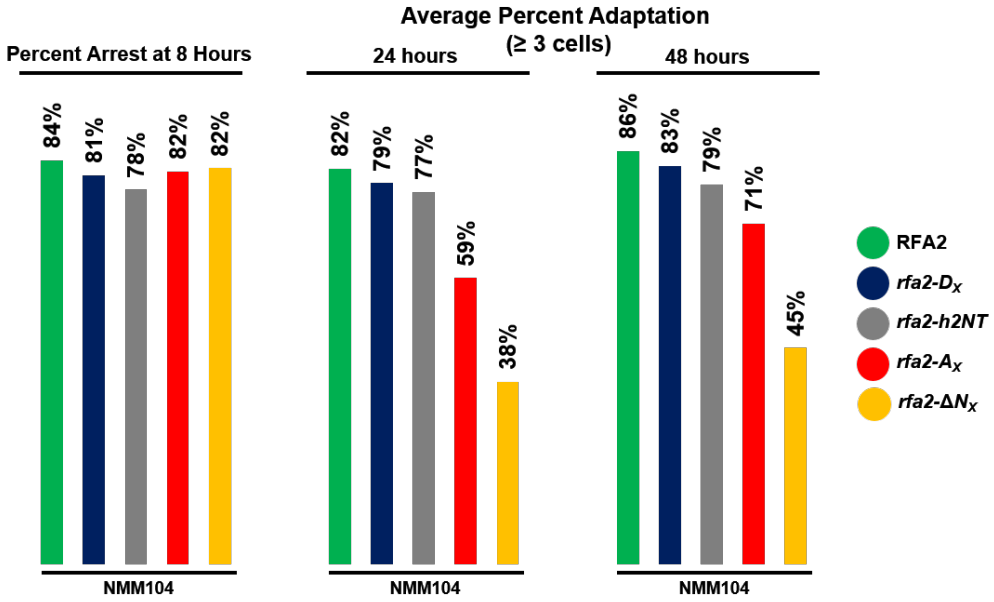

Figure 4.1. Rfa2 NT phosphorylation is required for checkpoint adaptation in wild-type cells. Microscopic analysis of checkpoint adaptation in NMM104 (JKM179 *rfa2*Δ::KanMX) cells. Broadly, rfa2 NT phospho-mimetic or naturally phosphorylatable mutations promote adaptation rescue, whereas an unphosphorylatable NT leads to a reduction in adaptation and an NT truncation severely impedes adaptation. Cells were harvested at 8 hours from culture induced to express HO endonuclease using galactose to a final concentration of 2%. 0.05 OD_{600} of cells were spread on YPRG plates using microbeads and analyzed at 8, 24, and 48 hours post-HO induction. Averages are from three independent experiments.

Table 4.1. Average Adaptation Percentages in NMM104 cells.

Strain	Percent of clusters ≥3 Cells at 8 Hours	Average Percent Adaptation by 24 hours	Average Percent Adaptation by 48 hours
WT	8%	82%	86%
rfa2-D$_X$	11%	79%	83%
rfa2-A$_X$	9%	59%	71%
rfa2-ΔN$_X$	10%	38%	45%
rfa2-h2NT	15%	77%	79%

Average adaptation was calculated by subtracting the total number of cells greater than or equal to three cells at 8 hours from total observed adaptation at 24 and 48 hours. Averages are from three independent experiments.

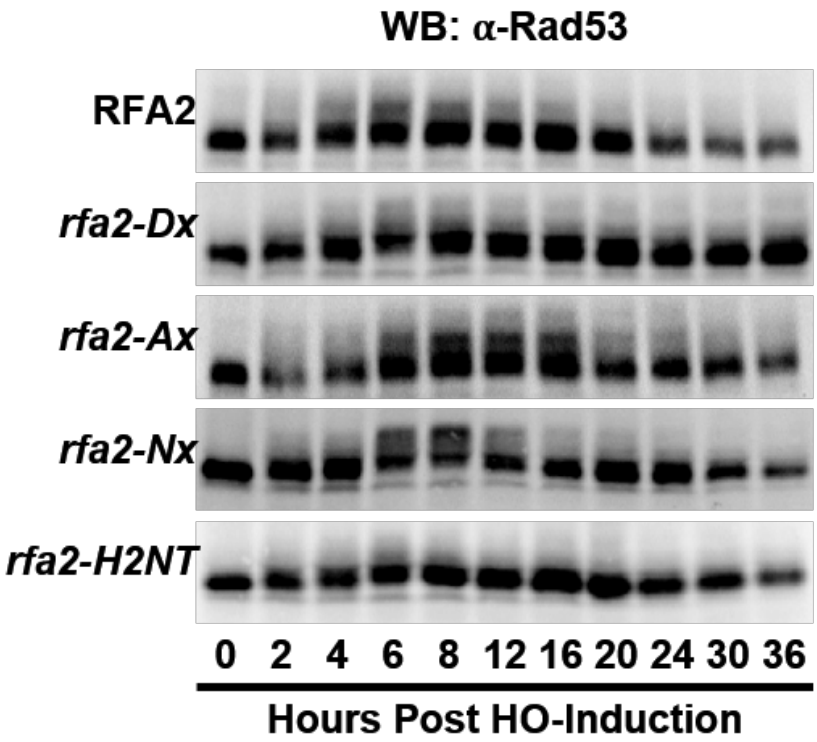

Figure 4.2. Rad53 phospho-state is correlated with checkpoint adaptation.
Rad53 immunoblots from NMM104 cells containing Rfa2 NT extensive mutations. Rad53 hyper-activation is not impaired in Rfa2 NT extensive mutations but becomes more rapidly inactivated with the *rfa2-D*$_X$ or *rfa2-h2NT* mutations, or more hyper-activated with the *rfa2-A*$_X$ or *rfa2-*Δ*N*$_X$ mutations at 6 hours and proceeding through 16 hours. 10 OD_{600} of cells were harvested at indicated time points and treated as described. 40 ug of whole cell lysate was used in SDS-PAGE.

4.4.B. The Rfa2 NT is required for checkpoint adaptation

Previous studies have shown that deletion of the DNA damage sensor kinase Tel1 leads to adaptation proficiency, and *tel1*Δ rescues adaptation deficiency caused by *mec1-ad* mutation, or *dna2*Δ, *sgs1*Δ, and *yku70*Δ (Clerici *et al.* 2014). In our adaptation assays, *tel1*Δ adapts slightly better than WT cells (Figure 4.5, Table 4.2) and *tel1*Δ Rfa2 NT extensive mutations adapt with a similar frequency to Tel1 proficient strains. However, *tel1*Δ is unable to rescue the adaptation defect conferred by *rfa2-*Δ*N*$_X$, suggesting that the physical presence of the Rfa2 NT is the most minimal requirement for checkpoint adaptation in budding yeast. Moreover, the *tel1*Δ mutation is both sensitive to DNA damaging agents, and all of the tested Rfa2 NT extensive mutations appear to enhance the observed sensitivity to genotoxic agents (Figures 4.6 and 4.7).

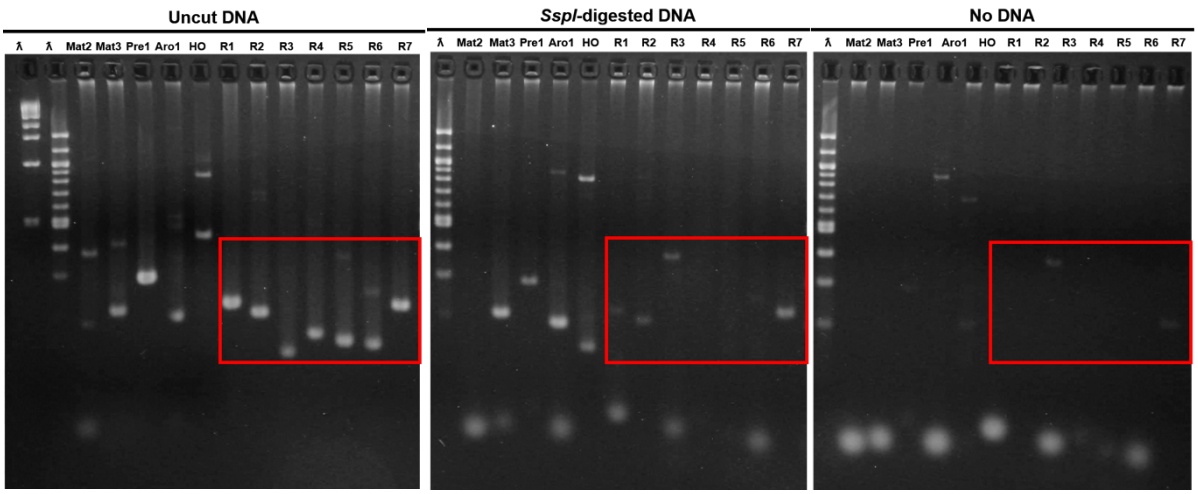

Figure 4.3. Proof of concept for resection qPCR assay.
Genomic DNA was harvested from 10 OD_{600} of exponentially growing cells and treated with or without *Ssp*I enzyme and then utilized in standard PCR as described in 4.3. PCR was also performed on primers without DNA revealing amplicons R1, R4, and R7 were dependent on, *Ssp*I-undigested DNA. Spurious amplification was observed in reactions using primers specific to R2, R3, and R6 in the absence of DNA template and in the presence of both digested and undigested DNA.

4.4.C. Rfa2 NT extensive mutations promote rescue of adaptation-deficient *rtt107*Δ and *slx4*Δ

As described previously, Rtt107 and Slx4 form a functional complex during lesion processing and repair (LPR) that has been shown to compete for binding of the BRCT-domain containing scaffold Dpb11 (a known activator of Mec1 kinase activity at break sites) with the Rad53 chaperone Rad9 (Ohouo *et al.* 2013). Preventing Rad9-Rad53 complex binding with Dpb11 is thought to lead to an attenuation or 'winding down' of the checkpoint signal and lead to mitotic exit (*ibid*). Moreover, rescue of *rtt107*Δ and *slx4*Δ adaptation deficiency has been demonstrated to be rescuable by overexpression of Rad9 and is thought to prevent extensive resection of DNA at the break site (Dibitetto *et al.* 2016). This led us to generate and test the effects of *rtt107*Δ and *slx4*Δ mutations in combination with Rfa2 NT extensive mutations. Initially, Diagnostic spot assays revealed that *rtt107*Δ mutations were sensitive to DNA damaging agents and combining *rtt107*Δ with Rfa2 NT extensive mutations led to a significant synthetic genetic defect (Figures 4.8 and 4.9). A similar effect was observed for *slx4*Δ cells containing the Rfa2 NT extensive mutations (Figures 4.10 and 4.11).

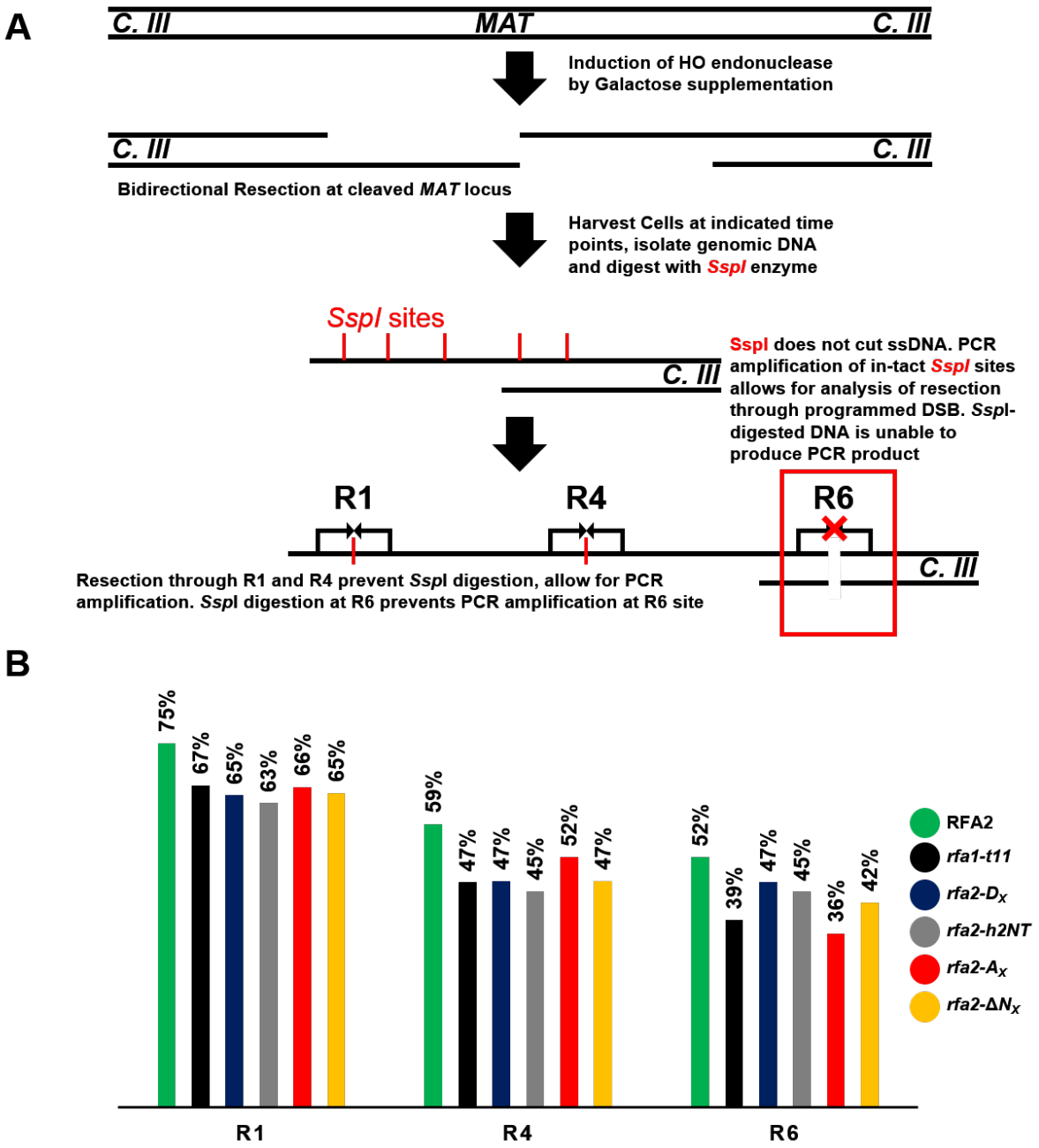

Figure 4.4. Rfa2 NT is dispensable for long-range resection of MAT locus.
A. Schematic of qPCR assay used. R1, R4, and R6 SspI sites exist at 1.7 kbp, 5.9 kbp, 8.9 kpb distal to the MAT locus on the right arm of chromosome III. **B.** Relative fold enrichment of qPCR products at R1, R4, and R6 of rfa2 NT mutations in NMM104 cells. All mutations appear to exhibit a moderate defect in resection when compared to WT. *rfa1-t11* does not exhibit a hyper-resection phenotype as previously reported. Cells were harvested at 4 hours from culture induced to express HO endonuclease using galactose to a final concentration of 2%. 10 OD_{600} of cells were harvested for genomic DNA isolation, and 100 ng of template DNA was used in each qPCR experiment. qPCR was performed using appropriate primers described in section 4.3.F, and are identical to that used in Dibettito *et al*. 2017 and are listed in Appendix C.

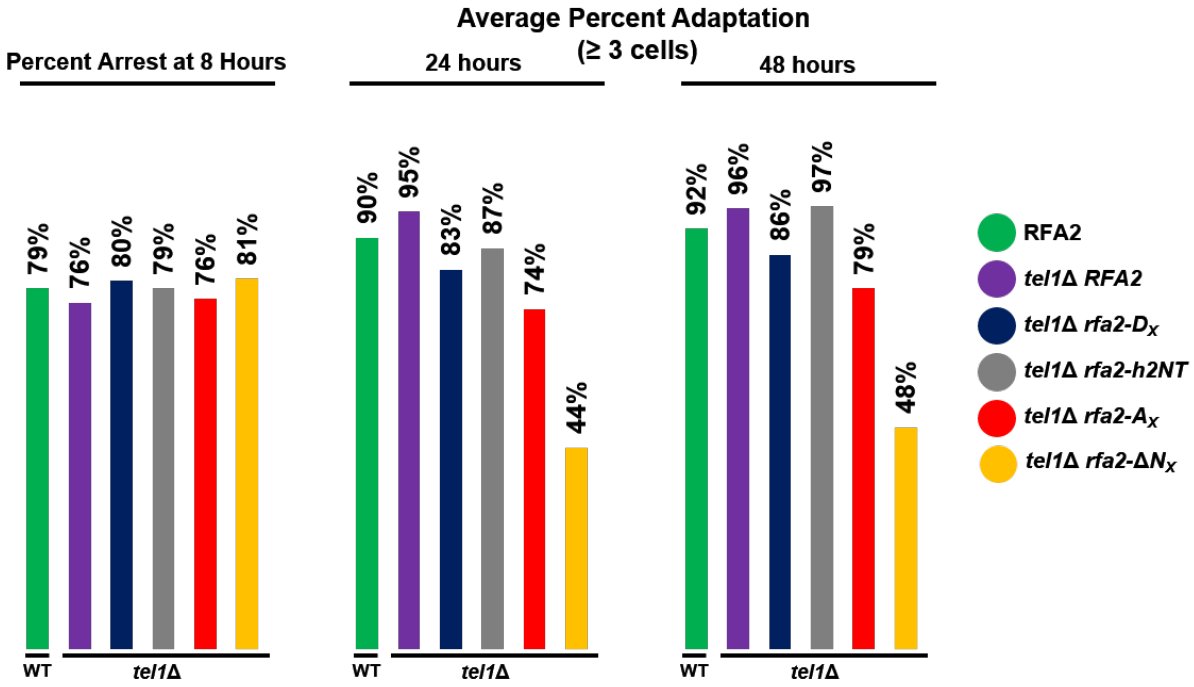

Figure 4.5. The Rfa2 NT is required for checkpoint adaptation in *tel1*Δ.
Microscopic analysis of checkpoint adaptation in *tel1*Δ Rfa2 NT extensive mutations. Broadly, rfa2 NT phospho-mimetic or naturally phosphorylatable mutations promote adaptation rescue, whereas an unphosphorylatable NT leads to a reduction in adaptation and an NT truncation severely impedes adaptation. Cells were harvested at 8 hours from culture induced to express HO endonuclease using galactose to a final concentration of 2%. 0.05 OD_{600} of cells were spread on YPRG plates using microbeads and analyzed at 8, 24, and 48 hours post-HO induction. Averages are from three independent experiments.

Table 4.2. Average Adaptation Percentages observed in NMM104 *tel1*Δ.

Strain	Percent of clusters ≥3 Cells at 8 hours	Average Percent Adaptation by 24 hours	Average Percent Adaptation by 48 hours
***tel1*Δ RFA2**	13%	95%	96%
***tel1*Δ + *rfa2-D*$_X$**	9%	83%	86%
***tel1*Δ + *rfa2-A*$_X$**	9%	74%	79%
***tel1*Δ + *rfa2-ΔN*$_X$**	7%	44%	48%
tel1*Δ + *rfa2-h2NT	11%	87%	97%

Average adaptation was calculated by subtracting the total number of cells greater than or equal to three cells at 8 hours from total observed adaptation at 24 and 48 hours. Averages are from three independent experiments.

Microscopic analysis of *rtt107*Δ Rfa2 NT extensive mutations during checkpoint adaptation reveals that *rtt107*Δ recapitulates its known adaptation-deficient phenotype, and this adaptation deficiency is rescued by phospho-mimetic *rfa2-D*$_X$ or the naturally phosphorylatable *rfa2-h2NT* (Figure 4.12). Biochemical analysis of the Rad53 phospho-state during adaptation reveals that *rtt107*Δ cells containing

rfa2-D$_X$ or *rfa2-h2NT* activate the Rad53-dependent checkpoint with near-WT kinetics; however, hyper-activation of Rad53 is not observed (Figure 4.13). Moreover, *rtt107*Δ *rfa2-A$_X$* or *rfa2-*Δ*N$_X$* mutations lead to the formation of hyper-phosphorylated Rad53 that persists through the observed time course (Figure 4.13, panels 2A, 3A, 3B and 4B). This hyper-phosphorylated species is detected in WT cells at approximately 8 hours (Figure 4.13B, panel 1), but is not present at 12 hours or later in the time-course. This demonstrates that in *rtt107*Δ, phospho-mimetic or naturally phosphorylatable forms of Rfa2 prevent hyper-activation of Rad53.

Microscopic analysis of *slx4*Δ Rfa2 NT extensive mutations during checkpoint adaptation reveals that not only does *slx4*Δ recapitulate its known adaptation-deficient phenotype, but that phospho-mimetic or naturally phosphorylated Rfa2 NT mutations promote checkpoint adaptation, similar to that observed for *rtt107*Δ cells (Figure 4.14). Biochemical analysis of Rad53 during adaptation in *slx4*Δ Rfa2 NT extensive mutations revealed that Rad53 phosphorylation and hyper activation occurs in a similar fashion to that observed for *rtt107*Δ mutations (Figure 4.15). While the biochemical data argues that these cells may not properly checkpoint, morphological observations of cells at 8 hours (Figure 4.12, Table 4.3; Figure 4.14, Table 4.4) reveal that approximately 80% of the cells display morphology that indicates proper checkpoint arrest. Consistently, the *rfa2-D$_X$* or *rfa2-h2NT* mutations prevented hyper-activation of Rad53 in *slx4*Δ cells. Taken together, our data suggests that both Rtt107 and Slx4 are required for full checkpoint activation, and that phosphorylation of the Rfa2 NT can prevent full hyper-activation of Rad53 during lesion processing and repair.

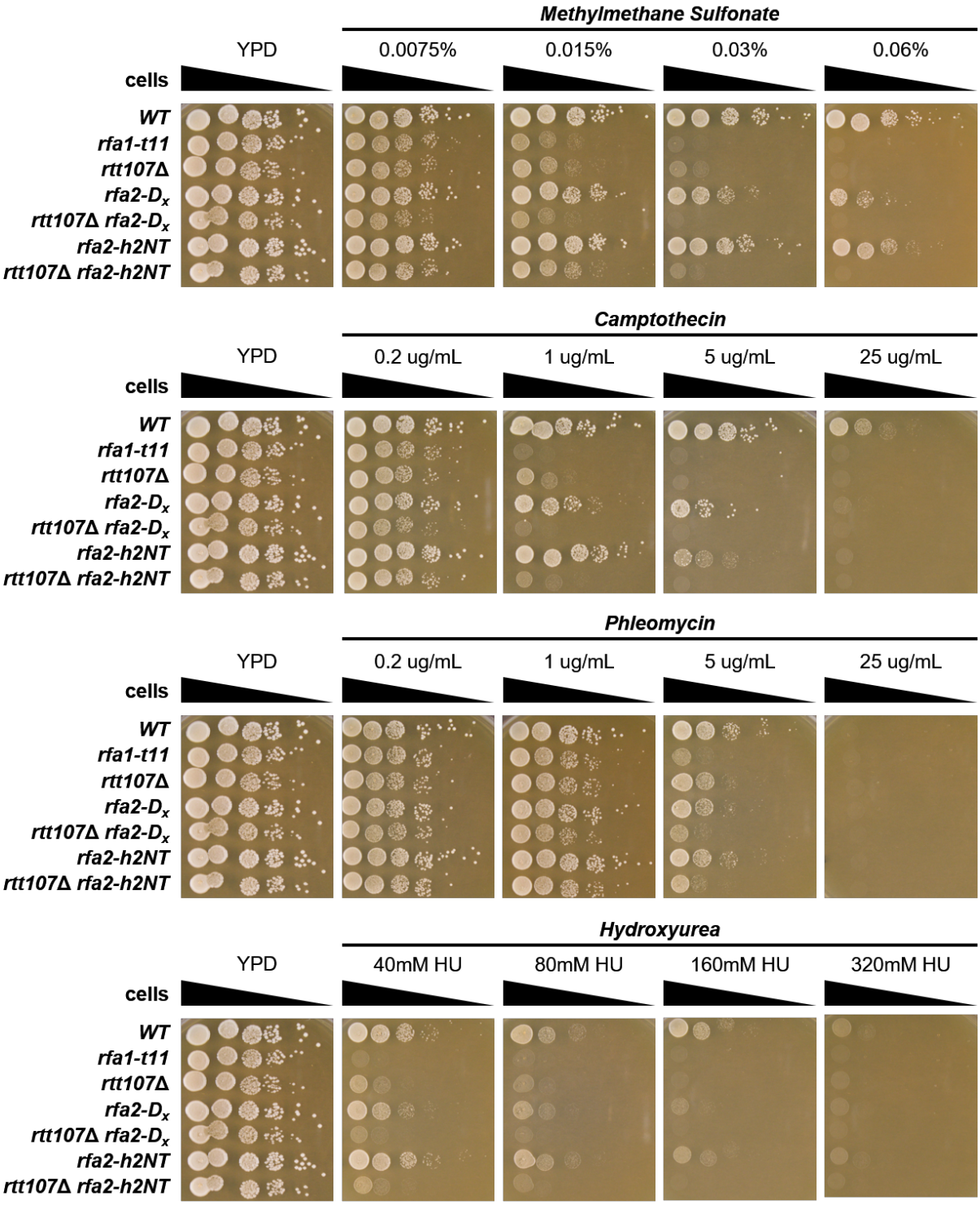

Figure 4.6. Diagnostic spot assay of *rtt107*Δ mutations (*rfa2-D$_X$* and *rfa2-h2NT*).
*rtt107*Δ Rfa2 NT mutations were harvested and an OD_{600} for the exponentially growing culture was determined. Starting at an OD_{600} of 1.0, six ten-fold serial dilutions were performed in sterile filtered water. 200 uL of the diluted culture was added to a 96-well microtiter plate and 5 uL of the dilution was then spotted onto the plates using a multi-channel pipetman.

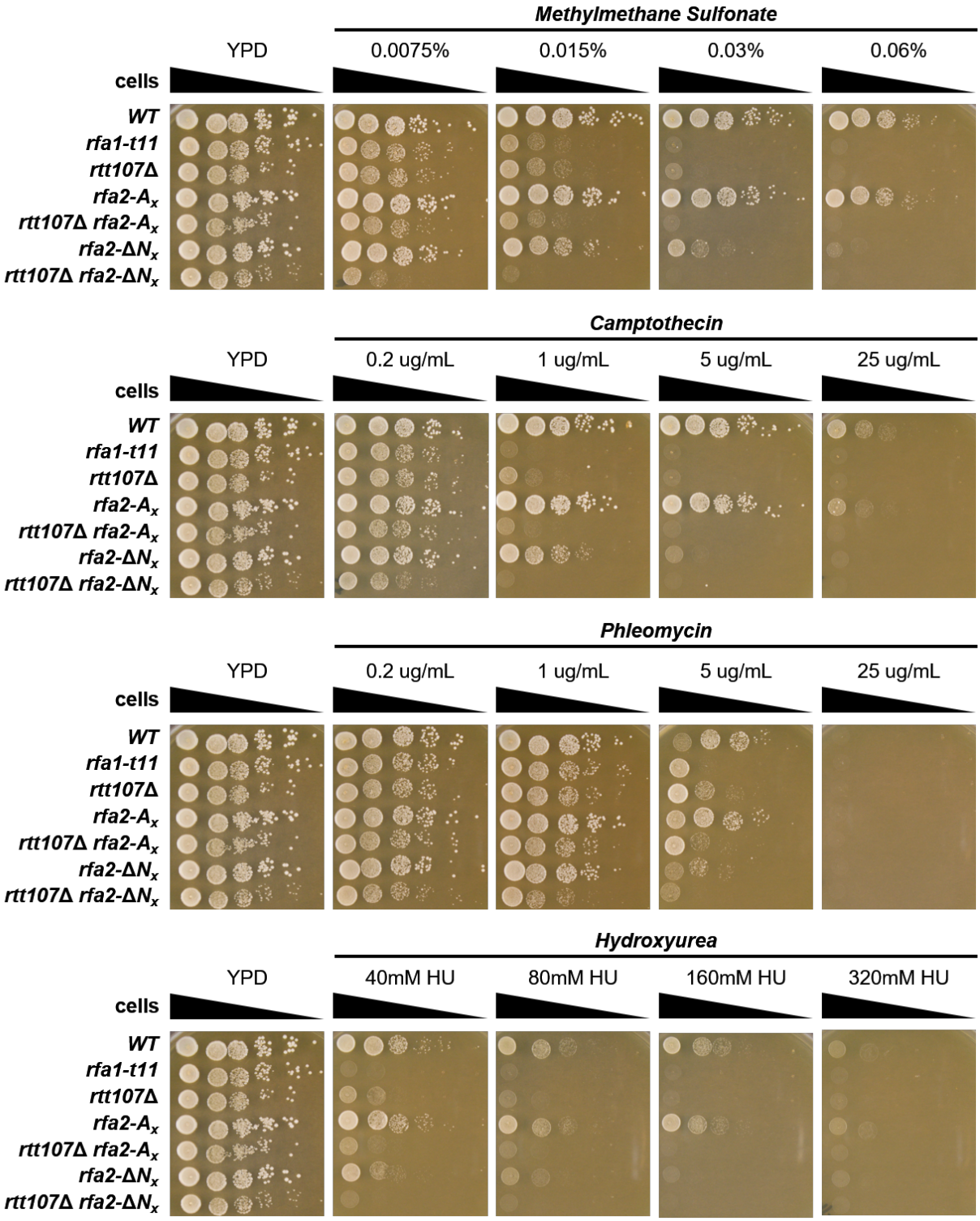

Figure 4.7. Diagnostic spot assay of *rtt107*Δ mutations (*rfa2-A*$_X$ and *rfa2-ΔN*$_X$).
*rtt107*Δ Rfa2 NT mutations were harvested and an OD_{600} for the exponentially growing culture was determined. Starting at an OD_{600} of 1.0, six ten-fold serial dilutions were performed in sterile filtered water. 200 uL of the diluted culture was added to a 96-well microtiter plate and 5 uL of the dilution was then spotted onto the plates using a multi-channel pipetman.

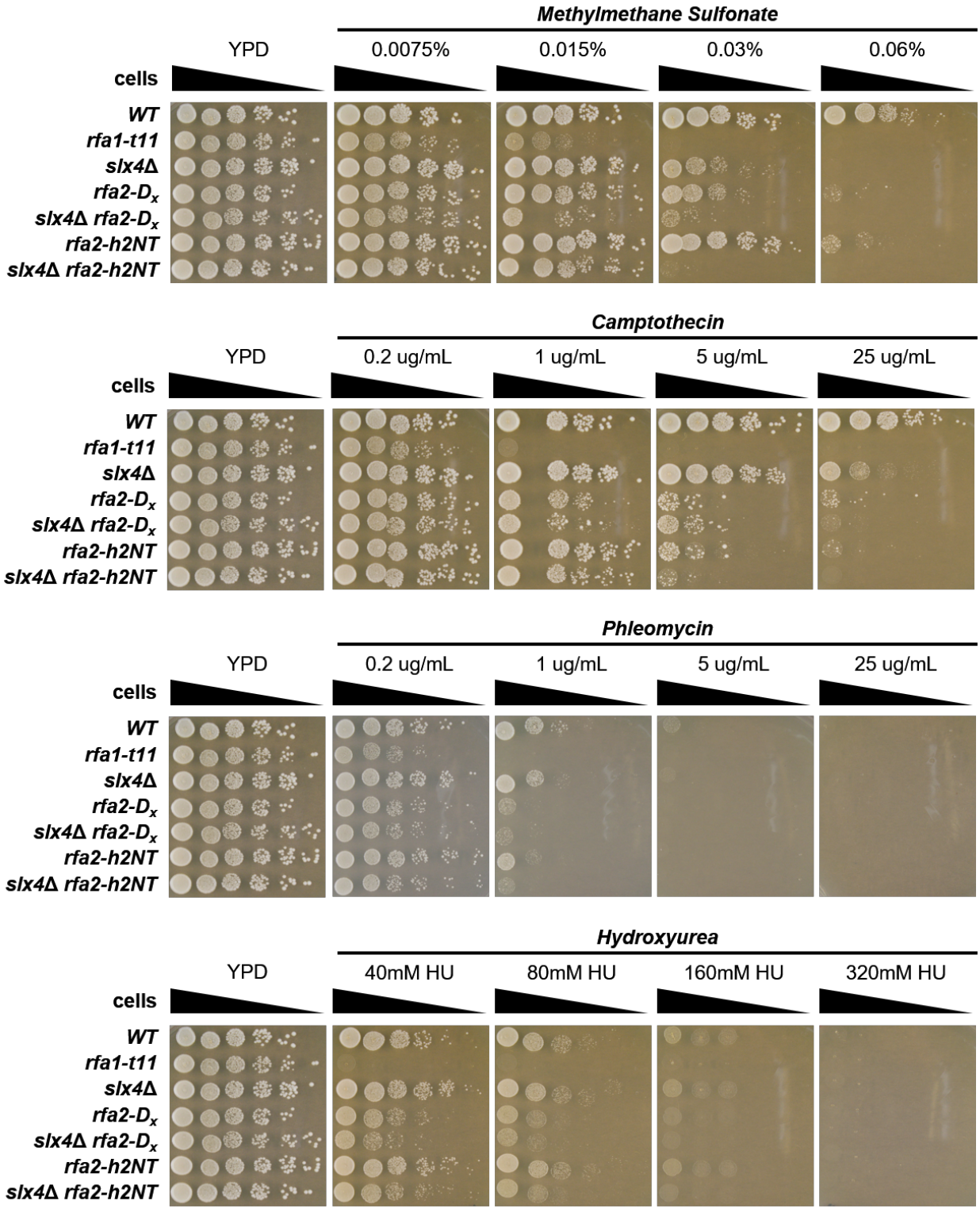

Figure 4.8. Diagnostic spot assay of *slx4*Δ mutations (*rfa2-Dx* and *rfa2-h2NT*).
*slx4*Δ Rfa2 NT mutations were harvested and an OD_{600} for the exponentially growing culture was determined. Starting at an OD_{600} of 1.0, six ten-fold serial dilutions were performed in sterile filtered water. 200 uL of the diluted culture was added to a 96-well microtiter plate and 5 uL of the dilution was then spotted onto the plates using a multi-channel pipetman.

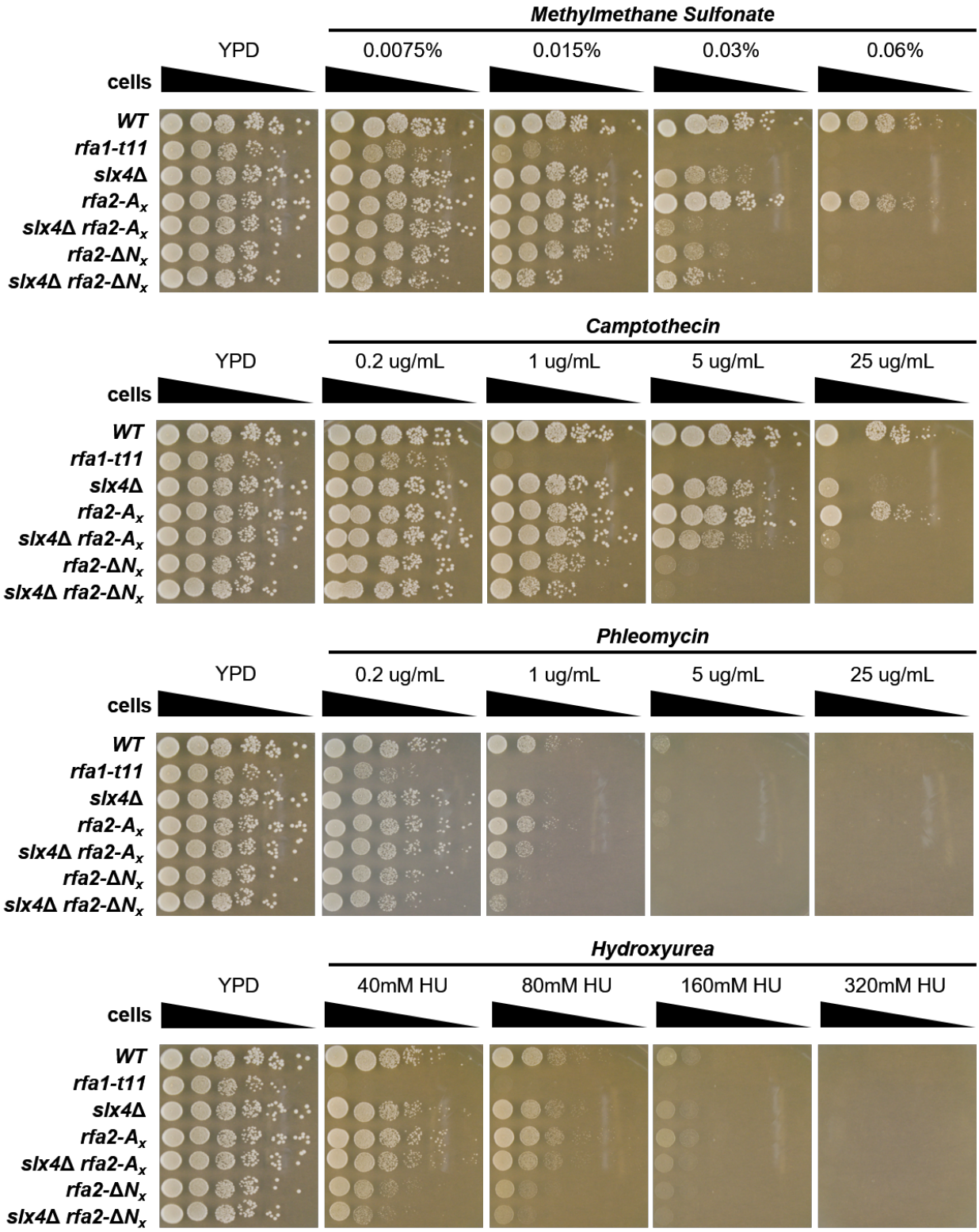

Figure 4.9. Diagnostic spot assay of *slx4*Δ mutations (*rfa2-A*$_X$ and *rfa2-*Δ*N*$_X$).
*slx4*Δ Rfa2 NT mutations were harvested and an OD_{600} for the exponentially growing culture was determined. Starting at an OD_{600} of 1.0, six ten-fold serial dilutions were performed in sterile filtered water. 200 uL of the diluted culture was added to a 96-well microtiter plate and 5 uL of the dilution was then spotted onto the plates using a multi-channel pipetman.

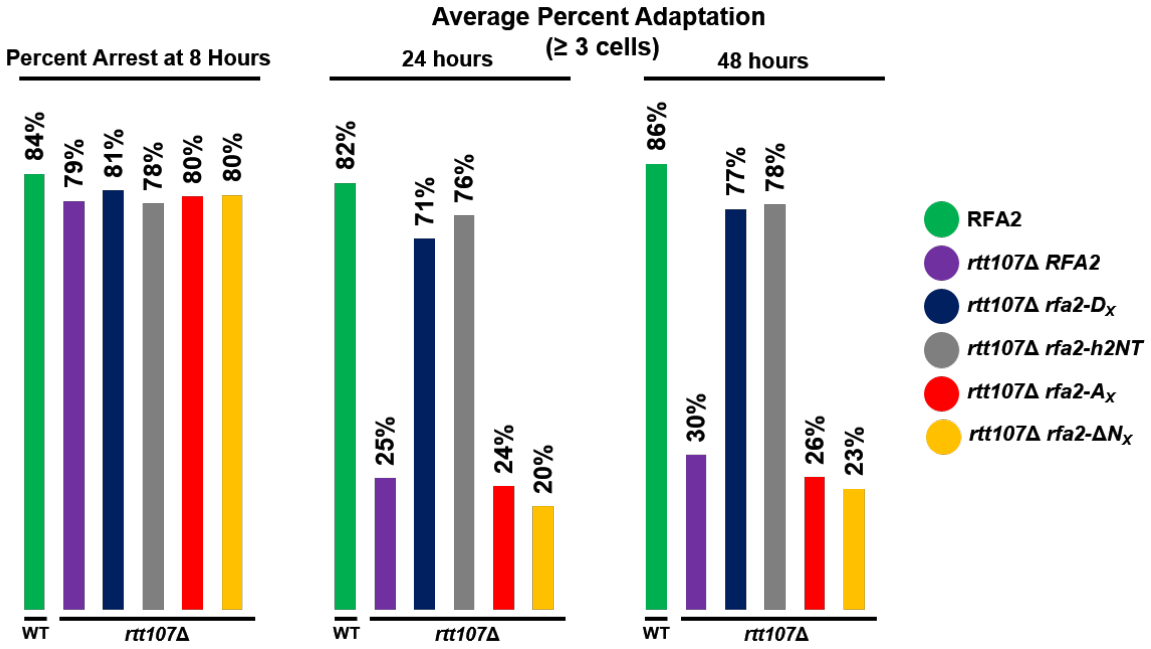

Figure 4.10. Rfa2 NT phosphorylation is required for checkpoint adaptation in *rtt107*Δ cells. Microscopic analysis of checkpoint adaptation in *rtt107*Δ Rfa2 NT extensive mutations. Broadly, Rfa2 NT phospho-mimetic or naturally phosphorylatable mutations promote adaptation rescue, whereas an unphosphorylatable NT leads to a reduction in adaptation and an NT truncation severely impedes adaptation. Cells were harvested at 8 hours from culture induced to express HO endonuclease using galactose to a final concentration of 2%. 0.05 OD_{600} of cells were spread on YPRG plates using microbeads and analyzed at 8, 24, and 48 hours post-HO induction. Averages are from three independent experiments.

Table 4.3. Average Adaptation Percentages observed in NMM104 *rtt107*Δ cells.

Strain	Percent of clusters ≥3 Cells at 8 Hours	Average Percent Adaptation by 24 hours	Average Percent Adaptation by 48 hours
rtt107Δ RFA2	15%	25%	30%
rtt107Δ rfa2-D_X	11%	71%	77%
rtt107Δ rfa2-A_X	11%	24%	26%
rtt107Δ rfa2-ΔN_X	13%	20%	23%
rtt107Δ rfa2-h2NT	15%	76%	78%

Average adaptation was calculated by subtracting the total number of cells greater than or equal to three cells at 8 hours from total observed adaptation at 24 and 48 hours. Averages are from three independent experiments.

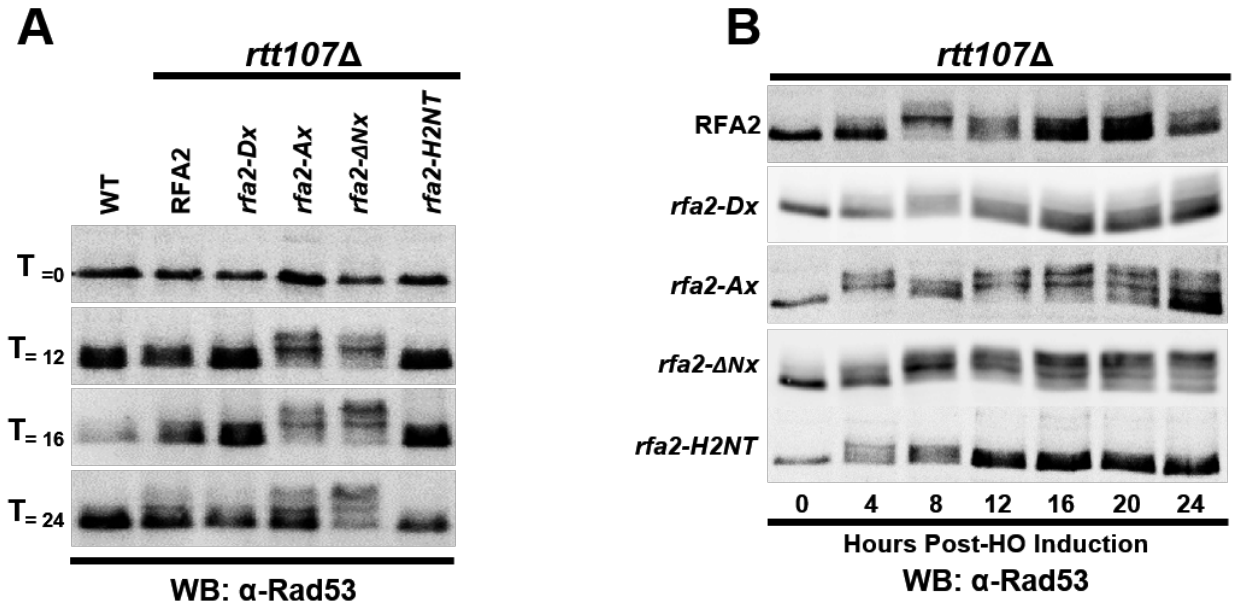

Figure 4.11. Rad53 inactivation during checkpoint adaptation requires Rfa2 NT phosphorylation in *rtt107*Δ.
Rad53 immunoblots from *rtt107*Δ cells. **A.** *rtt107*Δ cells containing *rfa2-D$_X$* or *rfa2-h2NT* display reduced Rad53 hyper-activation and faster deactivation during checkpoint adaptation, as observed in the 12-hour and 16-hour blots (panels 2 and 3, comparing *rfa2-D$_X$*/*rfa2-h2NT* with *rfa2-A$_X$*/*rfa2-*Δ*N$_X$*). *rfa2-A$_X$* and *rfa2-*Δ*N$_X$* maintain hyper-active Rad53 throughout the observed time course. 10 OD_{600} of cells were harvested at indicated time points and treated as described. 40 ug of whole cell lysate was used in SDS-PAGE. **B.** Rad53 immunoblots for each individual Rfa2 NT mutation in *rtt107*Δ mutant strain. Activation of Rad53 occurs indistinguishably from WT cells, however, *rtt107*Δ mutants containing the *rfa2-A$_X$* or *rfa2-*Δ*N$_X$* mutation display more hyper-phosphorylated Rad53 throughout the observed time course.

4.4.D. Effects of Rfa2 NT extensive mutations on *sae2*Δ adaptation-deficient mutations

During initiation of LPR, MRX localization to the DSB leads to the phosphorylation and localization of Sae2 to the MRX complex at the DSB site, and promotes MRXS endonucleolytic cleavage of nucleotides proximal to the DSB to promote resection (Nicolette *et al.* 2010). Deletion of Sae2 has been demonstrated to lead to checkpoint adaptation deficiency through a resection-dependent mechanism (Gobbini *et al.* 2015), as *sae2*Δ cells are unable to properly initiate the endonucleolytic activity of the MRXS complex at break sites, inhibiting resection by STR-Dna2 (Sgs1-Top3-Rmi1-Dna2 nuclease helicase complex). Because this mutation is reported to be resection-deficient, we tested whether Rfa2 NT phospho-mimetic or naturally phosphorylatable mutations could rescue the observed adaptation deficiency in *sae2*Δ. First, we assessed whether the generated *sae2*Δ and Rfa2 NT extensive mutation combinations recapitulated their known phenotypes via diagnostic spot assays (Figures 4.16 and 4.17), which revealed that the *sae2*Δ mutations generated in this study are sensitive to genotoxic

agents and that this sensitivity is exacerbated when in combination with *rfa2-D$_X$, rfa2-h2NT*, or *rfa2-ΔN$_X$*. Cells containing the *sae2*Δ *rfa2-A$_X$* mutation were no more sensitive to genotoxic agents than *sae2*Δ Rfa2 cells, suggesting that an unphopshorylated Rfa2 NT is required for clastogen resistance, as previously observed (Ghospurkar *et al.* 2015). Microscopic analysis of *sae2*Δ Rfa2 NT extensive mutations reveals that our generated *sae2*Δ recapitulates its known adaptation-deficient phenotype and is rescued by *rfa2-D$_X$* or *rfa2-h2NT* mutations, similar to that observed for *rtt107*Δ and *slx4*Δ mutations. Moreover, *rfa2-A$_X$* and *rfa2-ΔN$_X$* mutations consistently prevented adaptation or reduced the number of cells proceeding from 2 'big buds' to 3 or more cells (Figure 4.18, Table 4.5). Additionally, *sae2*Δ is dispensable for checkpoint activation, as previously described (Gobbini *et al.* 2015). Biochemical analysis of the Rad53 phospho-state in *sae2*Δ Rfa2 NT extensive mutants revealed that Rad53 hyper-activation occurs in all Rfa2 NT extensive mutations and more extensively than wild-type cells (Figure 4.19A, panel 2).

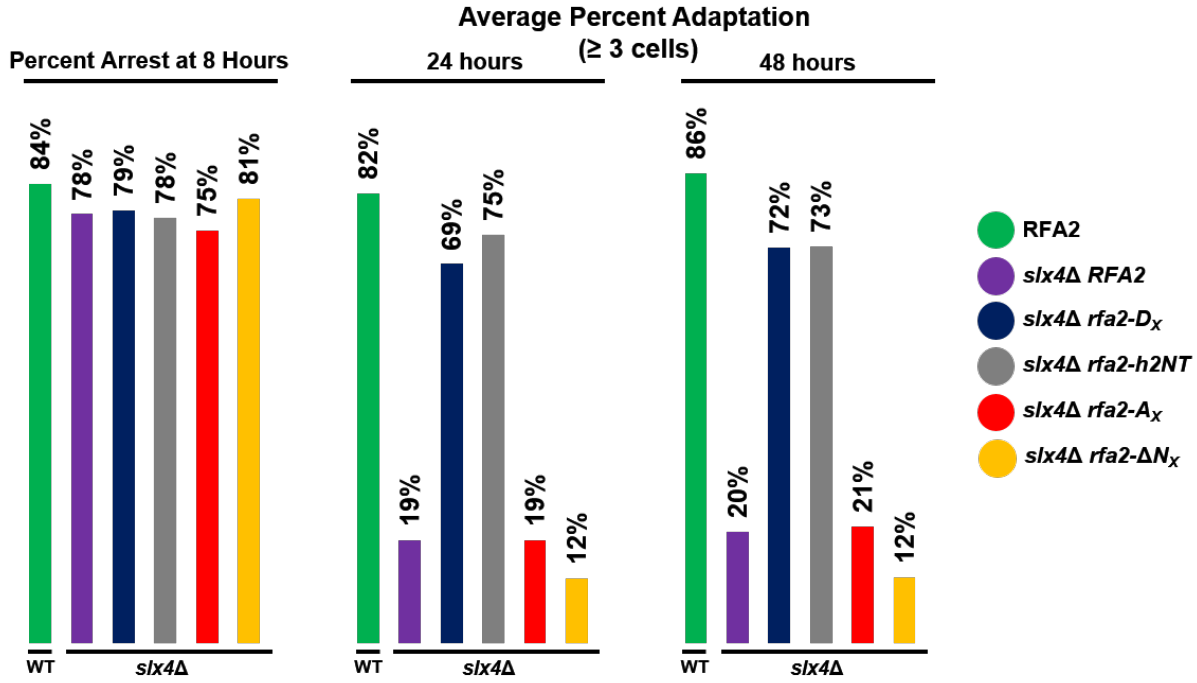

Figure 4.12. Rfa2 NT phosphorylation is required for checkpoint adaptation in *slx4*Δ cells. Microscopic analysis of checkpoint adaptation in *slx4*Δ Rfa2 NT extensive mutations. Broadly, Rfa2 NT phospho-mimetic or naturally phosphorylatable mutations promote adaptation rescue, whereas an unphosphorylatable NT leads to a reduction in adaptation and an NT truncation severely impedes adaptation. Cells were harvested at 8 hours from culture induced to express HO endonuclease using galactose to a final concentration of 2%. 0.05 OD_{600} of cells were spread on YPRG plates using microbeads and analyzed at 8, 24, and 48 hours post-HO induction. Averages are from three independent experiments.

Table 4.4. Average Adaptation Percentages observed in NMM104 *slx4Δ*.

Strain	Percent of clusters ≥3 Cells at 8 Hours	Average Percent Adaptation by 24 hours	Average Percent Adaptation by 48 hours
slx4Δ RFA2	15%	19%	20%
slx4Δ rfa2-D$_X$	15%	69%	72%
slx4Δ rfa2-A$_X$	20%	19%	21%
slx4Δ rfa2-ΔN$_X$	13%	12%	12%
slx4Δ rfa2-h2NT	16%	75%	73%

Average adaptation was calculated by subtracting the total number of cells greater than or equal to three cells at 8 hours from total observed adaptation at 24 and 48 hours. Averages are from three independent experiments.

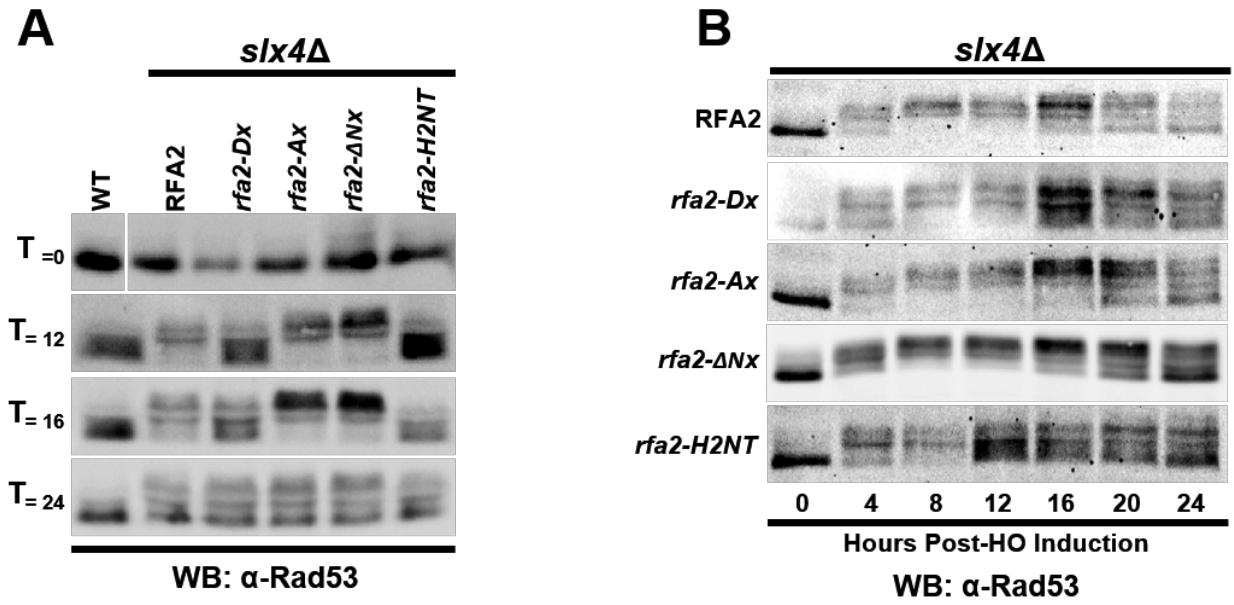

Figure 4.13. Rad53 inactivation during checkpoint adaptation requires Rfa2 NT phosphorylation in *slx4Δ*.
Rad53 immunoblots from *slx4*Δ cells. **A.** Persistent hyper-activation of Rad53 is observed in *rfa2-A$_X$* or *rfa2-ΔN$_X$*, but not *rfa2-D$_X$* or *rfa2-h2NT* mutations, specifically focusing on the temporal window within which checkpoint adaptation occurs (12-16 hours, panels 2 and 3). **B.** Rad53 immunoblots for each individual Rfa2 NT mutation in *slx4*Δ mutant strain. Activation of Rad53 occurs indistinguishably from WT cells, however, *slx4*Δ mutants containing the *rfa2-A$_X$* or *rfa2-ΔN$_X$* mutation display more hyper-phosphorylated Rad53 throughout the observed time course. 10 OD_{600} of cells were harvested at indicated time points and treated as described. 40 ug of whole cell lysate was used in SDS-PAGE.

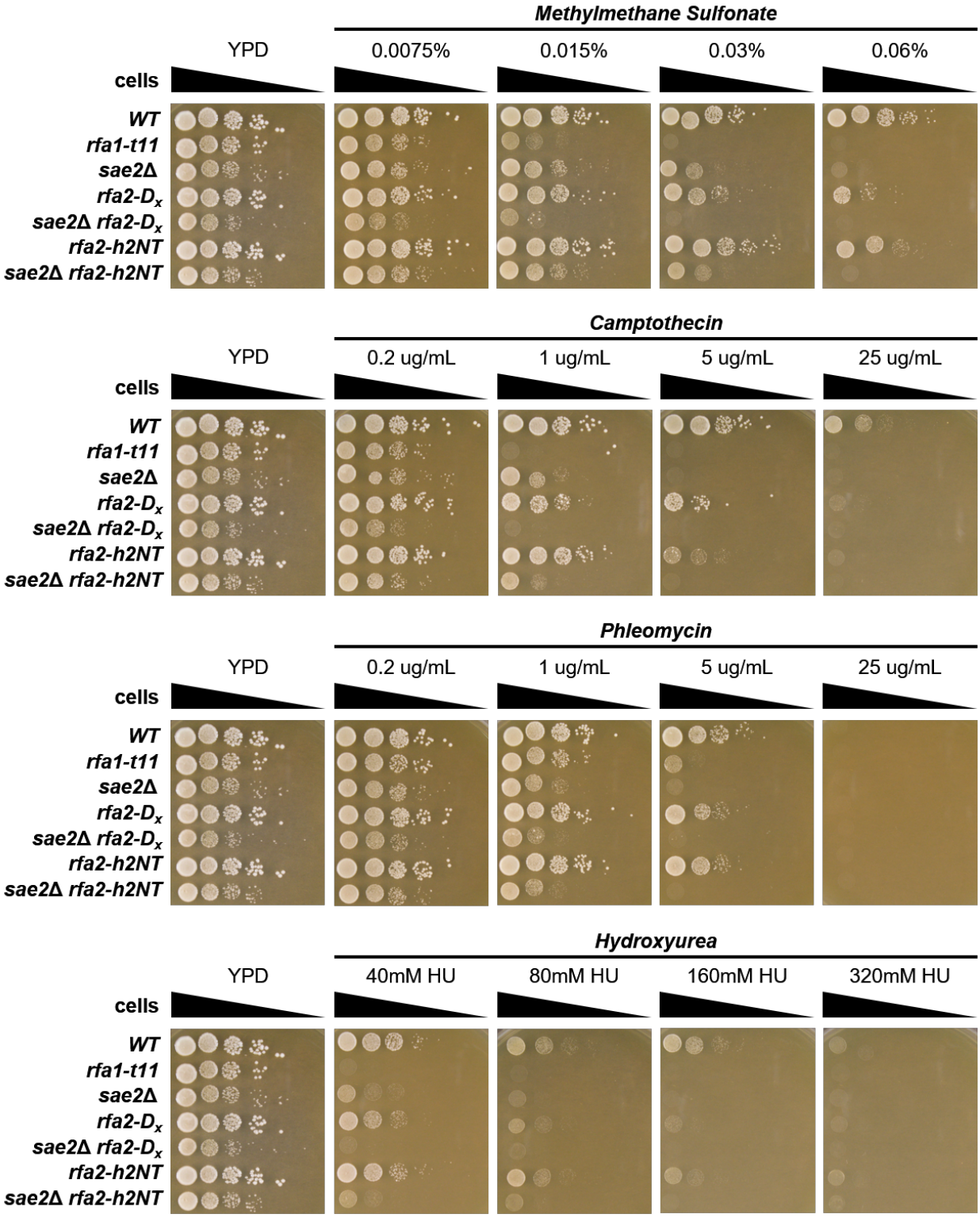

Figure 4.14. Diagnostic spot assay of *sae2*Δ mutations (*rfa2-Dx* and *rfa2-h2NT*).
*sae2*Δ Rfa2 NT mutations were harvested and an OD_{600} for the exponentially growing culture was determined. Starting at an OD_{600} of 1.0, six ten-fold serial dilutions were performed in sterile filtered water. 200 uL of the diluted culture was added to a 96-well microtiter plate and 5 uL of the dilution was then spotted onto the plates using a multi-channel pipetman.

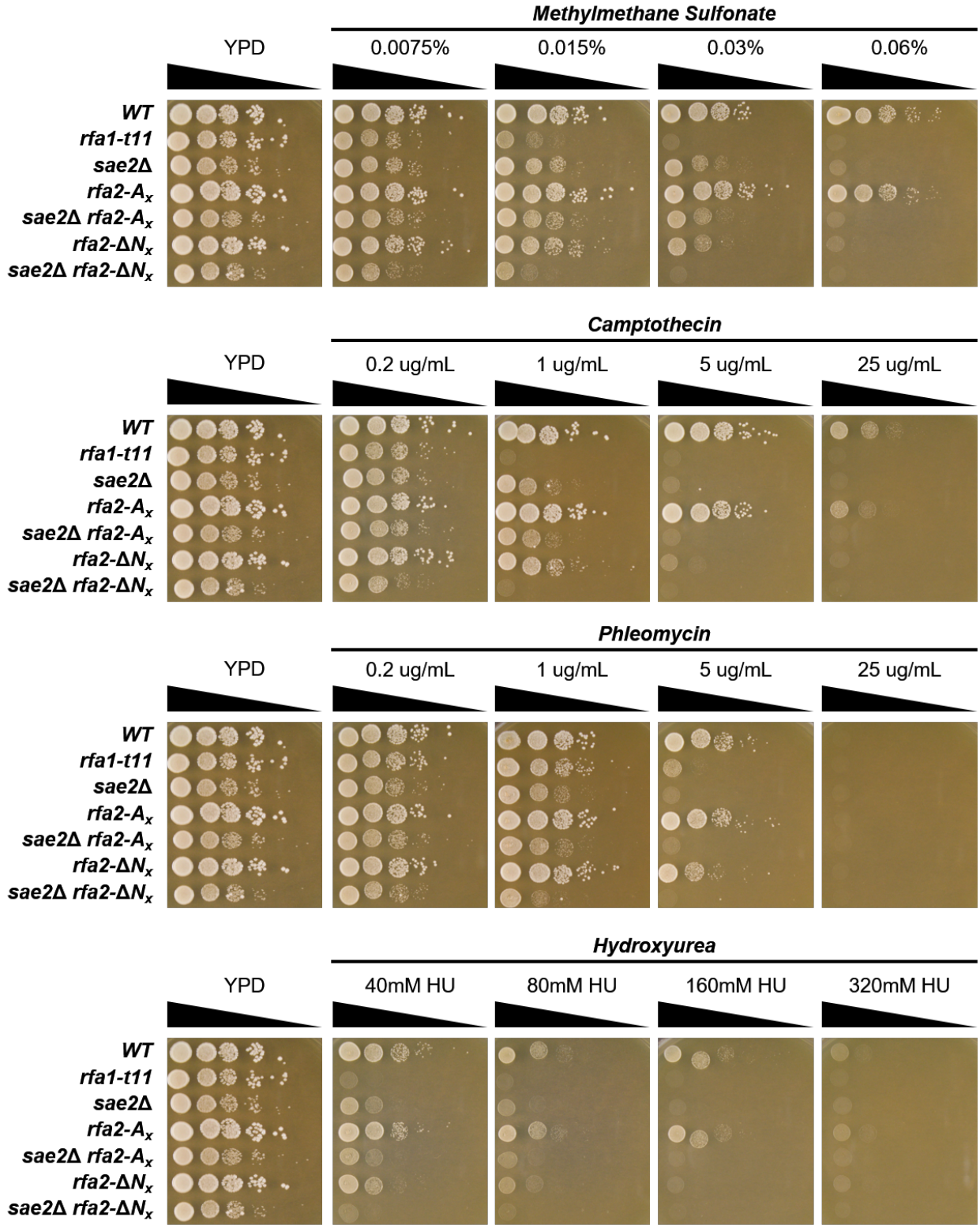

Figure 4.15. Diagnostic spot assay of *sae2*Δ mutations (*rfa2-A*$_X$ and *rfa2-ΔN*$_X$).
*sae2*Δ Rfa2 NT mutations were harvested and an OD_{600} for the exponentially growing culture was determined. Starting at an OD_{600} of 1.0, six ten-fold serial dilutions were performed in sterile filtered water. 200 uL of the diluted culture was added to a 96-well microtiter plate and 5 uL of the dilution was then spotted onto the plates using a multi-channel pipetman.

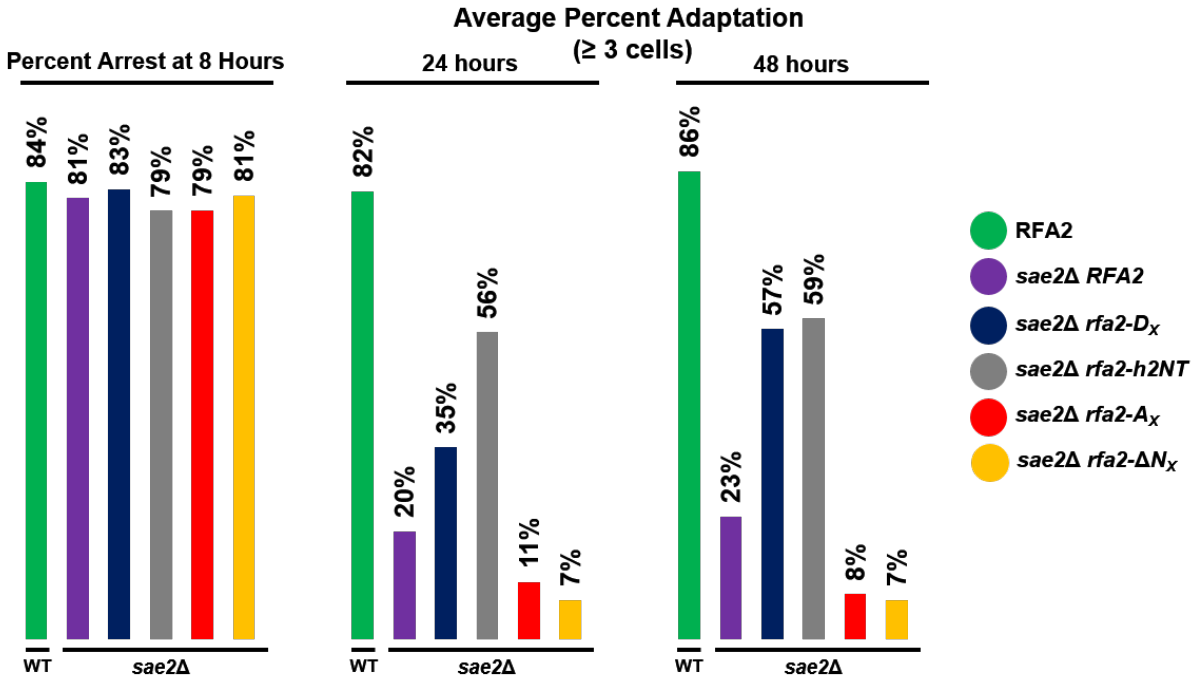

Figure 4.16. Rfa2 NT phosphorylation is required for checkpoint adaptation in *sae2*Δ cells. Microscopic analysis of checkpoint adaptation in *sae2*Δ Rfa2 NT extensive mutations. Broadly, rfa2 NT phospho-mimetic or naturally phosphorylatable mutations promote adaptation rescue, whereas an unphosphorylatable NT leads to a reduction in adaptation and an NT truncation severely impedes adaptation. Cells were harvested at 8 hours from culture induced to express HO endonuclease using galactose to a final concentration of 2%. 0.05 OD_{600} of cells were spread on YPRG plates using microbeads and analyzed at 8, 24, and 48 hours post-HO induction. Averages are from three independent experiments.

Table 4.5. Average Adaptation Percentages observed in NMM104 *sae2*Δ.

Strain	Percent of clusters ≥3 Cells at 8 Hours	Average Percent Adaptation by 24 hours	Average Percent Adaptation by 48 hours
sae2Δ RFA2	11%	20%	23%
sae2Δ rfa2-D$_X$	11%	35%	57%
sae2Δ rfa2-A$_X$	11%	11%	8%
sae2Δ rfa2-ΔN$_X$	12%	7%	7%
sae2Δ rfa2-h2NT	13%	56%	59%

Average adaptation was calculated by subtracting the total number of cells greater than or equal to three cells at 8 hours from total observed adaptation at 24 and 48 hours. Averages are from three independent experiments.

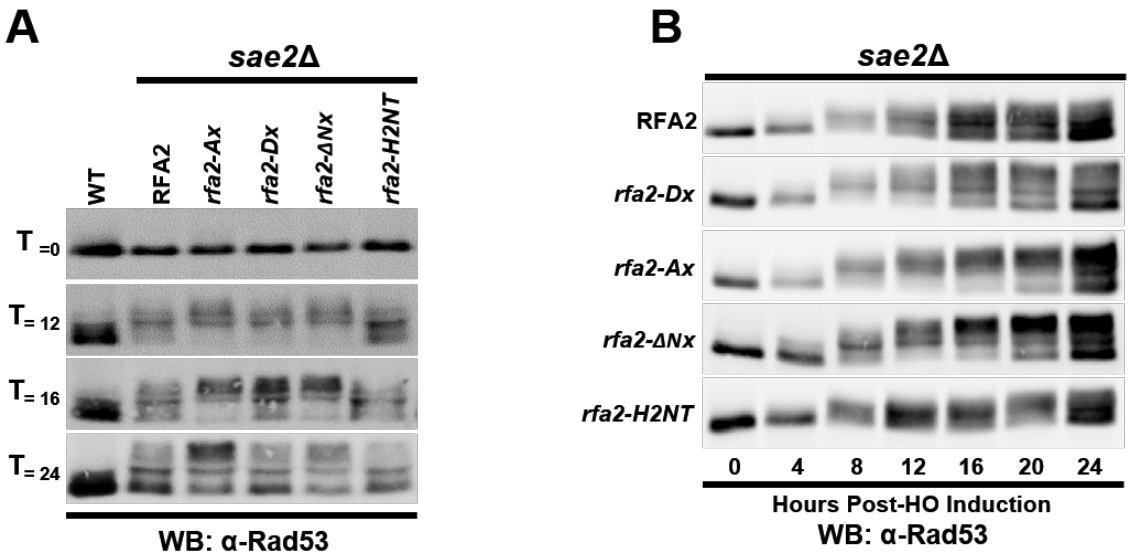

Figure 4.17. Rad53 inactivation during checkpoint adaptation requires Rfa2 NT phosphorylation in sae2Δ.
Rad53 immunoblots from *sae2*Δ cells. **A.** Rad53 hyper-activation is not impaired in *sae2*Δ cells but becomes more rapidly inactivated in *rfa2-D$_X$* or *rfa2-h2NT* mutations by 16 hours, as observed in *rtt107*Δ mutations. **B.** Rad53 immunoblots for each individual Rfa2 NT mutation in the *sae2*Δ mutant strain. Activation of Rad53 occurs indistinguishably from WT cells, however, *sae2*Δ mutants containing the *rfa2-A$_X$* or *rfa2-*Δ*N$_X$* mutation display more hyper-phosphorylated Rad53 throughout the observed time course. 10 OD_{600} of cells were harvested at indicated time points and treated as described. 40 ug of whole cell lysate was used in SDS-PAGE.

4.4.E. *rfa2-D$_X$* and *rfa2-h2NT* promote adaptation rescue more efficiently than *rfa1-t11* in *ckII*Δ adaptation-deficient mutations

In the late 1990's, Toczyski and Hartwell demonstrated that mutation of Cdc5 and Ckb2 (component of the CKII kinase complex) led to adaptation deficiency in yeast (Toczyski *et al.* 1997). Later, it was discovered that the *rfa1-t11* mutation could rescue the adaptation deficiency in *yku70*Δ and *rdh54*Δ cells, but are unable to overcome the checkpoint adaptation deficiency conferred by the *cdc5-AD* mutation (Lee *et al.* 2001). Our success in relieving checkpoint adaptation deficiency with phospho-mimetic or naturally phosphorylatable Rfa2 NT extensive mutations led us to test and compare the adaptation profiles of individual CKII complex-forming mutations *cka1*Δ, *cka2*Δ, *ckb1*Δ, and *ckb2*Δ in combination with the Rfa2 NT extensive mutations. Prior to analysis of adaptation, however, we sought to characterize the synthetic genetic interactions of individual *ckII*Δ subunit deletions with the Rfa2 NT extensive mutations. Deletion mutations of Cka1 (Figures 4.20 and 4.21) or Cka2 (Figures 4.22 and 4.23) are not hyper-sensitive to MMS or CPT but are hyper-sensitive to HU and PHL treatment. In combination with *rfa1-t11*, *cka1*Δ and *cka2*Δ are hyper-sensitive to all clastogens tested similar to that observed for

CKA1/CKA2 rfa1-t11, suggesting that *rfa1-t11* is the driver of this damage sensitive phenotype. Similar to that observed for the deletion mutations described in section 4.4.C and 4.4.D, combination of *cka1*Δ/*cka2*Δ with *rfa2-D*$_X$, *rfa2-h2NT,* or *rfa2-*Δ*N*$_X$ increase sensitivity to genotoxic agents, suggesting that there is a synthetic genetic interaction between Cka1/Cka2 and Rfa2. Moreover, deletions of Ckb1 and Ckb2 yield similar damage sensitive phenotypes to their *cka1*Δ or *cka2*Δ counterparts (Figures 4.24, 4.25, 4.26 and 4.27, respectively), suggesting a synthetic genetic interaction between the CKII kinase complex and Rfa2.

Microscopic analysis of individual *ckII*Δ subunit mutations during checkpoint adaptation, and in combination with Rfa2 NT extensive mutations, reveals a surprising separation of function during adaptation. Deletions of Cka1 and Cka2 are rescuable by *rfa2-D*$_X$, *rfa2-h2NT* and to a lesser extent *rfa1-t11* (Figure 4.28, Table 4.6; Figure 4.29, Table 4.7, respectively). Contrary to that observed in other deletion mutants tested in this study, the *rfa2-A*$_X$ mutation promotes a very minor adaptation proficiency in *cka1*Δ/*cka2*Δ (66% in *cka1*Δ versus 51% in *cka1*Δ *rfa2-A*$_X$; 37% in *cka2*Δ versus 49% in *cka2*Δ *rfa2-A*$_X$ at 48 hours), similar to that observed in NMM104 cells. The *rfa2-*Δ*N*$_X$ mutation reduces adaptation proficiency (*cka1*Δ *rfa2-*Δ*N*$_X$ adapts at 23%; *cka2*Δ *rfa2-*Δ*N*$_X$ adapts at 24% by 48 hours). Deletions of Ckb1 or Ckb2, however, produce slightly different adaptation phenotypes from their *cka1* and *cka2* counterparts. In both *ckb1*Δ and *ckb2*Δ (Figure 4.30; Table 4.8; Figure 4.31, Table 4.9, respectively), *rfa1-t11* is unable to promote robust rescue of the adaptation deficiency (26% in *ckb1*Δ versus 35% in *ckb1*Δ *rfa1-t11*; 25% in *ckb2*Δ versus 25% in *ckb2*Δ *rfa1-t11* at 48 hours). However, *rfa2-D*$_X$ and *rfa2-h2NT* are able to rescue the aforementioned adaptation deficiency to ~85% and 95%, respectively, in both *ckb1*Δ and *ckb2*Δ. Consistent with other adaptation-deficient mutations used in this study, the presence of either the *rfa2-A*$_X$ or *rfa2-*Δ*N*$_X$ mutation severely reduce the ability of *ckb1*Δ and *ckb2*Δ mutants to perform checkpoint adaptation. Biochemical analysis of the Rad53 phospho-state was not performed in these mutations, however, each individual *ckII*Δ subunit mutation and each combination with Rfa2 NT extensive mutations appeared to have G_2/M arrested morphology at 8 hours indicative of Rad53-damage-dependent checkpoint arrest. Taken together, our data suggests that, while each of the individual *ckII*Δ subunit deletions is adaptation-deficient, rescue of the observed adaptation deficiency is preferentially driven by the phospho-state of the Rfa2 NT and not the *rfa1-t11* mutation.

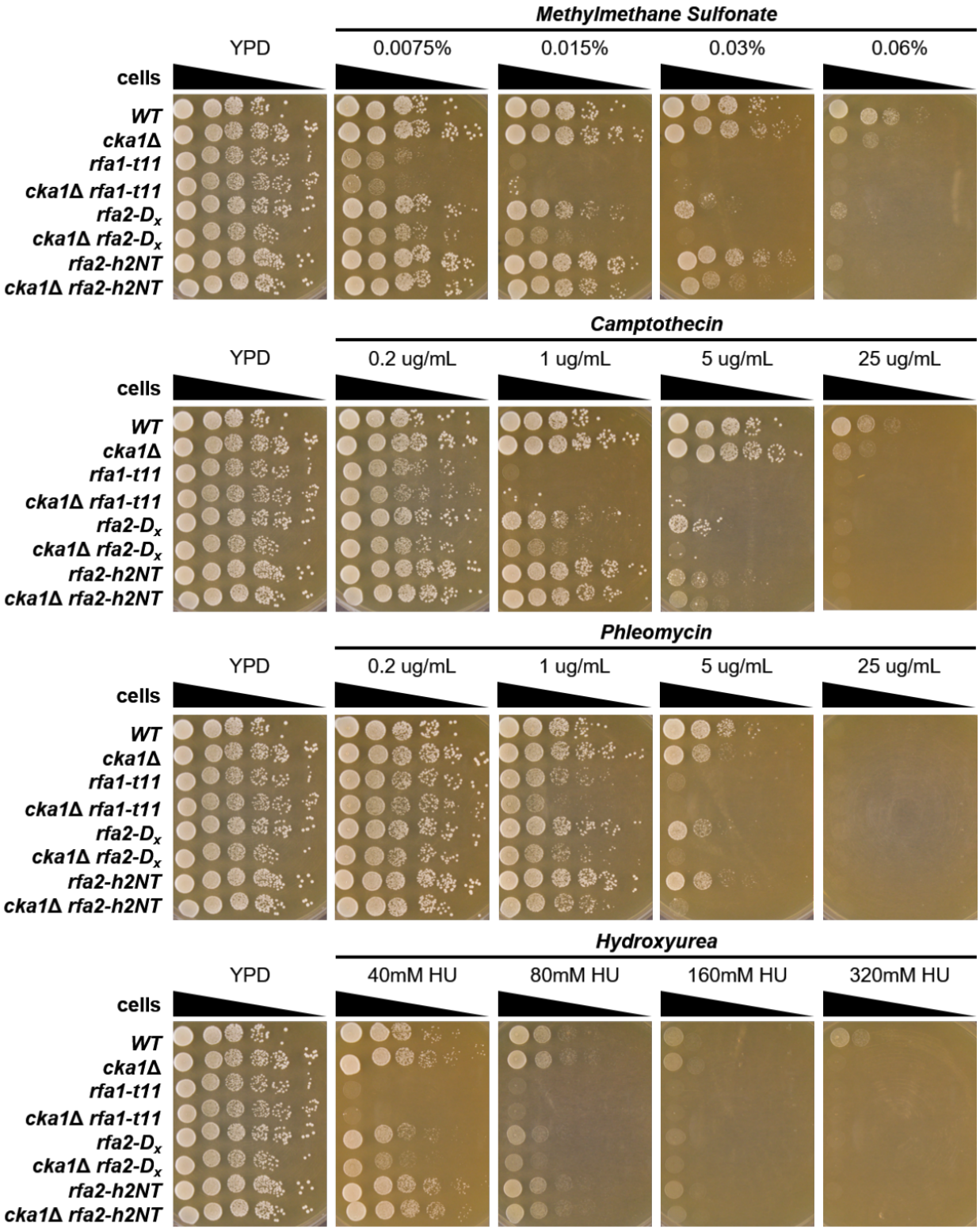

Figure 4.18. Diagnostic spot assay of *cka1*Δ mutations (*rfa2-Dx* and *rfa2-h2NT*).
*cka1*Δ Rfa2 NT mutations were harvested and an OD_{600} for the exponentially growing culture was determined. Starting at an OD_{600} of 1.0, six ten-fold serial dilutions were performed in sterile filtered water. 200 uL of the diluted culture was added to a 96-well microtiter plate and 5 uL of the dilution was then spotted onto the plates using a multi-channel pipetman.

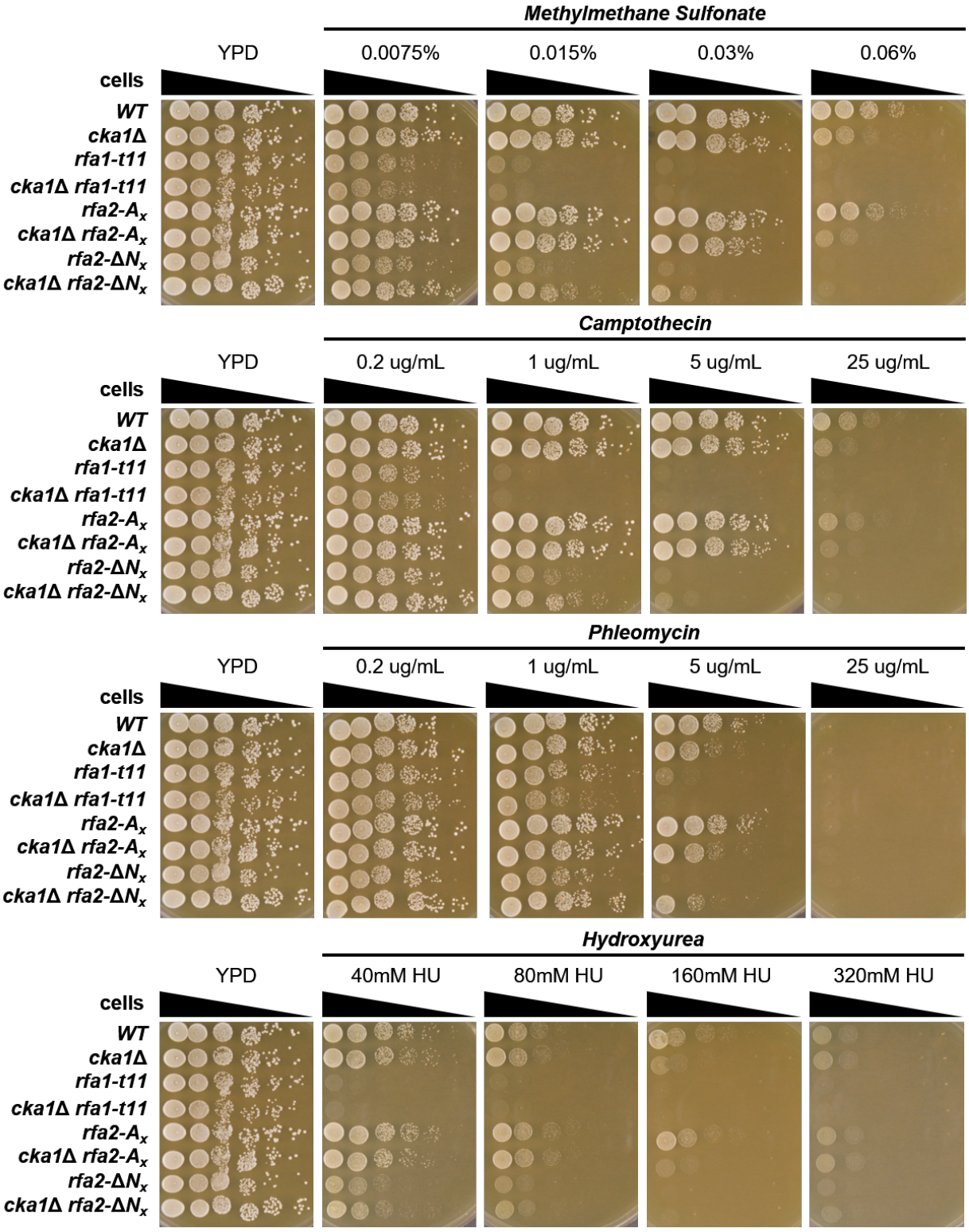

Figure 4.19. Diagnostic spot assay of *cka1*Δ mutations (*rfa2-A*$_X$ and *rfa2-*Δ*N*$_X$).
*cka1*Δ Rfa2 NT mutations were harvested and an OD_{600} for the exponentially growing culture was determined. Starting at an OD_{600} of 1.0, six ten-fold serial dilutions were performed in sterile filtered water. 200 uL of the diluted culture was added to a 96-well microtiter plate and 5 uL of the dilution was then spotted onto the plates using a multi-channel pipetman.

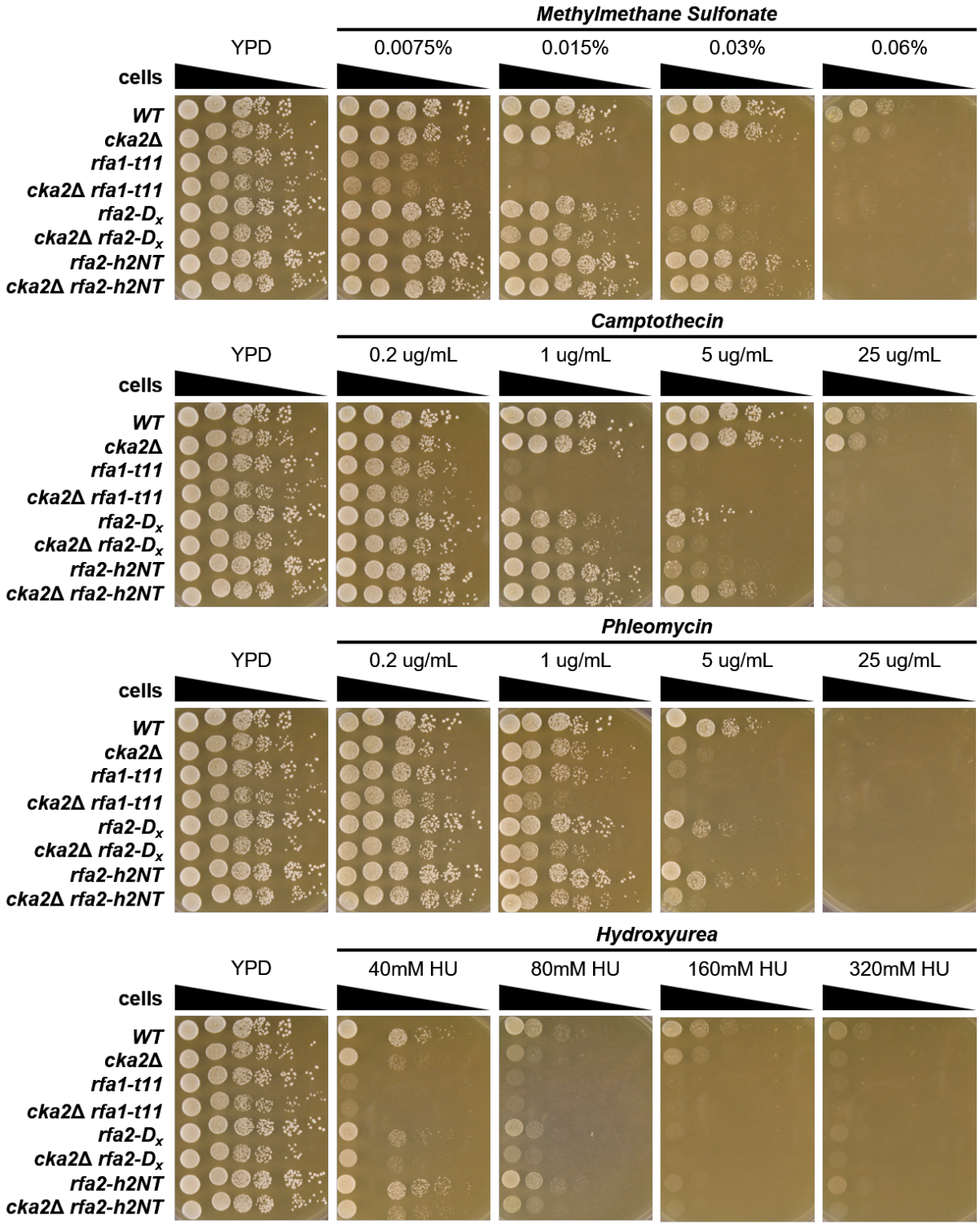

Figure 4.20. Diagnostic spot assay of *cka2*Δ mutations (*rfa2-D$_X$* and *rfa2-h2NT*).
*cka2*Δ Rfa2 NT mutations were harvested and an OD_{600} for the exponentially growing culture was determined. Starting at an OD_{600} of 1.0, six ten-fold serial dilutions were performed in sterile filtered water. 200 uL of the diluted culture was added to a 96-well microtiter plate and 5 uL of the dilution was then spotted onto the plates using a multi-channel pipetman.

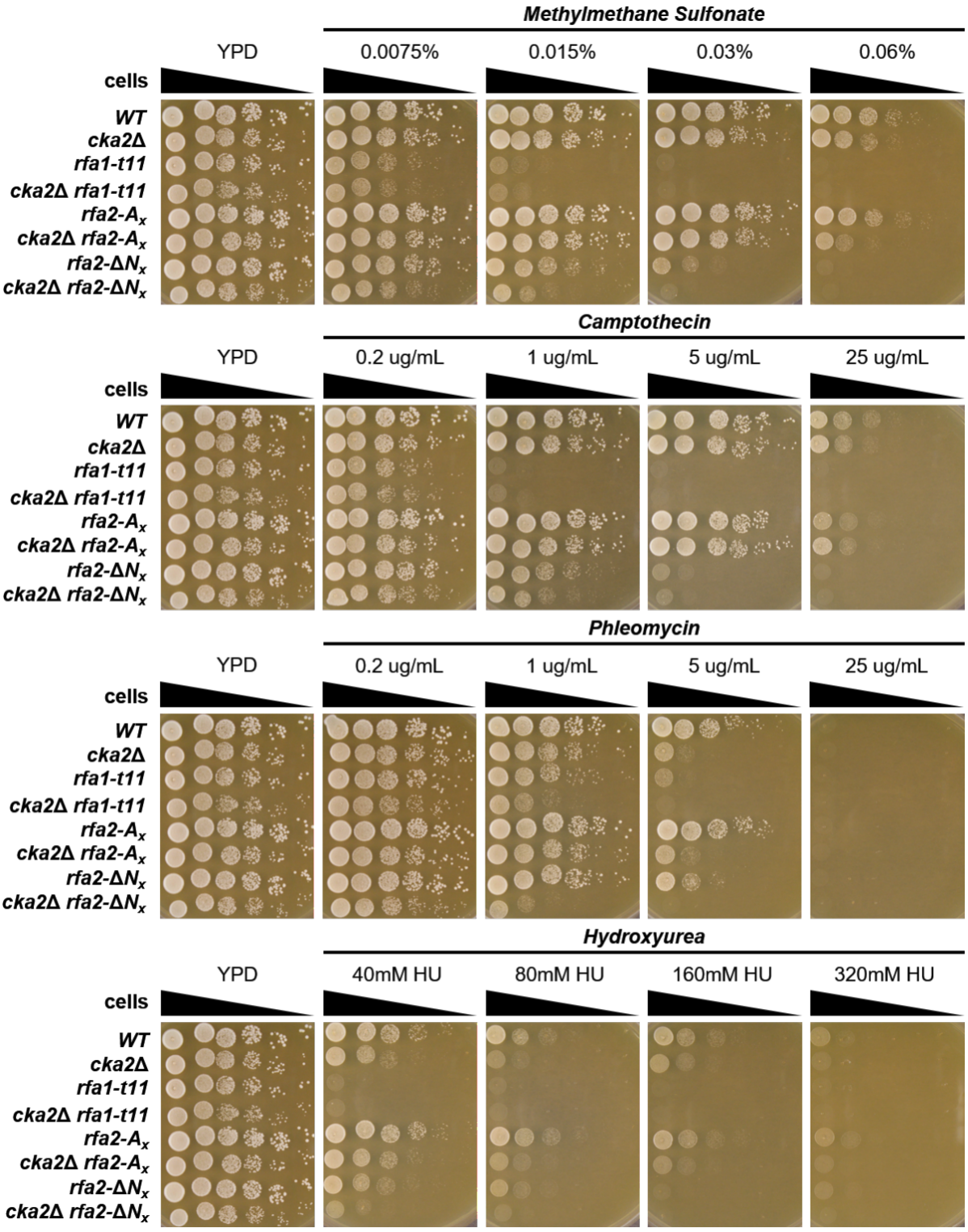

Figure 4.21. Diagnostic spot assay of *cka2*Δ mutations (*rfa2-A*$_X$ and *rfa2-ΔN*$_X$).
*cka2*Δ Rfa2 NT mutations were harvested and an OD_{600} for the exponentially growing culture was determined. Starting at an OD_{600} of 1.0, six ten-fold serial dilutions were performed in sterile filtered water. 200 uL of the diluted culture was added to a 96-well microtiter plate and 5 uL of the dilution was then spotted onto the plates using a multi-channel pipetman.

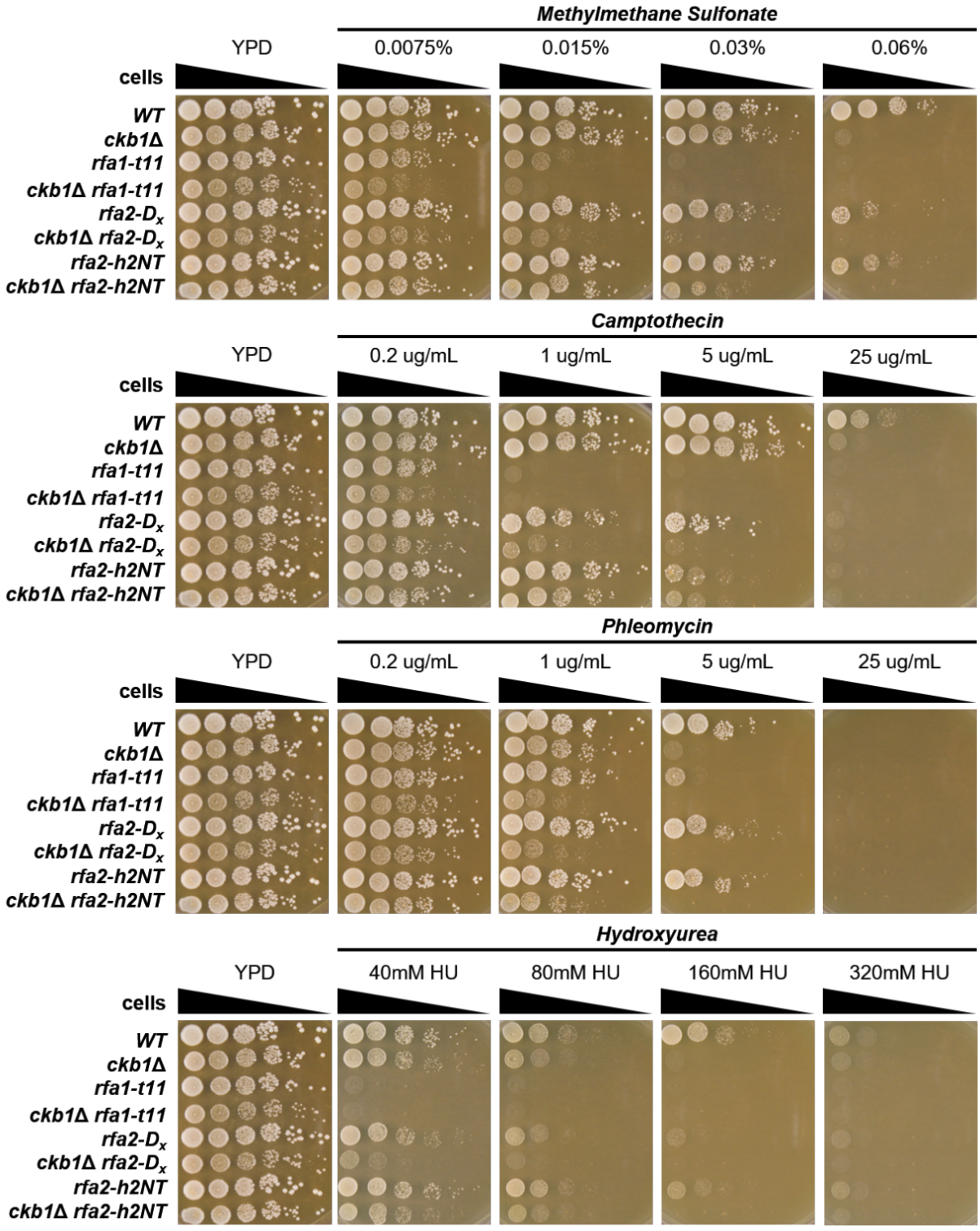

Figure 4.22. Diagnostic spot assay of *ckb1*Δ mutations (*rfa2-D$_X$* and *rfa2-h2NT*).
*ckb1*Δ Rfa2 NT mutations were harvested and an OD_{600} for the exponentially growing culture was determined. Starting at an OD_{600} of 1.0, six ten-fold serial dilutions were performed in sterile filtered water. 200 uL of the diluted culture was added to a 96-well microtiter plate and 5 uL of the dilution was then spotted onto the plates using a multi-channel pipetman.

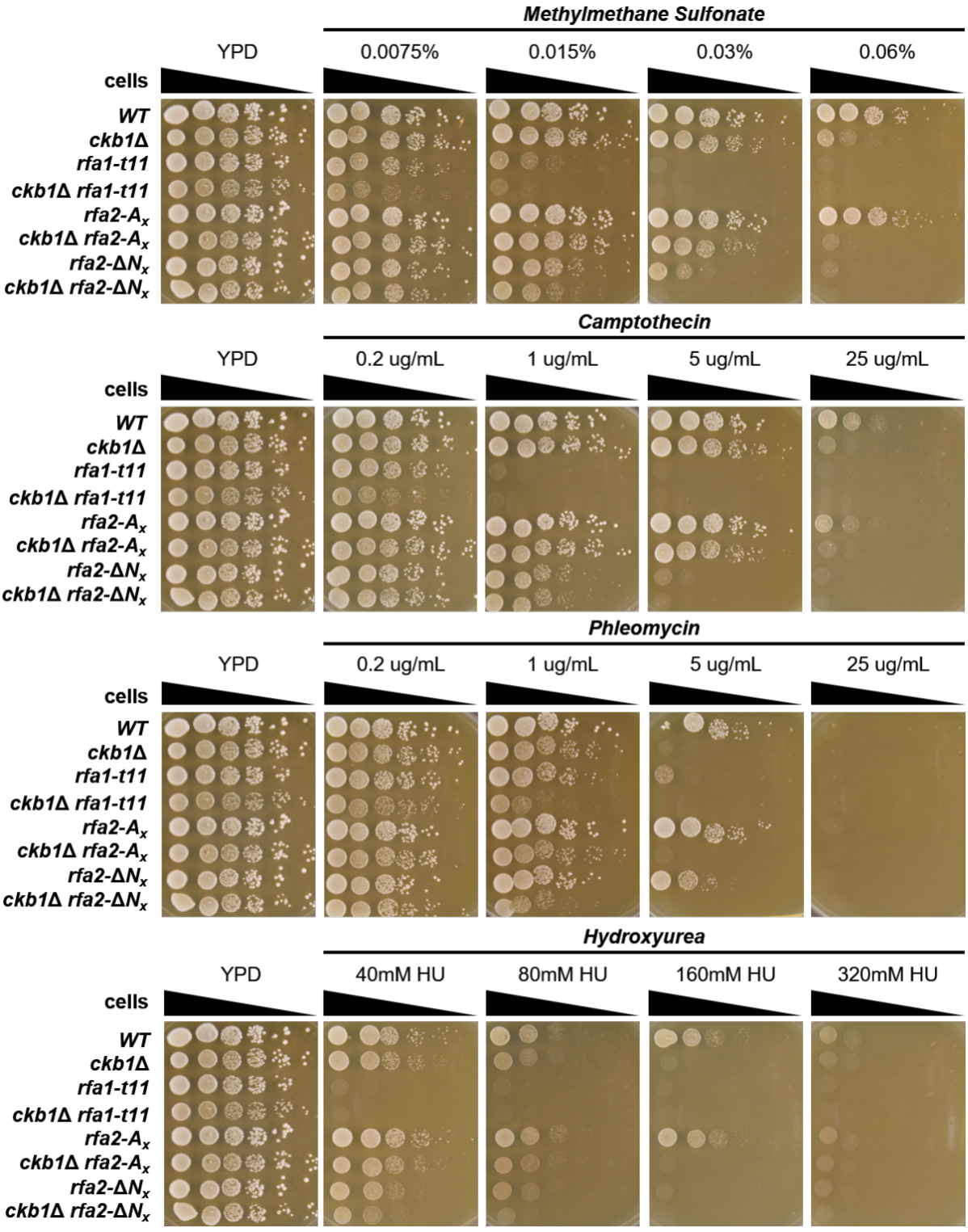

Figure 4.23. Diagnostic spot assay of *ckb1*Δ mutations (*rfa2-A*$_X$ and *rfa2-ΔN*$_X$).
*ckb1*Δ Rfa2 NT mutations were harvested and an OD_{600} for the exponentially growing culture was determined. Starting at an OD_{600} of 1.0, six ten-fold serial dilutions were performed in sterile filtered water. 200 uL of the diluted culture was added to a 96-well microtiter plate and 5 uL of the dilution was then spotted onto the plates using a multi-channel pipetman.

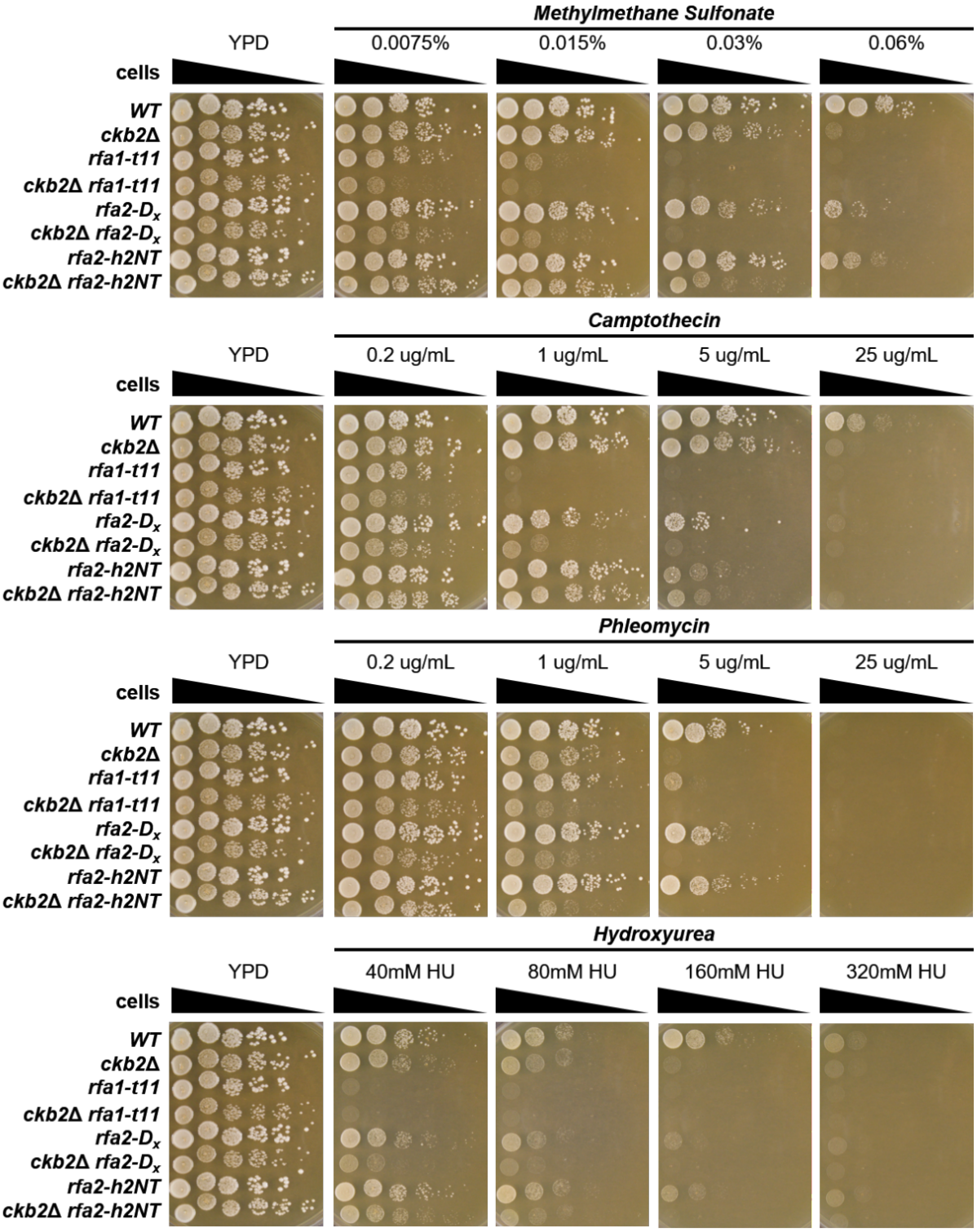

Figure 4.24. Diagnostic spot assay of *ckb2*Δ mutations (*rfa2-Dx* and *rfa2-h2NT*).
*ckb2*Δ ° mutations were harvested and an OD_{600} for the exponentially growing culture was determined. Starting at an OD_{600} of 1.0, six ten-fold serial dilutions were performed in sterile filtered water. 200 uL of the diluted culture was added to a 96-well microtiter plate and 5 uL of the dilution was then spotted onto the plates using a multi-channel pipetman.

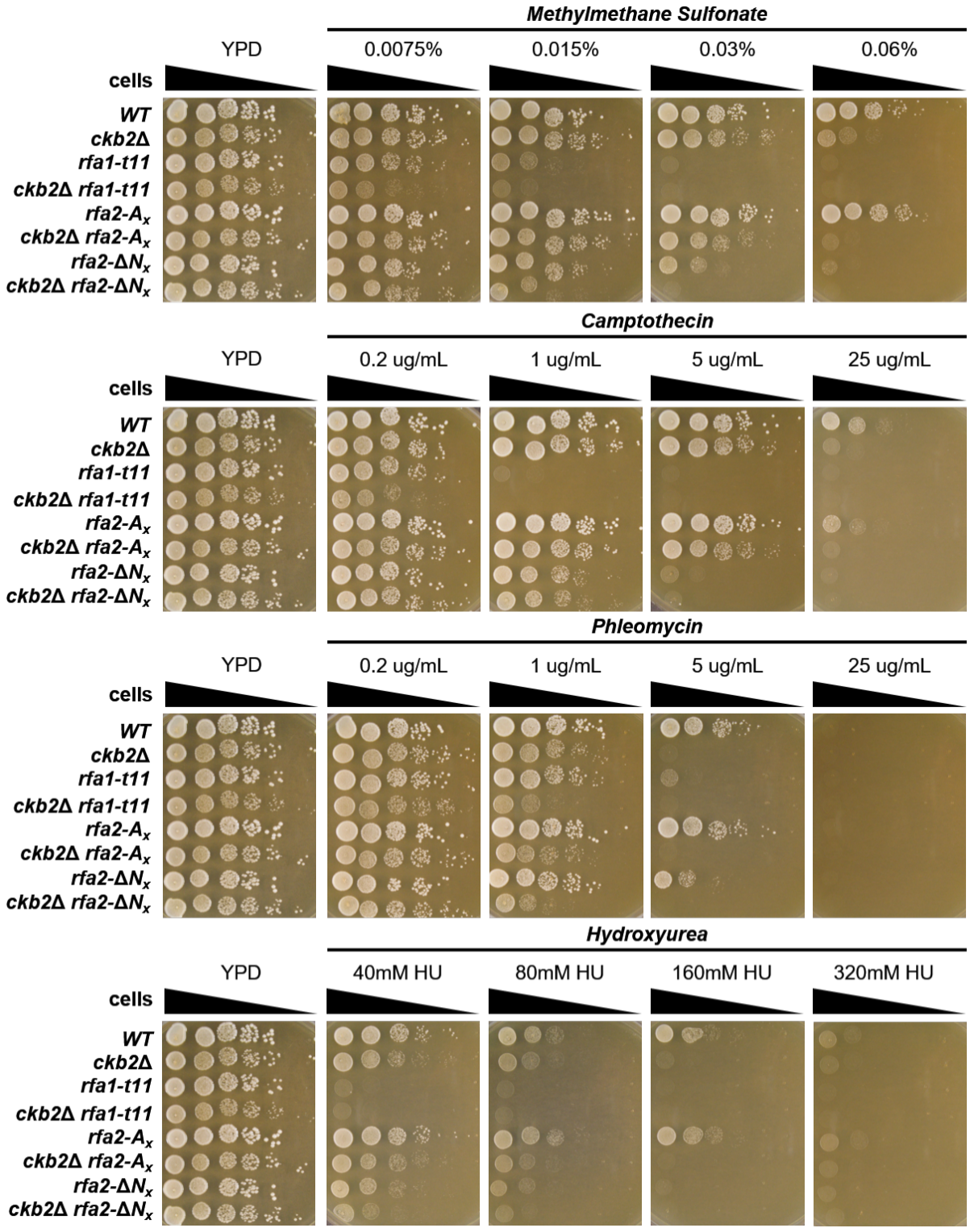

Figure 4.25. Diagnostic spot assay of *ckb2*Δ mutations (*rfa2-A*$_X$ and *rfa2-*Δ*N*$_X$).
*ckb2*Δ Rfa2 NT mutations were harvested and an OD_{600} for the exponentially growing culture was determined. Starting at an OD_{600} of 1.0, six ten-fold serial dilutions were performed in sterile filtered water. 200 uL of the diluted culture was added to a 96-well microtiter plate and 5 uL of the dilution was then spotted onto the plates using a multi-channel pipetman.

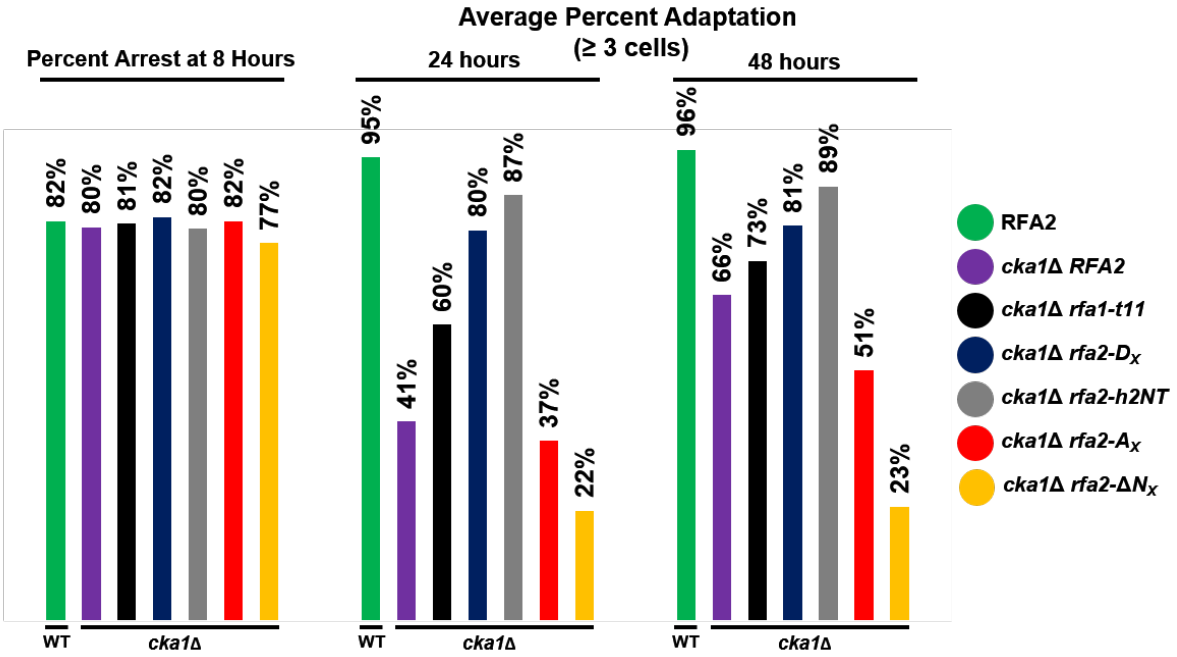

Figure 4.26. Rfa2 NT phosphorylation is required for checkpoint adaptation in adaptation-deficient *cka1*Δ mutations.
Microscopic analysis of checkpoint adaptation in *cka1*Δ Rfa2 NT extensive mutations. Similar to that observed for resection deficient mutations, rfa2 NT phospho-mimetic or naturally phosphorylatable mutations promote adaptation rescue in each resection deficient mutation, whereas an unphosphorylatable NT or NT truncation severely impedes adaptation. Adaptation rescue promoted by NT mutations exceeds that of *rfa1-t11*, a known checkpoint adaptation proficient mutation. Cells were harvested at 8 hours from culture induced to express HO endonuclease using galactose to a final concentration of 2%. 0.05 OD_{600} of cells were spread on YPRG plates using microbeads and analyzed at 8, 24, and 48 hours post-HO induction. Averages are from three independent experiments.

Table 4.6. Average Adaptation Percentages observed in NMM104 *cka1*Δ.

Strain	Percent of clusters ≥3 Cells at 8 Hours	Average Percent Adaptation by 24 hours	Average Percent Adaptation by 48 hours
***cka1*Δ**	12%	41%	66%
cka1*Δ *rfa1-t11	14%	60%	73%
***cka1*Δ + *rfa2-D*$_X$**	12%	80%	81%
***cka1*Δ + *rfa2-A*$_X$**	11%	37%	51%
***cka1*Δ + *rfa2-ΔN*$_X$**	11%	22%	23%
cka1*Δ + *rfa2-h2NT	12%	87%	89%

Average adaptation was calculated by subtracting the total number of cells greater than or equal to three cells at 8 hours from total observed adaptation at 24 and 48 hours. Averages are from three independent experiments.

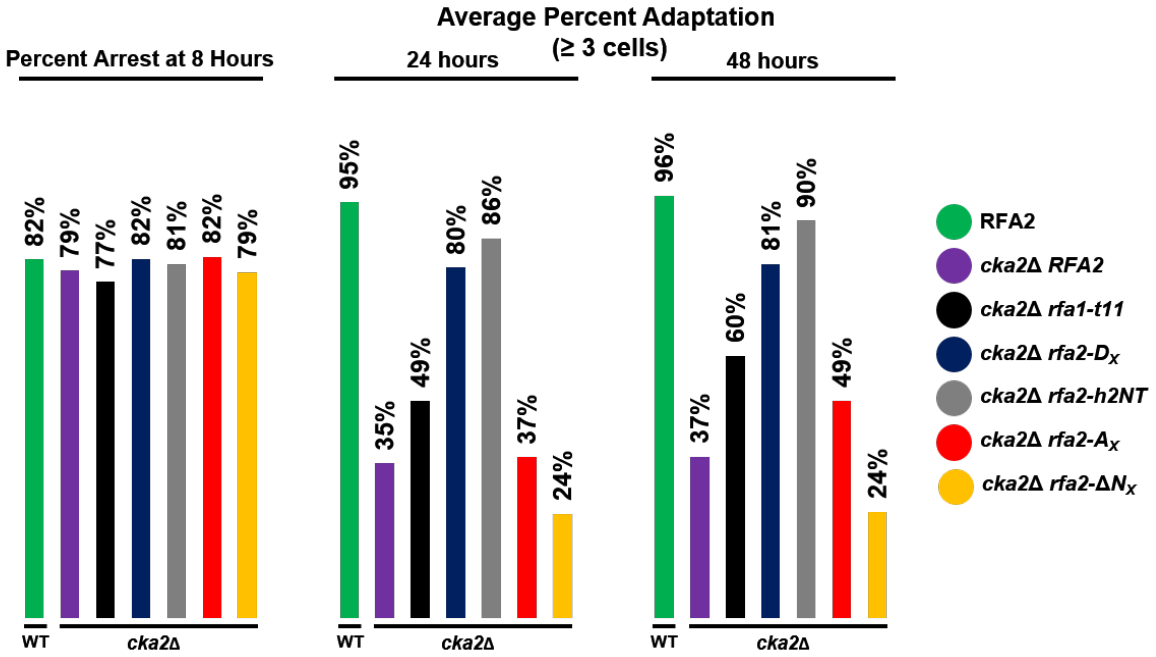

Figure 4.27. Rfa2 NT phosphorylation is required for checkpoint adaptation in adaptation-deficient *cka2*Δ mutations.
Microscopic analysis of adaptation in *cka2*Δ Rfa2 NT extensive mutations. Similar to that observed for resection deficient mutations, rfa2 NT phospho-mimetic or naturally phosphorylatable mutations promote adaptation rescue in each resection deficient mutation, whereas an unphosphorylatable NT or NT truncation severely impedes adaptation. Adaptation rescue promoted by NT mutations exceeds that of *rfa1-t11*, a known checkpoint adaptation proficient mutation. Cells were harvested at 8 hours from culture induced to express HO endonuclease using galactose to a final concentration of 2%. 0.05 OD_{600} of cells were spread on YPRG plates using microbeads and analyzed at 8, 24, and 48 hours post-HO induction. Averages are from three independent experiments.

Table 4.7. Average Adaptation Percentages observed in NMM104 *cka2*Δ.

Strain	Percent of clusters ≥3 Cells at 8 Hours	Average Percent Adaptation by 24 hours	Average Percent Adaptation by 48 hours
cka2Δ	12%	35%	37%
cka2Δ rfa1-t11	13%	49%	60%
cka2Δ + rfa2-D_X	17%	80%	81%
cka2Δ + rfa2-A_X	12%	37%	49%
cka2Δ + rfa2-ΔN_X	10%	24%	24%
cka2Δ + rfa2-h2NT	12%	86%	90%

Average adaptation was calculated by subtracting the total number of cells greater than or equal to three cells at 8 hours from total observed adaptation at 24 and 48 hours. Averages are from three independent experiments.

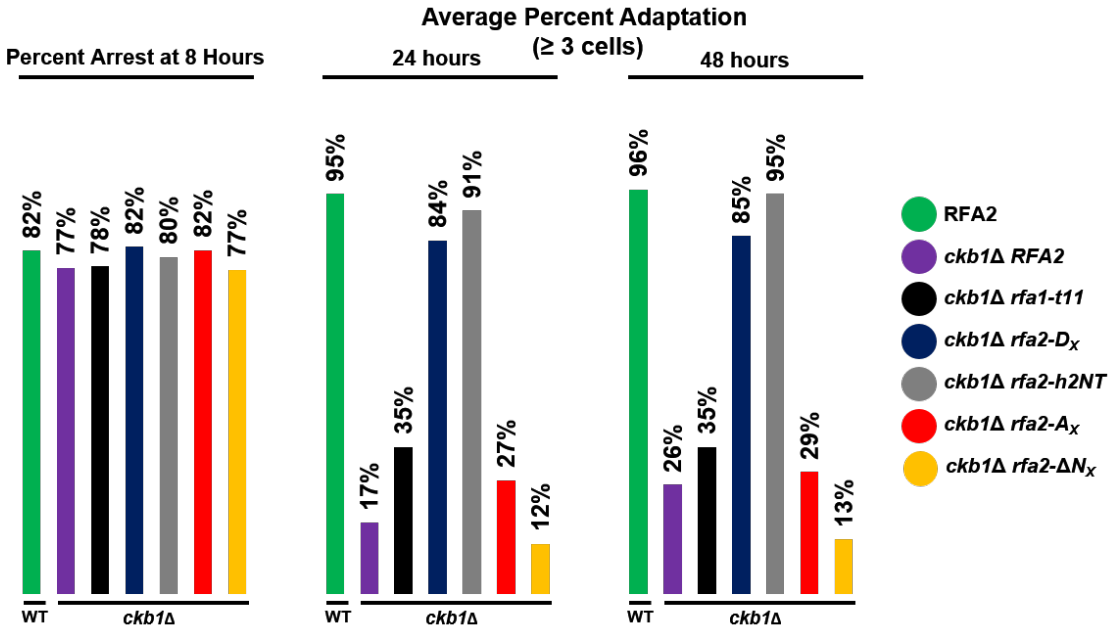

Figure 4.28. Rfa2 NT phosphorylation is required for checkpoint adaptation in adaptation-deficient *ckb1*Δ mutations.
Microscopic analysis of adaptation in *ckb1*Δ Rfa2 NT extensive mutations. Similar to that observed for resection deficient mutations, rfa2 NT phospho-mimetic or naturally phosphorylatable mutations promote adaptation rescue in each resection deficient mutation, whereas an unphosphorylatable NT or NT truncation severely impedes adaptation. Adaptation rescue promoted by NT mutations exceeds that of *rfa1-t11*, a known checkpoint adaptation proficient mutation. Cells were harvested at 8 hours from culture induced to express HO endonuclease using galactose to a final concentration of 2%. 0.05 OD_{600} of cells were spread on YPRG plates using microbeads and analyzed at 8, 24, and 48 hours post-HO induction. Averages are from three independent experiments.

Table 4.8. Average Adaptation Percentages observed in NMM104 *ckb1*Δ.

Strain	Percent of clusters ≥3 Cells at 8 Hours	Average Percent Adaptation by 24 hours	Average Percent Adaptation by 48 hours
***ckb1*Δ**	12%	17%	26%
ckb1*Δ *rfa1-t11	14%	35%	35%
ckb1*Δ + *rfa2-Dx	15%	84%	85%
ckb1*Δ + *rfa2-Ax	11%	27%	29%
ckb1*Δ + *rfa2-ΔNx	11%	12%	13%
ckb1*Δ + *rfa2-h2NT	12%	91%	95%

Average adaptation was calculated by subtracting the total number of cells greater than or equal to three cells at 8 hours from total observed adaptation at 24 and 48 hours. Averages are from three independent experiments.

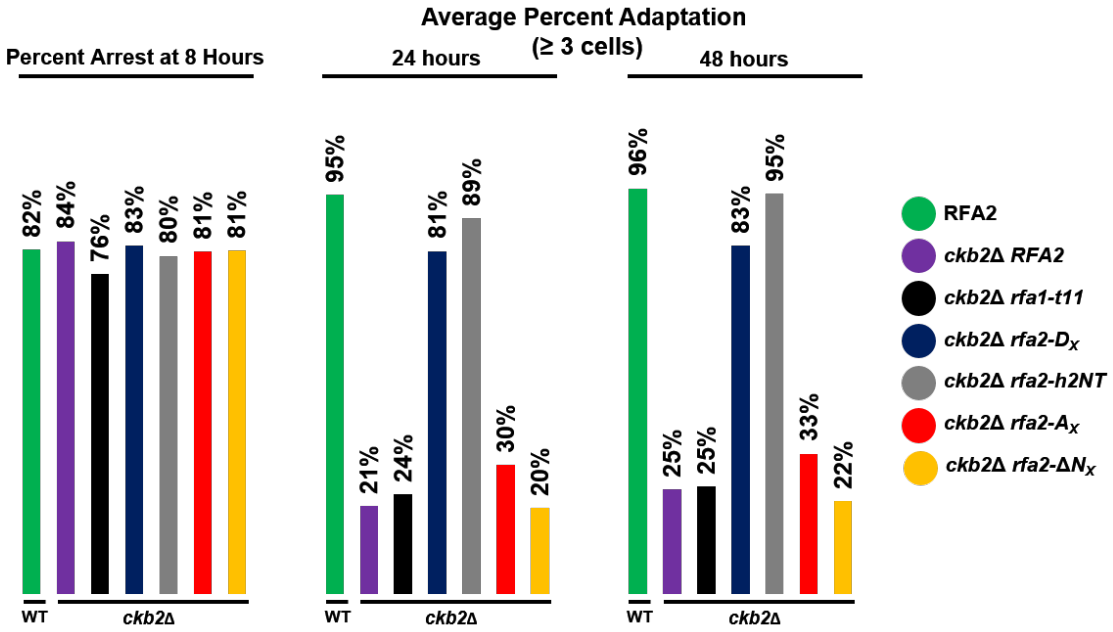

Figure 4.29. Rfa2 NT phosphorylation is required for checkpoint adaptation in adaptation-deficient *ckb2*Δ mutations.
Microscopic analysis of adaptation in *ckb2*Δ Rfa2 NT extensive mutations. Similar to that observed for resection deficient mutations, rfa2 NT phospho-mimetic or naturally phosphorylatable mutations promote adaptation rescue in each resection deficient mutation, whereas an unphosphorylatable NT or NT truncation severely impedes adaptation. Adaptation rescue promoted by NT mutations exceeds that of *rfa1-t11*, a known checkpoint adaptation proficient mutation. Cells were harvested at 8 hours from culture induced to express HO endonuclease using galactose to a final concentration of 2%. 0.05 OD_{600} of cells were spread on YPRG plates using microbeads and analyzed at 8, 24, and 48 hours post-HO induction. Averages are from three independent experiments.

Table 4.9. Average Adaptation Percentages observed in NMM104 *ckb2*Δ.

Strain	Percent of clusters ≥3 Cells at 8 Hours	Average Percent Adaptation by 24 hours	Average Percent Adaptation by 48 hours
***ckb2*Δ**	12%	21%	25%
ckb2*Δ *rfa1-t11	9%	24%	25%
***ckb2*Δ + *rfa2-D*$_X$**	16%	81%	83%
***ckb2*Δ + *rfa2-A*$_X$**	11%	30%	33%
***ckb2*Δ + *rfa2-ΔN*$_X$**	12%	20%	22%
ckb2*Δ + *rfa2-h2NT	10%	89%	95%

Average adaptation was calculated by subtracting the total number of cells greater than or equal to three cells at 8 hours from total observed adaptation at 24 and 48 hours. Averages are from three independent experiments.

4.4.F. Rpa2 NT phosphorylation during checkpoint adaptation is distinct from phosphorylation during genotoxic stress

As described in Chapter 2, phosphorylation of the Rfa2 NT is difficult to detect, at best, in response to genotoxic stressors. However, phosphorylation of the Rfa2 NT does occur and is observable via immunoblot. Figure 4.32 shows the Rfa2 phospho-state observed in response to global DSBs generated by phleomycin compared to that of cells that experience a single, controlled DSB at the *MAT* locus using HO endonuclease. In *rfa1-t11* cells Rfa2 phosphorylation can still occur. This additional distinct species is observed in *sae2*Δ, *rtt107*Δ, and to a lesser extent *slx4*Δ in response to PHL treatment and appears more prevalently in the same deletion mutations in response to the HO-induced DSB (Figure 4.32 A and B). Moreover, this distinct phosphorylation event that occurs in response to the HO-induced DSB is also observed in *tel1*Δ, *chk1*Δ, and *dun1*Δ mutants indicating that these DNA damage sensor or effector kinases are *not* responsible for the NT phosphorylation event observed. This distinct phosphorylation event is also observed in *cka1*Δ and *cka2*Δ mutant cells and is more abundant in the slower mobility species in *ckb1*Δ and *ckb2*Δ mutant cells in response to phleomycin (and possibly Gal-HO), suggesting that CKII activity may regulate the extent of phosphorylation on the Rfa2 NT through a yet unidentified mechanism.

4.5. Discussion

4.5.A. Checkpoint adaptation promoted by Rfa2 NT phospho-mutations is not dependent on resection

The results described in 4.4A revealed that each Rfa2 NT extensive mutations are proficient for both short- and long-range resection of the HO-induced DSB at the *MAT* locus. However, *rfa2-A$_X$* or *rfa2-*Δ*N$_X$* are generally incapable of promoting checkpoint adaptation, whereas *rfa2-D$_X$* and *rfa2-h2NT* are capable of rescuing all of the adaptation-deficient mutations tested in this study. Moreover, previous data has reported that resection of the DNA is not required for checkpoint adaptation (Eapen *et al.* 2012). Resection does provide cells with the ability to do alternative repair through single-strand annealing (SSA) (Helleday *et al.* 2007). If the DNA being resected on both ends of the break reaches a stretch of adequate homology between each, annealing between each of the generated overhangs occurs, followed by removal of non-homologous DNA ‘flaps’, DNA synthesis and completion of repair. However, this process

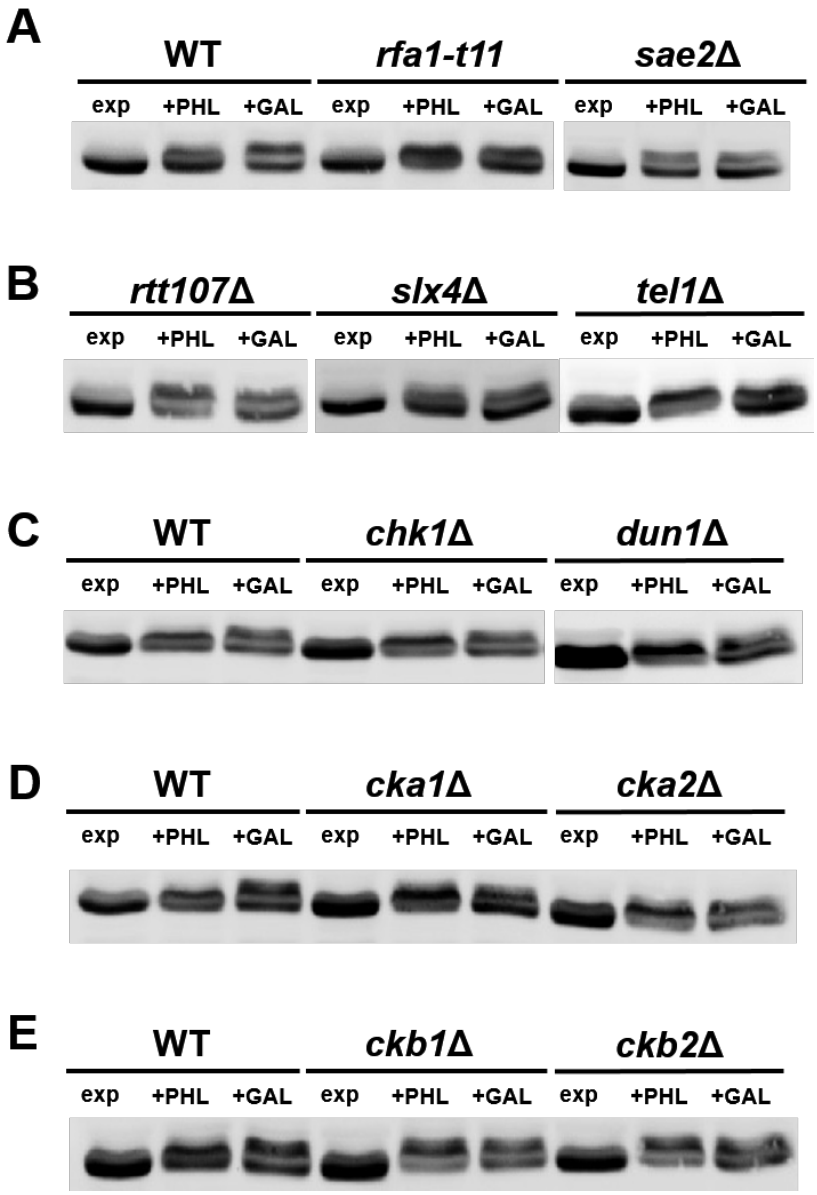

Figure 4.30. Rfa2 NT phosphorylation during checkpoint adaptation is distinct from that observed during genotoxic stress.
A. Rfa2 immunoblots from NMM104, *rfa1-t11* and *sae2*Δ cells treated with 5 ug/mL phleomycin or galactose-induced HO. **B.** Rfa2 immunoblots from *rtt107*Δ, *sae2*Δ, and *tel1*Δ cells. Phosphorylation in *tel1*Δ cells indicates that Tel1 is dispensable for Rfa2 NT phosphorylation during adaptation. **C.** Rfa2 immunoblots from *chk1*Δ and *dun1*Δ cells, treated as described in **A.** Phosphorylation in *chk1*Δ and *dun1*Δ cells indicates both kinases are dispensable for Rfa2 NT phosphorylation during adaptation. **D.** Rfa2 immunoblots from *cka1*Δ and *cka2*Δ cells, treated as described in **A. E.** Rfa2 immunoblots from *ckb1*Δ and *ckb2*Δ cells, treated as described in **A.** Phosphorylation of Rfa2 in CKII mutations indicates that CKII regulatory or kinase activity is dispensable for Rfa2 NT phosphorylation during adaptation. *ckb1*Δ and *ckb2*Δ mutations display NT phosphorylation during phleomycin challenge, indicating these genes may be important for controlling or reducing Rfa2 NT phosphorylation during the DNA damage response through an indirect mechanism. 10 OD_{600} of cells were harvested at indicated time points and treated as described. 20 ug of whole cell lysate was used in SDS-PAGE.

is incredibly mutagenic, as any genetic information contained within the DNA flaps that are removed prior to synthesis is lost forever. It is entirely possible that our Rfa2 NT extensive mutations are promoting a type of SSA repair of chromosome III, which would allow for reversal of the DDC and mitotic exit; however, further study will be required to determine whether this phenomenon is what is driving adaptation Rfa2 NT extensive mutations. Moreover, this also alludes to the possibility that Rfa2 possess some signaling activity in cells that is independent of the RFA complex binding to DNA.

4.5.B. Phospho-mimetic Rfa2 promotes adaptation rescue better than *rfa1-t11*

It is somewhat interesting that despite an impaired checkpoint, cells containing the *rfa1-t11* mutation are also as resection-proficient as the Rfa2 NT extensive mutations, albeit reduced from WT, but do not support checkpoint adaptation-proficiency to the same degree as Rfa2 NT extensive mutations in the mutant strain backgrounds tested. Previously, the *rfa1-t11* mutation was reported to lead to improper checkpoint maintenance through defective interactions with the 9-1-1 clamp loader complex Rad24-RFC, thus impairing 9-1-1 clamp loading (Kim *et al.* 2001, Majka *et al.* 2006). Cells containing the *rfa1-t11* mutation, however, still faithfully activate the Rad53-dependent checkpoint initially. Similarly, each of the Rfa2 NT extensive mutations tested herein all faithfully activate the Rad53-dependent checkpoint, however, preventing phosphorylation of the Rfa2 NT by alanine mutagenesis (*rfa2-A$_X$*) or truncation of the Rfa2 NT (*rfa2-*Δ*N$_X$*) lead to a more permanent arrest, whereas phospho-mimetic or naturally phosphorylatable forms of the Rfa2 NT (*rfa2-D$_X$* and *rfa2-h2NT,* respectively) lead to more rapid deactivation of the Rad53 checkpoint and appear to promote entry into mitosis, despite the presence of persistent DNA breaks. This phenomenon may explain the differences observed in clastogen sensitivity for each of the Rfa2 NT extensive mutations as well. For example, if *rfa2-D$_X$* is promoting aberrant checkpoint exit during LPR, these cells would divide continuously until their genomes were so unstable that the cells become inviable. Subsequently, *rfa2-*Δ*N$_X$* may lead to permanent arrest, rather than a repair defect, where cells do not exit the Rad53-dependent checkpoint regardless of whether DNA repair has occurred. Taken together, our results indicate that phosphorylation of the Rfa2 NT is required for checkpoint exit and mitotic entry, in a mechanism similar to that observed in human cells (Anantha *et al.* 2008).

Consistent with the hypothesis that Rfa2 NT phosphorylation promotes mitotic entry, regardless of the repair state of the DNA, is the observation that Rfa2 NT phosphorylation occurs in a distinct manner in cells experiencing an HO-induced DSB (Figure 4.24). Previously, it was demonstrated that CKII, the PP2 phosphatase complex, and Rad53 interact and this interaction is required for the dephosphorylation of Rad53 to alleviate checkpoint arrest and promote mitotic exit (Guillemain *et al.* 2007). Additionally, Figure 2.6 (Chapter 2) shows that *rfa2-h2NT* is more robustly phosphorylated in a *rad53*Δ mutation. Moreover, it was demonstrated that in a *set1*Δ or *mec3*Δ that Rad53 phosphorylates the Rfa2 NT (Schramke *et al.* 2001). It is entirely possible then that upon substantial hyper-activation of Rad53 that Rad53 inevitably targets the Rfa2 NT for phosphorylation in order to promote mitotic exit. It is also plausible that the Clb2/Cdc28 cyclin-dependent kinase complex would also phosphorylate the Rfa2 NT, similar to that observed in *Candida albicans* (Gao *et al.* 2014), as the Clb2/Cdc28-meiosis-specific homolog Ime2 phosphorylates Rfa2 at S27 during meiosis, prior to meiotic recombination (Clifford *et al.* 2004). Ultimately, cells must commit to permanent arrest or continued growth in order to survive, and it is plausible to think about the DDR program in a temporal fashion where cells only provide the DDR program with a certain amount of time to complete DNA repair and resume cell growth before the cell overrides the DDC and enters mitosis.

4.5.C. Potential therapeutic value in targeting Rpa2 phosphorylation during chemoradiation therapy in human disease

If phosphorylation of the Rfa2 NT is the predominant driver of mitotic entry, then it is also possible to speculate on the potential therapeutic value of promoting or inhibiting Rfa2 NT phosphorylation. In a *tel1*Δ, we observed that adaptation could not be rescued when combined with *rfa2*-ΔN_X to the same level as WT cells. Moreover, cells containing *rfa2*-ΔN_X are proficient for DNA replication in unstressed cells, similar to *rfa2*-D_X. Current therapeutic strategies for the treatment of cancer, a cellular disease caused by genetic mutations that cause dysregulation of cell growth, involve whole-organism exposure to genotoxic agents like MMS or CPT, in combination with radiation-induced DNA damage (chemoradiation therapy) with the idea that non-cancerous cells will be able to faithfully repair any lesions generated by the genotoxic agents, and cancer cells by virtue of their dysregulated growth cycle, will ultimately suffer enough genome-destabilizing mutations that the cancer cells will undergo apoptosis. While this is one of

the main therapeutic strategies used today, it still threatens the genomic fidelity of all cells within the affected host. A more effective treatment option may be a targeted therapy to inhibit Rpa2 phosphorylation through targeted kinase inhibition, or through promoting Rpa2 phosphorylation by stimulating the kinases that directly phosphorylate Rpa2 during mitotic entry (CDK). Recently, it was shown that the Rpa2 phospho-state correlates with cancer progression, as phosphorylated Rpa2 at S4/S8 were shown to be observed in higher concentration in dysplasias (abnormal cells within a tissue that may indicate pre-cancerous development), moderate concentrations in early grade tumors, and low concentrations in late-stage tumors (Rector *et al.* 2017). Moreover, RPA inhibitors to the Rpa1 N-terminal oligonucleotide-binding-fold-like domain have been demonstrated to increase replication stress and suppress tumor development in squamous cell carcinoma lines (Glanzer *et al.* 2014). Taken altogether, the findings presented here in context with what is currently known about Rpa2 phosphorylation mediating mitotic exit support a model where *preventing* phosphorylation of the Rpa2 NT may be a requirement of proper, concerted DNA repair, whereas promoting phosphorylation may be the signal that tells the cell that DNA repair is complete and that the cell can divide, safely preserving the fidelity of the genome. It is also possible that phosphorylation of the Rpa2 NT may be the biochemical signal that tells the cell to divide, irrespective of whether DNA repair has occurred.

CHAPTER 5: FUNCTION OF THE RFA2 NT IN MEIOSIS AND OTHER UNSOLVED MYSTERIES

5.1. Introduction

The process of meiosis (Chapter 1, Figure 1.2), or the generation of haploid gametes from diploid cells, is essential for the propagation of all sexually reproducing life (Martini *et al.* 2002). During meiosis, 180-200 programmed DSBs are generated by the recombination initiation complex (RIC) (described in Chapter 1, section 1.5) (Keeney *et al.* 1997). The role the RFA complex plays during meiosis remains poorly understood. Furthermore, the role Rfa2 NT phosphorylation plays during meiosis in *Saccharomyces cerevisiae* has not been examined.

In budding yeast, Rfa2 is known to be phosphorylated at S27 by the meiosis-specific Cdc28-homolog Ime2 (Clifford *et al.* 2004). This phosphorylation occurs independent of RFA complex binding to DNA, and occurs prior to meiotic recombination (*ibid*), however, the physiological relevance of this phosphorylation event remains unclear. Rfa2 is also known to be phosphorylated by the DNA damage sensor kinase Mec1 at S122 during meiosis, however, the role of this phosphorylation event appears mostly moot as cells expressing phospho-mutation forms of *rfa2-S122$_{A/D}$* produce only a modest change in crossover frequency with no impact on sporulation or spore viability (Bartrand *et al.* 2006).

In an effort to elucidate the function of the Rfa2 NT and its phospho-state during meiosis, a series of integrating vectors containing Rfa2 NT extensive mutations were generated. Using these Rfa2 NT extensive integrating vectors, chromosome replacements of the endogenous *RFA2* locus were performed in two meiotic yeast strain backgrounds, and the effects of extensive Rfa2 NT mutation were examined. I determined that the yeast Rfa2 NT phosphorylation plays a role in mediating meiosis, as cells containing mutant forms of the Rfa2 NT are defective in sporulation and produce high numbers of inviable spores. Moreover, I discovered that the Rfa2 NT is dispensable for the process of meiotic recombination, as cells containing *rfa2-*Δ*N$_X$* are able to recombine at diagnostic loci examined at the same frequency as cells containing *RFA2*.

While Rfa2 interaction with Rfa1 and Rfa3 are essential for complex formation and RFA activity, it is currently unknown what other yeast proteins involved in the lesion processing and repair (LPR) program Rfa2 interacts with. In an effort to examine Rfa2 interactions during both mitosis and meiosis, a series of yeast two hybrid vectors was generated with the assistance of Dr. Haring's Methods of

Recombinant DNA technology class during the spring semester in 2015. A list of the vectors generated can be found in Table 5.1. Unfortunately, however, the reporter vector used auto-activated on diagnostic media producing false-positive hits. As a result, the experiment was terminated until a new yeast two hybrid system could be obtained.

Table 5.1. List of yeast two hybrid vectors generated.

Gene Target	Vector	Sequence Verified?
Mre11	*pJG4-5-B42-MRE11*	Yes
Lge1	*pJG4-5-B42-LGE1*	Yes
Ybr137	*pJG4-5-B42-YBR137W*	Yes
Xrs2	*pJG4-5-B42-XRS2*	Yes
Sae2	*pJG4-5-B42-SAE2*	Yes
Cmr1	*pJG4-5-B42-CMR1*	Yes
Dmc1	*pJG4-5-B42-DMC1*	Yes
Rad50	*pJG4-5-B42-RAD50*	Yes
Rad51	*pJG4-5-B42-RAD51*	Yes
Rad52	*pJG4-5-B42-RAD52*	Yes
Rad54	*pJG4-5-B42-RAD54*	Yes
Rad55	*pJG4-5-B42-RAD55*	Yes
Rad57	*pJG4-5-B42-RAD57*	Yes
Rad59	*pJG4-5-B42-RAD59*	Yes

5.2. Materials and Methods

5.2.A. Construction and *In vitro* site-directed mutagenesis of pRS315-Rfa2 NT extensive vectors

Construction of pRS316-Rfa2 NT extensive mutant vectors was performed as follows. pRS315-derivative plasmids containing each Rfa2 NT mutation were digested with *Pvu*II in order to excise the Rfa2 NT mutant cassette from pRS315. Empty pRS316 plasmid was digested with *EcoR*V and *Pvu*II to

linearize the vector and create two homologous ends for *in vivo* homologous recombination in budding yeast. Linearized pRS316 and *Pvu*II digested pRS315-Rfa2 NT mutant DNA was then co-transformed into yeast. Transformants were plated on SD-Ura media in order to select for pRS316 vector recircularization. Following a four-day incubation, 1 mL of SD-Ura liquid media was used to flood the media plate, and total transformants were harvested by gently scrapping the plate and suspending the total cells into the liquid media. The resuspension was then added to 4 mL of SD-Ura media and grown overnight. Following yeast genomic DNA isolation, bacterial transformation into DH10B *E. coli* cells was performed and selection was done using LB-Amp plates. Bacterial transformants were then analyzed via colony cracking and restriction digest using diagnostic enzymes for each pRS316-Rfa2 NT extensive mutant (section 5.2.B.). Positive candidate plasmids were then sequenced by Eton Biosciences and used in *in vitro* site-directed mutagenesis.

I*n vitro* site-directed mutagenesis of pRS316-Rfa2 NT extensive mutation vectors (Appendix B) using a mutagenic primer (Appendix C) designed to remove the *CEN6/ARS4* centromeric and autonomously replicating sequence was performed under standard PCR conditions. Following a *Dpn*I digest, mutagenesis reactions were transformed into DH10B *E. coli* cells and plated on Luria Broth plates containing Ampicilin to select for transformants that had taken up in-tact vector. Candidate transformants were then harvested from the plate after 24 hours and manually screened via colony cracking, followed by a diagnostic digest (Figure 5.1). Vectors lacking the *CEN6/ARS4* site were then mini-prepped using the Omega Biotech E.Z.N.A Plasmid mini-prep kit, transformed back into *E. coli*, and added to the Haring lab permanent collection. pRS316-Rfa2 NT extensive vectors were accidentally discarded.

5.2.B. Integration of *pRS306*-Rfa2 NT extensive mutations into haploid yeast

RM26-26C and K264-10D yeast (Appendix A) were made competent and transformed with *SnaB*I-linearized *pRS306*-Rfa2 NT extensive mutation vectors. The *SnaB*I digest linearized the vector near the *rfa2* coding sequence and was necessary to target two-step gene replacement at the *RFA2* locus. Transformations were plated on SD-URA media. Positive transformants were struck to a master plate and tested via PCR to verify that the yeast were *RFA2/rfa2* positive. Overnight cultures of verified integrants were grown in YPD to stimulate pop-out of one of the *RFA2* sequences and were then spread out on 1.0 mg/mL 5'-FOA in order to select for cells that recombined out the *pRS306* vector sequence.

Cells that grew on 5'-FOA were then analyzed via PCR for integration of the Rfa2 NT extensive mutation. Positive candidate PCR fragments were then sent to Eton Biosciences for sequencing, and positive candidate yeast were replicated to YP-Glycerol media to ensure functional mitochondria. Verified candidates were then added to the Haring lab yeast permanent collection.

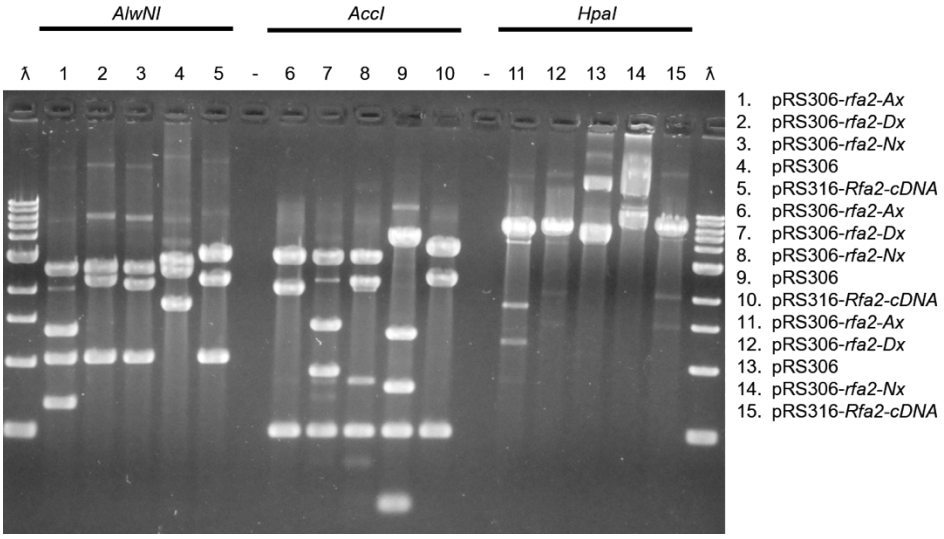

Figure 5.1. Restriction digest verification of Rfa2 NT extensive mutations in *pRS306* integrating vectors.
pRS306-Rfa2 NT extensive mutation vectors were digested with *AlwN*I, *Acc*I, and *Hpa*I in order to verify that each Rfa2 NT extensive mutation was present. pRS316-*Rfa2-cDNA* was used as a vector control for pRS306 or pRS316. *AlwN*I restriction digest is diagnostic for the presence of *rfa2-A*$_X$ as the coding sequence for *rfa2-A*$_X$ contains an additional *AlwN*I site that produces two additional fragments at ~1300 bp and ~650 bp from the 2 kbp fragment present in *rfa2-D*$_X$ and *rfa2*-Δ*N*$_X$ extensive mutation vectors. *Acc*I restriction digest is diagnostic for the presence of *rfa2-D*$_X$ and produces distinct digestion products from the 2 kbp fragment produced in the other extensive mutation vectors. *Hpa*I is diagnostic for *rfa2*-Δ*N*$_X$, as insertion of the *rfa2*-Δ*N*$_X$ coding sequence eliminates an *Hpa*I site present within the other Rfa2 NT extensive mutation vectors. PCR amplification was also used to verify

5.2.C. Mating of haploid yeast to create diploid cells

RM26-26C and K264-10D yeast integrants containing Rfa2 NT extensive mutations were mated by taking a patch of RM26-26C haploid cells and mashing them in with K264-10D haploid cells on SD-Com media. The following day. A streak from the mash was then taken from the haploid mash and struck out for single colonies on SD-His media to screen for diploids. Diploid yeast were verified as such by diagnostic replica plating to SD-His, SD-Leu, SD-Lys, and SD-Trp media.

5.2.D. Sporulation of diploid yeast and tetrad dissection

Diploids containing Rfa2 NT extensive mutations were patched to SpoII-Com media (minimal media) in order to induce sporulation via carbon/nitrogen starvation. Sporulation was monitored by

morphological analysis of cells following a three-minute zymolyase treatment using 3 uL of zylmolyase in 300 uL of ddH_2O on a hemocytometer. Zymolyase-treated tetrads were then spread finely on a YPD plate and dissected using a micro-dissection needle attached to an Olympus microscope. Spore viability was then quantitated from resulting spores after four days of growth.

5.2.E. Diagnostic replica plating

Diploid yeast patches from a master plate were replica plated onto diagnostic media (SD-His, SD-Leu, SD-Trp) to rapidly analyze effects on heteroallelic recombination. Plates were monitored over four days and results were documented.

5.2.F. Analysis of heteroallelic recombination

Diploid yeast grown in liquid SpoII-Com media were harvested, treated with zymolyase to remove the ascal coat and spread on SD-Leu or SD-Trp plates in order to assess heteroallelic recombination. Colonies that grew (positive recombinants) were then counted on each plate and quantitated.

5.2.G. qPCR of *MAT* locus during mating type switching

K264-10D cells containing Rfa2 NT extensive mutations cells were transformed with pGAL-HO (*URA3*+) and selected for positive transformants on SD-Ura media. Positive transformants were then plated to a master plate, and overnight cultures were started. The following day, cells were subcultured into 50 mL of SA-Ura (Synthetic complete media using acetate as a carbon source without uracil) and grown to an OD_{600} of 1.0. 10mL of 20% galactose in sterile filtered ddH_2O was then added to the media to a final concentration of 2% to induce expression of the HO endonuclease. Cells were harvested pre-HO induction ($T_{=0}$) and at 30-minute intervals following HO induction for four hours. Genomic DNA was harvested from samples isolated via phenol:chloroform:isoamyl alcohol (P:C:I) extraction and quantitated via spectroscopy. 10ng of DNA was used for qPCR with appropriate primers (Appendix C) diagnostic to determine the frequency of mating type switching from ‘A’ to ‘α’.

5.2.H. Generation of yeast two hybrid vectors

With the assistance of the Spring 2015 BIOC 474/674 Methods of Recombinant DNA technology course, pJG4-5 yeast two hybrid prey vectors to various lesion and processing repair proteins were generated. Vectors were analyzed during the course via diagnostic digest for proper insertion of desired target-prey genes. Positive candidate vectors were then sent to Eton Biosciences for sequence

verification. Vectors with whole gene insertions were then added to the Haring lab plasmid collection, and transformed into yeast with pEG202, and pSH18-34. Candidate yeast were then screened via diagnostic replica plating to SD-His/Trp/Leu media containing X-Gal. Unfortunately, all of the yeast two hybrid vectors auto-activated, producing blue colonies. Results were documented, and plates were discarded without photo documentation.

5.3. Results

5.3.A. Examination of the effects of Rfa2 NT extensive mutations during meiosis

Diploid yeast containing Rfa2 NT extensive mutations were pushed to undergo meiosis via carbon/nitrogen starvation as described above. Microscopic analysis of the cellular morphology of zymolyase treated yeast revealed that each Rfa2 NT extensive mutation was capable of facilitating meiosis in yeast. However, as Figure 5.2 shows, a severe meiotic deficiency was observed in homozygous diploids containing *rfa2-*Δ*N*$_X$. The wild-type yeast tested in this study were able to undergo meiosis roughly 52% of the time, whereas cells containing *rfa2-*Δ*N*$_X$ displayed only sporulated at 46%. Moreover, *rfa2-*Δ*N*$_X$ led to an increase in the number of 2-cell, incomplete spores, much more frequently than wild-type (~20% for *rfa2-*Δ*N*$_X$ versus ~12% for *RFA2*). The phospho-state of the Rfa2 NT, however, did not appear to play a major role in the ability of cells to undergo meiosis, as cells containing the *rfa2-D*$_X$ or *rfa2-A*$_X$ mutations sporulated at roughly the same frequency (~63% for each).

While each of the Rfa2 NT extensive mutations were able to promote and facilitate meiosis in budding yeast, their effects on tetrad formation (Figure 5.2, Tables 5.2 and 5.3) and spore viability was markedly different (Figure 5.3, Tables 5.4and 5.5). Analysis of the ability of Rfa2 NT extensive mutant diploids to form tetrads revealed that mutant cells containing *rfa2-D*$_X$ or *rfa2-A*$_X$ formed a tetrad containing four spores in approximately 50% of cells examined. Cells containing *RFA2* were only able to form tetrads 40% of the time, and the removal of the *RFA2* intron (*cDNA-WT*) led to a 7% increase in the ability of these diploids to form tetrads after meiosis. Mutant cells containing the *rfa2-*Δ*N*$_X$ mutation were only able to form tetrads in 26% of cells examined. This is potentially suggestive of a role for the intron of *RFA2* in regulating Rfa2 activity during meiosis and will require further study.

Further analysis of effects of Rfa2 NT extensive mutations during meiosis revealed markedly different spore survival phenotypes for each Rfa2 NT mutation. Cells containing *RFA2,* or the *rfa2-cDNA-WT* or *rfa2-A$_X$* mutations, produced 4 viable spores in at least 80% of tetrads dissected. Cells containing

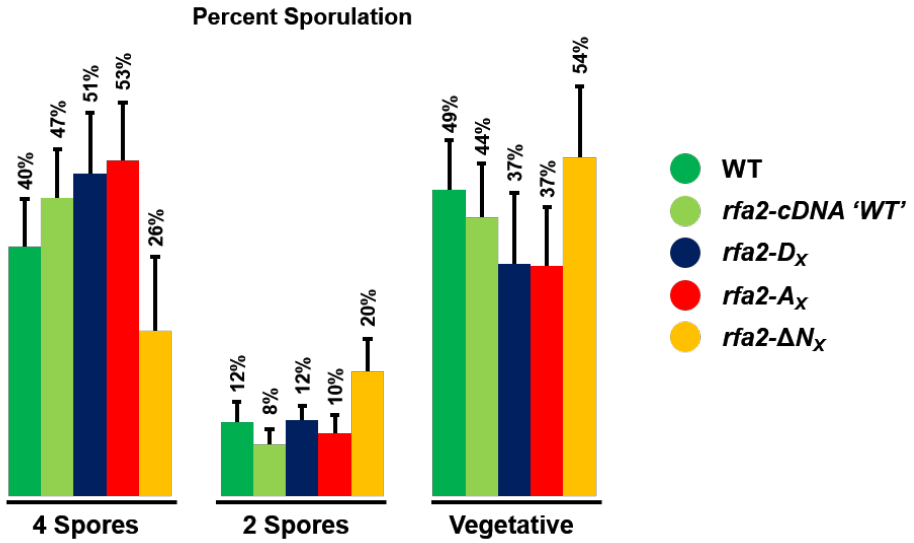

Figure 5.2. Effect of Rfa2 NT extensive mutations on meiosis in budding yeast.
Yeast diploids containing Rfa2 NT extensive mutations grown on YPD plates were replica plated to SpoIII-Com plates. After 4 days, a P-200 pipetman was used to harvest a small scrape of cells from the patch. Cells were then resuspended in 300 uL sterile ddH_2O and 3 uL of zymolyase was added and cells were zymolyase treated for 3 minutes. 20 uL of the reaction was then added to a hemocytometer slide and sporulation was counted via microscopic analysis of cellular morphology and quantitated. Averages and error bars presented were calculated from three independent replica platings and microscopic counts.

Table 5.2. Effect of Rfa2 NT extensive mutations on tetrad formation in budding yeast.

RFA2 Allele	4 Spores	2 Spores	Vegetative
RFA2	40%	12%	49%
cDNA-WT	47%	8%	44%
rfa2-D$_X$	51%	12%	37%
rfa2-A$_X$	53%	10%	37%
rfa2-ΔN$_X$	26%	20%	54%

Tetrads that form four spores were counted against a total population of cells scraped from the sporulating yeast patches on solid media plates. Two spores indicate dyads, whereas vegetative cells are single unbudded yeast cells.

Table 5.3. Effect of Rfa2 NT extensive mutations on meiosis in budding yeast.

RFA2 Allele:	*RFA2*	*RFA2-cDNA*	*rfa2-D$_X$*	*rfa2-A$_X$*	*rfa2-ΔN$_X$*
% Sporulated	51 ± 8%	56 ± 8%	63 ± 11%	63 ± 9%	46 ± 11%

Percent sporulation was calculated by adding the total of two and four spore meiotic products together.

the *rfa2-D$_X$* mutation only produced viable tetrads in approximately 60% of tetrads dissected, suggesting that permanent phospho-mimetic mutation of the Rfa2 NT leads to a meiotic defect. Cells containing the *rfa2-ΔN$_X$* were only able to produce four viable tetrads in 22% of tetrads dissected, demonstrating that the physical presence of the Rfa2 NT is a requirement for proper progression through meiosis in budding yeast.

After tetrad dissection, 92% of the spores analyzed from WT cells were viable, as well as 97% of the spores examined from *rfa2-cDNA* diploids. Spores containing the *rfa2-A$_X$* mutation were examined and determined to have a viability of 94%, in-line with wild-type cells. Examination of *rfa2-D$_X$* and *rfa2-ΔN$_X$* revealed that only 85% and 66% of spores analyzed, respectively, were viable. This indicates that phospho-mimetic mutation of the Rfa2 NT or deletion of the Rfa2 NT has a detrimental effect on the meiotic program during meiosis. Moreover, this data also indicates that the Rfa2 NT is required for proper meiotic progression.

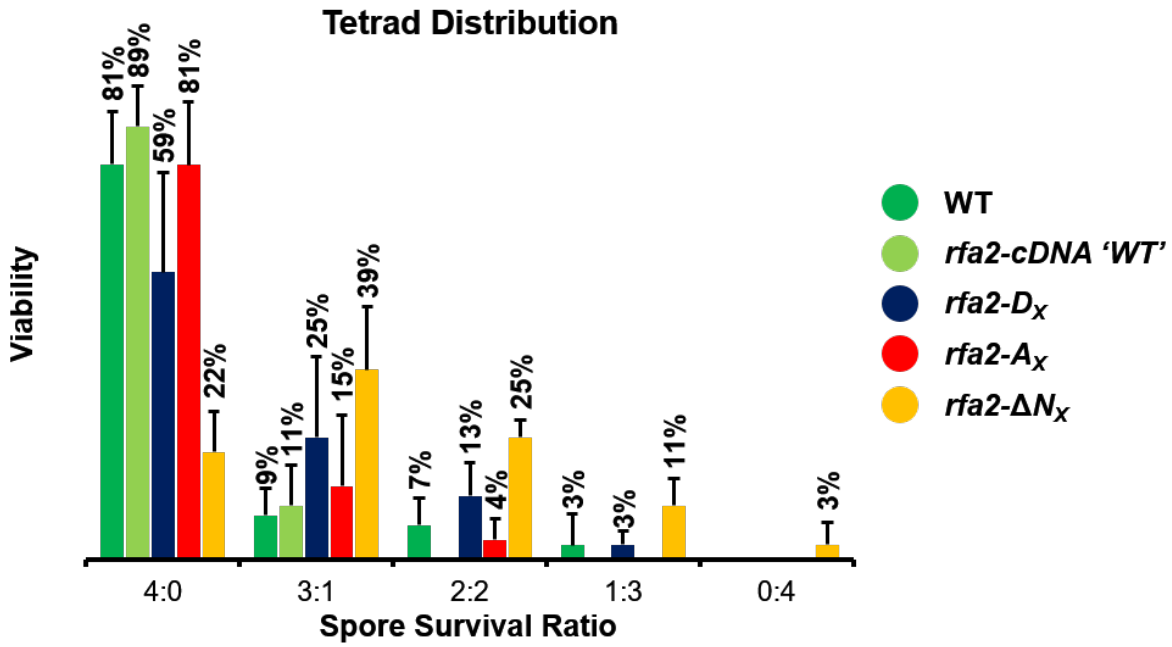

Figure 5.3. Effect of Rfa2 NT extensive mutations on spore viability in budding yeast.
Diploid cells containing Rfa2 NT extensive mutations were harvested as described in Figure 5.3. Following zymolyase treatment, cells were spread thinly onto a YPD plate using a sterilized inoculating loop. Tetrads were then micro-dissected using a pulled glass needle attached to an Olympus microscope and each spore's position on the plate was documented. Spore survival ratio was then calculated based on how many individual spores grew into single colonies at their respective positions. 4:0 indicates all four spores from the tetrad grew into colonies, 0:4 indicates none of the dissected tetrads grew into colonies. Viability percentages and error bars were calculated from a total of 160 (four independent experiments) dissected spores of each Rfa2 NT extensive mutation diploid.

Table 5.4. Effect of Rfa2 NT extensive mutations on spore survival ratio in budding yeast.

RFA2 Allele	4:0	3:1	2:2	1:3	0:4
RFA2	81%	9%	7%	3%	0%
cDNA-WT	89%	11%	0%	0%	0%
rfa2-D$_X$	59%	25%	13%	3%	0%
rfa2-A$_X$	81%	15%	4%	0%	0%
rfa2-ΔN$_X$	22%	39%	25%	11%	3%

Spore survival ratio was calculated by counting the number of live spores per row after tetrad dissection. A ratio of 4:0 indicates four live spores, zero dead spores, whereas 2:2 indicates two live cells, two dead spores.

Table 5.5. Effect of Rfa2 NT extensive mutations on spore viability in budding yeast.

RFA2 Allele:	RFA2	*RFA2-cDNA*	*rfa2-D$_X$*	*rfa2-A$_X$*	*rfa2-ΔN$_X$*
% Viability	92 ± 6%	97 ± 2%	85 ± 7%	94 ± 3%	66 ± 5%

Percent viability is calculated as a ratio of total colonies that grew from individual spores divided by the total number of spores dissected, irrespective of their spore survival ratio

5.3.B. Effects of Rfa2 NT extensive mutations on heteroallelic recombination

To analyze the effects of Rfa2 NT extensive mutations during homologous recombination, heteroallelic recombination was assayed in mitotically growing and meiotic products from Rfa2 NT extensive mutant diploids via qualitative replica plating (Figure 5.4) as well as a quantitative spore recombination assay (Figure 5.5). For cells to produce micro-colonies on diagnostic media, a single homologous recombination event must occur between auxotrophic mutant alleles (*e.g: lys2-2 and lys2-5*) to produce a prototrophic colony. During meiosis, the process of homologous recombination occurs at a nearly 100-fold increased frequency from that of mitotic cells. During diagnostic replica plating we observed micro-colony formation on two different diagnostic media. This demonstrates that diploids containing Rfa2 NT extensive mutations are proficient for both mitotic recombination and meiotic recombination and suggests that the Rfa2 NT is dispensable for the processes of homologous recombination in both mitotic and meiotic cells.

Further evidence of the dispensability for the Rfa2 NT during meiotic recombination was obtained through a quantitative assessment of heteroallelic recombination via random spore spreads. After treating tetrads with zymolyase, cells were spread on diagnostic media, allowed to grow, and then counted. Cells containing Rfa2 NT extensive mutations were able to perform heteroallelic recombination within 1-2-fold

total recombination frequency compared to wild-type Rfa2 or the *rfa2-cDNA-WT* mutation. If homologous recombination at any level were impacted by the state of the Rfa2 NT, then we would expect that less or no recombinants would be present. However, as indicated by both recombination assays the Rfa2 NT state does not play a major role in the ability of cells to perform homologous recombination during meiosis.

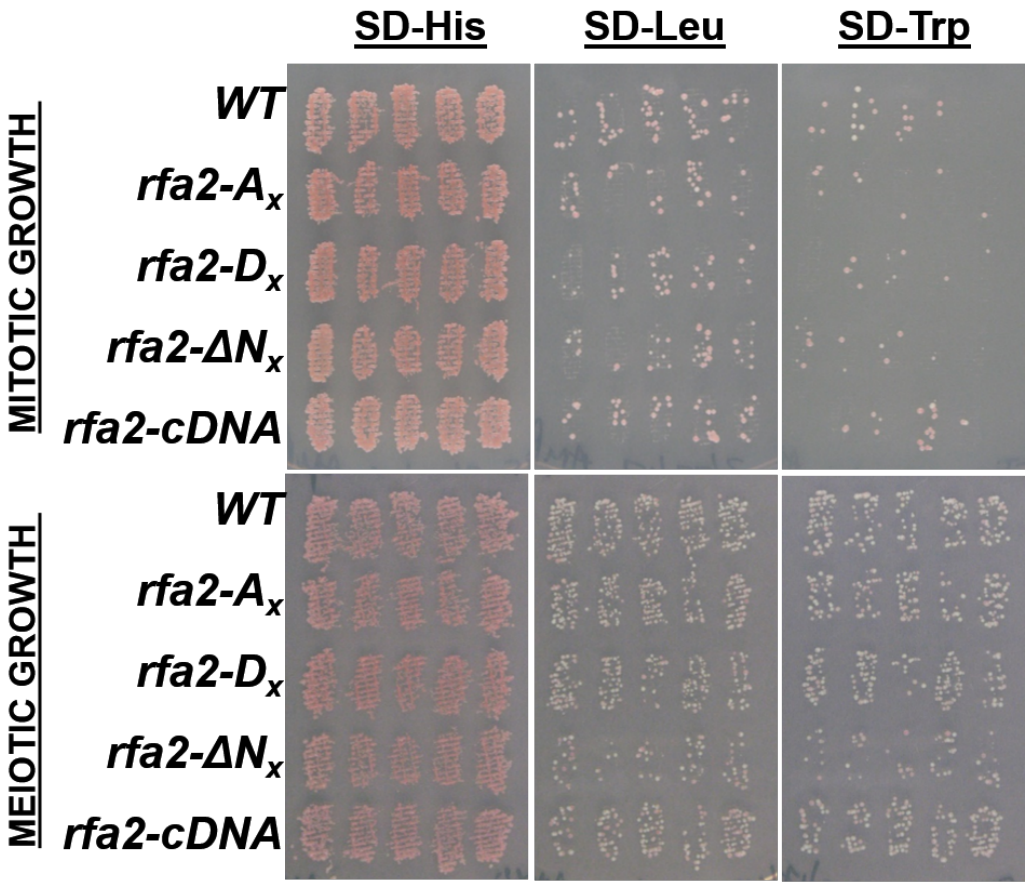

Figure 5.4. Effect of Rfa2 NT extensive mutations on heteroallelic recombination in budding yeast via diagnostic replica plating.
Diploid yeast containing Rfa2 NT extensive mutations were replica plated to SpoIII-Com plates in order to induce meiosis. The YPD master plate containing diploids was replica plated to SD-His, SD-Leu, and SD-Trp media to qualitatively analyze mitotic recombination frequency. After 4 days, SpoIII-Com replica plate was replica plated to SD-His, SD-Leu, and SD-Trp media to qualitatively analyze meiotic recombination frequency.

5.3.C. Effects of Rfa2 NT extensive mutations on mating type switching

Using qPCR analysis, I attempted to quantify the ability of cells to undergo a specialized type of recombination event that allows yeast to switch mating-type from A to α, and vice versa. During mating-type switching, donor sequence from the *HML*-α and *HMR*-a loci on chromosome III are used to repair the

MAT locus to the *opposite* mating type. Initiation of mating-type switching occurs via expression of HO endonuclease, which cleaves the *MAT* locus. However, the DSB generated in cells that are *HML*+ and

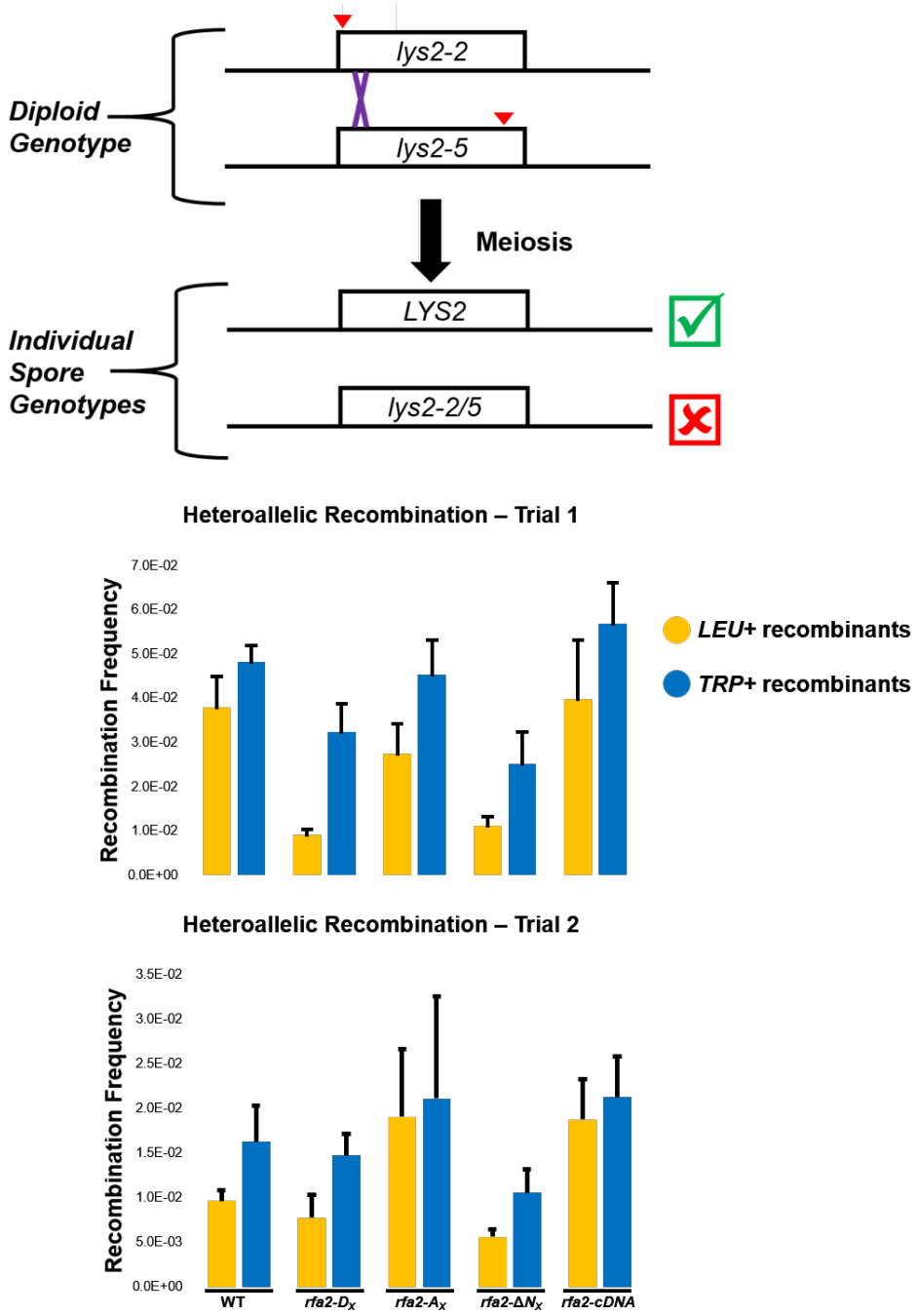

Figure 5.5. Effect of Rfa2 NT extensive mutations on heteroallelic recombination in budding yeast. Diploid yeast containing Rfa2 NT extensive mutations were grown in YPD rich media overnight, harvested, washed in ddH_2O and subcultured into YPA media. The following day, cells were harvested, washed once more, and subcultured into SpoII-Com liquid media and allowed to sporulate overnight. Presence of spores was examined microscopically. Cells were then harvested, treated with zymolyase, and equal numbers of cells were spread on SD-Leu or SD-Trp plates using microbeads. After four days of growth, colonies on each plate were calculated. Trial 1 and Trial 2 averages and error bars are from three independent platings following two independent liquid sporulation assays.

HMR+ does not lead to activation of Rad53-dependent checkpoint arrest and is repaired rapidly (Pellicioli *et al.* 2001). Because we had discovered a meiotic defect in diploids containing Rfa2 NT extensive mutations, we sought to understand if this defect was due to an inability to perform homologous recombination. However, results from heteroallelic recombination assays suggested that Rfa2 NT extensive mutations were proficient for recombination (section 5.3.B). Unfortunately, due to the experimental conditions we were using, I was unable to obtain a consistent result for the ability of the tested Rfa2 NT extensive mutations in K264-10D. Dr. Haring and I believe that this was largely due to the fact that we were doing glucose depletion in acetate media, rather than raffinose media. Induction or expression of HO was not measured. Furthermore, the cells we were using were expressing HO off of a plasmid that had a leaky promoter, and HO ended up being expressed at inopportune and unmeasurable times. As a result, the project was shelved. However, because yeast cells containing Rfa2 NT extensive mutations all progress through meiosis, albeit at differential rates and viabilities, and were successfully able to produce heteroallelic recombinants (Figure 5.5 and 5.6), we assessed that the defect in Rfa2 NT extensive mutation yeast was *not* due to an inability to perform homologous recombination.

5.3.D. Auto-activation of pJG4-5 bait vector prevented identification of Rfa2 interacting partners

Using the assistance of Dr. Haring's Recombinant DNA technology course at NDSU, we were able to successfully generate a number of yeast two hybrid (Y2H) prey vectors (Table 5.1) that we tested in a yeast two hybrid assay. During the Y2H assay, a reporter vector containing LexA operator sites recruits the LexA-DBD-Bait protein, in this case LexA-DBD-Rfa1, to the operator sequence. In order for transcription of the reporter gene *LacZ*, the B42-AD-Prey construct must come within close enough proximity to interact with the LexA-DBD-Bait protein. Reporter activity can be assessed by blue-white screening using X-Gal (5-bromo-4-chloro-3-indolyl-β-D-galactopyranoside), which when cleaved by LacZ leads to the formation of a blue pigment in the yeast. Yeast patches that turn blue after replica plating to X-Gal media are 'positive' hits indicative of a protein-protein interaction between bait and prey proteins, whereas white patches are indicative of a null interaction. During my attempts to perform the Y2H assay, it became apparent that the bait vector was auto-activating and producing blue colonies, even in the presence of empty pJG4-5 vector. When testing the prey vectors listed in Table 5.1, our reporter vector displayed auto-activation in the presence of an empty bait vector as recognized by blue tinted yeast,

suggesting that our Rfa1-prey vector was likely responsible for this auto-activation. As a result, the Y2H project was shelved, and it was determined that a new Y2H system with different reporter, bait, and prey vectors would be required.

5.4. Discussion

From the results above, it is clear that the Rfa2 NT is required for proper progression through the meiotic program but is dispensable for meiotic recombination during meiosis. It is fascinating to speculate as to why *rfa2-*Δ*N*$_X$ mutations were unable to promote proper meiotic progression, lead to an increase in the number of 2-cell spores, and also produced a much higher frequency of inviable haploids. Based on my research in previous chapters, I speculate that is likely caused by the lack of the Rfa2 NT, of which phosphorylation within this domain may be required during meiosis to promote both the reductional division during MI and the equational division during MII. However, it is possible that the lack of the Rfa2 NT and phospho-sites therein leads to a cell cycle timing defect. MII is often referred to as a mitotic-like equational division and if Rfa2 NT phosphorylation is required for mitotic exit, the lack of phospho-sites caused by the NT truncation would cause cells to accumulate in MII as dyads (two-cell spores). This idea is supported by the observation that DSBs generated during late meiosis (e.g. MII) typically lead to mitotic LPR signaling, Rad53 activation and normal mitotic DDC establishment (Cartagena-Lirola *et al.* 2008). Therefore, phosphorylation of the Rfa2 NT during meiosis may be a requirement of proper temporal progression of the meiotic program.

Moreover, defects in *rfa2-D*$_X$ allude to the idea that rapid modulation of the Rfa2 NT phospho-state may be required to produce viable spores, as cells containing *rfa2-D*$_X$ sporulated with the same frequency as *rfa2-A*$_X$ but also produced many more inviable cells. It is plausible then that the phospho-mimetic *rfa2-D*$_X$ mutation is promoting aberrant checkpoint exit during meiosis, as I have observed in mitotically growing cells. This aberrant exit from MII, for example, would cause missegregation of chromosomes and inviability due to progressing through the meiotic division faster than cells containing Rfa2 or *Rfa2-A*$_X$. While a disruption in the temporal meiotic program is enticing, analyzing which RFA-protein interactions are important for promoting proper meiotic progression will be a key area of research in the future as well. For example, it has been demonstrated that RPA interacts with both Rad51 and Dmc1 during meiosis (Golub *et al.* 1998, Murayama *et al.* 2013). The interaction between Dmc1 and RPA

has been demonstrated to be weak but still occur and may be a result of the programmed nature of the DSBs during meiotic recombination. Dmc1 is utilized preferentially during presynaptic filament formation during meiosis over Rad51 because Dmc1 drives interhomolog exchange (Schwacha *et al.* 1997) whereas Rad51 drives intersister exchange (Nimonkar *et al.* 2012). Understanding how these interactions are disrupted or impacted by the phospho-state of the Rfa2 NT may provide insight into the regulatory mechanisms utilized by cells during the MI and MII divisions.

Unfortunately, my current experimental design did not allow for adequate testing of RFA-protein interactions via Y2H due to auto-activation of the reporter vector pSH18-34. In order for Y2H to function properly, the LexA binding domain fused to a bait protein (Rfa1 in this case; pEG202-LexA-BD-Rfa1) and the LexA BD localizes to the LexA operator sites present on pSH18-34. In order for transcription of the reporter to occur, the B42 activation domain fused to a prey protein must come within close enough proximity to the LexA BD to interact, driving transcription of the reporter gene. During my attempts to perform the Y2H, our reporter vector auto-activated in the presence of empty pEG202-LexA-BD. Moreover, reporter auto-activation also occurred in the presence of each of our pJG4-5-B42-AD-Prey vectors making it impossible to distinguish positive hits from false positive results. Dr. Haring and I recently discussed some ways around this. Our main problem appears to be with our bait vector, and our collaborator Dr. Andre Walther from Cedar Crest College has offered his Y2H vector system as a replacement for our own. Once obtained, simple *in vivo* homologous recombination reactions could re-generate all of the vectors described in Table 5.1. Transformation and diagnostic replica plating would then yield strains ready to be tested via Y2H, hopefully with auto-activation free vectors.

Dr. Haring and I also discussed ways to better the qPCR mating-type switch assay in order to get a final result on whether the Rfa2 NT extensive mutations do not have a major effect on homologous recombination. First, each of the strains utilized should be grown in or on YPR media in order to deplete glucose stores and provide a better starting point for galactose induction. Second, DNA isolated for qPCR should be isolated via the methods described in chapter 4.3.E, as this yields the cleanest, contaminant-free DNA for qPCR. Third, our use of Applied Biological Materials (abm) *EvaGreen* qPCR mix has yielded exceptional results, where previously we had been using QuantaBioscience SYBR qPCR Fast mix. While it is unlikely that the age of the reagents used played a significant role in the failure of the aforementioned

qPCR experiments, care should be taken in the future to use the freshest reagents possible for optimal results.

5.5. Acknowledgements

Timothy M. Wilson planned and performed all meiosis experiments in this chapter. **Francis P. Landman** (undergraduate) assisted TMW in the diagnostic digests, sequence verification and permanent storage of yeast two hybrid vectors.

CHAPTER 6: CONCLUDING DISCUSSION AND FINAL REMARKS

Stable transfer of unadulterated genetic information during mitosis and meiosis is essential for the continued propagation of all life on Earth. Despite the wealth of information that is known about Rpa2 NT phosphorylation in human cells, the physiological consequences and impacts of phosphorylation of the Rpa2 NT remain elusive. The work described in Chapter 2 demonstrates a dispensability for phosphorylation of the Rfa2 NT in yeast and suggests that preventing cells from rapidly modulating the phospho-state of the Rfa2 NT may have negatively impact the ability of cells to perform stable genetic transfer. The work described in Chapters 3 and 4 contribute significantly to the understanding of the mechanisms of checkpoint adaptation in that phosphorylation of the Rfa2 NT appears to be the predominant driver of the molecular decisions to exit an established checkpoint in response to a permanent DNA lesion. Moreover, one question that remains unanswered is whether DSB resection is required for checkpoint adaptation. My results using a qPCR-based resection assay (Chapter 4, Figure 4.4) demonstrate that resection is not impacted by the Rfa2 NT phospho-state and suggest that Rfa2 NT phosphorylation promotes checkpoint adaptation independent of DNA resection and rescues all of the tested adaptation-deficient phenotypes generated by deletion of several recombination/repair and checkpoint factors. The brief studies performed in meiotic cells in Chapter 5 also allude to a role in Rfa2 NT phosphorylation in mediating successful meiotic progression and divisions. This chapter will focus on the results of my work and how they relate to previous and current work in the field of the DNA damage response (DDR), encompassing the processes of lesion processing and repair (LPR) and the DNA damage-dependent checkpoint (DDC), and provide a model for the role of Rfa2 NT phosphorylation in each process.

6.1. The role of the Rpa2 NT in LPR

Upon detection of a DNA lesion, the RPA complex localizes to the DSB and binds and protects the single-stranded DNA (ssDNA) generated during lesion processing, prior to DNA repair. Previous research in human cells has demonstrated that Rpa2 becomes phosphorylated by the damage sensor kinases DNA-PK, ATM, and ATR/ATRIP (Wang *et al.* 2001, Manthey *et al.* 2007, Liu *et al.* 2012). However, the physiological relevance of these phosphorylation events and their function in cells has remained elusive. Studies performed using permanent phospho-mimetic mutations has revealed that

preventing phosphorylation at damage-dependent phospho-sites leads to aberrant replication restart (Vassin *et al.* 2009) and deficiencies in homologous recombination repair (Liaw *et al.* 2011). Thus, rapid modulation of the Rpa2 NT phospho-state is a *requirement* for proper LPR, checkpoint maintenance, and mitotic exit.

6.1.A. Phosphorylation of the Rfa2 NT appears to be dispensable for LPR

As mentioned above, Rpa2 in human cells is robustly phosphorylated during the LPR program by DNA-PK, ATM, and ATR/ATRIP. In yeast, however, overt phosphorylation of the Rfa2 NT is not readily observable under short-term genotoxic conditions and only seems to appear during prolonged exposure to genotoxic agents. Phosphorylation of the yeast Rfa2 NT also appears to be dispensable for LPR, as the phospho-mimetic *rfa2-D$_X$* mutation leads to an increased sensitivity to genotoxic agents in wild-type cells, as well as cells already sensitive to genotoxic agents. Moreover, the *rfa2-A$_X$* mutation seems to confer clastogen resistance on par with wild-type cells, further suggestive that phosphorylation of the Rfa2 NT during LPR has negative consequences for the cell.

Phosphorylation of the Rpa2 NT has been reported to reduce interaction with the MRN complex *in vitro*, specifically impeding interaction with Nbs1 and Mre11 (Oakley *et al.* 2009). Moreover, phospho-mimetic Rpa2 displays impairs both interactions with DNA polymerase α and inhibits SV40 DNA replication (Oakley *et al.* 2003). The impaired interactions with the MRN complex and DNA polymerase α may explain the sensitivity to genotoxic agents conferred by *rfa2-D$_X$* in yeast, as well as repair deficiencies observed in human cells. While phospho-mimetic forms of Rpa2 have been demonstrated to be proficient during checkpoint activation, impairing an interaction with MRN could potentially lead to aberrant resection phenotypes that cause loss of genetic information or lead to mutation. Furthermore, impaired interactions with DNA polymerase α during repair synthesis at the D-loop pseudo-replication bubble would prevent adequate DNA synthesis from occurring, inhibiting repair and leading to the recombination deficient phenotypes observed in human cells. Moreover, the phospho-state of the Rpa2 NT does not appear to be required for localization of the RPA complex to DSB sites, as cells expressing the phospho-mimetic mutations of Rpa2 were still proficient for repair foci formation (Binz *et al.* 2003, Vassin *et al.* 2004). In the studies performed in Chapter 2, all of the Rfa2 NT extensive mutations were capable of activating the Rad53-dependent checkpoint indistinguishably from WT cells, demonstrating

that the phospho-state of Rfa2 or the physical presence of the Rfa2 NT is not a requirement for proper initiation of checkpoint signaling during the initial LPR events.

6.1.B. The Rfa2 NT is physically required for LPR

Previous research has demonstrated that the Rfa2 NT is physically required in order for cells to tolerate genotoxic stress by a number of clastogens (Ghospurkar *et al.* 2015). Similar results were observed in experiments carried out in Chapter 2. Together, these results demonstrate that the physical presence of the Rfa2 NT is required for proper genome maintenance during lesion processing and repair, but as mentioned above its phospho-state may be completely dispensable. Previous research by Anantha *et al*. (2009) indicated that Rpa2 NT phosphorylation is a requirement of proper mitotic exit, and prematurely stimulating phosphorylation of the Rpa2 NT via phospho-mimetic mutation leads to aberrant checkpoint exit despite the presence of lesions. Thus, being unable to modulate the phospho-state of the Rpa2 NT is detrimental to cells and genomic stability. Furthermore, if phosphorylation of the Rpa2 NT impairs interaction with DNA polymerase α, as reported, preventing phosphorylation during DNA synthesis would be essential for ensuring that DNA replication can initiate properly.

Additional evidence in human cells has demonstrated that phosphorylation of the Rpa2 NT is required for an interaction with the Prp19 ubiquitin ligase (Dubois *et al.* 2017). Ubiquitination of proteins involved in LPR have been described as a requirement for proper repair and checkpoint activation, however, this data is somewhat inconsistent with other evidence demonstrating that ubiquitin ligases are also required for inactivation of the DNA damage-dependent checkpoint (Zhang *et al.* 2005).

I propose a model (Figure 6.1) that involves dephosphorylated RPA recruiting in the initial repair machinery, which then would lead to phosphorylation of the Rpa2 NT driving an interaction with the Prp19 ligase. RPA would then sumoylated by the Pias1/Pias4 E3 sumo-ligases (Galanty *et al.* 2009), protecting it from ubiquitination and promoting DNA repair (Galanty *et al.* 2012). Upon initiation of repair, Senp6 desumoylase (Dou *et al.* 2010) would push RPA back into a hyposumoylated state which would allow RPA to be ubiquitinated. In this model, ubiquitination of RPA might then promote removal of RPA bound to the ssDNA at the DSB, facilitating Rad51 exchange. RPA-Prp19 could then ubiquitinate repair components to ensure proper strand invasion and repair synthesis (the D-loop would be bound by dephosphorylated RPA to promote proper association with DNA polymerase α). As repair synthesis

occurs, RPA bound in the D-loop would then be phosphorylated, bound by Prp19, and removed from the D-loop, tipping the balance of the number of inactive to active ubiquitin ligases attached to RPA which would drive ubiquitin-targeted degradation of repair components in a timely fashion, allowing the cells to spend a minimal amount of time arrested due to a DNA lesion.

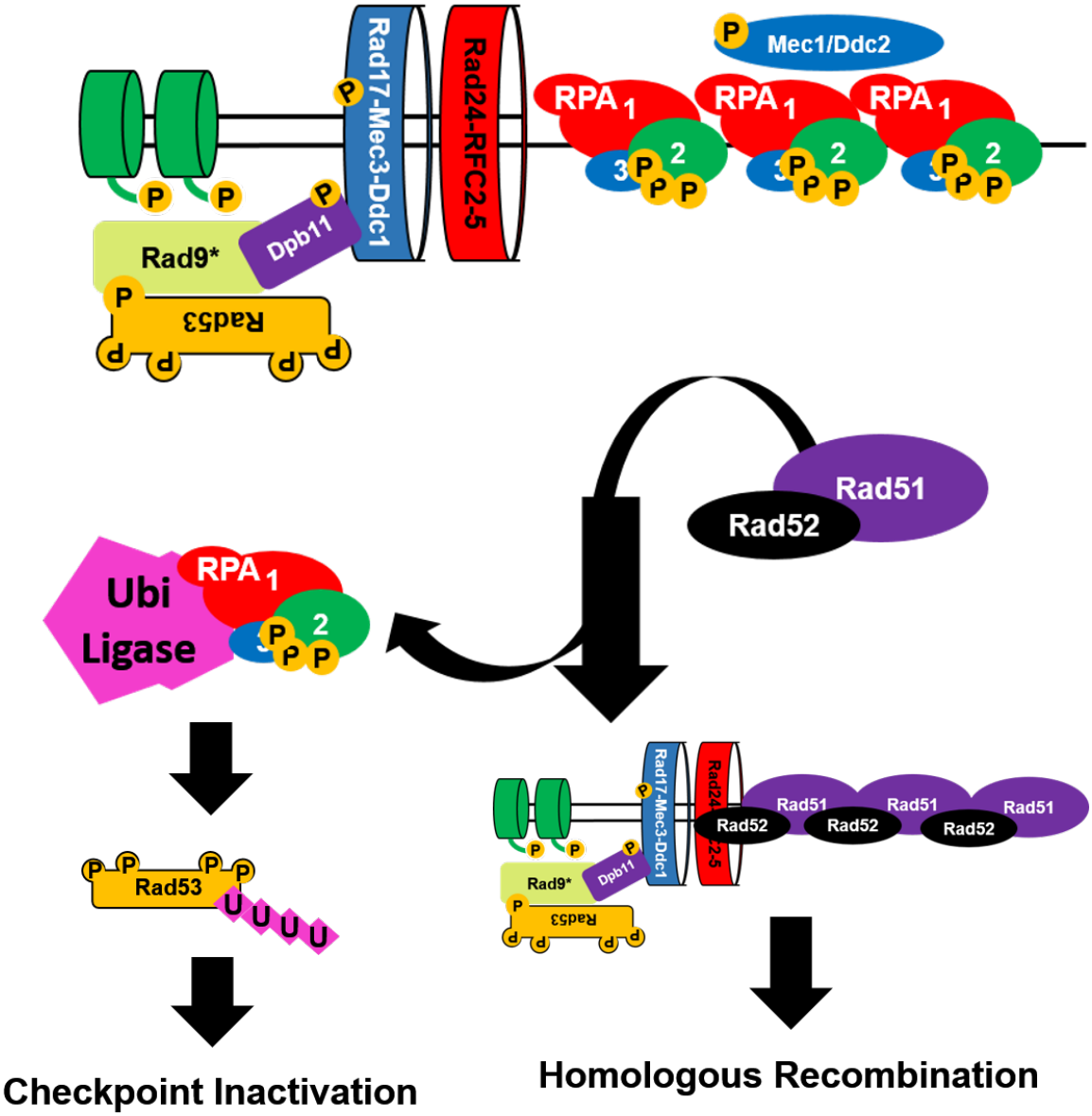

Figure 6.1. Model for Rfa2 NT phospho-regulation of ubiquitin and sumo ligase activity during LPR and adaptation
In this theoretical model, Rfa2 NT phosphorylation is achieved through an unknown kinase after S122 phosphorylation by Mec1/Ddc2. Phosphorylation of the Rfa2 NT leads to removal of RPA from ssDNA, allowing formation of the Rad51-presynaptic filament. Phospho-RPA then interacts with a ubiquitin ligase ('Ubi ligase'), simulating the ubiquitination of Rad53, targeting it for destruction by the proteasome. Targeted degradation of Rad53 leads to the inactivation of the DDC and promotes mitotic exit in cells that have either repaired the DNA lesion or are experiencing checkpoint adaptation due to the presence of a persistent DNA lesion.

It is also plausible that association of RPA with other ubiquitin ligases like Rfwd3 or the sumo-targeted ubiquitin ligase Rnf4 might drive the formation of ubiquitin super-complex that preferentially targets lesion processing and repair proteins for degradation through the ubiquitin-dependent proteasome. Another fascinating possibility would be that the phospho-state of Rpa2 preferentially inhibits checkpoint kinase activity through upregulation of phosphatase activity required to reverse checkpoint signaling and promote mitotic entry and will be discussed in 6.2.C.

6.1.C. Role for the Rfa2 NT in genome maintenance at telomeres

Telomere length has long been implicated in the life-span of a cell in that once a single cell has divided to the point where the telomeres are eroded as a result of shortening, the cells apoptose (Zhang *et al.* 1999). Telomere maintenance is somewhat similar to lesion processing and repair in that an ssDNA template, in the absence of the proteinaceous telomeric binding complex shelterin, can be bound by RPA and elicit a checkpoint response (Denchi *et al.* 2007, Guo *et al.* 2007). RPA at the telomeres is then displaced by the TERRA complex, leading to RPAs replacement at telomeres by the Pot1-Tpp1, which prevents RPA re-loading onto the telomeric ssDNA (Flynn *et al.* 2011, Flynn *et al.* 2012). In budding yeast, cells expressing the *rfa2-*ΔN_X mutation were deficient for Est1 recruitment to telomeres, leading to severely shortened telomeres (Schramke *et al.* 2004, Luciano *et al.* 2012). This demonstrates that the physical presence of the Rfa2 NT is required for adequate maintenance of telomeres and fidelity of the genome.

Moreover, the interaction between Est1 and RFA during S-phase may be a requirement during DNA replication when the shelterin complex is removed from telomeres. As discussed in 1.4, phospho-mimetic mutation of the Rpa2 NT has been reported to inhibit homologous recombination; however, the data presented in Chapter 5 demonstrates that homologous recombination is not impacted during meiosis where homologous recombination occurs at 100-fold higher frequency than in mitotic cells. Moreover, other members of the Haring lab have demonstrated that it is possible to integrate constructs into the genome in all of the yeast Rfa2 NT mutants. As such, in yeast, phosphorylation of the Rfa2 NT during S-phase or during mitotic exit may be required to prevent homologous recombination at telomeric DNA sequences that are preferentially kept in an ssDNA state when bound by shelterin.

6.2. Defining the role of Rfa2 NT phosphorylation during mitotic exit

It is abundantly clear from the studies in Chapters 3 and 4 that phospho-mimetic or naturally phosphorylatable Rfa2 NT mutations promote aberrant mitotic exit in response to a single, controlled, irreparable DSB. Moreover, Rfa2 NT phospho-mutations appear to rescue checkpoint adaptation deficiencies more often and more efficiently than that of *rfa1-t11*, as Rfa2 NT phospho-mutations were able to rescue every adaptation-deficient phenotype tested in the aforementioned studies and *rfa1-t11* was not. The idea that the Rpa2 NT phospho-state regulates mitotic exit is not entirely novel; however, it is currently unknown *how* and *why* Rpa2 NT phosphorylation promotes mitotic exit. Previous research has demonstrated that phospho-mimetic mutation of Rpa2 in human cells promotes mitotic exit despite the persistence of DNA lesions within the genome (Anantha *et al.* 2008). Furthermore, preventing phosphorylation at CDK-dependent phospho-sites on the Rpa2 NT has been reported to lead to accumulation of cells in S- and G_2/M phases of the cell cycle (Anantha *et al.* 2007, Anantha *et al.* 2008, Shi *et al.* 2010). Taken in context, the studies described in Chapters 3 and 4 reinforce the hypothesis that Rpa2 NT phosphorylation mediates mitotic exit, and may do so in the presence or absence of DNA lesions

6.2.A. Rfa2 NT phosphorylation causes aberrant checkpoint exit in the presence of a persistent lesion

In response to a persistent DNA lesion, Rfa2 in yeast becomes robustly phosphorylated as indicated by the studies done in Chapter 3. While certain factors may be required to stimulate the repair of DNA, such as those tested in Chapters 3 and 4, this phosphorylation even correlates well with the phospho-state of Rad53 returning to an inactive state. Moreover, phosphorylation of the Rfa2 NT is impaired in recombination deficient *rdh54*Δ cells, suggesting that these cells may not adapt on their own because Rfa2 NT phosphorylation is impaired. The phosphorylation events observed during checkpoint adaptation are distinct from those observed during mitotic genotoxic stress, highlighting a difference for Rfa2 NT phosphorylation in each process. During DNA repair, phosphorylation of the Rpa2 NT in human cells has been reported to inhibit homologous recombination. In yeast that cannot undergo homologous recombination at the *MAT* locus (due to the deletion of *HML* and *HMR*), Rfa2 phosphorylation occurs 12 hours after an HO-induced DSB is formed, and these cells readily adapt, starting at the 12-hour mark.

Furthermore, the addition of phospho-mimetic *rfa2-D$_X$* or the naturally phosphorylatable *rfa2-h2NT* rescue checkpoint adaptation in nearly every case examined. Thus, phosphorylation of the Rfa2 NT promotes checkpoint exit in the presence of a persistent lesion.

The studies described in Chapters 3 and 4 also provide some impetus for studying how promoting or inhibiting Rpa2 phosphorylation in human cells would contribute to diseases like cancer, which are driven by both mutation of the genome and dysregulated cell cycle pathways. Promoting Rpa2 phosphorylation, in combination with chemo/radiation therapy for example, may promote to a more effective response in cancer cells that would divide more rapidly than normal cells, and would be unable to tolerate additional DSBs generated by chemotherapeutic agents. Driving Rpa2 phosphorylation may allow cancerous cells to divide in the presence of significant DNA damage which would ultimately lead to severe genotoxic instability and potentially apoptosis. Alternatively, controlling the malignant growth of a tumor may be possible by developing ways to replace the endogenous Rpa2 with an N-terminal truncation. As described above in section 6.1.C, the *rfa2-ΔN$_X$* mutation prevents stable association of Est1 with telomeres and leads to severe telomere shortening. Cancer cells can survive severe genomic insult by performing genome rearrangements that elongate the telomeres artificially. Therapeutic use of *rpa2-ΔN$_X$* may lead to telomere shortening in cancer cells, sensitizing them to genotoxic agents or potentially returning them to a more tolerable growth level for treatment. Moreover, since cells containing N-terminal truncations of Rpa2 have been demonstrated to be sensitive to clastogens, finding a way to stably express the truncation mutation in human cancer cells may be an effective way to enhance treatment strategies and limit the negative impact chemo/radiation therapy has on the host.

6.2.B. A simple model for Rfa2 NT phosphorylation promoting checkpoint exit

In Chapter 2, I discovered that Rfa2 phosphorylation at S122 is impaired in *tel1*Δ mutants. S122 is a common marker for Mec1 activity on the RFA complex at DSB sites and reduced phosphorylation at S122 in *tel1*Δ mutant cells indicates that Mec1 activity is indicative of impaired Mec1 signaling. Moreover, in Chapters 3 and 4, the phospho-mimetic or naturally phosphorylatable Rfa2 NT mutants used during checkpoint adaptation studies (*rfa2-D$_X$* and *rfa2-h2NT*, respectively) were able to successfully promote mitotic exit in the presence of persistent DNA lesions in all adaptation-deficient mutants tested. Together, this data allows for the proposal of a simple model (Figure 6.2) where Rfa2 NT phosphorylation leads to

indirect inhibition of Mec1 checkpoint signaling and checkpoint exit through direct inhibition of hyper-phosphorylation of Rad53. Mec1 is the primary sensor kinase the phosphorylates Rad53 during LPR and the establishment of the DDC. The *rfa1-t11* mutation has been demonstrated to checkpoint initially as observed by Rad53 hyper-phosphorylation but leads to impaired checkpoint maintenance and aberrant checkpoint exit (Lee *et al.* 2001, Pellicioli *et al.* 2001, Ghospurkar *et al.* 2015). However, mutant forms of RFA containing the *rfa1-t11* mutation are still able to interact with Ddc2, as observed through crystallographic analysis (Deshpande *et al.* 2017), suggesting that the checkpoint maintenance defect conferred by *rfa1-t11* are not due to impaired interaction with Ddc2. Additional crystallographic studies using human RPA peptides have determined that NT phosphorylated Rpa2 interacts with a proteolyzed portion of Rpa2, specifically DBD-B (Liu *et al.* 2005). However, *in vivo* it is unlikely that the Rpa2 NT interacts with DBD-B while RPA is on ssDNA, as DBD-A and DBD-B of Rpa1 contain the strongest affinity for ssDNA compared to the other DBDs within RPA. Thus, it is plausible that NT phosphorylated Rpa2 may interact with the basic cleft of DBD-F, which is attached to Rpa2 via a highly-flexible linker region and has an OB-fold structure that does not bind ssDNA or contribute to RPA's ability to bind ssDNA. If NT phosphorylated Rfa2 in yeast is the negatively charged substrate that DBD-F interacts with during LPR, then the relocation of this flexibly linked interaction domain may cause reduced interaction with Ddc2, leading to reduced Mec1 activation through reduced interaction with RFA, Dbp11 and Ddc1. Moreover, the interaction between DBD-F of Rfa1 and the phosphorylated Rfa2 NT may be highly dynamic, providing rational for why cells containing the *rfa2-D$_X$* mutation are still able to activate the DDC with kinetics similar to wild-type cells. Preventing Mec1 activation would then inhibit Rad53 hyper-phosphorylation and lead directly to checkpoint exit. Further studies will be required to better analyze the effects of the phospho-state of Rfa2 and its impact on conformational changes of the RFA/RPA complexes when bound to ssDNA.

6.2.C. Phospho-mimetic Rfa2 NT mutations promote adaptation more efficiently than *rfa1-t11*

Previously, it was demonstrated that *rfa1-t11* promotes checkpoint adaptation in yeast cells (Pellicioli *et al.* 2001), however, the adaptation proficiency promoted by *rfa1-t11* is overshadowed by that of the phospho-mimetic Rfa2 mutations. The *rfa1-t11* mutation is thought to reduce interaction with

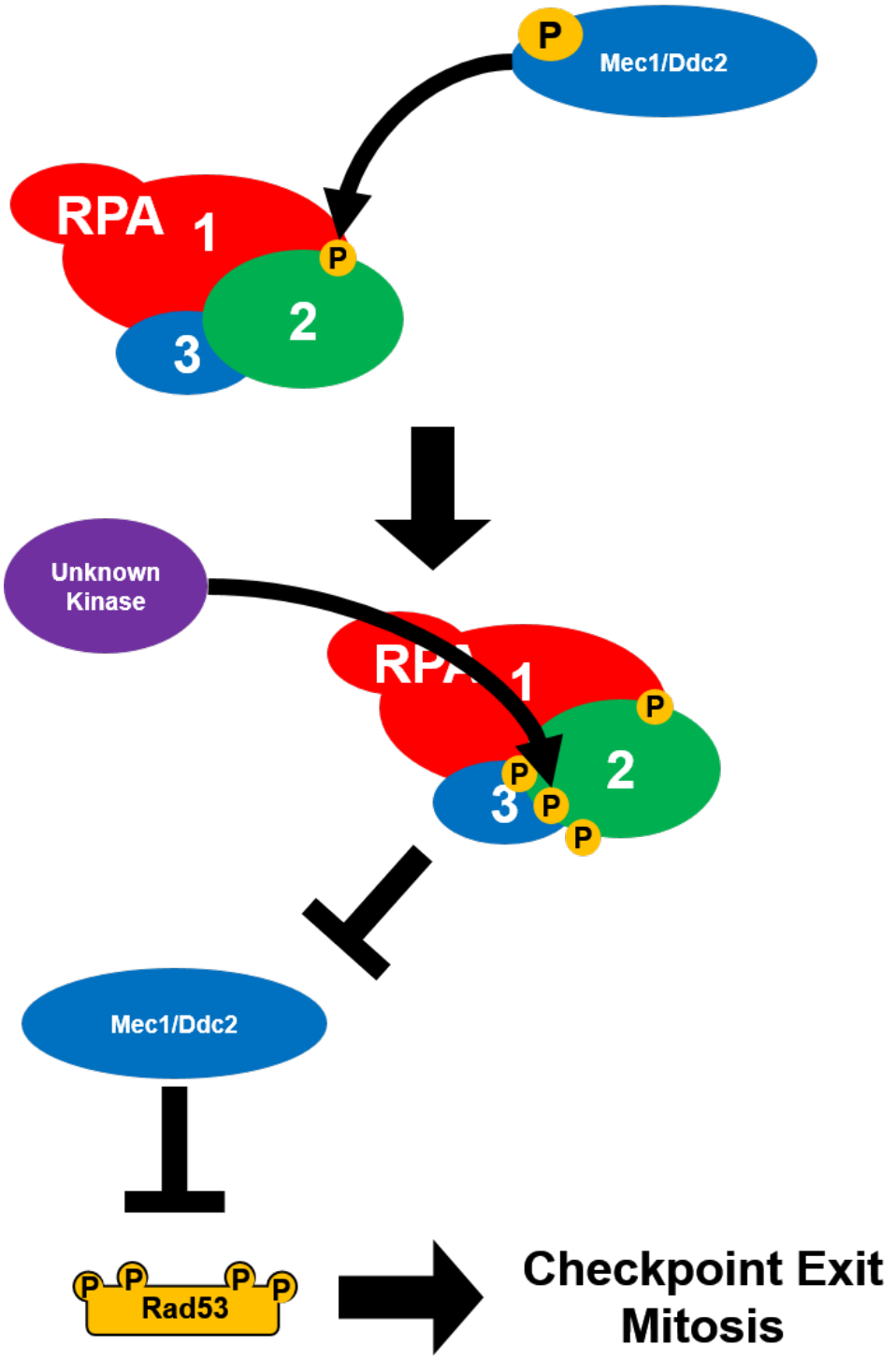

Figure 6.2. Rfa2 NT phosphorylation inhibits Mec1 potentiation of Rad53 phosphorylation leading to aberrant checkpoint exit

During initial LPR events, Mec1 recruitment to the DSB leads to phosphorylation of Rfa2 at S122. An unknown kinase then phosphorylates the Rfa2 NT allowing DBD-F of Rfa1 to interact with the phosphorylated Rfa2 NT. This attenuates and inhibits Mec1 signaling by destabilizing the interaction between Rfa1 and Ddc2 (Mec1 chaperone). Reduced Mec1 signaling at the DSB site leads reduced potentiation and maintenance of Rad53 hyper-phosphorylation and signaling, promoting exit from the established DNA damage-dependent checkpoint.

Rad24-RFC and by extension inhibit loading of the 9-1-1 clamp required for repair synthesis (Majka *et al.* 2006). While cells containing *rfa1-t11* are proficient for the initial activation of the damage-dependent checkpoint, they appear to have a deficiency in maintaining the required checkpoint signal so that faithful repair of a lesion can take place. Checkpoint initiation deficiencies were not observed for any of the Rfa2 NT extensive mutations, however, *rfa2-D$_X$* and *rfa2-h2NT* were able to rescue every adaptation deficiency tested in Chapters 3 and 4. It is likely then that these mutations and their effects on checkpoint maintenance are different. If *rfa1-t11* is preventing adequate loading of the 9-1-1 clamp, leading to an impaired checkpoint, how then do phospho-mimetic or naturally phosphorylatable Rfa2 NT mutations subvert the established checkpoint to promote mitotic exit in the presence of a persistent lesion?

A few enticing but complex hypotheses emerge. First, as described in 6.1.B, a model (Figure 6.1) surrounding the sumo and ubiquitin ligase complexes involved in DNA repair centered around RPA would lead to targeted degradation of checkpoint components, preferentially driven by phospho-Rpa2. Second, since the number of known interactors of the RPA complex continues to grow annually, it is possible that phospho-Rpa2 forms a complex with a yet unidentified interacting partner to drive mitotic exit. Phosphorylation of Rpa2 has been reported to cause disassembly of the RPA heterotrimer (Treuner *et al.* 1999), however, if this were true phospho-mimetic RPA mutations would be unable to support DNA replication or DNA repair in any capacity. However, this logic does not preclude the existence of a phospho-Rpa2 complex which has the sole purpose of promoting mitotic exit that also does not include Rpa1 or Rpa3, and forms after disassembly of the heterotrimer during the later stages of DNA repair. The third potential possibility is that Rpa2 NT phosphorylation is a signal that somehow intentionally suppresses kinase activity both at the DSB site and intracellularly to promote checkpoint exit and will be discussed below in 6.2.C. It is also plausible, that the entire mechanism governing the function of Rpa2 NT phosphorylation during mitotic exit, in the presence of absence of DNA lesions, is a complex combination of all three of the aforementioned hypotheses.

6.2.D. Rfa2 NT phosphorylation may drive signaling away from kinases and towards phosphatases

In Chapters 3 and 4, I demonstrated that the Rfa2 NT phospho-state impacts the phospho-state of the yeast master checkpoint regulator Rad53. Preventing phosphorylation of the Rfa2 NT leads to extensive Rad53 activation, whereas phospho-mimetic or naturally phosphorylatable forms lead to

noticeable dephosphorylation of Rad53 within the temporal window with which checkpoint adaptation occurs. The kinase activity of Rad53 during LPR, checkpoint maintenance, and checkpoint exit is not only modulated by ubiquitination, as described in section 6.1.B, but also on the activity of several kinases and phosphatases. As described in Chapter 1, phospho-activation of Rad53 is achieved by both sensor kinases Mec1 and Tel1, in a chaperone Rad9- or Mrc1- dependent fashion. This phospho-activation leads to the establishment of the DDC in yeast, leads to the activation of Chk1 through Tel1 activity, and prevents anaphase entry by Chk1 and Rad53 dependent phosphorylation of Pds1. During checkpoint exit, however, dephosphorylation and inactivation of Rad53 is achieved through a concerted network of phosphatases including the Ptc2, Ptc3, and Pph3 phosphatases (Guillemain *et al.* 2007, O'Neill *et al.* 2007, Kim *et al.* 2011). Deletions of the aforementioned phosphatases display checkpoint adaptation-deficient phenotypes in-line with that observed for other adaptation deficiencies (Leroy *et al.* 2003, Guillemain *et al.* 2007). Thus, phosphatase activity on proteins involved in the DDC and lesion processing and repair rare required for checkpoint recovery and mitotic exit once a break has been processed and repaired. Moreover, as described previously, Ptc2, Ckb1, and Rad53 interact *in vitro* and *in vivo* suggesting that CK2 phosphorylation of the PP2C phosphatase complex is required for checkpoint exit (Guillemain *et al.* 2007). It is currently unknown whether RFA and the CK2 kinase complex interact, or how the phospho-state of the Rfa2 NT would affect interaction with phosphatase complexes involved in the deactivation of the established DDC.

Large scale genetic-interaction screens have identified a negative genetic interaction (Costanzo *et al.* 2016) between Rfa2 and Ckb1 (catalytic subunit of CKII; Ackermann *et al.*2001), Cdc20 (Activator of the anaphase-promoting complex/cyclosome APC/C^{CDC20}; Charles *et al.* 1998, Cohen-Fix and Koshland 1999), and several components of the LPR program (Slx4, Dna2, Sgs1, Top3, Rmi1, Rad51, Rad52, Rad54, Rad55, Rad57; Costanzo *et al.* 2016). Moreover, negative synthetic genetic interactions have also been identified between CK2 components and Psy2 and Pph3 components of the PP4 phosphatase complex (*ibid*). Together with the studies performed in Chapters 3 and 4, as well as previous research using *rfa2* or *rpa2-NT* phospho-mutations, these negative genetic interactions suggest that mutations that loss of function or impaired regulation of RPA lead to synthetically sick or lethal phenotypes that impair a cell's ability to maintain its genome and provide a framework for RPA regulating kinase and phosphatase

activity during LPR and the DDC. Furthermore, work performed by Trevor Baumgartner in the Haring lab has demonstrated that phospho-mimetic or naturally phosphorylatable extensive mutation of the Rfa2 NT promotes checkpoint adaptation rescue in cells containing deletions of phosphatases Ptc2, Ptc3, and Pph3. Moreover, these phospho-forms of Rfa2 are also able to rescue the adaptation deficient *ptc2*Δ *ptc3*Δ double mutant, suggesting that dephosphorylation of Rad53 is not the only requirement of checkpoint exit.

Thus, a potential kinase-phosphatase regulatory model (Figure 6.3) that depends on the phospho-state of the Rpa2 NT can be proposed. Phosphorylation of the Rpa2 NT during HR is thought to be inhibitory towards homologous recombination (Liaw *et al.* 2011). Therefore, during LPR, the Rpa2 NT would be preferentially maintained in a dephosphorylated state prior to Rad51 exchange during presynaptic filament formation. Phosphorylation of the Rpa2 NT has been shown in human cells to be important for Rad52-Rad51 recruitment (Shi *et al.* 2010); however, *in vitro* studies have demonstrated that Rad51 can displace RPA from ssDNA independent of kinase activity (Ma *et al.* 2017, Ma *et al.* 2017). This data, combined with my studies, suggests a novel signaling function for the phospho-state of the Rfa2 NT. However, in the nuclear environment phosphorylation of Rpa2 may promote removal of the RPA complex from the ssDNA overhang, and RPA containing a dephosphorylated Rpa2 NT would be localized to the D-loop to promote DNA polymerase α recruitment. Phosphorylation of the Rpa2 NT would then remove RPA from the D-loop during repair synthesis. RPA containing phosphorylated Rpa2 NT could then drive interaction between a phosphatase complex (PP2C; Ptc2/Ptc3), and/or PP4; Pph3/Psy2) that would then begin dephosphorylation of multiple components involved in LPR once repair synthesis begins. Moreover, the formation of these phosphatase-RPA complexes may be directly responsible for the dephosphorylation of Rad53, promoting checkpoint recovery and mitotic exit. Direct interactions between Rpa2/Rfa2 and the aforementioned phosphatase complexes and their subunits has not been identified, and future research may better define a role for Rpa2/Rfa2 signaling activity outside of the RPA complexes main biochemical purpose of binding ssDNA and repair-scaffold formation. However, my research combined with what is known in the field clearly dictates that dysregulation of the Rpa2 NT phospho-state leads to mitotic exit in the presence of DNA lesions, and this process may be a direct

mechanism that leads to the accumulation of mutations within the genome that lead to cellular diseases like cancer in humans.

6.3. Role of the Rfa2 NT during meiosis unclear

Attempts to study the function of the Rfa2 NT during meiosis in yeast performed in Chapter 5 have provided the framework for additional study of the Rfa2 NT phospho-state during this critical cellular process. It is currently unknown that the cellular consequences of Rfa2 NT phosphorylation are during each stage of meiosis, however, it is clear that permanent phospho-mimetic mutation or truncation of the Rfa2 NT lead to the formation of inviable gametes in budding yeast. Further studies will be required to better define the role of the Rfa2 NT during meiosis.

6.3.A. Rfa2 NT extensive mutations lead to different meiotic phenotypes

During meiosis, yeast containing Rfa2 NT extensive mutations were all able to perform meiotic divisions leading to the formation of four spores, with truncation of the Rfa2 NT leading to a severe reduction in the ability of cells to generate gametes compared to wild-type cells. Cells containing either *rfa2-D$_X$* or *rfa2-A$_X$* mutations were able to produce tetrads at a higher frequency than wild-type cells, suggesting that the Rfa2 NT phospho-state are dispensable during meiosis. Fascinatingly, the wild-type, cDNA-less Rfa2 mutant (*Rfa2-cDNA-WT*) was also able to produce spores at a higher frequency than cells containing *RFA2* with an intron, suggestive of a role for the *RFA2* intron in meiosis. Further research will be required to analyze what role, if any, the intron of *RFA2* plays during the meiotic process.

However, the physical presence of the Rfa2 NT is a requirement of meiosis, as cells containing the *rfa2-*Δ*N$_X$* mutation produced fewer viable spores following meiosis. Moreover, cells containing the *rfa2-*Δ*N$_X$* mutation produce significantly more dyads (two-cell spores) than any of the other Rfa2 mutants tested, suggesting a defect in the ability of these cells to adequately complete the required meiotic divisions. The Rfa2 NT is known to be phosphorylated prior to meiotic recombination by Ime2 (Clifford *et al.* 2004). However, the physiological relevance of the Ime2-driven phosphorylation event remains elusive. It is plausible that this phosphorylation event is required to drive the MII division, which is often referred to as a mitotic-like equational division. However, if this event were required for proper meiotic progression, eliminating the S27 phosphorylation through mutagenesis should lead to MII arrest. My work in Chapter 5 using *rfa2-D$_X$* and *rfa2-A$_X$* extensive mutations suggest that this phosphorylation event does

not play a role in mediating the meiotic divisions during MI and MII, suggesting that this phosphorylation event is not required to promote entry or exit from both MI and MII. Moreover, this evidence also suggests that the physical presence of the NT is much more important during meiosis than the NT phospho-state. During meiotic recombination, it has also been reported that phosphorylation of Rfa2 outside of the NT at S122 controls meiotic crossover frequency (Bartrand *et al.* 2006). This further suggests that Rfa2 phosphorylation, generally, has no clear role during entry and exit from MI and MII. Future work by Angela Adsero in the Haring lab will better define a role for the Rfa2 NT during meiosis.

However, phosphorylation of Rfa2 during meiosis may play a role in mediating the signaling activity of the protein-interaction domain DBD-F of Rfa1. DBD-F is required for a number of protein-protein interactions during LPR and DDC establishment. During meiosis, phosphorylation of the Rfa2 NT may be required to prevent these interactions by driving an interaction between the positively charged cleft within the OB-fold of DBD-F and the negatively charged Rfa2 phospho-NT. In human cells, RPA interacts with MeioB and Spata22. MeioB is referred to as a meiosis-specific paralog to Rpa1 but lacks DBD-F (Ribeiro *et al.* 2016). MeioB and Spata22 may therefore take the place of Rpa1 and Rpa3 during meiosis, leading to the formation of a meiosis-specific MeioB-Rpa2-Spata22 ssDNA binding complex.

However, yeast lack a functional homolog to MeioB or Spata22. Moreover, Rfa1 is subjected to significant proteolysis during the meiotic program (Clifford *et al.* 2004), suggestive that DBD-F may be proteolytically removed from Rfa1 in order to prevent DDC signaling and Rad53 activation during meiotic recombination. In order to promote this conversion of mitotic-RPA (containing DBD-F) to meiotic-RPA (lacking DBD-F), Rfa2 NT phosphorylation may be required. Providing the positively charged DBD-F cleft with a negatively charged binding substrate would expose the flexible linker region to protease activity in cells, allowing this conversion to occur. However, more complex organisms may avoid this irreversible change to the RPA complex by utilizing alternative ssDNA binding complexes containing one or more of the individual RPA subunits. Moreover, identification of alternative RPA subunit-dependent complexes may further elucidate the multifunctional and dynamic roles these proteins have in mitotic and meiotic processes.

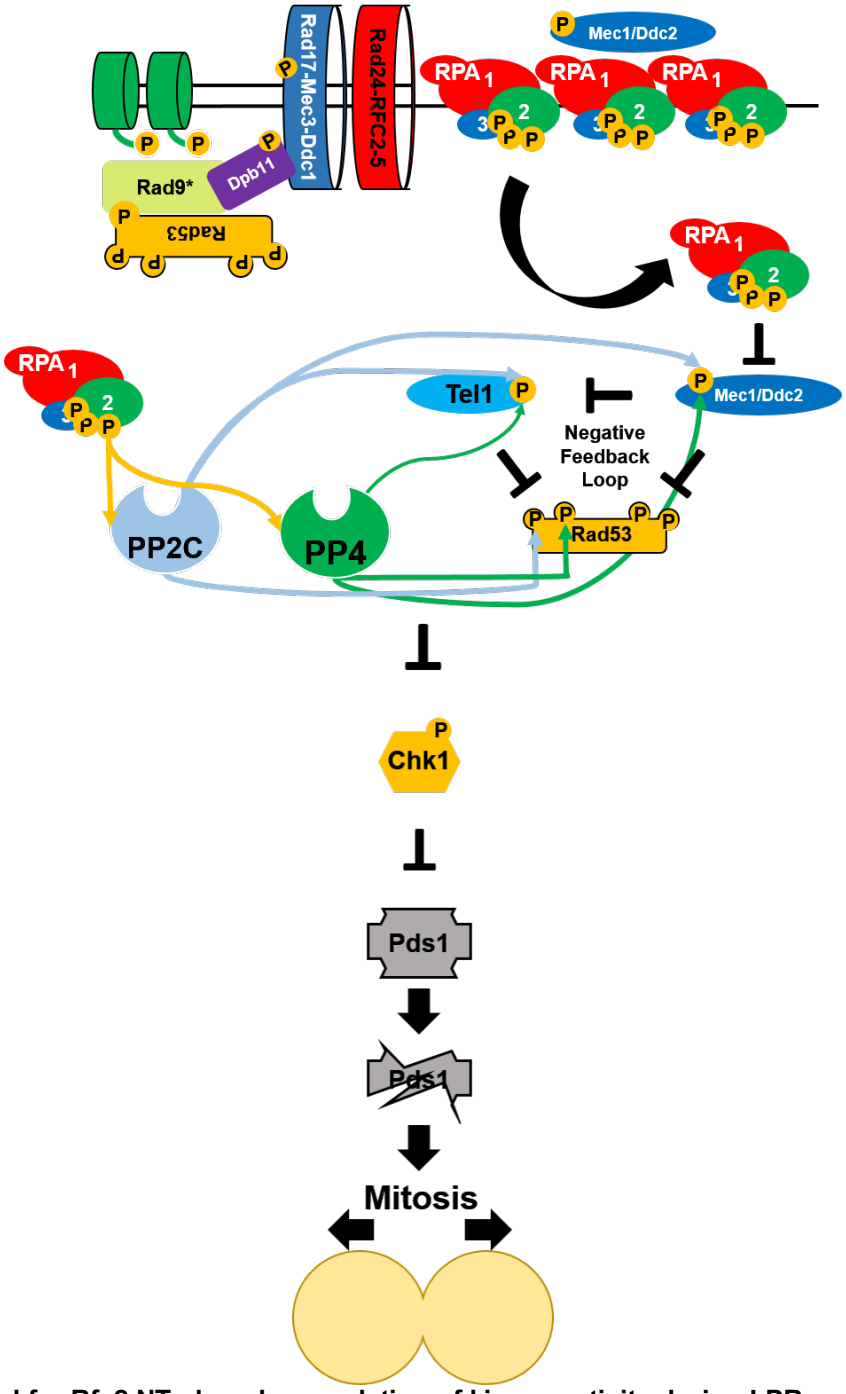

Figure 6.3. Model for Rfa2 NT phospho-regulation of kinase activity during LPR and adaptation
In this theoretical model for Rfa2 NT phospho-regulation of kinase activity during LPR and adaptation, Rfa2 NT phosphorylation leads to its dissociation from ssDNA and the formation of the Rad51-presynaptic filament, as described in Figure 6.1 and Figure 1.6. Phospho-RPA then, by an unknown mechanism, directly inhibits Mec1/Ddc2 activity at the break. Mec1 activity at the DSB attenuates Tel1 signaling (Clerici *et al.* 2014). Reduction in Mec1/Tel1 activity at the DSB further reduces Rad53 activation, and skews signaling towards PP2C and PP4 phosphatase complexes, leading to a further reduction in active, hyper-phosphorylated Rad53 and Chk1. Pds1 dephosphorylation leads to its destruction by the APC/C^{CDC20} complex, promoting mitotic entry. This is likely to occur once repair has completed during the LPR. During adaptation, the presence of phospho-RPA promotes mitotic exit irrespective of whether repair has occurred or not.

6.3.B. Timing of meiotic divisions may be affected by Rfa2 NT phosphorylation

While the ability of cells to form gametes during meiosis is not impacted in *rfa2-D$_X$* or *rfa2-A$_X$* extensive mutations, the viability of gametes produced by these two extensive mutations differs greatly. As described in Chapter 5, *rfa2-D$_X$* extensive mutation leads to a reduction in spore viability, whereas *rfa2-A$_X$* extensive mutations seem to promote spore viability in-line with that of wild-type cells. Not only does this reinforce the argument that Rfa2 NT phosphorylation is dispensable for the meiotic program, but it clearly argues that irreversible phosphorylation or phospho-mimetic mutation of the Rfa2 NT during meiosis leads to increased gamete inviability. However, the Rfa2 NT is required for meiosis as cells containing the *rfa2-*Δ*N$_X$* extensive mutation led to a significant decrease in four spore viability (WT cells 92%, *rfa2-*Δ*N$_X$* cells 67%) measured in my assays. Furthermore, the ability of cells to perform meiotic recombination, as measured by heteroallelic recombination, is unaffected in *any* of the Rfa2 NT extensive mutations, suggesting that the Rfa2 NT and the phospho-state of the Rfa2 NT are dispensable during recombination.

Since phosphorylation of the Rpa2 NT has been demonstrated in mitotic cells to regulate checkpoint exit (Anantha *et al.* 2008), and phospho-mimetic or naturally phosphorylatable mutation of the Rfa2 NT promotes checkpoint exit in response to irreparable lesions in yeast (Chapters 3 and 4; Wilson 2018b, Wilson *et al.* 2018c) , it is entirely plausible to speculate that the Rfa2 NT phospho-state may be impacting the timing of the meiotic divisions during MI and MII. If the phospho-state of Rfa2 NT is important for timely progression of divisions during MI and MII, I would hypothesize that preventing phosphorylation of this domain would lead to an arrest somewhere between MI and MII, leading to the formation of two-cell products. While this was not observed for *rfa2-A$_X$* extensive mutations, it was indeed the case for cells containing the NT truncation *rfa2-*Δ*N$_X$*. This suggests that the NT is required for timely progression during meiotic divisions. The reduction in viability exhibited by *rfa2-D$_X$* may be caused by a more rapid progression through the meiotic divisions, leading to inviability in some of the gametes formed during meiotic divisions. Thus, timely and well controlled phosphorylation and dephosphorylation of the Rfa2 NT may be required for proper progression through meiosis.

6.4. Final Remarks

Recent studies examining the effects of the Rpa2 NT phospho-state on cellular processes like apoptosis (controlled cell death) have reported that phosphorylation of the Rpa2 NT during replication leads to apoptosis in Chk1-inhibited cells using Gö6976 (Zuazua-Villar *et al.* 2015). Gö6976 is a known checkpoint inhibitor that inhibits protein kinase C (PKC), Chk1, and Chk2 activity leading to defective checkpoint signaling (Kohn *et al.* 2003). Normally, inhibition of Chk1 during DNA replication should also prevent adequate checkpoint maintenance, and thus lead to cellular division despite the presence of broken DNA or regressed/unstable replication forks and incomplete DNA replication. Anantha *et al.* 2008 reported that inhibition of Chk1 using UCN-01 (Chk1 inhibitor, synthetic derivative of staurosporine) prevented mitotic entry (Anantha *et al.* 2008). UCN-01 inhibits Chk1 function, but also induces cell cycle arrest and increases the effectiveness of DSB inducers like cisplatin, camptothecin, and ionizing radiation (Zhao *et al.* 2002). Conversely, Zuazua-Villar *et al*. also report that mutation forms of Rpa2 *(rpa2-S23/S29/S33A*) or depletion of Rpa2 through RNAi knockdown prevented apoptosis in their assays. S23 and S29 are known CDK phosphorylation sites and have been demonstrated by others to promote mitotic exit in the presence of DNA damage (Anantha *et al.* 2008).

It is possible then that direct inhibition of checkpoint function by inhibiting Chk1 and/or Chk2 activity directly leads to more robust phosphorylation of the Rpa2 NT, which would then drive mitotic exit as the DNA damage-dependent checkpoint is not properly maintained. Additionally, it may be possible that fragmented DNA that is unable to be repaired leads to the formation of a pseudo-telomeric structure at the break-site still attached to the centromere causing an aberrant checkpoint exit. Another intriguing possibility is that Rpa2 phosphorylation may drive apoptosis, or that irreversible apoptotic signaling may lead to Rpa2 phosphorylation. Previous research has demonstrated that Rpa2 phosphorylation is observed during the apoptotic process in cells (Zuazua-Villar *et al.* 2015); however, it is unknown whether increased fragmentation of DNA leads to increased phosphorylation of Rpa2 or if increased Rpa2 phosphorylation leads to increased DNA fragmentation. Future studies may better clarify whether Rpa2 phosphorylation causes or is a byproduct of DNA fragmentation. Moreover, if Rpa2 phosphorylation leads to increased DNA fragmentation, then a more effective treatment option for cancer may be to drive Rpa2 phosphorylation thus driving apoptosis in these cells. However, it is abundantly clear that, preventing

proper checkpoint maintenance leads directly to more robust Rpa2 NT phosphorylation, promoting aberrant mitotic exit and leading directly to genome instability and should be pursued from a therapeutic perspective.

My work done in Chapter 2 demonstrates that in yeast the Rfa2 NT is not overtly phosphorylated during LPR. Additionally, mimicking phosphorylation or the addition of a readily phosphorylatable Rfa2 NT leads to an increased sensitivity to genotoxic agents, likely due to the ability of the phospho-Rfa2 NT to promote checkpoint exit in the presence of unrepaired DNA lesions. This argument is reinforced by the work performed in Chapters 3 and 4, which demonstrate that phospho-mimetic or naturally phosphorylatable mutation of the Rfa2 NT leads to checkpoint exit in the presence of a persistent DNA lesion. The above combined with the work performed in Chapter 5 allude to a defined role for Rfa2 NT phosphorylation in the proper progression of the cell cycle during both mitosis and meiosis, and alteration of Rfa2 NT phospho-states has direct negative effects on each process, the ability of cells to maintain their genome, and viability when challenged with genotoxic stress.

There may be therapeutic value in preventing or promoting Rpa2 NT phosphorylation during genotoxic stress in human disease. Dysregulation of the cell cycle is a hallmark of cancer cells in humans, underscored by mass genome rearrangements that prevent telomere destruction that is critical for the aging process. Currently, inhibitors to checkpoint kinases like those mentioned above, are being used in combination with genotoxic DSB inducers to combat the dysregulated cell growth within tumors. However, the broader effects on the host caused by these inhibitors and genotoxic agents can directly lead to the formation of other cancers in different tissues. Rather than inhibiting checkpoint function in the presence of genotoxic agents through reductions in kinase activity, a more efficacious but more difficult approach may be to directly inhibit the phosphorylation of the Rpa2 NT or develop a novel strategy to remove the Rpa2 NT from malignant cells via a viral transfection or CRISPR-Cas9-like systems. Not only should this lead to permanent arrest in malignant cells and prevent Rpa2 NT phosphorylation-dependent mitotic exit, it would potentially lead to a restoration of telomere-dependent aging in these cells and also prevent the host from being exposed to any dose of genotoxic agent that would lead to the formation of malignancy in other tissues. As described above, yeast cells expressing the *rfa2-*ΔN_X mutation were defective for recruitment of Est1 to telomeres leading to severely shortened telomeres (Schramke *et al.*

2004). While the effects of NT truncations in humans has not been examined, there has already been some research done suggesting that regulating RPA function at telomeres, through association with TERRA and exchange for Pot1/Tpp1 (Flynn *et al.* 2011, Flynn *et al.* 2012), is important for proper regulation of telomeric DNA. Moreover, DNA-PK activity on hnRNP-A1 is thought to assist in mediating the switch from RPA to Pot1/Tpp1 at telomeres (Sui *et al.* 2015), and DNA-PK is also known to phosphorylate RPA on the Rpa2 NT when RPA is bound to ssDNA (Cruet-Hennequart *et al.* 2008, Liaw *et al.* 2011, Liu *et al.* 2012, Ashley *et al.* 2014). Taken together, the aforementioned studies in combination with what I have demonstrated in Chapters 3 and 4 regarding Rfa2 NT function during aberrant checkpoint release and mitotic exit, suggest that preventing phosphorylation or truncation of the Rpa2 NT in human cells may have significant therapeutic value in restoring malignant cells to a more normal growth state, or preventing cancer prior to the development of cellular dysregulation.

The work presented in this thesis makes one thing abundantly clear – dysregulation of the Rfa2 NT phospho-state in yeast has severe phenotypic consequences in both mitotic and meiotic cells, and alleviates checkpoint signaling in the face of DNA lesions. This may be the base mechanism by which malignancy or inherited cellular diseases, like Down and Turner syndromes caused by missegregation of chromosomes, forms in human cells and should be investigated further from a therapeutic angle. The core focus of the Haring lab is unraveling the molecular mechanisms by which cells prevent mutations within their genome, and this work performed and described within this thesis implicates the phospho-state of the Rfa2 NT as being a *direct contributor* to genomic instability in cells during genotoxic stress. While mutation of the genome is a requirement of evolution and population diversity within a species, too many mutations lead to cellular disease and genomic instability. In the future, more vigorous study of how the phospho-state of the Rpa2 NT regulates and promotes mitotic exit in the presence of DNA lesions will be critical in our understanding of how to combat cancer prior to the formation of malignancy, rather than treating cancer after the fidelity of a cell or organism's genome is compromised beyond the point of repair.

REFERENCES

Abdullah, U. B., J. F. McGouran, S. Brolih, D. Ptchelkine, A. H. El-Sagheer, T. Brown and P. J. McHugh (2017). "RPA activates the XPF-ERCC1 endonuclease to initiate processing of DNA interstrand crosslinks." EMBO J **36**(14): 2047-2060.

Ackermann, K., A. Waxmann, C. V. Glover and W. Pyerin (2001). "Genes targeted by protein kinase CK2: a genome-wide expression array analysis in yeast." Mol Cell Biochem **227**(1-2): 59-66.

Adams, D. J. and D. A. Clark (2015). "Common genetic and epigenetic syndromes." Pediatr Clin North Am **62**(2): 411-426.

Agarwal, R., Z. Tang, H. Yu and O. Cohen-Fix (2003). "Two distinct pathways for inhibiting pds1 ubiquitination in response to DNA damage." J Biol Chem **278**(45): 45027-45033.

Aklilu, B. B. and K. M. Culligan (2016). "Molecular Evolution and Functional Diversification of Replication Protein A1 in Plants." Front Plant Sci **7**: 33.

Aklilu, B. B., R. S. Soderquist and K. M. Culligan (2014). "Genetic analysis of the Replication Protein A large subunit family in Arabidopsis reveals unique and overlapping roles in DNA repair, meiosis and DNA replication." Nucleic Acids Res **42**(5): 3104-3118.

Alcasabas, A. A., A. J. Osborn, J. Bachant, F. Hu, P. J. Werler, K. Bousset, K. Furuya, J. F. Diffley, A. M. Carr and S. J. Elledge (2001). "Mrc1 transduces signals of DNA replication stress to activate Rad53." Nat Cell Biol **3**(11): 958-965.

Ali, S. I., J. S. Shin, S. H. Bae, B. Kim and B. S. Choi (2010). "Replication protein A 32 interacts through a similar binding interface with TIPIN, XPA, and UNG2." Int J Biochem Cell Biol **42**(7): 1210-1215.

Anantha, R. W. and J. A. Borowiec (2009). "Mitotic crisis: the unmasking of a novel role for RPA." Cell Cycle **8**(3): 357-361.

Anantha, R. W., E. Sokolova and J. A. Borowiec (2008). "RPA phosphorylation facilitates mitotic exit in response to mitotic DNA damage." Proc Natl Acad Sci U S A **105**(35): 12903-12908.

Anantha, R. W., V. M. Vassin and J. A. Borowiec (2007). "Sequential and synergistic modification of human RPA stimulates chromosomal DNA repair." J Biol Chem **282**(49): 35910-35923.

Arbel, A., D. Zenvirth and G. Simchen (1999). "Sister chromatid-based DNA repair is mediated by RAD54, not by DMC1 or TID1." EMBO J **18**(9): 2648-2658.

Arunkumar, A. I., M. E. Stauffer, E. Bochkareva, A. Bochkarev and W. J. Chazin (2003). "Independent and coordinated functions of replication protein A tandem high affinity single-stranded DNA binding domains." J Biol Chem **278**(42): 41077-41082.

Ashley, A. K., M. Shrivastav, J. Nie, C. Amerin, K. Troksa, J. G. Glanzer, S. Liu, S. O. Opiyo, D. D. Dimitrova, P. Le, B. Sishc, S. M. Bailey, G. G. Oakley and J. A. Nickoloff (2014). "DNA-PK phosphorylation of RPA32 Ser4/Ser8 regulates replication stress checkpoint activation, fork restart, homologous recombination and mitotic catastrophe." DNA Repair (Amst) **21**: 131-139.

Baker, B. S., A. T. Carpenter, M. S. Esposito, R. E. Esposito and L. Sandler (1976). "The genetic control of meiosis." Annu Rev Genet **10**: 53-134.

Ball, H. L., J. S. Myers and D. Cortez (2005). "ATRIP binding to replication protein A-single-stranded DNA promotes ATR-ATRIP localization but is dispensable for Chk1 phosphorylation." Mol Biol Cell **16**(5): 2372-2381.

Barnum, K. J. and M. J. O'Connell (2014). "Cell cycle regulation by checkpoints." Methods Mol Biol **1170**: 29-40.

Baroni, E., V. Viscardi, H. Cartagena-Lirola, G. Lucchini and M. P. Longhese (2004). "The Functions of Budding Yeast Sae2 in the DNA Damage Response Require Mec1- and Tel1-Dependent Phosphorylation." Molecular and Cellular Biology **24**(10): 4151-4165.

Bartrand, A. J., D. Iyasu and G. S. Brush (2004). "DNA stimulates Mec1-mediated phosphorylation of replication protein A." J Biol Chem **279**(25): 26762-26767.

Bartrand, A. J., D. Iyasu, S. M. Marinco and G. S. Brush (2006). "Evidence of meiotic crossover control in Saccharomyces cerevisiae through Mec1-mediated phosphorylation of replication protein A." Genetics **172**(1): 27-39.

Bastin-Shanower, S. A. and S. J. Brill (2001). "Functional analysis of the four DNA binding domains of replication protein A. The role of RPA2 in ssDNA binding." J Biol Chem **276**(39): 36446-36453.

Baudat, F., K. Manova, J. P. Yuen, M. Jasin and S. Keeney (2000). "Chromosome synapsis defects and sexually dimorphic meiotic progression in mice lacking Spo11." Mol Cell **6**(5): 989-998.

Berens, T. J. and D. P. Toczyski (2012). "Colocalization of Mec1 and Mrc1 is sufficient for Rad53 phosphorylation in vivo." Mol Biol Cell **23**(6): 1058-1067.

Bhargava, R., D. O. Onyango and J. M. Stark (2016). "Regulation of Single-Strand Annealing and its Role in Genome Maintenance." Trends Genet **32**(9): 566-575.

Binz, S. K., Y. Lao, D. F. Lowry and M. S. Wold (2003). "The phosphorylation domain of the 32-kDa subunit of replication protein A (RPA) modulates RPA-DNA interactions. Evidence for an intersubunit interaction." J Biol Chem **278**(37): 35584-35591.

Bishop, D. K., D. Park, L. Xu and N. Kleckner (1992). "DMC1: a meiosis-specific yeast homolog of E. coli recA required for recombination, synaptonemal complex formation, and cell cycle progression." Cell **69**(3): 439-456.

Bizard, A. H. and I. D. Hickson (2014). "The dissolution of double Holliday junctions." Cold Spring Harb Perspect Biol **6**(7): a016477.

Blackwell, L. J. and J. A. Borowiec (1994). "Human replication protein A binds single-stranded DNA in two distinct complexes." Mol Cell Biol **14**(6): 3993-4001.

Bochkarev, A., R. A. Pfuetzner, A. M. Edwards and L. Frappier (1997). "Structure of the single-stranded-DNA-binding domain of replication protein A bound to DNA." Nature **385**(6612): 176-181.

Bochkareva, E., S. Korolev, S. P. Lees-Miller and A. Bochkarev (2002). "Structure of the RPA trimerization core and its role in the multistep DNA-binding mechanism of RPA." EMBO J **21**(7): 1855-1863.

Bocquet, N., A. H. Bizard, W. Abdulrahman, N. B. Larsen, M. Faty, S. Cavadini, R. D. Bunker, S. C. Kowalczykowski, P. Cejka, I. D. Hickson and N. H. Thoma (2014). "Structural and mechanistic insight into Holliday-junction dissolution by topoisomerase IIIalpha and RMI1." Nat Struct Mol Biol **21**(3): 261-268.

Bonilla, C. Y., J. A. Melo and D. P. Toczyski (2008). "Colocalization of sensors is sufficient to activate the DNA damage checkpoint in the absence of damage." Mol Cell **30**(3): 267-276.

Brill, S. J. and B. Stillman (1989). "Yeast replication factor-A functions in the unwinding of the SV40 origin of DNA replication." Nature **342**(6245): 92-95.

Brill, S. J. and B. Stillman (1991). "Replication factor-A from Saccharomyces cerevisiae is encoded by three essential genes coordinately expressed at S phase." Genes Dev **5**(9): 1589-1600.

Brush, G. S., D. M. Clifford, S. M. Marinco and A. J. Bartrand (2001). "Replication protein A is sequentially phosphorylated during meiosis." Nucleic Acids Res **29**(23): 4808-4817.

Brush, G. S. and T. J. Kelly (2000). "Phosphorylation of the replication protein A large subunit in the Saccharomyces cerevisiae checkpoint response." Nucleic Acids Res **28**(19): 3725-3732.

Brush, G. S., D. M. Morrow, P. Hieter and T. J. Kelly (1996). "The ATM homologue MEC1 is required for phosphorylation of replication protein A in yeast." Proc Natl Acad Sci U S A **93**(26): 15075-15080.

Burgess, R. C., S. Rahman, M. Lisby, R. Rothstein and X. Zhao (2007). "The Slx5-Slx8 complex affects sumoylation of DNA repair proteins and negatively regulates recombination." Mol Cell Biol **27**(17): 6153-6162.

Burma, S., B. P. Chen, M. Murphy, A. Kurimasa and D. J. Chen (2001). "ATM Phosphorylates Histone H2AX in Response to DNA Double-strand Breaks." Journal of Biological Chemistry **276**(45): 42462-42467.

Cartagena-Lirola, H., I. Guerini, N. Manfrini, G. Lucchini and M. P. Longhese (2008). "Role of the Saccharomyces cerevisiae Rad53 checkpoint kinase in signaling double-strand breaks during the meiotic cell cycle." Mol Cell Biol **28**(14): 4480-4493.

Cejka, P., E. Cannavo, P. Polaczek, T. Masuda-Sasa, S. Pokharel, J. L. Campbell and S. C. Kowalczykowski (2010). "DNA end resection by Dna2-Sgs1-RPA and its stimulation by Top3-Rmi1 and Mre11-Rad50-Xrs2." Nature **467**(7311): 112-116.

Chang, Y., L. Gong, W. Yuan, X. Li, G. Chen, X. Li, Q. Zhang and C. Wu (2009). "Replication protein A (RPA1a) is required for meiotic and somatic DNA repair but is dispensable for DNA replication and homologous recombination in rice." Plant Physiol **151**(4): 2162-2173.

Charles, J. F., S. L. Jaspersen, R. L. Tinker-Kulberg, L. Hwang, A. Szidon and D. O. Morgan (1998). "The Polo-related kinase Cdc5 activates and is destroyed by the mitotic cyclin destruction machinery in S. cerevisiae." Curr Biol **8**(9): 497-507.

Chen, C., K. Umezu and R. D. Kolodner (1998). "Chromosomal rearrangements occur in S. cerevisiae rfa1 mutator mutants due to mutagenic lesions processed by double-strand-break repair." Mol Cell **2**(1): 9-22.

Chen, S. H. and H. Zhou (2009). "Reconstitution of Rad53 activation by Mec1 through adaptor protein Mrc1." J Biol Chem **284**(28): 18593-18604.

Chiruvella, K. K., Z. Liang, S. R. Birkeland, V. Basrur and T. E. Wilson (2013). "Saccharomyces cerevisiae DNA ligase IV supports imprecise end joining independently of its catalytic activity." PLoS Genet **9**(6): e1003599.

Chiruvella, K. K., Z. Liang and T. E. Wilson (2013). "Repair of double-strand breaks by end joining." Cold Spring Harb Perspect Biol **5**(5): a012757.

Chung, I. and X. Zhao (2015). "DNA break-induced sumoylation is enabled by collaboration between a SUMO ligase and the ssDNA-binding complex RPA." Genes Dev **29**(15): 1593-1598.

Chung, I. and X. Zhao (2015). "DNA break-induced sumoylation is enabled by collaboration between a SUMO ligase and the ssDNA-binding complex RPA." Genes & Development **29**(15): 1593-1598.

Ciccia, A. and S. J. Elledge (2010). "The DNA damage response: making it safe to play with knives." Mol Cell **40**(2): 179-204.

Clerici, M., D. Mantiero, I. Guerini, G. Lucchini and M. P. Longhese (2008). "The Yku70–Yku80 complex contributes to regulate double-strand break processing and checkpoint activation during the cell cycle." EMBO reports **9**(8): 810-818.

Clerici, M., D. Mantiero, G. Lucchini and M. P. Longhese (2005). "The Saccharomyces cerevisiae Sae2 Protein Promotes Resection and Bridging of Double Strand Break Ends." Journal of Biological Chemistry **280**(46): 38631-38638.

Clerici, M., D. Mantiero, G. Lucchini and M. P. Longhese (2006). "The Saccharomyces cerevisiae Sae2 protein negatively regulates DNA damage checkpoint signalling." EMBO Rep **7**(2): 212-218.

Clerici, M., C. Trovesi, A. Galbiati, G. Lucchini and M. P. Longhese (2014). "Mec1/ATR regulates the generation of single-stranded DNA that attenuates Tel1/ATM signaling at DNA ends." EMBO J **33**(3): 198-216.

Clifford, D. M., S. M. Marinco and G. S. Brush (2004). "The meiosis-specific protein kinase Ime2 directs phosphorylation of replication protein A." J Biol Chem **279**(7): 6163-6170.

Cohen-Fix, O. and D. Koshland (1997). "The anaphase inhibitor of Saccharomyces cerevisiae Pds1p is a target of the DNA damage checkpoint pathway." Proc Natl Acad Sci U S A **94**(26): 14361-14366.

Cohen-Fix, O. and D. Koshland (1999). "Pds1p of budding yeast has dual roles: inhibition of anaphase initiation and regulation of mitotic exit." Genes Dev **13**(15): 1950-1959.

Cohen-Fix, O., J. M. Peters, M. W. Kirschner and D. Koshland (1996). "Anaphase initiation in Saccharomyces cerevisiae is controlled by the APC-dependent degradation of the anaphase inhibitor Pds1p." Genes Dev **10**(24): 3081-3093.

Cortez, D., S. Guntuku, J. Qin and S. J. Elledge (2001). "ATR and ATRIP: partners in checkpoint signaling." Science **294**(5547): 1713-1716.

Costanzo, M., B. VanderSluis, E. N. Koch, A. Baryshnikova, C. Pons, G. Tan, W. Wang, M. Usaj, J. Hanchard, S. D. Lee, V. Pelechano, E. B. Styles, M. Billmann, J. van Leeuwen, N. van Dyk, Z.-Y. Lin, E. Kuzmin, J. Nelson, J. S. Piotrowski, T. Srikumar, S. Bahr, Y. Chen, R. Deshpande, C. F. Kurat, S. C. Li, Z. Li, M. M. Usaj, H. Okada, N. Pascoe, B.-J. San Luis, S. Sharifpoor, E. Shuteriqi, S. W. Simpkins, J. Snider, H. G. Suresh, Y. Tan, H. Zhu, N. Malod-Dognin, V. Janjic, N. Przulj, O. G. Troyanskaya, I. Stagljar, T. Xia, Y. Ohya, A.-C. Gingras, B. Raught, M. Boutros, L. M. Steinmetz, C. L. Moore, A. P. Rosebrock, A. A. Caudy, C. L. Myers, B. Andrews and C. Boone (2016). "A global genetic interaction network maps a wiring diagram of cellular function." Science **353**(6306).

Cremona, C. A., P. Sarangi, Y. Yang, L. E. Hang, S. Rahman and X. Zhao (2012). "Extensive DNA damage-induced sumoylation contributes to replication and repair and acts in addition to the mec1 checkpoint." Mol Cell **45**(3): 422-432.

Cremona, C. A., P. Sarangi and X. Zhao (2012). "Sumoylation and the DNA damage response." Biomolecules **2**(3): 376-388.

Cruet-Hennequart, S., M. T. Glynn, L. S. Murillo, S. Coyne and M. P. Carty (2008). "Enhanced DNA-PK-mediated RPA2 hyperphosphorylation in DNA polymerase eta-deficient human cells treated with cisplatin and oxaliplatin." DNA Repair (Amst) **7**(4): 582-596.

Cussiol, J. R., D. Dibitetto, A. Pellicioli and M. B. Smolka (2016). "Slx4 scaffolding in homologous recombination and checkpoint control: lessons from yeast." Chromosoma.

de la Torre-Ruiz, M. A., C. M. Green and N. F. Lowndes (1998). "RAD9 and RAD24 define two additive, interacting branches of the DNA damage checkpoint pathway in budding yeast normally required for Rad53 modification and activation." EMBO J **17**(9): 2687-2698.

Delacroix, S., J. M. Wagner, M. Kobayashi, K. Yamamoto and L. M. Karnitz (2007). "The Rad9-Hus1-Rad1 (9-1-1) clamp activates checkpoint signaling via TopBP1." Genes Dev **21**(12): 1472-1477.

Denchi, E. L. and T. de Lange (2007). "Protection of telomeres through independent control of ATM and ATR by TRF2 and POT1." Nature **448**(7157): 1068-1071.

Deshpande, I., A. Seeber, K. Shimada, J. J. Keusch, H. Gut and S. M. Gasser (2017). "Structural Basis of Mec1-Ddc2-RPA Assembly and Activation on Single-Stranded DNA at Sites of Damage." Mol Cell **68**(2): 431-445 e435.

Deshpande, R. A., G. J. Williams, O. Limbo, R. S. Williams, J. Kuhnlein, J. H. Lee, S. Classen, G. Guenther, P. Russell, J. A. Tainer and T. T. Paull (2014). "ATP-driven Rad50 conformations regulate DNA tethering, end resection, and ATM checkpoint signaling." EMBO J **33**(5): 482-500.

Desterro, J. M., M. S. Rodriguez and R. T. Hay (1998). "SUMO-1 modification of IkappaBalpha inhibits NF-kappaB activation." Mol Cell **2**(2): 233-239.

Diaz, R. L., A. D. Alcid, J. M. Berger and S. Keeney (2002). "Identification of residues in yeast Spo11p critical for meiotic DNA double-strand break formation." Mol Cell Biol **22**(4): 1106-1115.

Dibitetto, D., M. Ferrari, C. C. Rawal, A. Balint, T. Kim, Z. Zhang, M. B. Smolka, G. W. Brown, F. Marini and A. Pellicioli (2016). "Slx4 and Rtt107 control checkpoint signalling and DNA resection at double-strand breaks." Nucleic Acids Res **44**(2): 669-682.

Diener, A. C. and G. R. Fink (1996). "DLH1 is a functional Candida albicans homologue of the meiosis-specific gene DMC1." Genetics **143**(2): 769-776.

Din, S., S. J. Brill, M. P. Fairman and B. Stillman (1990). "Cell-cycle-regulated phosphorylation of DNA replication factor A from human and yeast cells." Genes Dev **4**(6): 968-977.

Dornreiter, I., L. F. Erdile, I. U. Gilbert, D. von Winkler, T. J. Kelly and E. Fanning (1992). "Interaction of DNA polymerase alpha-primase with cellular replication protein A and SV40 T antigen." EMBO J **11**(2): 769-776.

Dou, H., C. Huang, M. Singh, P. B. Carpenter and E. T. Yeh (2010). "Regulation of DNA repair through deSUMOylation and SUMOylation of replication protein A complex." Mol Cell **39**(3): 333-345.

Downs, J. A., N. F. Lowndes and S. P. Jackson (2000). "A role for Saccharomyces cerevisiae histone H2A in DNA repair." Nature **408**(6815): 1001-1004.

Dresser, M. E., D. J. Ewing, M. N. Conrad, A. M. Dominguez, R. Barstead, H. Jiang and T. Kodadek (1997). "DMC1 functions in a Saccharomyces cerevisiae meiotic pathway that is largely independent of the RAD51 pathway." Genetics **147**(2): 533-544.

Dubois, J. C., M. Yates, A. Gaudreau-Lapierre, G. Clement, L. Cappadocia, L. Gaudreau, L. Zou and A. Marechal (2017). "A phosphorylation-and-ubiquitylation circuitry driving ATR activation and homologous recombination." Nucleic Acids Res **45**(15): 8859-8872.

Dubrana, K., H. van Attikum, F. Hediger and S. M. Gasser (2007). "The processing of double-strand breaks and binding of single-strand-binding proteins RPA and Rad51 modulate the formation of ATR-kinase foci in yeast." J Cell Sci **120**(Pt 23): 4209-4220.

Eapen, V. V., N. Sugawara, M. Tsabar, W. H. Wu and J. E. Haber (2012). "The Saccharomyces cerevisiae chromatin remodeler Fun30 regulates DNA end resection and checkpoint deactivation." Mol Cell Biol **32**(22): 4727-4740.

Eggler, A. L., R. B. Inman and M. M. Cox (2002). "The Rad51-dependent pairing of long DNA substrates is stabilized by replication protein A." J Biol Chem **277**(42): 39280-39288.

Elia, A. E., D. C. Wang, N. A. Willis, A. P. Boardman, I. Hajdu, R. O. Adeyemi, E. Lowry, S. P. Gygi, R. Scully and S. J. Elledge (2015). "RFWD3-Dependent Ubiquitination of RPA Regulates Repair at Stalled Replication Forks." Mol Cell **60**(2): 280-293.

Elledge, S. J. (1996). "Cell cycle checkpoints: preventing an identity crisis." Science **274**(5293): 1664-1672.

Elmayan, T., F. Proux and H. Vaucheret (2005). "Arabidopsis RPA2: a genetic link among transcriptional gene silencing, DNA repair, and DNA replication." Curr Biol **15**(21): 1919-1925.

Eschbach, V. and D. Kobbe (2014). "Different replication protein A complexes of Arabidopsis thaliana have different DNA-binding properties as a function of heterotrimer composition." Plant Cell Physiol **55**(8): 1460-1472.

Fan, J. and N. P. Pavletich (2012). "Structure and conformational change of a replication protein A heterotrimer bound to ssDNA." Genes Dev **26**(20): 2337-2347.

Fang, F. and J. W. Newport (1993). "Distinct roles of cdk2 and cdc2 in RP-A phosphorylation during the cell cycle." J Cell Sci **106 (Pt 3)**: 983-994.

Feeney, L., I. M. Munoz, C. Lachaud, R. Toth, P. L. Appleton, D. Schindler and J. Rouse (2017). "RPA-Mediated Recruitment of the E3 Ligase RFWD3 Is Vital for Interstrand Crosslink Repair and Human Health." Mol Cell **66**(5): 610-621 e614.

Feng, J., T. Wakeman, S. Yong, X. Wu, S. Kornbluth and X. F. Wang (2009). "Protein phosphatase 2A-dependent dephosphorylation of replication protein A is required for the repair of DNA breaks induced by replication stress." Mol Cell Biol **29**(21): 5696-5709.

Ferrari, M., B. T. Nachimuthu, R. A. Donnianni, H. Klein and A. Pellicioli (2013). "Tid1/Rdh54 translocase is phosphorylated through a Mec1- and Rad53-dependent manner in the presence of DSB lesions in budding yeast." DNA Repair (Amst) **12**(5): 347-355.

Ferrari, S. R., J. Grubb and D. K. Bishop (2009). "The Mei5-Sae3 protein complex mediates Dmc1 activity in Saccharomyces cerevisiae." J Biol Chem **284**(18): 11766-11770.

Flynn, R. L., R. C. Centore, R. J. O'Sullivan, R. Rai, A. Tse, Z. Songyang, S. Chang, J. Karlseder and L. Zou (2011). "TERRA and hnRNPA1 orchestrate an RPA-to-POT1 switch on telomeric single-stranded DNA." Nature **471**(7339): 532-536.

Flynn, R. L., S. Chang and L. Zou (2012). "RPA and POT1: friends or foes at telomeres?" Cell Cycle **11**(4): 652-657.

Francon, P., J. M. Lemaitre, C. Dreyer, D. Maiorano, O. Cuvier and M. Mechali (2004). "A hypophosphorylated form of RPA34 is a specific component of pre-replication centers." J Cell Sci **117**(Pt 21): 4909-4920.

Fraune, J., S. Schramm, M. Alsheimer and R. Benavente (2012). "The mammalian synaptonemal complex: Protein components, assembly and role in meiotic recombination." Experimental Cell Research **318**(12): 1340-1346.

Fukushima, K., Y. Tanaka, K. Nabeshima, T. Yoneki, T. Tougan, S. Tanaka and H. Nojima (2000). "Dmc1 of Schizosaccharomyces pombe plays a role in meiotic recombination." Nucleic Acids Res **28**(14): 2709-2716.

Gaines, W. A., S. K. Godin, F. F. Kabbinavar, T. Rao, A. P. VanDemark, P. Sung and K. A. Bernstein (2015). "Promotion of presynaptic filament assembly by the ensemble of S. cerevisiae Rad51 paralogues with Rad52." Nat Commun **6**: 7834.

Galanty, Y., R. Belotserkovskaya, J. Coates and S. P. Jackson (2012). "RNF4, a SUMO-targeted ubiquitin E3 ligase, promotes DNA double-strand break repair." Genes Dev **26**(11): 1179-1195.

Galanty, Y., R. Belotserkovskaya, J. Coates, S. Polo, K. M. Miller and S. P. Jackson (2009). "Mammalian SUMO E3-ligases PIAS1 and PIAS4 promote responses to DNA double-strand breaks." Nature **462**(7275): 935-939.

Gao, J., H. Wang, A. H. Wong, G. Zeng, Z. Huang, Y. Wang, J. Sang and Y. Wang (2014). "Regulation of Rfa2 phosphorylation in response to genotoxic stress in Candida albicans." Mol Microbiol **94**(1): 141-155.

García-Rodríguez, N., R. P. Wong and H. D. Ulrich (2016). "Functions of Ubiquitin and SUMO in DNA Replication and Replication Stress." Frontiers in Genetics **7**: 87.

Gardner, R., C. W. Putnam and T. Weinert (1999). "RAD53, DUN1 and PDS1 define two parallel G2/M checkpoint pathways in budding yeast." EMBO J **18**(11): 3173-3185.

Gasior, S. L., H. Olivares, U. Ear, D. M. Hari, R. Weichselbaum and D. K. Bishop (2001). "Assembly of RecA-like recombinases: distinct roles for mediator proteins in mitosis and meiosis." Proc Natl Acad Sci U S A **98**(15): 8411-8418.

Gasior, S. L., A. K. Wong, Y. Kora, A. Shinohara and D. K. Bishop (1998). "Rad52 associates with RPA and functions with rad55 and rad57 to assemble meiotic recombination complexes." Genes Dev **12**(14): 2208-2221.

Germann, S. M., V. H. Oestergaard, C. Haas, P. Salis, A. Motegi and M. Lisby (2011). "Dpb11/TopBP1 plays distinct roles in DNA replication, checkpoint response and homologous recombination." DNA Repair **10**(2): 210-224.

Ghospurkar, P. L. (2015). "Characterization of Rpa2 N-terminal Function in the DNA Damage Response in Saccharomyces Cerevisiae.".

Ghospurkar, P. L., T. M. Wilson, S. Liu, A. Herauf, J. Steffes, E. N. Mueller, G. G. Oakley and S. J. Haring (2015). "Phosphorylation and cellular function of the human Rpa2 N-terminus in the budding yeast Saccharomyces cerevisiae." Exp Cell Res **331**(1): 183-199.

Ghospurkar, P. L., T. M. Wilson, A. L. Severson, S. J. Klein, S. K. Khaku, A. P. Walther and S. J. Haring (2015). "The DNA damage response and checkpoint adaptation in Saccharomyces cerevisiae: distinct roles for the replication protein A2 (Rfa2) N-terminus." Genetics **199**(3): 711-727.

Gilbert, C. S., C. M. Green and N. F. Lowndes (2001). "Budding Yeast Rad9 Is an ATP-Dependent Rad53 Activating Machine." Molecular Cell **8**(1): 129-136.

Glanzer, J. G., S. Liu, L. Wang, A. Mosel, A. Peng and G. G. Oakley (2014). "RPA inhibition increases replication stress and suppresses tumor growth." Cancer Res **74**(18): 5165-5172.

Gobbini, E., C. Cassani, M. Villa, D. Bonetti and M. P. Longhese (2016). "Functions and regulation of the MRX complex at DNA double-strand breaks." Microb Cell **3**(8): 329-337.

Gobbini, E., D. Cesena, A. Galbiati, A. Lockhart and M. P. Longhese (2013). "Interplays between ATM/Tel1 and ATR/Mec1 in sensing and signaling DNA double-strand breaks." DNA Repair (Amst) **12**(10): 791-799.

Gobbini, E., M. Villa, M. Gnugnoli, L. Menin, M. Clerici and M. P. Longhese (2015). "Sae2 Function at DNA Double-Strand Breaks Is Bypassed by Dampening Tel1 or Rad53 Activity." PLoS Genet **11**(11): e1005685.

Golub, E. I., R. C. Gupta, T. Haaf, M. S. Wold and C. M. Radding (1998). "Interaction of human rad51 recombination protein with single-stranded DNA binding protein, RPA." Nucleic Acids Res **26**(23): 5388-5393.

Gong, Z. and J. Chen (2011). "E3 ligase RFWD3 participates in replication checkpoint control." J Biol Chem **286**(25): 22308-22313.

Gospodinov, A., T. Vaissiere, D. B. Krastev, G. Legube, B. Anachkova and Z. Herceg (2011). "Mammalian Ino80 mediates double-strand break repair through its role in DNA end strand resection." Mol Cell Biol **31**(23): 4735-4745.

Grandin, N., A. Bailly and M. Charbonneau (2005). "Activation of Mrc1, a mediator of the replication checkpoint, by telomere erosion." Biol Cell **97**(10): 799-814.

Grandin, N. and M. Charbonneau (2007). "Control of the yeast telomeric senescence survival pathways of recombination by the Mec1 and Mec3 DNA damage sensors and RPA." Nucleic Acids Res **35**(3): 822-838.

Grenon, M., T. Costelloe, S. Jimeno, A. O'Shaughnessy, J. FitzGerald, O. Zgheib, L. Degerth and N. F. Lowndes (2007). "Docking onto chromatin via theSaccharomyces cerevisiae Rad9 Tudor domain." Yeast **24**(2): 105-119.

Grenon, M., C. Gilbert and N. F. Lowndes (2001). "Checkpoint activation in response to double-strand breaks requires the Mre11/Rad50/Xrs2 complex." Nature Cell Biology **3**(9): 844-847.

Grey, M., A. Dusterhoft, J. A. Henriques and M. Brendel (1996). "Allelism of PSO4 and PRP19 links pre-mRNA processing with recombination and error-prone DNA repair in Saccharomyces cerevisiae." Nucleic Acids Res **24**(20): 4009-4014.

Grudic, A., A. Jul-Larsen, S. J. Haring, M. S. Wold, P. E. Lonning, R. Bjerkvig and S. O. Boe (2007). "Replication protein A prevents accumulation of single-stranded telomeric DNA in cells that use alternative lengthening of telomeres." Nucleic Acids Res **35**(21): 7267-7278.

Guillemain, G., E. Ma, S. Mauger, S. Miron, R. Thai, R. Guerois, F. Ochsenbein and M. C. Marsolier-Kergoat (2007). "Mechanisms of checkpoint kinase Rad53 inactivation after a double-strand break in Saccharomyces cerevisiae." Mol Cell Biol **27**(9): 3378-3389.

Guo, X., Y. Deng, Y. Lin, W. Cosme-Blanco, S. Chan, H. He, G. Yuan, E. J. Brown and S. Chang (2007). "Dysfunctional telomeres activate an ATM-ATR-dependent DNA damage response to suppress tumorigenesis." EMBO J **26**(22): 4709-4719.

Haber, J. E. (2000). "Lucky breaks: analysis of recombination in Saccharomyces." Mutat Res **451**(1-2): 53-69.

Hagen, L., B. Kavli, M. M. Sousa, K. Torseth, N. B. Liabakk, O. Sundheim, J. Pena-Diaz, M. Otterlei, O. Horning, O. N. Jensen, H. E. Krokan and G. Slupphaug (2008). "Cell cycle-specific UNG2 phosphorylations regulate protein turnover, activity and association with RPA." EMBO J **27**(1): 51-61.

Hammet, A., C. Magill, J. Heierhorst and S. P. Jackson (2007). "Rad9 BRCT domain interaction with phosphorylated H2AX regulates the G1 checkpoint in budding yeast." EMBO reports **8**(9): 851-857.

Haring, S. J., T. D. Humphreys and M. S. Wold (2010). "A naturally occurring human RPA subunit homolog does not support DNA replication or cell-cycle progression." Nucleic Acids Res **38**(3): 846-858.

Haring, S. J., A. C. Mason, S. K. Binz and M. S. Wold (2008). "Cellular functions of human RPA1. Multiple roles of domains in replication, repair, and checkpoints." J Biol Chem **283**(27): 19095-19111.

Hartwell, L. H. and T. A. Weinert (1989). "Checkpoints: controls that ensure the order of cell cycle events." Science **246**(4930): 629-634.

Hayase, A., M. Takagi, T. Miyazaki, H. Oshiumi, M. Shinohara and A. Shinohara (2004). "A protein complex containing Mei5 and Sae3 promotes the assembly of the meiosis-specific RecA homolog Dmc1." Cell **119**(7): 927-940.

He, H., J. Wang and T. Liu (2017). "UV-Induced RPA1 Acetylation Promotes Nucleotide Excision Repair." Cell Rep **20**(9): 2010-2025.

Helleday, T., J. Lo, D. C. van Gent and B. P. Engelward (2007). "DNA double-strand break repair: from mechanistic understanding to cancer treatment." DNA Repair (Amst) **6**(7): 923-935.

Henriques, J. A., E. J. Vicente, K. V. Leandro da Silva and A. C. Schenberg (1989). "PSO4: a novel gene involved in error-prone repair in Saccharomyces cerevisiae." Mutat Res **218**(2): 111-124.

Herate, C., C. Vigne, C. A. Guenzel, M. Lambele, M. C. Rouyez and S. Benichou (2016). "Uracil DNA glycosylase interacts with the p32 subunit of the replication protein A complex to modulate HIV-1 reverse transcription for optimal virus dissemination." Retrovirology **13**: 26.

Heyer, W. D. (2004). "Recombination: Holliday junction resolution and crossover formation." Curr Biol **14**(2): R56-58.

Heyer, W. D., K. T. Ehmsen and J. A. Solinger (2003). "Holliday junctions in the eukaryotic nucleus: resolution in sight?" Trends Biochem Sci **28**(10): 548-557.

Heyer, W. D., M. R. Rao, L. F. Erdile, T. J. Kelly and R. D. Kolodner (1990). "An essential Saccharomyces cerevisiae single-stranded DNA binding protein is homologous to the large subunit of human RP-A." EMBO J **9**(7): 2321-2329.

Holliday, R. (2007). "A mechanism for gene conversion in fungi." Genet Res **89**(5-6): 285-307.

Hollingsworth, N. M., L. Goetsch and B. Byers (1990). "The HOP1 gene encodes a meiosis-specific component of yeast chromosomes." Cell **61**(1): 73-84.

Hong, E. L., A. Shinohara and D. K. Bishop (2001). "Saccharomyces cerevisiae Dmc1 protein promotes renaturation of single-strand DNA (ssDNA) and assimilation of ssDNA into homologous super-coiled duplex DNA." J Biol Chem **276**(45): 41906-41912.

Huyen, Y., O. Zgheib, R. A. DiTullio Jr, V. G. Gorgoulis, P. Zacharatos, T. J. Petty, E. A. Sheston, H. S. Mellert, E. S. Stavridi and T. D. Halazonetis (2004). "Methylated lysine 79 of histone H3 targets 53BP1 to DNA double-strand breaks." Nature **432**(7015): 406-411.

Iftode, C., Y. Daniely and J. A. Borowiec (1999). "Replication protein A (RPA): the eukaryotic SSB." Crit Rev Biochem Mol Biol **34**(3): 141-180.

Inano, S., K. Sato, Y. Katsuki, W. Kobayashi, H. Tanaka, K. Nakajima, S. Nakada, H. Miyoshi, K. Knies, A. Takaori-Kondo, D. Schindler, M. Ishiai, H. Kurumizaka and M. Takata (2017). "RFWD3-Mediated Ubiquitination Promotes Timely Removal of Both RPA and RAD51 from DNA Damage Sites to Facilitate Homologous Recombination." Mol Cell **66**(5): 622-634 e628.

Ira, G., A. Pellicioli, A. Balijja, X. Wang, S. Fiorani, W. Carotenuto, G. Liberi, D. Bressan, L. Wan, N. M. Hollingsworth, J. E. Haber and M. Foiani (2004). "DNA end resection, homologous recombination and DNA damage checkpoint activation require CDK1." Nature **431**(7011): 1011-1017.

Iyama, T. and D. M. Wilson, 3rd (2013). "DNA repair mechanisms in dividing and non-dividing cells." DNA Repair (Amst) **12**(8): 620-636.

Jablonowski, C. M., J. R. Cussiol, S. Oberly, A. Yimit, A. Balint, T. Kim, Z. Zhang, G. W. Brown and M. B. Smolka (2015). "Termination of Replication Stress Signaling via Concerted Action of the Slx4 Scaffold and the PP4 Phosphatase." Genetics **201**(3): 937-949.

Javaheri, A., R. Wysocki, O. Jobin-Robitaille, M. Altaf, J. Cote and S. J. Kron (2006). "Yeast G1 DNA damage checkpoint regulation by H2A phosphorylation is independent of chromatin remodeling." Proceedings of the National Academy of Sciences **103**(37): 13771-13776.

Kagey, M. H., T. A. Melhuish and D. Wotton (2003). "The Polycomb Protein Pc2 Is a SUMO E3." Cell **113**(1): 127-137.

Keeney, S., C. N. Giroux and N. Kleckner (1997). "Meiosis-specific DNA double-strand breaks are catalyzed by Spo11, a member of a widely conserved protein family." Cell **88**(3): 375-384.

Kelly, D. E., D. C. Lamb and S. L. Kelly (2001). "Genome-wide generation of yeast gene deletion strains." Comp Funct Genomics **2**(4): 236-242.

Kim, C., B. F. Paulus and M. S. Wold (1994). "Interactions of human replication protein A with oligonucleotides." Biochemistry **33**(47): 14197-14206.

Kim, C., R. O. Snyder and M. S. Wold (1992). "Binding properties of replication protein A from human and yeast cells." Mol Cell Biol **12**(7): 3050-3059.

Kim, H., J. Chen and X. Yu (2007). "Ubiquitin-binding protein RAP80 mediates BRCA1-dependent DNA damage response." Science **316**(5828): 1202-1205.

Kim, H. S. and S. J. Brill (2001). "Rfc4 interacts with Rpa1 and is required for both DNA replication and DNA damage checkpoints in Saccharomyces cerevisiae." Mol Cell Biol **21**(11): 3725-3737.

Kim, H. S. and S. J. Brill (2003). "MEC1-dependent phosphorylation of yeast RPA1 in vitro." DNA Repair (Amst) **2**(12): 1321-1335.

Kim, J. A., W. M. Hicks, J. Li, S. Y. Tay and J. E. Haber (2011). "Protein phosphatases pph3, ptc2, and ptc3 play redundant roles in DNA double-strand break repair by homologous recombination." Mol Cell Biol **31**(3): 507-516.

Klein, H. L. (1997). "RDH54, a RAD54 homologue in Saccharomyces cerevisiae, is required for mitotic diploid-specific recombination and repair and for meiosis." Genetics **147**(4): 1533-1543.

Kohn, E. A., C. J. Yoo and A. Eastman (2003). "The protein kinase C inhibitor Go6976 is a potent inhibitor of DNA damage-induced S and G2 cell cycle checkpoints." Cancer Res **63**(1): 31-35.

Kouznetsova, A., R. Benavente, A. Pastink and C. Höög (2011). "Meiosis in Mice without a Synaptonemal Complex." PLoS ONE **6**(12): e28255.

Kowalczykowski, S. C. (2000). "Some assembly required." Nat Struct Biol **7**(12): 1087-1089.

Kubara, P. M., S. Kerneis-Golsteyn, A. Studeny, B. B. Lanser, L. Meijer and R. M. Golsteyn (2012). "Human cells enter mitosis with damaged DNA after treatment with pharmacological concentrations of genotoxic agents." Biochem J **446**(3): 373-381.

Kumagai, A., J. Lee, H. Y. Yoo and W. G. Dunphy (2006). "TopBP1 activates the ATR-ATRIP complex." Cell **124**(5): 943-955.

Lazzaro, F., V. Sapountzi, M. Granata, A. Pellicioli, M. Vaze, J. E. Haber, P. Plevani, D. Lydall and M. Muzi-Falconi (2008). "Histone methyltransferase Dot1 and Rad9 inhibit single-stranded DNA accumulation at DSBs and uncapped telomeres." The EMBO Journal.

Lee, D. H., Y. Pan, S. Kanner, P. Sung, J. A. Borowiec and D. Chowdhury (2010). "A PP4 phosphatase complex dephosphorylates RPA2 to facilitate DNA repair via homologous recombination." Nat Struct Mol Biol **17**(3): 365-372.

Lee, J. and W. G. Dunphy (2010). "Rad17 plays a central role in establishment of the interaction between TopBP1 and the Rad9-Hus1-Rad1 complex at stalled replication forks." Mol Biol Cell **21**(6): 926-935.

Lee, J., A. Kumagai and W. G. Dunphy (2007). "The Rad9-Hus1-Rad1 checkpoint clamp regulates interaction of TopBP1 with ATR." J Biol Chem **282**(38): 28036-28044.

Lee, J. H. (2005). "ATM Activation by DNA Double-Strand Breaks Through the Mre11-Rad50-Nbs1 Complex." Science **308**(5721): 551-554.

Lee, J. H. and T. T. Paull (2005). "ATM activation by DNA double-strand breaks through the Mre11-Rad50-Nbs1 complex." Science **308**(5721): 551-554.

Lee, S. E., J. K. Moore, A. Holmes, K. Umezu, R. D. Kolodner and J. E. Haber (1998). "Saccharomyces Ku70, mre11/rad50 and RPA proteins regulate adaptation to G2/M arrest after DNA damage." Cell **94**(3): 399-409.

Lee, S. E., A. Pellicioli, A. Malkova, M. Foiani and J. E. Haber (2001). "The Saccharomyces recombination protein Tid1p is required for adaptation from G2/M arrest induced by a double-strand break." Curr Biol **11**(13): 1053-1057.

Lee, S. E., A. Pellicioli, M. B. Vaze, N. Sugawara, A. Malkova, M. Foiani and J. E. Haber (2003). "Yeast Rad52 and Rad51 recombination proteins define a second pathway of DNA damage assessment in response to a single double-strand break." Mol Cell Biol **23**(23): 8913-8923.

Leroy, C., S. E. Lee, M. B. Vaze, F. Ochsenbein, R. Guerois, J. E. Haber and M. C. Marsolier-Kergoat (2003). "PP2C phosphatases Ptc2 and Ptc3 are required for DNA checkpoint inactivation after a double-strand break." Mol Cell **11**(3): 827-835.

Leroy, C., S. E. Lee, M. B. Vaze, F. Ochsenbien, R. Guerois, J. E. Haber and M.-C. Marsolier-Kergoat (2003). "PP2C Phosphatases Ptc2 and Ptc3 Are Required for DNA Checkpoint Inactivation after a Double-Strand Break." Molecular Cell **11**(3): 827-835.

Lewis, C. W. and R. M. Golsteyn (2016). "Cancer cells that survive checkpoint adaptation contain micronuclei that harbor damaged DNA." Cell Cycle **15**(22): 3131-3145.

Li, G. M. (2008). "Mechanisms and functions of DNA mismatch repair." Cell Res **18**(1): 85-98.

Li, L., X. Lu, C. A. Peterson and R. J. Legerski (1995). "An interaction between the DNA repair factor XPA and replication protein A appears essential for nucleotide excision repair." Mol Cell Biol **15**(10): 5396-5402.

Li, X., Y. Chang, X. Xin, C. Zhu, X. Li, J. D. Higgins and C. Wu (2013). "Replication protein A2c coupled with replication protein A1c regulates crossover formation during meiosis in rice." Plant Cell **25**(10): 3885-3899.

Liaw, H., D. Lee and K. Myung (2011). "DNA-PK-dependent RPA2 hyperphosphorylation facilitates DNA repair and suppresses sister chromatid exchange." PLoS One **6**(6): e21424.

Lisby, M., J. H. Barlow, R. C. Burgess and R. Rothstein (2004). "Choreography of the DNA damage response: spatiotemporal relationships among checkpoint and repair proteins." Cell **118**(6): 699-713.

Liu, S., J. Chu, N. Yucer, M. Leng, S. Y. Wang, B. P. Chen, W. N. Hittelman and Y. Wang (2011). "RING finger and WD repeat domain 3 (RFWD3) associates with replication protein A (RPA) and facilitates RPA-mediated DNA damage response." J Biol Chem **286**(25): 22314-22322.

Liu, S., S. O. Opiyo, K. Manthey, J. G. Glanzer, A. K. Ashley, C. Amerin, K. Troksa, M. Shrivastav, J. A. Nickoloff and G. G. Oakley (2012). "Distinct roles for DNA-PK, ATM and ATR in RPA phosphorylation and checkpoint activation in response to replication stress." Nucleic Acids Res **40**(21): 10780-10794.

Liu, S., B. Shiotani, M. Lahiri, A. Marechal, A. Tse, C. C. Leung, J. N. Glover, X. H. Yang and L. Zou (2011). "ATR autophosphorylation as a molecular switch for checkpoint activation." Mol Cell **43**(2): 192-202.

Liu, Y., M. Kvaratskhelia, S. Hess, Y. Qu and Y. Zou (2005). "Modulation of Replication Protein A Function by Its Hyperphosphorylation-induced Conformational Change Involving DNA Binding Domain B." The Journal of biological chemistry **280**(38): 32775-32783.

Longhese, M. P., M. Foiani, M. Muzi-Falconi, G. Lucchini and P. Plevani (1998). "DNA damage checkpoint in budding yeast." EMBO J **17**(19): 5525-5528.

Lowndes, N. F. and J. R. Murguia (2000). "Sensing and responding to DNA damage." Curr Opin Genet Dev **10**(1): 17-25.

Lucca, C., F. Vanoli, C. Cotta-Ramusino, A. Pellicioli, G. Liberi, J. Haber and M. Foiani (2004). "Checkpoint-mediated control of replisome-fork association and signalling in response to replication pausing." Oncogene **23**(6): 1206-1213.

Luciano, P., S. Coulon, V. Faure, Y. Corda, J. Bos, S. J. Brill, E. Gilson, M. N. Simon and V. Geli (2012). "RPA facilitates telomerase activity at chromosome ends in budding and fission yeasts." EMBO J **31**(8): 2034-2046.

Luo, K., H. Zhang, L. Wang, J. Yuan and Z. Lou (2012). "Sumoylation of MDC1 is important for proper DNA damage response." EMBO J **31**(13): 3008-3019.

Luo, M., F. Yang, N. A. Leu, J. Landaiche, M. A. Handel, R. Benavente, S. La Salle and P. J. Wang (2013). "MEIOB exhibits single-stranded DNA-binding and exonuclease activities and is essential for meiotic recombination." Nat Commun **4**: 2788.

Ma, C. J., B. Gibb, Y. Kwon, P. Sung and E. C. Greene (2017). "Protein dynamics of human RPA and RAD51 on ssDNA during assembly and disassembly of the RAD51 filament." Nucleic Acids Res **45**(2): 749-761.

Ma, C. J., Y. Kwon, P. Sung and E. C. Greene (2017). "Human RAD52 interactions with Replication Protein A and the RAD51 presynaptic complex." J Biol Chem.

Majka, J., S. K. Binz, M. S. Wold and P. M. Burgers (2006). "Replication protein A directs loading of the DNA damage checkpoint clamp to 5'-DNA junctions." J Biol Chem **281**(38): 27855-27861.

Majka, J., S. K. Binz, M. S. Wold and P. M. J. Burgers (2006). "Replication Protein A Directs Loading of the DNA Damage Checkpoint Clamp to 5′-DNA Junctions." Journal of Biological Chemistry **281**(38): 27855-27861.

Majka, J., A. Niedziela-Majka and P. M. Burgers (2006). "The checkpoint clamp activates Mec1 kinase during initiation of the DNA damage checkpoint." Mol Cell **24**(6): 891-901.

Mallory, J. C., V. I. Bashkirov, K. M. Trujillo, J. A. Solinger, M. Dominska, P. Sung, W. D. Heyer and T. D. Petes (2003). "Amino acid changes in Xrs2p, Dun1p, and Rfa2p that remove the preferred targets of the ATM family of protein kinases do not affect DNA repair or telomere length in Saccharomyces cerevisiae." DNA Repair (Amst) **2**(9): 1041-1064.

Maniar, H. S., R. Wilson and S. J. Brill (1997). "Roles of replication protein-A subunits 2 and 3 in DNA replication fork movement in Saccharomyces cerevisiae." Genetics **145**(4): 891-902.

Manthey, K. C., S. Opiyo, J. G. Glanzer, D. Dimitrova, J. Elliott and G. G. Oakley (2007). "NBS1 mediates ATR-dependent RPA hyperphosphorylation following replication-fork stall and collapse." J Cell Sci **120**(Pt 23): 4221-4229.

Marechal, A., J. M. Li, X. Y. Ji, C. S. Wu, S. A. Yazinski, H. D. Nguyen, S. Liu, A. E. Jimenez, J. Jin and L. Zou (2014). "PRP19 transforms into a sensor of RPA-ssDNA after DNA damage and drives ATR activation via a ubiquitin-mediated circuitry." Mol Cell **53**(2): 235-246.

Marechal, A. and L. Zou (2015). "RPA-coated single-stranded DNA as a platform for post-translational modifications in the DNA damage response." Cell Res **25**(1): 9-23.

Martinez, J. S., C. von Nicolai, T. Kim, A. Ehlen, A. V. Mazin, S. C. Kowalczykowski and A. Carreira (2016). "BRCA2 regulates DMC1-mediated recombination through the BRC repeats." Proc Natl Acad Sci U S A **113**(13): 3515-3520.

Martini, E. and S. Keeney (2002). "Sex and the single (double-strand) break." Mol Cell **9**(4): 700-702.

Marwedel, T., T. Ishibashi, R. Lorbiecke, S. Jacob, K. Sakaguchi and M. Sauter (2003). "Plant-specific regulation of replication protein A2 (OsRPA2) from rice during the cell cycle and in response to ultraviolet light exposure." Planta **217**(3): 457-465.

Matos, J. and S. C. West (2014). "Holliday junction resolution: regulation in space and time." DNA Repair (Amst) **19**: 176-181.

Matsuoka, S., B. A. Ballif, A. Smogorzewska, E. R. McDonald, 3rd, K. E. Hurov, J. Luo, C. E. Bakalarski, Z. Zhao, N. Solimini, Y. Lerenthal, Y. Shiloh, S. P. Gygi and S. J. Elledge (2007). "ATM and ATR substrate analysis reveals extensive protein networks responsive to DNA damage." Science **316**(5828): 1160-1166.

Mazin, A. V., C. J. Bornarth, J. A. Solinger, W. D. Heyer and S. C. Kowalczykowski (2000). "Rad54 protein is targeted to pairing loci by the Rad51 nucleoprotein filament." Mol Cell **6**(3): 583-592.

McKee, A. H. and N. Kleckner (1997). "Mutations in Saccharomyces cerevisiae that block meiotic prophase chromosome metabolism and confer cell cycle arrest at pachytene identify two new meiosis-specific genes SAE1 and SAE3." Genetics **146**(3): 817-834.

Mer, G., A. Bochkarev, R. Gupta, E. Bochkareva, L. Frappier, C. J. Ingles, A. M. Edwards and W. J. Chazin (2000). "Structural basis for the recognition of DNA repair proteins UNG2, XPA, and RAD52 by replication factor RPA." Cell **103**(3): 449-456.

Mimitou, E. P. and L. S. Symington (2008). "Sae2, Exo1 and Sgs1 collaborate in DNA double-strand break processing." Nature **455**(7214): 770-774.

Mimitou, E. P. and L. S. Symington (2010). "Ku prevents Exo1 and Sgs1-dependent resection of DNA ends in the absence of a functional MRX complex or Sae2." EMBO J **29**(19): 3358-3369.

Mordes, D. A., G. G. Glick, R. Zhao and D. Cortez (2008). "TopBP1 activates ATR through ATRIP and a PIKK regulatory domain." Genes Dev **22**(11): 1478-1489.

Mordes, D. A., E. A. Nam and D. Cortez (2008). "Dpb11 activates the Mec1-Ddc2 complex." Proc Natl Acad Sci U S A **105**(48): 18730-18734.

Morrow, D. M., D. A. Tagle, Y. Shiloh, F. S. Collins and P. Hieter (1995). "TEL1, an S. cerevisiae homolog of the human gene mutated in ataxia telangiectasia, is functionally related to the yeast checkpoint gene MEC1." Cell **82**(5): 831-840.

Murayama, Y., Y. Kurokawa, Y. Tsutsui and H. Iwasaki (2013). "Dual regulation of Dmc1-driven DNA strand exchange by Swi5-Sfr1 activation and Rad22 inhibition." Genes Dev **27**(21): 2299-2304.

Murphy, A. K., M. Fitzgerald, T. Ro, J. H. Kim, A. I. Rabinowitsch, D. Chowdhury, C. L. Schildkraut and J. A. Borowiec (2014). "Phosphorylated RPA recruits PALB2 to stalled DNA replication forks to facilitate fork recovery." J Cell Biol **206**(4): 493-507.

Naiki, T., T. Wakayama, D. Nakada, K. Matsumoto and K. Sugimoto (2004). "Association of Rad9 with Double-Strand Breaks through a Mec1-Dependent Mechanism." Molecular and Cellular Biology **24**(8): 3277-3285.

Nakada, D. (2005). "Role of the C Terminus of Mec1 Checkpoint Kinase in Its Localization to Sites of DNA Damage." Molecular Biology of the Cell **16**(11): 5227-5235.

Nakada, D., Y. Hirano and K. Sugimoto (2004). "Requirement of the Mre11 complex and exonuclease 1 for activation of the Mec1 signaling pathway." Mol Cell Biol **24**(22): 10016-10025.

Nakada, D., Y. Hirano, Y. Tanaka and K. Sugimoto (2005). "Role of the C terminus of Mec1 checkpoint kinase in its localization to sites of DNA damage." Mol Biol Cell **16**(11): 5227-5235.

Nakada, D., K. Matsumoto and K. Sugimoto (2003). "ATM-related Tel1 associates with double-strand breaks through an Xrs2-dependent mechanism." Genes Dev **17**(16): 1957-1962.

Nakada, D., T. Shimomura, K. Matsumoto and K. Sugimoto (2003). "The ATM-related Tel1 protein of Saccharomyces cerevisiae controls a checkpoint response following phleomycin treatment." Nucleic Acids Res **31**(6): 1715-1724.

Namiki, Y. and L. Zou (2006). "ATRIP associates with replication protein A-coated ssDNA through multiple interactions." Proc Natl Acad Sci U S A **103**(3): 580-585.

Navadgi-Patil, V. M. and P. M. Burgers (2008). "Yeast DNA replication protein Dpb11 activates the Mec1/ATR checkpoint kinase." J Biol Chem **283**(51): 35853-35859.

Navadgi-Patil, V. M. and P. M. Burgers (2009). "A tale of two tails: activation of DNA damage checkpoint kinase Mec1/ATR by the 9-1-1 clamp and by Dpb11/TopBP1." DNA Repair (Amst) **8**(9): 996-1003.

Navadgi-Patil, V. M. and P. M. Burgers (2009). "The unstructured C-terminal tail of the 9-1-1 clamp subunit Ddc1 activates Mec1/ATR via two distinct mechanisms." Mol Cell **36**(5): 743-753.

Navadgi-Patil, V. M. and P. M. Burgers (2011). "Cell-cycle-specific activators of the Mec1/ATR checkpoint kinase." Biochem Soc Trans **39**(2): 600-605.

New, J. H. and S. C. Kowalczykowski (2002). "Rad52 protein has a second stimulatory role in DNA strand exchange that complements replication protein-A function." J Biol Chem **277**(29): 26171-26176.

New, J. H., T. Sugiyama, E. Zaitseva and S. C. Kowalczykowski (1998). "Rad52 protein stimulates DNA strand exchange by Rad51 and replication protein A." Nature **391**(6665): 407-410.

Nicolette, M. L., K. Lee, Z. Guo, M. Rani, J. M. Chow, S. E. Lee and T. T. Paull (2010). "Mre11–Rad50–Xrs2 and Sae2 promote 5′ strand resection of DNA double-strand breaks." Nature Structural & Molecular Biology **17**(12): 1478-1485.

Nimonkar, A. V., C. C. Dombrowski, J. S. Siino, A. Z. Stasiak, A. Stasiak and S. C. Kowalczykowski (2012). "Saccharomyces cerevisiae Dmc1 and Rad51 proteins preferentially function with Tid1 and Rad54 proteins, respectively, to promote DNA strand invasion during genetic recombination." J Biol Chem **287**(34): 28727-28737.

Niu, H., W. H. Chung, Z. Zhu, Y. Kwon, W. Zhao, P. Chi, R. Prakash, C. Seong, D. Liu, L. Lu, G. Ira and P. Sung (2010). "Mechanism of the ATP-dependent DNA end-resection machinery from Saccharomyces cerevisiae." Nature **467**(7311): 108-111.

O'Connell, M. J., N. C. Walworth and A. M. Carr (2000). "The G2-phase DNA-damage checkpoint." Trends Cell Biol **10**(7): 296-303.

O'Neill, B. M., S. J. Szyjka, E. T. Lis, A. O. Bailey, J. R. Yates, 3rd, O. M. Aparicio and F. E. Romesberg (2007). "Pph3-Psy2 is a phosphatase complex required for Rad53 dephosphorylation and replication fork restart during recovery from DNA damage." Proc Natl Acad Sci U S A **104**(22): 9290-9295.

Oakley, G. G., S. M. Patrick, J. Yao, M. P. Carty, J. J. Turchi and K. Dixon (2003). "RPA phosphorylation in mitosis alters DNA binding and protein-protein interactions." Biochemistry **42**(11): 3255-3264.

Oakley, G. G., K. Tillison, S. A. Opiyo, J. G. Glanzer, J. M. Horn and S. M. Patrick (2009). "Physical interaction between replication protein A (RPA) and MRN: involvement of RPA2 phosphorylation and the N-terminus of RPA1." Biochemistry **48**(31): 7473-7481.

Ohouo, P. Y., F. M. Bastos de Oliveira, B. S. Almeida and M. B. Smolka (2010). "DNA damage signaling recruits the Rtt107-Slx4 scaffolds via Dpb11 to mediate replication stress response." Mol Cell **39**(2): 300-306.

Ohouo, P. Y., F. M. Bastos de Oliveira, Y. Liu, C. J. Ma and M. B. Smolka (2013). "DNA-repair scaffolds dampen checkpoint signalling by counteracting the adaptor Rad9." Nature **493**(7430): 120-124.

Olsen, J. V., M. Vermeulen, A. Santamaria, C. Kumar, M. L. Miller, L. J. Jensen, F. Gnad, J. Cox, T. S. Jensen, E. A. Nigg, S. Brunak and M. Mann (2010). "Quantitative phosphoproteomics reveals widespread full phosphorylation site occupancy during mitosis." Sci Signal **3**(104): ra3.

Olson, E., C. J. Nievera, V. Klimovich, E. Fanning and X. Wu (2006). "RPA2 is a direct downstream target for ATR to regulate the S-phase checkpoint." J Biol Chem **281**(51): 39517-39533.

Olson, E., C. J. Nievera, E. Liu, A. Y. Lee, L. Chen and X. Wu (2007). "The Mre11 complex mediates the S-phase checkpoint through an interaction with replication protein A." Mol Cell Biol **27**(17): 6053-6067.

Osborn, A. J. and S. J. Elledge (2003). "Mrc1 is a replication fork component whose phosphorylation in response to DNA replication stress activates Rad53." Genes Dev **17**(14): 1755-1767.

Page, S. L. (2003). "Chromosome Choreography: The Meiotic Ballet." Science **301**(5634): 785-789.

Page, S. L. and R. S. Hawley (2003). "Chromosome choreography: the meiotic ballet." Science **301**(5634): 785-789.

Paques, F. and J. E. Haber (1999). "Multiple pathways of recombination induced by double-strand breaks in Saccharomyces cerevisiae." Microbiol Mol Biol Rev **63**(2): 349-404.

Park, M. S., D. L. Ludwig, E. Stigger and S. H. Lee (1996). "Physical interaction between human RAD52 and RPA is required for homologous recombination in mammalian cells." J Biol Chem **271**(31): 18996-19000.

Paull, T. T. and J. H. Lee (2005). "The Mre11/Rad50/Nbs1 complex and its role as a DNA double-strand break sensor for ATM." Cell Cycle **4**(6): 737-740.

Pellicioli, A., S. E. Lee, C. Lucca, M. Foiani and J. E. Haber (2001). "Regulation of Saccharomyces Rad53 checkpoint kinase during adaptation from DNA damage-induced G2/M arrest." Mol Cell **7**(2): 293-300.

Pellicioli, A., S. E. Lee, C. Lucca, M. Foiani and J. E. Haber (2001). "Regulation of Saccharomyces Rad53 Checkpoint Kinase during Adaptation from DNA Damage–Induced G2/M Arrest." Molecular Cell **7**(2): 293-300.

Petukhova, G., P. Sung and H. Klein (2000). "Promotion of Rad51-dependent D-loop formation by yeast recombination factor Rdh54/Tid1." Genes Dev **14**(17): 2206-2215.

Philipova, D., J. R. Mullen, H. S. Maniar, J. Lu, C. Gu and S. J. Brill (1996). "A hierarchy of SSB protomers in replication protein A." Genes Dev **10**(17): 2222-2233.

Piya, G., E. N. Mueller, H. K. Haas, P. L. Ghospurkar, T. M. Wilson, J. L. Jensen, C. L. Colbert and S. J. Haring (2015). "Characterization of the interaction between Rfa1 and Rad24 in Saccharomyces cerevisiae." PLoS One **10**(2): e0116512.

Psakhye, I. and S. Jentsch (2012). "Protein group modification and synergy in the SUMO pathway as exemplified in DNA repair." Cell **151**(4): 807-820.

Puddu, F., M. Granata, L. Di Nola, A. Balestrini, G. Piergiovanni, F. Lazzaro, M. Giannattasio, P. Plevani and M. Muzi-Falconi (2008). "Phosphorylation of the budding yeast 9-1-1 complex is required for Dpb11 function in the full activation of the UV-induced DNA damage checkpoint." Mol Cell Biol **28**(15): 4782-4793.

Pyerin, W., T. Barz and K. Ackermann (2005). "Protein kinase CK2 in gene control at cell cycle entry." Mol Cell Biochem **274**(1-2): 189-200.

Ratcliffe, S. G. (1981). "The effect of chromosome abnormalities on human growth." Br Med Bull **37**(3): 291-295.

Recolin, B. and D. Maiorano (2012). "Implication of RPA32 phosphorylation in S-phase checkpoint signalling at replication forks stalled with aphidicolin in Xenopus egg extracts." Biochem Biophys Res Commun **427**(4): 785-789.

Recolin, B., S. Van der Laan and D. Maiorano (2012). "Role of replication protein A as sensor in activation of the S-phase checkpoint in Xenopus egg extracts." Nucleic Acids Res **40**(8): 3431-3442.

Rector, J., S. Kapil, K. J. Treude, P. Kumm, J. G. Glanzer, B. M. Byrne, S. Liu, L. M. Smith, D. J. DiMaio, P. Giannini, R. B. Smith and G. G. Oakley (2016). "S4S8-RPA phosphorylation as an indicator of cancer progression in oral squamous cell carcinomas." Oncotarget.

Rector, J., S. Kapil, K. J. Treude, P. Kumm, J. G. Glanzer, B. M. Byrne, S. Liu, L. M. Smith, D. J. DiMaio, P. Giannini, R. B. Smith and G. G. Oakley (2017). "S4S8-RPA phosphorylation as an indicator of cancer progression in oral squamous cell carcinomas." Oncotarget **8**(6): 9243-9250.

Rhind, N. and P. Russell (1998). "Mitotic DNA damage and replication checkpoints in yeast." Curr Opin Cell Biol **10**(6): 749-758.

Ribeiro, J., E. Abby, G. Livera and E. Martini (2016). "RPA homologs and ssDNA processing during meiotic recombination." Chromosoma **125**(2): 265-276.

Robison, J. G., J. Elliott, K. Dixon and G. G. Oakley (2004). "Replication protein A and the Mre11.Rad50.Nbs1 complex co-localize and interact at sites of stalled replication forks." J Biol Chem **279**(33): 34802-34810.

Robison, J. G., L. Lu, K. Dixon and J. J. Bissler (2005). "DNA lesion-specific co-localization of the Mre11/Rad50/Nbs1 (MRN) complex and replication protein A (RPA) to repair foci." J Biol Chem **280**(13): 12927-12934.

Rodriguez, M. S., C. Dargemont and R. T. Hay (2001). "SUMO-1 conjugation in vivo requires both a consensus modification motif and nuclear targeting." J Biol Chem **276**(16): 12654-12659.

Romanienko, P. J. and R. D. Camerini-Otero (2000). "The mouse Spo11 gene is required for meiotic chromosome synapsis." Mol Cell **6**(5): 975-987.

Rouse, J. and S. P. Jackson (2002). "Interfaces between the detection, signaling, and repair of DNA damage." Science **297**(5581): 547-551.

Rouse, J. and S. P. Jackson (2002). "Lcd1p Recruits Mec1p to DNA Lesions In Vitro and In Vivo." Molecular Cell **9**(4): 857-869.

Sakofsky, C. J. and A. Malkova (2017). "Break induced replication in eukaryotes: mechanisms, functions, and consequences." Crit Rev Biochem Mol Biol **52**(4): 395-413.

Sanchez, Y., J. Bachant, H. Wang, F. Hu, D. Liu, M. Tetzlaff and S. J. Elledge (1999). "Control of the DNA damage checkpoint by chk1 and rad53 protein kinases through distinct mechanisms." Science **286**(5442): 1166-1171.

Sanchez, Y., B. A. Desany, W. J. Jones, Q. Liu, B. Wang and S. J. Elledge (1996). "Regulation of RAD53 by the ATM-Like Kinases MEC1 and TEL1 in Yeast Cell Cycle Checkpoint Pathways." Science **271**(5247): 357-360.

Sandell, L. L. and V. A. Zakian (1993). "Loss of a yeast telomere: arrest, recovery, and chromosome loss." Cell **75**(4): 729-739.

Santa Maria, S. R., Y. Kwon, P. Sung and H. L. Klein (2013). "Characterization of the interaction between the Saccharomyces cerevisiae Rad51 recombinase and the DNA translocase Rdh54." J Biol Chem **288**(30): 21999-22005.

Santocanale, C., H. Neecke, M. P. Longhese, G. Lucchini and P. Plevani (1995). "Mutations in the gene encoding the 34 kDa subunit of yeast replication protein A cause defective S phase progression." J Mol Biol **254**(4): 595-607.

Sarbajna, S. and S. C. West (2014). "Holliday junction processing enzymes as guardians of genome stability." Trends Biochem Sci **39**(9): 409-419.

Schleker, T., K. Shimada, R. Sack, B. L. Pike and S. M. Gasser (2010). "Cell cycle-dependent phosphorylation of Rad53 kinase by Cdc5 and Cdc28 modulates checkpoint adaptation." Cell Cycle **9**(2): 350-363.

Schramke, V., P. Luciano, V. Brevet, S. Guillot, Y. Corda, M. P. Longhese, E. Gilson and V. Geli (2004). "RPA regulates telomerase action by providing Est1p access to chromosome ends." Nat Genet **36**(1): 46-54.

Schramke, V., H. Neecke, V. Brevet, Y. Corda, G. Lucchini, M. P. Longhese, E. Gilson and V. Geli (2001). "The set1Delta mutation unveils a novel signaling pathway relayed by the Rad53-dependent hyperphosphorylation of replication protein A that leads to transcriptional activation of repair genes." Genes Dev **15**(14): 1845-1858.

Schubert, H. L., R. M. Blumenthal and X. Cheng (2006). 1 Protein Methyltransferases: Their Distribution Among the Five Structural Classes of AdoMet-Dependent Methyltransferases. The Enzymes. S. G. Clarke and F. Tamanoi, Academic Press. **24:** 3-28.

Schwacha, A. and N. Kleckner (1997). "Interhomolog bias during meiotic recombination: meiotic functions promote a highly differentiated interhomolog-only pathway." Cell **90**(6): 1123-1135.

Seroussi, E. and S. Lavi (1993). "Replication protein A is the major single-stranded DNA binding protein detected in mammalian cell extracts by gel retardation assays and UV cross-linking of long and short single-stranded DNA molecules." J Biol Chem **268**(10): 7147-7154.

Serrano, D. and D. D'Amours (2016). "Checkpoint adaptation: Keeping Cdc5 in the T-loop." Cell Cycle **15**(24): 3339-3340.

Sfeir, A. and L. S. Symington (2015). "Microhomology-Mediated End Joining: A Back-up Survival Mechanism or Dedicated Pathway?" Trends Biochem Sci **40**(11): 701-714.

Shi, W., Z. Feng, J. Zhang, I. Gonzalez-Suarez, R. P. Vanderwaal, X. Wu, S. N. Powell, J. L. Roti Roti, S. Gonzalo and J. Zhang (2010). "The role of RPA2 phosphorylation in homologous recombination in response to replication arrest." Carcinogenesis **31**(6): 994-1002.

Shim, E. Y., W. H. Chung, M. L. Nicolette, Y. Zhang, M. Davis, Z. Zhu, T. T. Paull, G. Ira and S. E. Lee (2010). "Saccharomyces cerevisiae Mre11/Rad50/Xrs2 and Ku proteins regulate association of Exo1 and Dna2 with DNA breaks." EMBO J **29**(19): 3370-3380.

Shima, H., H. Suzuki, J. Sun, K. Kono, L. Shi, A. Kinomura, Y. Horikoshi, T. Ikura, M. Ikura, R. Kanaar, K. Igarashi, H. Saitoh, H. Kurumizaka and S. Tashiro (2013). "Activation of the SUMO modification system is required for the accumulation of RAD51 at sites of DNA damage." J Cell Sci **126**(Pt 22): 5284-5292.

Shinohara, A., S. Gasior, T. Ogawa, N. Kleckner and D. K. Bishop (1997). "Saccharomyces cerevisiae recA homologues RAD51 and DMC1 have both distinct and overlapping roles in meiotic recombination." Genes Cells **2**(10): 615-629.

Shinohara, A., M. Shinohara, T. Ohta, S. Matsuda and T. Ogawa (1998). "Rad52 forms ring structures and co-operates with RPA in single-strand DNA annealing." Genes Cells **3**(3): 145-156.

Shinohara, M., S. L. Gasior, D. K. Bishop and A. Shinohara (2000). "Tid1/Rdh54 promotes colocalization of rad51 and dmc1 during meiotic recombination." Proc Natl Acad Sci U S A **97**(20): 10814-10819.

Shirayama, M., W. Zachariae, R. Ciosk and K. Nasmyth (1998). "The Polo-like kinase Cdc5p and the WD-repeat protein Cdc20p/fizzy are regulators and substrates of the anaphase promoting complex in Saccharomyces cerevisiae." EMBO J **17**(5): 1336-1349.

Sikorski, R. S. and P. Hieter (1989). "A system of shuttle vectors and yeast host strains designed for efficient manipulation of DNA in Saccharomyces cerevisiae." Genetics **122**(1): 19-27.

Sleeth, K. M., C. S. Sorensen, N. Issaeva, J. Dziegielewski, J. Bartek and T. Helleday (2007). "RPA mediates recombination repair during replication stress and is displaced from DNA by checkpoint signalling in human cells." J Mol Biol **373**(1): 38-47.

Smith, J., H. Zou and R. Rothstein (2000). "Characterization of genetic interactions with RFA1: the role of RPA in DNA replication and telomere maintenance." Biochimie **82**(1): 71-78.

Smolka, M. B., C. P. Albuquerque, S. H. Chen and H. Zhou (2007). "Proteome-wide identification of in vivo targets of DNA damage checkpoint kinases." Proc Natl Acad Sci U S A **104**(25): 10364-10369.

Sneeden, J. L., S. M. Grossi, I. Tappin, J. Hurwitz and W. D. Heyer (2013). "Reconstitution of recombination-associated DNA synthesis with human proteins." Nucleic Acids Res **41**(9): 4913-4925.

Souquet, B., E. Abby, R. Herve, F. Finsterbusch, S. Tourpin, R. Le Bouffant, C. Duquenne, S. Messiaen, E. Martini, J. Bernardino-Sgherri, A. Toth, R. Habert and G. Livera (2013). "MEIOB targets single-strand DNA and is necessary for meiotic recombination." PLoS Genet **9**(9): e1003784.

Soustelle, C., M. Vedel, R. Kolodner and A. Nicolas (2002). "Replication protein A is required for meiotic recombination in Saccharomyces cerevisiae." Genetics **161**(2): 535-547.

Stigger, E., R. Drissi and S. H. Lee (1998). "Functional analysis of human replication protein A in nucleotide excision repair." J Biol Chem **273**(15): 9337-9343.

Sugiyama, T., N. Kantake, Y. Wu and S. C. Kowalczykowski (2006). "Rad52-mediated DNA annealing after Rad51-mediated DNA strand exchange promotes second ssDNA capture." EMBO J **25**(23): 5539-5548.

Sui, J., Y.-F. Lin, K. Xu, K.-J. Lee, D. Wang and B. P. C. Chen (2015). "DNA-PKcs phosphorylates hnRNP-A1 to facilitate the RPA-to-POT1 switch and telomere capping after replication." Nucleic Acids Research **43**(12): 5971-5983.

Sung, P. (1997). "Function of yeast Rad52 protein as a mediator between replication protein A and the Rad51 recombinase." J Biol Chem **272**(45): 28194-28197.

Sung, P. (1997). "Yeast Rad55 and Rad57 proteins form a heterodimer that functions with replication protein A to promote DNA strand exchange by Rad51 recombinase." Genes Dev **11**(9): 1111-1121.

Sweeney, F. D., F. Yang, A. Chi, J. Shabanowitz, D. F. Hunt and D. Durocher (2005). "Saccharomyces cerevisiae Rad9 Acts as a Mec1 Adaptor to Allow Rad53 Activation." Current Biology **15**(15): 1364-1375.

Swift, L. H. and R. M. Golsteyn (2014). "Genotoxic anti-cancer agents and their relationship to DNA damage, mitosis, and checkpoint adaptation in proliferating cancer cells." Int J Mol Sci **15**(3): 3403-3431.

Symington, L. S. (2016). "Mechanism and regulation of DNA end resection in eukaryotes." Crit Rev Biochem Mol Biol **51**(3): 195-212.

Symington, L. S., R. Rothstein and M. Lisby (2014). "Mechanisms and regulation of mitotic recombination in Saccharomyces cerevisiae." Genetics **198**(3): 795-835.

Templado, C., F. Vidal and A. Estop (2011). "Aneuploidy in human spermatozoa." Cytogenet Genome Res **133**(2-4): 91-99.

Thompson, D. A. and F. W. Stahl (1999). "Genetic control of recombination partner preference in yeast meiosis. Isolation and characterization of mutants elevated for meiotic unequal sister-chromatid recombination." Genetics **153**(2): 621-641.

Thrower, J. S., L. Hoffman, M. Rechsteiner and C. M. Pickart (2000). "Recognition of the polyubiquitin proteolytic signal." Embo j **19**(1): 94-102.

Toczyski, D. P. (2006). "Methods for studying adaptation to the DNA damage checkpoint in yeast." Methods Enzymol **409**: 150-165.

Toczyski, D. P., D. J. Galgoczy and L. H. Hartwell (1997). "CDC5 and CKII control adaptation to the yeast DNA damage checkpoint." Cell **90**(6): 1097-1106.

Toh, G. W. L., A. M. O'Shaughnessy, S. Jimeno, I. M. Dobbie, M. Grenon, S. Maffini, A. O'Rorke and N. F. Lowndes (2006). "Histone H2A phosphorylation and H3 methylation are required for a novel Rad9 DSB repair function following checkpoint activation." DNA Repair **5**(6): 693-703.

Torseth, K., B. Doseth, L. Hagen, C. Olaisen, N. B. Liabakk, H. Graesmann, A. Durandy, M. Otterlei, H. E. Krokan, B. Kavli and G. Slupphaug (2012). "The UNG2 Arg88Cys variant abrogates RPA-mediated recruitment of UNG2 to single-stranded DNA." DNA Repair (Amst) **11**(6): 559-569.

Treuner, K., M. Findeisen, U. Strausfeld and R. Knippers (1999). "Phosphorylation of replication protein A middle subunit (RPA32) leads to a disassembly of the RPA heterotrimer." J Biol Chem **274**(22): 15556-15561.

Trujillo, K. M., D. H. Roh, L. Chen, S. Van Komen, A. Tomkinson and P. Sung (2003). "Yeast xrs2 binds DNA and helps target rad50 and mre11 to DNA ends." J Biol Chem **278**(49): 48957-48964.

Tsubouchi, H. and G. S. Roeder (2004). "The budding yeast mei5 and sae3 proteins act together with dmc1 during meiotic recombination." Genetics **168**(3): 1219-1230.

Umezu, K., N. Sugawara, C. Chen, J. E. Haber and R. D. Kolodner (1998). "Genetic analysis of yeast RPA1 reveals its multiple functions in DNA metabolism." Genetics **148**(3): 989-1005.

Van Komen, S., G. Petukhova, S. Sigurdsson, S. Stratton and P. Sung (2000). "Superhelicity-driven homologous DNA pairing by yeast recombination factors Rad51 and Rad54." Mol Cell **6**(3): 563-572.

Vassin, V. M., R. W. Anantha, E. Sokolova, S. Kanner and J. A. Borowiec (2009). "Human RPA phosphorylation by ATR stimulates DNA synthesis and prevents ssDNA accumulation during DNA-replication stress." J Cell Sci **122**(Pt 22): 4070-4080.

Vassin, V. M., M. S. Wold and J. A. Borowiec (2004). "Replication protein A (RPA) phosphorylation prevents RPA association with replication centers." Mol Cell Biol **24**(5): 1930-1943.

Vaze, M. B., A. Pellicioli, S. E. Lee, G. Ira, G. Liberi, A. Arbel-Eden, M. Foiani and J. E. Haber (2002). "Recovery from checkpoint-mediated arrest after repair of a double-strand break requires Srs2 helicase." Mol Cell **10**(2): 373-385.

Vialard, J. E. (1998). "The budding yeast Rad9 checkpoint protein is subjected to Mec1/Tel1-dependent hyperphosphorylation and interacts with Rad53 after DNA damage." The EMBO Journal **17**(19): 5679-5688.

Vidanes, G. M., F. D. Sweeney, S. Galicia, S. Cheung, J. P. Doyle, D. Durocher and D. P. Toczyski (2010). "CDC5 inhibits the hyperphosphorylation of the checkpoint kinase Rad53, leading to checkpoint adaptation." PLoS Biol **8**(1): e1000286.

Viscardi, V., D. Bonetti, H. Cartagena-Lirola, G. Lucchini and M. P. Longhese (2007). "MRX-dependent DNA Damage Response to Short Telomeres." Molecular Biology of the Cell **18**(8): 3047-3058.

Wan, L. and J. Huang (2014). "The PSO4 protein complex associates with replication protein A (RPA) and modulates the activation of ataxia telangiectasia-mutated and Rad3-related (ATR)." J Biol Chem **289**(10): 6619-6626.

Wang, G., G. Unger, K. A. Ahmad, J. W. Slaton and K. Ahmed (2005). "Downregulation of CK2 induces apoptosis in cancer cells--a potential approach to cancer therapy." Mol Cell Biochem **274**(1-2): 77-84.

Wang, H., J. Gao, A. H. Wong, K. Hu, W. Li, Y. Wang and J. Sang (2013). "Rfa2 is specifically dephosphorylated by Pph3 in Candida albicans." Biochem J **449**(3): 673-681.

Wang, H., J. Guan, H. Wang, A. R. Perrault, Y. Wang and G. Iliakis (2001). "Replication protein A2 phosphorylation after DNA damage by the coordinated action of ataxia telangiectasia-mutated and DNA-dependent protein kinase." Cancer Res **61**(23): 8554-8563.

Wang, H., D. Liu, Y. Wang, J. Qin and S. J. Elledge (2001). "Pds1 phosphorylation in response to DNA damage is essential for its DNA damage checkpoint function." Genes Dev **15**(11): 1361-1372.

Wang, M., A. Mahrenholz and S. H. Lee (2000). "RPA stabilizes the XPA-damaged DNA complex through protein-protein interaction." Biochemistry **39**(21): 6433-6439.

Wang, X. and J. E. Haber (2004). "Role of Saccharomyces single-stranded DNA-binding protein RPA in the strand invasion step of double-strand break repair." PLoS Biol **2**(1): E21.

Wang, Y., X. Y. Zhou, H. Wang, M. S. Huq and G. Iliakis (1999). "Roles of replication protein A and DNA-dependent protein kinase in the regulation of DNA replication following DNA damage." J Biol Chem **274**(31): 22060-22064.

Wanrooij, P. H. and P. M. Burgers (2015). "Yet another job for Dna2: Checkpoint activation." DNA Repair (Amst) **32**: 17-23.

Wanrooij, P. H., E. Tannous, S. Kumar, V. M. Navadgi-Patil and P. M. Burgers (2016). "Probing the Mec1ATR Checkpoint Activation Mechanism with Small Peptides." J Biol Chem **291**(1): 393-401.

Ward, I. M. and J. Chen (2001). "Histone H2AX Is Phosphorylated in an ATR-dependent Manner in Response to Replicational Stress." Journal of Biological Chemistry **276**(51): 47759-47762.

Weinert, T. (1998). "DNA damage checkpoints update: getting molecular." Curr Opin Genet Dev **8**(2): 185-193.

West, S. C., M. G. Blanco, Y. W. Chan, J. Matos, S. Sarbajna and H. D. Wyatt (2015). "Resolution of Recombination Intermediates: Mechanisms and Regulation." Cold Spring Harb Symp Quant Biol **80**: 103-109.

Wilson, T. M., T. A. Baumgartner, W. A. Larson, E. M. Richards, B. L. Senger, N. M. Miles and S. J. Haring (2018). "Rfa2 N-terminal phosphorylation rescues Checkpoint Adaptation Deficiency in Resection Deficient and Phosphatase Deficient Yeast." *In Preparation*.

Wilson, T. M., W. A. Larson, A. L. Severson, E. M. Richards, B. L. Senger, N. M. Miles and S. J. Haring (2018). "Replication Factor A2 amino-terminal phosphorylation facilitates checkpoint adaptation in yeast." *In Preparation*.

Wilson, T. M., E. M. Richards, B. L. Senger and S. J. Haring (2018). "Prolonged DNA Damage Causes Delayed Replication Factor A2 N-Terminal Phosphorylation." *In Preparation*.

Wold, M. S. (1997). "Replication protein A: a heterotrimeric, single-stranded DNA-binding protein required for eukaryotic DNA metabolism." Annu Rev Biochem **66**: 61-92.

Wold, M. S. and T. Kelly (1988). "Purification and characterization of replication protein A, a cellular protein required for in vitro replication of simian virus 40 DNA." Proc Natl Acad Sci U S A **85**(8): 2523-2527.

Wyatt, H. D. and S. C. West (2014). "Holliday junction resolvases." Cold Spring Harb Perspect Biol **6**(9): a023192.

Xu, L., B. M. Weiner and N. Kleckner (1997). "Meiotic cells monitor the status of the interhomolog recombination complex." Genes Dev **11**(1): 106-118.

Xu, X., S. Vaithiyalingam, G. G. Glick, D. A. Mordes, W. J. Chazin and D. Cortez (2008). "The basic cleft of RPA70N binds multiple checkpoint proteins, including RAD9, to regulate ATR signaling." Mol Cell Biol **28**(24): 7345-7353.

Yamamoto, A. (1996). "Pds1p, an inhibitor of anaphase in budding yeast, plays a critical role in the APC and checkpoint pathway(s)." The Journal of Cell Biology **133**(1): 99-110.

Yin, Y., A. Seifert, J. S. Chua, J. F. Maure, F. Golebiowski and R. T. Hay (2012). "SUMO-targeted ubiquitin E3 ligase RNF4 is required for the response of human cells to DNA damage." Genes Dev **26**(11): 1196-1208.

Yuzhakov, A., Z. Kelman, J. Hurwitz and M. O'Donnell (1999). "Multiple competition reactions for RPA order the assembly of the DNA polymerase delta holoenzyme." EMBO J **18**(21): 6189-6199.

Zaki, M. S., A. A. Kamel and M. El-Ruby (2005). "Double aneuploidy in three Egyptian patients: Down-Turner and Down-Klinefelter syndromes." Genet Couns **16**(4): 393-402.

Zhang, X., V. Mar, W. Zhou, L. Harrington and M. O. Robinson (1999). "Telomere shortening and apoptosis in telomerase-inhibited human tumor cells." Genes & Development **13**(18): 2388-2399.

Zhang, Y. W., D. M. Otterness, G. G. Chiang, W. Xie, Y. C. Liu, F. Mercurio and R. T. Abraham (2005). "Genotoxic stress targets human Chk1 for degradation by the ubiquitin-proteasome pathway." Mol Cell **19**(5): 607-618.

Zhao, B., M. J. Bower, P. J. McDevitt, H. Zhao, S. T. Davis, K. O. Johanson, S. M. Green, N. O. Concha and B. B. Zhou (2002). "Structural basis for Chk1 inhibition by UCN-01." J Biol Chem **277**(48): 46609-46615.

Zhao, M., R. Geng, X. Guo, R. Yuan, X. Zhou, Y. Zhong, Y. Huo, M. Zhou, Q. Shen, Y. Li, W. Zhu and J. Wang (2017). "PCAF/GCN5-Mediated Acetylation of RPA1 Promotes Nucleotide Excision Repair." Cell Rep **20**(9): 1997-2009.

Zhu, Z., W.-H. Chung, E. Y. Shim, S. E. Lee and G. Ira (2008). "Sgs1 Helicase and Two Nucleases Dna2 and Exo1 Resect DNA Double-Strand Break Ends." Cell **134**(6): 981-994.

Zickler, D. and N. Kleckner (1999). "Meiotic Chromosomes: Integrating Structure and Function." Annual Review of Genetics **33**(1): 603-754.

Zou, L. and S. J. Elledge (2003). "Sensing DNA damage through ATRIP recognition of RPA-ssDNA complexes." Science **300**(5625): 1542-1548.

Zou, L., D. Liu and S. J. Elledge (2003). "Replication protein A-mediated recruitment and activation of Rad17 complexes." Proc Natl Acad Sci U S A **100**(24): 13827-13832.

Zuazua-Villar, P., A. Ganesh, G. Phear, M. E. Gagou and M. Meuth (2015). "Extensive RPA2 hyperphosphorylation promotes apoptosis in response to DNA replication stress in CHK1 inhibited cells." Nucleic Acids Res **43**(20): 9776-9787.

APPENDIX A. YEAST STRAINS

Strain	Genotype	Source
B9B-A	*MAT-A ade3 his5-2 leu1-c trp5-20 ura1 cyh^r*	SJH
B9B-α	*MAT-α ade3 his5-2 leu1-c trp5-20 ura1 cyh^r*	SJH
AWY 111	*JKM179 cdc5-AD*	Andre Walther
AWY 112	*JKM179 mec1Δ::natMX sml1Δ::G418*	Andre Walther
AWY 113	*JKM179 sml1Δ::G418*	Andre Walther
AWY 115	*JKM179 tel1Δ::URA3*	Andre Walther
AWY 134	*JKM179 rad53Δ::natMX sml1Δ::G418*	Andre Walther
AWY 182	*JKM179 chk1Δ::G418*	Andre Walther
AWY 190	*JKM179 dun1Δ::G418*	Andre Walther
JKM 179A	*MAT-A ura3-52 lys5 trp1::hisG leu2-3 112 ade1-100 ade3::GAL-HO ho Δ hmr1 Δ::ADE1 hml Δ::ADE1*	(Lee *et al.* 1998)
JKM 179α	*MAT-α ura3-52 lys5 trp1::hisG leu2-3 112 ade1-100 ade3::GAL-HO ho Δ hmr1 Δ::ADE1 hml Δ::ADE1*	(Lee *et al.* 1998)
AWY 292	*JKM179 rfa2-A$_X$*	Andre Walther
AWY 295	*JKM179 rfa2-D$_X$ ku70 Δ::G418*	Andre Walther
AWY 296	*JKM179 rdh54Δ::URA3*	Andre Walther
AWY 298	*JKM179 rfa2-D$_X$ rdh54Δ::URA3*	Andre Walther
AWY 301	*JKM179 rfa2-A$_X$ rdh54Δ::URA3*	Andre Walther
AWY 308	*JKM179 rfa2-D$_X$ cdc5-AD*	Andre Walther
AWY 309	*JKM179 rfa2-A$_X$ cdc5-AD*	Andre Walther
AWY 32	*JKM179 ku70::KAN*	Andre Walther
AWY 38	*JKM179 rfa1-t11*	Andre Walther
AWY 39	*JKM179 ku70::KAN rfa-t11*	Andre Walther
AWY 556	*JKM179 tel1Δ::TRP1*	Andre Walther
AWY 92	*JKM179 rfa2-A$_X$*	Andre Walther
AWY 96	*JKM179 rfa2-D$_X$*	Andre Walther
AWY 97	*JKM179 rfa2-ΔN$_X$*	Andre Walther
AWY 99	*JKM179 rfa1-t11 rfa2-D$_X$*	Andre Walther

Strain	Genotype	Source
BLS 106	*NMM104 pRS315-rfa2-R$_X$*	This Study
BLS 107	*NMM104 pRS315-rfa2-R$_X$*	This Study
EMR 001	*NMM104 pRS315-rfa2-ΔN$_X$-S122D-I*	This Study
EMR 002	*NMM104 pRS315-rfa2-ΔN$_X$-S122D-II*	This Study
EMR 003	*NMM104 pRS315-rfa2-ΔN$_X$-S122A-I*	This Study
EMR 004	*NMM104 pRS315-rfa2-ΔN$_X$-S122A-II*	This Study
EMR 006	*TMW150 pRS315-rfa2-D$_X$-S122A*	This Study
EMR 007	*TMW150 pRS315-rfa2-D$_X$-S122D*	This Study
EMR 008	*TMW150 pRS315-rfa2-ΔN$_X$-S122A*	This Study
EMR 009	*TMW150 pRS315-rfa2-ΔN$_X$-S122D*	This Study
EMR 010	*TMW163 pRS315-rfa2-D$_X$-S122A*	This Study
EMR 011	*TMW163 pRS315-rfa2-D$_X$-S122A*	This Study
EMR 012	*TMW163 pRS315-rfa2-D$_X$-S122D*	This Study
EMR 013	*TMW163 pRS315-rfa2-D$_X$-S122D*	This Study
NMM 101	*JKM179 rfa1Δ::G418 pJM132*	This Study
NMM 102	*JKM179 rfa1Δ::G418 pJM132*	This Study
NMM 103	*JKM179 rfa1Δ::G418 pJM132*	This Study
NMM 104	*JKM179 rfa2Δ::G418 pJM132*	This Study
NMM 105	*JKM179 rfa2Δ::G418 pJM132*	This Study
NMM 106	*JKM179 rfa2Δ::G418 pJM132*	This Study
TAB 113	*NMM104 pRS315-rfa2-D$_X$-S122A*	This Study
TAB 114	*NMM104 pRS315-rfa2-D$_X$-S122D*	This Study
TAB 115	*NMM104 pRS315-rfa2-A$_X$-S122A*	This Study
TAB 116	*NMM104 pRS315-rfa2-A$_X$-S122D*	This Study
TAB 117	*NMM104 pRS315-rfa2-S122A*	This Study
TAB 118	*NMM104 pRS315-rfa2-S122D*	This Study
TAB 123	*JKM179 yku70Δ::G418*	This Study

Strain	Genotype	Source
TMW 101	*RMY122A pRS313-RFA1 pRS315-rfa2-h2NT*	(Ghospurkar *et al.* 2015)
TMW 102	*RMY122A pRS313-RFA1 pRS315-rfa2-h2D$_X$*	(Ghospurkar *et al.* 2015)
TMW 103	*RMY122A pRS313-RFA1 pRS315-rfa2-h2A$_X$*	(Ghospurkar *et al.* 2015)
TMW 104	*RMY122A pRS313-RFA1 pRS315-rfa2-h2ΔN$_X$*	(Ghospurkar *et al.* 2015)
TMW 105	*RMY122A pRS313-RFA1 pRS315-rfa2-h24$_{PD}$*	(Ghospurkar *et al.* 2015)
TMW 106	*RMY122A pRS313-RFA1 pRS315-rfa2-h2L34*	(Ghospurkar *et al.* 2015)
TMW 107	*RMY122A pRS313-RFA1 pRS315-rfa2-h4L34*	(Ghospurkar *et al.* 2015)
TMW 108	*RMY122A pRS313-rfa1-S178A pRS315-rfa2-S122A*	(Ghospurkar *et al.* 2015)
TMW 109	*RMY122A pRS313-rfa1-S178A pRS315-rfa2-S122D*	(Ghospurkar *et al.* 2015)
TMW 110	*RMY122A pRS313-rfa1-S178D pRS315-rfa2-S122A*	(Ghospurkar *et al.* 2015)
TMW 111	*RMY122A pRS313-rfa1-S178D pRS315-rfa2-S122D*	(Ghospurkar *et al.* 2015)
TMW 112	*RMY122A pRS313-rfa1-S178A pRS315-RFA2*	(Ghospurkar *et al.* 2015)
TMW 113	*RMY122A pRS313-rfa1-S178D pRS315-RFA2*	(Ghospurkar *et al.* 2015)
TMW 114	*RMY122A pRS313-RFA1 pRS315-rfa2-S122A*	(Ghospurkar *et al.* 2015)
TMW 115	*RMY122A pRS313-RFA1 pRS315-rfa2-S122D*	(Ghospurkar *et al.* 2015)
TMW 116	*RMY122A pRS313-rfa1-LexA-S178A pRS315-RFA2*	(Ghospurkar *et al.* 2015)
TMW 117	*RMY122A pRS313-rfa1-LexA-S178D pRS315-RFA2*	(Ghospurkar *et al.* 2015)
TMW 118	*JKM139 rfa1Δ::G418 pJM132*	This Study
TMW 119	*JKM139 rfa2Δ::G418 pJM132*	This Study
TMW 130	*NMM101 cka1Δ::natMX*	This Study
TMW 131	*NMM101 cka1Δ::natMX*	This Study
TMW 132	*NMM101 cka2Δ::natMX*	This Study
TMW 133	*NMM101 cka2Δ.::natMX*	This Study
TMW 134	*NMM101 ckb1Δ::natMX*	This Study
TMW 135	*NMM101 ckb1Δ::natMX*	This Study
TMW 136	*NMM101 ckb2Δ::natMX*	This Study
TMW 137	*NMM101 ckb2Δ::natMX*	This Study

Strain	Genotype	Source
TMW 138	*NMM104 cka1Δ::natMX*	This Study
TMW 139	*NMM104 cka2Δ::natMX*	This Study
TMW 140	*NMM104 ckb1Δ::natMX*	This Study
TMW 141	*NMM104 ckb2Δ::natMX*	This Study
TMW 142	*JKM179 cdc5-AD rfa2-D$_X$*	This Study
TMW 143	*JKM179 cdc5-AD rfa2-D$_X$*	This Study
TMW 144	*JKM179 cdc5-AD rfa2-A$_X$*	This Study
TMW 145	*JKM179 cdc5-AD rfa2-A$_X$*	This Study
TMW 146	*JKM179 cdc5-AD rfa2-ΔN$_X$*	This Study
TMW 147	*JKM179 cdc5-AD rfa2-ΔN$_X$*	This Study
TMW 148	*NMM104 dun1Δ::natMX*	This Study
TMW 149	*NMM104 chk1Δ::natMX*	This Study
TMW 150	*NMM104 tel1Δ::natMX*	This Study
TMW 151	*NMM104 sml1Δ::hphNX*	This Study
TMW 152	*NMM104 rtt107Δ::hphNX*	This Study
TMW 153	*NMM104 rtt107Δ::hphNX*	This Study
TMW 154	*NMM104 slx4Δ::hphNX*	This Study
TMW 155	*NMM104 slx4Δ::hphNX*	This Study
TMW 156	*NMM104 sae2Δ::hphNX*	This Study
TMW 157	*NMM104 sae2Δ::hphNX*	This Study
TMW 158	*NMM104 sae2::hphNX*	This Study
TMW 159	*NMM104 rdh54Δ::natMX*	This Study
TMW 160	*NMM104 rdh54Δ::natMX*	This Study
TMW 161	*NMM104 rdh54Δ::natMX*	This Study
TMW 162	*NMM104 rdh54Δ::natMX*	This Study
TMW 163	*TMW151 mec1Δ::natMX*	This Study
TMW 164	*NMM104 cdc5-AD rfa1-t11 pRS315-RFA2*	This Study

Strain	Genotype	Source
TMW 165	*NMM104 cdc5-AD rfa1-t11 pRS315-RFA2*	This Study
TMW 166	*NMM104 rfa1-t11 pRS315-RFA2*	This Study
TMW 167	*NMM104 rfa1-t11 pRS315-RFA2*	This Study
TMW 168	*TMW154 pRS315-RFA2*	This Study
TMW 169	*TMW154 pRS315-rfa2-D_X*	This Study
TMW 170	*TMW154 pRS315-rfa2-A_X*	This Study
TMW 171	*TMW154 pRS315-rfa2-ΔN_X*	This Study
TMW 172	*TMW154 pRS315-rfa2-h2NT*	This Study
TMW 173	*TMW159 pRS315-RFA2*	This Study
TMW 174	*TMW159 pRS315-D_X*	This Study
TMW 175	*TMW159 pRS315-A_X*	This Study
TMW 176	*TMW159 pRS315-ΔN_X*	This Study
TMW 177	*TMW159 pRS315-h2NT*	This Study
TMW 178	*NMM104 pRS315-A_{M1}*	This Study
TMW 179	*NMM104 pRS315-A_{M2}*	This Study
TMW 180	*NMM104 pRS315-A_{M3}*	This Study
TMW 181	*NMM104 pRS315-rfa2-ΔN_1*	This Study
TMW 182	*NMM104 pRS315-rfa2-ΔN_2*	This Study
TMW 183	*NMM104 pRS315-rfa2-ΔN_3*	This Study
TMW 184	*TMW184 rfa1-t11*	This Study
TMW 185	*TMW184 cka1::natMX pRS315-rfa1-t11*	This Study
TMW 186	*TMW184 cka2::natMX pRS315-rfa1-t11*	This Study
TMW 187	*TMW184 ckb1::natMX pRS315-rfa1-t11*	This Study
TMW 188	*TMW184 ckb2::natMX pRS315-rfa1-t11*	This Study
TMW 189	*NMM104 pRS315-RFA2*	This Study
TMW 190	*NMM104 pRS315-rfa2-D_X*	This Study
TMW 191	*NMM104 pRS315-rfa2-A_X*	This Study

Strain	Genotype	Source
TMW 193	*TMW156 pRS315-RFA2*	This Study
TMW 194	*TMW156 pRS315-rfa2-D_X*	This Study
TMW 195	*TMW156 pRS315-rfa2-A_X*	This Study
TMW 196	*TMW156 pRS315-rfa2-ΔN_X*	This Study
TMW 197	*TMW156 pRS315-rfa2-h2NT*	This Study
TMW 198	*TMW152 pRS315-RFA2*	This Study
TMW 199	*TMW152 pRS315-rfa2-D_X*	This Study
TMW 200	*TMW152 pRS315-rfa2-A_X*	This Study
TMW 201	*TMW152 pRS315-rfa2-ΔN_X*	This Study
TMW 202	*TMW152 pRS315-rfa2-h2NT*	This Study
TMW 203	*NMM104 pRS315-rfa2-h2NT*	This Study
TMW 204	*NMM104 pRS315-rfa2-A_{M2+3}*	This Study
TMW 205	*NMM104 pRS315-rfa2-A_{M1+3}*	This Study
TMW 206	*NMM104 pRS315-rfa2-A_{M1+2}*	This Study
TMW 207	*TMW159 pRS315-rfa2-D_{M1}*	This Study
TMW 208	*TMW159 pRS315-rfa2-D_{M2}*	This Study
TMW 209	*TMW159 pRS315-rfa2-D_{M3}*	This Study
TMW 210	*TMW159 pRS315-rfa2-D_{M1+2}*	This Study
TMW 211	*TMW159 pRS315-rfa2-D_{M1+3}*	This Study
TMW 212	*TMW159 pRS315-rfa2-D_{M2+3}*	This Study
TMW 213	*TMW159 pRS315-rfa2-D_{I3}*	This Study
TMW 214	*TMW159 pRS315-rfa2-D_{I11}*	This Study
TMW 215	*TMW159 pRS315-rfa2-D_{I12}*	This Study
TMW 216	*TMW159 pRS315-rfa2-D_{I14}*	This Study
TMW 217	*TMW159 pRS315-rfa2-D_{I21}*	This Study
TMW 218	*TMW159 pRS315-rfa2-D_{I27}*	This Study
TMW 219	*TMW159 pRS315-rfa2-D_{I30}*	This Study

Strain	Genotype	Source
TMW 220	*TMW159 pRS315-rfa2-D_{I32}*	This Study
TMW 221	*TMW159 pRS315-rfa2-D_{I34}*	This Study
TMW 222	*TMW159 pRS315-rfa2-D_{I38}*	This Study
TMW 223	*TMW151 pRS315-rfa2-h2NT*	This Study
TMW 224	*TMW150 pRS315-rfa2-h2NT*	This Study
TMW 225	*TMW148 pRS315-rfa2-h2NT*	This Study
TMW 226	*TMW156 pRS315-rfa2-h2NT*	This Study
TMW 227	*TMW163 pRS315-rfa2-h2NT*	This Study
TMW 228	*TMW149 pRS315-rfa2-h2NT*	This Study
TMW 229	*TMW152 pRS315-rfa2-h2NT*	This Study
TMW 230	*TMW154 pRS315-rfa2-h2NT*	This Study
TMW 231	*TMW159 pRS315-rfa2-h2NT*	This Study
TMW 232	*TMW156 pRS315-RFA2*	This Study
TMW 233	*TMW156 pRS315-rfa2-D_X*	This Study
TMW 234	*TMW156 pRS315-rfa2-A_X*	This Study
TMW 235	*TMW156 pRS315-rfa2-ΔN_X*	This Study
TMW 236	*TMW156 pRS315-rfa2-h2NT*	This Study
TMW 237	*TMW152 pRS315-RFA2*	This Study
TMW 238	*TMW152 pRS315-rfa2-D_X*	This Study
TMW 239	*TMW152 pRS315-rfa2-A_X*	This Study
TMW 240	*TMW152 pRS315-rfa2-ΔN_X*	This Study
TMW 241	*TMW152 pRS315-rfa2-h2NT*	This Study
TMW 242	*TMW154 pRS315-RFA2*	This Study
TMW 243	*TMW154 pRS315-rfa2-D_X*	This Study
TMW 244	*TMW154 pRS315-rfa2-A_X*	This Study
TMW 245	*TMW154 pRS315-rfa2-ΔN_X*	This Study
TMW 246	*TMW154 pRS315-rfa2-h2NT*	This Study

Strain	Genotype	Source
TMW 247	*TMW159 pRS315-RFA2*	This Study
TMW 248	*TMW159 pRS315-rfa2-D_X*	This Study
TMW 249	*TMW159 pRS315-rfa2-A_X*	This Study
TMW 250	*TMW159 pRS315-rfa2-ΔN_X*	This Study
TMW 251	*TMW159 pRS315-rfa2-h2NT*	This Study
TMW 252	*TMW150 pRS315-RFA2*	This Study
TMW 253	*TMW150 pRS315-rfa2-D_X*	This Study
TMW 254	*TMW150 pRS315-rfa2-A_X*	This Study
TMW 255	*TMW150 pRS315-rfa2-ΔN_X*	This Study
TMW 256	*TMW150 pRS315-rfa2-h2NT*	This Study
TMW 257	*TMW163 pRS315-RFA2*	This Study
TMW 258	*TMW163 pRS315-rfa2-D_X*	This Study
TMW 259	*TMW163 pRS315-rfa2-A_X*	This Study
TMW 260	*TMW163 pRS315-rfa2-ΔN_X*	This Study
TMW 261	*TMW163 pRS315-rfa2-h2NT*	This Study
TMW 262	*TMW149 pRS315-RFA2*	This Study
TMW 263	*TMW149 pRS315-rfa2-D_X*	This Study
TMW 264	*TMW149 pRS315-rfa2-A_X*	This Study
TMW 265	*TMW149 pRS315-rfa2-ΔN_X*	This Study
TMW 266	*TMW149 pRS315-rfa2-h2NT*	This Study
TMW 267	*TMW148 pRS315-RFA2*	This Study
TMW 268	*TMW148 pRS315-rfa2-D_X*	This Study
TMW 269	*TMW148 pRS315-rfa2-A_X*	This Study
TMW 270	*TMW148 pRS315-rfa2-ΔN_X*	This Study
TMW 271	*TMW148 pRS315-rfa2-h2NT*	This Study
TMW 272	*TMW151 pRS315-RFA2*	This Study
TMW 273	*TMW151 pRS315-rfa2-D_X*	This Study

Strain	Genotype	Source
TMW 274	*TMW151 pRS315-rfa2-A$_X$*	This Study
TMW 275	*TMW151 pRS315-rfa2-ΔN$_X$*	This Study
TMW 276	*TMW151 pRS315-rfa2-h2NT*	This Study
TMW 277	*TMW138 pRS315-RFA2*	This Study
TMW 278	*TMW138 pRS315-rfa2-D$_X$*	This Study
TMW 279	*TMW138 pRS315-rfa2-A$_X$*	This Study
TMW 280	*TMW138 pRS315-rfa2-ΔN$_X$*	This Study
TMW 281	*TMW138 pRS315-rfa2-h2NT*	This Study
TMW 282	*TMW130 pRS315-rfa1-t11*	This Study
TMW 283	*TMW139 pRS315-RFA2*	This Study
TMW 284	*TMW139 pRS315-rfa2-D$_X$*	This Study
TMW 285	*TMW139 pRS315-rfa2-A$_X$*	This Study
TMW 286	*TMW139 pRS315-rfa2-ΔN$_X$*	This Study
TMW 287	*TMW139 pRS315-rfa2-h2NT*	This Study
TMW 288	*TMW132 pRS315-rfa1-t11*	This Study
TMW 289	*TMW140 pRS315-RFA2*	This Study
TMW 290	*TMW140 pRS315-rfa2-D$_X$*	This Study
TMW 291	*TMW140 pRS315-rfa2-A$_X$*	This Study
TMW 292	*TMW140 pRS315-rfa2-ΔN$_X$*	This Study
TMW 293	*TMW140 pRS315-rfa2-h2NT*	This Study
TMW 294	*TMW134 pRS315-rfa1-t11*	This Study
TMW 295	*TMW141 pRS315-RFA2*	This Study
TMW 296	*TMW141 pRS315-rfa2-D$_X$*	This Study
TMW 297	*TMW141 pRS315-rfa2-A$_X$*	This Study
TMW 298	*TMW141 pRS315-rfa2-ΔN$_X$*	This Study
TMW 299	*TMW141 pRS315-rfa2-h2NT*	This Study
TMW 300	*TMW136 pRS315-rfa1-t11*	This Study

Strain	Genotype	Source
TMW 301	*RM26-26C: MATα ade2-1, ade5, can^{r}, CYH^{s}, his1, HIS7, leu1-12, lys2-1, trp5-2, ura3-1, RFA2*	This Study
TMW 302	*Isogenic to RM26-26C, rfa2-A$_X$*	This Study
TMW 303	*Isogenic to RM26-26C, rfa2-D$_X$*	This Study
TMW 304	*Isogenic to RM26-26C, rfa2-ΔN$_X$*	This Study
TMW 305	*Isogenic to RM26-26C, rfa2-cDNA-WT*	This Study
TMW 306	*K264-10D: MATa, ade2-1 cyh^{r}, HIS1, leu1-c, lys2-2, met13-c, trp5-c, tyr1-2, ura3-1*	This Study
TMW 307	*Isogenic to K264-10D, rfa2-A$_X$*	This Study
TMW 308	*Isogenic to K264-10D, rfa2-D$_X$*	This Study
TMW 309	*Isogenic to K264-10D, rfa2-ΔN$_X$*	This Study
TMW 310	*Isogenic to K264-10D, rfa2-cDNA-WT*	This Study
TMW 311	*RMY122A pRS313-RFA1 pRS315-RFA2*	(Ghospurkar et al. 2015)
TMW 312	*RMY122A pRS313-rfa1-t11 pRS315-RFA2*	(Ghospurkar et al. 2015)
TMW 313	*RMY122A pRS313-RFA1 pRS315-rfa2-D$_X$*	(Ghospurkar et al. 2015)
TMW 314	*RMY122A pRS313-RFA1 pRS315-rfa2-A$_X$*	(Ghospurkar et al. 2015)
TMW 315	*RMY122A pRS313-RFA1 pRS315-rfa2-ΔN$_X$*	(Ghospurkar et al. 2015)
TMW 316	*TMW159 pRS315-rfa2-D$_{M1}$*	This Study
TMW 317	*TMW159 pRS315-rfa2-D$_{M2}$*	This Study
TMW 318	*TMW159 pRS315-rfa2-D$_{M3}$*	This Study
TMW 319	*TMW159 pRS315-rfa2-D$_{M1+2}$*	This Study
TMW 320	*TMW159 pRS315-rfa2-D$_{M1+3}$*	This Study
TMW 321	*TMW159 pRS315-rfa2-D$_{M2+3}$*	This Study
TMW 322	*TMW159 pRS315-RFA2*	This Study
TMW 323	*TMW159 pRS315-rfa2-D$_X$*	This Study
TMW 324	*TMW159 pRS315-rfa2-A$_X$*	This Study
TMW 325	*TMW159 pRS315-rfa2-ΔN$_X$*	This Study
TMW 326	*TMW159 pRS315-rfa2-h2NT*	This Study
TMW 327	*TMW159 pRS315-rfa2-D$_{I3}$*	This Study

Strain	Genotype	Source
TMW 328	*TMW159 pRS315-rfa2-D_{I11}*	This Study
TMW 329	*TMW159 pRS315-rfa2-D_{I12}*	This Study
TMW 330	*TMW159 pRS315-rfa2-D_{I14}*	This Study
TMW 331	*TMW159 pRS315-rfa2-D_{I21}*	This Study
TMW 332	*TMW159 pRS315-rfa2-D_{I23}*	This Study
TMW 333	*TMW159 pRS315-rfa2-D_{I27}*	This Study
TMW 334	*TMW159 pRS315-rfa2-D_{I30}*	This Study
TMW 335	*TMW159 pRS315-rfa2-D_{I32}*	This Study
TMW 336	*TMW159 pRS315-rfa2-D_{I34}*	This Study
TMW 337	*TMW159 pRS315-rfa2-D_{I38}*	This Study
TMW 338	*TMW159 pRS315-rfa2-E-Q*	This Study
TMW 339	*NMM104 pRS315-rfa2-A_{M1}*	This Study
TMW 340	*NMM104 pRS315-rfa2-A_{M2}*	This Study
TMW 341	*NMM104 pRS315-rfa2-A_{M3}*	This Study
TMW 342	*NMM104 pRS315-rfa2-ΔN_1*	This Study
TMW 343	*NMM104 pRS315-rfa2-ΔN_2*	This Study
TMW 344	*NMM104 pRS315-rfa2-ΔN_3*	This Study

APPENDIX B. PLASMIDS

Name	Plasmid	Genotype/Description
pRS313-*rfa1-t11*	pRS313-rfa1-t11	Derivative pRS313-*RFA1* on HIS3+ vector
pRS313-RFA1	pRS313-RFA1	Derivative pRS313-*RFA1* on HIS3+ vector
pAW07	pRS315-RFA2	Derivative pRS315-*RFA2* on LEU2+ vector
pAW08	pRS315-rfa2-D_X	Derivative pRS315-*rfa2-*D_X on LEU2+ vector
pAW09	pRS315-rfa2-A_X	Derivative pRS315-*rfa2-*A_X on LEU2+ vector
pAW10	pRS315-rfa2-ΔN_X	Derivative pRS315-*rfa2-*ΔN_X on LEU2+ vector
pPLG1	pRS315-rfa2-S3D	Derivative pRS315-*rfa2-S3D*
pPLG2	pRS315-rfa2-S11D	Derivative pRS315-*rfa2-S11D*
pPLG3	pRS315-rfa2-S12D	Derivative pRS315-*rfa2-S12D*
pPLG4	pRS315-rfa2-T14D	Derivative pRS315-*rfa2-T14D*
pPLG5	pRS315-rfa2-S21D	Derivative pRS315-*rfa2-S21D*
pPLG6	pRS315-rfa2-S23D	Derivative pRS315-*rfa2-S23D*
pPLG7	pRS315-rfa2-S27D	Derivative pRS315-*rfa2-S27D*
pPLG8	pRS315-rfa2-S30D	Derivative pRS315-*rfa2-S30D*
pPLG9	pRS315-rfa2-T32D	Derivative pRS315-*rfa2-T32D*
pPLG10	pRS315-rfa2-T34D	Derivative pRS315-*rfa2-T34D*
pPLG11	pRS315-rfa2-T38D	Derivative pRS315-*rfa2-T38D*
pPLG12	pRS315-rfa2-S3A	Derivative pRS315-*rfa2-S3A*
pPLG13	pRS315-rfa2-S11A	Derivative pRS315-*rfa2-S11A*
pPLG14	pRS315-rfa2-S12A	Derivative pRS315-*rfa2-S12A*
pPLG15	pRS315-rfa2-T14A	Derivative pRS315-*rfa2-T14A*
pPLG16	pRS315-rfa2-S21A	Derivative pRS315-*rfa2-S21A*
pPLG17	pRS315-rfa2-S23A	Derivative pRS315-*rfa2-S23A*

Name	Plasmid	Genotype/Description
pPLG18	pRS315-rfa2-S27A	Derivative pRS315-*rfa2-S27A*
pPLG19	pRS315-rfa2-S30A	Derivative pRS315-*rfa2-S30A*
pPLG20	pRS315-rfa2-T32A	Derivative pRS315-*rfa2-T32A*
pPLG21	pRS315-rfa2-T34A	Derivative pRS315-*rfa2-T34A*
pPLG22	pRS315-rfa2-T38A	Derivative pRS315-*rfa2-T38A*
pPLG23	pRS315-rfa2-Am1	Derivative pRS315-*rfa2-Am1*
pPLG24	pRS315-rfa2-Am2+3	Derivative pRS315-*rfa2-Am2+3*
pPLG25	pRS315-rfa2-Am2	Derivative pRS315-*rfa2-Am2*
pPLG26	pRS315-rfa2-Am3	Derivative pRS315-*rfa2-Am3*
pPLG27	pRS315-rfa2-Am1+2	Derivative pRS315-*rfa2-Am1+3*
pPLG28	pRS315-rfa2-Am1+3	Derivative pRS315-*rfa2-Am1+3*
pPLG29	pRS315-rfa2-Dm1	Derivative pRS315-*rfa2-Dm1*
pPLG30	pRS315-rfa2-Dm2+3	Derivative pRS315-*rfa2-Dm2+3*
pPLG31	pRS315-rfa2-Dm2	Derivative pRS315-*rfa2-Dm2*
pPLG32	pRS315-rfa2-Dm3	Derivative pRS315-*rfa2-Dm3*
pPLG33	pRS315-rfa2-Dm1+2	Derivative pRS315-*rfa2-Dm1+3*
pPLG34	pRS315-rfa2-Dm1+3	Derivative pRS315-*rfa2-Dm1+3*
pFA6-hphNT1	P30347	pFA6 empty vector, hphNX resistance cassette
pFA6-natNT2	P30346	pFA6 empty vector, natMX resistance cassette
pAMH1	pRS315-rfa2-Hs2PD	pRS315-*rfa2-h2NT*
pAMH2	pRS315-rfa2-Hs2PD	pRS315-*rfa2-h2NT*
pAMH3	pRS315-rfa2-Hs2Asp9	pRS315-*rfa2-h2D$_X$*
pAMH4	pRS315-rfa2-Hs2Ala10	pRS315-*rfa2-h2A$_X$*
pAMH5	pRS315-rfa2-Hs2Ala10	pRS315-*rfa2-h2A$_X$*

Name	Plasmid	Genotype/Description
pAMH6	pRS315-rfa2-Hs2ΔN33	pRS315-*rfa2-h2ΔN$_{33}$*
pAMH7	pRS315-rfa2-Hs4PD	pRS315-*rfa2-h4NT*
pENM10	pJG4-5-B42-HA-RFA1	pJG4-5-B42-HA-*RFA1*
pENM11	pJG4-5-B42-HA-RFA2	pJG4-5-B42-HA-*RFA2*
pENM12	pJG4-5-B42-HA-RFA3	pJG4-5-B42-HA-*RFA3*
pEG202	pEG202	Y2H Vector
pSH18-34	pSH18-34	Y2H vector
pEG202K	pEG202KAN	pEG202 amp marker replaced by KanMX
pJG4-5	pJG4-5	pJG4-5 empty vector, HA tag, B42 activation domain
pBLS1	pHs2S4A	*pHs2S4A*
pBLS2	pHs2S8A-6	*pHs2S8A-6*
pBLS2	pHs2S8A-7	*pHs2S8A-7*
pBLS3	pHs2S11A-4	*pHs2S11A-4*
pBLS3	pHs2S11A-5	*pHs2S11A-5*
pBLS4	pHs2S12A	*pHs2S12A*
pBLS5	pHs2S13A	*pHs2S13A*
pBLS6	pHs2T21A	*pHs2T21A*
pBLS7	pHs2S23A	*pHs2S23A*
pBLS8	pHs2S29A	*pHs2S29A*
pBLS9	pHs2S33A	*pHs2S33A*
pPLG61	pEG202K	pEG202 amp marker replaced by kan
pPLG62	pSH18-34K	pSH18-34 amp marker replaced by kan
LexA-S178A	pRS313-LexA-rfa1-S178A	Y2H construct, S178A rfa1 mutation
LexA-S178D	pRS313-LexA-rfa1-S178D	Y2H construct, S178D rfa1 mutation

Name	Plasmid	Genotype/Description
S178A	pRS313-rfa1-S178A	Derivative pRS313-*rfa1-S178A*
S178D	pRS313-rfa1-S178D	Derivative pRS313-*rfa1-S178D*
S122A	pRS315-rfa2-S122A	Derivative pRS315-*rfa2-S122A*
S122D	pRS315-rfa2-S122D	Derivative pRS315-*rfa2-S122D*
pTMW01	pRS306-rfa2-WT(cDNA)	pRS305-*rfa2-cDNA-WT*, integrating vector
pTMW02	pRS306-rfa2-D_X	pRS306-*rfa2-*D_X, integrating vector
pTMW03	pRS306-rfa2-A_X	pRS306-*rfa2-*A_X, integrating vector
pTMW04	pRS306-rfa2-ΔN_X	pRS306-*rfa2-*ΔN_X, integrating vector
pTMW10	pJG4-5-B42-MRE11	pJG4-5 Prey - MRE11
pTMW11	pJG4-5-B42-LGE1	pJG4-5 Prey - LGE1
pTMW12	pJG4-5-B42-YBR137W	pJG4-5 Prey - YBR137W
pTMW13	pJG4-5-B42-XRS2	pJG4-5 Prey - XRS2
pTMW14	pJG4-5-B42-SAE2	pJG4-5 Prey - SAE2
pTMW15	pJG4-5-B42-CMR1	pJG4-5 Prey - CMR1
pTMW16	pJG4-5-B42-DMC1	pJG4-5 Prey - DMC1
pTMW17	pJG4-5-B42-DMC1	pJG4-5 Prey - DMC1
pTMW18	pJG4-5-B42-DMC1	pJG4-5 Prey - DMC1
pTMW19	pJG4-5-B42-DMC1	pJG4-5 Prey - DMC1
pTMW20	pJG4-5-B42-RAD50	pJG4-5 Prey - RAD50
pTMW21	pJG4-5-B42-RAD50	pJG4-5 Prey - RAD50
pTMW22	pJG4-5-B42-RAD51	pJG4-5 Prey - RAD51
pTMW23	pJG4-5-B42-RAD52	pJG4-5 Prey - RAD52
pTMW24	pJG4-5-B42-RAD54	pJG4-5 Prey - RAD54
pTMW25	pJG4-5-B42-RAD55	pJG4-5 Prey - RAD55

Name	Plasmid	Genotype/Description
pTMW26	pJG4-5-B42-RAD57	pJG4-5 Prey - RAD57
pTMW27	pJG4-5-B42-RAD59	pJG4-5 Prey - RAD59
pPLG13	pRS315-Rfa2-S11A	Identical to B708, Sequenced
pPLG14	pRS315-Rfa2-S12A	Identical to B709, Sequenced
pPLG15	pRS315-Rfa2-T14A	Identical to B710, Sequenced
pPLG16	pRS315-Rfa2-S21A	Identical to B711, Sequenced
pPLG17	pRS315-Rfa2-S23A	Identical to B712, Sequenced
pPLG18	pRS315-Rfa2-S27A	Identical to B713, Sequenced
pPLG19	pRS315-Rfa2-SS30A	Identical to B714, Sequenced
pPLG20	pRS315-Rfa2-T32A	Identical to B715, Sequenced
pPLG21	pRS315-Rfa2-T34A	Identical to B716, Sequenced
pPLG22	pRS315-Rfa2-T38A	Identical to B717, sequenced
pTMW28	pKU2-Rfa1-T11-BsaHI-1	rfa1-T11 integrating vector BsaHI site
pTMW29	pKU2-Rfa1-T11-BsaHI-2	rfa1-T11 integrating vector BsaHI site
pTMW30	pKU2-Rfa1-T11-BsaHI-3	rfa1-T11 integrating vector BsaHI site
pPLG12	pRS315-Rfa2-S3A	Identical to B707, Sequenced
pBLS1-1	B109/O-284-3	Derivative pRS315-*rfa2-D$_X$-S122D*
pBLS1-2	B109/O-284-4	Derivative pRS315-*rfa2-D$_X$-S122D*
pBLS1-3	B109/O-284-7	Derivative pRS315-*rfa2-D$_X$-S122D*
pBLS2-1	B109/O-285-2	Derivative pRS315-*rfa2-D$_X$-S122A*
pBLS2-2	B109/O-285-4	Derivative pRS315-*rfa2-D$_X$-S122A*
pBLS2-3	B109/O-285-8	Derivative pRS315-*rfa2-D$_X$-S122A*
pBLS3-1	B110/O-284-2	Derivative pRS315-*rfa2-A$_X$-S122D*
pBLS3-2	B110/O-284-8	Derivative pRS315-*rfa2-A$_X$-S122D*

Name	Plasmid	Genotype/Description
pBLS3-3	B110/O-284-10	Derivative pRS315-*rfa2-A$_X$-S122D*
pBLS4-1	B110/O-285-3	Derivative pRS315-*rfa2-A$_X$-S122A*
pBLS4-2	B110/O-285-5	Derivative pRS315-*rfa2-A$_X$-S122A*
pBLS4-3	B110/O-285-7	Derivative pRS315-*rfa2-A$_X$-S122A*
pNPT1	pRS316-RFA1	RFA1 full length into pRS316
pNPT2	pRS316-rfa-t11	rfa1-t11 in vivo cloned into pRS316
pSA39	pSA39	pSA empty vector, Lys5(MX) cassette
pPLG1	pRS315-Rfa2-DI3	Derivative pRS315-*rfa2-D$_{I3}$*
pPLG2	pRS315-Rfa2-DI11	Derivative pRS315-*rfa2-D$_{I11}$*
pPLG3	pRS315-Rfa2-DI12	Derivative pRS315-*rfa2-D$_{I12}$*
pPLG4	pRS315-Rfa2-DI14	Derivative pRS315-*rfa2-D$_{I14}$*
pPLG5	pRS315-Rfa2-DI21	Derivative pRS315-*rfa2-D$_{I21}$*
pPLG7	pRS315-Rfa2-DI27	Derivative pRS315-*rfa2-D$_{I27}$*
pPLG8	pRS315-Rfa2-DI30	Derivative pRS315-*rfa2-D$_{I30}$*
pPLG9	pRS315-Rfa2-DI32	Derivative pRS315-*rfa2-D$_{I32}$*
pPLG10	pRS315-Rfa2-DI34	Derivative pRS315-*rfa2-D$_{I34}$*
pPLG11	pRS315-Rfa2-DI38	Derivative pRS315-*rfa2-D$_{I38}$*
pPLG29	pRS315-Rfa2-Dm1	Derivative pRS315-*rfa2-D$_{M1}$*
pPLG31	pRS315-Rfa2-Dm2	Derivative pRS315-*rfa2-D$_{M2}$*
pPLG32	pRS315-Rfa2-Dm3	Derivative pRS315-*rfa2-D$_{M3}$*
pPLG33	pRS315-Rfa2-DM1+2	Derivative pRS315-*rfa2-D$_{M1+2}$*
pPLG34	pRS315-Rfa2-DM1+3	Derivative pRS315-*rfa2-D$_{M1+3}$*
pPLG31	pRS315-Rfa2-DM2+3	Derivative pRS315-*rfa2-D$_{M2+3}$*
pEMR001	B111 / O284 - 4c	Derivative pRS315-*rfa2-ΔN$_X$-S122D*

Name	Plasmid	Genotype/Description
pEMR002	B111 / O284 - 4d	Derivative pRS315-*rfa2*-ΔN_X-*S122D*
pEMR003	B111 / O285 - 5e	Derivative pRS315-*rfa2*-ΔN_X-*S122A*
pEMR004	B111 / O285 - 5g	Derivative pRS315-*rfa2*-ΔN_X-*S122A*

APPENDIX C. PRIMERS

Name	Sequence	Purpose
RFA2-UP-NEW	TAGCAATTCCTTTGGCCTCGATGAG CTTCC	Upstream RFA2 primer
RFA2-DOWN-NEW	GATAAAACCCTGGTCAGTCAAGGT CGTAC	Downstream RFA2 primer
pJG4-5-UP-Sequence	GATCCAGCCTGACTGGCTGAAATC GAATGG	pJG4-5 sequencing primer
pJG4-5-UP-Recover	TGGCGGATCAGGCGATTAACGTGG TGCCGG	pJG4-5 sequencing primer
pJG4-5-DOWN-Recover	TCAACAACGTATCTACCAACGATTT GACCC	pJG4-5 sequencing primer
RFA2-UP-NEW-O-338	TAGCAATTCCTTTGGCCTCGATGAG CTTCC	Upstream RFA2 primer
RFA2-DOWN-NEW-O-339	GATAAAACCCTGGTCAGTCAAGGT CGTAC	Downstream RFA2 primer
MATα-HO-UP-Proximal	TGCAGCAGCGAATATGGGACTACT TC	HO qPCR primer
MATα-HO-DOWN-Proximal	CAAGATCGTTTATGGTTAAGATAAG AACAAAGAATGATGC	HO qPCR primer
MATα-HO-UP-Distal	CACGCGGACAAAATGCAGCAC	HO qPCR primer
MATα-HO-DOWN-Distal	GCCAATTCGTTCAAATTACAAAAGT CACATCAAGATC	HO qPCR primer
rfa1-t11-REV	GGAAATCATGATCAAATTCTCTCTG TTGCTGTTGGCGCCATCAGATTTCT TGGTGTTATA	*rfa1-t11* mutagenic primer w/ BsaHI diagnostic site
HIS4-qPCR-REV	GTTAAGGATGCCACCTCTTCC	His4 qPCR control
HIS4-qPCR-FOR	TGATAGGTATGAAGCCACAATACAA	His4 qPCR control
HO-BglII-Distal-REV	GCACTTTGCATGAGATGAAGTT	HO qPCR primer
HO-BglII-Distal-FOR	GGATCAACGGAATGATTATTATAGT AGC	HO qPCR primer
HO-Xho1-REV	GAAGGCACCGATGATACTACAC	HO qPCR primer
HO-Xho1-FOR	TCGGTAAATCACCAGACATAGC	HO qPCR primer
HO-HindIII-REV	CGGAATTGACAGGAATGATAATG	HO qPCR primer
HO-HindIII-FOR	ACAAGGGCATCCTTGTTT	HO qPCR primer

Name	Sequence	Purpose
HO-StyI-Proximal-REV	GCAAATACATGATCTTGTTAGGG	HO qPCR primer
HO-StyI-Proximal-FOR	CCTTCTTCATTACTATTCATCTTCG	HO qPCR primer
ARE1-qPCR-REV	CGACCAGAGTGCAGCATATC	ARE1 qPCR control
ARE1-qPCR-FOR	GGTAGAACTGGGCCACAAAT	ARE1 qPCR control
MATa-HO-UP-Distal	ATCCTATACTAACAATTTGTAGTTC ATAAATAAACGTATGAGATC	HO qPCR primer
MATa-HO-UP-Proximal	TCGTTTTCAATGATTAAAATAGCAT AGTCGGGTTT	HO qPCR primer
MATa-FOR	ACTTCAAGTAAGAGTTTGGGTATGT	HO qPCR primer
MATα-FOR	GCACGGAATATGGGACTACTTC	HO qPCR primer
MAT-REV	GTCACATCAAGATCGTTTATGGTTA AG	HO qPCR primer
pJG4-5-CMR1-FOR	ATTATGCCTCTCCCGAATTCATGCC GGAATTAACAGAATT	CMR1 Forward primer - Y2H project pJG4-5 homology
pJG4-5-CMR1-REV	GAAGTCCAAAGCTTCTCGAGTCATT CTTCCTGCTTTATGG	CMR1 Reverse primer - Y2H project pJG4-5 homology
pJG4-5-CSM3-FOR	ATTATGCCTCTCCCGAATTCATGGA TCAAGATTTTGACAG	CSM3 Forward primer - Y2H project pJG4-5 homology
pJG4-5-CSM-REV	GAAGTCCAAAGCTTCTCGAGCTAA AAGCCCATTTCCTTCA	CSM3 Reverse primer - Y2H project pJG4-5 homology
pJG4-5-MRC1-FOR	ATTATGCCTCTCCCGAATTCATGGA TGATGCCTTGCATGC	MRC1 Forward primer - Y2H project pJG4-5 homology
pJG4-5-MRC1-REV	GAAGTCCAAAGCTTCTCGAGCTAAT TATCAAAGCTATCTT	MRC1 Reverse primer - Y2H project pJG4-5 homology
pJG4-5-TOF1-FOR	ATTATGCCTCTCCCGAATTCATGTC TGCTGATTTGCAACA	TOF1 Forward primer - Y2H project pJG4-5 homology
pJG4-5-TOF1-REV	GAAGTCCAAAGCTTCTCGAGTCAAT CATCACTATCACCTT	TOF1 Reverse primer - Y2H project pJG4-5 homology
pJG4-5-MRE11-FOR	ATTATGCCTCTCCCGAATTCATGGA CTATCCTGATCCAGA	MRE11 Forward primer - Y2H project pJG4-5 homology
pJG4-5-MRE11-REV	GAAGTCCAAAGCTTCTCGAGCTATT TTCTTTTCTTAGCAA	MRE11 Reverse primer - Y2H project pJG4-5 homology
pJG4-5-RAD50-FOR	ATTATGCCTCTCCGGAATTCATGAG CGCTATCTATAAATT	RAD50 Forward primer - Y2H project pJG4-5 homology
pJG4-5-RAD50-REV	GAAGTCCAAAGCTTCTCGAGTCAAT AAGTGACTCTGTTAA	RAD50 Reverse primer - Y2H project pJG4-5 homology

Name	Sequence	Purpose
pJG4-5-XRS2-FOR	ATTATGCCTCTCCCGAATTCATGTG GGTAGTACGATACCA	XRS2 Forward primer - Y2H project pJG4-5 homology
pJG4-5-XRS2-REV	GAAGTCCAAAGCTTCTCGAGTTATC CTTTTCTTCTTTTGA	XRS2 Reverse primer - Y2H project pJG4-5 homology
pJG4-5-SAE2-FOR	ATTATGCCTCTCCCGAATTCATGGT GACTGGTGAAGAAAA	SAE2 Forward primer - Y2H project pJG4-5 homology
pJG4-5-SAE2-REV	GAAGTCCAAAGCTTCTCGAGTTAAC ATCTAGCATATATCT	SAE2 Reverse primer - Y2H project pJG4-5 homology
pJG4-5-DMC1-FOR	ATTATGCCTCTCCCGAATTCATGTC TGTTACAGGAACTGA	DMC1 Forward primer - Y2H project pJG4-5 homology
pJG4-5-DMC1-REV	GAAGRCCAAAGCTTCTCGAGCTAG TCACTTGAATCGGTAA	DMC1 Reverse primer - Y2H project pJG4-5 homology
pJG4-5-RAD51-FOR	ATTATGCCTCTCCCGAATTCATGTC TCAAGTTCAAGAACA	RAD51 Forward primer - Y2H project pJG4-5 homology
pJG4-5-RAD51-REV	GAAGTCCAAAGCTTCTCGAGCTAC TCGTCTTCTTCTCTGG	RAD51 Reverse primer - Y2H project pJG4-5 homology
pJG4-5-RAD52-FOR	ATTATGCCTCTCCCGAATTCATGAA TGAAATTATGGATAT	RAD52 Forward primer - Y2H project pJG4-5 homology
pJG4-5-RAD52-REV	GAAGTCCAAAGCTTCTCGAGTCAA GTAGGCTTGCGTGCAT	RAD52 Reverse primer - Y2H project pJG4-5 homology
pJG4-5-RAD54-FOR	ATTATGCCTCTCCCGAATTCATGGC AAGACGCAGATTACC	RAD54 Forward primer - Y2H project pJG4-5 homology
pJG4-5-RAD54-REV	GAAGTCCAAAGCTTCTCGAGTCAAT GTGAAATATATTGAA	RAD54 Reverse primer - Y2H project pJG4-5 homology
pJG4-5-RAD55-FOR	ATTATGCCTCTCCCGAATTCATGTC GCTTGGTATACCACT	RAD55 Forward primer - Y2H project pJG4-5 homology
pJG4-5-RAD55-REV	GAAGTCCAAAGCTTCTCGAGTTAAC CCTCACTATCATAAA	RAD55 Reverse primer - Y2H project pJG4-5 homology
pJG4-5-RAD57-FOR	ATTATGCCTCTCCCGAATTCATGCC TAGGGCCTTATCAAT	RAD57 Forward primer - Y2H project pJG4-5 homology
pJG4-5-RAD57-REV	GAAGTCCAAAGCTTCTCGAGTCAG GCTGTTTCTATTCCTC	RAD57 Reverse primer - Y2H project pJG4-5 homology
pJG4-5-RAD59-FOR	ATTATGCCTCTCCCGAATTCATGAC GATACAAGCGAAGCC	RAD59 Forward primer - Y2H project pJG4-5 homology
pJG4-5-RAD59-REV	GAAGTCCAAAGCTTCTCGAGTTATT TGATATGCGTGCCTT	RAD59 Reverse primer - Y2H project pJG4-5 homology
pJG4-5-RDH54-FOR	ATTATGCCTCTCCCGAATTCATGGC GGTAATAAGCGTTAA	RDH54 Forward primer - Y2H project pJG4-5 homology
pJG4-5-RDH54-REV	GAAGTCCAAAGCTTCTCGAGTCATT GTTCTCTGAGACATA	RDH54 Reverse primer - Y2H project pJG4-5 homology
pJG4-5-LGE1-FOR	ATTATGCCTCTCCCGAATTCATGAG CGGATACACGGGAAA	LGE1 Forward primer - Y2H project pJG4-5 homology

Name	Sequence	Purpose
pJG4-5-LGE1-REV	GAAGTCCAAAGCTTCTCGAGCTAC TGCATTAATAACAATG	LGE1 Reverse primer - Y2H project pJG4-5 homology
rfa1-del-for	CTGCAGTAGGCAAAGTTCCAGATA ACACACCAC	Rfa1 deletion diagnostic primer (Forward)
rfa1-del-rev	GGTAATAACTTGCTTGTAGAACGGT TCACAATCCC	Rfa1 deletion diagnostic primer (Reverse)
rfa2-del-for	GCTGTACTAGCTGGTATGATTCACC ACTGATG	Rfa2 deletion diagnostic primer (Forward)
rfa2-del-rev	CAGTAATGAGCCCTGAATCAGACA TTCACCACAC	Rfa2 deletion diagnostic primer (Reverse)
pJG4-5-UP-Sequence	GATCCAGCCTGACTGGCTGAAATC GAATGG	pJG4-5 sequencing primer
pJG4-5-DOWN-Recover	TCAACAACGTATCTACCAACGATTT GACCC	pJG4-5 sequencing primer
UBC6-FOR	AACCACCGGCTATCAGAATG	For detection of Rfa1 expression via qPCR
UBC6-REV	TTCCAAGTATCAGGGTGGTAATC	For detection of Rfa1 expression via qPCR
cdc5-ad-FOR	TCCAAATTAAGGACGATTCAGGCG	Used to amplify cdc5-AD for *in vivo* cloning
cdc5-ad-REV	GTCAAAGAGGGCCTTTCTATTGG	Used to amplify cdc5-AD for in vivo cloning
MEC1-UP-FOR	CAAGGCTCCATAACTATATGGAGC	Upstream MEC1 Forward primer
MEC1-DOWN-REV	TAACTTATATGGTGTCAACATCCC	Downstream MEC1 Reverse primer
RAD53-UP-FOR	TGGCAGAAAAATCATCACCGTGGG	Upstream RAD53 Forward primer
RAD53-DOWN-REV	CCACATCAAGCAGGATTATGTTTT	Downstream RAD53 Reverse primer
SML1-UP-FOR	AGCCCAAACGGGCTCCACTACCCG	Upstream SML1 Forward primer
SML1-DOWN-REV	GGCGCTAGCGATATCTAGCTGTAT	Downstream SML1 Reverse primer
TEL1-UP-FOR	GATATTATGAGCGTGATAGGAGGG	Upstream TEL1 Forward primer
TEL1-DOWN-REV	CCCTTTGTATCTTACTGTTCTCAT	Downstream TEL1 Reverse primer
CHK1-UP-FOR	TTCAACATTACTACGAGGCCTGCC	Upstream CHK1 Forward primer
CHK1-DOWN-REV	GGCTCGAATATTACTCAAACAGGG	Downstream CHK1 Reverse primer

Name	Sequence	Purpose
DUN1-UP-FOR	TAGTAATACGATGGTATGTGTGTG	Upstream DUN1 Forward primer
DUN1-DOWN-REV	ACTGTGACATTTTTTATATGCGGG	Downstream DUN1 Reverse primer
RDH54-UP-FOR	ATCTTCAACAACGCGCTGTTGGAG	Upstream RDH54 Forward primer
RDH54-DOWN-REV	GCCCTACTTAATATGTGACTTGAA	Downstream RDH54 Reverse primer
cka1-natMX-F	CAAAAATAGGGGGTTGTAGAAGGA ATATTTGATTCGAACTGACATGGAG GCCCAGAATAC	natMX based deletion primers for Cka1
cka1-natMX-R	CAGTGATTTTTTTTTTTTTATTTCAT TCATTATTTATTTCCAGTATAGCGA CCAGCATTC	Natmx based deletion primer for Cka1
cka2-natMX-F	ATAGAAGGAACAATAAACCTAAAAG AATAGAAGAAACAGAGACATGGAG GCCCAGAATAC	Natmx based deletion primer for *cka2*
cka2-natMX-R	GGTGGAAAAAGAATTGCCTTGCTA AGAGTATTGTTGTCCACAGTATAGC GACCAGCATTC	Natmx based deletion primer for *cka2*
ckb1-natMX-F	GTATTTAGAAGCGACCATTAGCTAA AAGAGAGAGAAAACTGACATGGAG GCCCAGAATAC	Natmx based deletion primer for *ckb1*
ckb1-natMX-R	ATATGTATATGGTAGGGCAAAGAG GAAAATAAATCAAGGGCAGTATAG CGACCAGCATTC	natmx based deletion primer for *ckb1*
ckb2-natMX-F	CAAGATTAAGGGACTTAGAGAACT GATAGAAAAGCAGATCGACATGGA GGCCCAGAATAC	natmx based deletion primer for *ckb2*
ckb2-natMX-R	CTAGGATTTCATTTCGAATTTTTTCT TCTTTCTTTAATAGCAGTATAGCGA CCAGCATTC	natmx based deletion primer for *ckb2*
CKA1-UP-FOR	ACATACAGCAGCACTAAGTGGTAG	Forward primer to amplify CKA1
CKA1-DOWN-REV	TATGAAATTTGCTCGTGTCAACCC	Reverse primer to amplify CKA1
CKA2-UP-FOR	CCTTGCGTAGCCCGCTTTTCGCCC	Forward primer to amplify CKA2
CKA2-DOWN-REV	GTAGACATCGCTACCGTCGGCAGG	Reverse primer to amplify CKA2
CKB1-UP-FOR	AGAATATCGCTACCGCTGCTGCCC	Forward primer to amplify CKB1
CKB1-DOWN-REV	GACGACGAAGCTGGTGTGAAGCTG	Reverse primer to amplify CKB1
CKB2-UP-FOR	AGCGAATAAATGGAGGTGTATTGG	Forward primer to amplify CKB2

Name	Sequence	Purpose
CKB2-DOWN-REV	ATATATAACAGGCTAACTTCGGAG	Reverse primer to amplify CKB2
RFA2-UP-FOR-NEW-O-338	TAGCAATTCCTTTGGCCTCGATGAG CTTCC	Upstream RFA2 primer
RFA2-UP-REV-NEW-O-339	GATAAAACCCTGGTCAGTCAAGGT CGTAC	Downstream RFA2 primer
natMX-DOWN-FOR	CCCTGTACGACGGCACCGCCTCGG	natMX amplicon - Forward
natMX-UP-REV	GGTGCGGTACCGGTAAGCCGTGTC	natMX amplicon - Reverse
tel1-natMX-F	AAGCCTTCAAAGAAAAAGGGAAAT CAGTGTAACATAGACGGACATGGA GGCCCAGAATAC	natMX based deletion primers for *tel1*
tel1-natMX-R	TATAAACAAAAAAAAGAAGTATAAA GCATCTGCATAGCAACAGTATAGC GACCAGCATTC	natMX based deletion primers for *tel1*
sml1-TRP1-F	TCTCACTAACCTCTCTTCAACTGCT CAATAATTTCCCGCTGTTAACGACA TTACTATATA	natMX based deletion primers for sml1
sml1-TRP1-R	GGGAAATGGAAAGAGAAAAGAAAA GAGTATGAAAGGAACTCTGCAGGC AAGTGCACAAAC	natMX based deletion primers for sml1
rfa1-natMX-F	AGGCGAAACCAGCAAGAAGACCAG ATTATACTTACAAGAGGACATGGAG GCCCAGAATAC	natMX based deletion primers for rfa1
rfa1-natMX-R	TATGTTACATAGATTAAATAGTACTT GATTATTTGATACACAGTATAGCGA CCAGCATTC	natMX based deletion primers for rfa1
rdh54-natMX-F	TACTATAAATAACCGATTAGAATCG AGTTTTTGTATTGAAGACATGGAGG CCCAGAATAC	natMX based deletion primers for rdh54
rdh54-natMX-R	CGCCAAATATGGACACTTATATACT AAATAAAATAGCTATCAGTATAGCG ACCAGCATTC	natMX based deletion primers for rdh54
rad53-natMX-F	AATAGTGAGAAAAGATAGTGTTACA CAACATCAACTAAAAGACATGGAG GCCCAGAATAC	natMX based deletion primers for rad53
rad53-natMX-R	TTAAAAAGGGGCAGCATTTTCTATG GGTATTTGTCCTTGGCAGTATAGC GACCAGCATTC	natMX based deletion primers for rad53
mec1-natMX-F	ACAAGAACGACATACACCGCGTAA AGGCCCACAAGACTGCGACATGGA GGCCCAGAATAC	natMX based deletion primers for *mec1*
mec1-natMX-R	AAGAGGAAGTTCGTCTGTTGCCGA AAATGGTGGAAAGTCGCAGTATAG CGACCAGCATTC	natMX based deletion primers for *mec1*
dun1-natMX-F	AGGGGCTTAACATACAGTAAAAAA GGCAATTATAGTGAAGGACATGGA GGCCCAGAATAC	natMX based deletion primers for *dun1*

Name	Sequence	Purpose
dun1-natMX-R	CCAGATTCAAACAATGTTTTTGAAA TAATGCTTCTCATGTCAGTATAGCG ACCAGCATTC	natMX based deletion primers for *dun1*
chk1-natMX-F	GTATATCATAAGTTGCTGTATATGG GCAGCACGTATTACTGACATGGAG GCCCAGAATAC	natMX based deletion primers for *chk1*
chk1-natMX-R	TGATCAGTGCATCTTAACCCTTCTT TTGTCTCCATTTTTTCAGTATAGCG ACCAGCATTC	natMX based deletion primers for *chk1*
mec1-natmx-ext-F	TGAAGAGAGATGATTAATGAAGACA AAGTGAGGCTGGACAACAAGAACG ACATACACCGC	extension primer for *mec1* deletion natMX cassette
mec1-natmx-EXT-R	AACTCCGCCGGAGAAAAGCACCTG CAGTGATGGTTAGATCAAGAGGAA GTTCGTCTGTTG	extension primer for *mec1* deletion natMX cassette
rad53-natmx-EXT-F	TTTGTATATGCATTCGATTTTCTTAA GCTTTAAAAGAGAGAATAGTGAGAA AAGATAGT	extension primer for rad53 deletion natMX cassette
rad53-natmx-EXT-R	ATAGATGAATTCTGAGTATTGGTAT CTACCATCTTCTCTCTTAAAAAGGG GCAGCATTTT	extension primer for rad53 deletion natMX cassette
sml1-trp1-ext-F	CATTTTTAAATGTCTTATCTGCTCCT TTGTGATCTTACGGTCTCACTAACC TCTCTTCAA	TRP1 based deletion prrimer for sml1
sml1-trp1-ext-R	AAAAGAAGGGTATCTAAGAGAAGA AAAGAACAGAACTAGTGGGAAATG GAAAGAGAAAAG	TRP1 based deletion prrimer for sml1
rtt107-hphN-F	CAAAAGAATTCAGACATTTCTATTG AACCATTCCAGAAATGACATGGAG GCCCAGAATAC	hphNX based deletion primer for *rtt107*
rtt107-hphN-R	AAATTGTAGAAAAATTAAAAGGTTT GCGGATAAAGTGTGGTTAAAGCCT TCGAGCGTCCC	hphNX based deletion primer for *rtt107*
sml1-hphN-F	TCTCACTAACCTCTCTTCAACTGCT CAATAATTTCCCGCTGACATGGAG CGCAAGAATAC	hphNX based deletion primer for sml1
sml1-hphN-R	GGGAAATGGAAAGAGAAAAGAAAA GAGTATGAAAGGAACTTTAAAGCCT TCGAGCGTCCC	hphNX based deletion primer for sml1
sae2-hphN-F	CTCTTTCTTCTTCTTTTTCGTCTTAT TTTTGGGTTTCGTGGACATGGAGG CCCAGAATAC	hphNX based deletion primer for *sae2*
sae2-hphN-R	CGAAAATAACGTCGACGTTCTCTAT CATAATAAAACCCTGTTAAAGCCTT CGAGCGTCCC	hphNX based deletion primer for *sae2*
slx4-hphN-F	TATATGAATTTACAATCATTGTAGG GAAAAGAAAACTTGTGACATGGAG GCCCAGAATAC	hphNX based deletion primer for *slx4*
slx4-hphN-R	AAATGTTAAAGTAAAGGCTTTGCAG AGAATGACCTGGTGATTAAAGCCTT CGAGCGTCCC	hphNX based deletion primer for *slx4*

Name	Sequence	Purpose
ura3-hphN-F	TGCCCAGTATTCTTAACCCAACTGCACAGAACAAAAACCTGACATGGAGGCCCAGAATAC	hphNX based deletion primer for ura3
ura3-hphN-R	TAATAACTGATATAATTAAATTGAAGCTCTAATTTGTGAGTTAAAGCCTTCCAGCGTCCC	hphNX based deletion primer for ura3
RFA1-SEQ	TCACGCGTAAAAATTAGACGAGGCG	Rfa1 sequencing primer
hphN-1406-1465-F	CGTCTGGACCGATGGCTGTGTAGAAGTACTCGCCGATAGTGGAAACCGACGCCCCAGCAC	C-terminal Forward primer for hphN knockout verification
hphN-915-975-R	CGCACTGACGGTGTCGTCCATCACAGTTTGCCAGTGATACACATGGGGATCAGCAATCGC	N-terminal Reverse primer for hphN knockout verification
natMX-882-941-F	GAGCAGGCGCTCTACATGAGCATGCCCTGCCCCTAATCAGTACTGACAATAAAAAGATTC	C-terminal Forward primer for hphN knockout verification
natMX-541-600-R	CGTACGCGACGAACGTCCGGGAGTCCGGGTCGCCGTCCTCCCCGTCGTCCGATTCGTCGT	N-terminal Reverse primer for natMX knockout verification
SAE2-EXT-R	GTCGTTCCCGTGGTAGAAATGCTTTGATTTTCAGATATGCCGAAAATAACGTCGACGTTC	Extension primers for Sae2
SAE2-EXT-F	CTATCAAAGAAGTTTTGTCTGAGTTAGCGTCTGATTTTGACTCTTTCTTCTTCTTTTTCG	Extension primers for Sae2
SLX4-EXT-R	AGAGAAGCAATGGTCGCGGCTCCGCCAAGAAGAAGAATCTAAATGTTAAAGTAAAGGCTT	extension primers for *slx4*
SLX4-EXT-F	ACGGGTTTTTGTTCGATGAAAAATCACCAGTAGAGCACCATATATGAATTTACAATCATT	extension primers for *slx4*
RTT107-EXT-F	TTCTTCGACATTAGAAATCTCTTGTATTTTTTGTACATCCCAAAAGAATTCAGACATTTC	extension primers for *rtt107*
RTT107-EXT-R	TGCTTTACGCATTCTGGCCATGAATCTGTTTTTATCCATGAAATTGTAGAAAAATAAAAA	extension primers for *rtt107*
RTT107-UP-F	GGAACTCAAGGGCTTTTCTGTATTTTCTCATAGACATTATTTATCAGTAATTGCAGCTGT	Upstream primer for *rtt107* (-500bp)
RTT107-DOWN-R	TAAGATTTCTGACGTAAATCTATGGATGTAACCTGTTTAATTATTAGATCAAAAAGTTCT	Downstream primer for *rtt107* (+500bp)
SLX4-UP-F	TTTTAGCGAAAGATTTTTATTCACAAGCTTTTTTTATCCTTAATGCTCGAATACTACAAC	Upstream primer for *slx4* (-500bp)
SLX4-DOWN-R	AGCCCTGTGTGAATTGGGAGAAACTAGGTTATTGTCCTTATGGCAGAAGATGCTGCTTCA	Downstream primer for *slx4* (+500bp)
SAE2-UP-F	GCCAGTAATTGACGATGCGGAAGGATGTGTTATTGCATGGGAAAGCTCGTTTGTTTCCAG	Upstream primer for *sae2* (-500bp)

Name	Sequence	Purpose
SAE2-DOWN-R	AATGCGATGCATACTGCATATTTAA ACCAATCATGTACTTTTCATATGAT AAAGGGCGAA	Downstream primer for *sae2* (+500bp)
RDH54-EXT-F	AAAAATAAAACGCGAAGAGCTAAAA AAAAAAAAGAAAACCTACTATAAAT AACCGATTAG	extension primer for rdh54 deletion cassettes
RDH54-EXT-R	ATACAATCAGTGATTAAATAATAGC TATTTTATTTAGTATCGCCAAATATG GACACTTAT	extension primer for rdh54 deletion cassettes
LysMX-Mid-For	TATCGCTTCTCCGTGCAATT	LysMX diagnostic primer. Forward primer
LysMX-Mid-REV	TTTACGAGGAACATAGCTAC	LysMX diagnostic primer., Reverse primer
cka1-up-for	ATGAGAAATCTATTGGAAAC	CKA1 external Forward primer
cka2-up-for	GTCGATTGCTCCAAAGTTGG	*cka2* external Forward primer
ckb1-up-for	ATAGAGTTGTTGAATTCTTT	*ckb1* external Forward primer
ckb2-up-for	CCAATATGATATAGGGACCA	*ckb2* external Forward primer
cka1-down-rev	TAGAAGGTGGTAAGGATCCA	*cka1* external Reverse primer
cka2-down-rev	CTTCTTCATTGCTGAAAAAA	*cka2* external Reverse primer
ckb1-down-rev	GCCCAACAAGGTAGTGAACA	*ckb1* external Reverse primer
ckb2-down-rev	GCCGAAAGAAATTTGCTGCA	*ckb2* external Reverse primer
TRP1-up-rev	CAAGTATTTCGGAGTGCCTG	internal gene primer for confirmation of knockout
TRP1-down-for	CGATTTCTGACTGGGTTGGA	internal gene primer for confirmation of knockout
RAD53-UP-NEW-FOR	ATGGACTGTTCTTTCTGCACAGGC GACTAA	Upstream RAD53 Forward primer
RAD53-DOWN-NEW-REV	GGTTGGCGCTGACCAACAACAAGG CCAATGG	Downstream RAD53 Reverse primer
MEC1-UP-NEW-FOR	GCGGTACTCAGACGATAACTATGA GTACAGG	Upstream MEC1 Forward primer
MEC1-DOWN-NEW-REV	CAATCCACTTATAGTTAAGCAGGCA TAGGGG	Downstream MEC1 Reverse primer
RFA1-SEQ	TCACGCTAAAAATTAGACGAGGCG	Rfa1 sequencing primer

Name	Sequence	Purpose
RFA2-UP-F	TAGCAATTCCTTTGGCCTCGATGAG CTTCC	Rfa2 upstream Forward primer
rad53-gblock-FOR	CATCACCGTGGGTAGACTTGGAAA TGAAAACATTTATAGA	Amplification of G-42 for rad53 knockouts
rad53-gblock-REV	CTTTTTCTGATTCAAAAATTCATTAA GCATAACTAAAACT	Amplification of G-42 for rad53 knockouts
cka1-up-new-FOR	AGATGTTATTTTCACATCACATGTC GCTAATTTG	Upstream CKA1 primer
cka1-down-new-REV	GTTTTGGTGAGCACAACGGTGTTT CATTCAAGAA	Downstream CKA1 primer
cka2-up-new-FOR	CAACTCTGAAGTTGATTTACTTGCT GTAGGTCGA	Upstream CKA2 primer
cka2-down-new-REV	ATTTTACTCAAAAGGTAAATGGCTC TCTCAGCGT	Downstream CKA2 primer
ckb1-up-new-FOR	TGAAGATGGGCCTGAAAGGCTTTA TTTTCTGATT	Upstream CKB1 primer
ckb1-down-new-REV	CAATCCAGATTAAGGAAGGAGTATA GGCAATTAC	Downstream CKB1 primer
ckb2-up-new-FOR	GAGATCACCTGTTATGAAAAAAATA TCACCGGTA	Upstream CKB2 primer
ckb2-down-new-REV	GTAAATAACTATAATTGACACCACC TGTCAACCA	Downstream CKB2 primer
QMAT2.F	ATTGCGACAAGGCTTCACCC	MAT qPCR (Rsa1 -5kbp)
QMAT2.R	CACATCACAGGTTTATTGGTTCC	MAT qPCR (Rsa1 -5kbp)
QMAT3.1.F	GGTTCAACAACTGCCACCTTTG	MAT qPCR (Rsa1 -10kbp)
QMAT3.1.R	GGTGATGGAGATGGAGTAGGAACG	MAT qPCR (Rsa1 -10kbp)
QPRE1.F	CCCACAAGTCCTCTGATTTACATTC G	Pre1 control qPCR primers
QPRE1.R	ATTCGATTGACAGGTGCTCCCTTTT C	Pre1 control qPCR primers
QARO1.F	GAGTCGTTACAAGGTGATGCCAG	Aro1 control qPCR primers
QARO1.R	AATAGCGGCAACAACACATGC	Aro1 control qPCR primers
MAT-HO-F	AATGGCACGCGGACAAA	PCR @ Mat locus during resection (+break control)
MAT-HO-R	CATCTTCCCAATATCCGTCACC	PCR @ Mat locus during resection (+break control)

Name	Sequence	Purpose
MAT-Ssp1-r1.1-F	ACCATTCTCATTATAAACAAGAATATCCAG	R1 Forward
MAT-Ssp1-r1.1-R	TACTGCCGGTGTTAAGCATTTA	R1 Reverse
MAT-Ssp1-r2.1-F	AGCCACAGGATTAATTATCTGAAATATG	R2 Forward
MAT-Ssp1-r2.1-R	AAGAAGAAGAGGAAGGCGAAAG	R2 Reverse
MAT-Ssp1-r3.1-F	AGTATTTAAGTGTTACCCGGTTACTT	R3 Forward
MAT-Ssp1-r3.1-R	ATTCTTGCGGATATCGTGCTAC	R3 Reverse
MAT-Ssp1-r4.1-F	GTTCTCTCAATAAGGAAGCATCAAG	R4 Forward
MAT-Ssp1-r4.1-R	CGCTCTTTCTGTATGTATAGAACTAAAT	R4 Reverse
MAT-Ssp1-r5.2-F	CAGTGAACGCTTGTGCTATCTT	R5 Forward
MAT-Ssp1-r5.2-R	CGGTCTTTCACTGTCGTGATTT	R5 Reverse
MAT-Ssp1-r6.1-F	GTTAGAGGATGTCTAGCACTTGAG	R6 Forward
MAT-Ssp1-r6.1-R	CGTAGTGATGACGTACGTGTATAG	R6 Reverse
MAT-Ssp1-r7.1-F	AGAGTCATTACAACGAGGAAATAGAA	R7 Forward
MAT-Ssp1-r7.1-F	CGTGGATCTGGTAGATCTGTAAAC	R7 Reverse

APPENDIX D. APPENDIX FIGURES

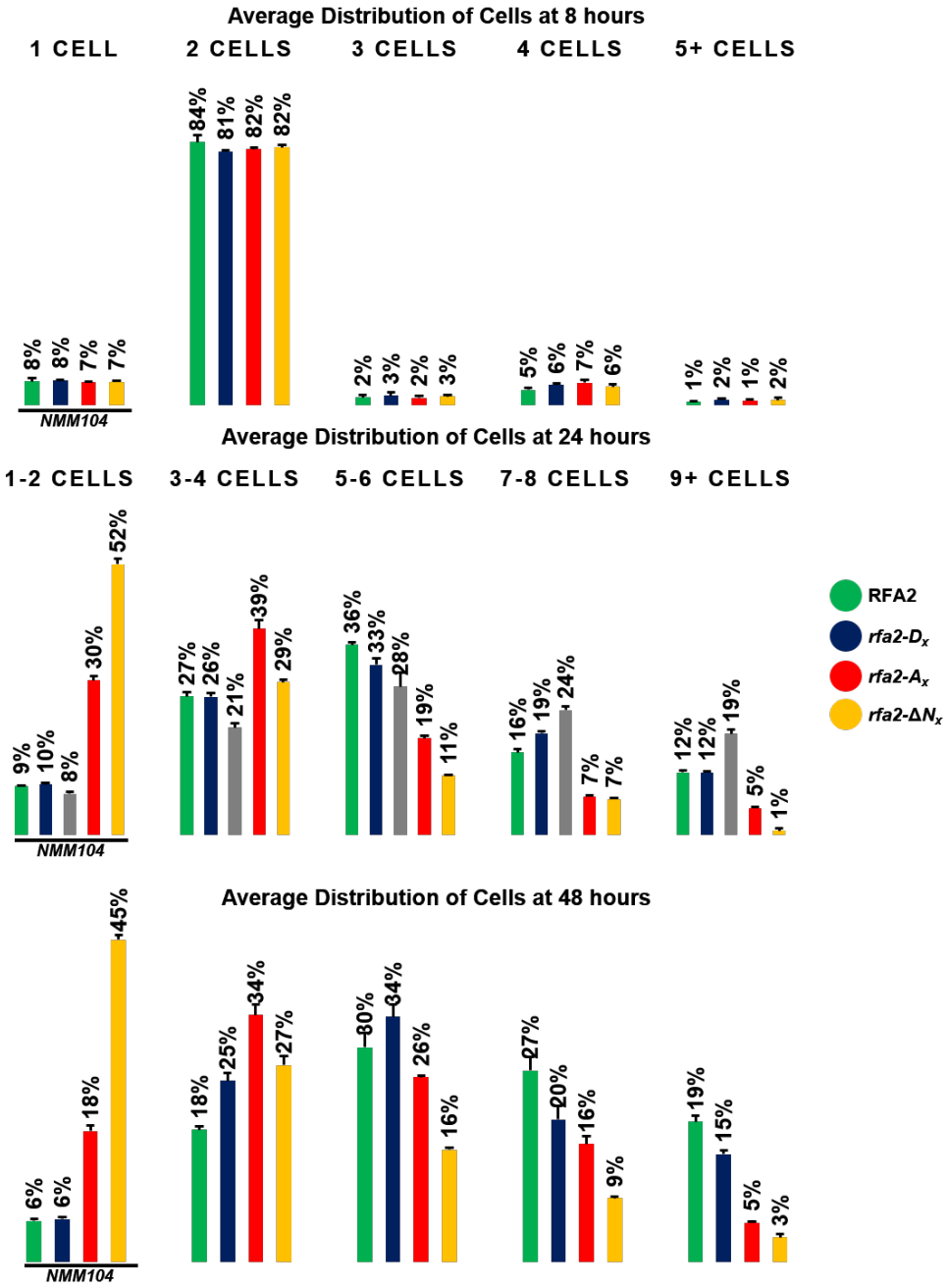

Figure D.1. Distribution of cells in Rfa2 NT extensive mutations during adaptation time course. NMM104 cells containing Rfa2 NT mutations were harvested from HO-induced culture at 8 hours, diluted, spread on YPRG plates using glass beads, and then analyzed microscopically and quantitated at 8, 24, and 48 hours post-HO induction. Cells were categorized based on morphology of 1 unbudded cell, 2 cells or bilobal 'big' buds, 3 cells, 4 cells, or 5 or more cells per cluster at 8 hours. At 24 and 48 hours, cells were categorized as 1-2 'arrested' cells, 3-4 cells, 5-6 cells, 7-8 cells, or 9 or more cells per cluster. Averages are from three independent replicate data sets. Errors bars represent standard deviation from averages obtained in replicate data sets. HO expression was induced in exponentially growing cells by adding 2% galactose to the media.

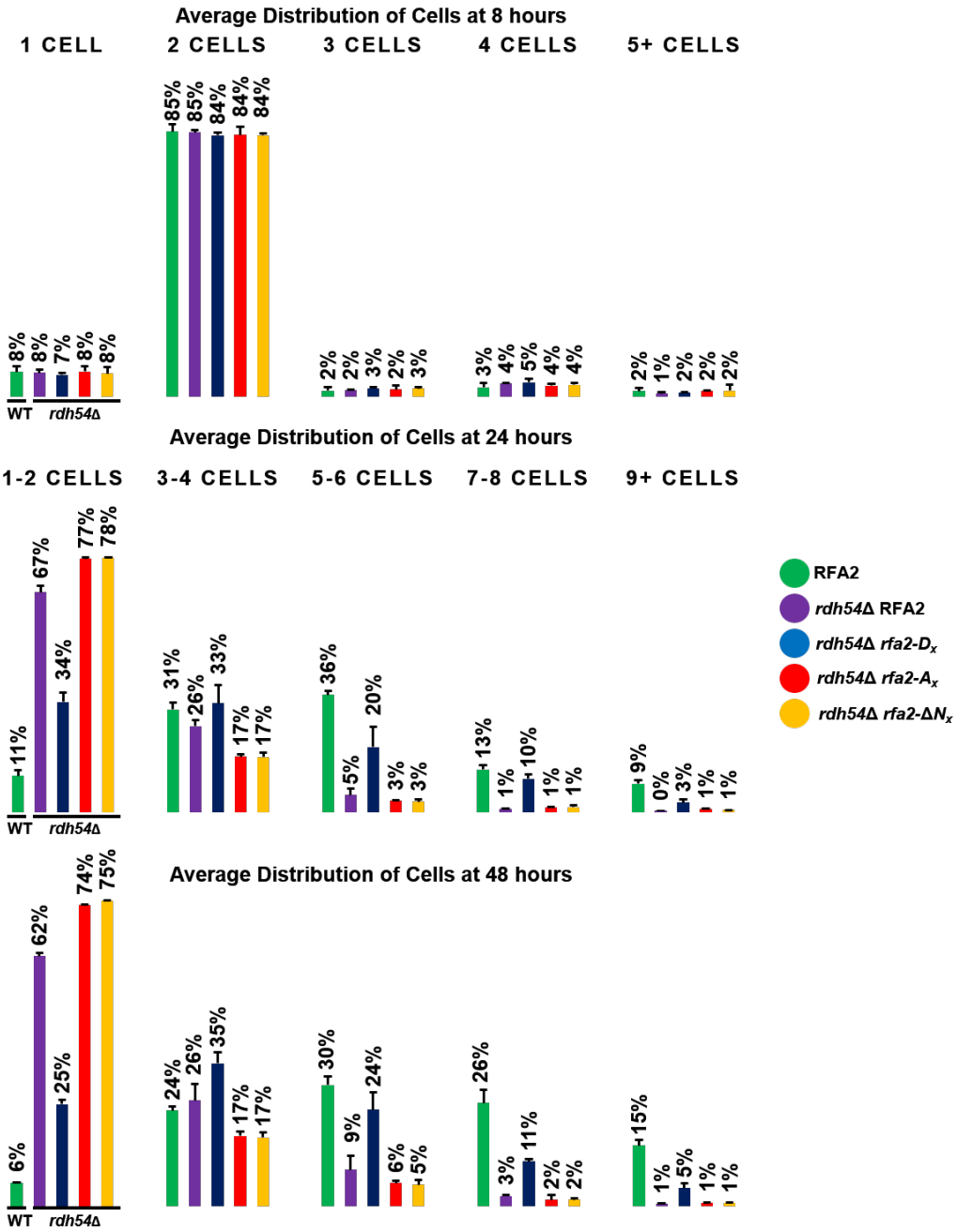

Figure D.2. Distribution of cells in *rdh54Δ rfa2* NT extensive mutations during adaptation time course.

rdh54Δ cells containing Rfa2 NT mutations were harvested from HO-induced culture at 8 hours, diluted, spread on YPRG plates using glass beads, and then analyzed microscopically and quantitated at 8, 24, and 48 hours post-HO induction. Cells were categorized based on morphology of 1 unbudded cell, 2 cells or bilobal 'big' buds, 3 cells, 4 cells, or 5 or more cells per cluster at 8 hours. At 24 and 48 hours, cells were categorized as 1-2 'arrested' cells, 3-4 cells, 5-6 cells, 7-8 cells, or 9 or more cells per cluster. Averages are from three independent replicate data sets. Errors bars represent standard deviation from averages obtained in replicate data sets. HO expression was induced in exponentially growing cells by adding 2% galactose to the media.

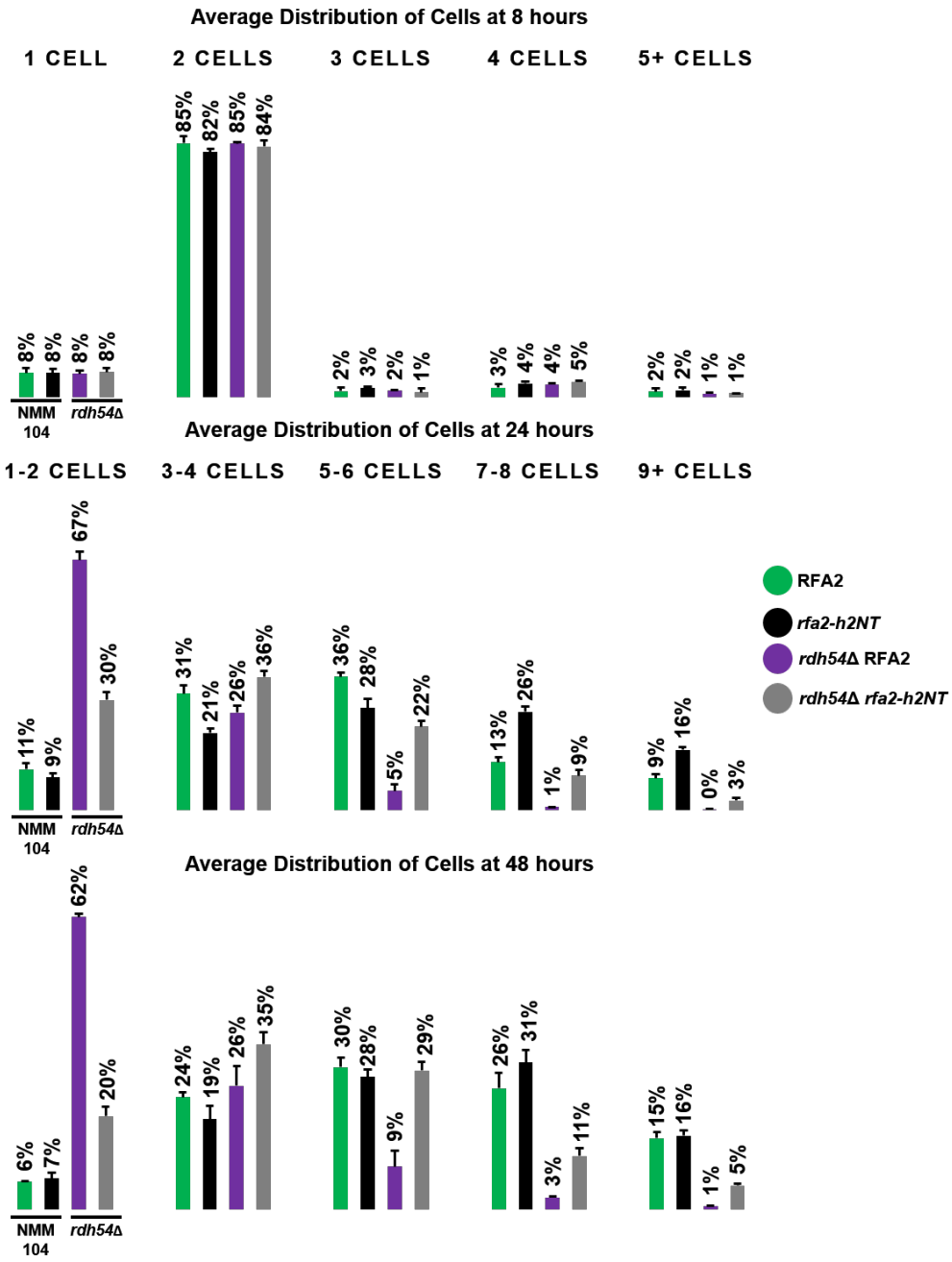

Figure D.3. Distribution of cells in *rdh54Δ rfa2-h2NT* mutations during adaptation time course. NMM104 or *rdh54Δ* cells containing *rfa2-h2NT* were harvested from HO-induced culture at 8 hours, diluted, spread on YPRG plates using glass beads, and then analyzed microscopically and quantitated at 8, 24, and 48 hours post-HO induction. Cells were categorized based on morphology of 1 unbudded cell, 2 cells or bilobal 'big' buds, 3 cells, 4 cells, or 5 or more cells per cluster at 8 hours. At 24 and 48 hours, cells were categorized as 1-2 'arrested' cells, 3-4 cells, 5-6 cells, 7-8 cells, or 9 or more cells per cluster. Averages are from three independent replicate data sets. Errors bars represent standard deviation from averages obtained in replicate data sets. HO expression was induced in exponentially growing cells by adding 2% galactose to the media.

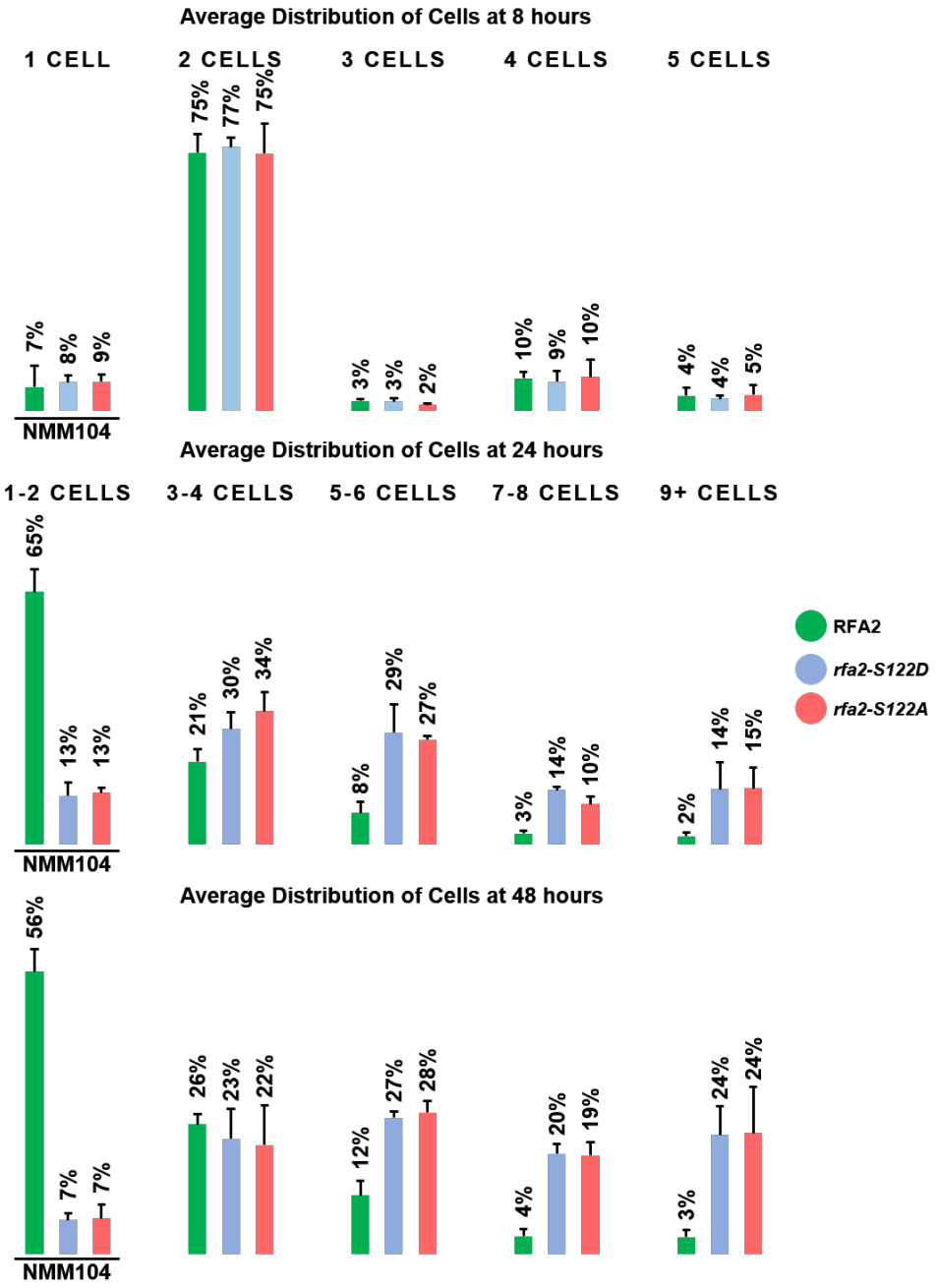

Figure D.4. Distribution of cells in *rfa2-S122*$_{D/A}$ mutations during adaptation time course. NMM104 containing *rfa2-S122D* or *rfa2-S122A* were harvested from HO-induced culture at 8 hours, diluted, spread on YPRG plates using glass beads, and then analyzed microscopically and quantitated at 8, 24, and 48 hours post-HO induction. Cells were categorized based on morphology of 1 unbudded cell, 2 cells or bilobal 'big' buds, 3 cells, 4 cells, or 5 or more cells per cluster at 8 hours. At 24 and 48 hours, cells were categorized as 1-2 'arrested' cells, 3-4 cells, 5-6 cells, 7-8 cells, or 9 or more cells per cluster. Averages are from three independent replicate data sets. Errors bars represent standard deviation from averages obtained in replicate data sets. HO expression was induced in exponentially growing cells by adding 2% galactose to the media.

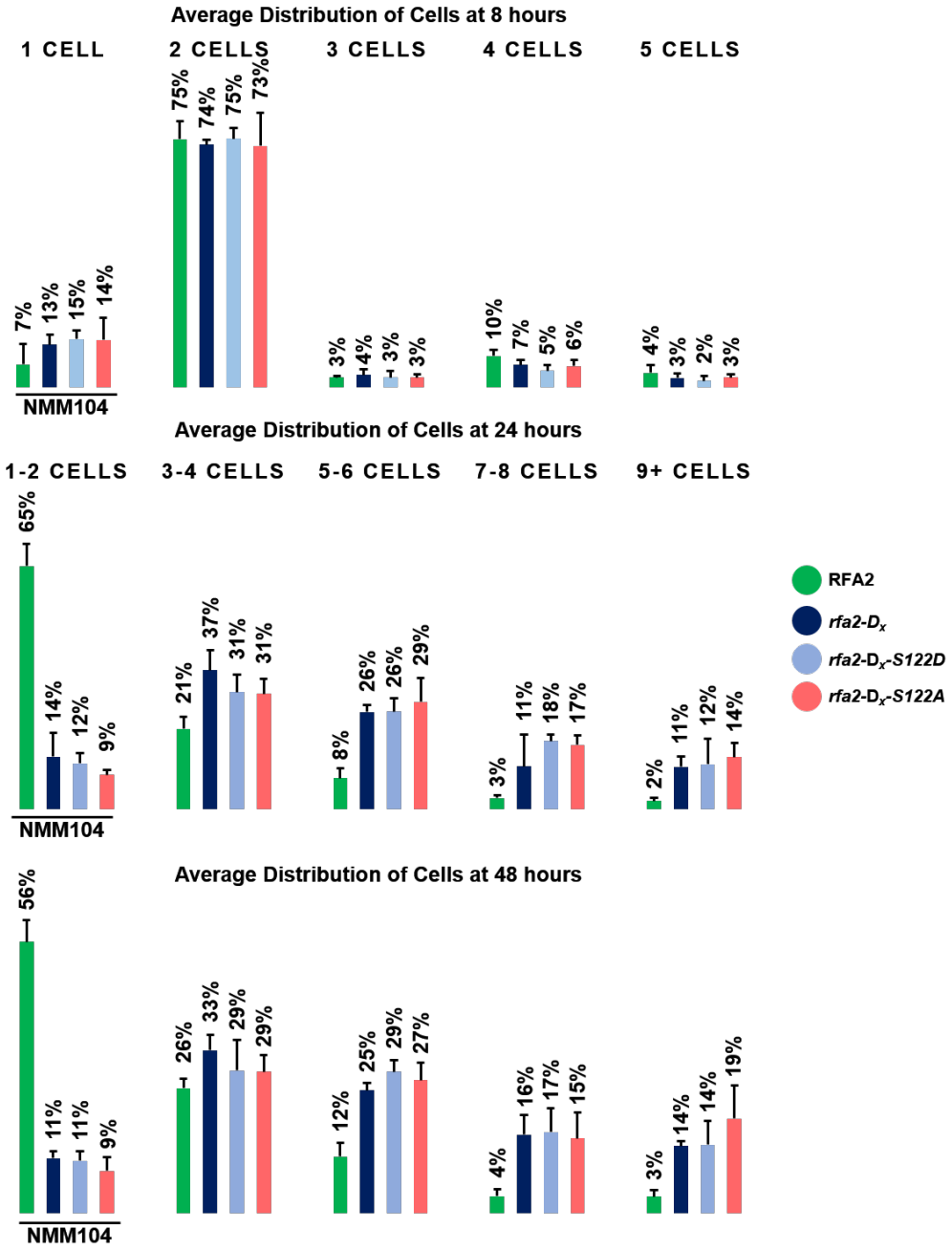

Figure D.5. Distribution of cells in *rfa2-Dx-S122D/A* mutations during adaptation time course. NMM104 containing *rfa2-Dx-S122D* or *rfa2-Dx-S122A* were harvested from HO-induced culture at 8 hours, diluted, spread on YPRG plates using glass beads, and then analyzed microscopically and quantitated at 8, 24, and 48 hours post-HO induction. Cells were categorized based on morphology of 1 unbudded cell, 2 cells or bilobal 'big' buds, 3 cells, 4 cells, or 5 or more cells per cluster at 8 hours. At 24 and 48 hours, cells were categorized as 1-2 'arrested' cells, 3-4 cells, 5-6 cells, 7-8 cells, or 9 or more cells per cluster. Averages are from three independent replicate data sets. Errors bars represent standard deviation from averages obtained in replicate data sets. HO expression was induced in exponentially growing cells by adding 2% galactose to the media.

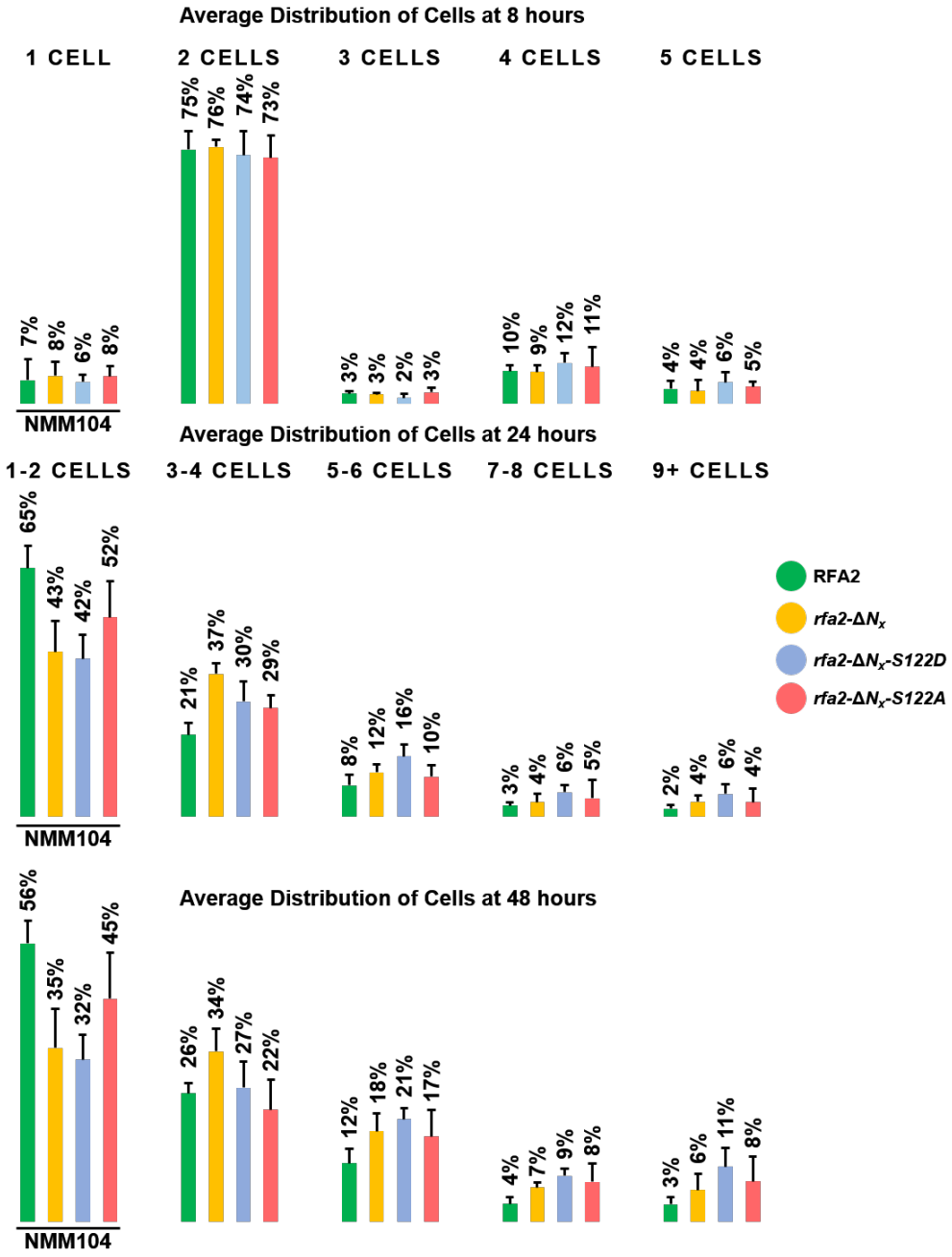

Figure D.6. Distribution of cells in *rfa2-ΔNX-S122D/A* mutations during adaptation time course. NMM104 containing *rfa2-ΔNX-S122D* or *rfa2-ΔNX-S122A* were harvested from HO-induced culture at 8 hours, diluted, spread on YPRG plates using glass beads, and then analyzed microscopically and quantitated at 8, 24, and 48 hours post-HO induction. Cells were categorized based on morphology of 1 unbudded cell, 2 cells or bilobal 'big' buds, 3 cells, 4 cells, or 5 or more cells per cluster at 8 hours. At 24 and 48 hours, cells were categorized as 1-2 'arrested' cells, 3-4 cells, 5-6 cells, 7-8 cells, or 9 or more cells per cluster. Averages are from three independent replicate data sets. Errors bars represent standard deviation from averages obtained in replicate data sets. HO expression was induced in exponentially growing cells by adding 2% galactose to the media.

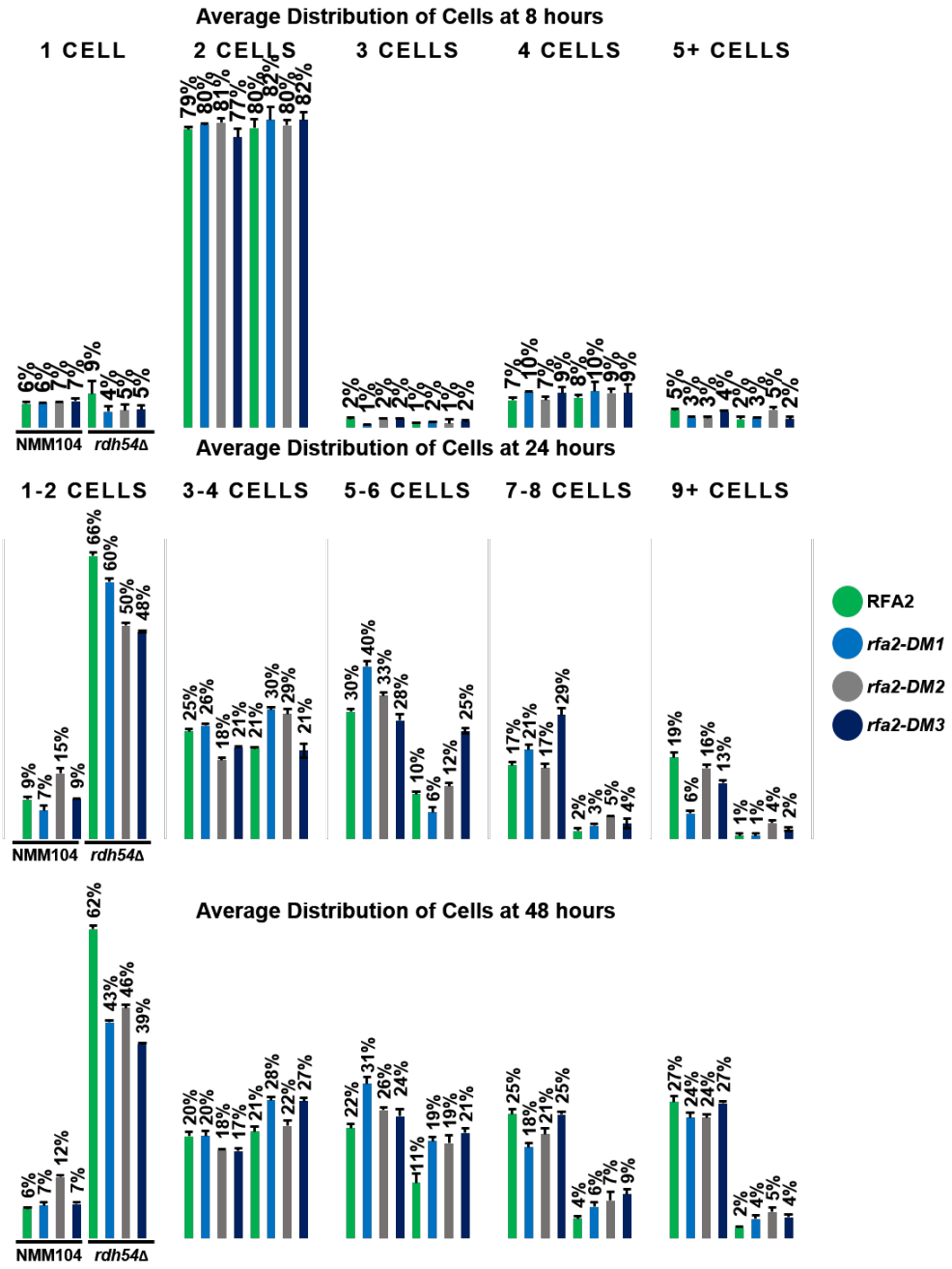

Figure D.7. Distribution of cells in *rfa2-D$_M$* mutations during adaptation time course.
NMM104 or *rdh54*Δ cells containing *rfa2-D$_{M1}$*, *rfa2-D$_{M2}$*, or *rfa2-D$_{M3}$*, were harvested from HO-induced culture at 8 hours, diluted, spread on YPRG plates using glass beads, and then analyzed microscopically and quantitated at 8, 24, and 48 hours post-HO induction. Cells were categorized based on morphology of 1 unbudded cell, 2 cells or bilobal 'big' buds, 3 cells, 4 cells, or 5 or more cells per cluster at 8 hours. At 24 and 48 hours, cells were categorized as 1-2 'arrested' cells, 3-4 cells, 5-6 cells, 7-8 cells, or 9 or more cells per cluster. Averages are from three independent replicate data sets. Errors bars represent standard deviation from averages obtained in replicate data sets. HO expression was induced in exponentially growing cells by adding 2% galactose to the media.

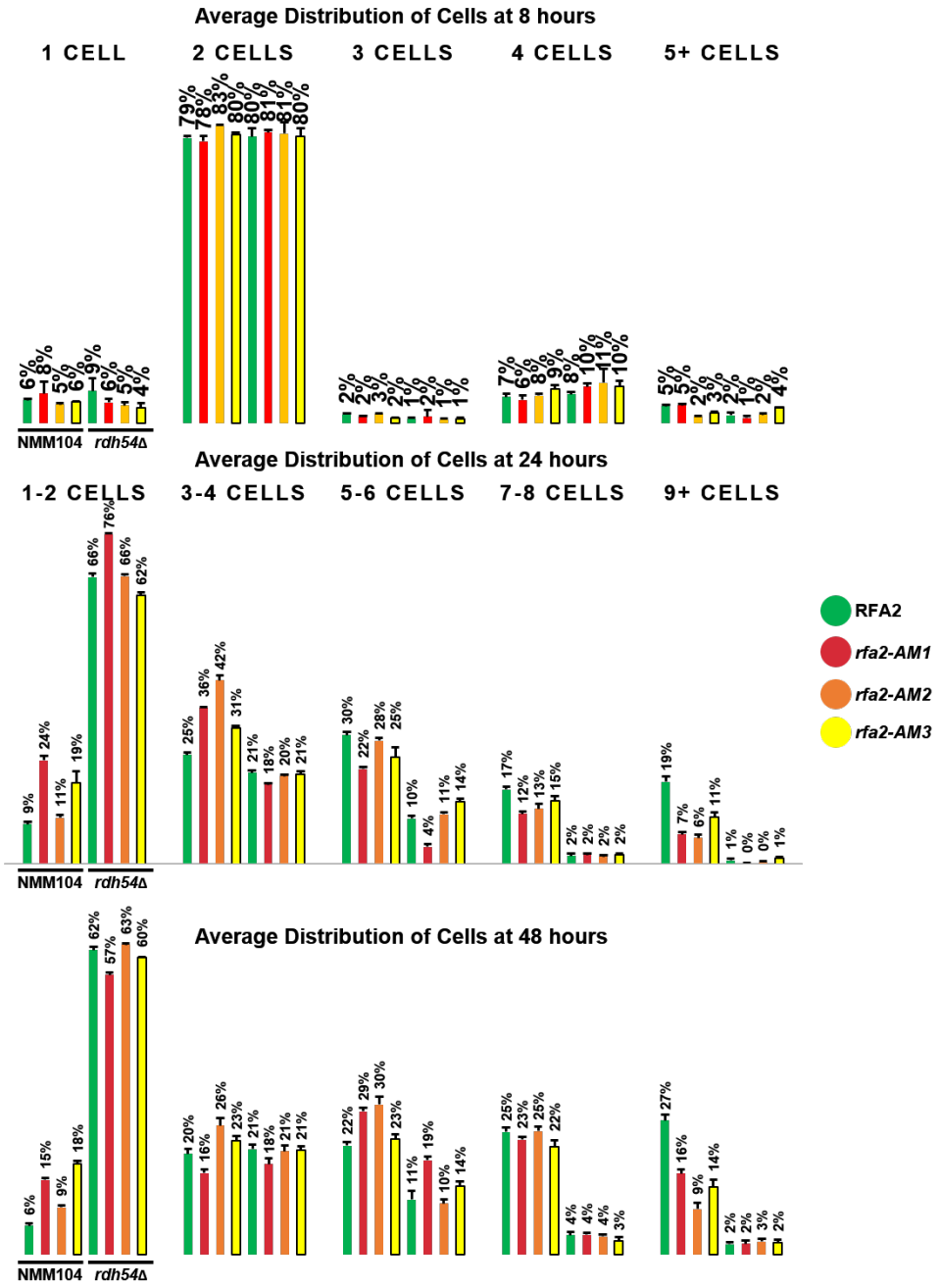

Figure D.8. Distribution of cells in *rfa2-A$_M$* mutations during adaptation time course.
NMM104 or *rdh54*Δ cells containing *rfa2-A$_{M1}$*, *rfa2-A$_{M2}$*, or *rfa2-A$_{M3}$*, were harvested from HO-induced culture at 8 hours, diluted, spread on YPRG plates using glass beads, and then analyzed microscopically and quantitated at 8, 24, and 48 hours post-HO induction. Cells were categorized based on morphology of 1 unbudded cell, 2 cells or bilobal 'big' buds, 3 cells, 4 cells, or 5 or more cells per cluster at 8 hours. At 24 and 48 hours, cells were categorized as 1-2 'arrested' cells, 3-4 cells, 5-6 cells, 7-8 cells, or 9 or more cells per cluster. Averages are from three independent replicate data sets. Errors bars represent standard deviation from averages obtained in replicate data sets. HO expression was induced in exponentially growing cells by adding 2% galactose to the media.

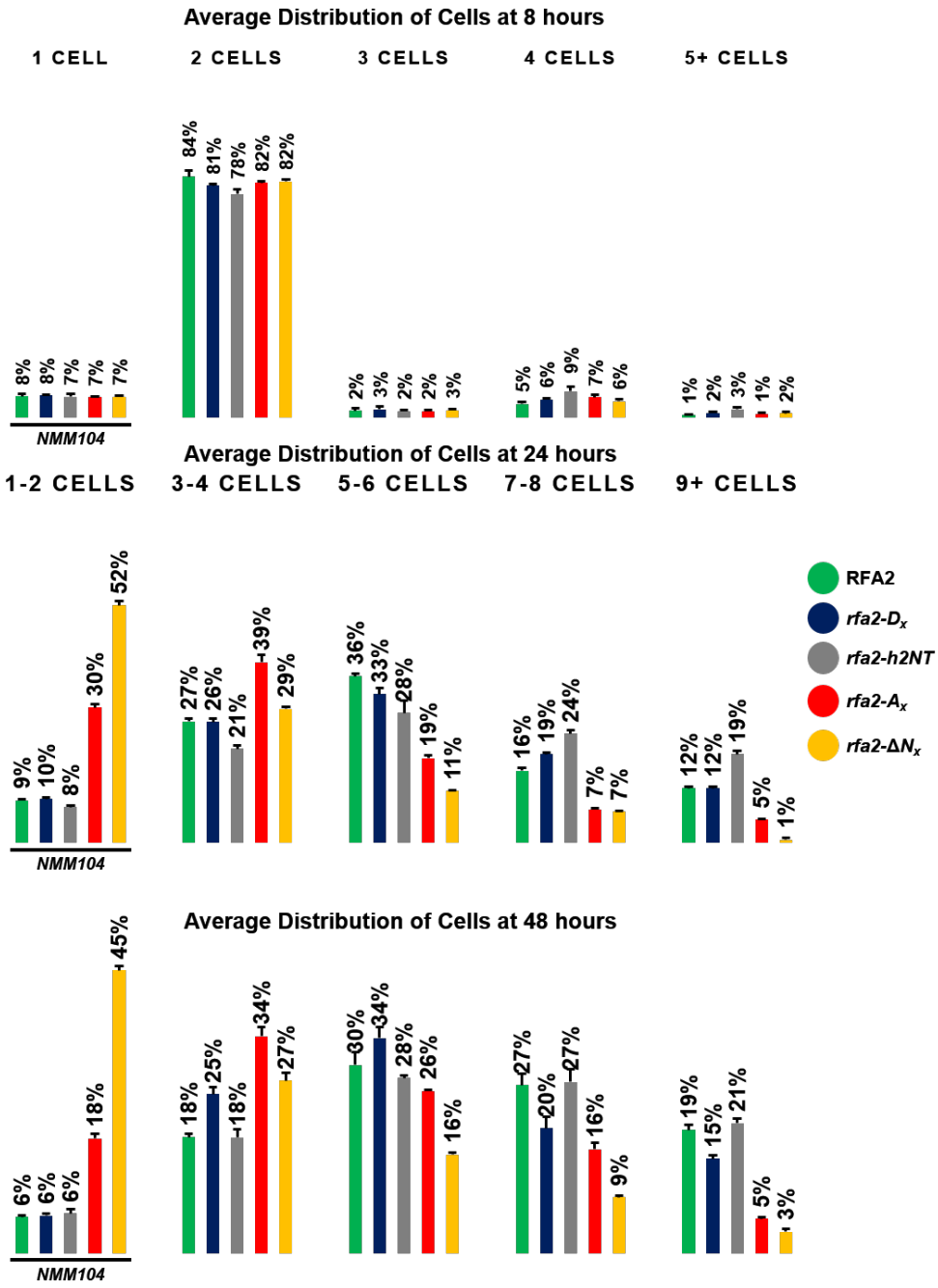

Figure D.9. Distribution of cells in NMM104 Rfa2 NT extensive mutations during adaptation time course.
NMM104 cells containing Rfa2 NT mutations were harvested from HO-induced culture at 8 hours, diluted, spread on YPRG plates using glass beads, and then analyzed microscopically and quantitated at 8, 24, and 48 hours post-HO induction. Averages are from three independent replicate data sets. HO expression was induced in exponentially growing cells by adding 2% galactose to the media. *rfa2-A*$_X$ or *rfa2-*Δ*N*$_X$ display reduced average adaptation compared to RFA2 cells. *rfa2-D*$_X$ adapts indistinguishably from RFA2 cells.

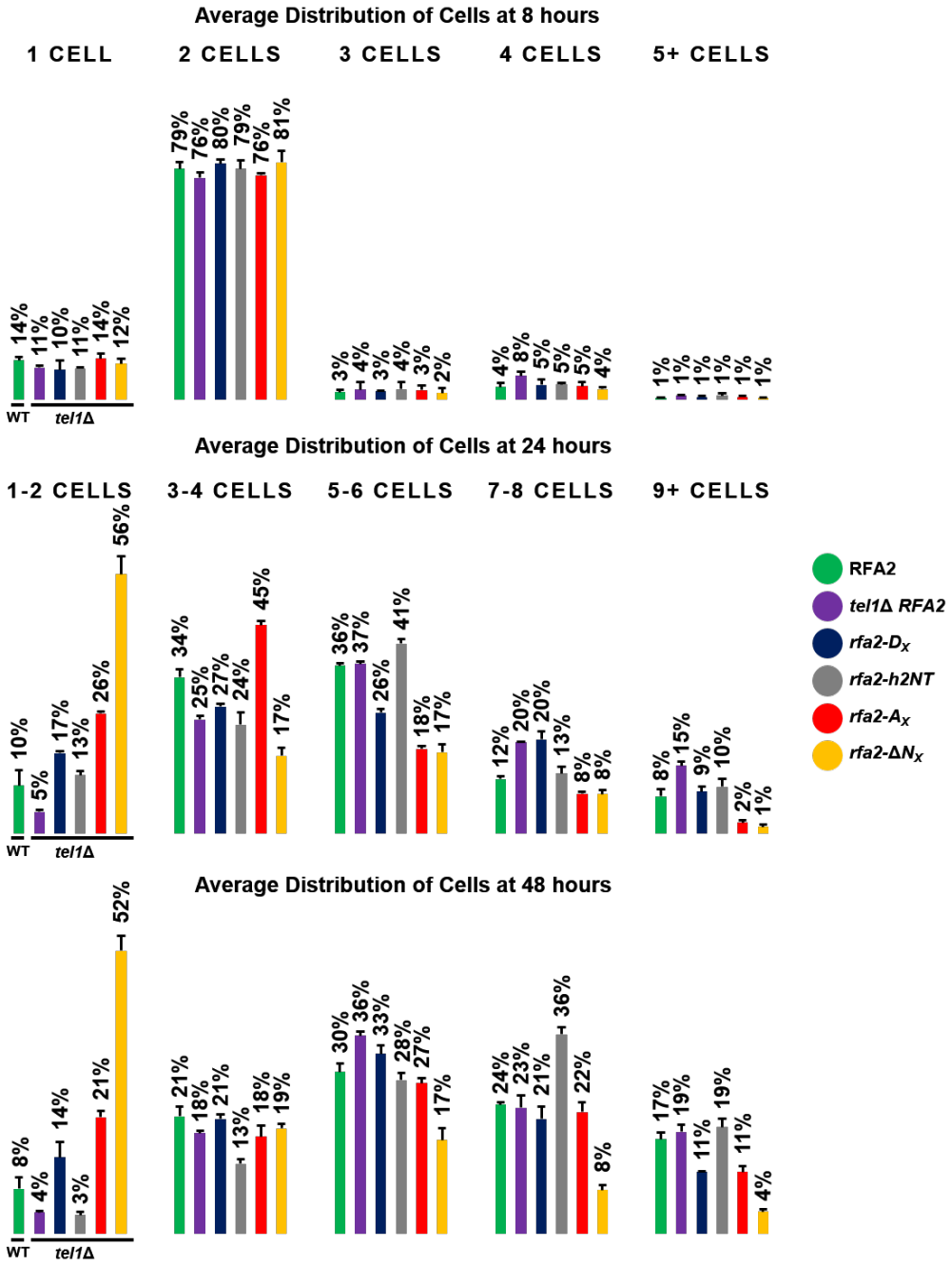

Figure D.10. Distribution of cells in *tel1*Δ Rfa2 NT extensive mutations during adaptation time course.
*tel1*Δ cells containing Rfa2 NT mutations were harvested from HO-induced culture at 8 hours, diluted, spread on YPRG plates using glass beads, and then analyzed microscopically and quantitated at 8, 24, and 48 hours post-HO induction. Averages are from three independent replicate data sets. HO expression was induced in exponentially growing cells by adding 2% galactose to the media. *rfa2-A*$_X$ or *rfa2-*Δ*N*$_X$ display reduced average adaptation compared to RFA2 cells. *rfa2-D*$_X$ adapts indistinguishably from RFA2 cells.

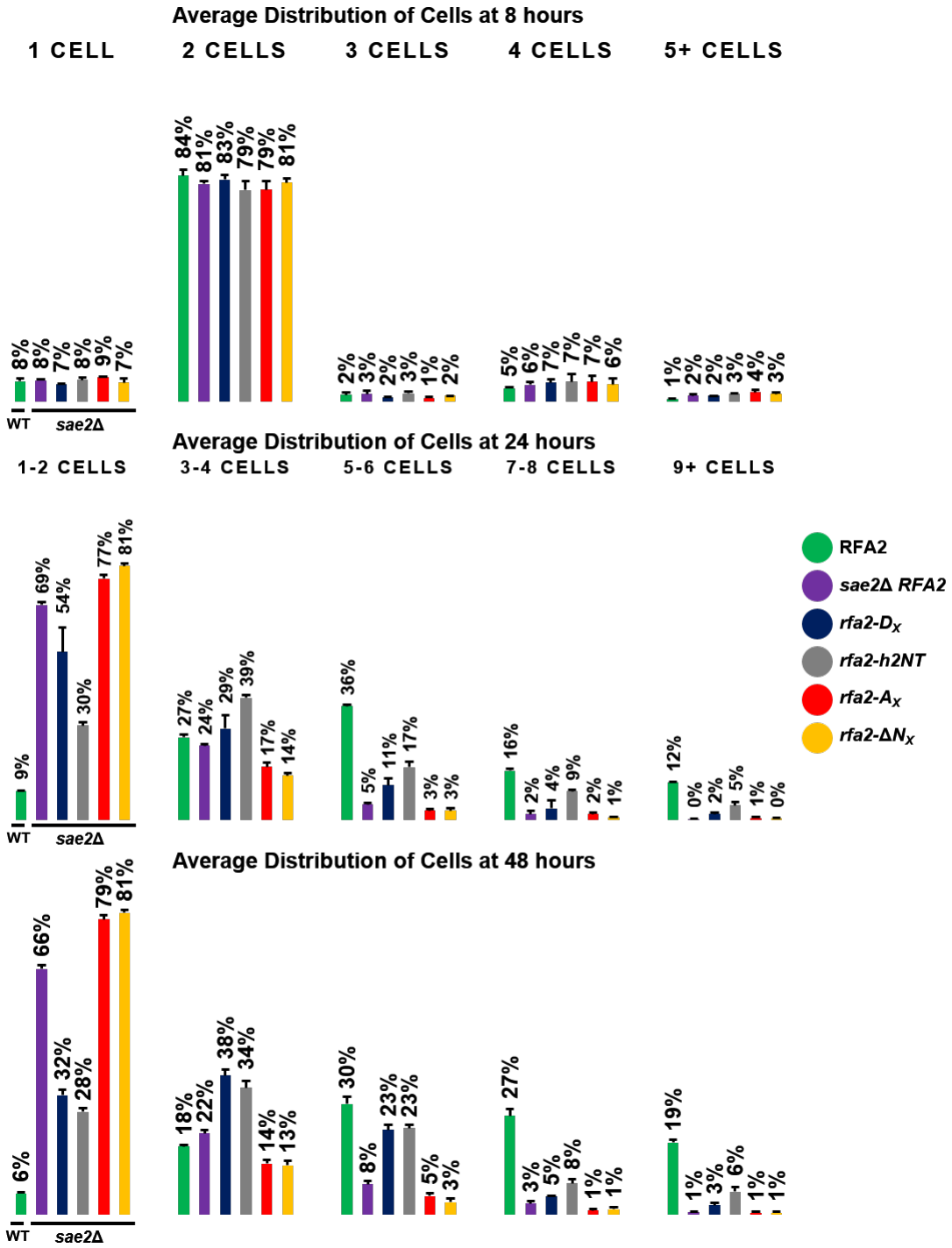

Figure D.11. Distribution of cells in *sae2*Δ Rfa2 NT extensive mutations during adaptation time course.
*sae2*Δ cells containing Rfa2 NT mutations were harvested from HO-induced culture at 8 hours, diluted, spread on YPRG plates using glass beads, and then analyzed microscopically and quantitated at 8, 24, and 48 hours post-HO induction. Averages are from three independent replicate data sets. HO expression was induced in exponentially growing cells by adding 2% galactose to the media.

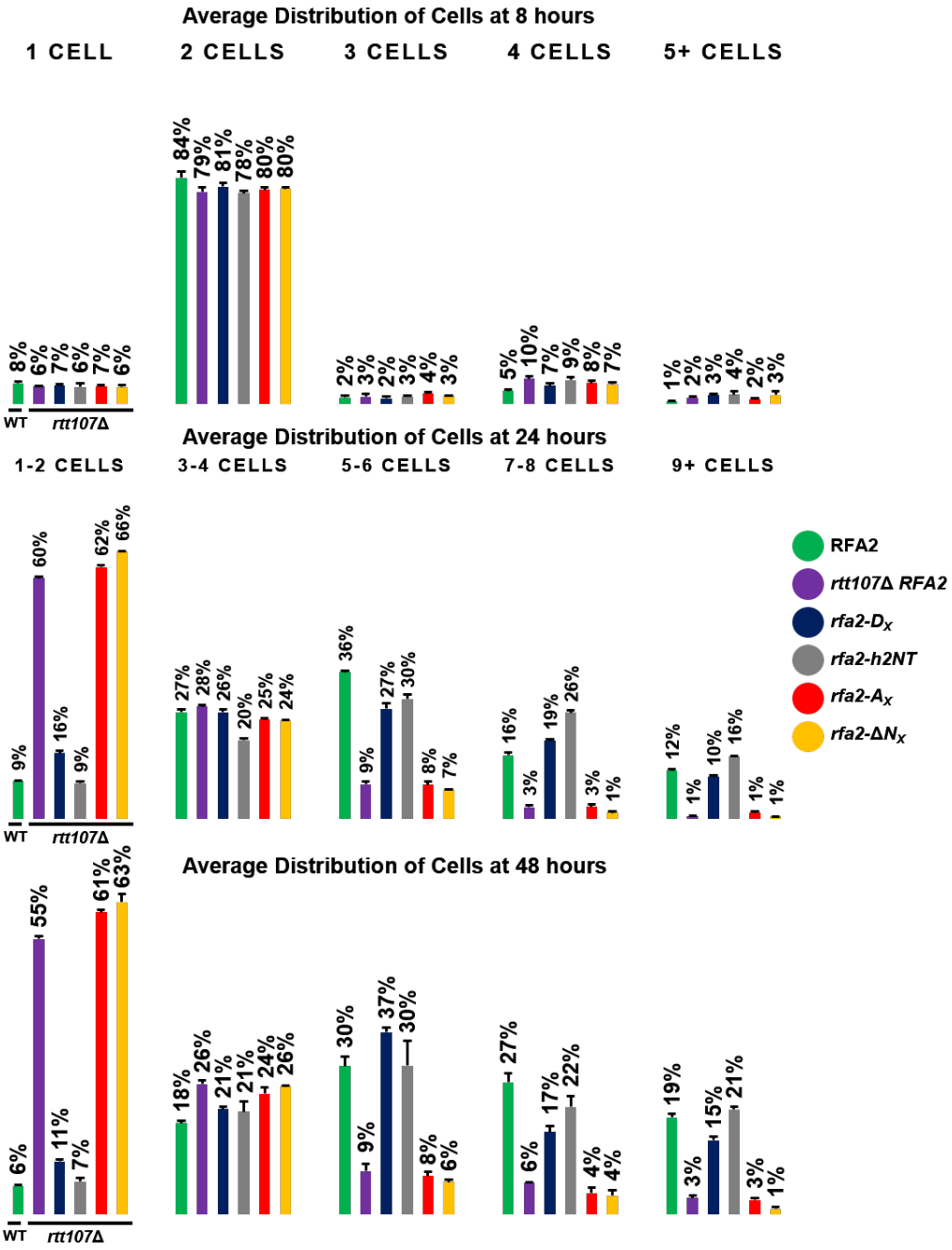

Figure D.12. Distribution of cells in *rtt107*Δ Rfa2 NT extensive mutations during adaptation time course.
*rtt107*Δ cells containing Rfa2 NT mutations were harvested from HO-induced culture at 8 hours, diluted, spread on YPRG plates using glass beads, and then analyzed microscopically and quantitated at 8, 24, and 48 hours post-HO induction. Averages are from three independent replicate data sets. HO expression was induced in exponentially growing cells by adding 2% galactose to the media.

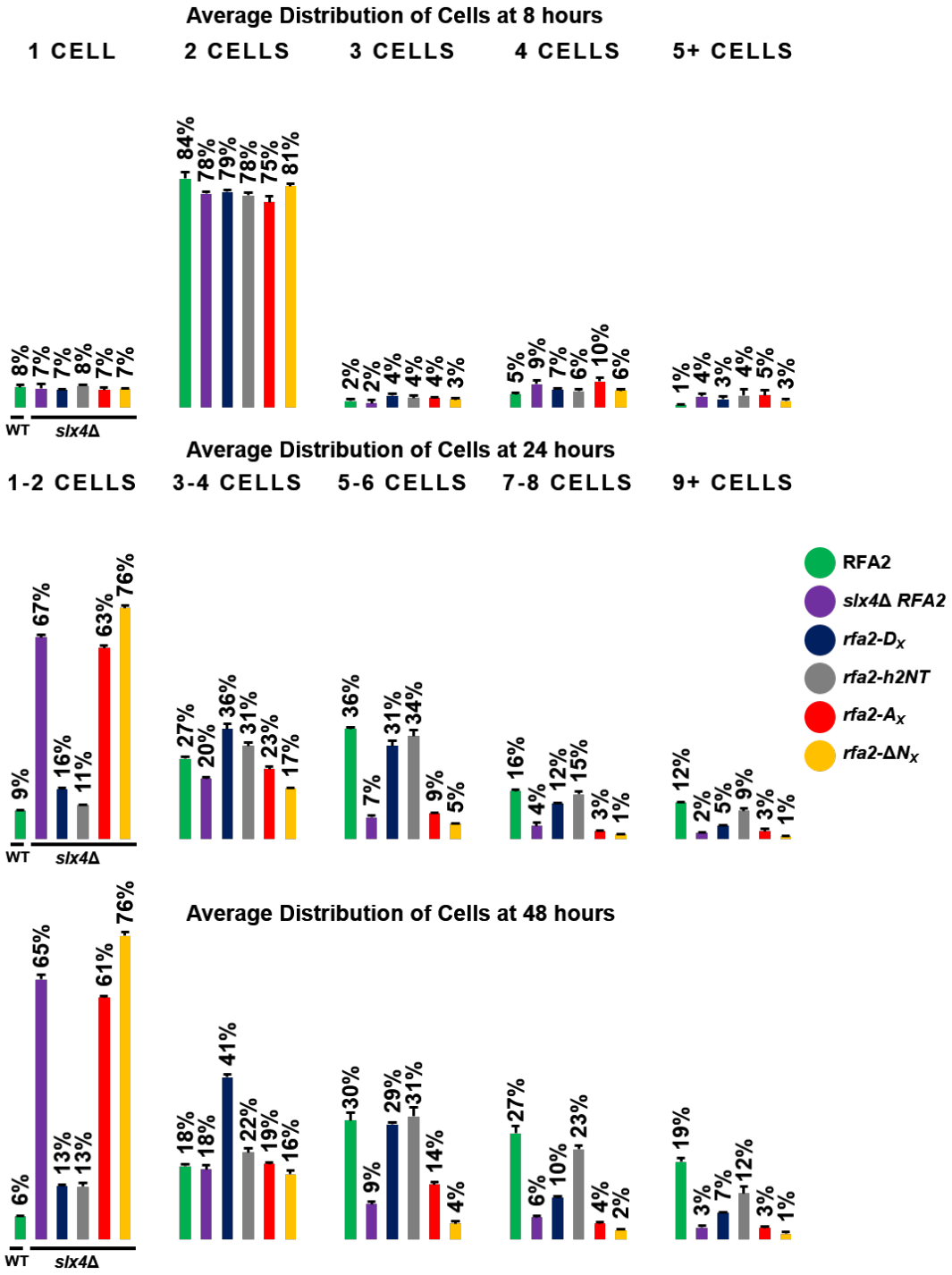

Figure D.13. Distribution of cells in *slx4*Δ Rfa2 NT extensive mutations during adaptation time course.
*slx4*Δ cells containing Rfa2 NT mutations were harvested from HO-induced culture at 8 hours, diluted, spread on YPRG plates using glass beads, and then analyzed microscopically and quantitated at 8, 24, and 48 hours post-HO induction. Averages are from three independent replicate data sets. HO expression was induced in exponentially growing cells by adding 2% galactose to the media.

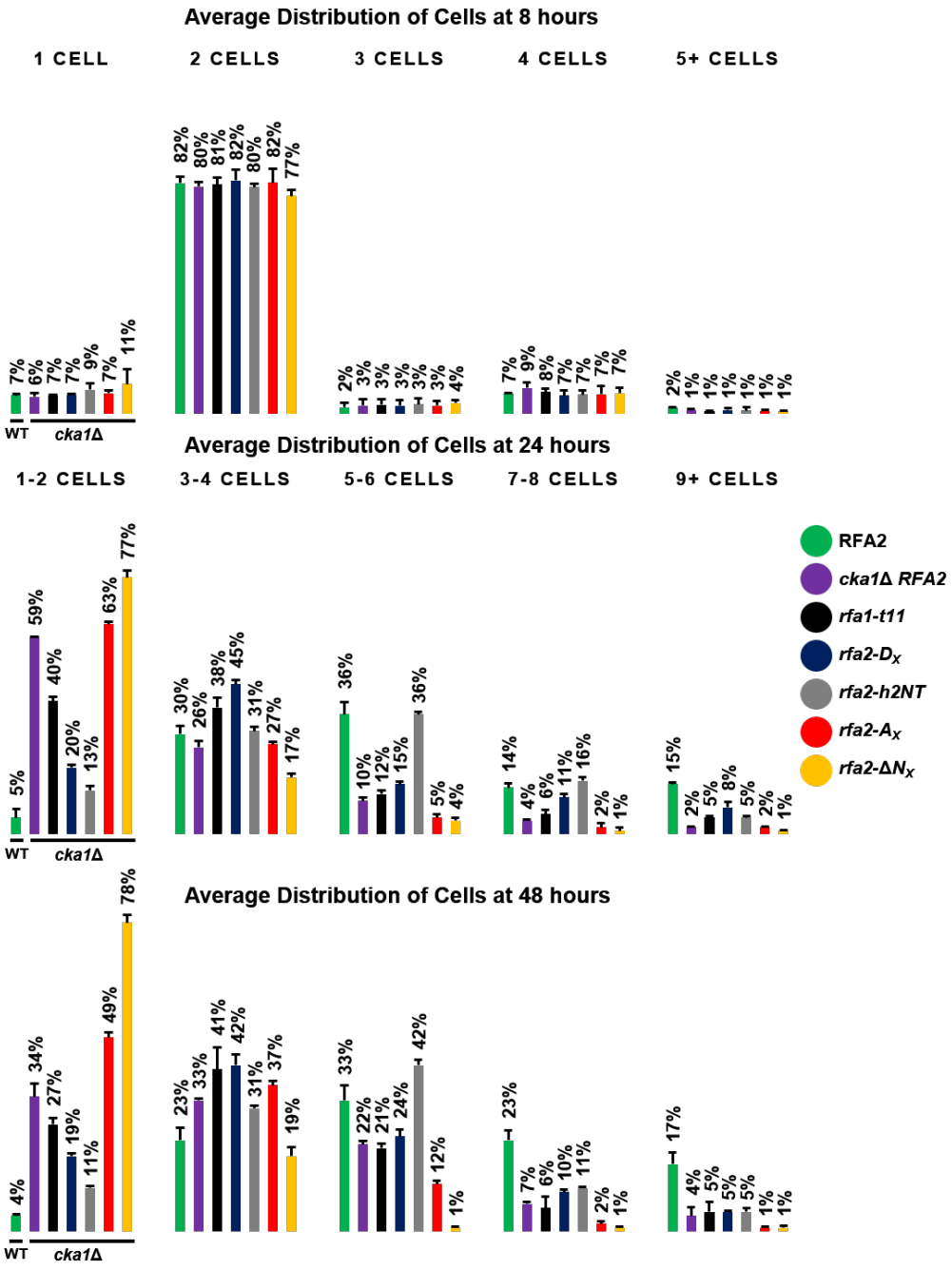

Figure D.14. Distribution of cells in *cka1*Δ Rfa2 NT extensive mutations during adaptation time course.

*cka1*Δ cells containing Rfa2 NT mutations were harvested from HO-induced culture at 8 hours, diluted, spread on YPRG plates using glass beads, and then analyzed microscopically and quantitated at 8, 24, and 48 hours post-HO induction. Averages are from three independent replicate data sets. HO expression was induced in exponentially growing cells by adding 2% galactose to the media.

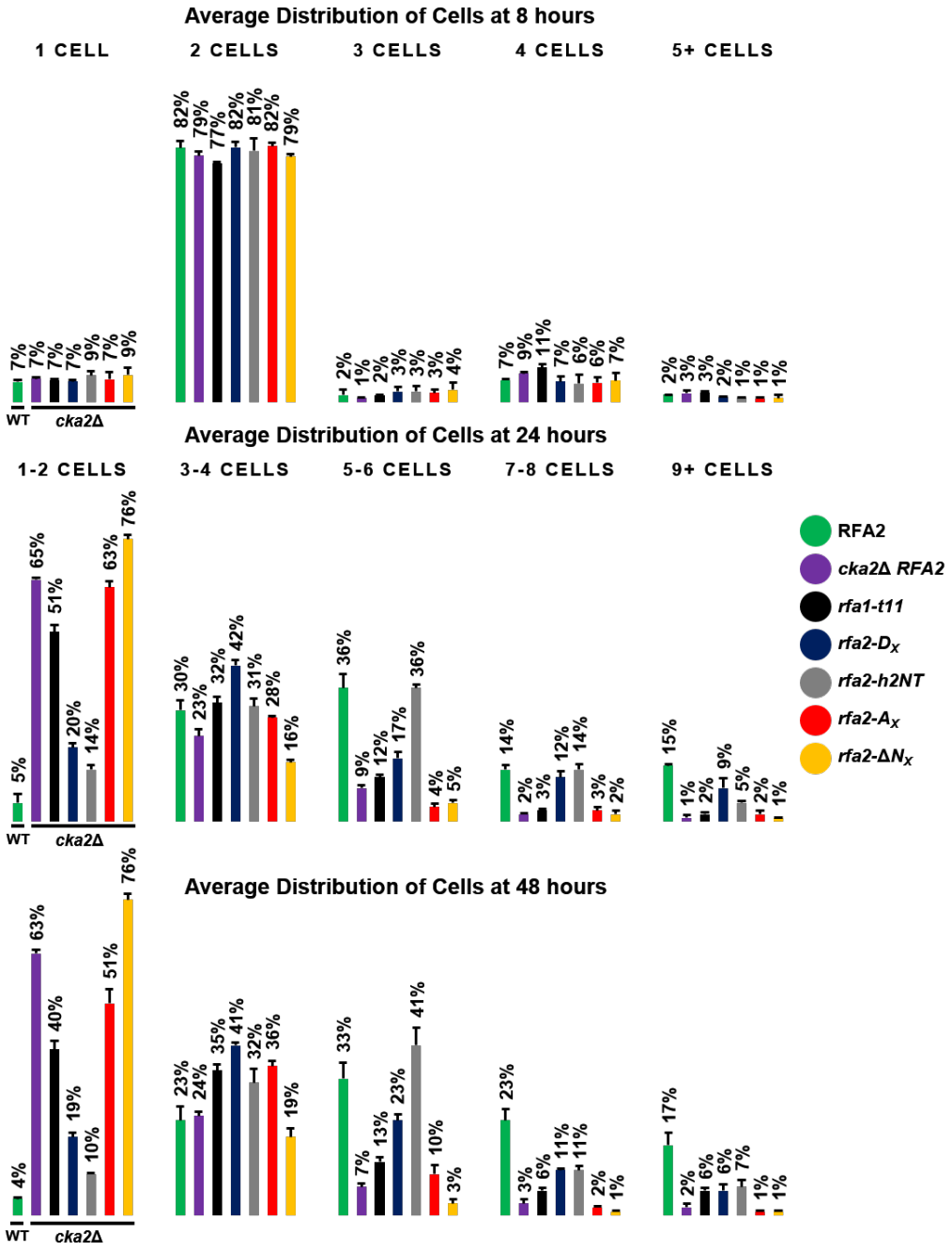

Figure D.15. Distribution of cells in *cka2*Δ Rfa2 NT extensive mutations during adaptation time course.

*cka2*Δ cells containing Rfa2 NT mutations were harvested from HO-induced culture at 8 hours, diluted, spread on YPRG plates using glass beads, and then analyzed microscopically and quantitated at 8, 24, and 48 hours post-HO induction. Averages are from three independent replicate data sets. HO expression was induced in exponentially growing cells by adding 2% galactose to the media.

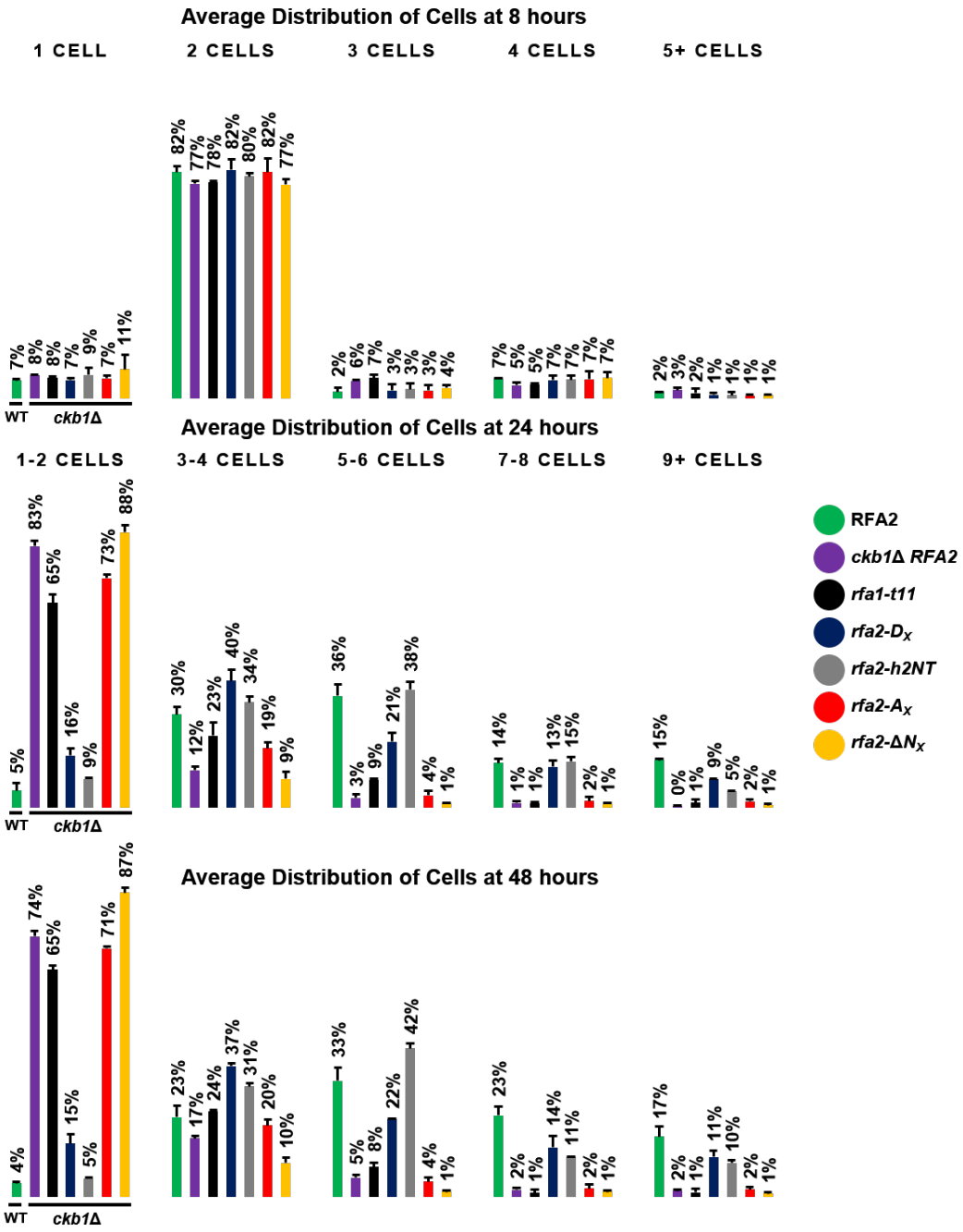

Figure D.16. Distribution of cells in *ckb1*Δ Rfa2 NT extensive mutations during adaptation time course.

*ckb1*Δ cells containing Rfa2 NT mutations were harvested from HO-induced culture at 8 hours, diluted, spread on YPRG plates using glass beads, and then analyzed microscopically and quantitated at 8, 24, and 48 hours post-HO induction. Averages are from three independent replicate data sets. HO expression was induced in exponentially growing cells by adding 2% galactose to the media.

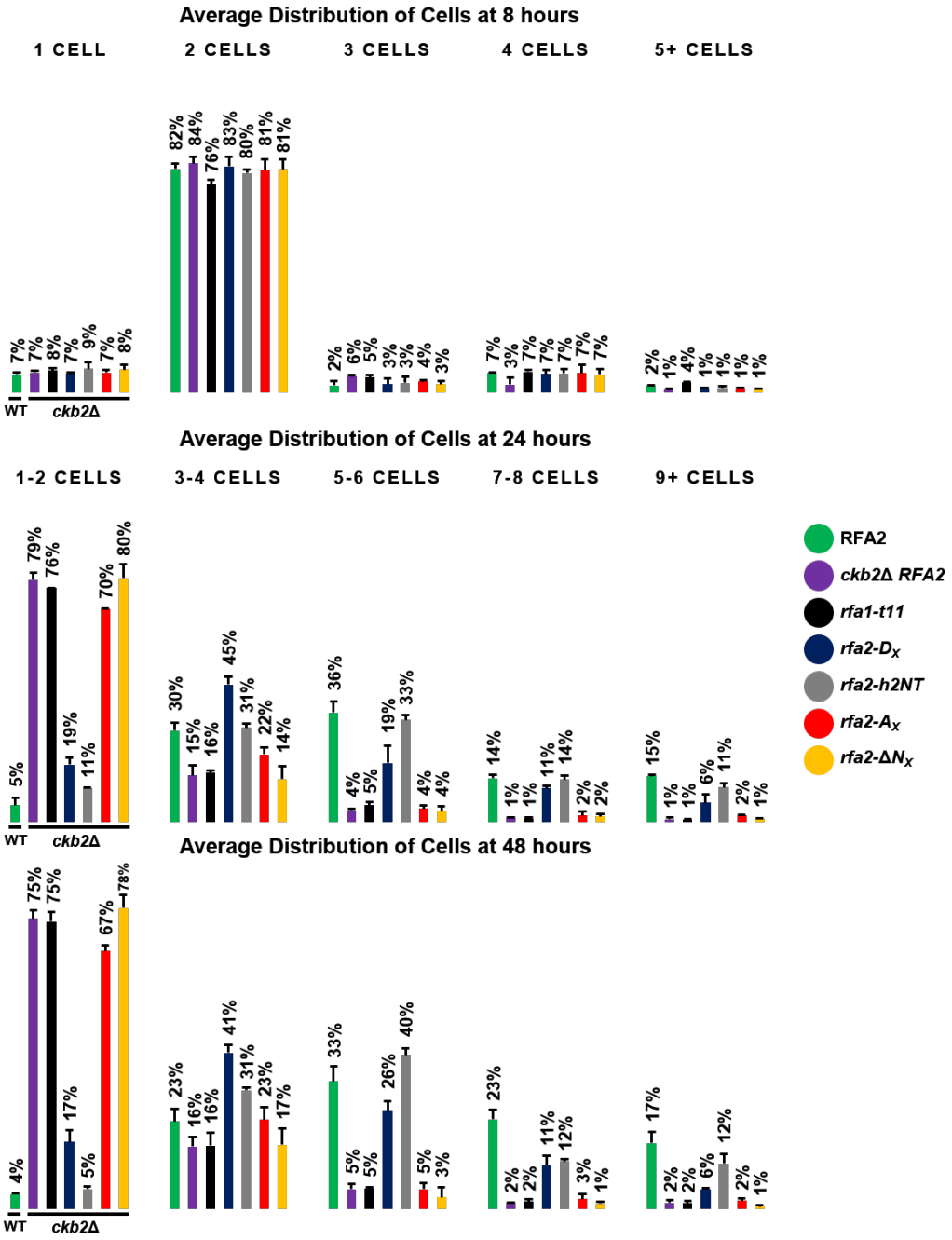

Figure D.17. Distribution of cells in *ckb2*Δ Rfa2 NT extensive mutations during adaptation time course.

*ckb2*Δ cells containing Rfa2 NT mutations were harvested from HO-induced culture at 8 hours, diluted, spread on YPRG plates using glass beads, and then analyzed microscopically and quantitated at 8, 24, and 48 hours post-HO induction. Averages are from three independent replicate data sets. HO expression was induced in exponentially growing cells by adding 2% galactose to the media.